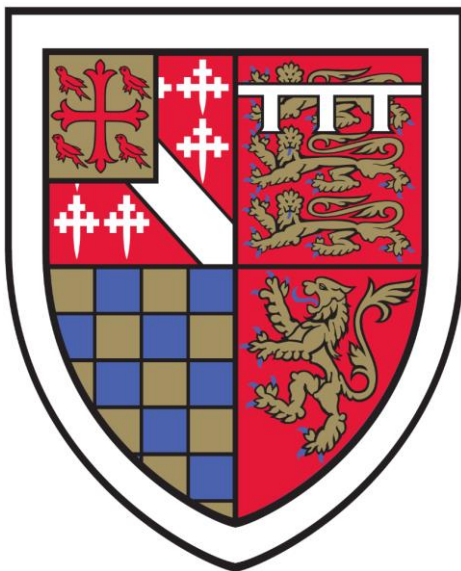


C-H ACTIVATION OF FUNCTIONAL MATERIALS



Png Zhuang Mao

St Edmund's College

University of Cambridge

This dissertation is submitted for the Degree of Doctor of Philosophy

Department of Chemistry, University of Cambridge

Lensfield Road

Cambridge

CB2 1EW

6th April 2020

I DECLARATION

This dissertation is submitted in partial fulfilment of the requirements for the degree of Doctor of Philosophy in Chemistry. It describes work carried out in the Department of Chemistry, University of Cambridge, from the April of 2016 to the April of 2018, as well as work carried out in the Institute of Materials, Research, and Engineering (IMRE), Singapore, from April of 2018 to April of 2020. Unless otherwise indicated, the research described is my own, and not the product of collaboration. It is not substantially the same as any that I have submitted, or, is being concurrently submitted for a degree or diploma or other qualification at the University of Cambridge or any other University or similar institution except as declared in the Preface and specified in the text. I further state that no substantial part of my thesis has already been submitted, or, is being concurrently submitted for any such degree, diploma or other qualification at the University of Cambridge or any other University or similar institution except as declared in the Preface and specified in the text.

Png Zhuang Mao

6th April 2020

II STATEMENT OF LENGTH

This dissertation does not exceed the word limit of 60 000 as set by the Degree Committee for the faculty of Physics and Chemistry.

Png Zhuang Mao

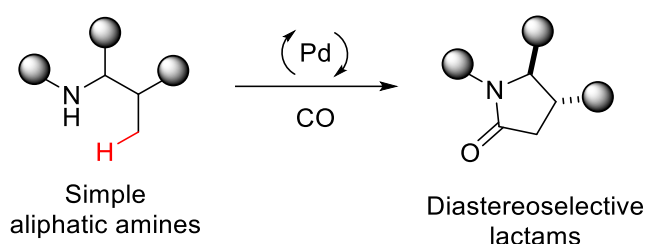
6th April 2020

III ABSTRACT

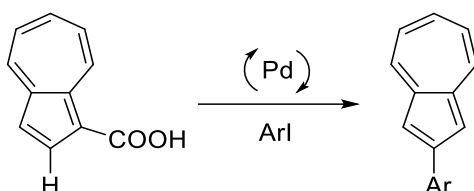
C-H Activation of Functional Materials, PNG Zhuang Mao

This thesis comprises three projects on the theme of C-H activation for the synthesis of functional materials.

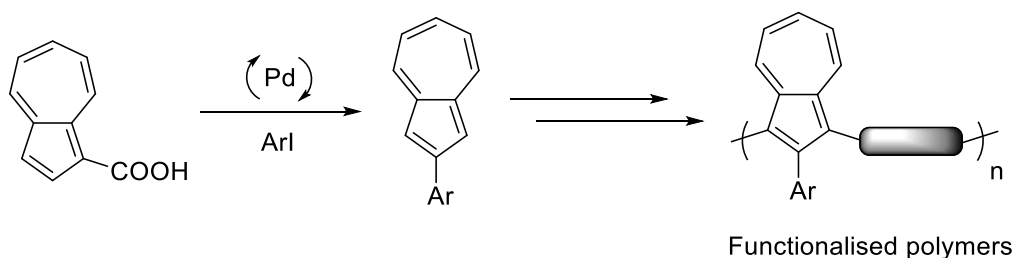
Chapter 1 describes the development of gamma C-H carbonylation of free aliphatic secondary amines to form secondary lactams. The diastereoselectivity of the reaction was found to be significantly influenced by the choice of reaction conditions. Under optimised conditions, a wide range of lactams were delivered in high yields and good *d.r.*, with many different functional groups and substitution patterns being tolerated. Further transformation of the lactam was also demonstrated, yielding pyrrolidines and functionalised lactams.



Chapter 2 describes the development of a carboxylate directed C-H arylation of azulene at the 2-position. This methodology enables the overriding of the natural reactivity of the 1, 3-position to conveniently access 2-arylated azulene, without regioselectivity issues and in moderate to high yields. The reaction was found to tolerate a wide range of aryl groups, including some heteroarenes. In-situ decarboxylation was also observed, allowing the carboxylate to act as a traceless directing group.



This methodology was subsequently applied to the preparation of 2-functionalised azulene – fluorene polymers in chapter 3. These polymers were then tested for electrochromic applications and optical sensitivity to acidic environment. Functionalisation of azulene was found to significantly influence the properties of these polymers. In particular, electron-donating aryl groups were found to enhance the sensitivity of the polymers to acidic environments.



IV ACKNOWLEDGEMENTS

This work would have been impossible for all the help and support which I had received over the past four years. I would like to thank Professor Matthew Gaunt who gave me this opportunity to work in this amazing group, as well as for his valuable insights and guidance. In the same way, I would also like to thank Dr Xu Jianwei for his continual faith in me and supporting me in the pursuit of this PhD.

To my mentors and collaborators, Jaime Cabrera, Darren Wilcox and Jorge Piero Cadahia, thank you all for all your guidance and support. Thank you also to my IMRE colleagues, Kang Yi, Shermin, Ming Hui, Debbie, Hui Ning, Georgina, Xi Ping, Anqi, Seok Hong, and Teck Huat for all your help and support in all areas of keeping and maintaining a safe and effective working environment in the lab. Special thanks goes to Shermin and Ming Hui for helping me to proof read this thesis. To my colleagues in the Gaunt group and in IMRE, thank you for your friendship and laughter, creating a pleasant working environment, especially in times where scientific results deviate from ideality.

I would also like to thank A*STAR AGA for supporting me in this PhD Program. Thank you for believing in us and cultivating the scientific community in Singapore. Thanks also to IMRE for hosting me during the past two years. I look forward to being able to contribute to A*STAR in the coming years.

My thanks also goes out to my family for always being supportive and always being there. This journey would have been impossible otherwise. Love you all!

Thanks to my awesome churchmates and cell group who are always keeping me in prayer, and hearing me out even when I speak in another tongue.

Special thanks goes to Prof Robert Phipps and Prof Simon Lewis for the great project discussion and all the encouragement.

Most of all, thank you God for giving me life, health, and everything to be able to pursue this PhD.

V LIST OF ABBREVIATIONS

| | |
|-------------------------|--|
| °C | Degrees Celsius |
| Ac | acetyl |
| Ad | 1-adamantyl |
| aq | aqueous |
| Ar | aryl |
| Bn | benzyl |
| BQ | 1,4-benzoquinone |
| Bu | butyl |
| calc. | calculated |
| CMD | concerted metallation/deprotonation |
| <i>d.r.</i> | diastereomeric ratio |
| DG | directing group |
| DMF | <i>N,N</i> -dimethylformamide |
| DMSO | dimethyl sulfoxide |
| eq | equivalents |
| ESI | electron spray ionisation |
| Et | ethyl |
| FG | functional group |
| g | grams |
| GCMS | gas chromatography-mass spectrometry |
| Hrs | hours |
| HOMO | highest occupied molecular orbital |
| HPLC | high performance liquid chromatography |
| HRMS | high resolution mass spectrometry |
| Hz | hertz |
| IR | infrared |
| <i>J</i> | coupling constant (in Hertz) |
| LUMO | lowest unoccupied molecular orbital |
| <i>m</i> | meta |
| M | Molarity |
| MOF | Metal organic framework |
| Me | methyl |
| mL | milliliter |
| mmol | millimole |
| mol | mole |
| NFSI | N-Fluorobenzenesulfonimide |
| NMR | nuclear magnetic resonance |
| <i>o</i> | ortho |
| <i>p</i> | para |
| Ph | phenyl |
| Piv | pivaloyl |
| ppm | parts per million |
| R | variable group |
| rt | room temperature |
| <i>t</i> or <i>tert</i> | tertiary |
| TCE | 1,1,2,2-tetrachloroethane |
| TFA | trifluoroacetyl/trifluoroacetic acid |
| THF | tetrahydrofuran |
| TLC | thin layer chromatography |
| TMEDA | tetramethylethylenediamine |
| TRIPS | 2,4,6-triisopropylbenzoic acid |
| Ts | tosyl |

UV

ultraviolet

VI CONTENTS

| | |
|--|----|
| I Declaration | 2 |
| II Statement of Length | 2 |
| III Abstract | 4 |
| IV Acknowledgements | 3 |
| V List of Abbreviations | 4 |
| VI Contents | 7 |
| Chapter 1: C-H Carbonylation of Free Aliphatic Amines to Form Functionalized γ -Lactams | 9 |
| 1.1 Introduction | 9 |
| 1.1.1 Introduction to C-H Activation | 9 |
| 1.1.1.1 Mechanism of C-H Activation | 10 |
| 1.1.1.2 Directing Groups and Cyclometallation | 11 |
| 1.1.2 Palladium Catalysed C-H Activation in Aliphatic Amines | 12 |
| 1.1.2.1 C(sp ³)-H Activation Directed by Amine Derivatives | 12 |
| 1.1.2.3 Free Amine Directed C(sp ³)-H Activation | 21 |
| 1.2 Results and Discussion | 29 |
| 1.2.1 Early Leads and Hypothesis | 29 |
| 1.2.2 Optimisation of Reaction Selectivity | 31 |
| 1.2.3 Optimisation of Reaction Efficacy | 36 |
| 1.2.4 Optimisation of Reaction Diastereoselectivity | 39 |
| 1.2.5. Substrate Scope | 47 |
| 1.2.6 Functionalisation of Lactams | 52 |
| 1.2.7 Reaction Mechanism | 54 |
| 1.3 Summary | 55 |
| Chapter 2: Carboxylate Directed C-H Arylation of Azulene | 56 |
| 2.1 Introduction | 56 |
| 2.1.1 Functionalisation at the 1, 3-Position of Azulene | 56 |
| 2.1.2 Functionalisation at the 4 – 8-Position of Azulene | 58 |
| 2.1.3 Functionalisation at the 2-Position of Azulene | 61 |
| 2.2 C-H Activation of Azulene | 63 |
| 2.3 Results and Discussion | 64 |
| 2.3.1 Optimisation of Reaction | 65 |

| | |
|--|-----|
| 2.3.2 Scope of Reaction..... | 72 |
| 2.4 Reaction Mechanism..... | 77 |
| 2.5 Summary..... | 78 |
| Chapter 3: Polymeric Azulene with Functionalisation at the 2-Position..... | 79 |
| 3.1 Introduction | 79 |
| 3.1.1 Polyazulenes Connected on the Five-Membered Ring | 79 |
| 3.1.2 Polyazulenes Connected on the Seven-Membered Ring..... | 88 |
| 3.1.3 Miscellaneous Polymeric Azulene Structure | 93 |
| 3.2 2-Functionalised Azulene in Polymeric Materials..... | 97 |
| 3.3 Results and Discussion | 98 |
| 3.4 Summary | 108 |
| 4. Experimental | 109 |
| 4.1 General Experimental Procedure | 109 |
| 4.2 Experimental Conditions for Carbonylation | 109 |
| 4.3 Synthesis of Amines | 110 |
| 4.4 Carbonylation of Amines | 128 |
| 4.5 Functionalisation of Lactams..... | 143 |
| 4.6 Palladacycle Studies | 145 |
| 4.7 Synthesis of Azulene-1-Carboxylic Acids..... | 147 |
| 4.8 C-H Arylation of Azulene-1-Carboxylic Acid..... | 149 |
| 4.9 Bromination of 2-Functionalised Azulene..... | 160 |
| 4.10 Suzuki Polymerisation..... | 163 |
| 4.11 Miscellaneous Spectra | 165 |
| 5. References..... | 169 |
| Appendix A..... | 174 |
| Appendix B..... | 181 |
| Appendix C: Proton and Carbon NMRs..... | 186 |

CHAPTER 1: C-H CARBONYLATION OF FREE ALIPHATIC AMINES TO FORM FUNCTIONALIZED γ -LACTAMS.

This chapter describes the development of C-H carbonylation of free aliphatic secondary amines to form secondary γ -lactams. The diastereoselectivity of the reaction was found to be significantly influenced by the choice of reaction conditions. Under optimised conditions, a wide range of lactams were delivered in high yields and good *d.r.*, with many different functional groups and substitution patterns being tolerated.

1.1 INTRODUCTION

1.1.1 Introduction to C-H Activation

Transition metal catalysed reactions (figure 1) have completely transformed the area of organic synthesis and can be considered the cornerstone of modern chemistry. These reactions have completely changed the way chemists view chemical synthesis, paving the way for transformations which would be difficult to carry out using classical methods. Some of the best known transformations include the Suzuki,¹ Negishi,² and Heck³ reactions, which were first reported in the late 1960s and 1970s, and won the Nobel Prize in Chemistry in 2010.

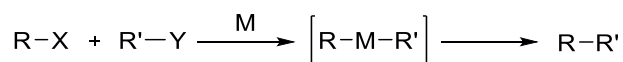


Figure 1: General scheme of transition metal catalysed cross coupling reactions.

Although remarkable in its scope of applications, these reactions often require the use of pre-activated substrates such as organotin, organoborates, or organohalides prior to the cross-coupling step. In contrast, C-H bonds are usually less reactive, given their high bond energy ($\sim 95 - 110 \text{ kcal mol}^{-1}$ compared to $\sim 70 - 85 \text{ kcal mol}^{-1}$ for C-Br bonds⁴), low acidity (pK_a up to 56 in the case of methane⁵), and low polarity. The most unreactive C-H bonds, namely in alkanes, usually react only under harsh conditions such as in combustion, or in the presence of high energy reactants such as superacids,⁶ free radicals,⁷ carbenes⁸ and nitrenes.⁹ Typically unselective and often destructive, these processes tend to be functional group intolerant and less useful for targeted chemical synthesis.

Yet mild, direct, and selective reaction of the C-H bond is possible. For instance, in nature, enzymes such as Cytochrome P450 mono-oxygenase are able to selectively oxidise unactivated C-H bonds.¹⁰ As C-H bonds are ubiquitous in organic molecules, a general method to selectively transform these bonds without pre-functionalisation (C-H activation) would be a highly useful reaction. Some of the earliest reports of stoichiometric C-H activation include Dubeck's cleavage of a $\text{C}(\text{sp}^2)$ -H bond using a Cp_2Ni complex to form organonickel complex **1b** in 1963¹¹ (figure 2a), and Murahashi's cobalt catalysed carbonylation of 1-diphenylmethanimine **2a** to form 2-phenylisoindolin-1-one **2b** in 1955¹² (figure 2b). In 1993, Murai reported the first catalytic C-H activation, using an organometallic ruthenium complex¹³ (figure 2c).

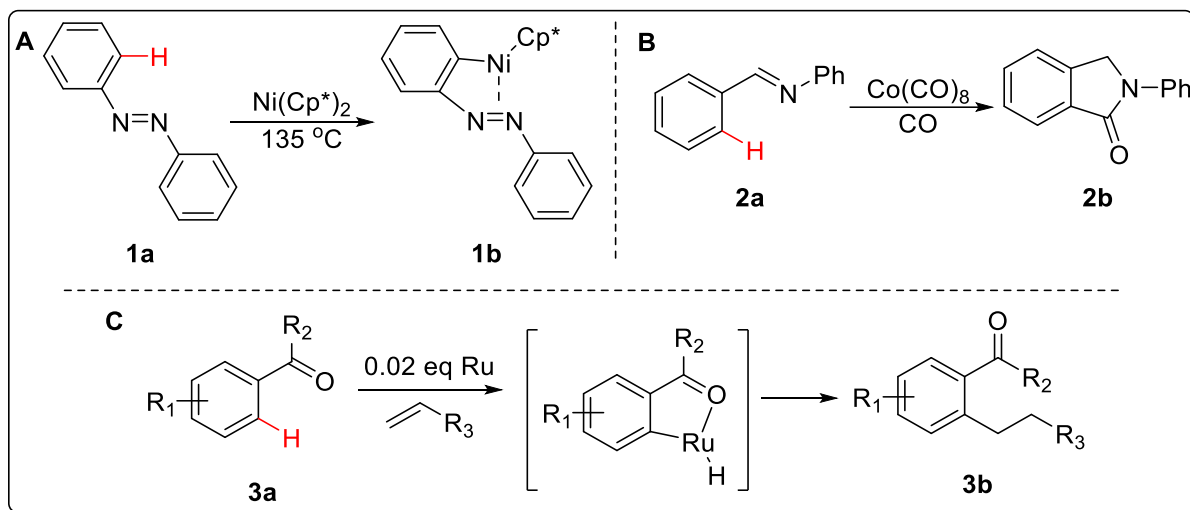


Figure 2: Early reports of C-H activation (a) Dubeck's cleavage of a C-H bond using nickel (II) cyclopentadiene. (b) Murahashi's carbonylation of 1-diphenylmethanimine. (c) Murai's seminal catalytic C-H activation.

Since then, the field of C-H activation has exploded, such that it is now one of the most important fields in chemistry. While earlier works typically activate either $\text{C}(\text{sp}^2)\text{-H}$ bonds or $\text{C}(\text{sp})\text{-H}$ bonds, advances in the field have meant that even the more unreactive $\text{C}(\text{sp}^3)\text{-H}$ bonds can be activated.^{14,15} Today, a vast range of chemical transformation is possible, including alkoxy carbonylation,^{16,17} arylation,¹⁸ halogenation,¹⁹ oxidation,²⁰ and polymerisation.²¹ Control of regioselectivity has also been achieved in many cases with directing groups such as amides²² and sulfoxides²³ enabling selective functionalization at either the β or γ positions.²⁴ On aromatic rings, apart from the commonly reported *ortho* directed C-H activation,^{25–28} *meta* directed C-H activation has also been achieved in some cases by using templates.^{29–31} In some cases, mild condition C-H activation have also been reported, with reactions occurring at room temperature, without strong oxidant, reductants, acids or bases, enabling more functional groups to survive the reaction.³² Our fundamental understanding of C-H activation has also been improved by mechanistic studies of these reactions.^{33–36}

1.1.1.1 Mechanism of C-H Activation

There are five main mechanisms of C-H activation, namely concerted metalation deprotonation (CMD), oxidative addition, σ -bond metathesis, 1,2 insertion, and metalloradical mechanism.^{37,38} However, the lines between these mechanisms are blurred and can be difficult to distinguish experimentally.³⁹

Early mechanistic studies on palladium C-H activation found that the acetate counterion is generally the best for reactivity. There are a few reasons for this. Firstly, the acetate acts reversibly as either a monodentate ligand, or a bidentate ligand (figure 3a). It also increases the electrophilicity of palladium, and acts as an intramolecular base.⁴⁰ Studies by Ryabov's group in 1985 on the *ortho*-palladation of *N,N*-dimethylbenzylamine, found evidence for an ordered, compact transition state, consistent with intramolecular deprotonation by the acetate.⁴¹ Computational studies by Davies in 2005 supports this observation, demonstrating that the most favourable route is via an agostic interaction⁴² with the C-H bond, which helps to increase the acidity of the proton, lowering the energy barrier for deprotonation. Subsequent deprotonation by the acetate ligand, with simultaneous formation of the Pd-C bond takes place via a six membered transition state³⁹ (figure 3b). This is usually known as

the CMD mechanism, although other names such as the internal electrophilic substitution,⁴³ and ambiphilic metal-ligand activation,⁴⁴ had also been used interchangeably. Other possible mechanisms for C-H activation are also briefly illustrated in figure 3c.

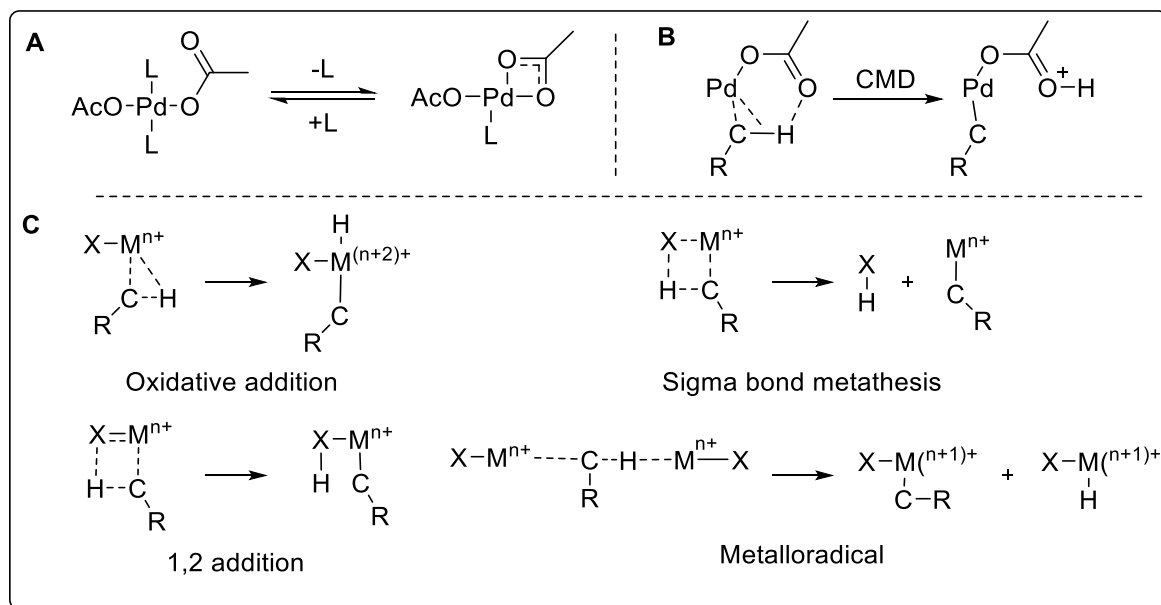


Figure 3: (a) Acetate's ability to act as either a monodentate ligand or a bidentate ligand. (b) General CMD mechanism, involving an agnostic C-H interaction with palladium and a concerted deprotonation of the proton by the acetate ligand. (c) Other proposed mechanisms for C-H activation: Oxidative addition, sigma bond metathesis, 1,2 addition, and metalloradical mechanism.

1.1.1.2 Directing Groups and Cyclometallation

While CMD and other C-H activation mechanisms can in-principle occur intermolecularly, the presence of a Lewis base can pre-coordinate the molecule to the metal centre,^{34,45} resulting in a more favoured intramolecular C-H activation. This Lewis basic group thus acts as a directing group for C-H activation to form the metallocyclic complex. Two main types of directing groups strategies exist. The first is to attach an auxiliary to the molecule, which chelates the metal centre, positioning it for C-H activation (figure 4a). Some examples include amino quinolines as reported by Daugulis's group,²⁴ and oxazolecarboxamide by Liu's group.⁴⁶ Other auxiliaries such as oximes,^{47,48} pyridine *N*-oxides,⁴⁹ and oxosilanes⁵⁰ function by modulating the electronic properties of the parent molecule rather than directing chelating the metal centre. However, this strategy has the inherent drawback of increasing the number of synthetic steps required. Furthermore, removal of the auxiliary post-reaction may sometimes be non trivial, requiring harsh conditions. The second strategy is to make use of native directing groups, whereby functional groups already present in the molecule act as directing groups for C-H activation (figure 4b). Over the last two decades, functional groups such as carboxylic acids,^{51,52} alcohols,⁵⁰ ketones,¹³ sulfoxides,⁶¹ furans and thiophenes,⁵⁴ esters,^{55,56} and amides⁵⁷ have been used as native directing groups for cyclometallation. However, this strategy is not yet generalised, and reaction conditions have to be carefully tuned so as to cater to different directing groups.

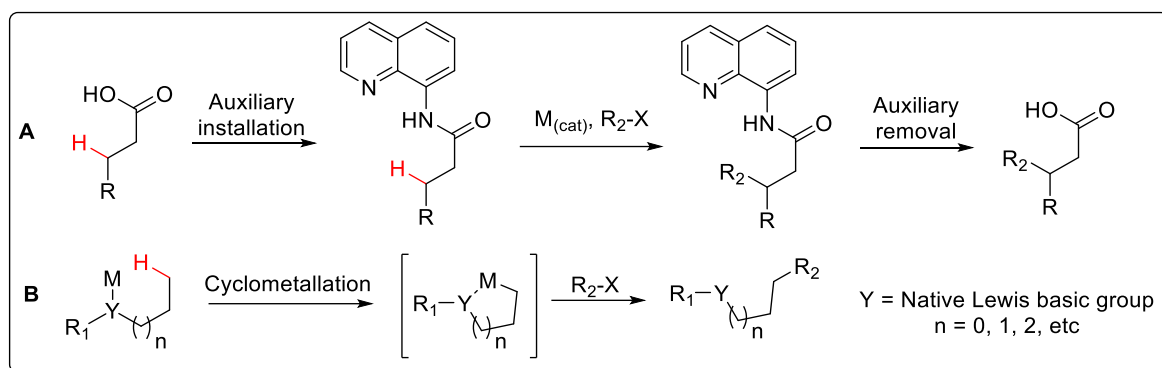


Figure 4: Directing group strategy for C-H activation (a) Auxiliary modulated C-H activation, with amino quinoline as a typical example. (b) Native directing group strategy for C-H activation.

1.1.2 Palladium Catalysed C-H Activation in Aliphatic Amines

Amines are common in many compounds, especially in the areas of pharmaceuticals and agrochemicals. As such, their exploitation as a synthetic handle would be a useful and convenient transformation, enabling simple functionalisation of the molecule. Indeed, classical methods such as alkylation,⁵⁸ and reductive amination⁵⁹ as well as more modern methods including cross coupling,⁶⁰ hydroamination,⁶¹ and photoredox catalysis,⁶² are frequently used to build complex amines. Given that amines are generally excellent ligands, it would be expected that they would also be able to function as a directing group for cyclometallation. This has indeed been achieved for C(sp²)-H functionalisation. As early as 2004, Orito's group reported the carbonylation of benzyl amine to form benzolactams.⁶³ *Ortho*-arylation of benzylamines was also achieved by Daugulis,⁶⁴ Zhang,⁶⁵ and Dixon,⁶⁶ while Shi's group reported *ortho*-olefination in 2007.⁶⁷ On the other hand, prior to 2015, reports of free aliphatic amines directing C(sp³)-H functionalisation are comparatively rarer. The problem is two-fold. Firstly, being such strong ligands, amines typically form the highly stable, but off catalytic-cycle bis(amine) Pd(II) complex with electrophilic palladium salts^{33,68} (figure 5a). Secondly, β -hydride elimination can often be a competing reaction leading to degradation of the starting amine⁶⁹ (figure 5b). As such, C-H activation of amines typically make use of auxiliaries or protecting groups to facilitate the reaction. The following section is an overview of various amine and amine derivatives directed C-H activation.

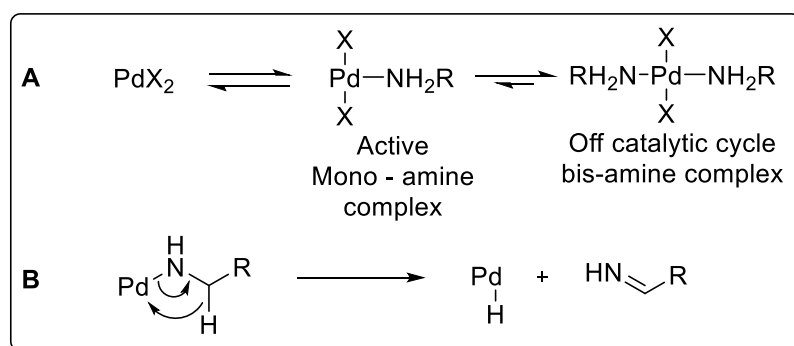


Figure 5: Two main issues for simple amine C-H activation: (a) Formation of an off-catalytic-cycle stable bis-amine complex. (b) General mechanism of β -hydride elimination.

1.1.2.1 C(sp³)-H Activation Directed by Amine Derivatives

The first report of an amine derivative directed C(sp³)-H activation was in 2005 by Daugulis' group (figure 6).²⁴ This was inspired by an earlier report by the same group demonstrating that pyridine is able to act as a directing group for C(sp³)-H arylation (figure 6a). Furthermore, the additional chelating group was also thought to help stabilise high energy Pd(IV) intermediates.⁷⁰ Picolinic acid was attached to various amines as an auxiliary, and the resulting picolinamides were coupled with aryl-iodide under palladium catalysed conditions. Both primary, and secondary γ C-H bonds were arylated in high yields, although longer reaction times is required for the secondary positions (figure 6b). Branching at the α - position was also tolerated and caused no loss in yield. The palladium amide **5c** was isolated, and a preliminary Pd(II) – Pd(IV) pathway was proposed but no extensive mechanistic investigation was carried out (figure 6c).

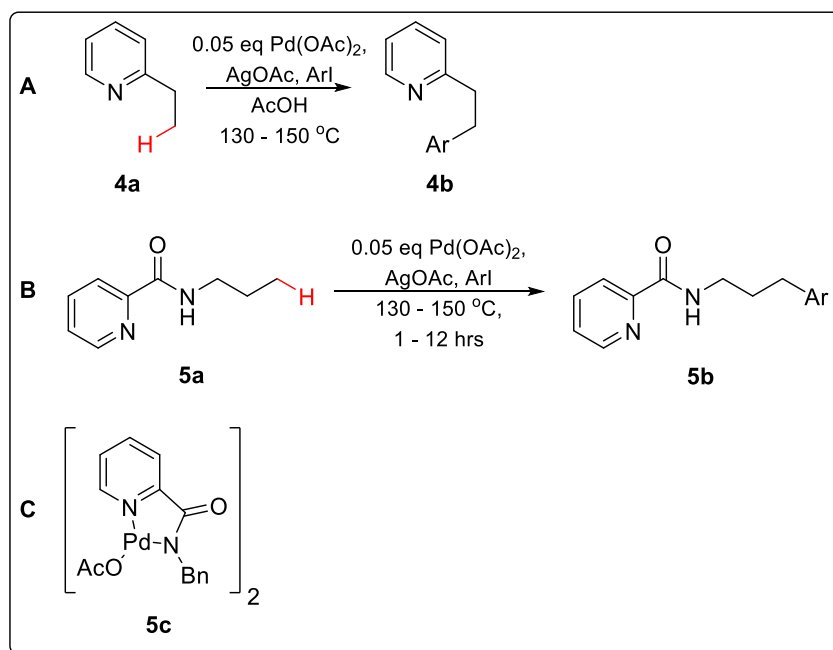


Figure 6: (a) Prior report of pyridine directed arylation. (b) First report of amine derivative (picolinamide) directed C-H arylation. (c) Palladium amide as a possible intermediates of the reaction.

In 2011, Chen's group reported further studies of the picolinamide auxiliary.⁷¹ Screening of picolinamide derivatives revealed a trend: electron donating groups on the pyridine, such as OMe in **6a_{ii}**, improved the yield of the reaction, while the converse was true for electron withdrawing groups such as CF₃ on **6a_{iii}** (figure 7a). Despite this finding, the unmodified picolinamide in **6a_i** was still the preferred auxiliary as its performance is almost comparable with that of 4-methoxypicolinamide in **6a_{ii}**, while having significantly lower cost, commercial availability, and synthetic simplicity. Only the monoarylated product was observed in all cases, although two γ positions are available. Mechanistic studies were not conclusive, but favour a sequential C-H activation / ArI-coupling pathway. The scope of the reaction was also expanded to alkenylation (figure 7b). Coupling with vinyl iodides required somewhat elevated temperatures, as well as the addition of 0.1 equivalent of benzoquinone, with typically modest yields.

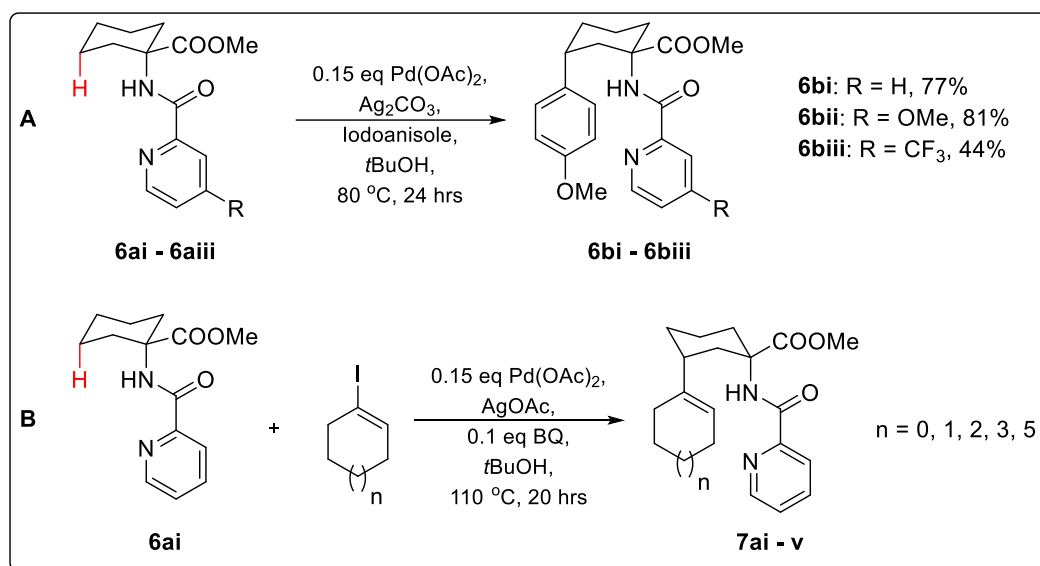


Figure 7: (a) Electronic effects on picolinamide on yields of reaction. (b) Alkenylation of picolinamide protected amines.

Although the picolinamide auxiliary is useful, its post-reaction removal is non-trivial, with conventional amide cleavage methods proving to be unsatisfactory.⁷¹ As such, in 2011, Chen's group made use of a modified picolinamide with a methylene hydroxy group at the ortho position (**8a**), which could help to facilitate cleavage of the amide via an intramolecular acyl transfer (figure 8). This modified picolinamide was removable by treatment with HCl at 80 °C in 70% yield. However, the harsh condition required to remove the picolinamide group highlights one of the main drawbacks of the auxiliary strategy.

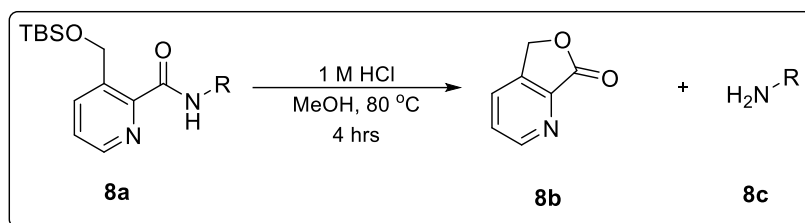


Figure 8: Modified picolinamide auxiliary to enable removal by acidic hydrolysis.

In the same year, Chen's group reported the oxidative ring closure reaction from picolinamide substrates.⁷² The choice of oxidant proved essential to the reaction, with only the hypervalent (diacetoxyiodo)benzene giving promising initial results. The ring strained azetidine product **9b** was favoured even when the five-membered pyrrolidine product **9c** could also be formed via a putative six-membered palladacycle (figure 9). However, in the absence of γ CH₃ groups, pyrrolidines were also formed in good yields. This is attributed to five-membered palladacycles being more kinetically favoured as compared to six-membered palladacycles. The same methodology was also applied to the synthesis of indolines, and the reaction proceeded smoothly even at a lower temperature of 60 °C.

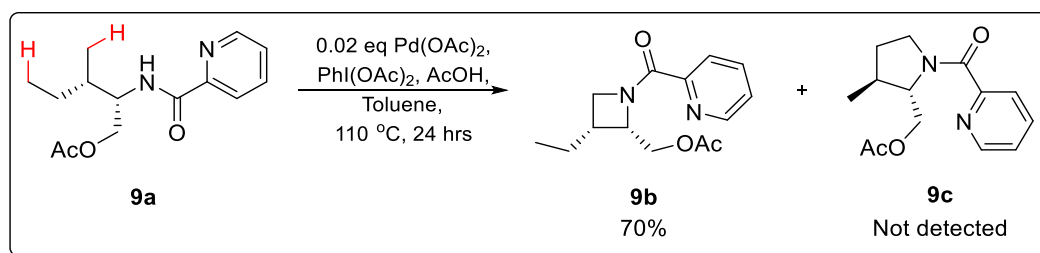


Figure 9: Azetidine selectively formed over pyrrolidines in picolinamide directed oxidative ring closure.

In 2013, alkylation of picolinamide protected aliphatic amines at the γ position was also achieved (figure 10).⁷³ Careful optimisation of the reaction conditions was required, as conditions previously optimised for the alkylation of picolinamide protected benzylamine⁷⁴ failed to produce any desired product for aliphatic amines. Firstly, silver was added as an iodide scavenger. Dibenzyl phosphate was also an essential additive, presumably acting as a phase transfer catalyst for silver carbonate.⁷⁵ Further improvement was also found by addition of sodium iodide and copper (II) chloride, although their functional roles in the reaction is not known. The previously developed more easily removable auxiliary (in **8a**) was also usable in this alkylation reaction.

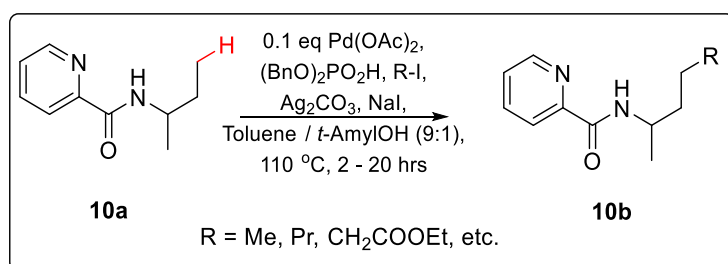


Figure 10: C(sp³)-H alkylation of protected amine at the γ position.

A *N*-(2-pyridyl)sulfonyl derivative of the picolinamide group was employed in 2013 by Carretero's group for the arylation of amino acid derivatives.⁷⁶ This *N*-(2-pyridyl)sulfonyl group has previously been employed in the alkenylation of indoles and pyrroles,^{77,78} as well as the olefination of anilines and arylalkylamines.⁷⁹ In comparison with picolinamide, the *N*-(2-pyridyl)sulfonyl group can be removed under milder conditions, by treatment with zinc at room temperature. Arylation of *L*-valine derivative **11a** was achieved with high diastereoselectivity of more than 20 : 1 (figure 11a). This is likely due to the accessibility of the C-H bond for palladation, as well as the stability of the resulting palladacycle.⁸⁰ Control of mono/bisarylation was also achievable by varying the temperature, as well as the molar equivalence of aryl-iodide used. This methodology could also be employed for functionalisation of dipeptides with good selectivity for monoarylation at the γ -methyl group. The bimetallic palladacycle intermediate (**11d**) was also characterised by single crystal X-ray diffraction.

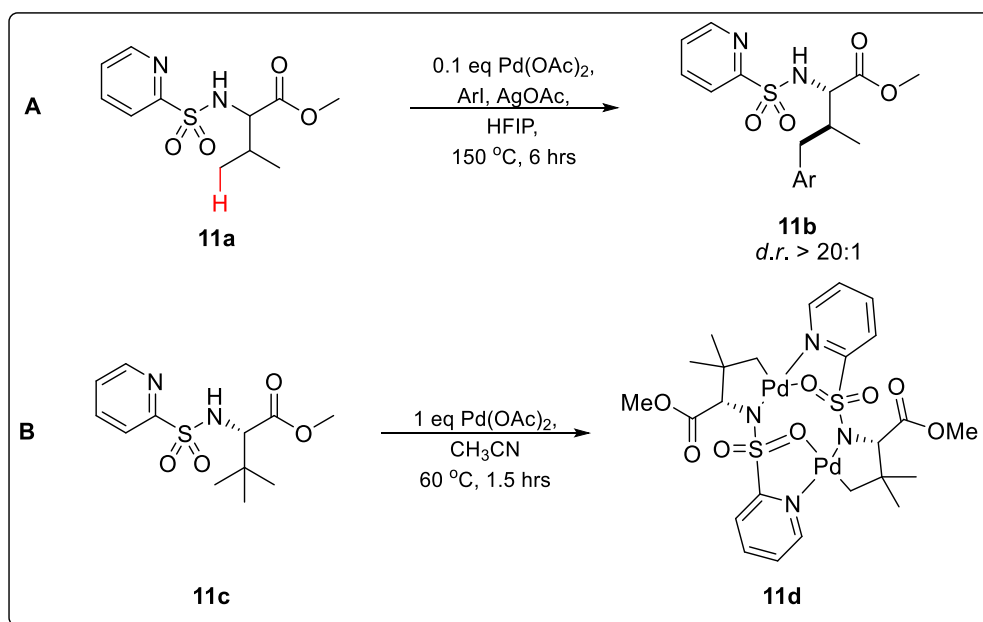


Figure 11: (a) γ Arylation of 2-pyridylsulfonyl protected amino acid derivatives. (b) Stoichiometric palladium reaction generating bimetallic five-membered ring palladacycle complex.

In 2013, Ma's group reported the use of 2-methoxyiminoacetyl as an auxiliary for γ arylation of amino acid (figure 12a).⁸¹ This auxiliary was also easily removable by hydrolysis with KOH in dioxane at room temperature. Furthermore, the auxiliary could also be directly transformed into a glycine residue via hydrogenation, which may be useful in peptide synthesis (figure 12b).

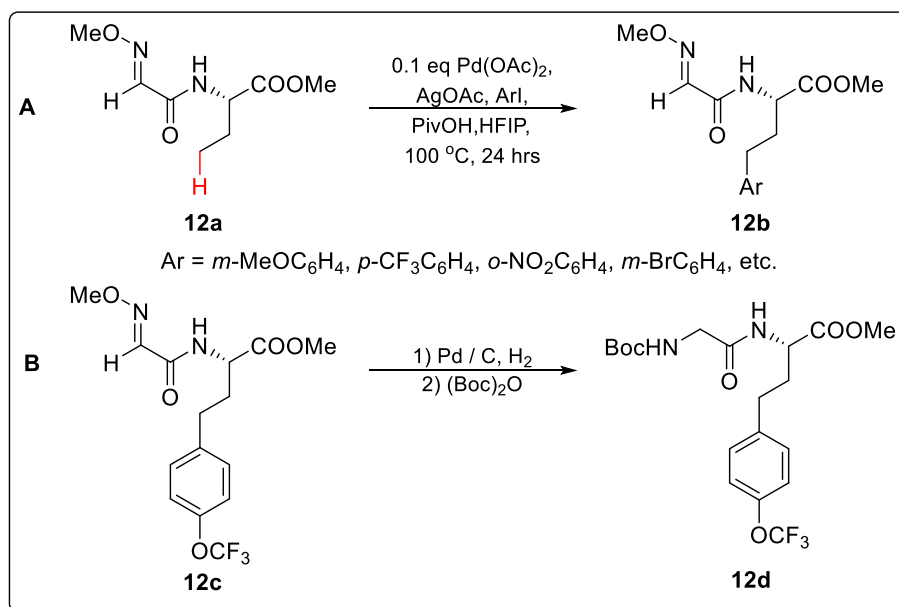


Figure 12: (a) γ -Arylation of amino acids enabled by 2-methoxyiminoacetyl auxiliary. (b) Direct transformation of auxiliary into glycine residue.

Building on Ma's work, Liu's group reported the use of the structurally related 5-methylisoxazole-3-carboxamides as an auxiliary in 2015.⁴⁶ The 5-methyl group on **23a** was found to be crucial for stability of the auxiliary under reaction conditions. Apart from arylation, alkylation of the amine derivative was also found to proceed in good

yields (figure 13a). The auxiliary was also removable under mildly basic conditions (figure 13b).

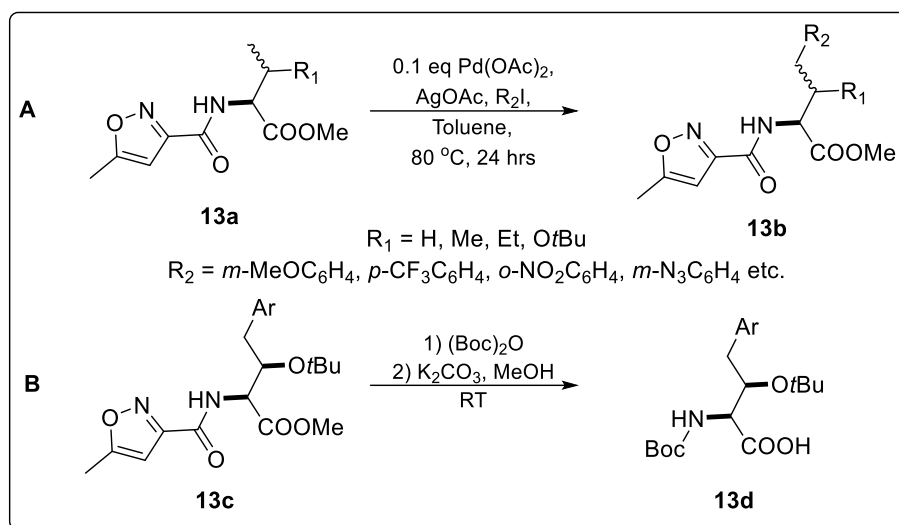


Figure 13: (a) 5-Methylisoxazole-3-carboxamides as an auxiliary to direct alkylation and arylation. (b) Removal of 5-methylisoxazole-3-carboxamides auxiliary under mildly basic conditions to generate Boc protected amino acid.

In 2013, Shi reported the use of 1,2,3-triazole-4-carboxylic acid as an auxiliary for either cyclization or acetoxylation of amines.⁸² The conditions employed for cyclisation were similar to those reported by Chen's group (see figure 9),⁷² and the reaction profile was also similar, with the azetidine product favoured over the pyrrolidine product, and no acetoxylation being observed (figure 14a). However, under very similar conditions, Shi also demonstrated that modification of the auxiliary changed the reaction profile entirely, with the acetoxylation being the dominant product (figure 14b). The switch in reactivity was attributed to the tridentate coordination, which forces the Pd-C bond into the axial position. This intermediate then reductively eliminates to form the acetoxylation product (figure 14c).

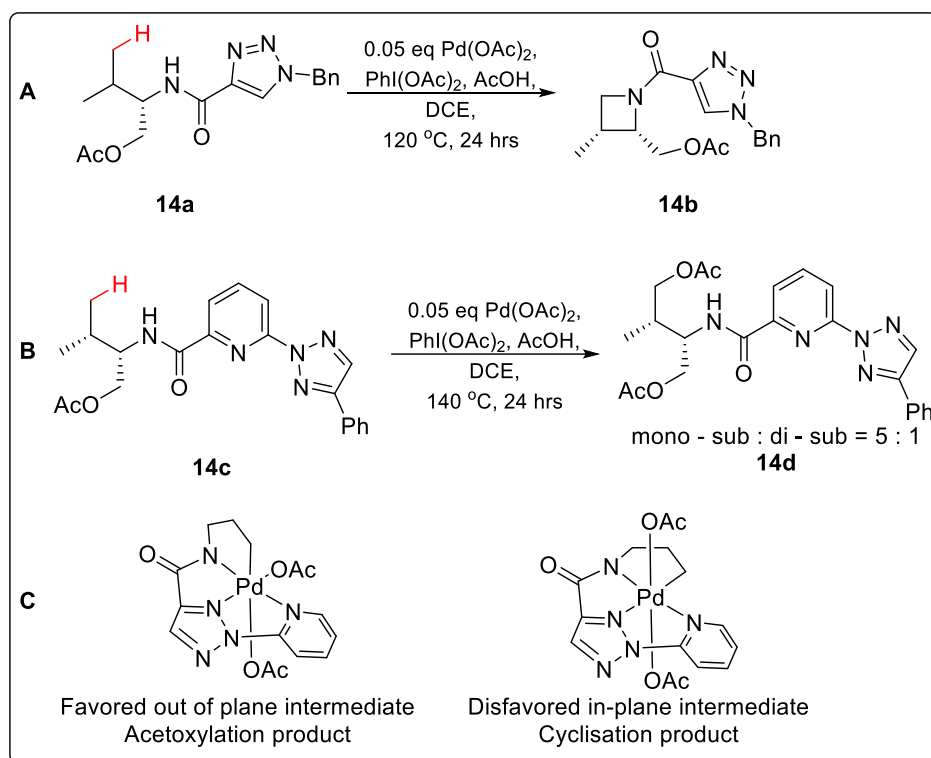


Figure 14: (a) Oxidative cyclisation mediated by a triazole auxiliary. (b) Modification of auxiliary to promote acetoxylation product. (c) Out of plane intermediate leading to acetoxylation product favoured.

In 2014, Zhao's group reported the use of oxalyl amides as auxiliary for cyclisation of amines to form pyrrolidines (figure 15).⁸³ A range of amines with δ CH_3 groups were smoothly cyclised to form the corresponding pyrrolidines. However, unlike previous report by Chen's group, Valine derivatives was not cyclised to form the corresponding azetidine. Instead, only the acetoxylated product was found in 49% yield. The synthetic practicality of the oxalyl amide auxiliary was also demonstrated by the reaction's scalability to gram scale, followed by deprotection by refluxing in NaOH.

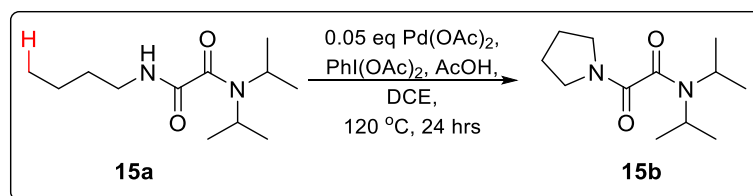


Figure 15: Oxalyl amide as auxiliary for δ cyclisation of amines to form pyrrolidines.

In contrast with the previous reports employing strongly coordinating auxiliaries, Yu's group reported use of the pentafluorophenyl group as an auxiliary in 2014 (figure 16).⁸⁴ Addition of a mono-*N*-protected amino acid ligand was also found to be crucial for the reaction. Furthermore, the enantiomer of the ligand was found to be important for the efficacy of the reaction. When *L*-amino esters were used as the substrates in the reaction, the *D*-enantiomer was found to be much more effective in the reaction, providing evidence for the steric impact of the ligand on the reactivity of the catalytic system. Although the reaction was optimised for coupling with boronic esters, aryl iodides could also be employed for the coupling. In 2016, a similar system was also reported for γ olefination, although the ligands employed were pyridine, quinoline or

phenanthridine based.⁸⁵ The more commonly employed 4-nitrobenzenesulfonyl group could also be used as an auxiliary instead of the triflyl group.

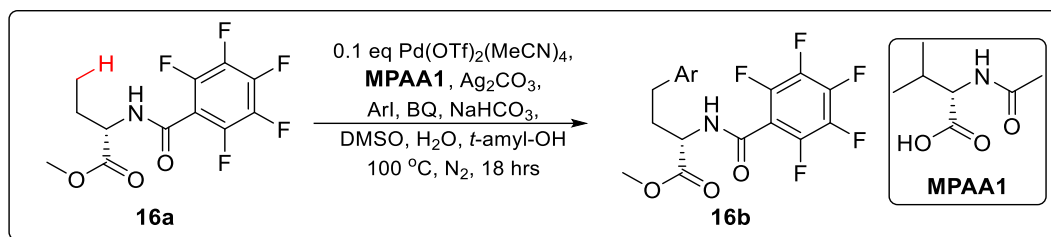


Figure 16: C-H activation enabled by an acetyl protected sterically bulky amino acid ligand.

Of particular importance to this project are the following three reports of γ C-H carbonylation of aliphatic amines mediated by different auxiliaries.

In 2015, Wang's group reported γ carbonylation of picolinamide protected alkyl amines to form γ -lactams (figure 17a).⁸⁶ Unlike previous reports of undirected C-H carbonylation requiring 10 to 50 atm of CO,⁸⁷ this reaction only required 1 atm of CO. TEMPO was found to be an essential additive, while other commonly used oxidants such as Cu(OAc)₂ and AgOAc gave no product. However, where both the α and β positions of the amine are branched, low diastereoselectivity of only up to 1.5:1 was observed in the reaction. The product formed could either be treated with NaOH to obtain the unprotected γ -lactam or hydrolysed by refluxing with HCl to obtain γ -amino acids (figure 17b). The synthetic utility of this transformation was demonstrated by the preparation of racemic Pregabalin⁸⁸ in three steps from the simple amine **17e** (figure 17c).

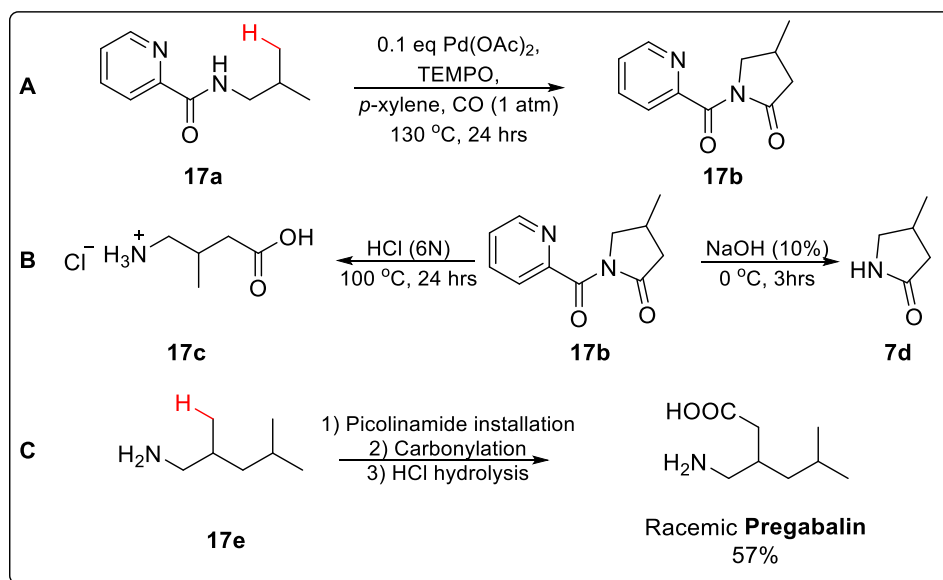


Figure 17: (a) Carbonylation of picolinamide protected amines to form γ -lactams. (b) Deprotection of product to obtain γ -lactams or γ -amino acids. (c) Synthesis of racemic Pregabalin in three steps.

In the same year, Yao and Zhao's group reported that oxalyl amides are also effective auxiliaries for γ carbonylation of aliphatic amines (figure 18).⁸⁹ Under optimised conditions, methyl groups at the γ position, as well as cyclopropane methylene groups were smoothly carbonylated. Addition of an acidic additive was found to be beneficial for the reaction, with 3-(trifluoromethyl)benzoic acid being the most effective. This was

ascribed to the additional stabilising effect of the electron deficient acid on the palladium (0) species in the catalytic cycle, while it performed the role of acetic acid or pivalic acid during the C-H activation step.⁹⁰ The reaction condition was specific to the oxalyl amide auxiliary, as the use of other auxiliaries such as picolinamide did not give rise to significant yields of the corresponding product. The oxalyl auxiliary was also removable by heating at 50 °C with 3 equivalents of NaOH to yield the γ -lactam **18c**.

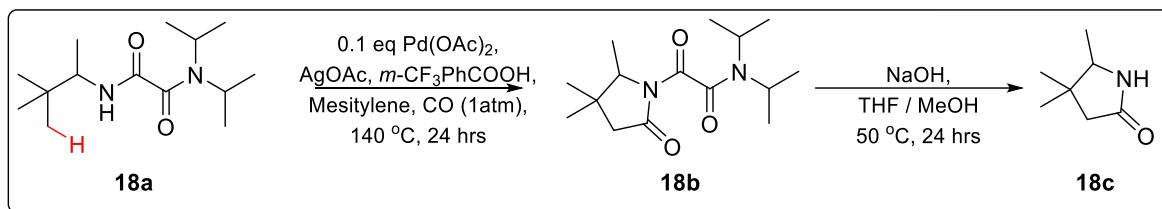


Figure 18: Carbonylation of oxalyl amide protected amine, followed by removal of the oxalyl amide auxiliary by hydrolysis with NaOH.

In 2016, Carretero's group applied their previously developed (2-pyridyl)sulfonyl auxiliary to the γ carbonylation of amino acids and peptides (figure 19a).⁹¹ $\text{Mo}(\text{CO})_6$ was chosen to be the CO source so as to better control the amount of CO present in the reaction mixture. A slight molar excess of 0.33 equivalent of $\text{Mo}(\text{CO})_6$ was found to be optimal, presumably due to the deactivating effect of excess CO on Pd(II). Apart from the usual γ methyl carbonylation, methylene groups of cyclopropane, norborane, and adamantane were also carbonylated (figure 19b), though 20 – 30 mol% of palladium was required for these transformations. The utility of this reaction was also demonstrated by the selective late stage functionalization of an estrogen derivative **19f**, giving the γ lactam **19g** in 40% yield (figure 19c).

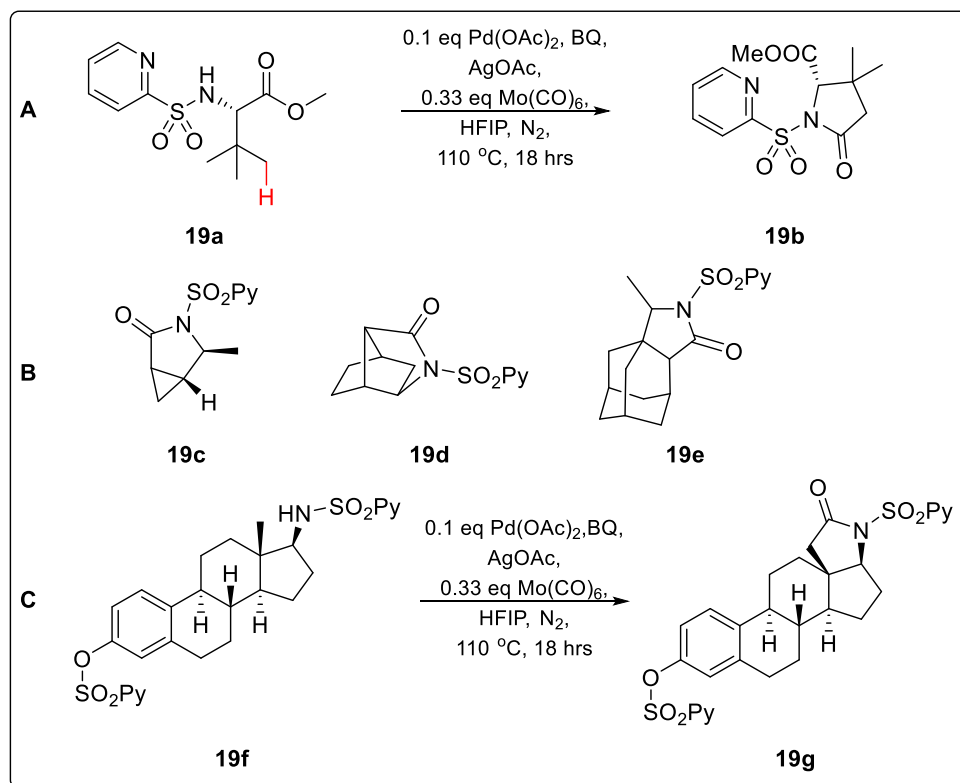


Figure 19: (a) Carbonylation of 2-pyridylsulfonyl protected amino acid derivatives. (b) Carbonylation at the γ methylene site of cyclopropane, norborane, and adamantane. (e) Late stage carbonylation of an estrogen derivative.

1.1.2.3 Free Amine Directed $\text{C}(\text{sp}^3)\text{-H}$ Activation

The first report of a catalytic free amine directed $\text{C}(\text{sp}^3)\text{-H}$ activation was in 2014 by Gaunt's group.⁹² When 3,3,5,5-tetramethylmorpholin-2-one **20ai** was reacted with a stoichiometric amount of palladium acetate, a 4-membered ring **20bi** was formed (figure 20a). Surprisingly, when **20aii** was subjected to the same conditions, the 4-membered palladacycle was still obtained, although a classical 5-membered palladacycle could in-principle also be formed. Upon treatment with $\text{PhI}(\text{OAc})_2$, the corresponding azetidine was formed through a putative Pd(IV) intermediate. From these initial results, a catalytic reaction was developed (figure 20b). A range of functional groups were tolerated at the R_1 position, with the same 4-membered palladacycle selectivity being observed. However, steric factors were essential for the reaction; removal of any of the substituents around the secondary amine led to complete shutdown of the reaction. Under these reaction conditions, non-

morpholinone substrates were also reactive at the same β -methyl position, but the acetoxyated product was formed instead of the expected azetidine, suggesting that the lactone group plays a subtle but important role in the reaction. Aziridination of morpholinone **20ai**, and subsequent nucleophilic ring opening, was also translated into a flow-synthesis setup in 2016,⁹³ while a BINOL phosphoric acid mediated enantioselective aziridination was also reported in 2017.⁹⁴ In 2018, the γ -ring closure to form azetidines was also achieved (figure 20c).⁹⁵ The choice of oxidant (Koser's reagent⁹⁶) was found to be crucial for this reaction; when $\text{PhI}(\text{OAc})_2$ was used instead, only the acetoxyated product was obtained.⁹⁷ Alkenylation of morpholinone substrates to form pyrrolidines was also reported in 2017 (figure 20d).⁹⁸

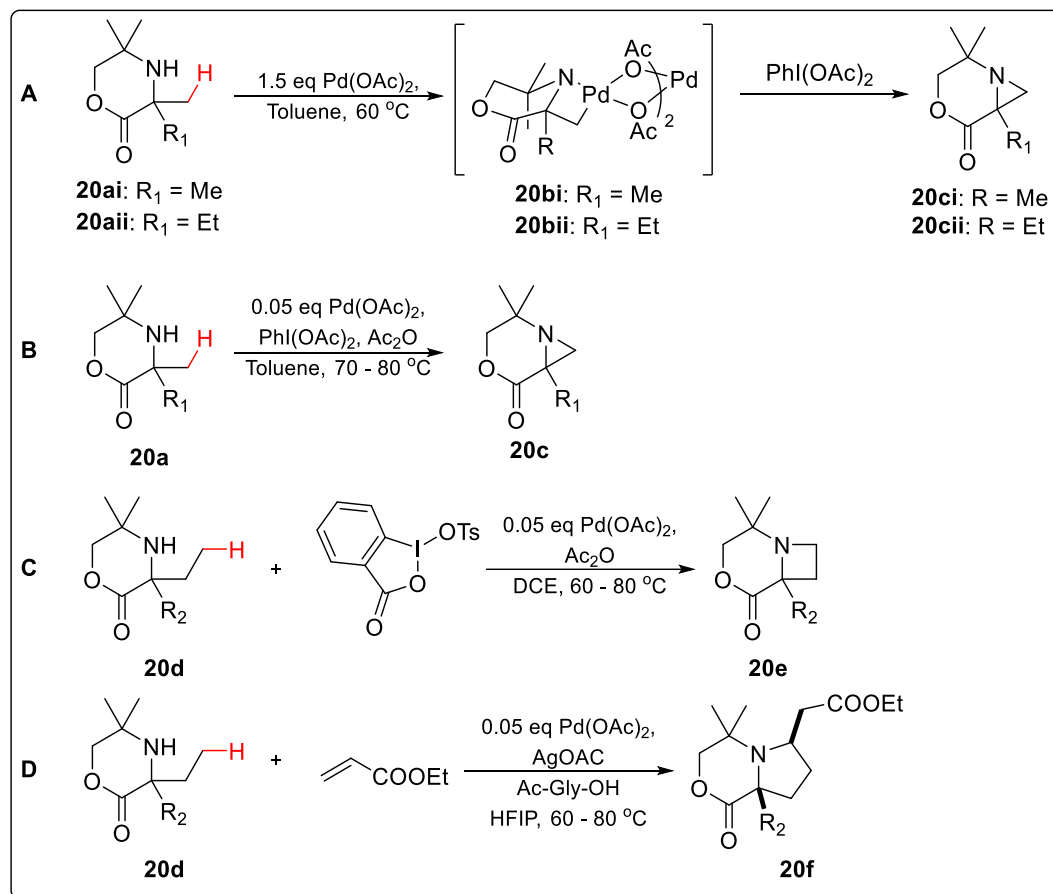


Figure 20: (a) Stoichiometric reaction between morpholinone and palladium acetate generating azetidine via a four membered palladacycle intermediate. (b) Catalytic C-H ring closure of morpholinone to form aziridines. (c) Oxidant controlled azetidination of morpholinone substrates. (d) Alkenylation of morpholinones to form pyrrolidines.

Like morpholinone **20ai**, Tetramethylpiperidine **21a** ($\text{X} = \text{CH}_2$) also generates a four membered palladacycle when reacted with palladium acetate.⁹² Treatment of this palladacycle with carbon monoxide gives the corresponding β -lactam **21b**. On this basis, a catalytic β -carbonylation of various piperidine derivatives was also developed (figure 21a). In 2015, this four membered palladacycle reaction pathway was also exploited to conduct arylation (figure 21b).⁹⁹ As Yu's group had previously reported,¹⁰⁰ addition of an amino acid ligand was essential for reaction efficacy, without which, no arylation product was obtained. *N*-acetyl phenylalanine was found to be the most effective ligand. Apart from piperidine derivatives, azepines and morpholines scaffolds were also tolerated in the reaction. Asymmetric arylation was also investigated, and a

modest ee of 60% was obtained by employing a β -phenyl-phenylalanine with a bulky acyl side chain.

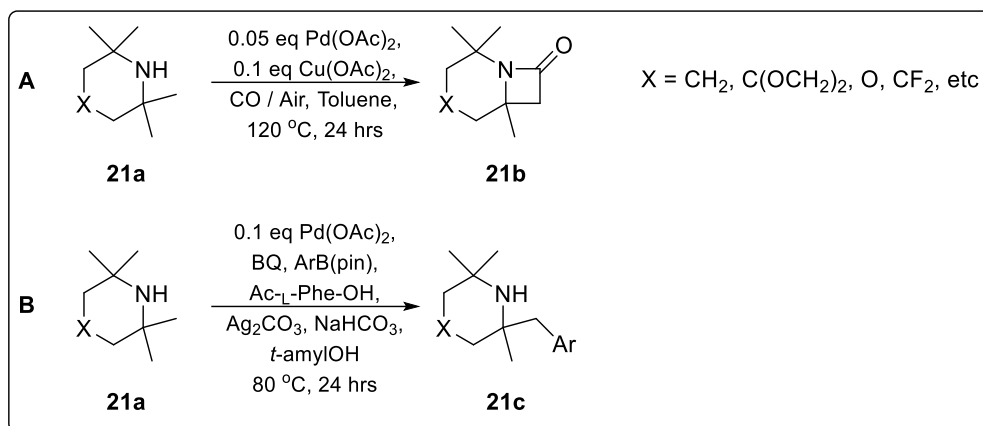


Figure 21: (a) β Carbonylation of tetramethylpiperidine substrates to give β -lactams. (b) Arylation of aliphatic amines via a 4-membered palladacycle.

Although these free amines directed C-H functionalisation may be useful transformations, the bi- α -tertiary structural requirements of the substrate limits the scope of the reaction. In 2015, the Gaunt group developed a methodology utilising a steric tether to modulate the reaction.¹⁰¹ Cyclohexanone was employed to bridge the amino alcohol substrate, forming a sterically hindered spiral oxazolidine **22b** (figure 22a). This motif was remarkably reactive towards palladium acetate. Even at room temperature, no bis-amine complex could be detected. Instead, the five membered cyclopalladated complex **22c** was directly obtained. This palladacycle intermediate was amendable to a wide number of transformations, the substrate was successfully acetoxylated (**22d**), arylated (**22e**), carbonylated (**22f**), and alkenylated (**22g**) (figure 22b). The synthetic utility of this strategy was demonstrated by the synthesis of the multiple sclerosis drug, Gilenya (**22i**), from amino alcohol **22h** in four steps with an overall yield of 51% (figure 22c). The carbonylation of a spiro ketals was also reported in 2019 (figure 22d).¹⁰²

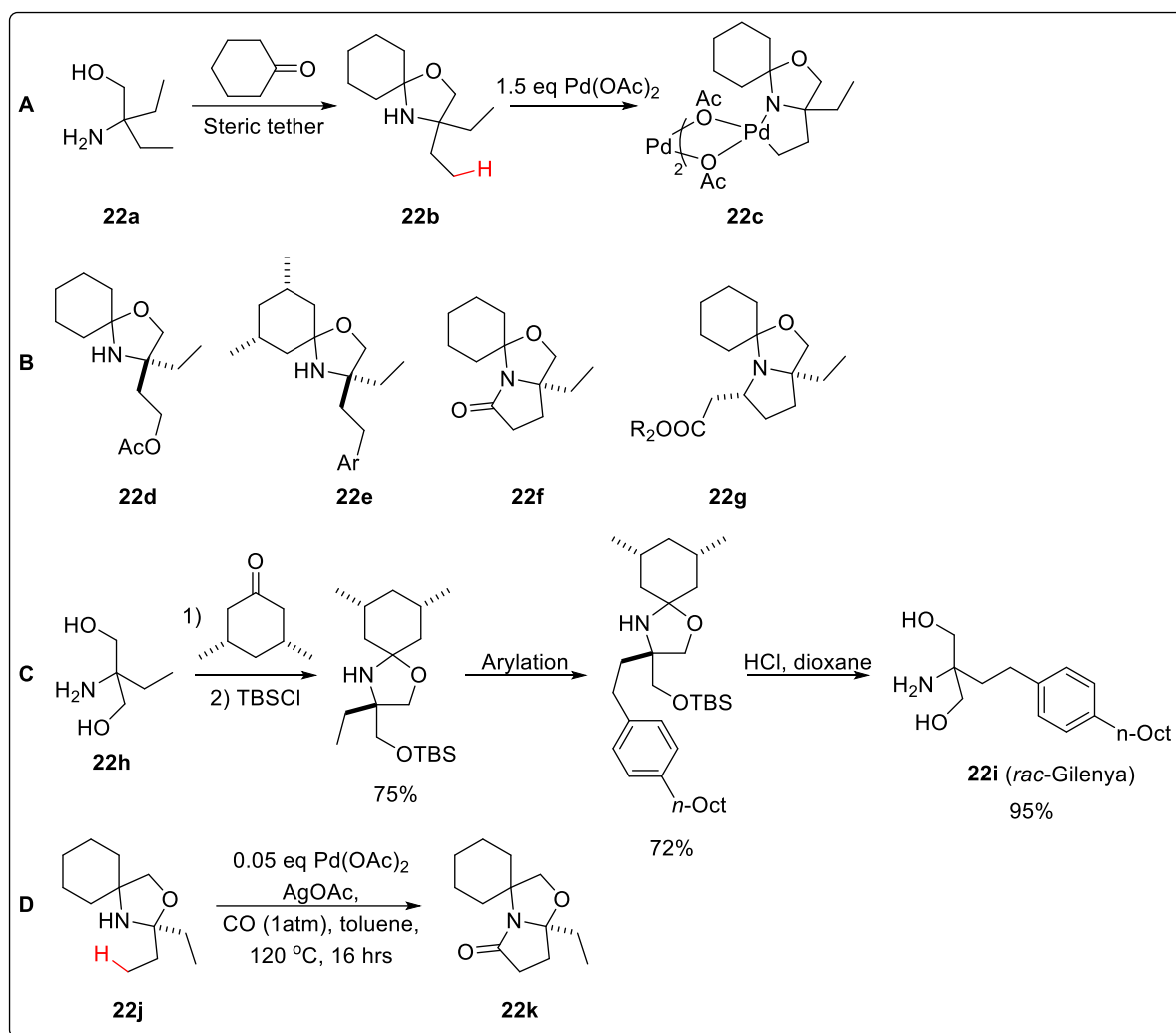


Figure 22: (a) Simple ketone as steric tether. Resultant spiral oxazolidine easily cyclopalladated at room temperature (b) Examples of transformations possible including, acetoxylation, arylation, carbonylation and alkenylation. (c) Synthesis of Gilenya in 4 steps. (d) Carbonylation of a spiro-ketal.

In 2016, Sanford's group reported the transannular C-H functionalisation of alicyclic amine (figure 23a).¹⁰³ The alicyclic amine **23a** is proposed to occupy a boat-like conformation **23b** to position the palladium for C-H activation, in the process generating a bicyclic-palladacycle **23c** which is subsequently functionalized to form **23d** (figure 23a). Although trace yields of the C-H arylated product was observed with the free amine, the reaction was found to work best with an additional coordinating *p*-CF₃C₆F₄ aniline amide group in **23e** (figure 20b). Various classes of alicyclic amines were tolerated in the arylation, including piperidines (**23f**), azabicyclo[3.1.0]hexanes (**23g**), and octahydrocyclopentapyrroles (**23h**) (figure 23c). Although the yields of this reaction are usually modest due to the thermodynamically unfavourable boat conformation required, this methodology could be useful in cases where traditional synthetic pathways would be challenging, as exemplified by the late-stage arylation of Varenicline¹⁰⁴ (figure 23d). In 2018, Sanford reported improvements in reaction efficacy via the use of pyridine or quinoline carboxylate ligands.¹⁰⁵ This effect was attributed to the increased turnover rate of the active catalyst.

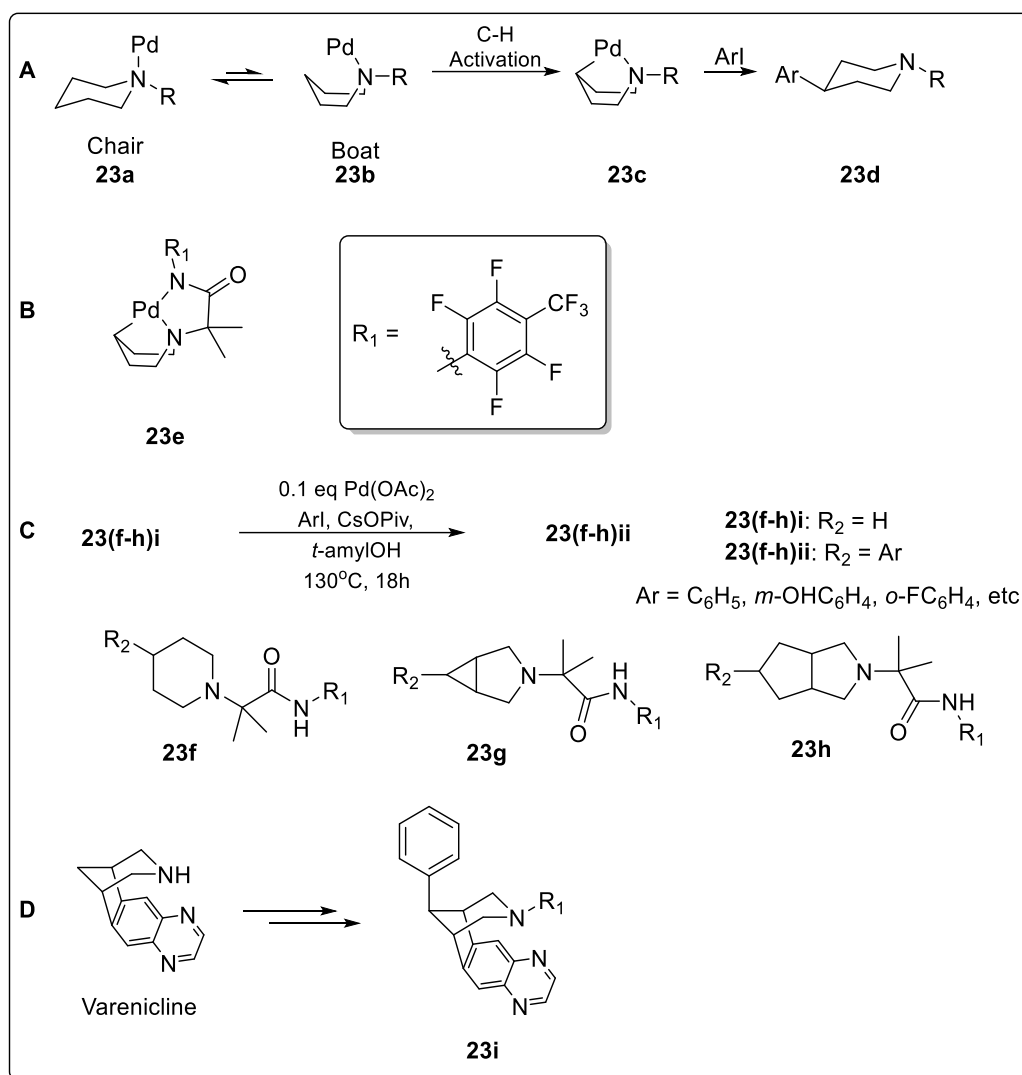


Figure 23: (a) Transannular C-H activation *via* a boat-like conformation. (b) Addition of a coordinating *p*-CF₃C₆F₄ aniline amide group to improve reaction efficacy. (c) C-H arylation of various fused ring configuration. (d) Late stage arylation of Varenicline.

In 2016, Gaunt's group reported a general β -carbonylation of simple aliphatic amines to form β lactams.¹⁰⁶ Unlike the previous work, even simple, less sterically hindered secondary amines can undergo carbonylation in high yields (figure 24a). Carbonylation takes place at the β -position even in the presence of primary γ -methyl groups. This is attributed to the mechanism of the reaction (Figure 24b). First, carbon monoxide binds to the palladium carboxylate. An internal nucleophilic attack by the carboxylate on carbon monoxide results in the formation of a palladium anhydride intermediate. This anhydride is then attacked by the amine to form a carbamoyl-palladium species. Although two possible positions of attack on the anhydride is possible, using a bulky carboxylate such as adamantanoic acid blocks the attack on the undesired position. Subsequent C-H activation on the β -position then results in a five membered cyclopalladation complex, which upon reductive elimination, gives rise to the corresponding β -lactam product. The reaction was also remarkably selective, with even complex molecules such as forming the corresponding β -lactams (**24c-e**) with good selectivity and yields (figure 24c).

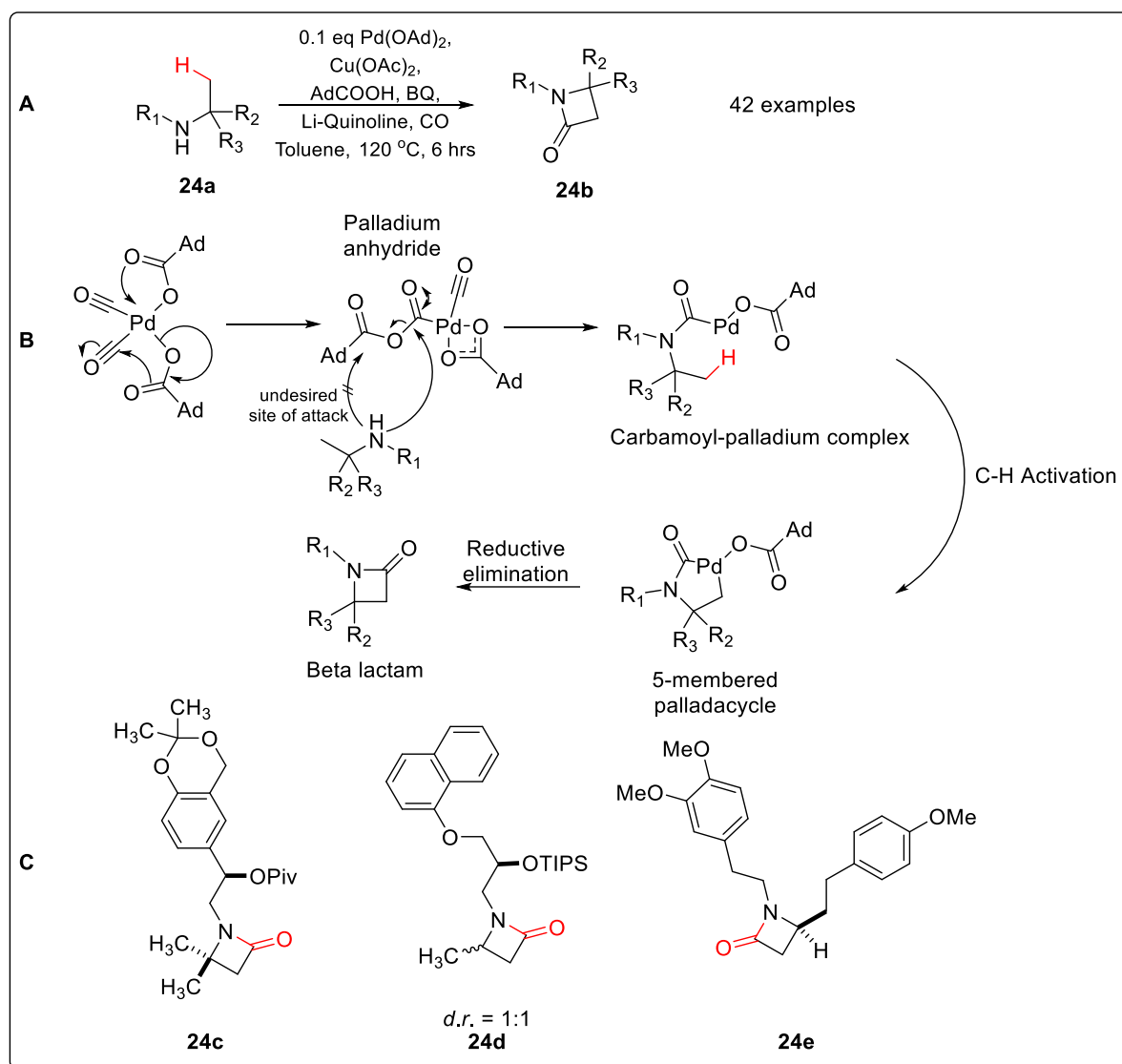


Figure 24: (a) Carbonylation of simple aliphatic amines to give β lactams. (b) Proposed mechanism of carbonylation accounting for β -selectivity (c) Late stage functionalization of complex molecules.

The remarkable β -selectivity of the carbonylation is illustrated in two follow-up publications from the Gaunt group in 2017. Even in the presence of multiple γ -methyl groups, carbonylation takes place exclusively at the β -methylene position (figure 25a).¹⁰⁷ Xantphos was found to be an essential ligand, although its role in the reaction is not fully known. Where an α – tertiary center exists, the reaction is β -methylene selective even over the traditionally more reactive $\text{C(sp}^2\text{)}\text{-H}$ bonds (figure 25b).¹⁰⁸ This selectivity governed by the reaction conditions. When the same substrate was subjected to Orito's benzylamine carbonylation conditions,⁶³ the isoindolinone was the only product formed, though in low yields of 16%.

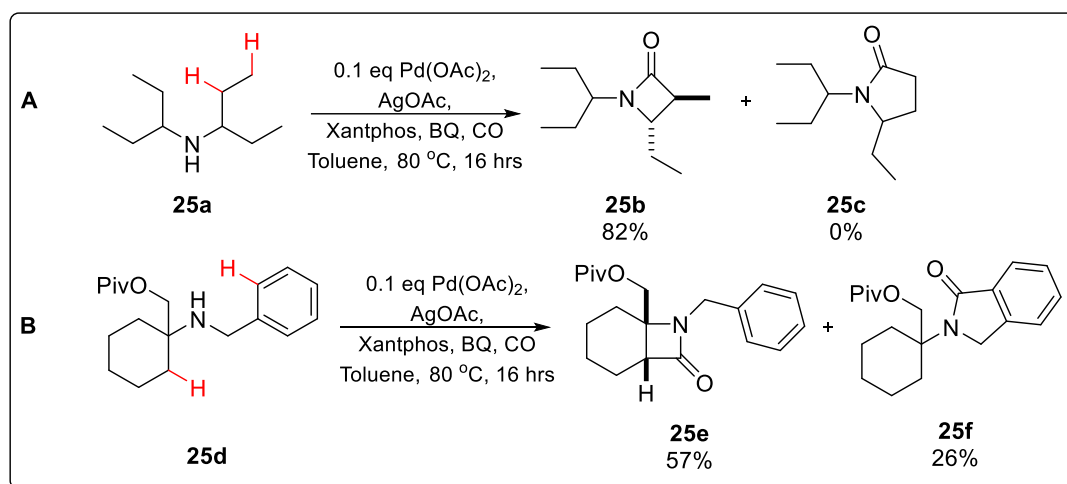


Figure 25: (a) β-Methylene selectivity over γ-methyl position. (b) α – Tertiary moiety driving β-methylene selectivity even over C(sp²)-H bonds.

Since 2016, the use of transient directing groups to direct amine C-H activation has seen increased research interest. The earliest reports focus on generating an imine *in-situ* via condensation of the amine with an aldehyde. γ – arylation via this strategy has been reported by the groups of Dong,¹⁰⁹ Yu,¹¹⁰ Ge,¹¹¹ and Murakami,¹¹² each employing a different aldehyde (figure 26a). Apart from masking the primary amine, the imine also provides a bidentate coordination system, helping to position the palladium for C-H activation. Evidence for this was the isolation of an intermediate palladacycle by Dong and Ge (figure 26b). The imine is then hydrolysed at the end of the reaction to yield the functionalised amine directly. In 2018, Young's group also reported that carbon dioxide can function as a transient directing group for amine arylation *via* a putative carbamate intermediate (figure 26c).¹¹³ This method is also able to arylate secondary amines, though at a somewhat reduced yield. A single example of acetoxylation of free primary amines was also reported by Shi's group in 2017.¹¹⁴ Acetic acid was used as the solvent to protonate the amine, thus limiting the coordination of the amine to palladium, thereby suppressing the formation of the off cycle bis(amine)complex.

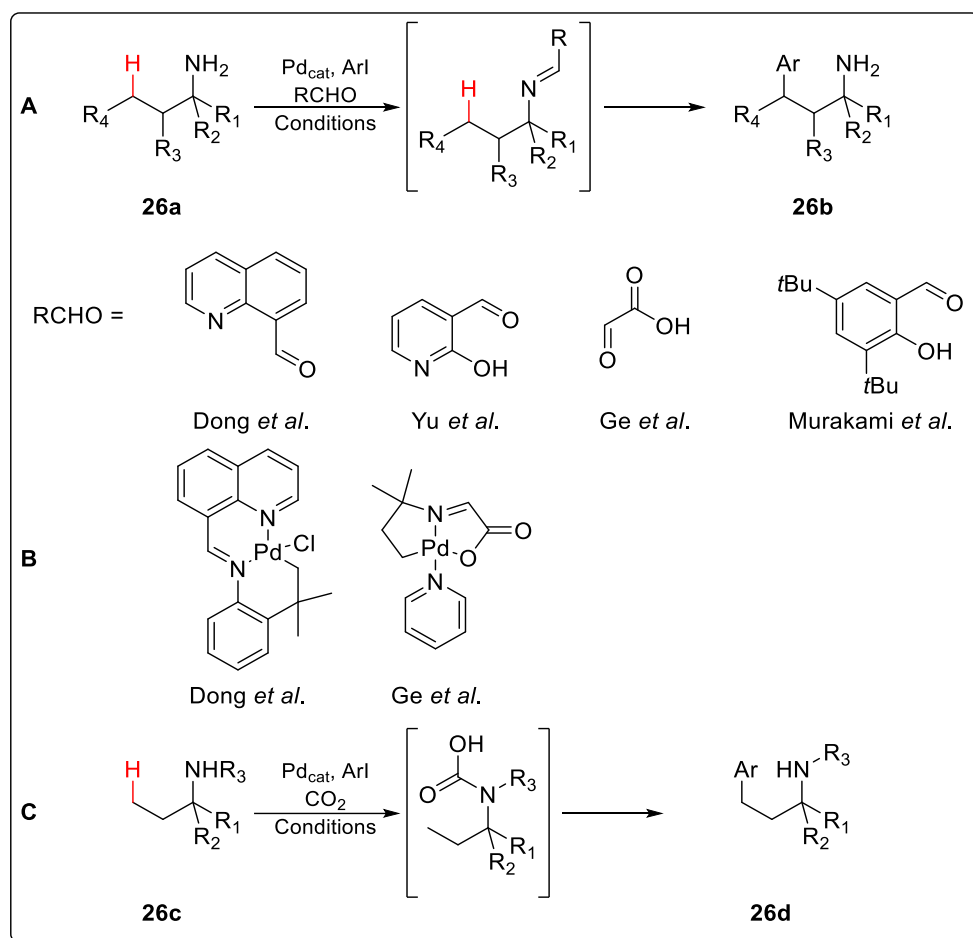


Figure 26: (a) Arylation of free amines via transient directing group. (b) Isolated palladacycles by Dong and Ge's group. (c) Carbon dioxide as a transient directing group for arylation of amines.

1.2 RESULTS AND DISCUSSION

1.2.1 Early Leads and Hypothesis

Previous work in the group has demonstrated that the β -position carbonylation of aliphatic amines is highly facile, with over 100 published examples.^{106–108} This selectivity holds true even in cases where traditionally more reactive sites are present on the same molecule; β -methylene positions are usually selectively carbonylated even over traditionally more reactive positions such as the γ -methyl positions or γ -C(sp²)-H positions. However, there were instances in which the γ -lactams was observed. Firstly, where stoichiometric amount of palladium was pre-heated with the amine before addition of carbon monoxide, the corresponding γ -lactam was exclusively formed (figure 27a). Secondly, when the CO concentration was reduced from 100% to the commercially available 6.25 % CO / air mixture, about 20 % of the γ lactam was also formed (figure 27b).

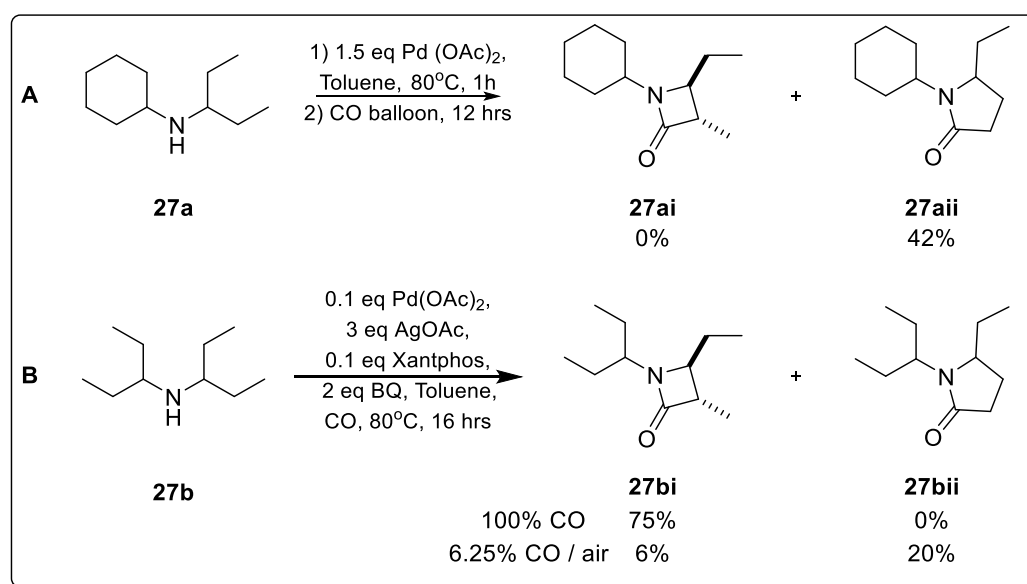


Figure 27: Instances where the γ lactam is observed (a) Pre-heating with stoichiometric amounts of palladium. (b) Reducing the concentration of CO.

These observations can be understood by considering the reaction mechanism leading to the formation of the β lactams. Computational and experimental studies suggest that a key intermediate towards β -lactams formation is the carbamoyl-palladium complex.¹⁰⁶ This species undergoes C-H activation on the β position to form a 5 membered cyclopalladation complex, which upon reductive elimination, affords the corresponding β lactam (figure 28a). However, conceptually, it is also possible for the amine directed γ C-H activation to take place first, leading to the classical 5-membered palladacycle. This palladacycle could then undergo CO insertion and yield the corresponding γ lactam upon reductive elimination (figure 28b). This alternate mechanism would account for the cases where the γ -lactam is observed. In pre-heating stoichiometric amounts of palladium, the 5-membered palladacycle is pre-formed, and proceeds on to form the corresponding γ lactam exclusively. Where the CO concentration is reduced, it is likely that the rate of formation of the carbamoyl-palladium complex is reduced, such that the alternate mechanism becomes rate significant, and thus the γ lactam is observed alongside the β lactam.

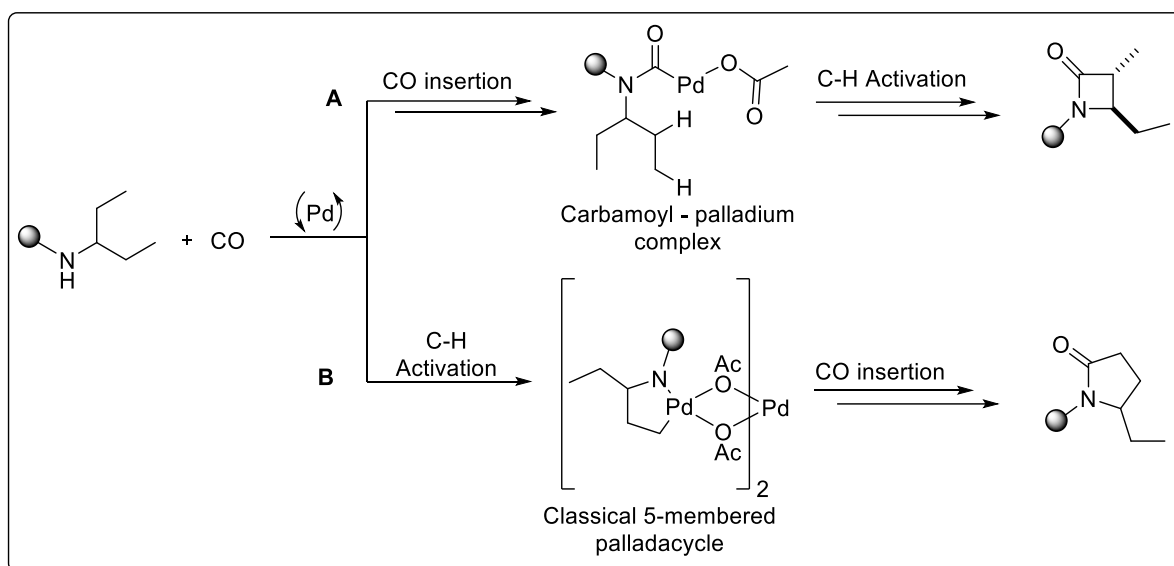


Figure 28: Different mechanistic pathways for formation of β and γ lactams. (a) Insertion of CO first, followed by C-H activation of the carbamoyl palladium complex, generating the β lactam. (b) C-H activation taking place first, generating the γ lactam.

Based on this mechanistic rationalisation, we attempted to find conditions which would favour the formation of the γ lactam over the β lactam by changing the reaction mechanism. Amine **27a** was used as the test subject for our optimisation studies. We began with the conditions shown in figure 29, which was previously found to form 7% of the γ lactam. The reaction conditions (temperature, solvent, counterion, oxidant(s) and ligands) were then systematically modified to examine their effects on selectivity between the β lactam formation and the γ lactam formation.

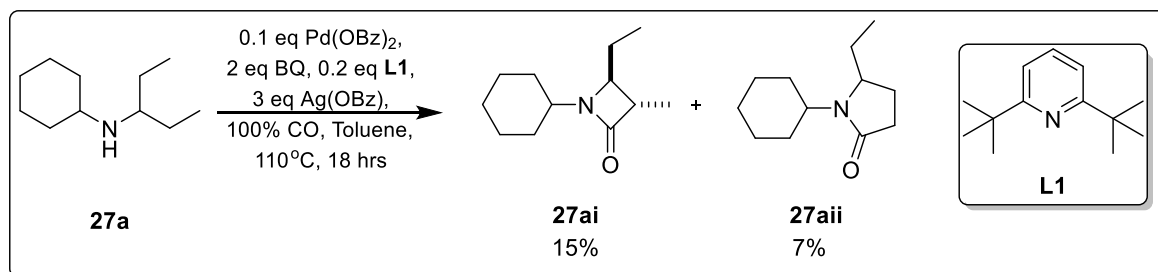
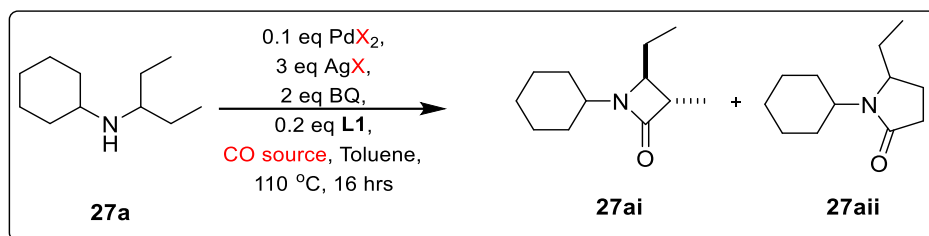


Figure 29: Most promising conditions from previous optimisation forming the starting point of this work. Reactions conducted on a 0.1 mmol scale in a microwave vial. Yields determined by ^1H NMR of the crude reaction sample against TCE as an internal standard

1.2.2 Optimisation of Reaction Selectivity

We began our optimisation by screening the counterions of the reaction (figure 30). When either the commonly used palladium acetate / silver acetate (entry 2) or palladium pivalate / silver pivalate (entry 3) couple were used, no γ – lactam was formed. Pleasingly, when the concentration of CO was lowered to 6.25% CO / air, a slight improvement in γ – lactam yield to 11% was observed (entry 4).



| Entry | X | CO source | 27ai / % | 27aii / % | 27aii : 27ai |
|-------|------|----------------|----------|-----------|--------------|
| 1 | OBz | 100% CO | 15 | 7 | 0.5 : 1 |
| 2 | OAc | 100% CO | 26 | - | - |
| 3 | OPiv | 100% CO | 47 | - | - |
| 4 | OBz | 6.25% CO / Air | 23 | 11 | 0.5 : 1 |

Figure 30: Screening of counter-ions at different temperature and CO concentration. Reactions conducted on a 0.1 mmol scale in a microwave vial. Yields determined by ¹H NMR of the crude reaction sample against TCE as an internal standard.

We went on to examine the ligand control on the reaction, on the premise that ligands could potentially compete with carbon monoxide for binding sites on palladium and thus lowering the rate of CO binding. A range of ligands was screened, and the electron rich 4-methoxypyridine gave the most promising results, with a 16% yield of the γ lactam, and a selectivity of 2.7 : 1 over the β lactam (figure 31, entry 2). We found that increasing the ligand loading to 0.5 eq gave a further increase in yield and selectivity of 5.7 : 1 (entry 7). However, increasing the loading even further to 1 eq greatly inhibited the reaction (entry 8).

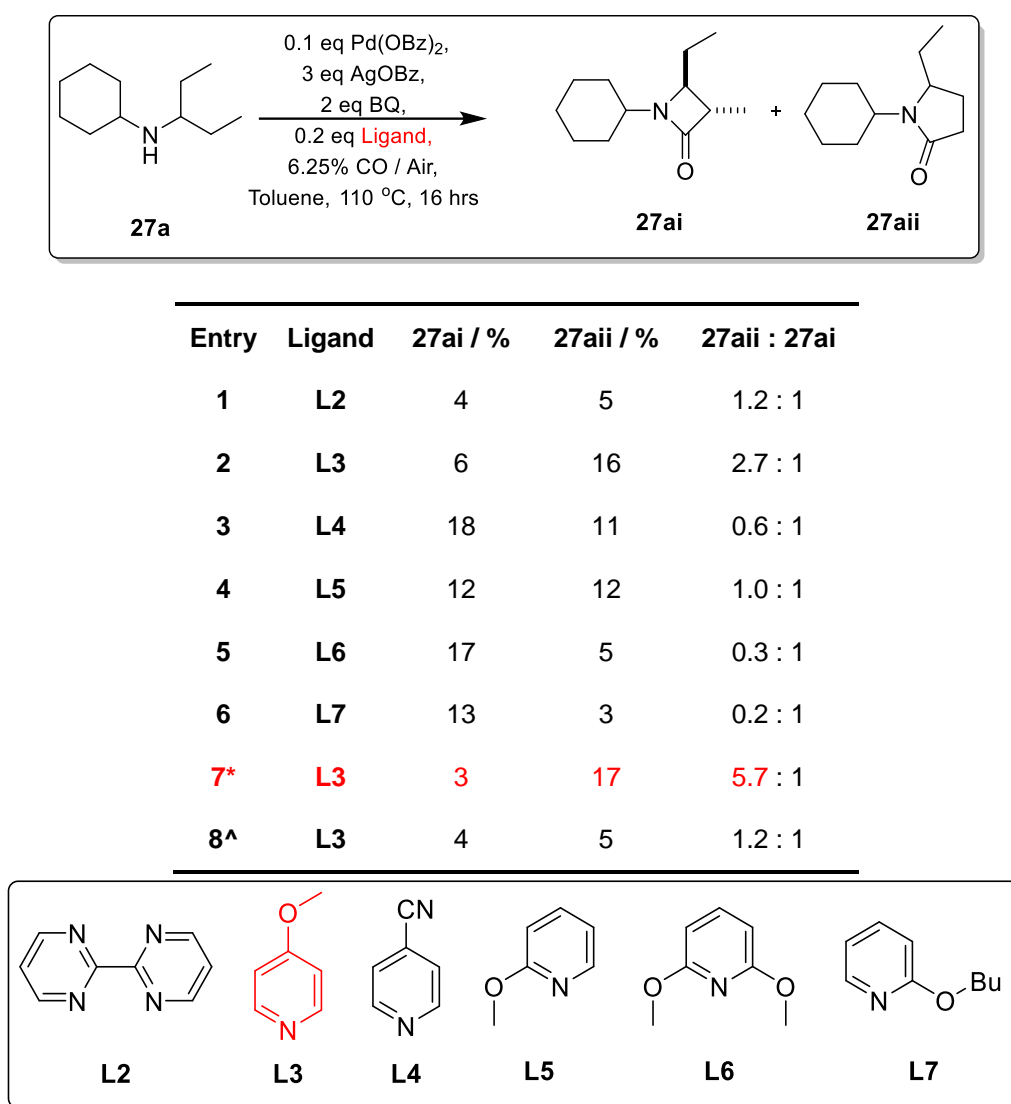
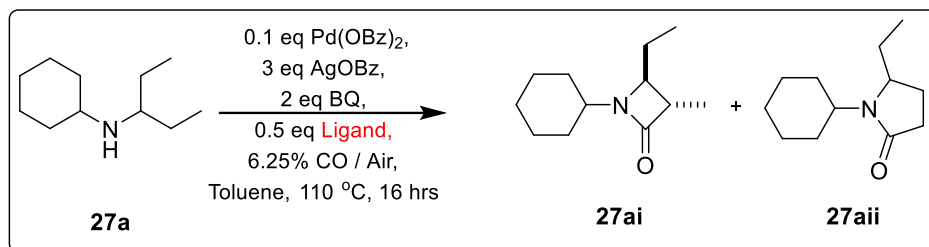


Figure 31: Screening for ligand control of reaction. Conducted on a 0.1 mmol scale in a microwave vial. Yields determined by ^1H NMR of the crude reaction sample against TCE as an internal standard. *0.5 eq of ligand. ^ 1 eq of ligand

With this lead, we went on to screen a range of similar ligands (figure 32). Both electronic (entry 2 – 6) and steric (entry 7-9) factors on pyridine were varied, while the related imidazole (entry 10, 11) and isoquinoline (entry 12) derivatives were also tested. Although both the electron rich **L8** and **L9** ligands gave comparable yields and selectivity, the original 4-methoxypyridine still gave the highest yield and selectivity.



| Entry | Ligand | 27ai / % | 27aai / % | 27aai : 27ai |
|-----------|------------|----------|-----------|----------------|
| 1 | L3 | 3 | 17 | 5.7 : 1 |
| 2 | L8 | 4 | 15 | 3.8 : 1 |
| 3 | L9 | 3 | 11 | 3.7 : 1 |
| 4 | L10 | 6 | 8 | 1.3 : 1 |
| 5 | L11 | 1 | 4 | 4.0 : 1 |
| 6 | L12 | 8 | 9 | 1.1 : 1 |
| 7 | L13 | 7 | 9 | 1.3 : 1 |
| 8 | L14 | 4 | 8 | 2.0 : 1 |
| 9 | L15 | 3 | 8 | 2.7 : 1 |
| 10 | L16 | 4 | 5 | 1.3 : 1 |
| 11 | L17 | - | - | - |
| 12 | L18 | 5 | 12 | 2.4 : 1 |

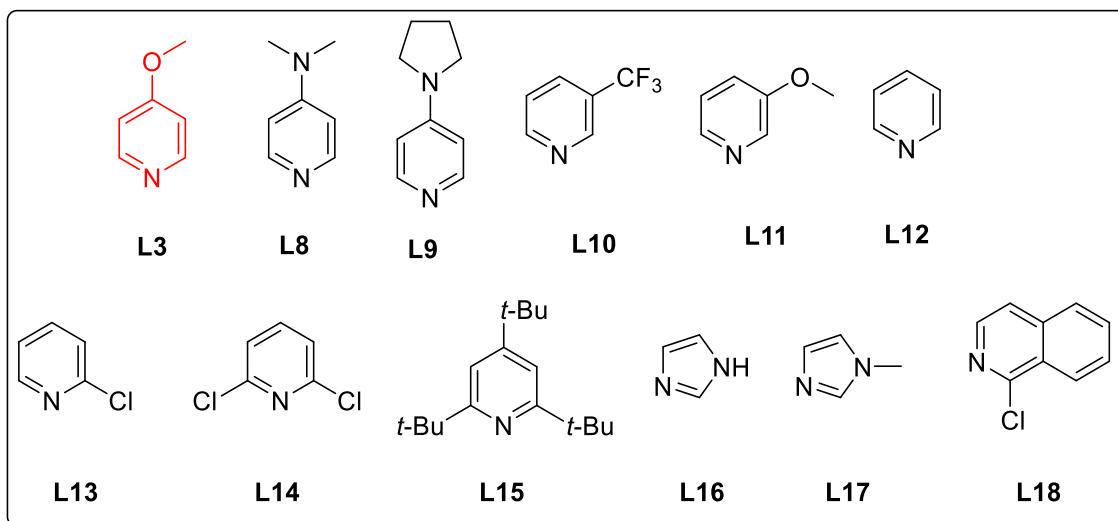
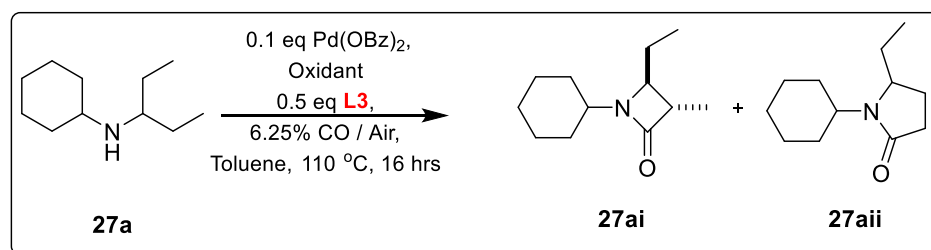


Figure 32: Further screening for ligand control of reaction with pyridine-related ligands. Conducted on a 0.1 mmol scale in a microwave vial. Yields determined by ^1H NMR of the crude reaction sample against TCE as an internal standard.

Although selectivity of the reaction could somewhat be achieved via ligand control, the overall reaction was plagued by low conversion rates, with a significant amount of unreacted starting material at the end of the reaction. This was partially attributed to the formation of palladium black, resulting in deactivation of the active catalyst. As such, a range of commonly used oxidants were screened to improve catalyst turnover (figure 33). However, none of these gave higher yields of the γ lactam than the original conditions.



| Entry | Oxidant | Co-oxidant | 27ai / % | 27aii / % |
|-------|--------------------------------------|------------|----------|-----------|
| 1 | 2 eq chloranil | - | Traces | - |
| 2 | 2 eq TEMPO | 3 eq AgOBz | Traces | Traces |
| 3 | 2 eq TEMPO | - | Traces | Traces |
| 4 | 2 eq PhI(OAc) ₂ | - | - | - |
| 5 | 2 eq Ag ₂ CO ₃ | - | Traces | Traces |
| 6 | 0.2 eq Cu(OAc) ₂ | 2 eq TEMPO | Traces | - |
| 7 | 0.2 eq Cu(OAc) ₂ | 2 eq BQ | 47 | Traces |

Figure 33: Oxidant screening of reaction. Conducted on a 0.1 mmol scale in a microwave vial. Yields determined by ¹H NMR of the crude reaction sample against TCE as an internal standard.

1.2.3 Optimisation of Reaction Efficacy

Given the low overall efficacy of the reaction, with no obvious method to improve it, we believed that a new starting point for the reaction was required. The reaction which gave the highest overall C-H carbonylation yield in the lab is shown in figure 34. A yield of 99% of the β lactam was achieved. The reaction made use of copper acetate as an oxidant, with oxygen being the co-oxidant. An amino acid derivative was also used as an additive to the reaction, and quinuclidine was the base / ligand.

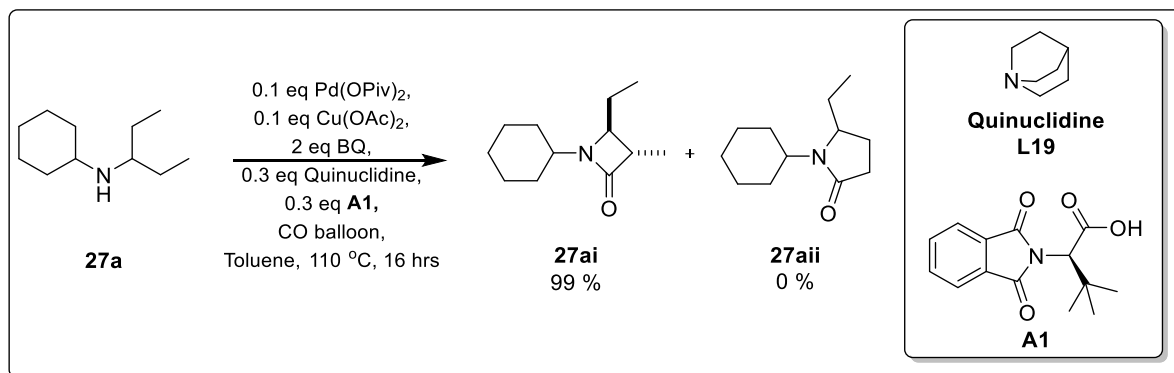
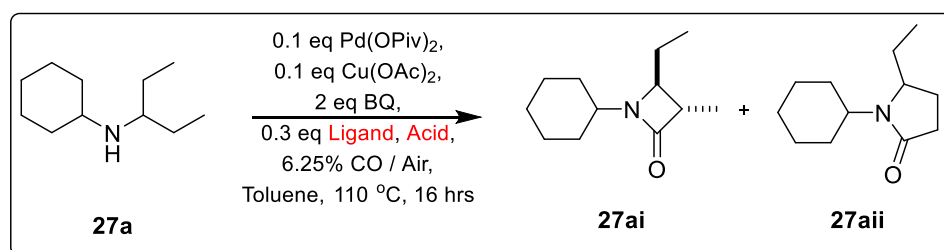


Figure 34: Conditions from other projects which gave high overall conversion of 99 %. Yields determined by ¹H NMR of the crude reaction sample against TCE as an internal standard.

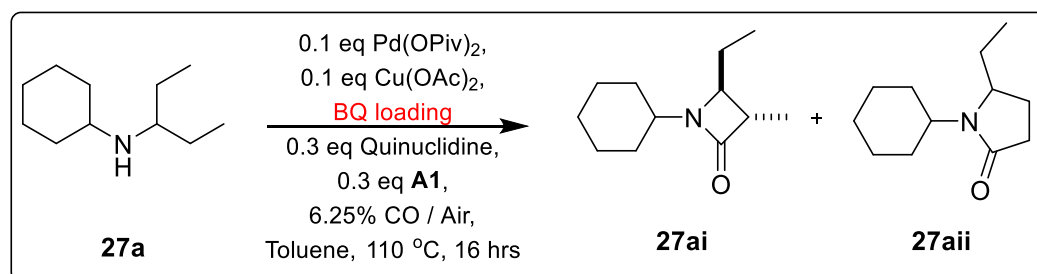
Taking lessons learnt from the previous optimisation, we lowered the concentration of carbon monoxide to 6.25 % CO / air, and obtained 29 % of the γ lactam (entry 1). Although the γ selectivity for this reaction was somewhat lower, with 42% of the β lactam being formed, the yield was higher than any of the other conditions. It was found that both the acid and the ligand was essential to the formation of γ lactam; removal of either component resulted in lowering of yields (entry 2-3). Unfortunately, the use of 4-methoxypyridine, which had previously given good selectivity, was unsuccessful in mediating this set of reaction conditions (entry 4).



| Entry | Acid | Ligand | 27ai / % | 27aai / % | 27aai : 27ai |
|----------|-----------|------------|----------|-----------|--------------|
| 1 | A1 | L19 | 42 | 29 | 0.7 : 1 |
| 2 | - | L19 | 91 | Traces | > 20 : 1 |
| 3 | A1 | - | 30 | 16 | 0.5 : 1 |
| 4 | A1 | L3 | 32 | Traces | - |

Figure 35: The role of the acid and ligand in determining reaction efficacy. Yields determined by ¹H NMR of the crude reaction sample against TCE as an internal standard.

Although extensive optimisation of the reaction was carried out, with the catalyst, copper source, ligand, acid, and solvent being varied, none of these modifications gave better γ lactam yields (see appendix A for details). The only component which made a significant improvement was the removal of benzoquinone (figure 36, entry 6). At the end of all the optimisation, the highest yield that was achievable was about 38%, with a selectivity of 2.2 : 1 in favour of the γ lactam.



| Entry | BQ Loading / mol% | 27ai / % | 27aii / % | 27aii : 27ai |
|-------|-------------------|----------|-----------|--------------|
| 1 | 200 | 42 | 29 | 0.7 : 1 |
| 2 | 100 | 47 | 30 | 0.6 : 1 |
| 3 | 50 | 41 | 29 | 0.6 : 1 |
| 4 | 40 | 36 | 27 | 0.8 : 1 |
| 5 | 30 | 32 | 28 | 0.9 : 1 |
| 6 | 0 | 17 | 38 | 2.2 : 1 |

Figure 36: Optimisation of benzoquinone loading. Yields determined by ¹H NMR of the crude reaction sample against TCE as an internal standard.

Although the removal of benzoquinone led to an increase in γ lactam yield and selectivity, the overall C-H activation yield fell to 55%, which is significantly lower than the total 71% when benzoquinone was present. We suspected that this could be due to decomposition of the starting material via β -hydride elimination. As such, the same reaction was conducted in deuterated toluene, and the reaction mixture was directly used for NMR without further work-up. About 10 mol% of 3-pentanone, the product of β -hydride elimination followed by hydrolysis, was discernible together with the β and γ lactams.

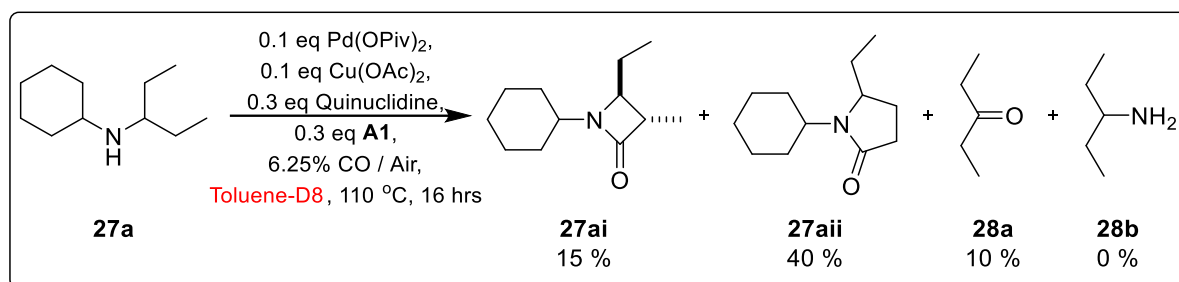


Figure 37: Study to determine mass balance of reaction by direct NMR of crude product without work-up. Yields determined by ¹H NMR with TCE as an internal standard.

We also studied the substrate dependence of the reaction. Both symmetrical amine **27b** and sterically challenged **27c** were subjected to the reaction conditions (figure 38). Although **27c** gave complete selectivity towards the γ lactam, with no trace of the β lactam being formed, the overall yield was still moderate at 45%.

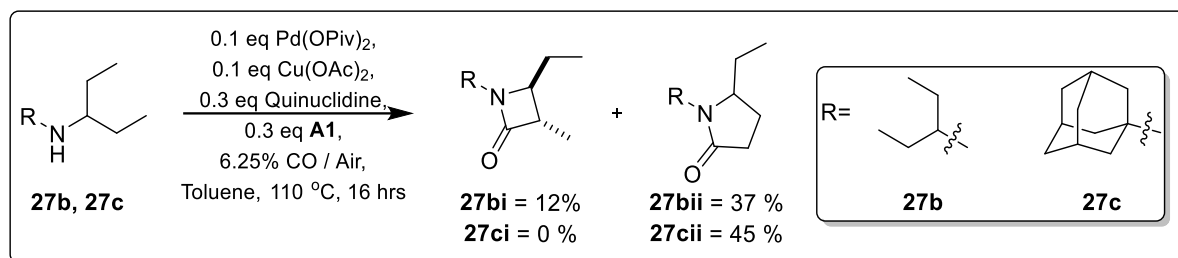


Figure 38: Substrate dependence of reaction conditions.

From these results, it appears that although the selectivity of the reaction can be controlled to a certain extent, this often comes at the price of overall reaction efficacy. An alternate approach would be required for this reaction.

1.2.4 Optimisation of Reaction Diastereoselectivity

Thus far, the reaction has been optimised based on the 3-pentylamine scaffold. However, the mass balance experiment conducted previously suggests that decomposition of the starting material could be an important competitive route. We believed that including a β -branch to the amine would help to prevent the molecule from adopting the co-planar conformation required for β -hydride elimination to take place.¹¹⁵ As such, a new substrate class was proposed.

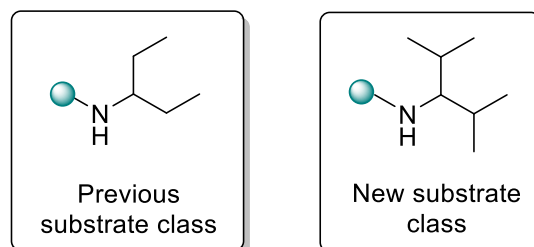


Figure 29: New substrate classes for carbonylation.

Sterically hindered amine **29a** was prepared and subjected to the reaction conditions (figure 30), and pleasingly, a 56 % yield of the corresponding γ lactam was obtained ($d.r.$ = 5 : 1). The major diastereomer was identified as the *trans* product by comparison of its NMR spectrum with previously reported *trans* lactams¹¹⁶. As the competing β -lactam is unlikely to be formed, the concentration of CO could be increased. When a CO balloon was used instead of the 6.25 % CO / air mixture, a yield of 75% was achieved, with a $d.r.$ of 6 : 1.

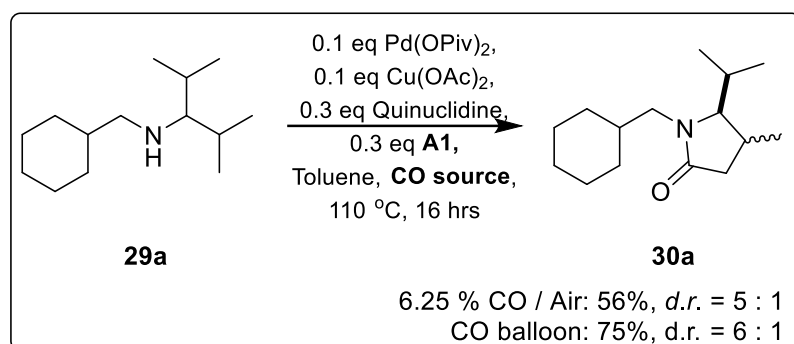


Figure 30: Reaction of new amine substrates with best conditions previously. Yields determined by ¹H NMR of the crude reaction sample against TCE as an internal standard.

Although the reaction yield was high enough to be synthetically useful, we still wanted to improve the diastereoselectivity of the reaction. As such, we continued to optimise the reaction. One possible method could be ligand or counterion control, where steric factors around palladium could promote the formation of one diastereomer over the other. As such, a screen of the acids used was first carried out (figure 31).

We began our screen by focusing on sterically bulky acids (**A2** – **A6**) in hopes that the sterics would help to modulate the diastereoselectivity of the reaction. This strategy was moderately successful, with reaction $d.r.$ ranging from about 10 : 1 to 12 : 1. Unfortunately, the reaction yield also fell to about significantly. Next, we tested various benzoic acids with different sterics (eg **A12**, **A13**), and electronics. Two results were particularly remarkable. Firstly, the bulky 2, 4, 6-triisopropylbenzoic acid (TRIPS, **A12**) gave good yields of 70% with reasonable diastereoselectivity of about 10 : 1. The less

bulky **A13** also gave similar diastereoselectivity, though with modest yields. Secondly, amongst all the acids screened, **A14** gave the highest yields of 81%, although the diastereoselectivity was comparatively lower at about 5 : 1. The other electron deficient benzoic acids (**A15** – **A22**) which we screened also gave similar results, though with slightly lower yields. Conversely, electron deficient aliphatic acids **A7** and **A8** did not give the same enhancement in yields. Electron rich benzoic acids **A10** and **A11** also gave somewhat lower yields. As **A12** gave the best overall yield with reasonable diastereoselectivity, we decided to carry forward our optimisation with it.

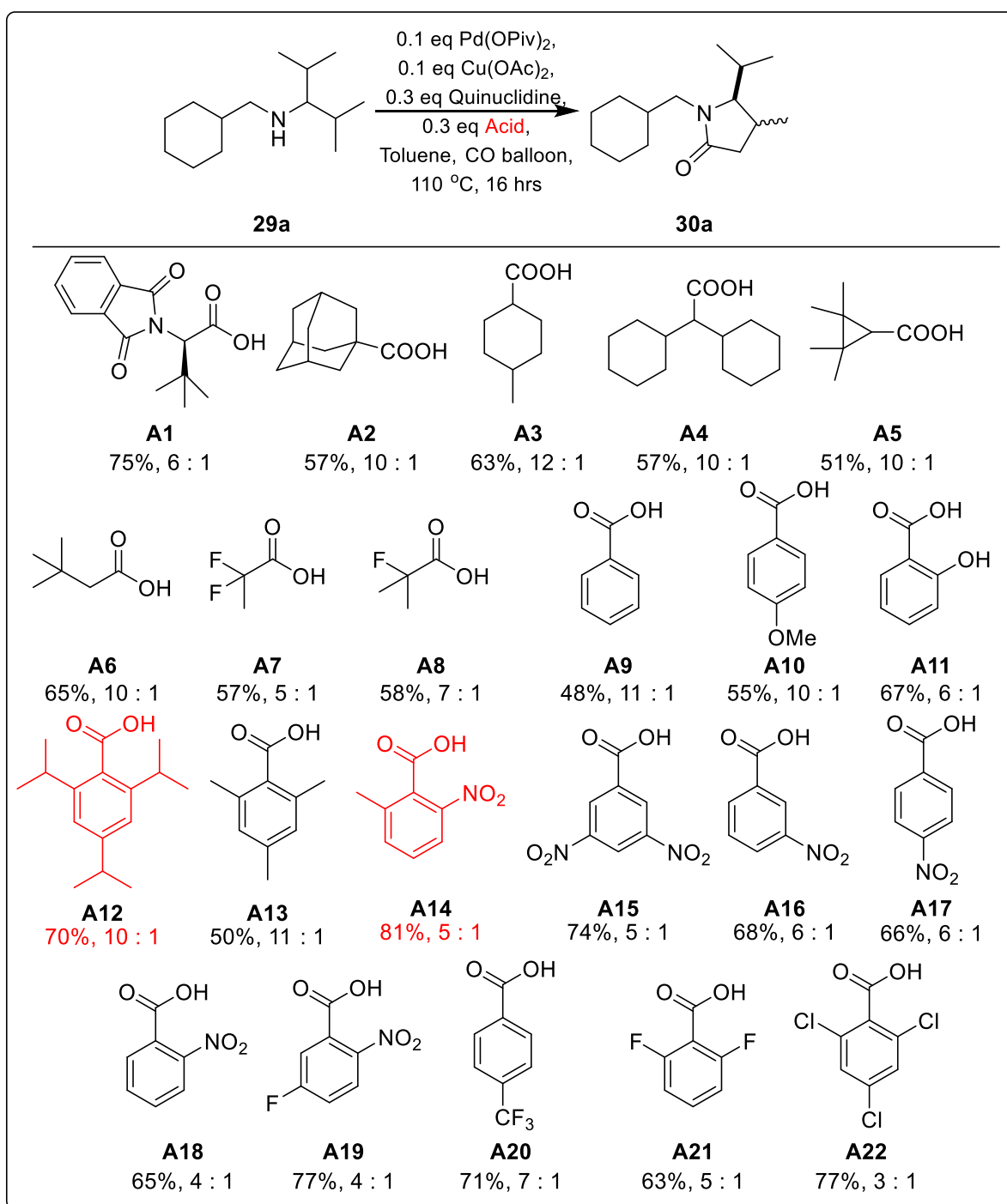


Figure 31: Screening of acids for optimisation of yields and d.r.. Yields determined by ¹H NMR of the crude reaction sample against TCE as an internal standard. d.r. determined by GC – FID.

Next, we carried out a screen of the additive used in the reaction (figure 32). Quinuclidine analogues such as **L20** and **L21**, as well as piperidine (**L22**) and morpholine (**L23**) gave lower yields as compared to quinuclidine, though the dibasic **L21** gave better diastereoselectivity of about 15:1. We also screened pyridine (**L12**), and found that although the yield was modest at 46%, the diastereoselectivity was excellent at 18 : 1. A range of pyridine was then screened, with varying sterics (**L24**, **L25**), and electronics (**L3**, **L9**, **L10**, **L11**, **L13**, **L26** – **L28**) at various positions on the pyridine ring. Although exceptional diastereoselectivity could be achieved by some of the electron rich pyridines, (**L3**, **L9**), the yield was still moderate. We also tested

various diazines (**L29** – **L31**) and triazines (**L32**), indole (**L33**), and quinolines (**L34**), diadentate ligands (**L35**, **L36**), and phosphate ligands (**L37**, **L38**) though without much success. In the end, we concluded that that quinuclidine still gave the best balance between yields and diastereoselectivity, and carried forward our optimisation with it. However, in cases where diastereoselectivity is much more important, such that the yields can be sacrificed, it would be possible to use either 4-methoxypyridine (**L3**) or DMAP (**L9**) as the basic additive.

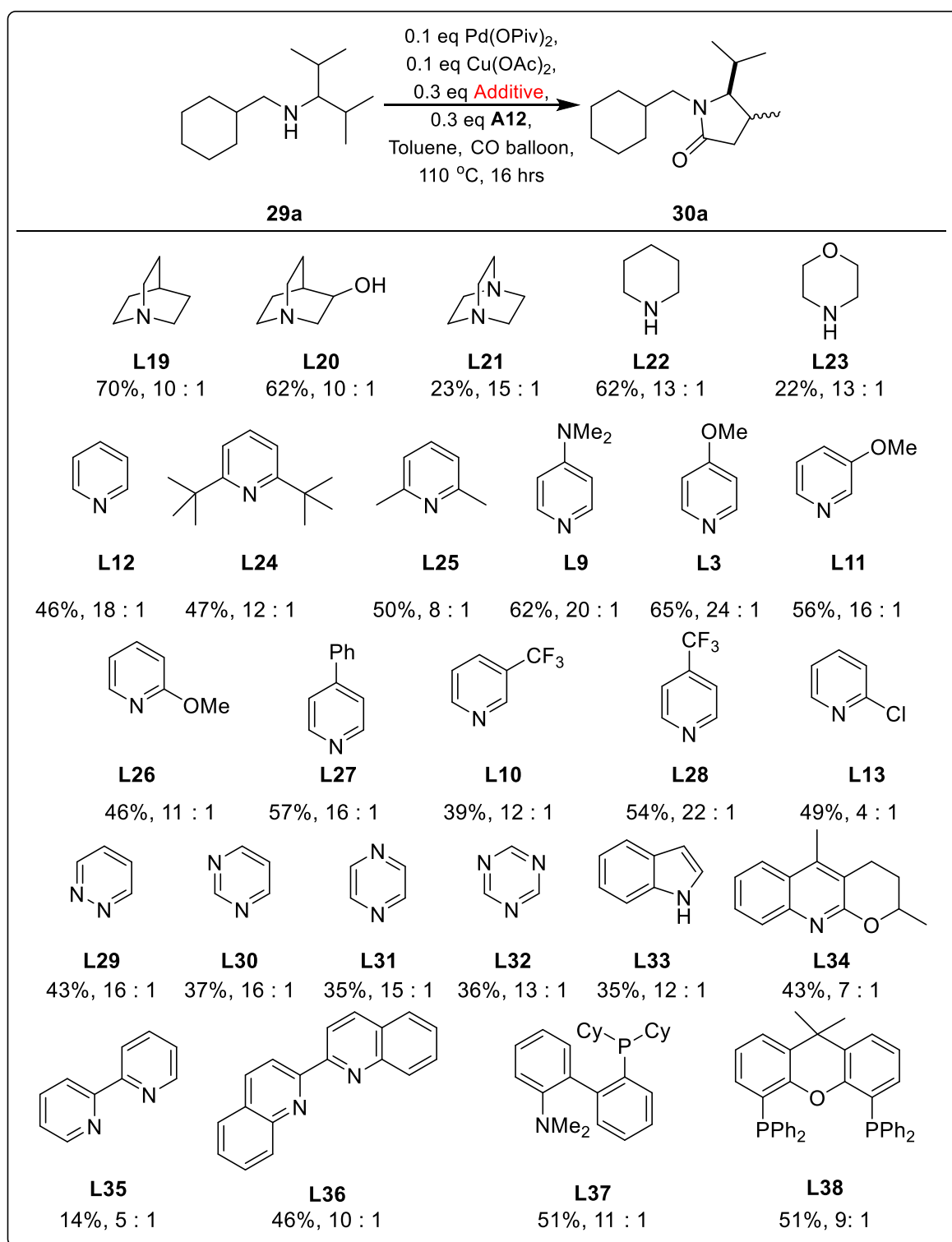
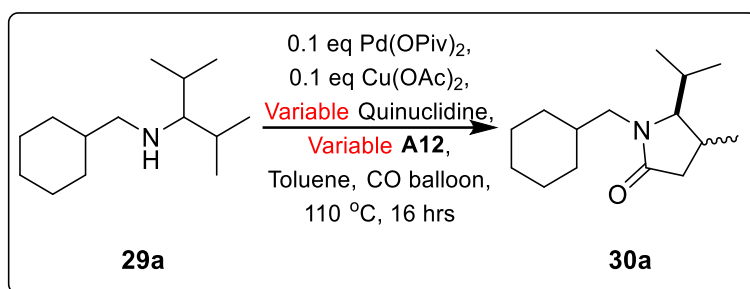


Figure 32: Screening of different additive to improve *d.r.* of reaction. Yields determined by ¹H NMR of the crude reaction sample against TCE as an internal standard. *d.r.* determined by GC – FID.

As both the choice of the acid and additive appears to have profound impact on both the yields and diastereoselectivity of the reaction, we carried out further investigations on the impact of the loading of these components on the reaction (figure 33). We first carried out the control experiment without both acid and quinuclidine (entry 1). Although the native diastereoselectivity of the reaction was high at 17 : 1, the yield

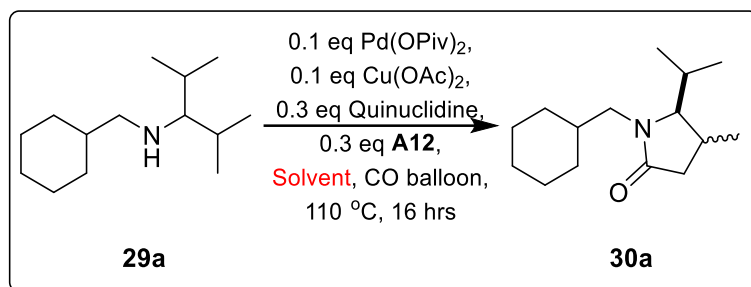
was poor at 35%. Next, the loading of the acid was kept at 0.3 eq, while the loading of quinuclidine was varied between 0 to 1.0 eq (entry 2-6). Apart from the example without any quinuclidine, where the yield dropped significantly to 39%, only minor differences in the yields and the diastereoselectivity was observed. We then kept the loading of quinuclidine constant at 0.3 eq, while the amount of acid was varied (entry 7-10), the yields of the reaction dropped significantly to the about 40%. Finally, we varied both the amount of quinuclidine and acid together between 0.1 eq and 1.0 eq (entry 11-13). Again, all the yields were modest at about 40%, while the diastereoselectivity was maximum at lower acid and quinuclidine loadings. At the end of this screen, we found that the maximum yield and diastereoselectivity was still obtained with equal loading of acid and quinuclidine at 0.3 eq each (entry 4).



| Entry | Quinuclidine / eq | A12 / eq | Yield / % | d.r. |
|-------|-------------------|----------|-----------|--------|
| 1 | 0 | 0 | 35 | 17 : 1 |
| 2 | 0 | 0.3 | 39 | 10 : 1 |
| 3 | 0.1 | 0.3 | 67 | 10 : 1 |
| 4 | 0.3 | 0.3 | 70 | 10 : 1 |
| 5 | 0.5 | 0.3 | 68 | 9 : 1 |
| 6 | 1.0 | 0.3 | 67 | 10 : 1 |
| 7 | 0.3 | 0 | 37 | 17 : 1 |
| 8 | 0.3 | 0.1 | 39 | 17 : 1 |
| 9 | 0.3 | 0.5 | 42 | 10 : 1 |
| 10 | 0.3 | 1.0 | 37 | 10 : 1 |
| 11 | 0.1 | 0.1 | 35 | 19 : 1 |
| 12 | 0.5 | 0.5 | 43 | 10 : 1 |
| 13 | 1.0 | 1.0 | 42 | 7 : 1 |

Figure 33: Screening of different ligand and acid loading. Yields determined by ^1H NMR of the crude reaction sample against TCE as an internal standard. *d.r.* determined by GC – FID.

A solvent screen was also carried out (figure 34). Aromatic solvents such as *o*-xylene and chlorobenzene (entry 1, 2) performed similarly to toluene, though with slightly lower yields. Dioxane and DMF both gave poorer yields with only slightly better diastereoselectivity (entry 3, 4). Other solvents screened (entry 5 – 8) did not give any discernible product.



| Entry | Solvent | Yield / % | d.r. |
|-------|------------------|-----------|--------|
| 1 | <i>o</i> -Xylene | 61 | 10 : 1 |
| 2 | Chlorobenzene | 66 | 8 : 1 |
| 3 | Dioxane | 47 | 12 : 1 |
| 4 | DMF | 16 | 12 : 1 |
| 5 | Dichloroethane | - | - |
| 6 | Ethylene Glycol | - | - |
| 7 | Ethyl Acetate | - | - |
| 8 | THF | - | - |

Figure 34: Screening of different solvents. Yields determined by ¹H NMR of the crude reaction sample against TCE as an internal standard. *d.r.* determined by GC – FID.

Figure 35 shows the optimal reaction conditions for diastereoselective carbonylation of aliphatic amines forming γ -lactams. The additives were found to play an important role in controlling both the yields and the diastereoselectivity of the reaction. Although other acids and basic additive may give higher yields or diastereoselectivity, we found these conditions to give the best compromise between increasing yields and diastereoselectivity. With these conditions in hand, we proceeded to test the scope of the reaction.

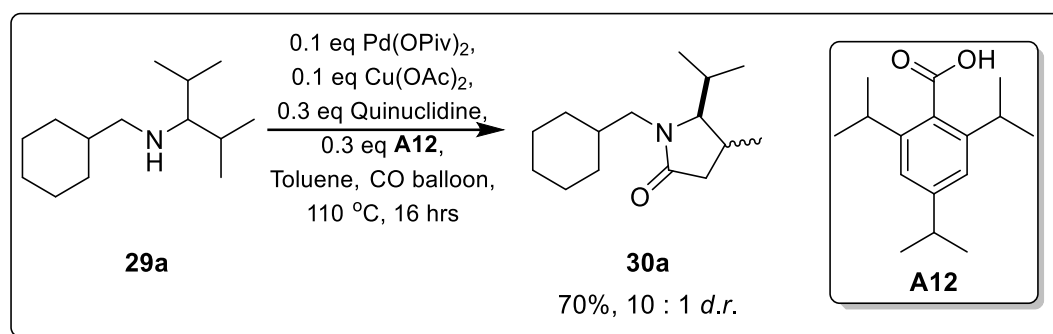


Figure 35: Optimised conditions for diastereoselective carbonylation of aliphatic amines to form γ -lactams.

1.2.5. Substrate Scope

With the optimised conditions at hand, we proceeded to evaluate the substrate scope of the reaction. Amine substrates were typically prepared by reductive amination of the corresponding ketone. Functionalised ketones were prepared by Grignard alkylation of the aldehyde, followed by oxidation by Dess–Martin periodinane. We began by modifying the functional groups on the non-reacting side of the amine (figure 36). Branching at the α -position on the non-reacting side of the amine was well tolerated and provided the corresponding γ -lactams in good yields and d.r.. Substituents including five and six membered carbocycles, tetrahydropyran, protected piperidine and difluorocycloalkanes, were tolerated in the reaction, and delivered the desired lactams efficiently (**30b** – **30f**). Protecting groups such as ketals and 1,3, diols (**30g**, **30h**) were also accommodated with no deprotection observed after the reaction. Protected azetidines and oxetanes (**30i**, **30j**) were also tolerated in the reaction, though with somewhat lowered yields. TIPS protected amino alcohols also gave moderate yields in the reaction (**30k**). Pleasingly, the lewis basic pyridine motif was also accommodated by the reaction despite its potential to competitively coordinate with palladium (**30l**, **30m**), with moderate to high yields being achieved.

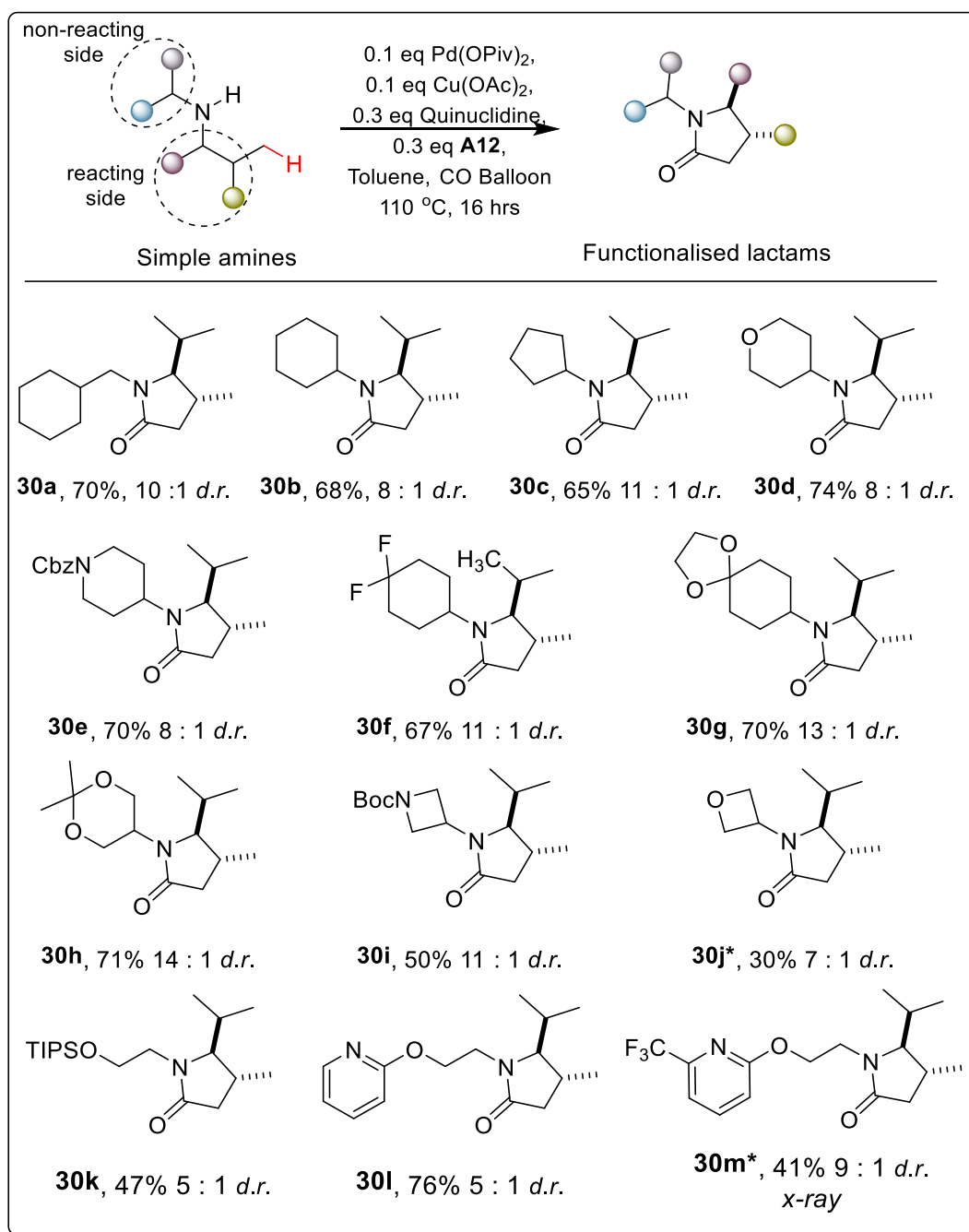


Figure 36: Functionalisation of the N-substituent of the lactam. *In collaboration with Dr Jorge Peiró Cadahía

We then moved on to examine the substrate scope of the reactive side of the amine (figure 37). The 5-position of the lactam was readily functionalised, with cyclohexane, cyclopentane, tetrahydropyrans, and protected piperidine motifs adjacent to the nitrogen atom delivered γ -lactams in reasonable yields and diastereoselectivity (**30n** – **30q**). However, introduction of an acetal substituent in the same position completely removed the diastereoselectivity of the reaction (**30r**), though the corresponding orthoester derivative of valine gave diastereoselectivity of 5 : 1 (**30s**). In the case of isoleucine derivative **29t**, where both γ -methyl and γ -methylene C–H bonds were available, carbonylation was only observed at the γ -methyl group. Consequently, the *cis* lactam was the only isomer observed in 57% yield (**30t**). As the diastereomer obtained is determined solely by the starting material, we made use of acid **A14** in

place of **A12**, which has been shown to increase the yield of the reaction. Similarly, amine **29u** was also subjected to modified reaction conditions, and the corresponding 4-ethyl lactam **30u** was obtained.

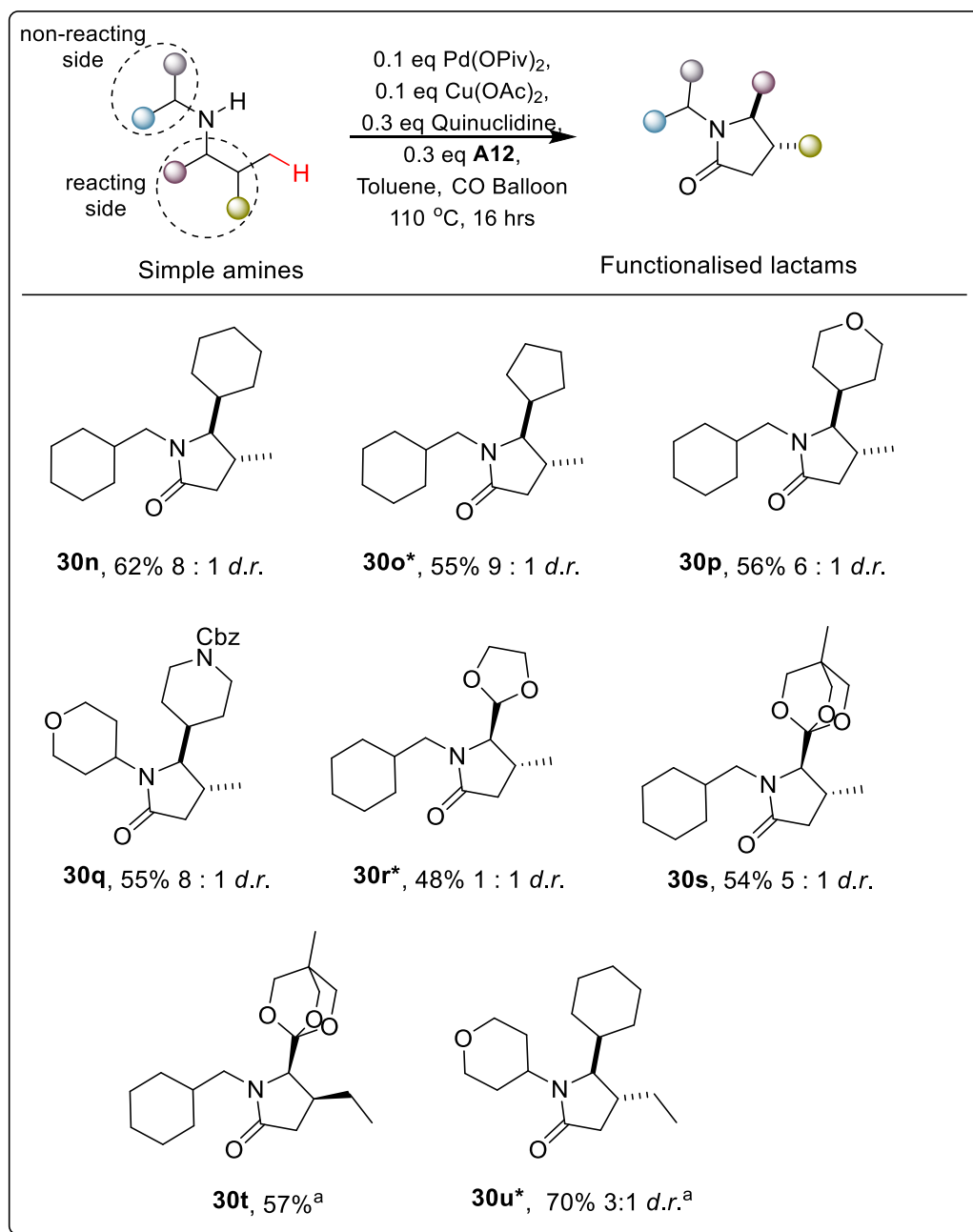
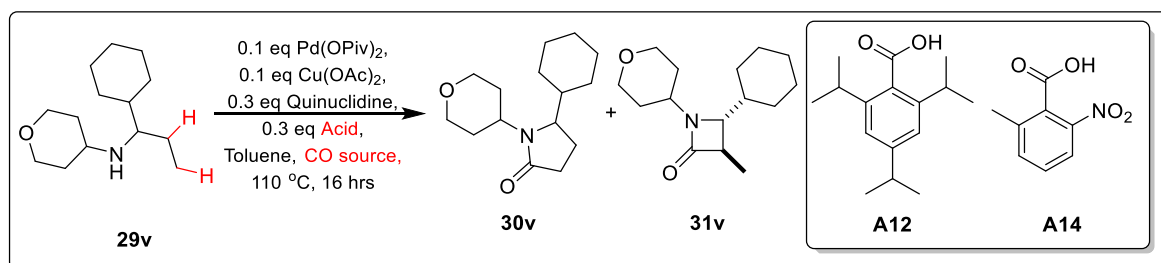


Figure 37: Functionalisation of the 4- and 5-position of the lactam. ^aWith **A14** instead of **A12** *In collaboration with Dr Jorge Peiró Cadahía.

We were also still interested in the γ -carbonylation of amines with a β -methylene site. Previous work in the group has demonstrated the β -selectivity of amine carbonylation. Indeed, when amine **29v** was subjected to previously reported methylene carbonylation conditions, the β -lactam **31v** was exclusively formed in 40% yield.¹⁰⁷ Even under our optimised γ -carbonylation conditions (figure 38, entry 1), only 11% of the γ -lactam was obtained, while 26% of the β -lactam was formed. However, modification of the reaction conditions to make use of **A14** in place of **A12** gave a remarkable increase in γ -lactam yield to 41%, while the amount of β -lactam remained

similar (entry 2). Taking lessons from previous optimisations, we lowered the concentration of carbon monoxide to the commercially available 6.25% CO / air mixture (entry 3), which also gave rise to an increase yield of γ -lactam. Pleasingly, combining both effects together improved both the yields and selectivity of the reaction (entry 4), with a 50% yield of the γ -lactam, and only a 2% yield of the β -lactam. We were thus able to tune the reaction conditions to override the preference for β -carbonylation.



| Entry | Acid | CO Source | 30v | 31v | 30v / 31v |
|-------|------------|------------------------|-----|-----|-----------|
| 1 | A12 | 100% CO balloon | 11 | 26 | 0.4 |
| 2 | A14 | 100% CO balloon | 41 | 25 | 1.6 |
| 3 | A12 | 6.25% CO / Air balloon | 36 | 23 | 1.6 |
| 4 | A14 | 6.25% CO / Air balloon | 50 | 2 | 25 |

Figure 38: γ -Carbonylation of amines in the presence of competing β -methylene positions.

With these conditions at hand, we proceeded to examine the scope of substrates with competing β -methylene groups (figure 39). Pleasingly, the reaction was γ -selective for a variety of substituents on the 5-position of the lactam with a moderate yield (**30v** – **30x**). In all these cases, the γ -lactam was the main product, and the β -lactam was typically found in less than 10% yield. Lactam **30y** with a β -methylene position on the non-reacting side of the amine was also found to be γ -selective, with only about traces of the β -lactam being obtained.

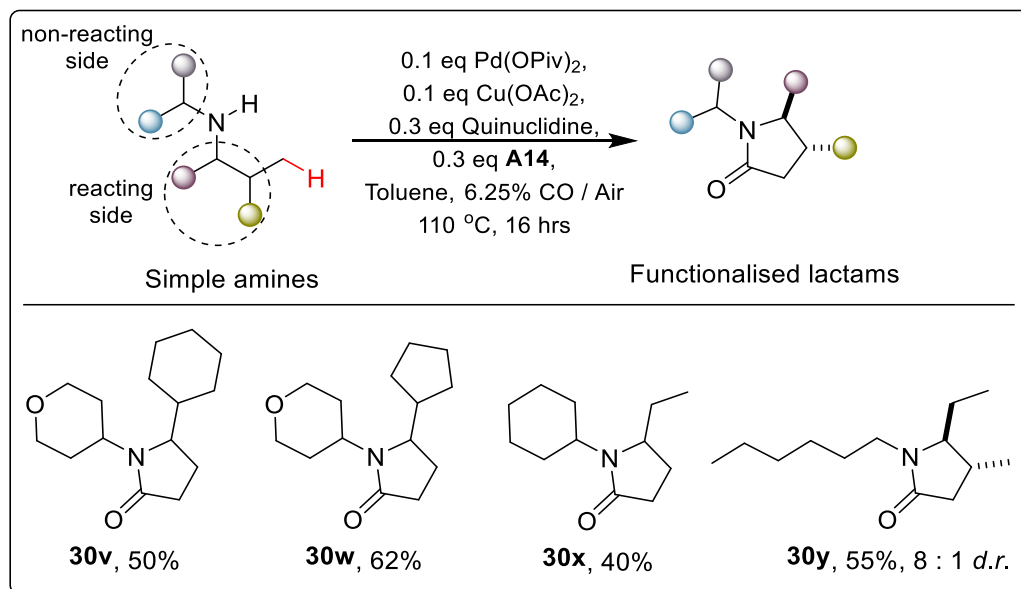


Figure 39: Substrate scope for amines with competing β -methylene positions.

Figure 40 shows some of the substrates which were less successful for this reaction. While we obtained about 22% of the γ -lactam **30z**, we were unable to outcompete the sp^2 C-H activation, and about 55% of the corresponding isoindolione was formed as the major product. The reaction also did not succeed for substrates without α -branching on the reacting side of the amine. At the end of the reaction, most of the starting material has been consumed without formation of the lactam. This could be attributed to β -hydride degradation of the starting amine, which would be more facile without α -branching.

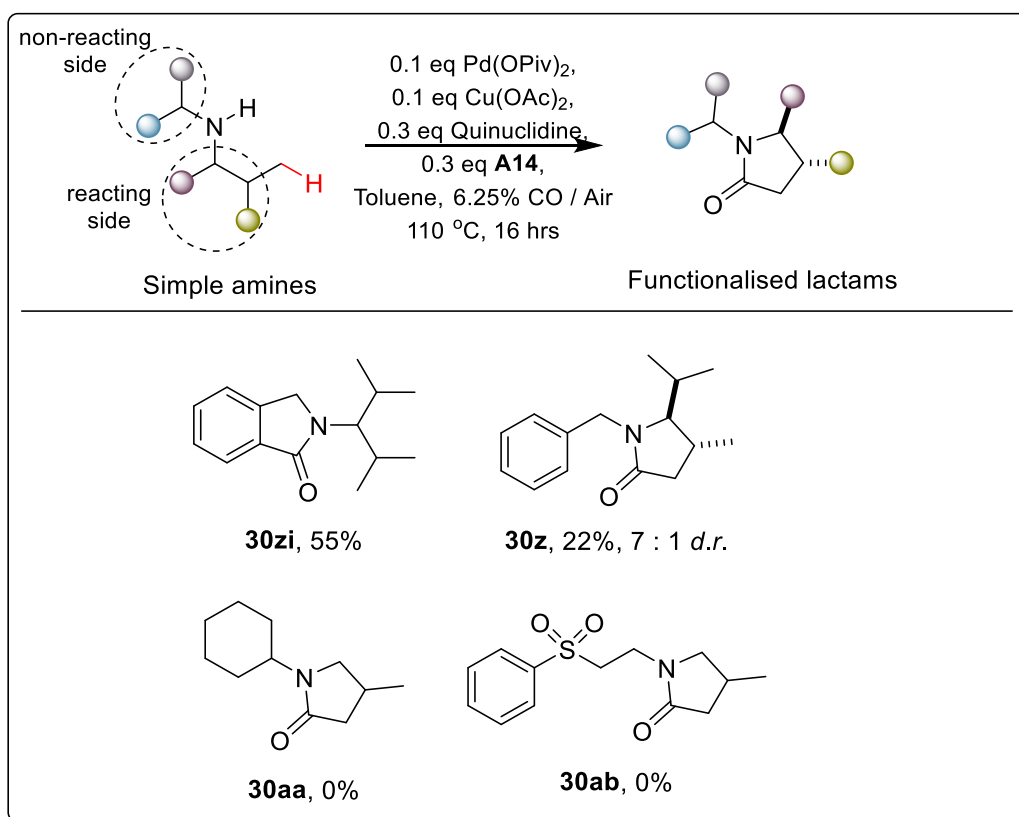


Figure 40: Selected unsuccessful substrates.

1.2.6 Functionalisation of Lactams

We went on to demonstrate the synthetic utility of this reaction by further functionalisation of the obtained lactams into useful building blocks (figure 41). Reduction of the lactam delivers the corresponding 2,3-disubstituted pyrrolidine (**32a-i**), which would be non-trivial to access by other methods. We also made use of enolate chemistry to functionalise the 3-position with either alkyl groups (**32a-ii**), or fluorination with NSFI (**32a-iii**), giving rise to 3, 4, 5-trifunctionalised lactams. Notably, lactam **32a-iii** is structurally related to a kinases inhibitor (IRAK4) at nanomolar potency in cell based assays.¹¹⁷

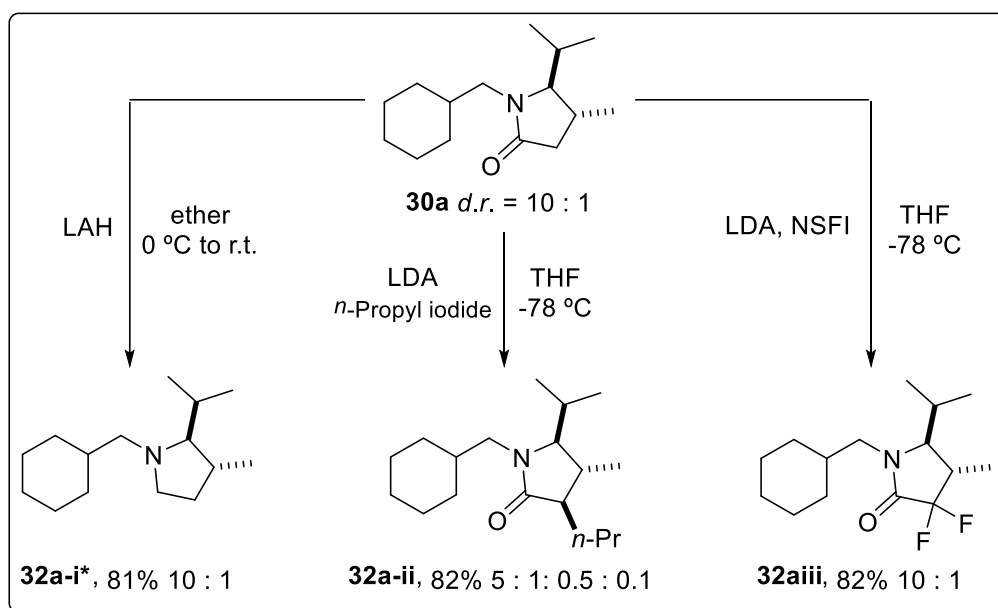


Figure 41: Functionalisation of lactams via reduction or enolate chemistry. *In collaboration with Dr Jorge Peiró Cadahía.

1.2.7 Reaction Mechanism

To study the reaction mechanism, we first prepared the five membered palladacycle by heating amine **29f** with stoichiometric palladium acetate. The palladacycle was isolated in 72% yield, with single crystal x-ray crystallography confirming its structure. The palladacycle was then subjected to carbon monoxide and heated at 80 °C. Pleasingly, the corresponding γ -lactam was obtained in quantitative yield (figure 42a). An alternative mechanistic pathway is via C-H activation of the carbamoyl-palladium complex (as described in figure 24).¹⁰⁶ However, when we prepared carbamoyl chloride **34a** and treated it with tetrakis(triphenylphosphine) palladium, the corresponding lactam was not formed (figure 42b). On this basis, we propose a preliminary catalytic cycle for the carbonylation reaction (figure 42c). Coordination of the amine to palladium forms the mono-amine palladium complex, which undergoes C-H activation to form the palladacycle. Subsequent CO insertion, followed by reductive elimination yields the corresponding γ lactam. Oxidation of palladium (0) by copper acetate and air regenerates palladium (II) for another catalytic cycle.

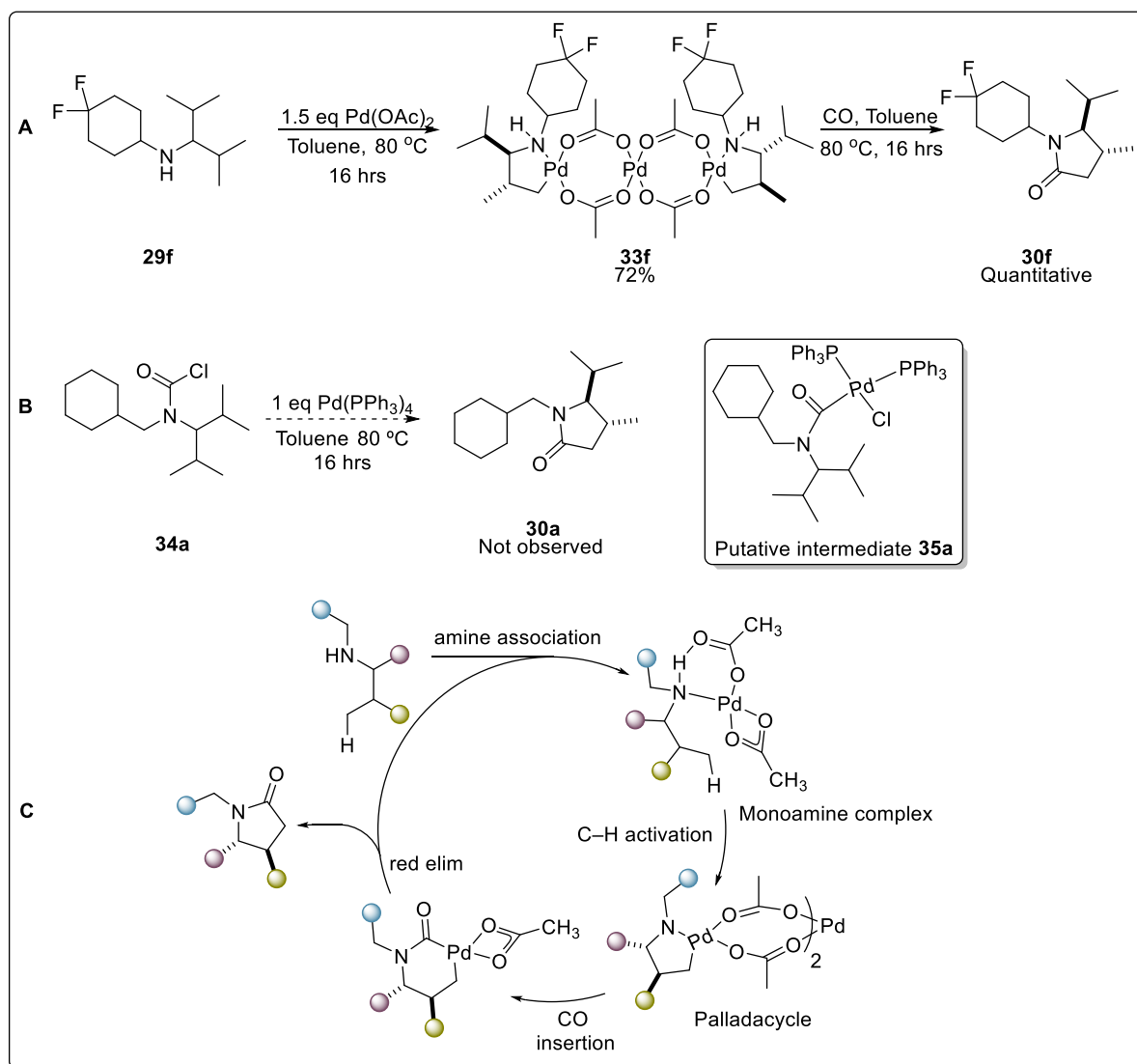


Figure 42: Study of the reaction mechanism. (a) Testing of the 5-membered palladacycle pathway. (b) Testing of the carbamoyl palladium pathway. (c) Proposed catalytic cycle.

1.3 SUMMARY

In summary, we have developed a diastereoselective C-H carbonylation reaction for unprotected secondary amines to yield γ -lactams. Both the yields and diastereoselectivity are strongly influenced by the reaction conditions, especially the carboxylic acid and ligand used. The reaction is feasible for a wide range of functional groups and substitution patterns, providing an abridged route to functionalised secondary lactams. Preliminary mechanistic studies suggest that the reaction proceeds via a classical five- membered palladacycle. We have also demonstrated the ease of further transformation of the lactam by either reduction to obtain the pyrrolidine, or enolate chemistry to functionalise the 5-position of the lactam. As such, we believe that this reaction would be of significant interest to synthetic and medicinal chemists.

CHAPTER 2: CARBOXYLATE DIRECTED C-H ARYLATION OF AZULENE

This chapter describes the development of carboxylic acid directed C-H arylation of azulene at the 2-position. The choice of reaction conditions was found to significantly influence the efficacy of the reaction, with the phosphate base and bulky acid playing a key role. A wide range of 2-functionalised azulene could be prepared, notably including some heterocycles.

2.1 INTRODUCTION

Azulene (**36**), discovered in 1863 by Piesse, is a deeply dark blue isomer of naphthalene. Over the years, azulene and its derivatives have attracted the interest of chemists due to its unique properties. For instance, azulene has an inherent dipole moment of about 1.08 D, with the seven membered ring being slightly electron deficient, while the five membered ring is electron rich.¹¹⁸ Azulene is also the first known and probably the most well-known exception to Kasha's rule, exhibiting fluorescence from the S₂ → S₀ state with a quantum yield of about 0.2, in contrast with a S₁ → S₀ quantum yield of about 10⁻⁴.¹¹⁹ Azulene and its related polymers can also be tuned either by functionalization at appropriate positions,¹²⁰ or by regioisomerism.¹²¹ All these properties have led to azulene being explored in many diverse fields, including sensory materials,¹²² Near IR materials,^{123,124} electrochromic materials,^{125,126} organic photovoltaics materials,^{127,128} photocatalysts,¹²⁹ conducting polymers,¹³⁰ liquid crystals,¹³¹ capacitance,¹³² and even medicinal purposes.^{133–135}

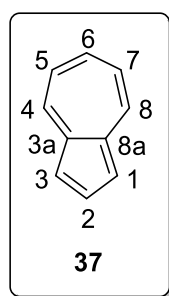


Figure 49: Azulene and its numbering.

However, a major challenge inhibiting azulene research is in its functionalization. Azulene has highly reactive 1,3-nucleophilic positions which dominates most of its chemical transformation. As such, preparation of azulene functionalized at other positions is often cumbersome and require long synthetic routes. Furthermore, derivatives of azulene are often unstable with many possible decomposition pathways. For instance, the aerobic autooxidation of alkyl azulenes has been reported, with extremely complicated mixtures comprising more than ten different compounds being observed.^{136,137} Azulene is also often responsive to acidic environment as it is able to form a tropylium cation upon protonation.¹³⁸ All these contribute to the difficulties in preparing azulene analogues apart from the readily accessible 1,3-position.

The following section will discuss methods of azulene functionalization which has previously been developed and employed. Particular attention will be paid to the methods employed to functionalize the 2-position.

2.1.1 Functionalisation at the 1, 3-Position of Azulene

The 1, 3-positions of azulene are highly reactive towards electrophilic substitution. As early as 1948, Brown predicted this reactivity via quantum mechanical calculations.¹³⁹ This reactivity pattern was verified experimentally by Anderson and Nelson in 1950, who demonstrated that methyl chloride, acetic anhydride, and copper nitrate reacts with azulene at the 1-position to obtain the corresponding products.¹⁴⁰ In 1953, the same group demonstrated that other electrophilic reactions, including Friedel Crafts acylation, chlorination, bromination, and nitration, also takes place in the 1-, 3-position.¹⁴¹ Fluorination by means of N-fluoro-pyridinium salts proved to be unsatisfactory, but is highly efficient when employing Selectfluor™ in the reaction.¹⁴² Figure 49 shows a range of 1, 3-substituted azulene which can be prepared by electrophilic substitution reaction.

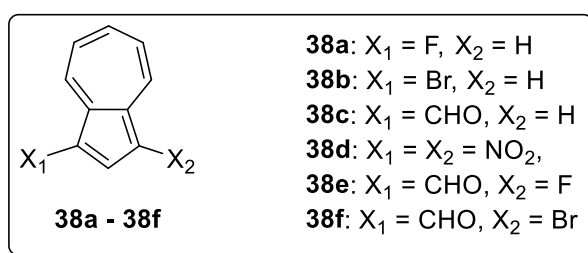


Figure 49: Various 1, 3-substituted azulenes directly prepared by electrophilic substitution reaction.

Access to a wide variety of substituents is possible by further chemical transformation of these azulene derivatives (figure 50). For instance, 1, 3-di-halo substituted azulene substrates can be further functionalized to obtain 1,3-diarylazulene products via the Suzuki-Miyaura coupling as first reported by Daub in 1997,¹⁴³ and optimised by Murafuji and Sugihara in 2002.¹⁴⁴ However, preparation of mono substituted halo-azulene is non-trivial as these reactions often result in a mixture of mono and di substituted azulenes. Furthermore, the mixture is also susceptible to decomposition upon separation with silica. In 2016, Cowper's group demonstrated the preparation and application of 1-azulenesulfonium salts which are bench stable, and can be used as halide substitutes in Suzuki-Miyaura coupling reactions.¹⁴⁵ This methodology enables the preparation of 1-mono-arylated azulenes without complex separation steps.

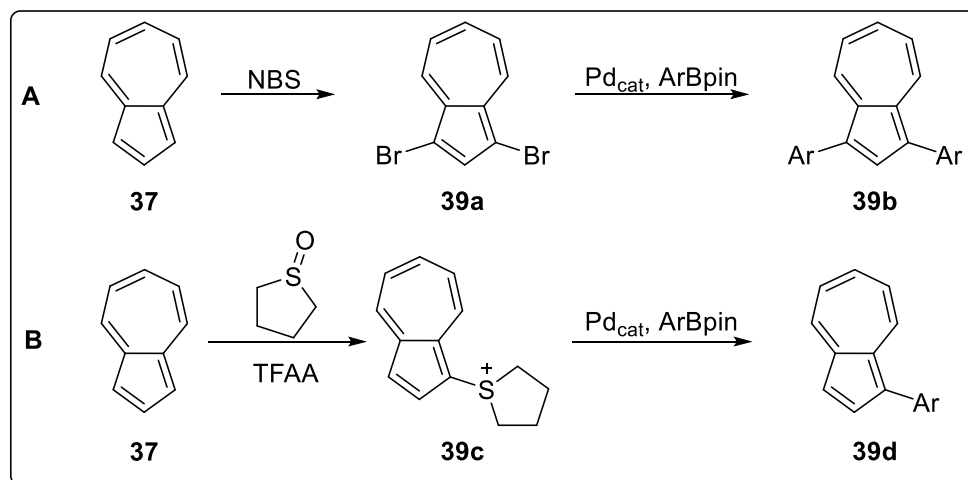


Figure 50: Further functionalisation of azulene at the 1,3-position from (a) 1,3-dihaloazulene (b) 1-azulenesulfonium salts to obtain 1-arylazulenes

The first instance of direct C-H arylation of azulene was reported in 2000 by Dyker's group (figure 51a).¹⁴⁶ Reacting azulene with a fivefold excess of 1-chloro-4-nitrobenzene with palladium catalyst gave a 28% yield of the corresponding 1-arylazulene. This reaction was thought to proceed via an electrophilic attack on an aryl-palladium(II)-halide species, followed by reductive elimination to form the arylated product. Improvements to this was achieved by Murai's group in 2016 by making use of XPhos and pivalic acid as additives.¹⁴⁷ Under these new conditions, both mono and diarylated products were obtainable with a maximum of 62% yield of the diarylated azulene. In 2013, a similar reaction was reported for guaiazulene by Doucet's group (figure 51b).¹⁴⁸ The reaction condition has to be carefully chosen as the arylation could take place on the 1-position, 2-position, as well as the 4-methyl position.

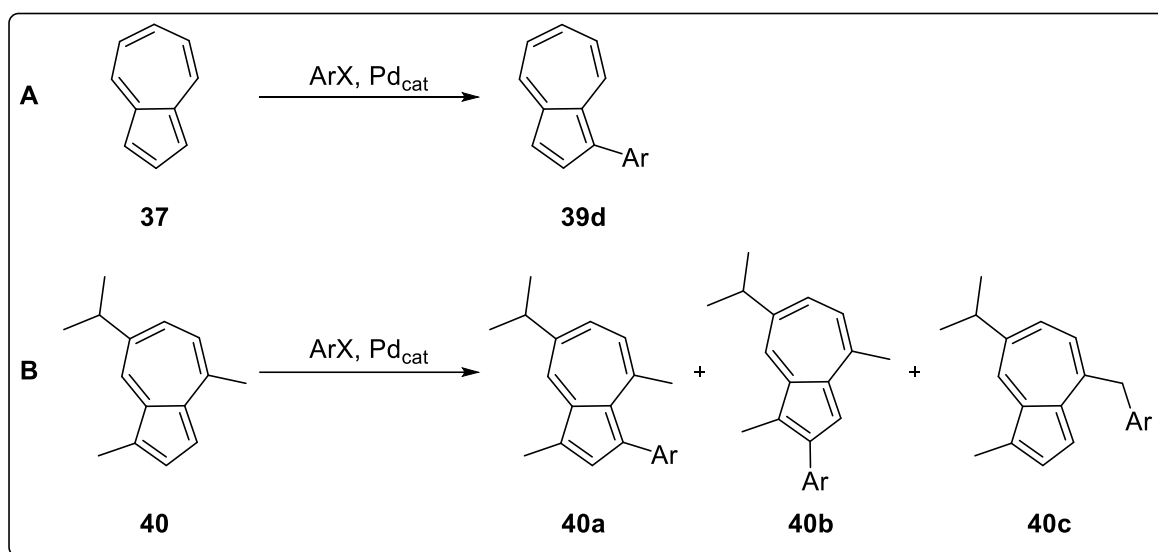


Figure 51: (a) Direct arylation of azulene at the 1-position by palladium catalyst. (b) Direct arylation of guaiazulene at the 1, 2, and 4-methyl positions.

Liu's group reported the arylation of azulene under irradiation with UV light in 2001.¹⁴⁹ Careful selection of the reaction conditions is required as azulene is itself a strong chromophore. Figure 52 shows a range of 1-aryl azulene obtainable by this method. However, when the same methodology was attempted with bromoarenes and chloroarenes, no product was observed. This was attributed to the faster homolysis of aryl iodides due to the weaker C – I bond.

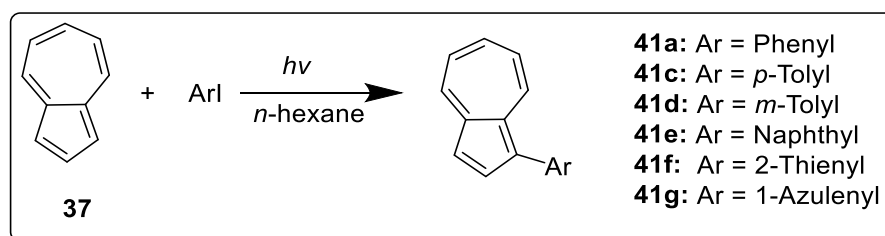


Figure 52: Arylation at the 1-position via photo arylation.

2.1.2 Functionalisation at the 4 – 8-Position of Azulene

Compared to 1, 3-functionalization, the direct functionalization of the seven membered ring of azulene is challenging and often depends on the availability of synthetic

handles put in place during the formation of the azulene backbone. The main methods for construction of the azulene ring are the methods of Nozoe,^{150–152} Ziegler and Hafner,¹⁵³ and Houk.¹⁵⁴

Nozoe's method of azulene construction begins with an activated tropone **41b** (figure 53a). Reaction with diethylmalonate gives an furan-2-one intermediate **41c**, which further reacts to form the 1,2,3-trisubstituted azulene **41d**. Other substituents can also be obtained by replacing diethylmalonate with malonitrile, ethylcyanoacetate, or cyanoacetamide. These trisubstituted azulenes are highly versatile. For instance, as the 1,3-positions are already occupied, reaction with bromine yields azulene brominated at the 6-position (**41f**). Removal of the functionalization at the 1, 2, and 3 positions is key to obtaining 6-bromo azulene. This strategy was employed by Gao's group to prepare biazulene diimides linked at the 6-position (figure 53b).¹⁵⁵

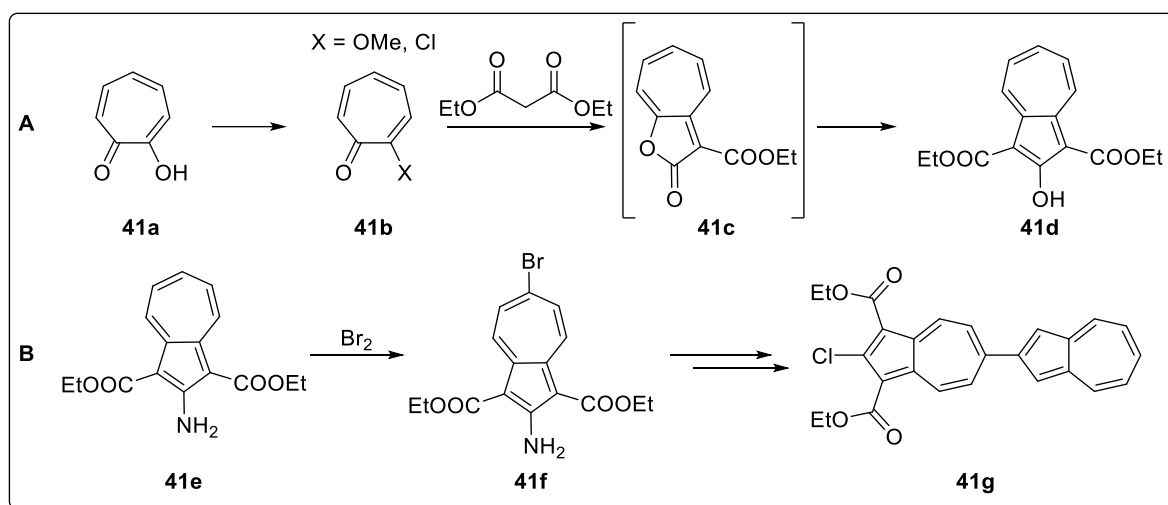


Figure 53: (a) Nozoe's method of constructing azulene from activated tropones. (b) Functionalization of azulene at the 6-position by Gao to construct biazulene moieties.

Another important method was developed by Ziegler and Hafner in 1955 involving a reaction between cyclopentadiene, and a pyridine derived Zincke salt.¹⁵³ While earlier methods made of Zincke salts were derived from 2, 4 dinitrochlorobenzene, alkylation of pyridine with bromobutane has also been employed.¹⁵⁶ Wallen's group found that optimization of the reaction condition, together with the use of microwave irradiation greatly improved the reaction yield and speed (figure 54a).¹⁵⁷ This methodology is quite versatile, with many substitution patterns possible on both the five membered ring and six membered ring. However, the yields are often extremely low and the products can be difficult to purify, especially for products with substituents in the 5, 7-positions.¹⁵⁸ Figure 54b shows some of these azulene derivatives prepared via the method of Ziegler and Hafner.^{159–161}

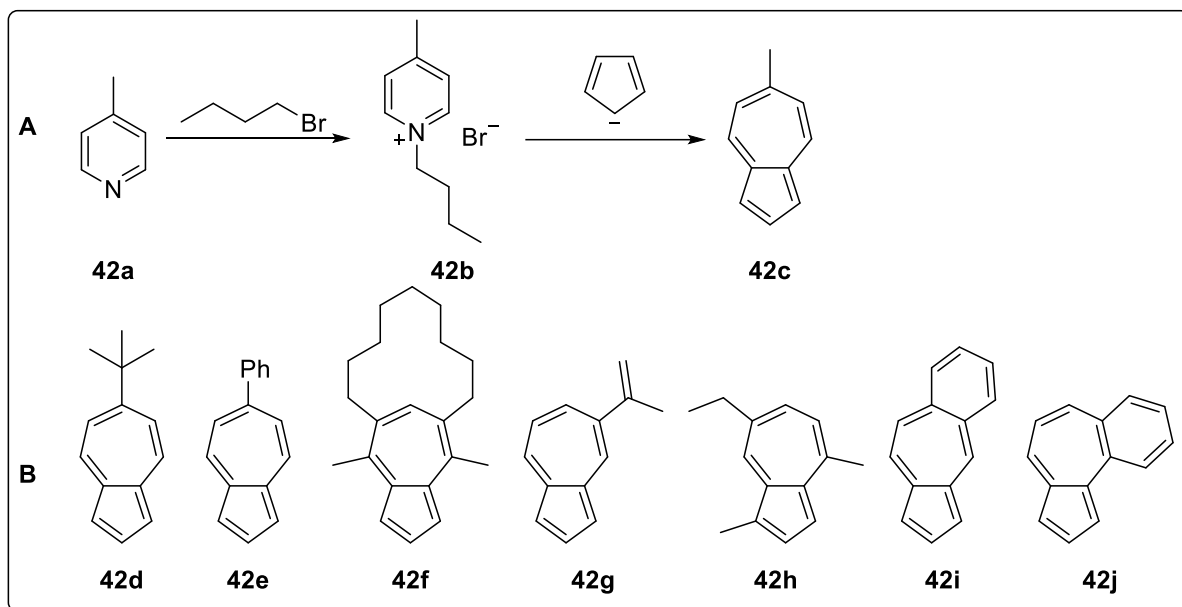


Figure 54: (a) Preparation of 6-methylazulene by method of Ziegler and Hafner. (b) Some representative azulene derivatives prepared by this method.

In 1977, Houk's group reported the [6+4] cycloaddition of aminofulvenes to thiophene S,S-dioxides to form 6-methylazulene in 25% yield.¹⁵⁴ In the same year, Leaver's group also reported this reaction, forming the previously unknown 5, 6-dichloroazulene in 46% yield.¹⁶² This method would later be more fully explored by Hawker's group in 2011.¹⁶³ The substitution pattern of the seven membered ring would be pre-determined by the substitution pattern on the thiophene precursor (figure 55). The dibromo-azulene products would then be precursors for further reaction, and azulene oligomers and polymers connected at the seven membered ring were prepared and studied.^{164,165}

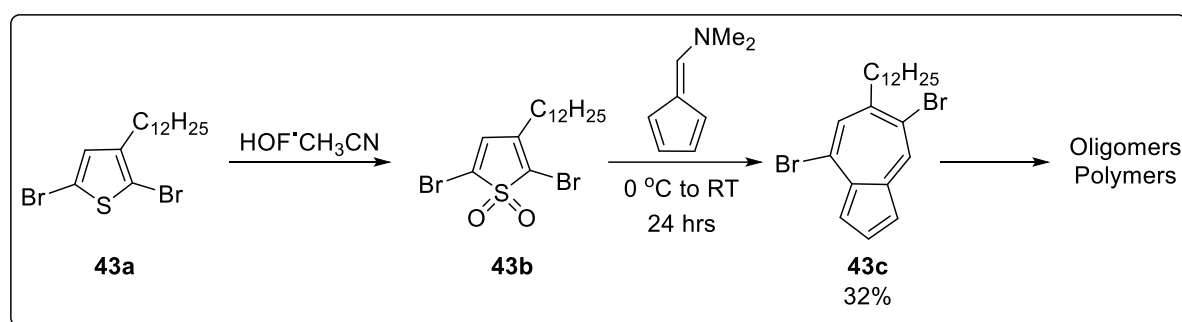


Figure 55: Preparation of azulene functionalised at the seven membered ring by [6+4] cyclisation.

Some other isolated methods also exist for functionalisation of the 6-position. The 4, 6-position of azulene is in principle susceptible to nucleophilic attacks, though using a bulkier nucleophile could tune the selectivity towards the 6-position. Sugihara's group made use of this strategy to prepare azulene-6-carboxylic acid (figure 56).¹⁶⁶ Reacting azulene with lithium tris(methylthio)methanide, followed by treatment with *p*-chloranil gave compound **44a** exclusively. Subsequent reaction with silver nitrate and hydrolysis by sodium hydroxide yielded azulene-6-carboxylic acid in good yields.

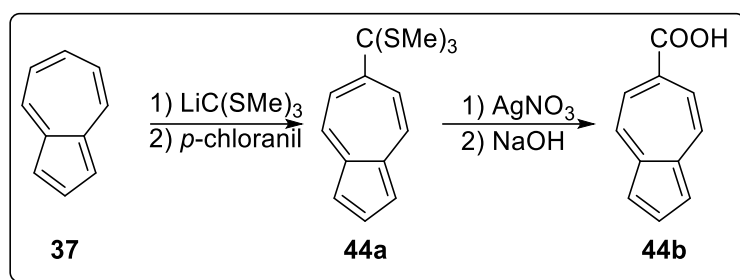


Figure 56: Preparation of azulene-6-carboxylic acid by nucleophilic attack on the 6-position.

2.1.3 Functionalisation at the 2-Position of Azulene

In 1948, Brown's group conducted quantum mechanical calculations which suggested that even positions of azulene could be susceptible to nucleophilic attacks.¹³⁹ However, the low orbital coefficient at the 2-position makes this challenging, and this was never achieved in practice, with reactions preferentially occurring at the 4, 6, and 8-positions. Classically, to obtain a relatively simple 2-iodoazulene, one would first make use of Nozoe's methodology to obtain azulene **41e** from 2-methoxy tropone (figure 57a).¹⁶⁷ Hydrochloride gas would substitute the amino group for a chloride via the Sandmeyer's reaction, while hydrolysis, followed by treatment with phosphoric acid gives the decarboxylated azulene. The chloride could then be converted into the iodide via treatment with potassium iodide. 2-iodoazulene would be a useful precursor to further functionalization via lithiation, or cross coupling reactions.¹⁶⁸ Another method developed by Murafuji's group generates 2-azulenyl-lithiums directly from 1,3-dichloroazulene (figure 57b). Treatment of **45d** with lithium diethylamide gives the corresponding 2-azulenyl-lithium species directly. The 2-azulenyllithium species was stabilized by *ortho*-coordination of the two adjacent halogens. These lengthy methodologies required to obtain a relatively simple molecule illustrate the difficulties of 2-functionalization of azulene.

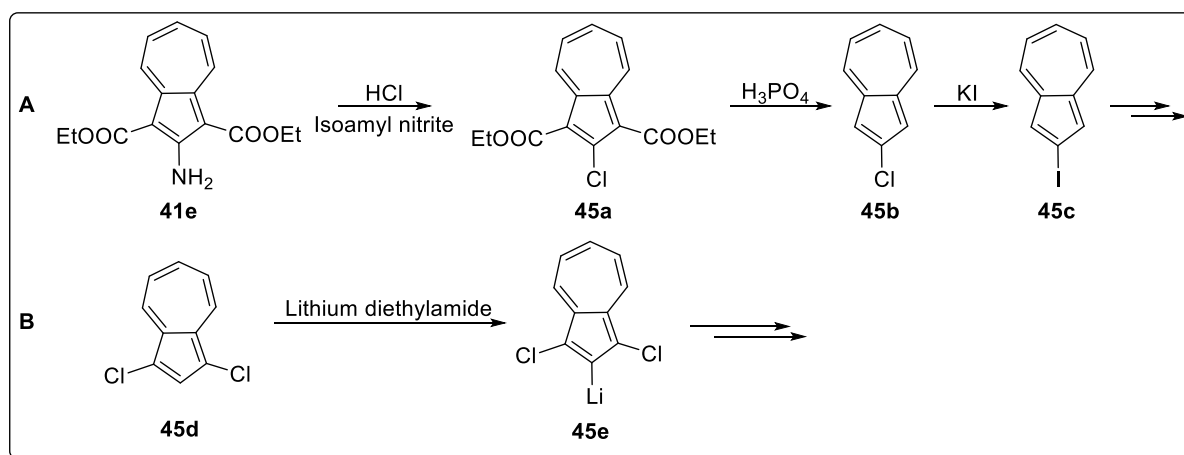


Figure 57: (a) Preparation of 2-iodoazulene from trisubstituted azulene obtained by Nozoe's methodology. (b) Direct lithiation of 1,3 dichloroazulene.

A significant advancement in the field was achieved in 2003, where Sugihara's group developed the direct borylation of azulene at the 2-position *via* the use of iridium catalysis, with a selectivity of 7 : 1 over the 1-position (Figure 58a).¹⁶⁹ This was inspired by the work of Hartwig^{170,171} and Smith,^{172,173} who developed the iridium catalyzed borylation of aromatic hydrocarbons. The selectivity of the borylation was attributed to

the formation of a π complex between the 5-membered ring and the iridium center, as well as steric factors. The boronic ester could then be further reacted via Suzuki coupling to form other 2-functionalized azulenes.^{174–177} More recently, Murafuji's group also developed the copper mediated iododeborylation of **46b**, allowing access to 2-iodoazulene in only two steps.¹⁷⁸ A complementary iridium catalyzed 2-silylation of azulene was also developed by Murai and Takai's group in 2015 (figure 58b).¹⁷⁹ This silylation was even more regioselective than the borylation, with 2-silylazulene being the only regiomer of the reaction, and the electronic properties of the silane only had a slight influence on the efficacy of the reaction.

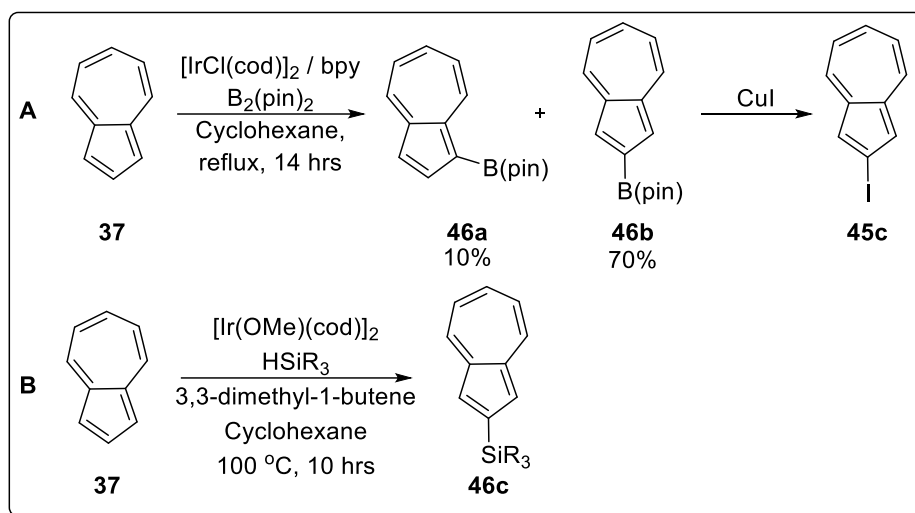


Figure 58: (a) Iridium catalyzed 2-borylation of azulene. (b) Complementary iridium catalyzed 2-silylation of azulene.

2.2 C-H ACTIVATION OF AZULENE

In the last two decades, the field of C-H activation has seen great progress. C-H activation has also been applied to the field of azulene chemistry. However, most of such examples focus on direct functionalization of the 1,3-position, making use of its natural reactivity.^{146–148,159} Sugihara's use of iridium catalyst to functionalize the 2-position is a remarkable advance in the chemistry of azulene (figure 59b), but sometimes suffers from regioselectivity issues. Furthermore, the boronic ester would have to be further reacted in order to obtain functional materials.

We envisioned a novel mechanism of functionalization, whereby a directing group at the 1-position would enable C-H activation at the 2-position. To our knowledge, this strategy has never been applied to the functionalization of azulene. To test out this principle, we chose the carboxylate group to direct arylation towards the 2-position. The use of carboxylic acids as directing group for C-H activation is well documented, though not in the context of azulene.^{180–182} Furthermore, the carboxylic group can be easily installed at the 1-position via operationally convenient and scalable methodologies.¹⁸³ If necessary, the carboxylic acid could also be removed either post reaction or *in-situ* if so desired, thus acting as a traceless directing group.

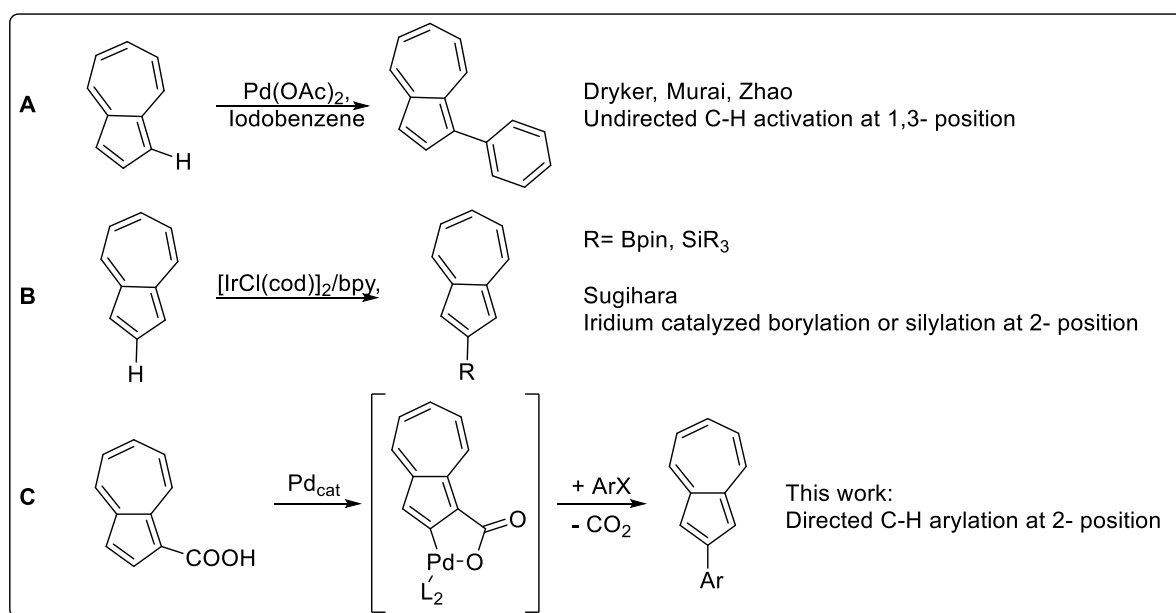


Figure 59: Summary of C-H activation methods for azulene functionalization. (a) Undirected palladium catalyzed C-H activation at the 1, 3-position. (b) Iridium catalyzed borylation / silylation at the 2-position. (c) This work: directed C-H arylation at the 2-position.

2.3 RESULTS AND DISCUSSION

To begin our investigation, we started with carboxylic directed arylation conditions developed by Yu's group and Su's group, using either aryl iodides or aryl borates as the coupling partner (figure 60a-c).¹⁸⁴⁻¹⁸⁶ Unfortunately, none of these conditions gave us any discernable product, although the starting material was completely consumed. However, an initial hit was obtained when we applied the conditions developed by Larrosa's group, where a 3.5% yield of the arylated product was obtained (figure 60d).¹⁸⁷ Although this reaction was originally optimized to prevent decarboxylation, we found that the decarboxylation appears to still have taken place *in-situ*. As such, we took this as the starting point of our optimization.

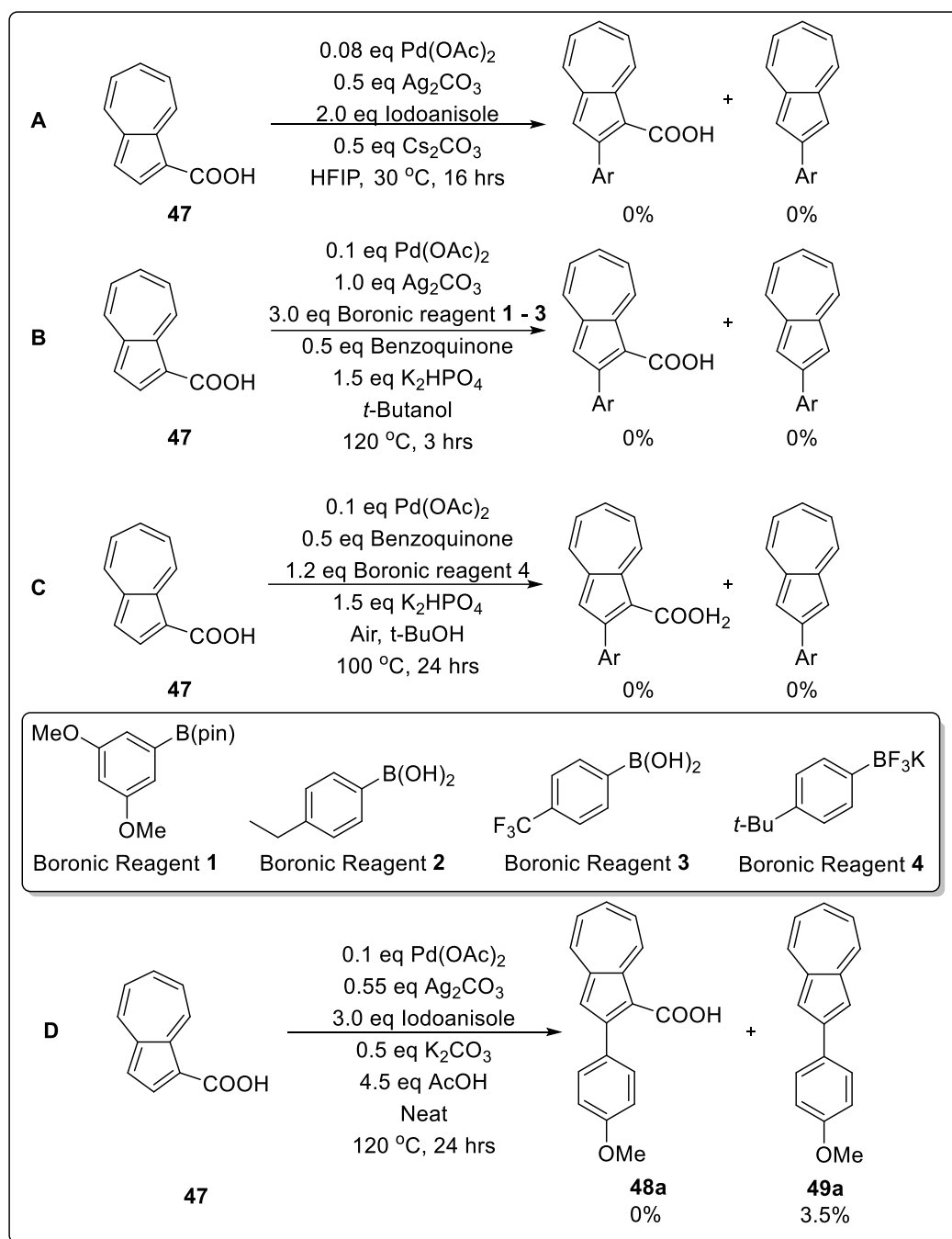
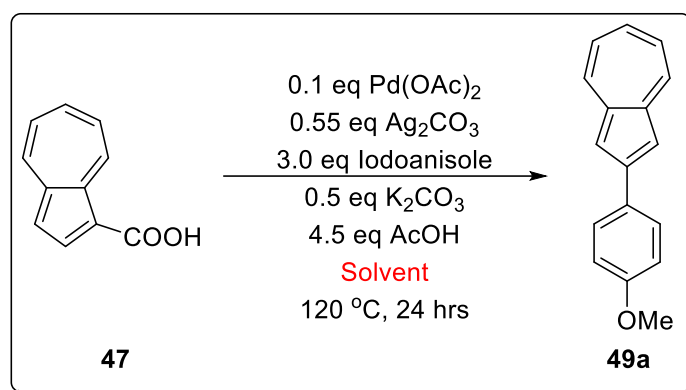


Figure 60: Attempts at using carboxylic acid directed C-H arylation conditions developed by (a) Su's group. (b, c) Yu's Group (d) Larrosa's group with initial hit.

2.3.1 Optimisation of Reaction

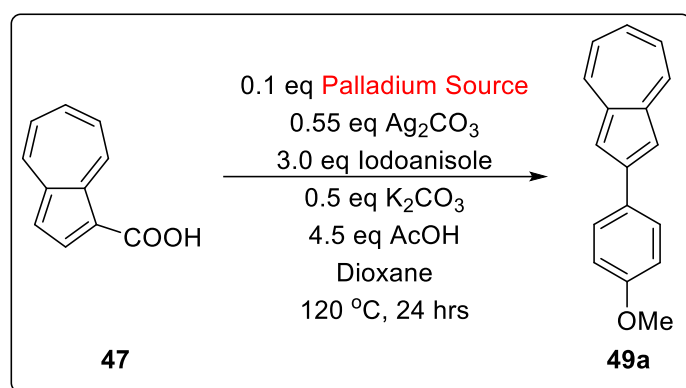
As the original reaction was conducted neat, we began our optimization by first introducing and varying the solvent used (figure 61). Using commonly used solvents such as dichloroethane, toluene, and dioxane (entry 2 - 4) saw an increase in yield ranging from 15% to 20%. The closely related *p*-xylene only gave a 7% yield (entry 5). Using acetic acid and DMF saw no reaction (entry 1, 6), while only trace product was observed with hexanol as the solvent (entry 7). As such, the dioxane was used as the solvent of choice for the optimization.



| Entry | Solvent | 49a / % |
|----------|------------------|-----------|
| 1 | Acetic Acid | - |
| 2 | Dichloroethane | 16 |
| 3 | Toluene | 15 |
| 4 | Dioxane | 20 |
| 5 | <i>p</i> -xylene | 7 |
| 6 | DMF | - |
| 7 | Hexanol | 2 |
| 8 | Neat | 4 |

Figure 61: Optimisation of solvent for reaction. Yields determined by ^1H NMR of the crude reaction sample against TCE as an internal standard.

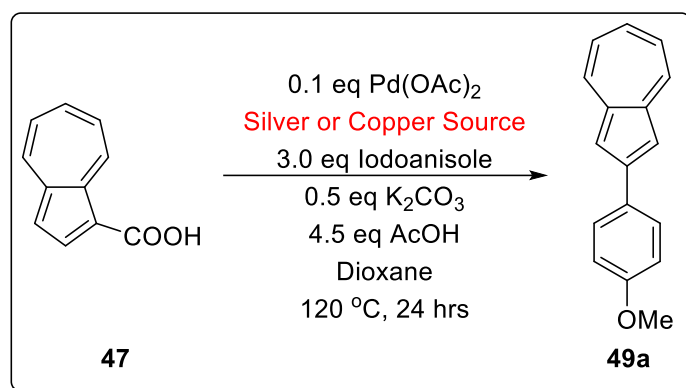
We went on to vary the palladium source of the reaction (figure 62). Both palladium pivalate and palladium bromide performed almost as well as palladium acetate (entry 2, 3). Palladium (0) sources such as $\text{Pd}_2(\text{dba})_3$ and $\text{Pd}(\text{PPh}_3)_4$ (entry 4, 5) also gave some product, but the yield was somewhat lower. Addition of a strongly coordinating bipyridine ligand to the catalyst inhibited the reaction (entry 6), while a weaker bisbenzonitrile ligand (entry 7) performed similarly to the reaction without ligand (entry 3). Since the palladium (II) sources all performed similarly, we carried on the optimisation with palladium acetate.



| Entry | Pd Source | 49a / % |
|----------|---|-----------|
| 1 | $\text{Pd}(\text{OAc})_2$ | 20 |
| 2 | $\text{Pd}(\text{OPiv})_2$ | 18 |
| 3 | PdCl_2 | 19 |
| 4 | $\text{Pd}_2(\text{dba})_3$ | 7 |
| 5 | $\text{Pd}(\text{PPh}_3)_4$ | 8 |
| 6 | (2,2'-Bipyridine)dichloropalladium(II) | - |
| 7 | Bisbenzonitriledichloropalladium(II) | 19 |

Figure 62: Optimisation of palladium source for reaction. Yields determined by ^1H NMR of the crude reaction sample against TCE as an internal standard.

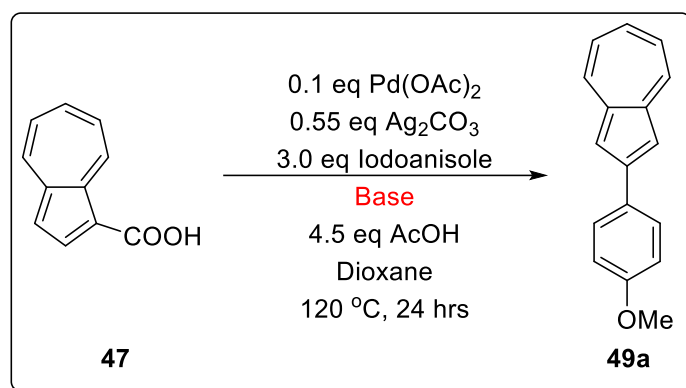
Next, the choice and loading of the metal salt was examined (figure 63). Replacing silver carbonate with copper salts completely shut down the reaction (entry 5 – 7). The role of silver as a re-oxidant, halide scavenger, and even as a facilitator of the C-H activation has been well documented.^{188,189} Silver carbonate is also shown to be a superior salt compared to silver acetate (entry 3 – 4). However, the loading of silver needs to be precise. Increasing the amount of silver resulted in lower yields being observed. This could be due to competitive coordination of **47** with silver, preventing it from binding with palladium, resulting in lower activities. As such, we continued the optimisation with the original silver loading of 0.55 eq.



| Entry | Silver / Copper Salt | Loading / eq | 49a / % |
|-------|---------------------------------|--------------|---------|
| 1 | Ag ₂ CO ₃ | 0.55 | 21 |
| 2 | Ag ₂ CO ₃ | 1.1 | 15 |
| 3 | AgOAc | 1.1 | 16 |
| 4 | AgOAc | 2.2 | 17 |
| 5 | Cu(OAc) ₂ | 1.1 | - |
| 6 | CuCl ₂ | 1.1 | - |
| 7 | CuBr ₂ | 1.1 | - |

Figure 63: Optimisation of silver or copper salt for reaction. Yields determined by ¹H NMR of the crude reaction sample against TCE as an internal standard.

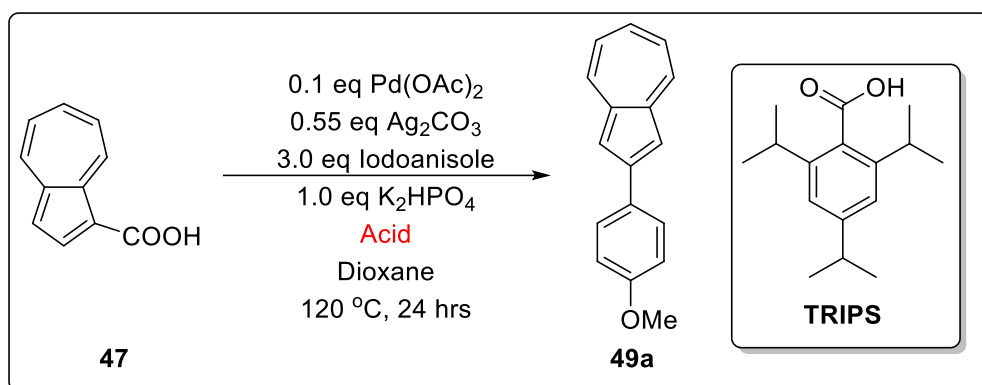
We also optimised the base used in the reaction (figure 64). Changing the metal ion to lithium, sodium, cesium and calcium did not result in any improvements in the yield (entry 3 – 6). Meanwhile, using stronger and weaker bases such as potassium hydroxide and potassium acetate did not seem to affect the yield of the reaction (entry 1, 2). We also tried the organic base quinuclidine, but that only gave a 7% yield in the reaction. However, surprisingly, when potassium phosphate (dibasic) was employed in the reaction, a significant jump in yield to 36% was observed (entry 8). The loading was optimal at 1 eq of base, as reduction in the loading resulted in lower yields of the reaction (entry 9).



| Entry | Base | Loading / eq | 49a / % |
|----------|-------------------------------------|--------------|-----------|
| 1 | KOH | 1 | 19 |
| 2 | KOAc | 1 | 19 |
| 3 | Li ₂ CO ₃ | 0.5 | 11 |
| 4 | Na ₂ CO ₃ | 0.5 | 7 |
| 5 | Cs ₂ CO ₃ | 0.5 | 9 |
| 6 | CaCO ₃ | 0.5 | 2 |
| 7 | Quinuclidine | 1 | 7 |
| 8 | K₂HPO₄ | 1 | 36 |
| 9 | K ₂ HPO ₄ | 0.5 | 13 |

Figure 64: Optimisation of base used in the reaction. Yields determined by ¹H NMR of the crude reaction sample against TCE as an internal standard.

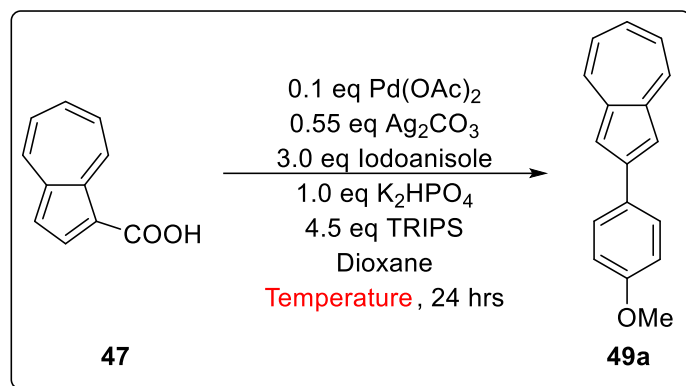
We went on to optimise the acid used in the reaction (figure 65). Either increasing or decreasing the amount of acetic acid used resulted in decreased yields of the reaction (entry 2, 3). Stronger acids such as trifluoroacetic acid and *p*-toluenesulfonic acid resulted in complete shut down of the reaction (entry 4, 5). A hit was obtained in triisopropylbenzoic acid (TRIPS), which saw the yield jump to 68% (entry 6). *N*-protected isoleucine and 2-methyl-6-nitrobenzoic acid both saw reduced yields (entry 7, 8). As such, we attempted to optimise the loading of TRIPS in the reaction, ranging from 0.1 eq to 6.0 eq (entry 9 – 14). However, the original 4.5 eq was found to be optimal, with both higher and lower loadings of the acid giving lower yields.



| Entry | Acid | Loading / eq | 49a / % |
|----------|---------------------------------|--------------|-----------|
| 1 | Acetic Acid | 4.5 | 33 |
| 2 | Acetic Acid | 2.0 | 6 |
| 3 | Acetic Acid | 6.0 | 16 |
| 4 | Trifluoroacetic Acid | 4.5 | - |
| 5 | <i>p</i> -toluene sulfonic acid | 4.5 | - |
| 6 | TRIPS | 4.5 | 68 |
| 7 | <i>N</i> -Acetyl isoleucine | 4.5 | 2 |
| 8 | 2-methyl-6-nitrobenzoic acid | 4.5 | 8 |
| 9 | TRIPS | 0.1 | 12 |
| 10 | TRIPS | 0.3 | 11 |
| 11 | TRIPS | 1.0 | 20 |
| 12 | TRIPS | 2.0 | 31 |
| 13 | TRIPS | 4.0 | 45 |
| 14 | TRIPS | 6.0 | 54 |

Figure 65: Optimisation of acid used in the reaction. Yields determined by ¹H NMR of the crude reaction sample against TCE as an internal standard.

The final parameter which we optimised was the reaction temperature (figure 66). The reaction worked well between the range of 100 °C to 120 °C, though a slight increase was observed at 100 °C, with a yield of 72% (entry 2 – 4). Both higher and lower temperatures saw the reaction yield sharply dropping (entry 1, 5).



| Entry | Temperature / °C | 49a / % |
|----------|------------------|-----------|
| 1 | 90 | 25 |
| 2 | 100 | 72 |
| 3 | 110 | 66 |
| 4 | 120 | 68 |
| 5 | 130 | 54 |

Figure 66: Optimisation of temperature of reaction. Yields determined by ¹H NMR of the crude reaction sample against TCE as an internal standard.

Control experiments were also conducted to ensure that no further improvement in yields could be obtained. These experiments can be found in section 2.4, Appendix B.

2.3.2 Scope of Reaction

With these optimal conditions at hand, we went on to examine the scope of the reaction. We began by studying the scope of aryl-iodides tolerated in the reaction (figure 67). Both iodobenzene and 4-iodotoluene worked well in the reaction to give **49b** and **49c** with yields of 67% and 75% respectively. The highly electron deficient trifluoromethyl group was also tolerated, though with lower yields of 31% (**49d**). This could be due to the lower solubility of the resultant azulene. Both fluoro and chloro groups were also tolerated by the reaction, giving the corresponding products in moderate yields (**49e**, **49f**). Pleasingly, esters (**49g**) and cyano (**49h**) groups which could be further functionalized also worked in reasonable yields. Boc protected amino groups was also tolerated in the reaction (**49i**), giving high yields of 76%.

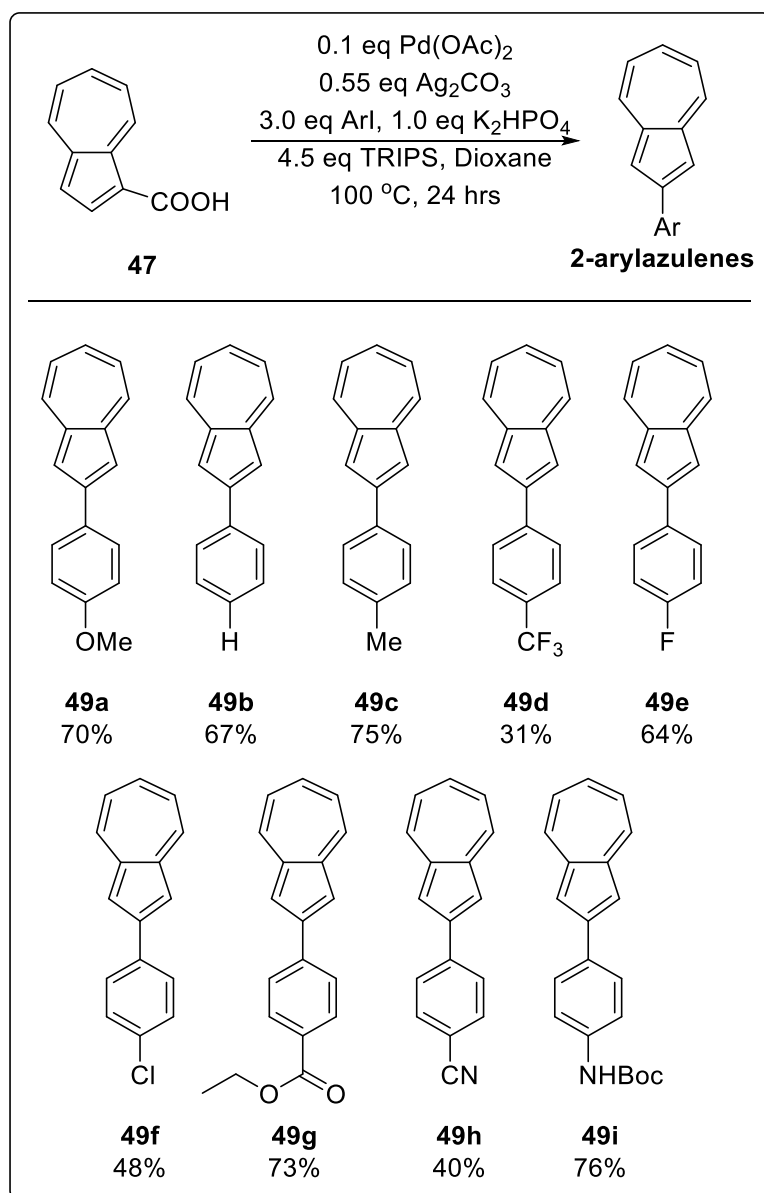


Figure 67: Substrate scope of reaction, functional group tolerance

We went on to examine the scope of substitution patterns of the aryl group. Both 3-iodoanisole and 3'-iodoacetophenone gave the corresponding products (**49j**, **49k**), though **49k** was obtained in somewhat lower yields. Pleasingly, 3, 5 dimethyl substitution was also tolerated, affording **49l** in 82% yield. Similarly, 5-iodo-2,3-dihydrobenzofuran also gave the corresponding **49m** in moderate yields.

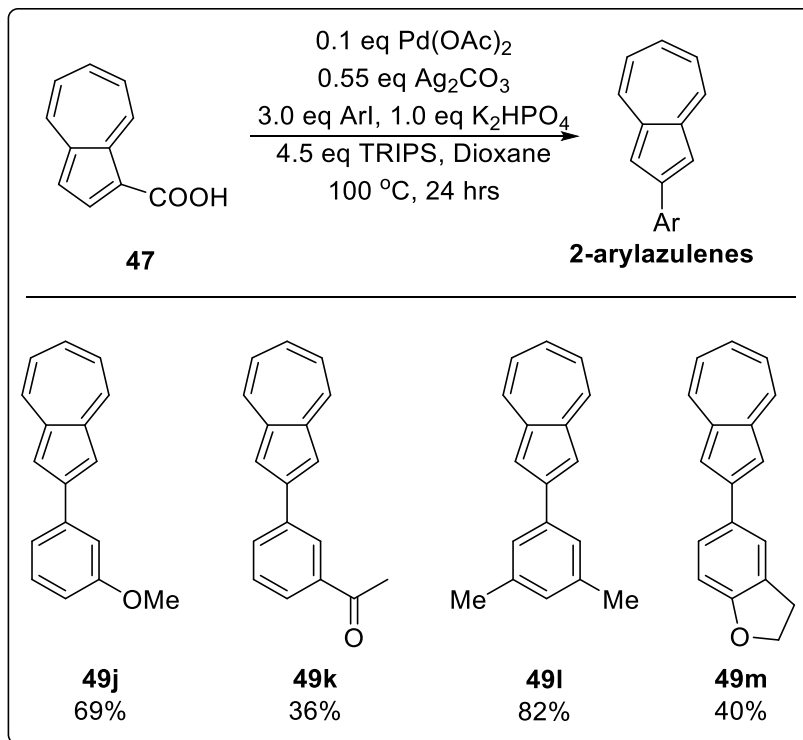


Figure 68: Substrate scope of reaction, substitution pattern on aryl group

Next, we tested some heteroarenes in the reaction (figure 69). Both 2-iodothiophene and 3-iodothiophene gave the corresponding products (**49n**, **49o**), though in somewhat lower yields. Pleasingly, the 2,6-dichloropyridine group could be attached to azulene at the 4-position with high yields of 73% (**49p**).

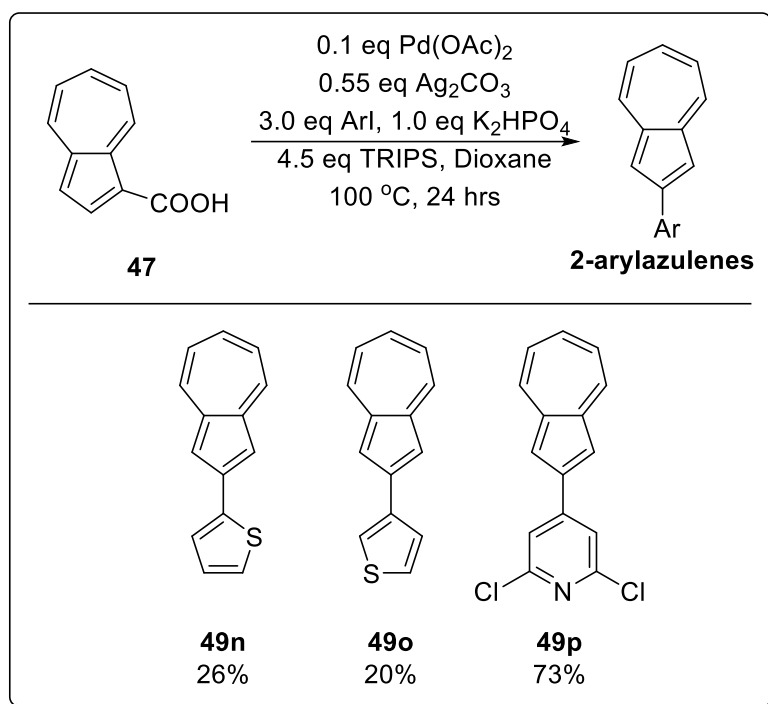


Figure 69: Substrate scope of reaction, reaction of heteroarenes

Finally, we also examined the effects of substituents on azulene at the 6-position (figure 70). The carboxylic acid precursors were prepared stepwise by method of Hafner and Ottoman.¹⁵⁷ Both 6-methylazulene-1-carboxylic acid and 6-*tert*-butylazulene-1-carboxylic acid were amenable to the reaction, giving the corresponding arylated products in moderate yields (**50a**, **50b**, **51a**, **51b**). This methodology gives convenient access to 2, 6 bi-functionalized azulenes, which could be further functionalized to tune the properties of the resultant azulene.

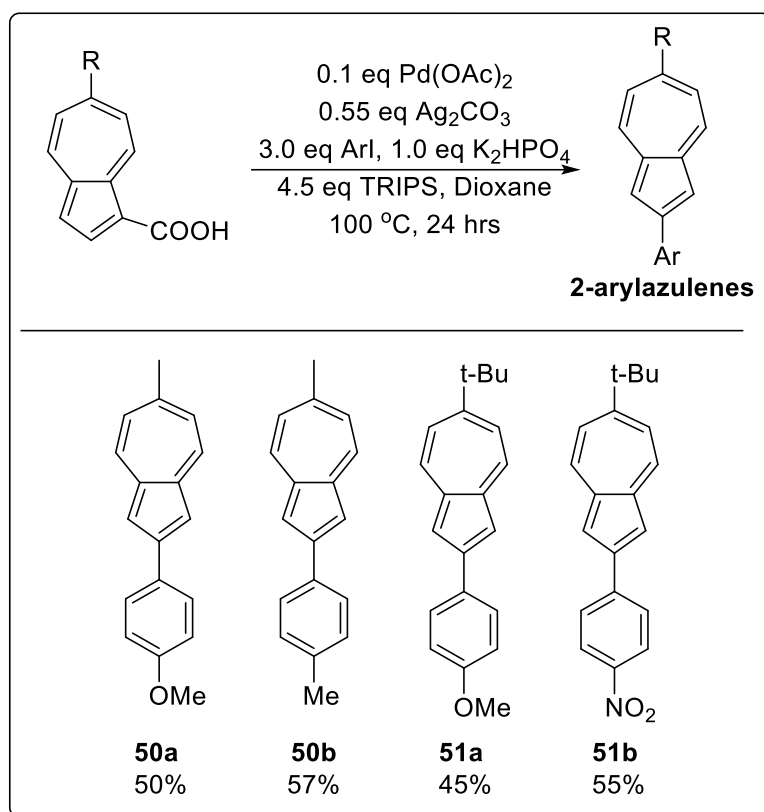


Figure 70: Substrate scope of reaction, functional group on azulene

Some notable substrates that do not work in this reaction include naphthalene substrates (**52a**), 2-iodoarenes (**52b**, **52c**), 2-pyridines (**52d**), as well as iodoalkenes (**52e**) (figure 71). The starting material is mostly recoverable at the end of the reaction. We also attempted the reaction with bromobenzene as the coupling partner, but only recovered the starting material after 16 hours. Attempting the same reaction with elevated temperatures of 120 °C only led to starting material decomposition.

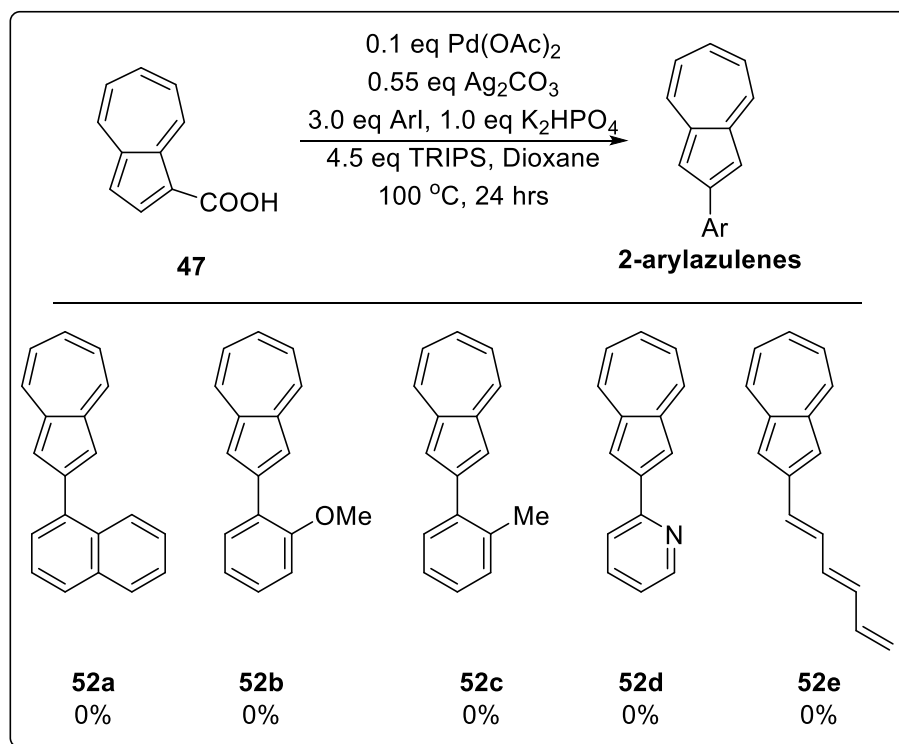


Figure 71: Substrate scope of reaction, selected unsuccessful substrates

2.4 REACTION MECHANISM

Like previous reports by the groups of Daugulis¹⁹⁰ and Yu¹⁸⁵, we believe that the reaction goes through a palladacycle dimer intermediate,¹⁹¹ which then undergoes oxidative addition by the aryl iodide to form a Pd(IV) intermediate (figure 72). Subsequent reductive elimination followed by decarboxylation would yield the corresponding 2-aryl azulene product. In principle, C-H activation could also take place at the 8-position of azulene. However, none of the 8-aryl azulene product was observed in any of our reactions. This is probably due to the five membered palladacycle being more favoured as compared to the six membered palladacycle. Furthermore, the seven membered ring of azulene is more electron deficient, which may also be more unfavourable for the C-H activation. However, further mechanistic studies would have to be conducted to understand both the selectivity and the exact role of each reagent.

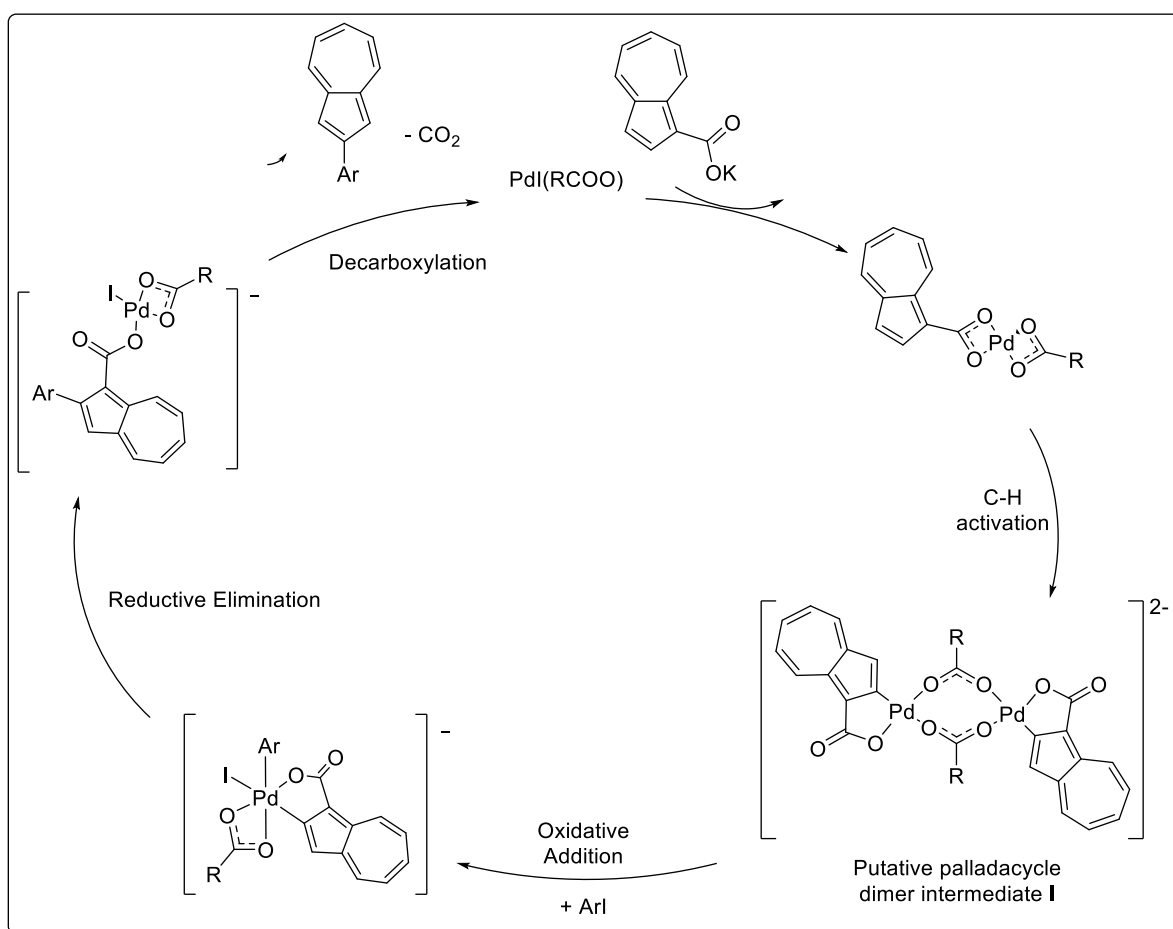


Figure 72: Proposed reaction mechanism for carboxylic acid directed C-H arylation

2.5 SUMMARY

In summary, we have developed a new methodology for arylating the 2-position of azulene *via* carboxylic acid directed C-H activation. This strategy allows for the less available 2-position to be activated preferentially over the far more reactive 1, 3-positions. The choice of reaction condition was found to be crucial for its success, with the phosphate base and the bulky acid TRIPS being key reagents. This strategy works with a wide variety of aryl-iodides as the coupling partner, including some heteroarenes. Pre-existing functionality on azulene is also tolerated by the reaction. In all, we believe that this methodology would be of significant interest to the material chemist in enabling 2-arylation of azulene.

CHAPTER 3: POLYMERIC AZULENE WITH FUNCTIONALISATION AT THE 2-POSITION

3.1 INTRODUCTION

The unique electronic and optical properties of azulene makes it highly interesting for material chemists. In particular, azulene has been incorporated into many different polymers. These polymers can be classified according to their connectivity on azulene. The 1, 3-connectivity is a natural place to begin, as its high reactivity lends it to many different possible reactions. More recently, with Hawker's exploration of [6+4] cyclisation to form azulene functionalised on the seven membered ring (see figure 55), some azulene polymers connected by the seven membered ring has also been prepared. Other methods of incorporating azulene in polymers include having it appended as a side chain, or forming a network polymer with it. The following section will discuss the methods of preparing these polymers as well as their properties and applications.

3.1.1 Polyazulenes Connected on the Five-Membered Ring

The most common method by which polyazulene is formed is by electropolymerisation. The polyazulene modified electrode has been tested for a wide variety of applications including detection of metal ions,^{122,192} glucose,¹⁹³ hydrogen peroxide,¹⁹⁴ 4-nitrophenol,¹⁹⁵ and even as capacitance materials.^{196,197} In all of these cases, the properties of the polyazulene film formed depends greatly on the conditions in which they are prepared. For instance, the solvent, electrolyte, and even the polymerisation potential has all been reported to form films with different properties. However, chemical characterisation of the film is usually non-trivial as the polymer formed is usually completely insoluble in all solvents. The poor solubility also limits its processability and applications.

One of the earliest reports of chemically formed polyazulene was reported by Lai's group in 2003.¹³⁰ 1,3-dibromoazulene was polymerised by method of Yamamoto (figure 73a).¹⁹⁸ The polymer was formed as a yellow-green powder which was soluble in organic solvents such as chloroform, xylenes, and THF. Like the parent azulene, polyazulene reacts with strong acids such as TFA and sulphuric acid with a visible change in colour, which was attributed to the formation of azulonium cation radicals or polycations (figure 73b). While the neutral polyazulene film was essentially non-conductive, exposure to iodine or TFA vapour resulted in it greatly increased conductivity in the range of 1 Scm^{-1} .

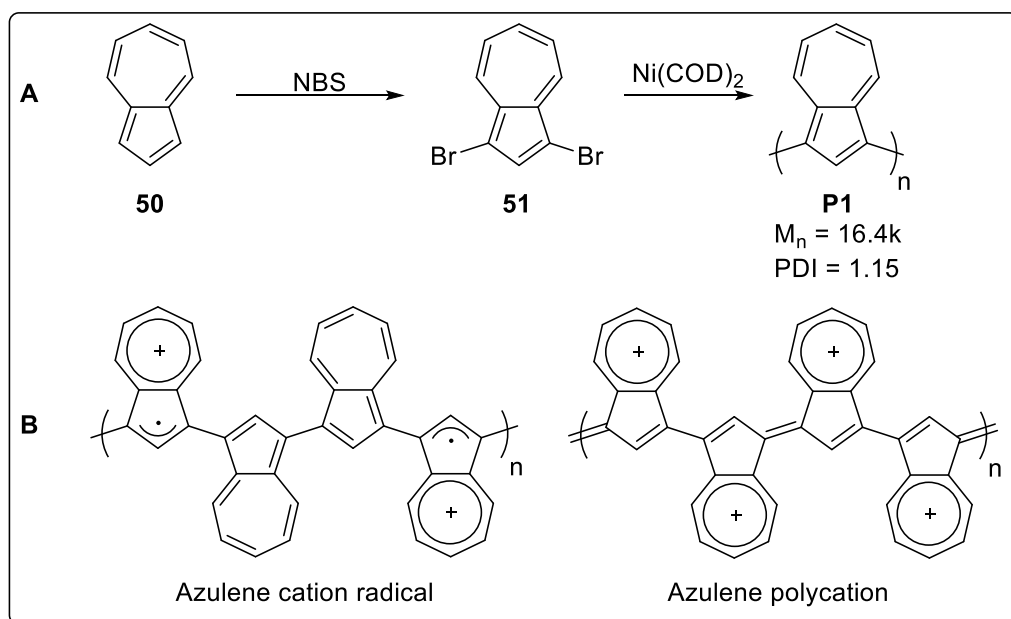


Figure 73: (a) Polyazulene prepared by nickel mediated homocoupling. (b) Protonation of polyazulene leading to azulene cationic radical or azulene polycation.

Apart from azulene homopolymers, azulene has also often be copolymerised with other moieties. In 2003, Lai's group prepared a series of azulene-thiophene polymers by oxidative polymerisation with iron(III) chloride (figure 74a).¹⁹⁹ Like polyazulene, the polymer solution was optically responsive towards TFA, with a new absorption band being formed at 694 nm, and bleaching of the azulene 386 nm band (figure 74b). The new band at 694 nm was attributed to the formation of azulenium cations and dications. This protonation was also reported to be reversible by simply washing with water and methanol. The polymer film could also be protonated by TFA vapor, and an increase in conductivity to 0.34 Scm^{-1} was observed. Further studies in 2004 also showed that the polymer could also be doped by iron(III) chloride to form two new bands at 668 and 1060 nm (figure 74c).²⁰⁰ This was attributed to the formation of polarons and bipolarons. However, upon exposure to air for 10 mins, these bands started to decrease in intensity, suggesting that the polarons formed were unstable.

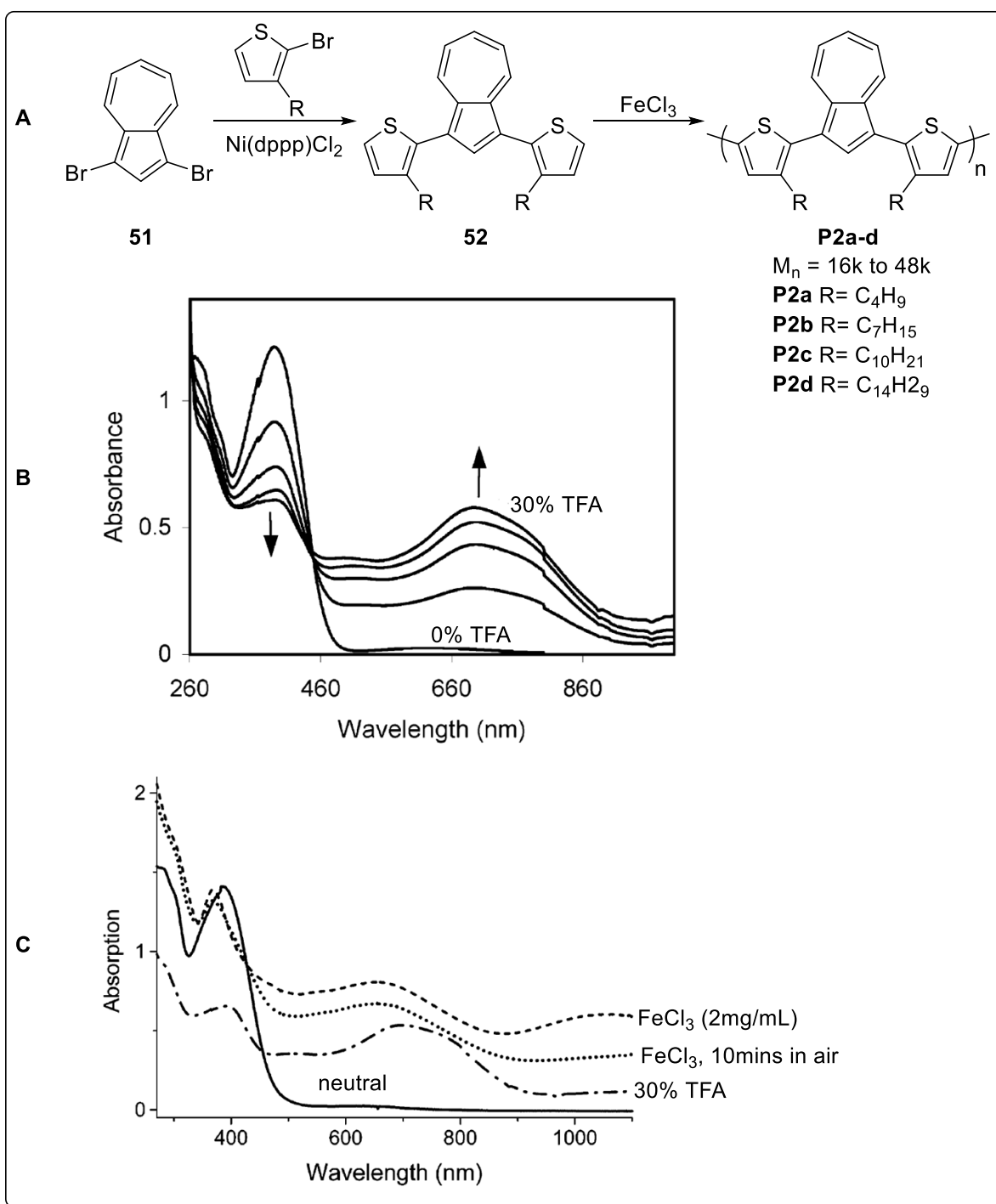


Figure 74: (a) Preparation of azulene thiophene copolymers by oxidative coupling. (b) UV spectrum of **P2c** in chloroform with varying TFA concentrations. (c) UV spectrum of **P2c** in chloroform after different doping treatment. Adapted (b) and (c) from reference 200 with permission from the American Chemical Society Copyright (2003).

In 2008, Xu's group reported a series of azulene – fluorene polymers by Suzuki polymerisation. (figure 75a).¹²⁵ Polymers with a single fluorene repeating unit (**P3a – d**) were yellow in THF, but turned light brown in the presence of TFA. Meanwhile, polymers with triple fluorene repeating unit (**P3e, f**) were orange in THF, but turned green upon addition of TFA. The protonation was non reversible, and addition of triethylamine did not lead to recovery of the original colour. This was attributed to oxidation or decomposition of the protonated azulene. **P3a – P3d** were reported to have no observable fluorescence even upon addition of TFA, while **P3e** and **P3f** did show increasing fluorescence upon protonation. The electrochromic properties of the polymer films were also reported. The color of **P3c** changed from pale yellowish-green in the neutral and reduced (-2.0 V) state light brown in the oxidised (+2.8 V) state (figure 75b). A few cycles of the oxidation and reduction was demonstrated (figure 75c); the oxidative switching time was 8.1s for oxidation and 6.8s for bleaching.

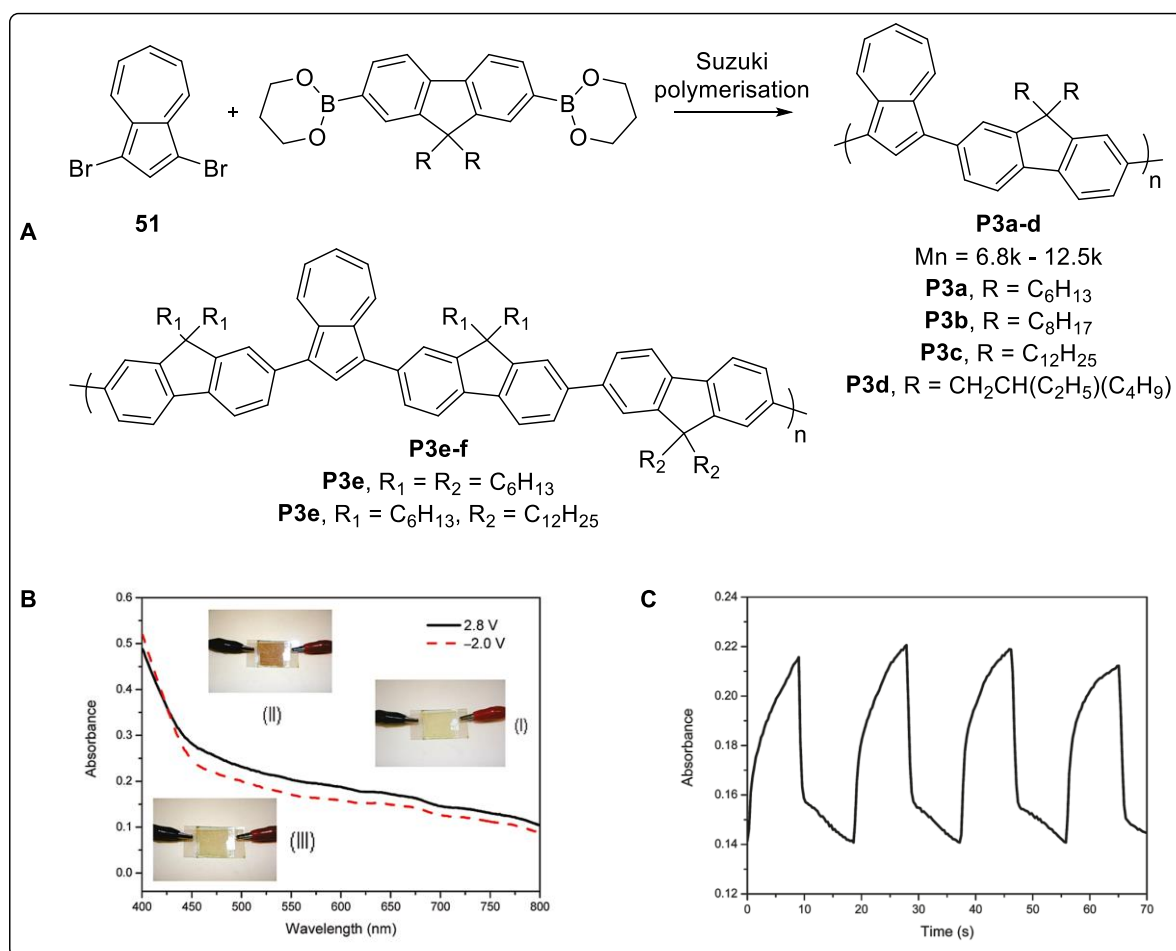


Figure 75: (a) Preparation of azulene – fluorene copolymers by Suzuki coupling. (b) Colour change of **P3c** upon electrochemical oxidation. (c) Absorbance (at 540 nm) – time profile of **P3c** upon multiple cycles of oxidation and reduction. Adapted (b) and (c) from reference 126 with permission from the American Chemical Society Copyright (2008).

In 2013, Xu's group reported a series of azulene – carbazole – benzothiadiazole (BTD) polymers with different feed ratios (figure 76a).¹²⁶ In electrochromic experiments, it was shown that **P4d**, with just 5% of BTD units, exhibited the greatest optical contrast between reduced and oxidised state (figure 76b). This was attributed to the lower oxidation potentials of **P4d** caused by the donor acceptor (D-A) effect. Faster switching times was also observed for **P4d** as compared to **P4a**. When combined with poly(4-styrene sulfonic acid)-doped poly(3,4-ethylenedioxythiophene) (PEDOT:PSS) in an electrochromic device, their complementary absorption spectrum enables black to transmissive electrochromic transition (figure 76b,c). At 600 nm, their combined transmittance was about 65% at bleached state, but less than 10% throughout the whole visible spectrum during coloration.

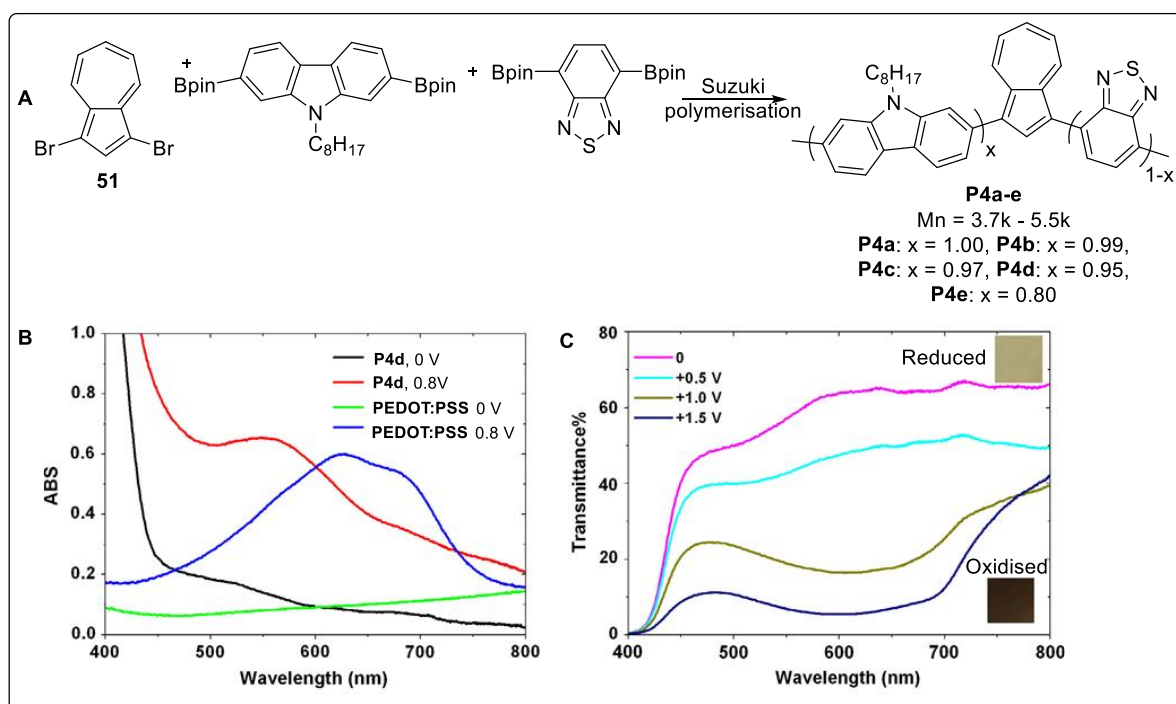


Figure 76: (a) Preparation of azulene – carbazole – BTD polymers. (b) UV spectrum of **P4d** and PEDOT:PSS under neutral and oxidised conditions. (c) Combined transmittance spectrum of **P4d** and PEDOT:PSS under electrochemical switching, exhibiting black to transmissive electrochromic behaviour. Adapted (b) and (c) from reference 127 with permission from Elsevier B.V. (2013).

In 2013, He's group reported a series of IR active azulene polymers (figure 77a).¹²⁴ This was an extension of a previous work on IR active azulene small molecules, which were found to crystallise when fabricated into films, making them unsuitable for fabrication of organic devices.¹²³ In contrast, the polymer films were found to have high thermal stability (up to 380 °C in air), and easy film fabrication. The UV-Vis spectrum of the polymer solution shows an absorption maxima at about 380 nm (figure 77b). Upon addition of TFA, the yellow-green solution immediately changed to dark brown. New peaks were observable in the visible (~480 nm, 570 nm) and IR (~1600 nm) range, while the 380 nm peak decreased in intensity. The new peaks were attributed to intramolecular charge transfer (ICT) in the polymers. The polymer film also saw similar colour change upon exposure to TFA. Upon further neutralisation with ammonia vapor, the colour change was reversible many time until the films were broken by solvent swelling.

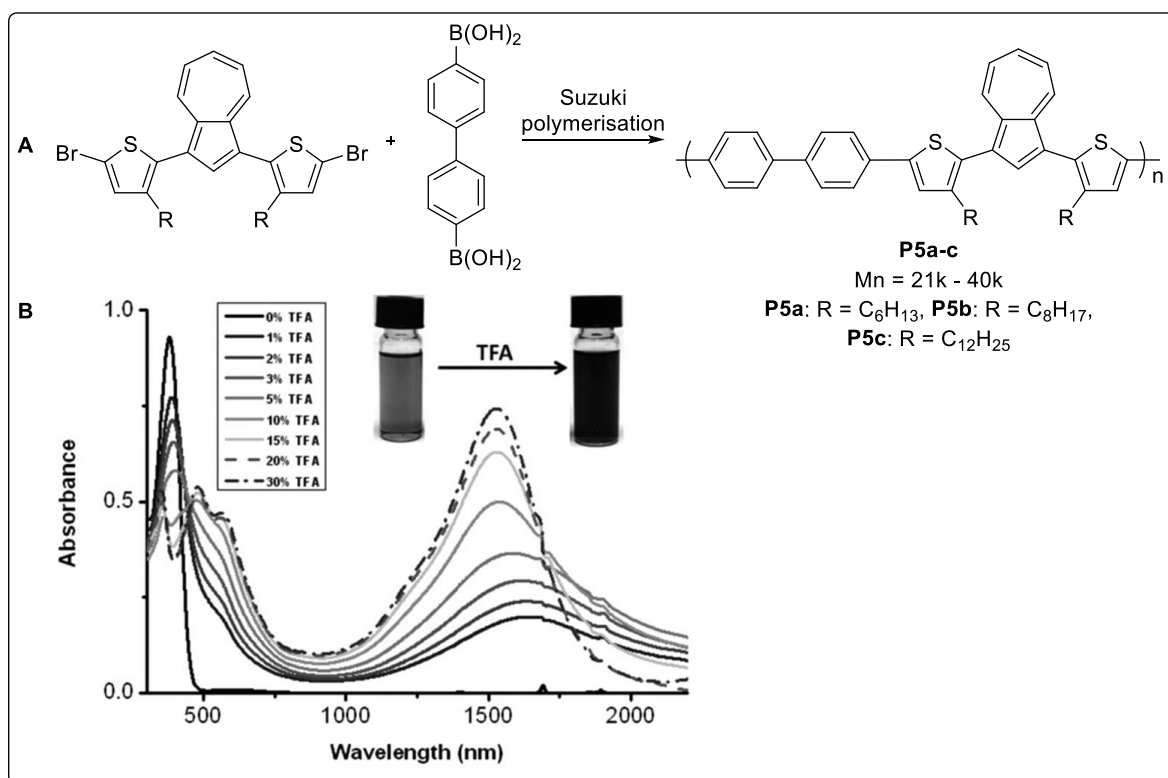


Figure 77: (a) Preparation of azulene – thiophene – biphenyl polymers for NIR applications. (b) UV-vis-NIR spectra change of **P5c** with increasing TFA concentration. Adapted (b) from reference 125 with permission from Wiley Copyright (2013).

An extension of the work on IR active azulene polymers was reported in 2014 by He's group (figure 78a).²⁰¹ While the previous report gave major absorption up to 1500 nm, molecular engineering of the polymer enabled the absorption to extend to the 2500 nm range. The UV-vis spectrum of the polymer solution all showed redshifts of between 20 nm to 150 nm compared to the previously reported **P5c** (figure 78b). When protonated, all the polymers showed strong absorption in the IR region, covering nearly the full NIR spectrum from 1000 nm to 2500 nm (figure 78c).

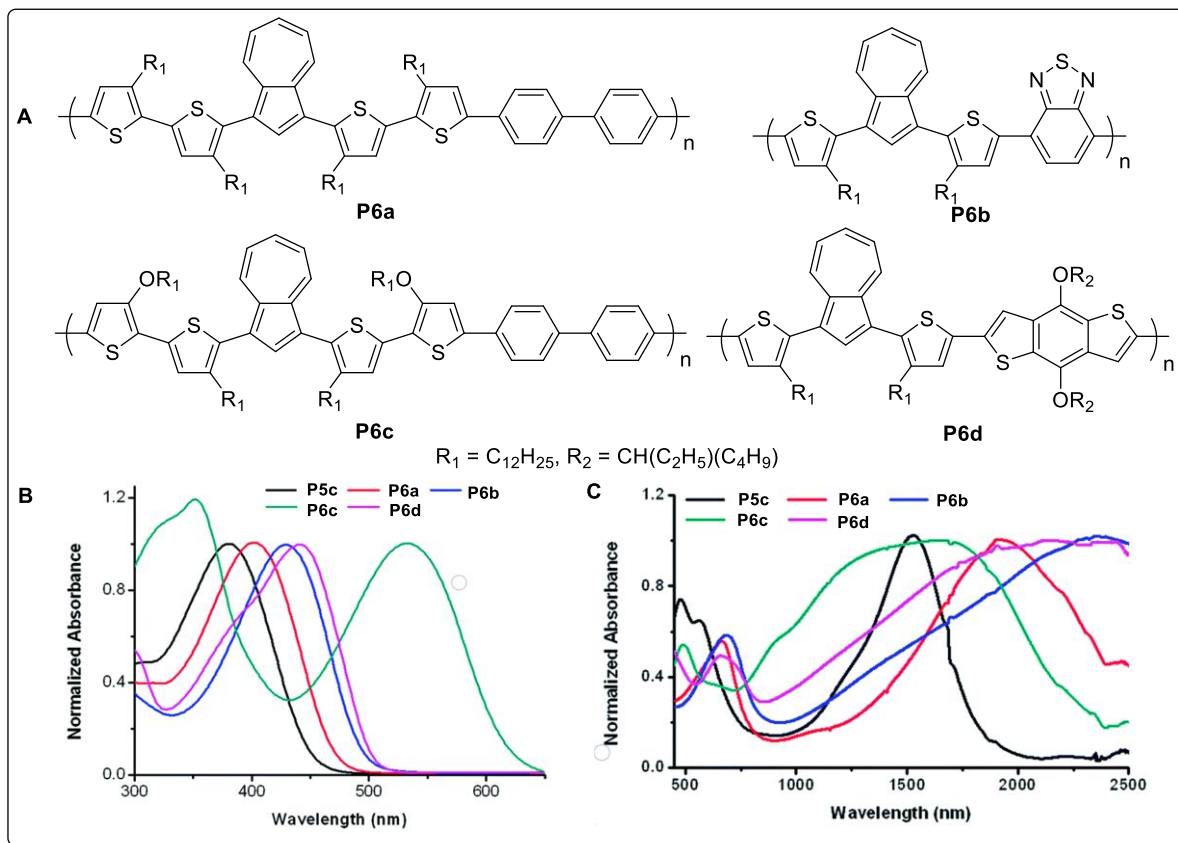


Figure 78: (a) Azulene based NIR polymers. (b) UV-vis spectrum of polymers **5c** – **6d** in chloroform. (c) UV-vis-IR spectrum of polymers **5c** – **6d** with 30% TFA – chloroform solution. Adapted (b) and (c) from reference 201 with permission from The Royal Society of Chemistry Copyright (2014).

In 2015, Imahori's group reported a series of azulene – thiophene – diketopyrrolo[3,4-c]pyrrole-1,4-dione (DPP) and azulene – thiophene – 2,1,3-benzothiadiazole (BTD) polymers (figure 79). The electron rich five membered ring of azulene was treated as a donor unit, while the DPP and BTD units functioned as the acceptor units. However, **P7b** was found to be poorly soluble in any common organic solvent. As such, additional hexyl groups were added to the thiophene units at different positions. These polymers were then incorporated into photovoltaic (PV) devices and tested for their efficacy. However, none of these polymers had particularly striking photovoltaic properties, with a maximum power conversion efficiency (PCE) of 0.39% for **P7b**. This was attributed to the fast nonradiative vibrational relaxation of the polymer's excited state to the ground state (fluorescence lifetime of 2.09 ns to 8.85 ns).

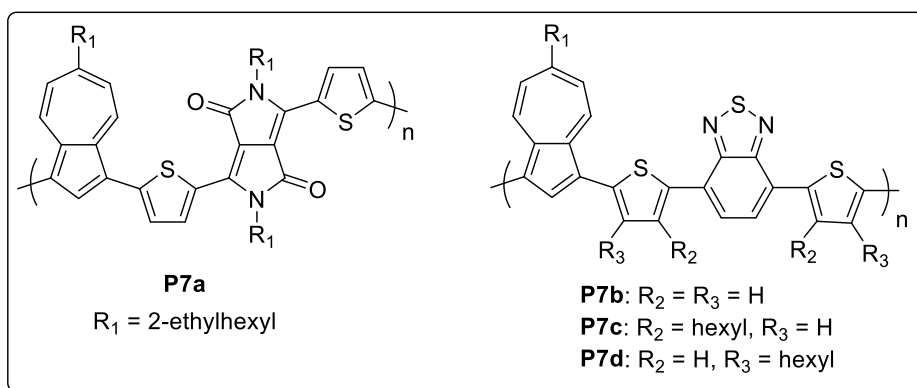


Figure 79: Azulene – DPP and azulene - BTD polymers prepared for solar cell applications

3.1.2 Polyazulenes Connected on the Seven-Membered Ring

Polyazulene connected at the seven membered ring is comparatively less common, becoming more common only after Hawker's group popularised Houk's method of preparing azulene via [6+4] cyclisation.¹⁶³ This method enabled relatively simple preparation of 5, 7-dibromoazulene from 2, 5-dibromothiophene (see figure 55), which could be useful synthetic handles for polymerisation.

In 2012, Hawker's group reported the preparation of a series of 5,7-connected polyazulenes (figure 80a).¹⁶⁴ **P8a-c** were prepared by method of Yamamoto. Both **P8a** and **P8b** has absorption spectra similar to that of the parent azulene, with absorption maxima of about 348 nm (figure 80b). In contrast, **P8c** with no alkyl group showed a red shifted absorption band at 409 nm. This was slightly red shifted compared to 1,3 polyazulene **P1** with an absorption band at 404 nm. The difference was attributed to the poorer conjugation of **P8a** and **P8b** due to steric hindrance from the 6-alkyl group, resulting in a high degree of twisting away from planarity. As a result, the optical properties of **P8a** and **P8b** are very similar to those of individual azulene units. To improve the conjugation, linkers were incorporated into the polymer, with **P8d** having an acetylene spacer and **P8e** having a thiophene spacer. The polymers were then subjected to treatment with TFA. As previously reported for **P1**, immediate colour changes were observed (figure 80c). More remarkably, **P8d** and **P8e** were found to undergo reversible acid base cycling with no significant variation over different cycles. On the other hand, neutralisation of acidic **P1** did not recover the original spectrum. This difference was attributed to the more effective stabilisation of the formed tropylium cationic species formed due to direct linkage to the seven-membered ring. As a result, oxidative degradation would be slower than for 1,3 polyazulene **P1**.

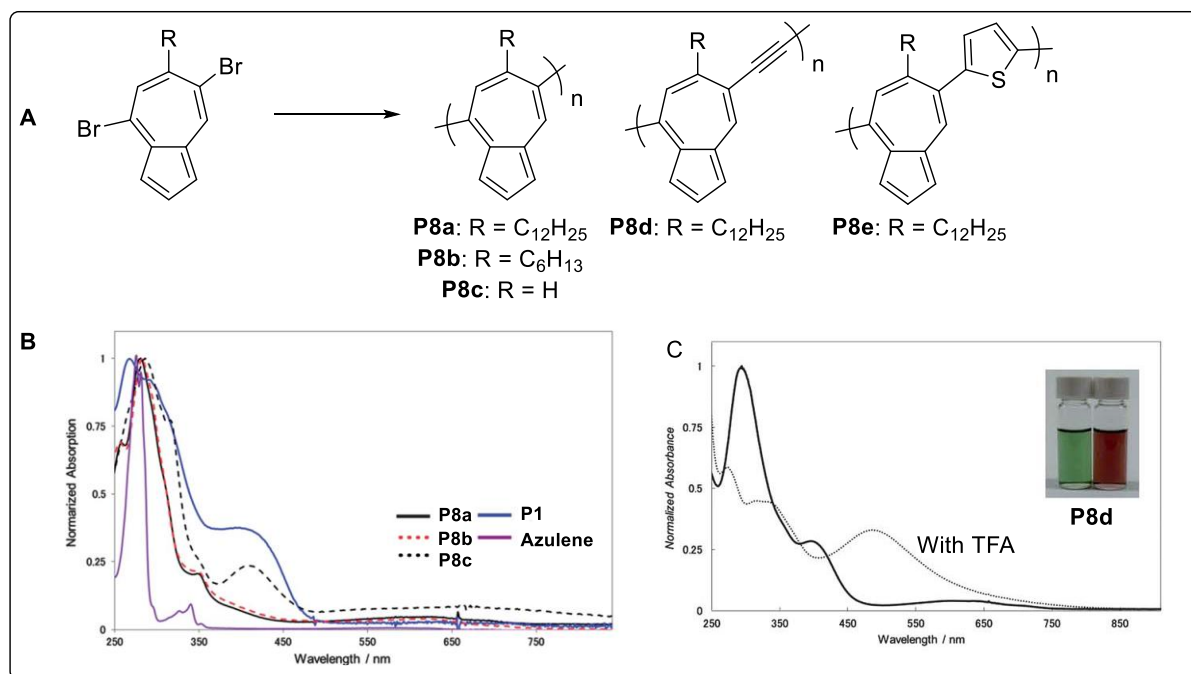


Figure 80: (a) 5,7-connected polyazulenes prepared by method of Yamamoto, Sonogashira, and Stille. (b) UV-vis spectrum of **P8a** – **P8c** compared with **P1** and azulene. (c) UV vis of **P8d** before and after addition of 20% TFA. Adapted (b) and (c) from reference 165 with permission from The Royal Society of Chemistry Copyright (2012).

In 2014, Hawker's group reported two other series of azulene random polymers.¹²¹ Different ratios of azulene units connected via the 5-membered ring or 7-membered

ring were co-polymerised with bithiophene or fluorene monomers (figure 81a). The optical properties were then studied by UV-Vis spectroscopy. For both series of polymers, a gradual transition from a single absorption peak for **P9a** and **P10a**, with entirely 1, 3-connected azulene units, to two distinct absorption peak for **P9e** and **P10e** was observed (figure 81b). The S0 – S1 transition at 650 nm is also stronger for **P9e** and **P10e**. The optical response to TFA was also measured. For the fluorene containing series of polymers, **P9e** had a much sharper response to TFA as compared to the rest of the series, with a strong peak at 520 nm (figure 81c). In thin film state, the protonation for **P9e** was also shown to be reversible, with the original green colour recoverable upon exposure to a flow of argon. A similar but less pronounced result was observed for the bi-thiophene series, although in this case, both **P10d** and **P10e** had similar absorptivity in the 600 nm region upon addition of TFA (figure 81d). This work illustrates how the properties of azulene polymers can be modulated simply by changing the connectivity of azulene.

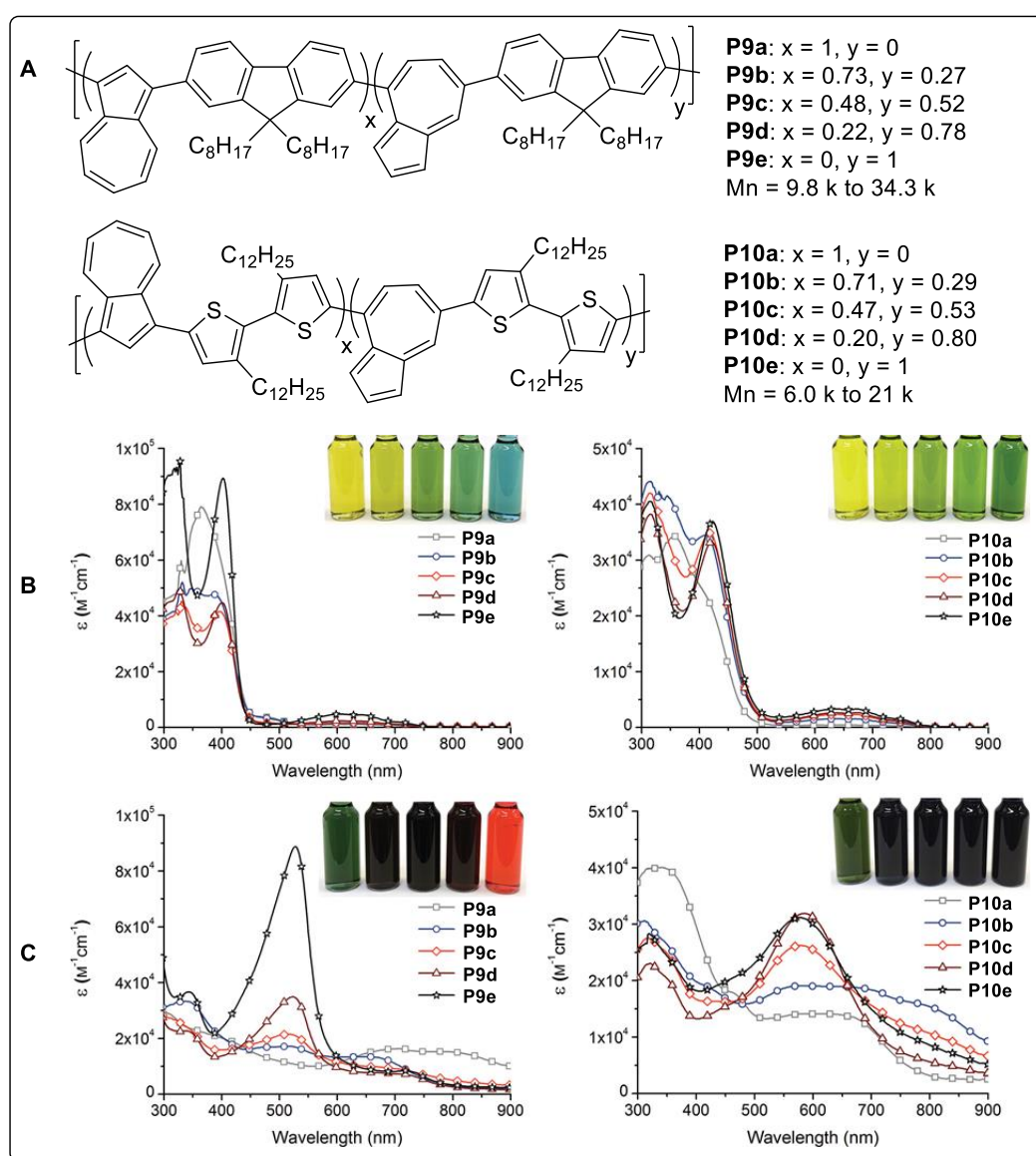


Figure 81: (a) Preparation of random azulene – thiophene and azulene – fluorene copolymers with different ratios of regioisomeric azulene units. (b) UV-Vis spectrum of **P9a-e** and **P10a-e**. (c) UV-Vis of TFA protonated **P9a-e** and **P10a-e**. Adapted (b) and (c) from reference 122 with permission from Wiley Copyright (2014).

In the 2015, Zhang's group reported the characterisation of a series of three azulene - DPP co-polymers (figure 82a).¹²⁷ Azulene was incorporated into the polymer due to its small HOMO - LUMO gap. While **P11a** and **P11b** uses azulene connected at the 1, 3-position, **P11c** contains azulene connected at the 5, 7-position. When tested for their field effect transistor (FET) properties, **P11a** and **P11b** exhibit p-type semiconducting behaviour, with hole mobilities of up to $0.97 \text{ cm}^2\text{V}^{-1}\text{s}^{-1}$ while **P11c** with the 5, 7-connectivity on azulene shows ambipolar character, with hole and electron mobilities of up to 0.062 and $0.021 \text{ cm}^2\text{V}^{-1}\text{s}^{-1}$ respectively. These polymers were also blended with PC₇₁BM (a fullerene electron acceptor) and incorporated into photovoltaic devices to function as electron donors. However, the overall photovoltaic performance was low, with a maximum PCE of 2.04% achieved by a blend of **P11a** with PC₇₁BM in a ratio of 1:1.5, while the **P11b** and **P11c** only achieved a maximum of 0.26% and 0.40% respectively. The poor performance of the film was attributed to their rough surface morphologies, as large domains of over 200 nm were observed after blending the polymer with PC₇₁BM.

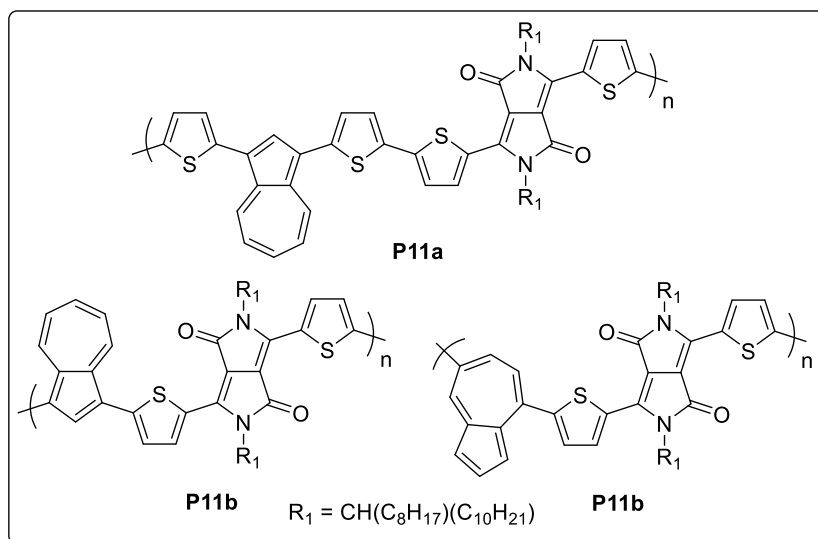


Figure 82: Azulene – DPP polymers prepared for solar cell applications.

In 2018, Gao's group reported the first 2,6-connected azulene polymer (figure 83a, b).²⁰² The key intermediate was compound **41f**, prepared by method of Nozoe as described earlier (see figure 53). Coupling of the bromine with thiophene provided the 6-connectivity, while transformation of the 2-amino group to a chloride enabled Yamamoto coupling, providing the 2-connectivity (**53b**). Subsequent cyclisation and bromination gave the monomer **53c** which was coupled with *N*-dodecylthieno[3,4-*c*]pyrrole-4,6-dione (TPD) and 1,2,4,5-tetrafluorobenzene (TFB) to form polymers **P12a** and **P12b** respectively. Density functional theory calculations indicate that the electron density distribution of the HOMO and LUMO are well delocalised over both monomer units, which would be beneficial for charge transport. This is corroborated by a strong absorption at the 650 nm region in the UV spectra, which is assigned to intramolecular charge transport. The polymers were also tested for transistor and photovoltaic properties. Both polymers exhibited n-type charge transport properties, with electron mobility of $0.42 \text{ cm}^2\text{V}^{-2}\text{s}^{-1}$ for **P12a** and $0.24 \text{ cm}^2\text{V}^{-2}\text{s}^{-1}$ for **P12b**. **P12a** was blended with PTB7 and fabricated into a photovoltaic device. The power conversion efficiency was found to be 1.82%. The somewhat low efficiency was attributed to the poor film morphology as seen through AFM imaging.

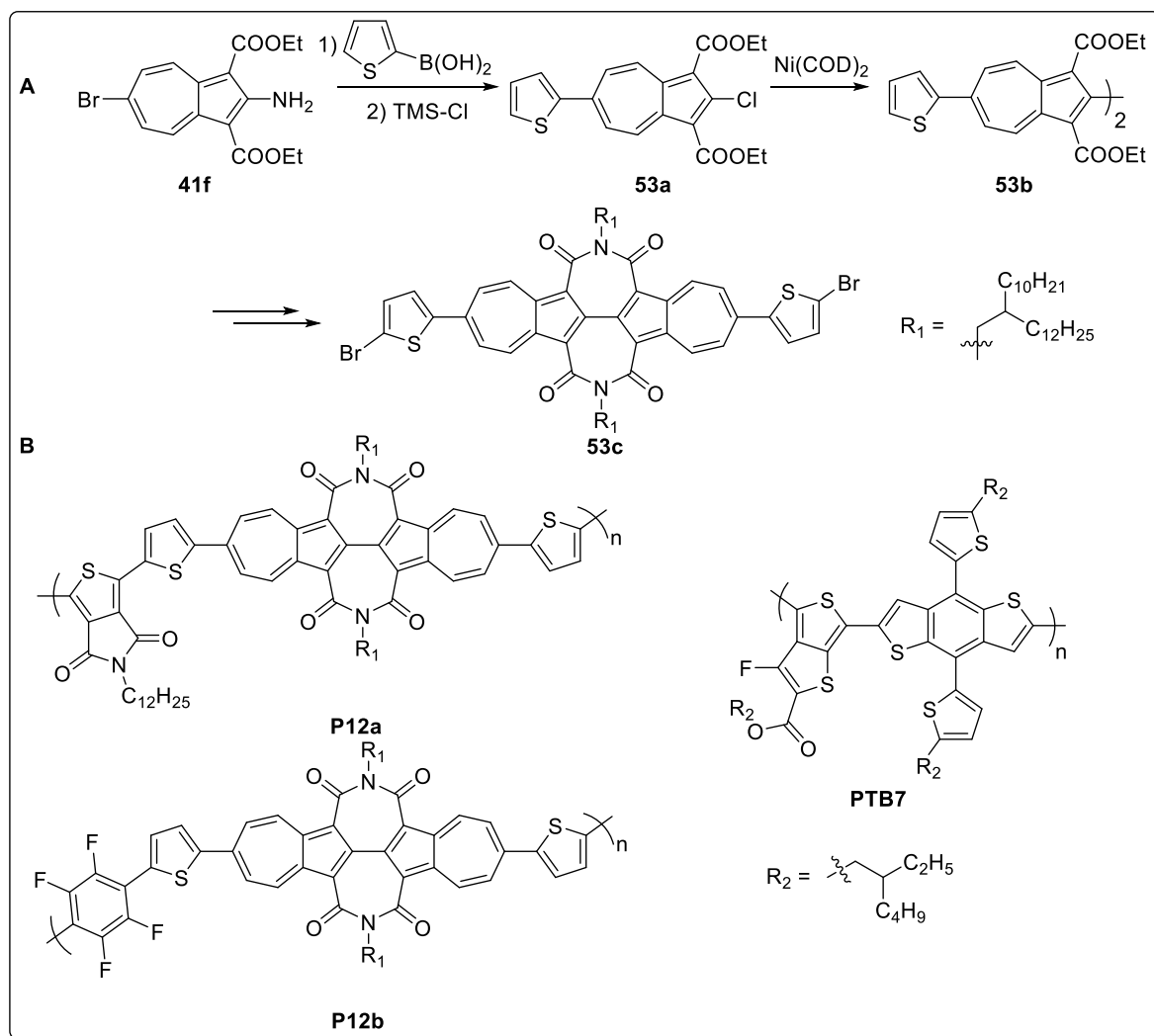


Figure 83: (a) Preparation of 2,6-connected azulene based monomers. (b) 2,6-connected azulene polymers evaluated for transistor and photovoltaics applications.

A second series of 2,6-connected azulene polymers was reported by Gao's group in 2019. **P13a** and **P13b**, with fluorene connected at the 2,6-position and the 1,3-position vacant, were prepared (figure 84a).²⁰³ Previously reported **P3b**, with fluorene connected at the 1,3-position, was also prepared as reference. The UV spectra for both **P13a** and **P13b** shows a band at 400 – 550 nm which was attributed to intramolecular charge transfer. As compared to **P13b**, both **P13a** and **P13b** were also much more sensitive to TFA, with drastic changes to the spectrum with just 2% of TFA added to the solution, and a new band appearing at 630 nm (figure 84b). This band was attributed to the formation of the azulenum cation. Neutralisation of the acid with triethylamine also resulted in recovery of the original absorption spectrum. The electrical conductivity of the thin films were also tested. Neutral films of both **P13a** and **P13b** had conductivity of about 10^{-4} S/cm, while protonation of the film by exposure with triflic acid vapor led to conductivity of 2.94 and 0.32 S/cm for **P13a** and **P13b** respectively. In contrast, **P3b** only had conductivity in the range of 10^{-3} S/cm even when protonated.

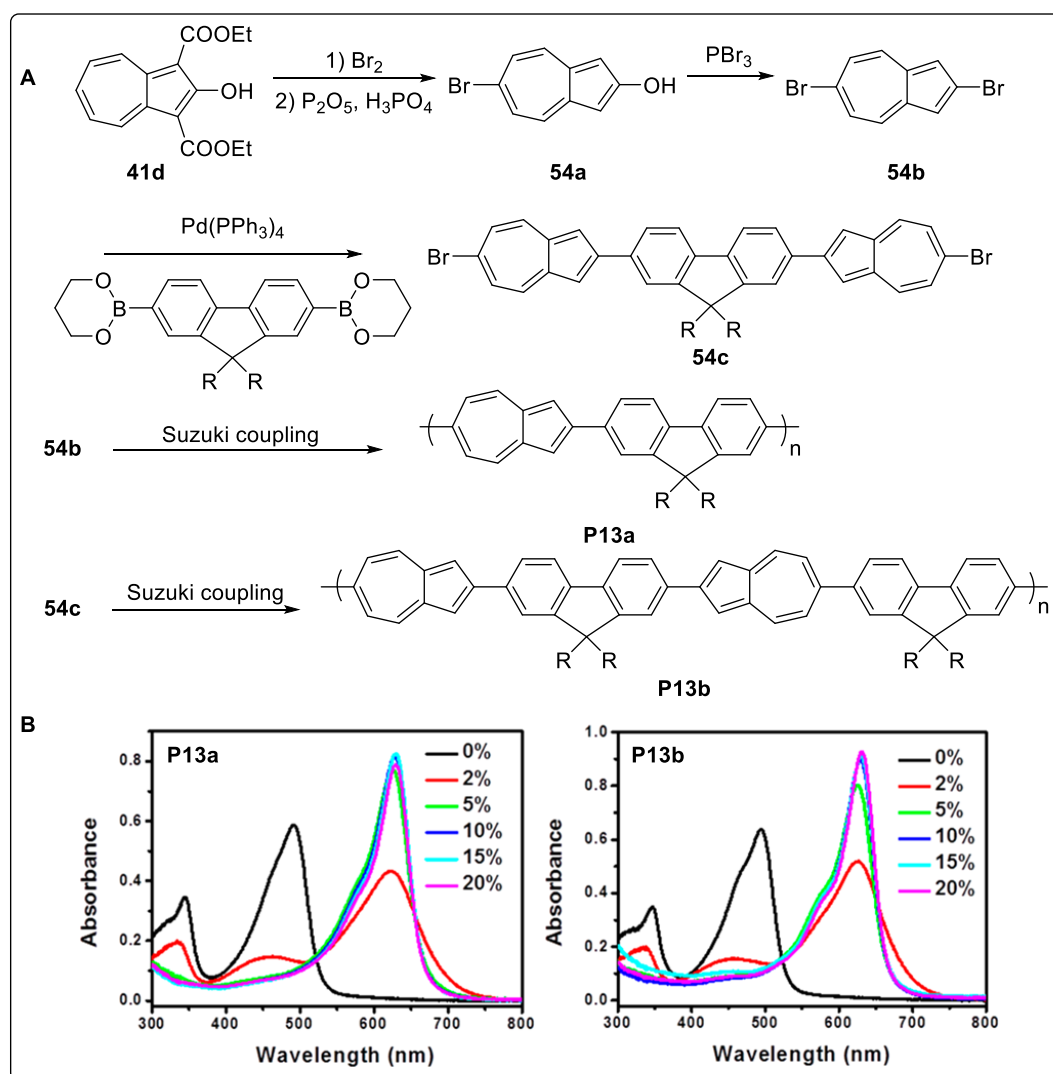


Figure 84: (a) Preparation of 2,6-connected azulene-fluorene polymers. (b) Change in UV spectrum of **P13a** and **P13b** in response to TFA in solution state. Adapted (b) from reference 203 with permission from American Chemical Society Copyright (2019).

3.1.3 Miscellaneous Polymeric Azulene Structure

Apart from direct incorporation into the backbone of the linear polymer, there has also been some isolated reports of azulene being appended to the polymer backbone and azulene as part of a network polymer.

The first attempt to incorporate azulene into a acrylate type polymer was by Okawara's group in 1978 (figure 85a).²⁰⁴ However, subjecting monomer **55a** to AIBN did not result in any polymerisation. Attempting to copolymerise **55a** with 15 equivalent of styrene only resulted in about 5% incorporation of azulene into the polymer. This was attributed to azulene inhibiting the chain radical process. In 2014, Emrick's group revisited this and prepared monomers **55b** and **55c** to incorporate into methylacrylate polymers (figure 85b).²⁰⁵ Subjecting these monomers to free radical polymerisation using AIBN initiation gave homopolymers **14a** and **14f** respectively (figure 85c). Copolymerisation with different feed ratios of methyl methacrylate or sulfobetaine methacrylate also gave the corresponding polymers (**14b-e**, **14g-k**). Polymer **14l** without azulene was also prepared as a control. Zwitterionic polymers are often attractive work function modifiers due to their orthogonal solubility and absence of external counterions. As such, **P14d-e**, **i-l** were incorporated into photovoltaic devices as cathode modification layers. The active layer was PTB7:PC₇₁BM, while the cathode was silver. In general, increasing azulene content was beneficial for the PCE; the control **P14l** gave a PCE of 3.7% while **P14k** with a 75 mol% of azulene gave the highest PCE of 7.6%. Both **P14d** and **P14e** were also effective interlayers, giving PCE of 6.0% and 7.1% respectively.

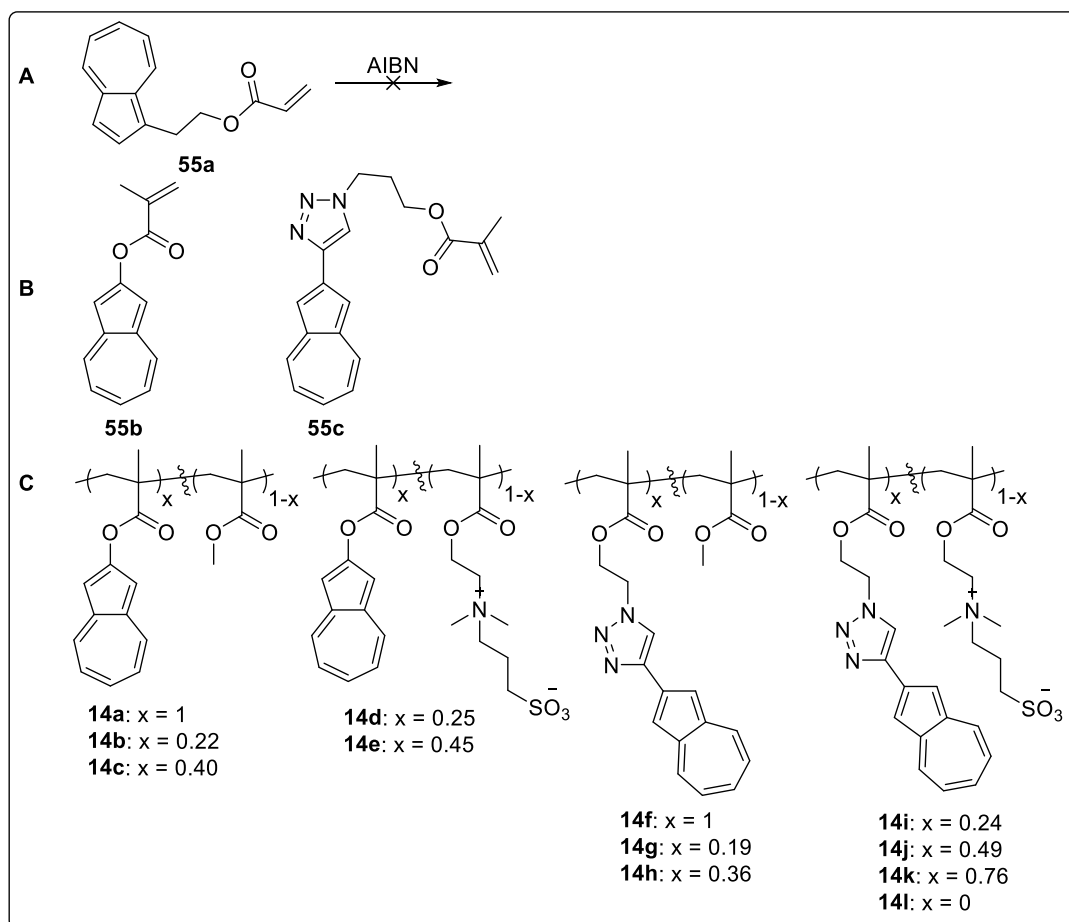


Figure 85: (a) First unsuccessful attempt at incorporating azulene into an acrylate type polymer by Okawara's group. (b) Monomers for azulene methacrylate polymers by Emrick's group. (c) Azulene methacrylate polymers prepared and tested as cathode modification materials.

Azulene has also been incorporated into microporous networks. Zhang's group reported the preparation of **P15a** and **P15b** by Sonagashira coupling (figure 86a).¹²⁹ Upon protonation by TFA, these polymers became hydrophilic and were dispersible in water. The pore diameters were about 1.5 nm in size. Upon protonation, the conduction band and valence band of **P15a** was found to be -0.84 V and 1.22 V (vs standard calomel electrode) respectively, implying a band gap of 2.06 eV. This was sufficient for the reduction of Cr(VI) to Cr(III), which requires a potential of 1.57 V. While protonated **P15a** was able to directly reduce Cr(VI) to Cr(III) photocatalytically within 60 mins, addition of formic acid, Fe(III), or Cu(II), increased the efficiency of the reduction (figure 86b). The polymer was also reusable, and reduction of Cr(VI) occurred almost quantitatively over five repeating cycles.

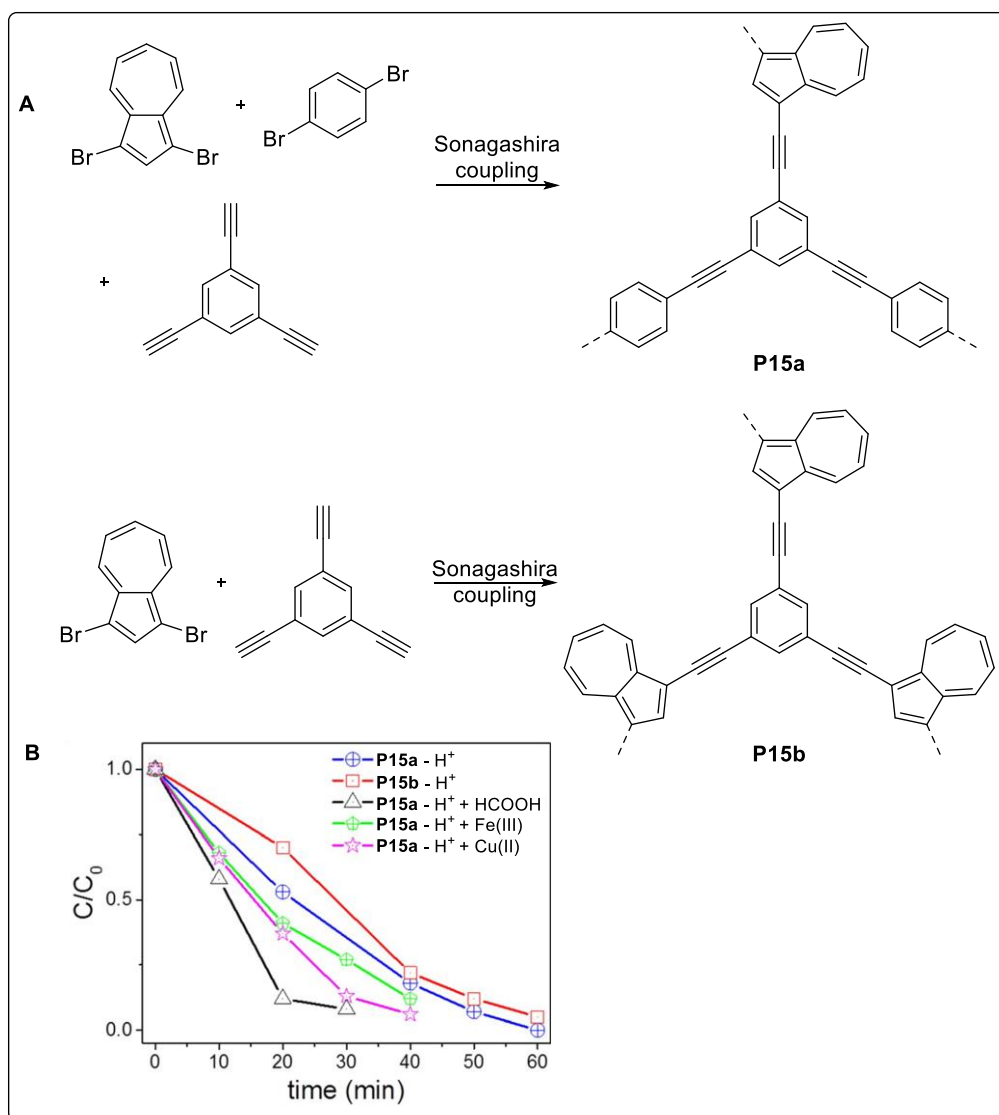


Figure 86: (a) Preparation of network azulene polymers by Sonagashira coupling. (b) Rate of photocatalytic reduction of Cr(IV) to Cr(III) by the polymers with and without additives. Adapted (b) from reference 130 with permission from Wiley Copyright (2016).

In 2010, Berke's group reported metal organic frameworks (MOF) comprising 1,3-azulenedicarboxylate and zinc (figure 87).²⁰⁶ **MOF1** was found to have void space of 41%. These were then evaluated for hydrogen storage applications. Considerable hydrogen uptake of 17.5 mgg⁻¹ at 77 K and 1 bar was observed for **MOF2**. Strong **MOF2** – H₂ interaction values of about 7.1 kJmol⁻¹ was also observed, which is one of the highest values for physisorption compounds.

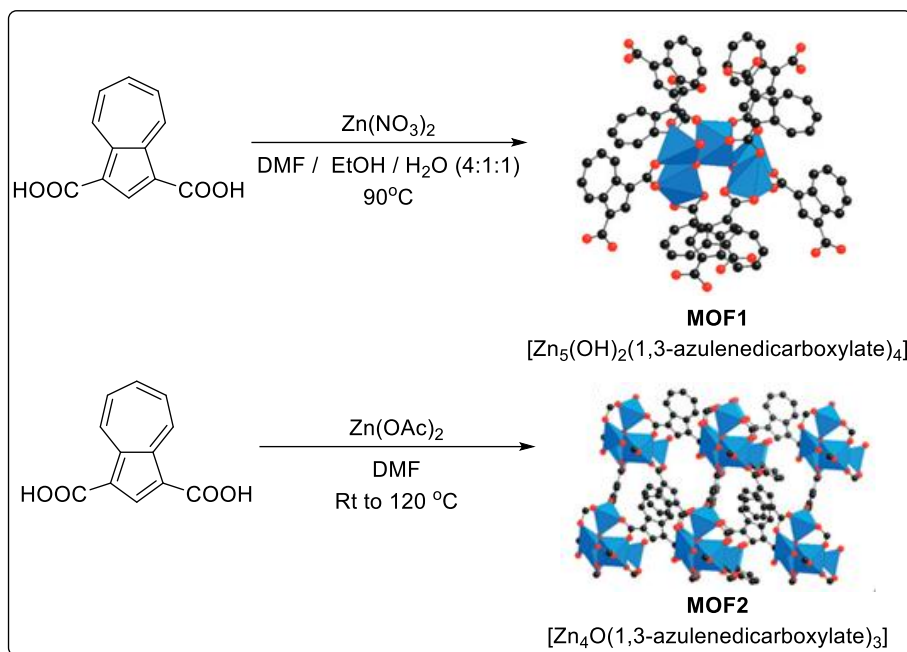


Figure 87: MOF comprising 1,3-azulenedicarboxylate and zinc.

3.2 2-Functionalised Azulene in Polymeric Materials.

Figure 90a summaries the range of azulene polymers and co-polymers which have been previously reported, including those with 1,3-connectivity, 4,7-connectivity, and even 2,6-connectivity. However, most of these have been with unfunctionalised azulene. Some exceptions include polymer series **P7** and **P8** with alkyl groups at the 6-position to improve polymer solubility, and polymer series **P12** with the diimide functionality. The effect of azulene functionalisation on the properties of polymeric material has been largely unexplored. Yet, in small molecular material, the effect of functionalisation on azulene properties are well documented. Introducing electron withdrawing and electron donating substituents on azulene results in drastic changes in the colour of resultant molecule, with colours including red, purple, green, and blue possible.¹²⁰ Likewise, the emission spectrum of azulene has also been tuned from 443 nm to 750 nm by varying the substituent on the 2-position.²⁰⁷ We have recently developed a methodology to conveniently arylate azulene on the 2-position. As such, we were interested to apply this methodology to incorporate these 2-arylated azulene into polymers, and to explore the effect of functionalisation on the properties of the material (figure 90b).

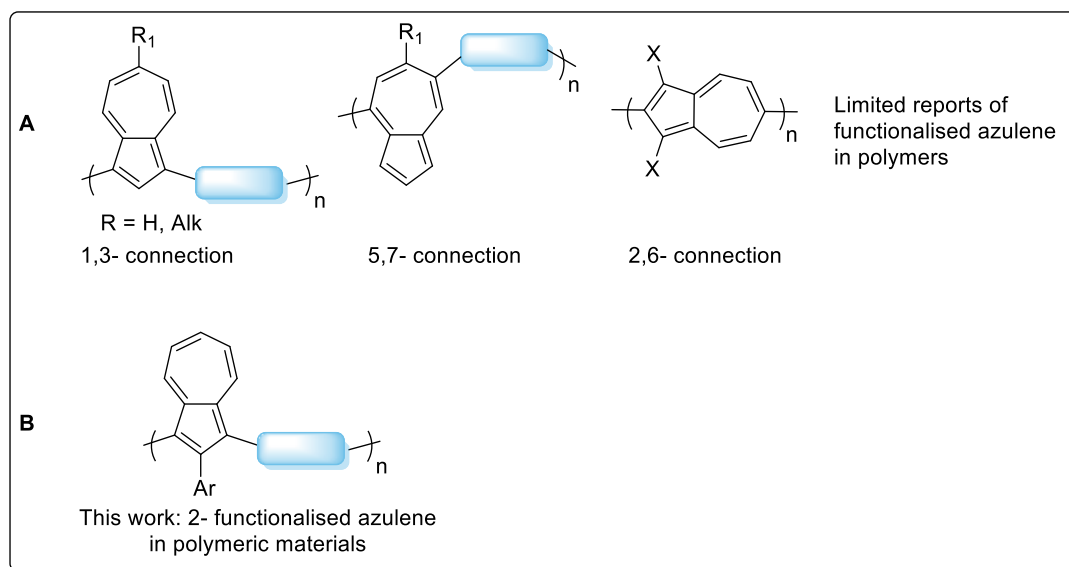


Figure 90: (a) Existing azulene polymers in literature, including 1,3-connectivity, 5,7-connectivity, and 2,6-connectivity. (b) Exploring the effect of 2-functionalisation of azulene on material properties.

As an initial starting point, we chose to co-polymerise these functionalised azulene with fluorene. Properties of the variations of the unfunctionalized azulene-fluorene copolymer have been reported by Xu's group (1,3-connectivity),¹²⁵ Hawker's group (5,7-connectivity),¹²¹ and most recently, by Gao's group (2,6-connectivity).²⁰³ However, no functionalised variant has been reported to our knowledge.

3.3 RESULTS AND DISCUSSION

Applying the methodology developed in the previous chapter, we prepared four 2-functionalised azulenes with different electronics (figure 91, **56b-e**). The reactions proceeded smoothly on 5 mmol scale with yields between 50 to 75%. These functionalised azulene were then brominated with NBS, which were all completed within 2 hours for all the substrates.

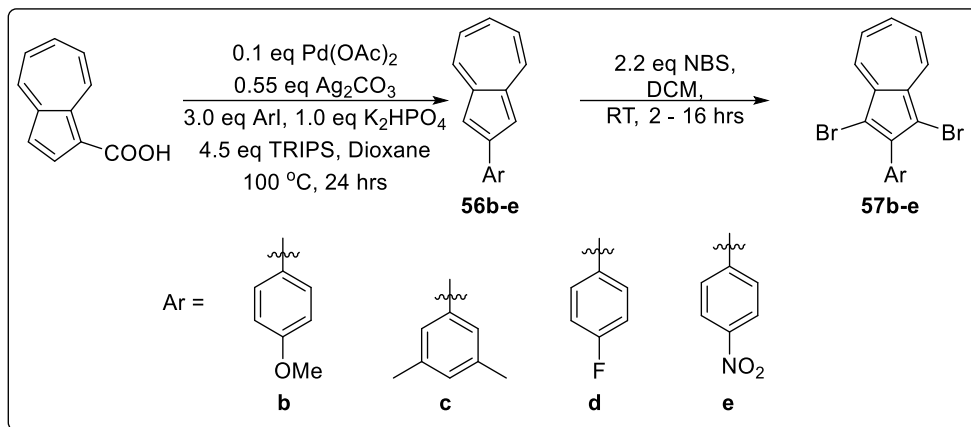
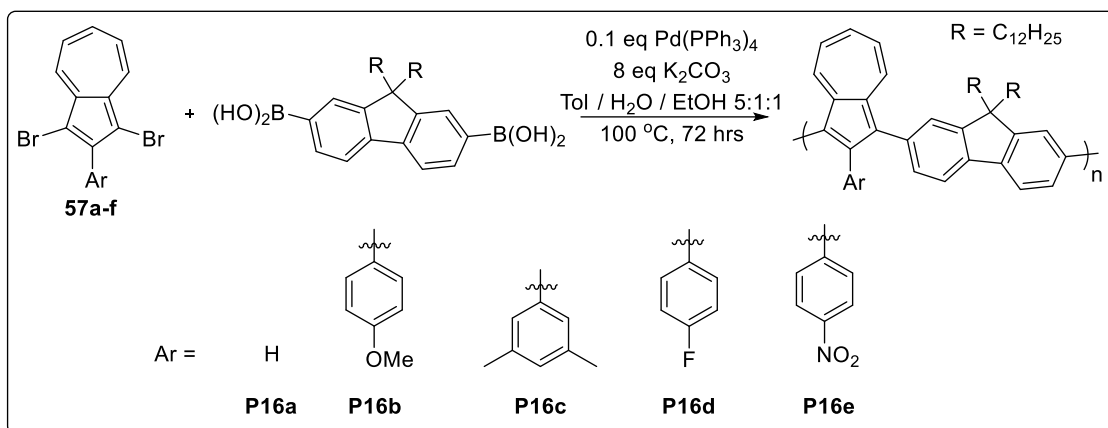


Figure 91: Preparation of monomers by C-H arylation, followed by NBS bromination.

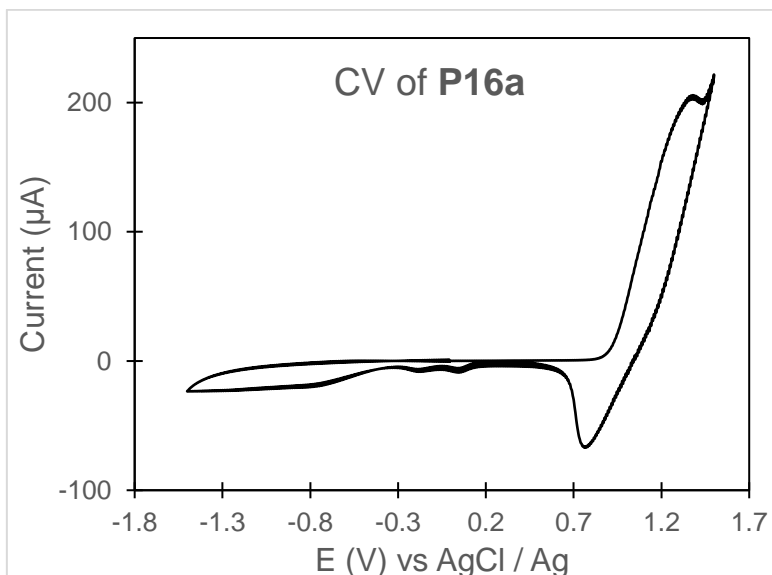
The dibrominated azulenes were then subjected to Suzuki coupling with (9,9-didodecyl-9H-fluorene-2,7-diyl)diboronic acid to obtain the corresponding polymers (Figure 92, **P16a-e**). **P16a**, the unfunctionalized azulene polymer was also prepared to act as a standard. The polymers were purified by precipitation in methanol, followed by Soxhlet extraction using hexane, acetone, and finally chloroform. GPC analysis of the polymers showed that the polymers have molecular weights ranging from 8.2 kDa to 15.1 kDa, while the polydispersity index (PDI) ranged from 1.4 to 2.3. The polymers were also characterised by thermogravimetric analysis (TGA) and found to be stable up to about 400 °C in N₂.



| Polymer | Yield / % | Mn / kDa | Mw / kDa | PDI | T _d / °C |
|-------------|-----------|----------|----------|-----|---------------------|
| P16a | 30 | 15.1 | 30.6 | 2.0 | 405 |
| P16b | 65 | 10.3 | 23.4 | 2.3 | 437 |
| P16c | 52 | 11.2 | 15.6 | 1.4 | 423 |
| P16d | 67 | 8.2 | 12.1 | 1.5 | 437 |
| P16e | 51 | 12.9 | 21.0 | 1.6 | 442 |

Figure 92: Suzuki polymerisation of dibromo monomers to obtain 2-arylated azulene polymers. These polymers were characterised by GPC (polystyrene standard) and TGA. TGA was carried out at a ramp rate of 20 °C / min under an N₂ atmosphere up to 800 °C. Decomposition temperature (T_d) is the temperature at which 5% weight loss occurs

The HOMO and LUMO of the polymers were estimated from the onset of oxidation and reduction (figure 93). A representative sample is shown below (see experimental for remaining CV spectra). The spectra showed irreversible oxidation and reduction of the polymers. The HOMO ranged from -5.3 eV to - 5.5 eV, while the LUMO ranged from -4.05 eV to - 3.95 eV. The optical band gap (E_g) was also estimated from the UV spectrum of the polymers (shown in figure 94), and matched the value of the HOMO – LUMO gap (estimated from CV) fairly well.

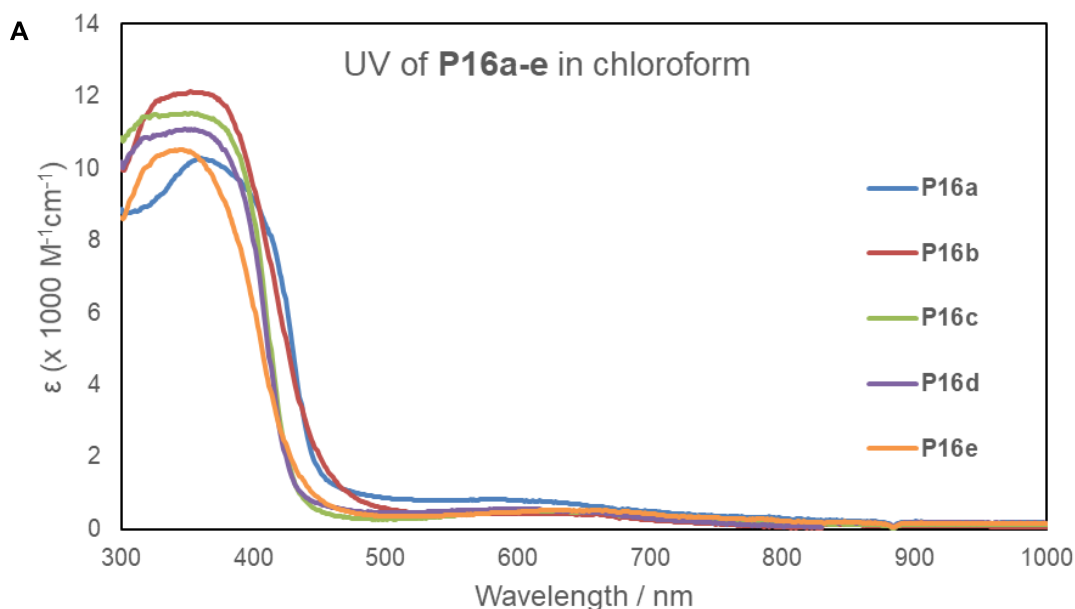


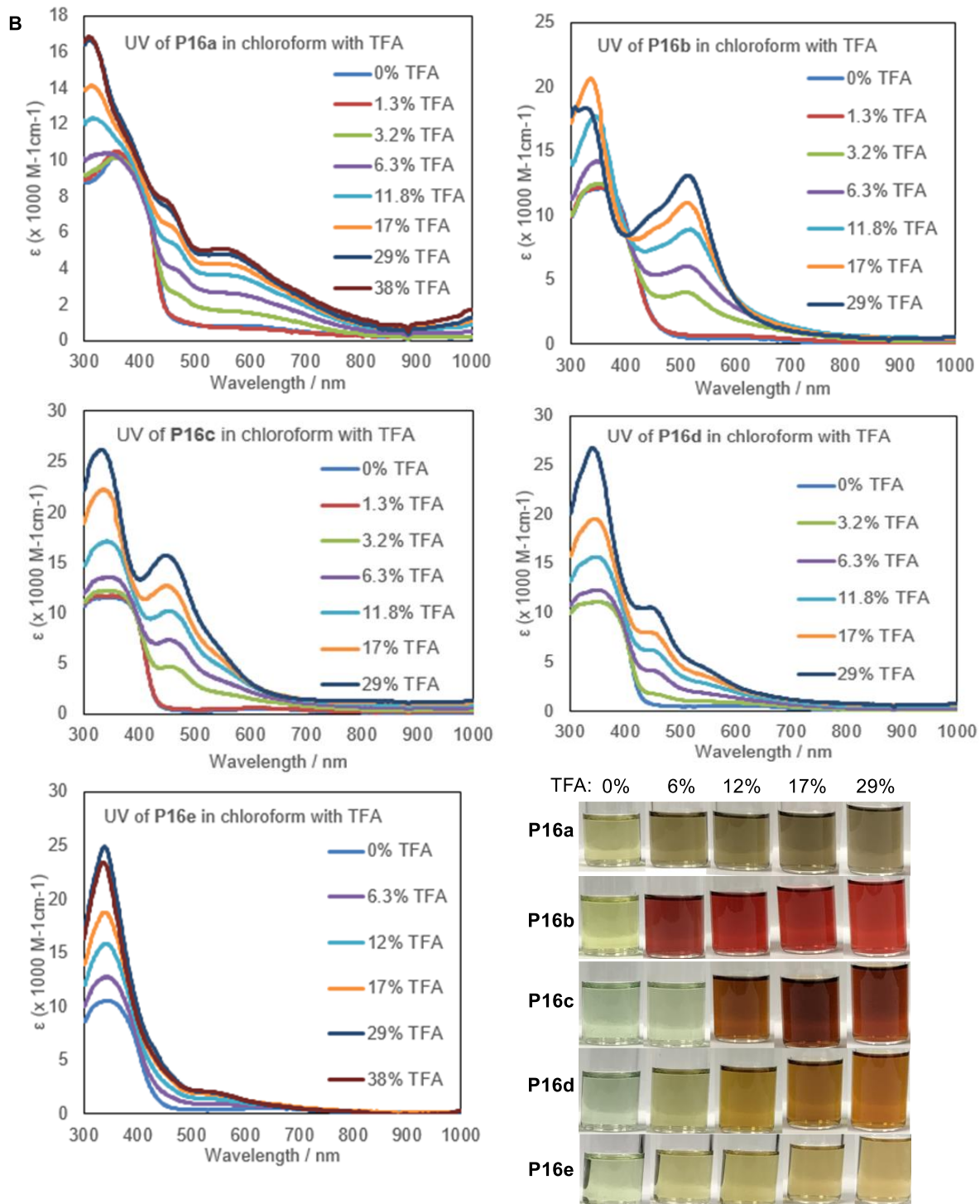
| Polymer | Abs λ_{onset} (nm) | E_g (eV) | HOMO (eV) | LUMO (eV) | LUMO – HOMO (eV) |
|-------------|-----------------------------------|------------|-----------|-----------|------------------|
| P16a | 769 | 1.61 | -5.30 | -3.69 | 1.61 |
| P16b | 825 | 1.50 | -5.30 | -3.73 | 1.57 |
| P16c | 785 | 1.57 | -5.50 | -3.85 | 1.65 |
| P16d | 800 | 1.55 | -5.50 | -3.95 | 1.55 |
| P16e | 820 | 1.51 | -5.55 | -3.90 | 1.65 |

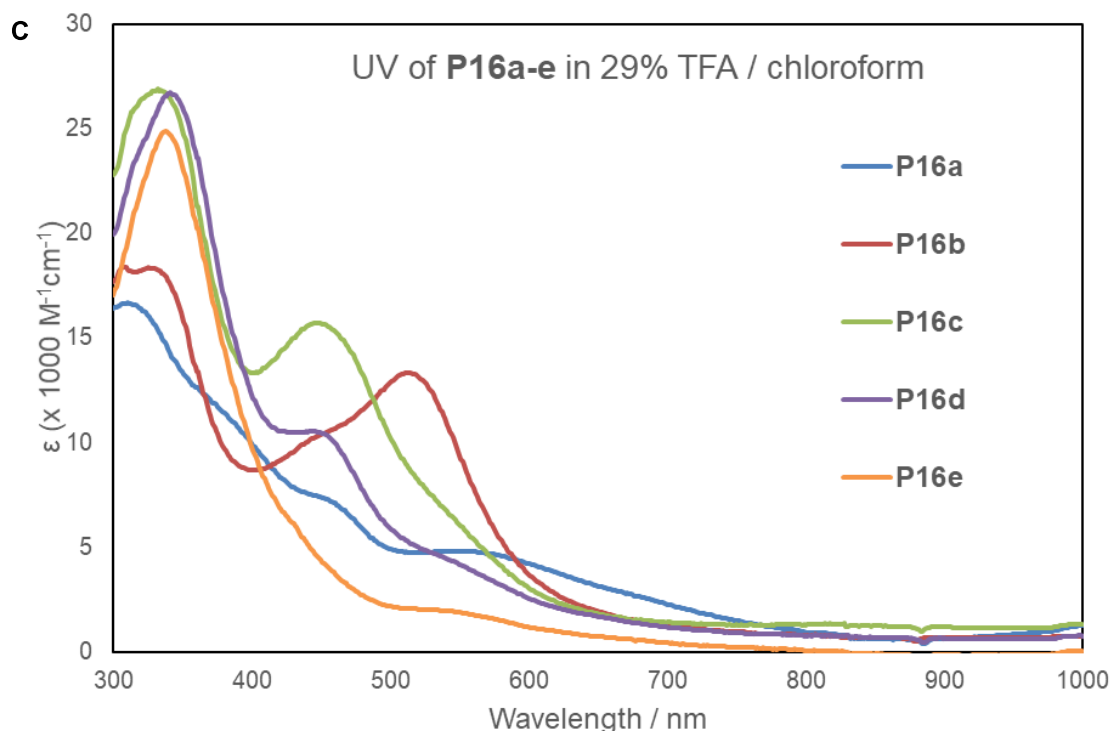
Figure 93: CV of **P16a** on ITO-coated glass substrate in 0.1M LiClO₄ / acetonitrile at a scan rate of 100 mV/s. Summary of HOMO and LUMO values for the polymers estimated by onset of oxidation and reduction. The spectrum was calibrated by ferrocene, then the HOMO and LUMO calculated by the formula $E_{\text{HOMO/LUMO}} = -(4.80 + E_{\text{onset}}^{\text{ox}} / E_{\text{onset}}^{\text{red}})$ eV. Optical band gap was calculated by the equation $E_g = 1240 / \text{Abs } \lambda_{\text{onset}}$.

Figure 94a shows the UV-vis spectra of **P16a** – **P16e** in chloroform. Only small variations in the spectrums were observed with strong peaks being observed in the 350 nm region. The band at about 600 nm corresponds to the $S_0 - S_1$ band of azulene, while the strong peaks between 300 nm to 400 nm correspond to the $\pi - \pi$ absorption band of both azulene and fluorene. The polymers were then titrated with varying concentrations of TFA and the UV-vis spectra were recorded (figure 94b ,c). Colour change was observed for the polymers in varying degree. **P16a**, **c**, **d** and **e** turned from green to brown while **P16b** turned from yellow to red. The intramolecular charge transfer (ICT) transition at about 450 nm and the azulenium cation band at about 600 nm were clearly visible for **P16a**.^{121,125,203} These bands increased in intensity with increasing concentrations of TFA up to 29%, after which no further changes were observed, suggesting a saturation of protonation in the polymer. Protonation of the polymer was also not reversible, with addition of triethylamine being unable to restore the original colour of the polymer. This irreversibility has been attributed to either oxidation or decomposition of the protonated azulene in earlier works.¹²⁵

Differences in the sensitivity and colour changes of the polymer were prominent, particularly in the 400 – 600 nm region. **P16b**, with its strongly electron donating methoxy group, was the most sensitive to TFA, turning bright red with just 3 - 6% of TFA being added. A strong band at 513 nm was also observed. **P16c** with a 3,5-dimethylbenzene group was slightly less sensitive to TFA as compared to **P16b**, only exhibiting obvious colour changes after about 12% of TFA being added. The new peak formed was also blue-shifted at 447 nm compared to **P16b**. Meanwhile, **P16d** had a broad-spectral profile similar to **P16a**, with two new peaks at about 450 nm and 550 nm. **P16e**, with its strongly electron-withdrawing nitro group, saw only a small increase in absorbance in the 400 – 600 nm region, and the polymer solution only became slightly brown.







| Polymer | Chloroform | | 29% TFA in Chloroform | |
|-------------|------------------------------|------------------------------|------------------------------|------------------------------|
| | λ_{max1} (nm) | λ_{max2} (nm) | λ_{max1} (nm) | λ_{max2} (nm) |
| P16a | 359 | 583 | 310 | 554 |
| P16b | 352 | 660 | 327 | 513 |
| P16c | 353 | 659 | 331 | 447 |
| P16d | 347 | 658 | 341 | 445 |
| P16e | 344 | 647 | 336 | 535 |

Figure 94: UV-vis spectrum of **P16a-e** (a) Before addition of TFA. (b) Titration of polymer solutions with TFA. Insert shows photos of the polymer solutions at various TFA concentrations. (c) After addition of 29% TFA. Measurements were done in chloroform, at a polymer concentration of $\sim 10^{-5}$ M.

The differences in the polymer's response to TFA could be understood by considering the structure of the polymer. Protonation of azulene at the 1-position is well documented, and in the unfunctionalized polymer, the azulenium cation would help to stabilise the charge. In the case of functionalised azulene with electron donating groups, such as in **P16b**, there could be additional stabilisation of the positive charge by resonance of the 4-methoxy group (figure 95). Likewise, **P16c** with the dimethyl groups could help to stabilise the positive charge, though to a lesser degree. As such, these two polymers would be more susceptible to acids as compared to **P16a**. On the other hand, **P16d**, with the 4-fluorine functionalisation, is both inductively withdrawing and resonance donating. As such, its effect cancels out and results in similar acid response as compared to **P16a**. Meanwhile, **P16e** has a strongly electron withdrawing nitro group, which destabilises the azulenium cation. As such, the polymer has much

less response to TFA as compared to all the other polymers. These results illustrates how the polymer's properties may be tuned by functionalisation of azulene.

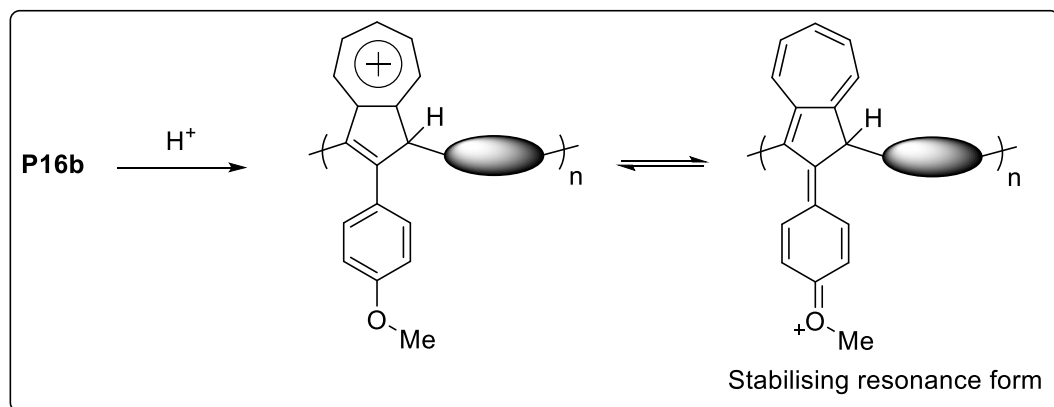


Figure 95: Increased acid sensitivity of **P16b** due to stabilising resonance of the 4-methoxy group.

Electrochromic devices with a structure of ITO / polymer / PMMA-PC-LiClO₄ / ITO were fabricated. The UV-vis spectra of these devices were then measured. They were then subjected to varying oxidative potential, and the spectra of the film were measured again. Finally, the oxidised film was subjected to reducing potential, and the spectrum was measured once again. The results are shown in figure 96. All the films showed some changes upon oxidation. However, only **P16a** and **P16b** showed a further difference upon reduction. **P16a** turned from yellowish green (neutral) to brown (oxidised) and back to yellowish green (reduced). **P16b** turned from yellow (neutral) to dark red (oxidised) to light red (reduced). Further increase or decrease in the potentials did not result in further changes in the spectrum.

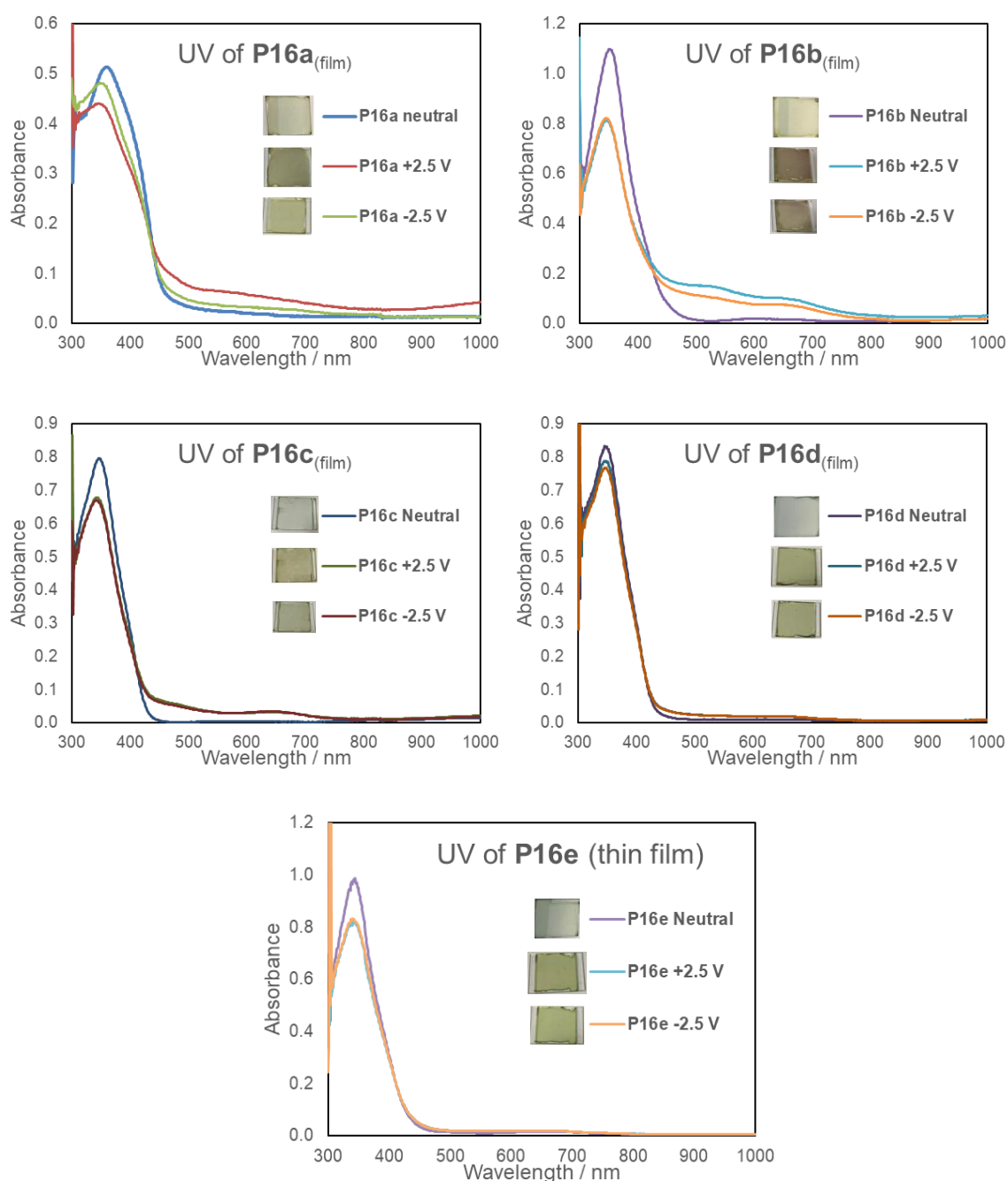


Figure 96: UV spectrum of **P16a-e** electrochromic devices when subjected to oxidising and reducing potentials.

We went on to investigate the longevity of the films upon repeated oxidising and reducing switching (figure 96). The absorbance of **P16a** was followed at 351nm while **P16b** was followed at 528 nm, corresponding to the points of greatest difference in absorption between the oxidised state and reduced states. The colour switching time (time taken for 95% of the full change in absorbance) of **P16a** was 15s for oxidation and 6s for reduction. The colour switching time for **P16b** was 42s for oxidation and 20s for reduction, which is comparatively much slower. **P16a** could switch between oxidised and reduced state for about 15 cycles before rapidly degrading. Meanwhile, **P16b** showed significantly lower stability to electrochromic switching as compared to **P16a**, rapidly degrading after about 5 cycles.

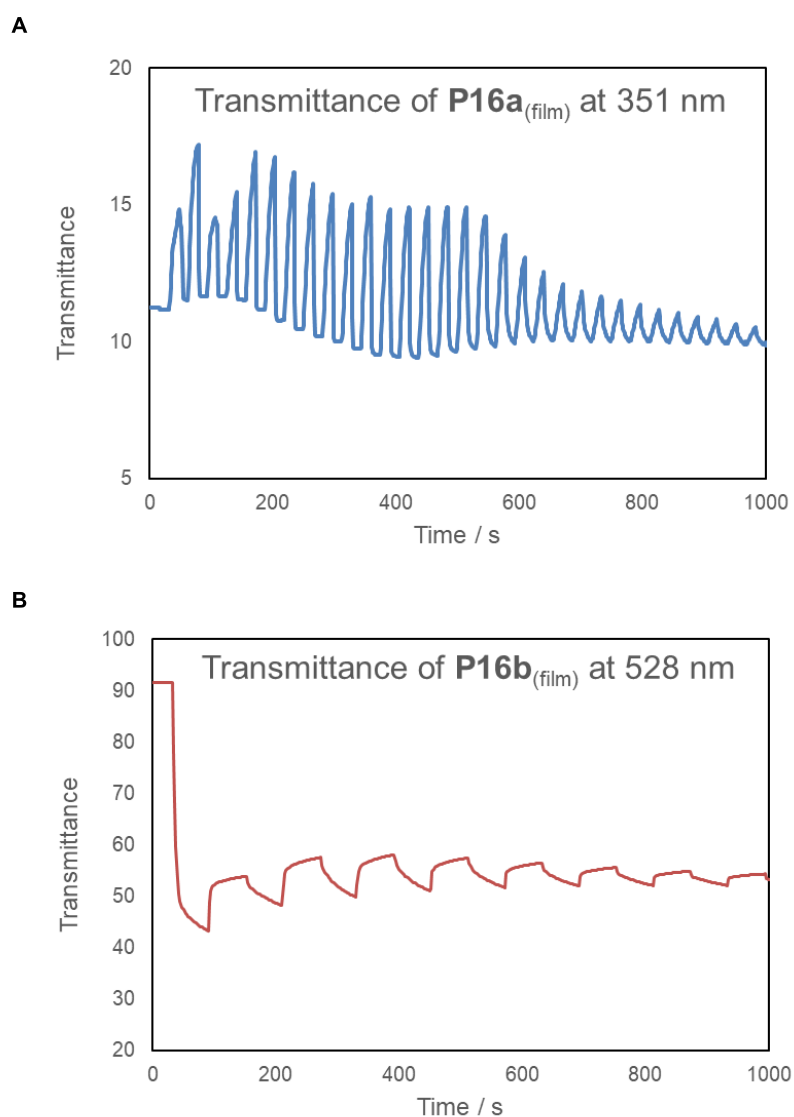


Figure 96: Transmittance – time profile of (a) **P16a** and (b) **P16b** when subjected to oxidative and reductive potentials.

The electrochromic behaviour of functionalised polymers **P16b-e** differs significantly from that **P16a**, most notably by exhibiting irreversible electrooxidation. This can be attributed to overcrowding on the 2-position. During electrooxidation, an electron is first removed from the electron rich five membered ring, forming a cationic radical (figure 97).²⁰⁸ This radical then rearranges to form a stable closed shell structure.

Notably, this structure is not favoured when the 2-position of azulene is occupied due to overcrowding, preventing the planar structure from being adopted.²⁰⁹ As a result, the cationic radical structure rapidly decomposes, and cannot be recovered by further reduction. However, **P16b**, is still able to undergo a few cycles of oxidation and reduction before no further change is observed. This could be due to the 4-methoxy group providing some stabilisation to the cationic radical, slowing down the decomposition pathways. These results suggest that while the 2-position is not suitable for improving electrochromic properties of these polymers, functionalisation at other positions of the seven membered ring may still help to stabilise the azulenium cation and improve electrochromic cycling properties.

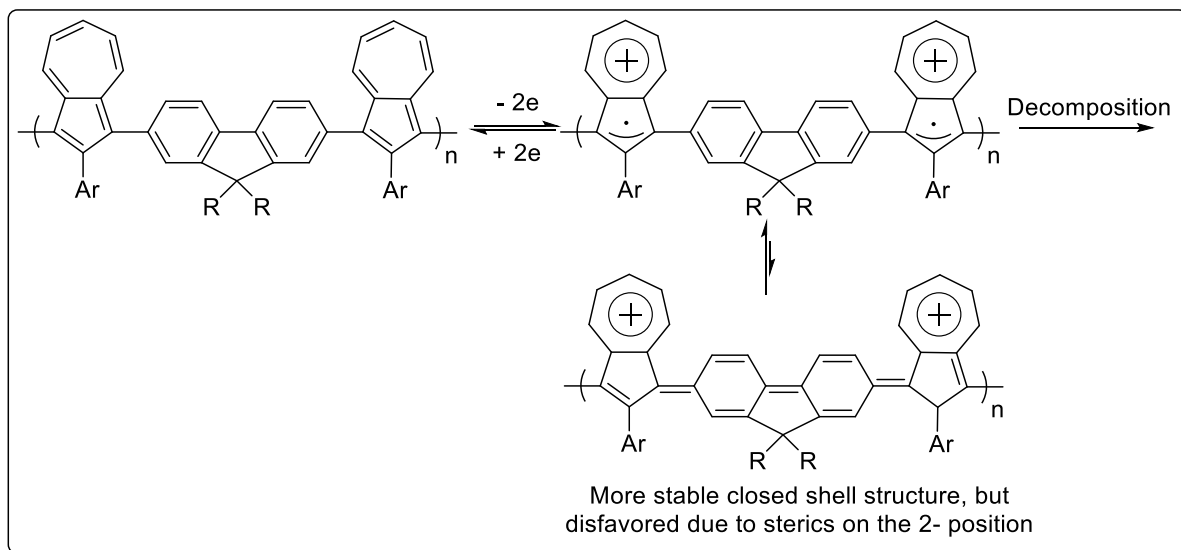


Figure 97: Electrooxidation of azulene polymer forming cationic radical, which is unable to rearrange to a more stable closed shell structure due to overcrowding on the 2-position.

3.4 SUMMARY

In summary, we have prepared and characterised a novel series of 2-functionalised azulene-fluorene polymers. The polymer's colorimetric response to acid correlated to the electronics of the functionalisation at the 2-position; substituents with greater electron donating ability resulted in a greater ease of protonation, and a more red-shifted spectrum. The polymer's response to electrochemical oxidation was likewise affected by the functionality at the 2-position, and all the functionalised polymers showed much less change when subjected to electrochemical oxidation and reduction in comparison to unfunctionalized **P16a**. While unfunctionalized azulene-fluorene polymer could undergo about 15 cycles of electrochemical oxidation and reduction, **P16b** could only undergo about 5 cycles, while the other polymers could not be reduced. This is attributed to overcrowding on the 2-position hindering the formation of a stable closed shell configuration. In all, the substituent at the 2-position has a significant effect on the properties of the polymer. This strategy could be applied to other positions on azulene to further enable tuning of the polymer's properties.

4. EXPERIMENTAL

4.1 General Experimental Procedure

All reactions were conducted using standard techniques using oven-dried glassware. Anhydrous solvents were obtained from solvent stills (DCM and toluene were distilled from CaH_2). Commercial reagents were used as supplied from Sigma Aldrich, Alfa Aesar, or Fluorochem, except for 1-4-benzoquinone, which was recrystallized from hexane and stored in the dark. 6-substituted azulenes were prepared as previously described in literature, with the spectra corresponding to previous reports.¹⁵⁹

Thin-layer chromatography (TLC) was performed on Merck Kiesegel 60 F254 0.20 mm precoated, glass backed, silica gel plates; visualisation was achieved by aqueous KMnO_4 . Flash column chromatography was performed using silica gel (Merck Geduran Si 60 [40-63 μm]) with the relevant solvent.

Nuclear magnetic resonance (NMR) spectra were recorded on a Bruker DPX 400 or on a Jeol 500 MHz with chemical shifts (δ) reported in ppm from TMS with the CDCl_3 as internal standard (^1H , 7.26 ppm; ^{13}C , 77.16 ppm). Data is reported as follows: chemical shift (integration, splitting (s = singlet, d = doublet, t = triplet, q = quartet, qt = quintet, sxt = sextet, spt = septet, m = multiplet), coupling constant, assignment).

Infrared spectra (FT-IR) were recorded using a Perkin-Elmer Paragon 1000 Fourier transform Spectrometer equipped with ATR and analysed as neat thin films or pelletized with KBr, with absorption maxima (λ_{max}) being quoted in wavenumbers (cm^{-1}). UV spectra were recorded on a Shimadzu UV3101PC UV-vis-NIR spectrophotometer. TGA was conducted in a TA Instruments TGA Q500 in nitrogen at a heating rate of 20 $^\circ\text{Cmin}^{-1}$ up to 800 $^\circ\text{C}$. High Resolution Mass Spectrometry (HRMS) was carried out by the ESPRC Mass Spectrometry Service at the University of Swansea using an LTQ Orbitrap XL spectrometer with positive ion nano-electrospray or by the National University of Singapore Mass Spectrometry Service using an Bruker MicroTOF-QII positive ion nano-electrospray.

Cyclic voltammograms were obtained by spin coating the polymer film (10 mg/mL in chloroform) on an indium tin oxide (ITO) – coated glass substrate in 0.1 M LiClO_4 / acetonitrile at a scan rate of 100 mVs^{-1} , using an Autolab PGSTAT30 electrochemical workstation. Electrochromic devices were prepared by spin coating the polymer on a ITO – glass substrate, followed by a gel electrolyte (left to dry for 2 hours), then finally another ITO – glass substrate. The gel electrolyte was prepared by mixing poly(methacrylate) (PMMA, $M_w = 120\,000\text{ g/mol}$, 2.8g), LiClO_4 (0.512g), and propylene carbonate (6.65 mL) in dry acetonitrile (28 mL).

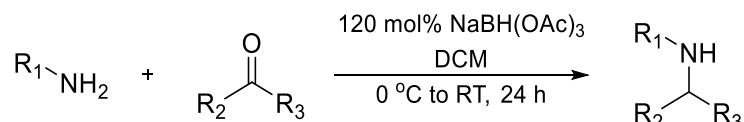
4.2 Experimental Conditions for Carbonylation

Various conditions involving carbon monoxide at different concentrations are described in this work. Where relevant, the following conventions are used to describe experimental techniques. “CO” refers to 100% CO, with evacuation and backfilling of the reaction vessel with three times. “CO balloon” refers to 100% CO being used, but with no evacuation and backfilling. “6.25% CO / air” refers to the commercially available mixture being used, with evacuation and backfilling of the reaction vessel. “6.25% CO / air balloon” refers to the same mixture used with no evacuation and backfilling. As such, the concentration of CO decreases in the order of CO > CO

balloon > 6.25% CO / air > 6.25% CO / air balloon. In all cases, the balloon was left attached to the reaction vessel until the end of the reaction. Reaction optimisation was carried out on a 0.1 mmol scale in a boiling tube with a 12 mm stirrer at 400 rpm, sealed with a new B24 suba seal and parafilm. Reaction scope was carried out on a 0.3 mmol scale in a 100 mL RBF with an oval stirrer at 400 rpm, also sealed with a new B24 suba seal and parafilm. The reaction was also scaled to a 5 mmol scale, which was carried out in a 1 L RBF with an oval stirrer at 600 rpm.

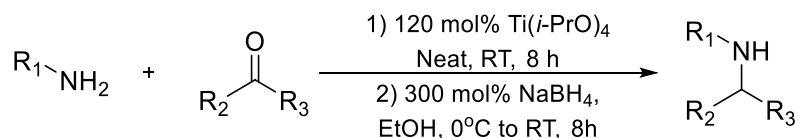
4.3 Synthesis of Amines

General Procedure A for Reductive Amination



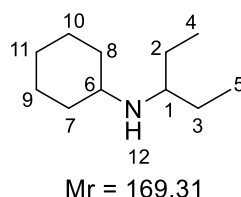
To a stirred solution of amine (1 eq) and ketone / aldehyde (1 – 1.5 eq) in dichloromethane (0.2 M) at 0 °C under nitrogen, sodium triacetoxyborohydride (1.2 eq) was slowly added over 10 mins. The reaction mixture was stirred for 24 hours, warming up to room temperature. 1 M sodium hydroxide was added to quench the reaction mixture until the bubbling stops and stirred for an additional 30 mins. The mixture was extracted with dichloromethane and the combined organic extracts were washed with brine and dried with magnesium sulphate. Removal of the solvent *in vacuo* gave the crude amine. Further purification by kugelrohr or column chromatography gave the pure amine as a colourless liquid.

General Procedure B for Reductive Amination



A solution of the amine (1 eq), ketone (1 - 1.2 eq), and Ti(*i*-PrO)₄ (2 eq) was stirred neat for 8 hours at room temperature under nitrogen. The mixture was cooled to 0 °C. Absolute ethanol (dilute to 0.25 M) was then added, followed by sodium borohydride (3 eq) portion-wise over 10 mins, and the resulting mixture was stirred for an additional 8 hours, warming up to room temperature. The mixture was then poured into NaOH (10 mol%), filtered, and washed with acetone. The mixture was extracted with DCM and the combined organic extracts were washed with brine and dried with MgSO₄. Removal of the solvent *in vacuo* gave the crude amine. Further purification by kugelrohr or column chromatography gave the pure amine as a colourless liquid.

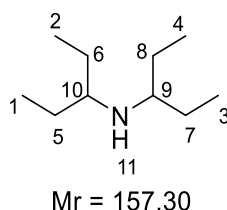
N-(pentan-3-yl)cyclohexylamine (27a)



General procedure A was applied using cyclohexylamine (5.7 g, 57 mmol) and 3-pentanone (4.9 g, 57 mmol) in dichloromethane (250 mL) with addition of sodium

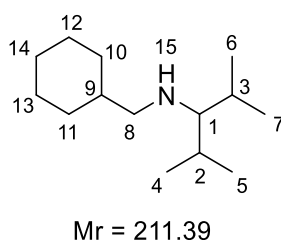
triacetoxyborohydride (14.5 g, 68 mmol). Purification by kugelrohr (80 °C, 3 mbar) gave **27a** as a colourless liquid (5.8 g, 60%). IR ($\lambda_{\text{max}}/\text{cm}^{-1}$) 2960, 2924, 2853, 1450, 1112. ^1H NMR (400 MHz, CDCl_3) 2.46 – 2.42 (2H, m, H1, H6), 1.85 (2H, dd, $J_1 = 11.9$ Hz, $J_2 = 2.6$ Hz, H7a, H8a), 1.71 (2H, dt, $J_1 = 12.8$ Hz, $J_2 = 3.4$ Hz, H9a, H10a), 1.60 (1H, dt, $J_1 = 11.9$ Hz, $J_2 = 3.4$ Hz, H11a), 1.38 (4H, m, H2, H3), 1.29 - 1.09 (3H, m, H9b, H10b, H11b), 1.02 (2H, dq, $J_1 = 11.2$ Hz, $J_2 = 3.1$ Hz, H7b, H8b), 0.86 (6H, t, $J = 7.4$ Hz, H4, H5), 0.71 (1H, b, H12). ^{13}C NMR (101 MHz, CDCl_3) 56.6 (C8), 53.9 (C1), 34.4 (C2, C3), 26.7 (C9, C10), 26.2 (C6), 25.3 (C4, C5), 10.0 (C11, C12). HRMS (FTMS +p NSI) m/z : $[\text{M} + \text{H}]^+$ calculated for $\text{C}_{11}\text{H}_{24}\text{N}$ 170.1903, found = 170.1901, $\Delta = -1.3$ ppm.

Di(pentan-3-yl)amine (27b)



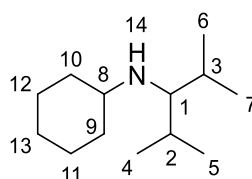
General procedure A was applied using 3-aminopentane (4.36 g, 50 mmol) and 3-pentanone (4.31 g, 49 mmol) in dichloromethane (250 mL) with addition of sodium triacetoxyborohydride (12.71 g, 60 mmol). Purification by kugelrohr (45 °C, 3 mbar) gave **27b** as a colourless liquid (3.5 g, 45 %). IR ($\lambda_{\text{max}}/\text{cm}^{-1}$) 2959, 2924, 2852, 1449, 1112. ^1H NMR (400 MHz, CDCl_3) 2.38 (2H, p, $J = 5.8$ Hz, H9, H10), 1.39 (8H, m, H5, H6, H7, H8), 0.865 (12H, t, $J = 7.7$ Hz, H1, H2, H3, H4) ^{13}C NMR (101 MHz, CDCl_3) 57.0 (C9, C10), 26.3 (C5, C6, C7, C8), 9.9 (C1, C2, C3, C4) HRMS (FTMS +p NSI) m/z : $[\text{M} + \text{H}]^+$ calculated for $\text{C}_{10}\text{H}_{23}\text{N}$ 158.1903, found = 158.1900, $\Delta = -1.9$ ppm.

N-(cyclohexylmethyl)-2,4-dimethylpentan-3-amine (29a)



General procedure B was applied to cyclohexylmethylamine (1.1 g, 10 mmol), 2,4-dimethylpentanone (1.1 g, 10 mmol) and $\text{Ti}(\text{i-PrO})_4$ (5.7 g, 20 mmol) neat. After stirring for 8 hours, the mixture was cooled to 0°C. Absolute ethanol (40 mL) was added, followed by sodium borohydride (1.1 g, 30 mmol) portion wise and the resultant mixture was stirred for another 8 hours. Purification by kugelrohr (155 °C, 3mbar) gave **29a** as a colourless liquid (1.3 g, 61%). IR ($\lambda_{\text{max}}/\text{cm}^{-1}$) 2955, 2921, 2852, 1448, 1116. ^1H NMR (400 MHz, CDCl_3) 2.45 (2H, d, $J = 6.7$ Hz, H8), 1.80 - 1.63 (8H, m, H10a, H11a, H12a, H13a, H14a, H1, H2, H3), 1.39 (1H, m, H9), 1.29 – 1.09 (3H, m, H10b, H11b, H14b), 0.92 (2H, td, $J_1 = 12.7$ Hz, $J_2 = 3.5$ Hz, H12b, H13b), 0.89 (12H, d (overlap), $J = 6.6$ Hz, H4, H5, H6, H7). ^{13}C NMR (101 MHz, CDCl_3) 66.4 (C1), 59.2 (C8), 39.1 (C9), 31.6 (C10, C11), 30.9 (C2, C3), 26.8 (C12, C13), 26.1 (C14), 20.8 (C4, C5), 18.2 (C6, C7). HRMS (FTMS +p NSI) m/z : $[\text{M} + \text{H}]^+$ calculated for $\text{C}_{14}\text{H}_{29}\text{N}$ 212.2372, found = 212.2373, $\Delta = 0.5$ ppm.

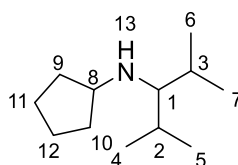
***N*-(2,4-dimethylpentan-3-yl)cyclohexanamine (29b)**



Mr = 197.36

General procedure B was applied to cyclohexylamine (1.0 g, 10 mmol), 2,4-dimethylpentanone (1.1 g, 10 mmol) and $\text{Ti}(\text{i-PrO})_4$ (5.7 g, 20 mmol) neat. After stirring for 8 hours, the mixture was cooled to 0 °C. Absolute ethanol (40 mL) was added, followed by sodium borohydride (1.1 g, 30 mmol) portion wise and the resultant mixture was stirred for another 8 hours. Purification by kugelrohr (150 °C, 4mbar) gave **29b** as a colourless liquid (1.1 g, 55%). IR ($\lambda_{\text{max}}/\text{cm}^{-1}$) 2955, 2925, 2852, 1465, 1449, 1366, 1112. ^1H NMR (400 MHz, CDCl_3) 2.35 (1H, tt, $J_1 = 11.1$ Hz, $J_2 = 3.9$ Hz, H8), 2.00 (1H, t, $J = 5.62$ Hz, H1), 1.90 – 1.82 (2H, m, 9a, 10a), 1.77 – 1.66 (4H, m, H2, H3, H11a, H12a), 1.62 – 1.54 (1H, m, H13a), 1.28 – 1.08 (3H, m, H11b, H12b, H13b), 1.08 – 0.94 (2H, m, H9b, H10b), 0.90 (6H, d $J = 7.2$ Hz, H4, H5), 0.87 (6H, d $J = 7.2$ Hz, H6, H7). ^{13}C NMR (101 MHz, CDCl_3) 65.5 (C1) 57.1 (C8), 34.7 (C9, C10), 31.0 (C2, C3), 26.2 (C13), 25.5 (C11, C12), 21.1 (C4, C5), 18.4 (C6, C7). HRMS (FTMS +p NSI) m/z : $[\text{M} + \text{H}]^+$ calculated for $\text{C}_{13}\text{H}_{27}\text{N}$ 198.2250, found = 198.2248, $\Delta = -1.0$ ppm.

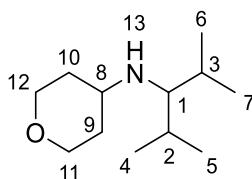
***N*-(2,4-dimethylpentan-3-yl)cyclopentanamine (29c)**



Mr = 183.34

General procedure B was applied to cyclopentylamine (425 mg, 5 mmol), 2,4-dimethylpentanone (550 mg, 5 mmol) and $\text{Ti}(\text{i-PrO})_4$ (2.4 g, 10 mmol) neat. After stirring for 8 hours, the mixture was cooled to 0 °C. Absolute ethanol (20 mL) was added, followed by sodium borohydride (550 mg, 15 mmol) portion wise and the resultant mixture was stirred for another 8 hours. Purification by silica column (5% to 20% ethyl acetate / petroleum ether) gave **29c** as a colourless liquid (450 mg, 49%). IR ($\lambda_{\text{max}}/\text{cm}^{-1}$) 2954, 2870, 1464, 1383, 1359, 1123, 1066. ^1H NMR (400 MHz, CDCl_3) 3.09 (1H, p, $J = 6.8$ Hz, H8), 1.97 (1H, t, $J = 5.4$ Hz, H1), 1.83 – 1.61 (6H, m, H2, H3, H9a, H10a, H11a, H12a), 1.55 – 1.43 (2H, m, H11b, H12b), 1.31 – 1.20 (2H, m, H9b, H10b), 0.91 (6H, d, $J = 6.9$ Hz, H4, H5), 0.88 (6H, d, $J = 6.9$, H6, H7). ^{13}C NMR (101 MHz, CDCl_3) 67.1 (C1), 60.5 (C8), 33.7 (C9, C10), 30.8 (C2, C3), 23.5 (C11, C12), 21.1 (C4, C5), 18.4 (C6, C7). HRMS (FTMS +p NSI) m/z : $[\text{M} + \text{H}]^+$ calculated for $\text{C}_{14}\text{H}_{29}\text{N}$ 184.2060, found = 184.2059, $\Delta = -0.5$ ppm.

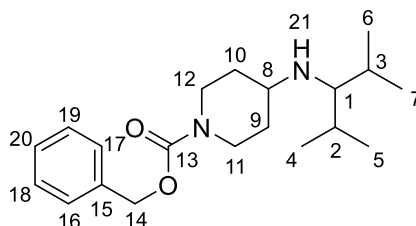
***N*-(2,4-dimethylpentan-3-yl)tetrahydro-2H-pyran-4-amine (29d)**



Mr = 199.33

General procedure B was applied to 4-aminotetrahydropyran (1.0 g, 10 mmol), 2,4-dimethylpentanone (1.1 g, 10 mmol) and $\text{Ti}(i\text{-PrO})_4$ (5.7 g, 20 mmol) neat. After stirring for 8 hours, the mixture was cooled to 0 °C. Absolute ethanol (40 mL) was added, followed by sodium borohydride (1.1 g, 30 mmol) portion wise and the resultant mixture was stirred for another 8 hours. Purification by kugelrohr (120 °C, 5mbar) gave **29d** as a colourless liquid (0.8 g, 41%). IR ($\lambda_{\text{max}}/\text{cm}^{-1}$) 2954, 2839, 1466, 1383, 1363, 1236, 1120. ^1H NMR (400 MHz, CDCl_3) 3.99 – 3.92 (2H, m, H11b, H12b), 3.36 (2H, td, $J_1 = 12.0$ Hz, $J_2 = 3.0$ Hz, H11a, H12a), 2.67 (1H, tt, $J_1 = 10.5$ Hz, $J_2 = 4.1$ Hz, H8), 2.02 (1H, t, $J = 6.2$ Hz, H1) 1.84 – 1.77 (2H, m, H9, H10), 1.73 (2H, oct, $J = 6.2$ Hz, H2, H3), 1.42 – 1.29 (2H, m, H9, H10) 0.91 (6H, d, $J = 6.7$ Hz, H4, H5), 0.88 (6H, d, $J = 6.7$ Hz, H6, H7). ^{13}C NMR (101 MHz, CDCl_3) 67.1 (C11, C12), 65.2 (C1), 54.3 (C8), 34.8 (C9, C10), 30.8 (C2, C3), 21.1 (C4, C5), 18.3 (C6, C7). HRMS (FTMS +p NSI) m/z : $[\text{M} + \text{H}]^+$ calculated for $\text{C}_{12}\text{H}_{25}\text{NO}$ 201.2043, found = 201.2042, $\Delta = -0.5$ ppm.

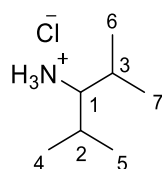
Benzyl 4-((2,4-dimethylpentan-3-yl)amino)piperidine-1-carboxylate (29e)



Mr = 332.48

General procedure B was applied to benzyl 4-aminopiperidine-1-carboxylate (1.0 g, 10 mmol), 2,4-dimethylpentanone (1.1 g, 10 mmol) and $\text{Ti}(i\text{-PrO})_4$ (5.7 g, 20 mmol) neat. After stirring for 8 hours, the mixture was cooled to 0 °C. Absolute ethanol (40 mL) was added, followed by sodium borohydride (1.1 g, 30 mmol) portion wise and the resultant mixture was stirred for another 8 hours. Purification by silica column (20% to 40% ethyl acetate / petroleum ether) gave **29e** as a colourless liquid (1.1 g, 33%). IR ($\lambda_{\text{max}}/\text{cm}^{-1}$) 2954, 2870, 1694, 1429, 1225, 1116. ^1H NMR (400 MHz, CDCl_3) 7.37 – 7.28 (5H, m, H16, H17, H18, H19, H20), 5.12 (2H, s, H14), 4.09 (2H, br, H11, H12), 2.85 (2H, br, H11, H12), 2.61 (1H, tt, $J_1 = 10.1$ Hz, $J_2 = 3.8$ Hz, H8), 2.00 (1H, t, $J = 5.5$ Hz, H1), 1.89 – 1.79 (2H, m, H9, H10), 1.73 (2H, oct, $J = 7.7$ Hz, H2, H3), 1.31 – 1.16 (2H, m, H9, H10), 0.90 (6H, d, $J = 6.7$ Hz, H4, H5), 0.87 (6H, d, $J = 6.7$ Hz, H6, H7). ^{13}C NMR (101 MHz, CDCl_3) 155.3 (C13), 137.0 (C15), 128.5 (C16, C17), 127.9 (C20), 127.8 (C18, C19), 67.0 (C14), 65.4 (C1), 54.9 (C8), 43.0 (C11, C12), 33.4 (C9, C10), 30.9 (C2, C3), 21.1 (C4, C5), 18.3 (C6, C7). HRMS (FTMS +p NSI) m/z : $[\text{M} + \text{H}]^+$ calculated for $\text{C}_{20}\text{H}_{32}\text{N}_2\text{O}_2$ 334.25705, found = 334.25687, $\Delta = -0.5$ ppm.

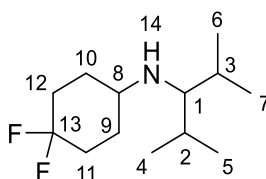
2,4-Dimethylpentan-3-amine hydrochloride (29f-i)



Mr = 151.67

General procedure B was applied to 2,4-dimethylpentanone (2.2 g, 20 mmol), ammonia (7.1 mL, 7 M in MeOH), and $\text{Ti}(\text{O}i\text{Pr})_4$ (12 mL, 40 mmol). After stirring for 8 hours, the mixture was cooled to 0 °C. Absolute ethanol (40 mL) was added, followed by sodium borohydride (1.1 g, 30 mmol) portion wise and the resultant mixture was stirred for another 8 hours. The crude was quenched with 10% aq. NaOH and the resulting white solid was filtered off and washed with Et_2O . The aqueous phase was washed with Et_2O (3 x 100 mL), and the combined organic layers extracted with 1 M aq. HCl (3 x 50 mL), followed by basification with 10% aq. NaOH (until pH ~ 10). The aqueous phase was extracted with Et_2O (3 x 50 mL) and the combined organic layers dried over MgSO_4 , filtered, treated with 2 M HCl in Et_2O (20 mL) and concentrated *in vacuo* to afford the title compound **29f-i** as a white solid (2.5 g, 83%). m.p.: 192 – 195°C (lit. 160°C). IR ($\lambda_{\text{max}}/\text{cm}^{-1}$): 3027, 2959, 2889, 1578, 1507, 1463, 1137, 1070, 960. ^1H NMR (400 MHz, D_2O) 2.85 (1H, t, J = 6.1 Hz, H1), 2.08 (2H, m, H2, H3), 1.04 (6H, d, J = 6.9 Hz, H4, H5), 0.98 (6H, d, J = 6.9 Hz, H6, H7). ^{13}C NMR (101 MHz, D_2O) 63.4 (C1), 27.6 (C2, C3), 19.0 (C4, C5), 16.17 (C6, C7). HRMS (ESI) m/z : calculated for $\text{C}_7\text{H}_{18}\text{N}_1\text{Cl}_1\text{Na}_1$ $[\text{M}+\text{Na}]^+$ 174.1017, found 174.1020, Δ = 1.7 ppm.

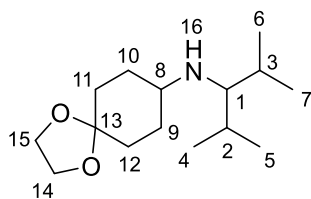
***N*-(2,4-dimethylpentan-3-yl)-4,4-difluorocyclohexan-1-amine (29f)**



Mr = 233.35

General procedure B was applied to 2,4-dimethylpentylamine (550 mg, 5 mmol), 4,4-difluorocyclohexanone (670 mg, 5 mmol) and $\text{Ti}(i\text{-PrO})_4$ (2.4 g, 10 mmol) neat. After stirring for 8 hours, the mixture was cooled to 0 °C. Absolute ethanol (20 mL) was added, followed by sodium borohydride (550 mg, 15 mmol) portion wise and the resultant mixture was stirred for another 8 hours. Purification by silica column (5% to 20% ethyl acetate / petroleum ether) gave the **29f** as a colourless liquid (500 mg, 43%). IR ($\lambda_{\text{max}}/\text{cm}^{-1}$) 2957, 2871, 1470, 1448, 1376, 1107. ^1H NMR (400 MHz, CDCl_3) 2.66 – 2.58 (1H, m, H8), 2.16 – 2.03 (2H, m, H11a, H12a) 1.98 (1H, t, J = 5.5 Hz, H1), 1.90 – 1.82 (2H, m, H9, H10), 1.79 – 1.67 (4H, m, H2, H3, H11b, H12b), 1.50 – 1.38 (2H, m, H9b, H10b), 0.91 (6H, d, J = 6.7 Hz, H4, H5), 0.87 (6H, d, J = 6.7 Hz, H6, H7). ^{13}C NMR (101 MHz, CDCl_3) 123.6 (C13), 65.8 (C1), 54.0 (C8), 31.9 (C11, C12), 30.9 (C2, C3), 29.7 (C9, C10), 21.1 (C4, C5), 18.3 (C6, C7) ^{19}F NMR (MHz, CDCl_3) -96.5 (d, 240 Hz), -99.9 (d, 240 Hz) HRMS (FTMS +p NSI) m/z : $[\text{M} + \text{H}]^+$ calculated for $\text{C}_{13}\text{H}_{25}\text{F}_2\text{N}$ 234.2028, found = 234.2029, Δ = 0.4 ppm.

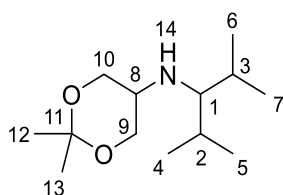
***N*-(2,4-dimethylpentan-3-yl)-1,4-dioxaspiro[4.5]decan-8-amine (29g)**



Mr = 225.40

General procedure B was applied to 2,4-dimethylpentylamine (550 mg, 5 mmol), 2,4-1,4-dioxaspiro[4.5]decan-8-one (780 mg, 5 mmol) and $\text{Ti}(i\text{-PrO})_4$ (2.4 g, 10 mmol) neat. After stirring for 8 hours, the mixture was cooled to 0 °C. Absolute ethanol (20 mL) was added, followed by sodium borohydride (550 mg, 15 mmol) portion wise and the resultant mixture was stirred for another 8 hours. Purification by silica column (10% to 30% ethyl acetate / petroleum ether) gave **29g** as a colourless liquid (710 mg, 63%). IR ($\lambda_{\text{max}}/\text{cm}^{-1}$) 2950, 2871, 1473, 1378, 1245, 1195, 1152, 1039. ^1H NMR (400 MHz, CDCl_3) 3.92 (4H, s, H14, H15), 2.50 (1H, tt, $J_1 = 9.9$ Hz, $J_2 = 3.6$ Hz, H8), 1.92 (1H, t, $J = 5.9$ Hz, H1), 1.88 – 1.64 (6H, m, H9a - 12a, H2, H3), 1.51 (2H, td, $J_1 = 13.2$ Hz, $J_2 = 4.0$ Hz, H11b, H12b), 1.42 – 1.30 (2H, m, H9b, H10b), 0.89 (6H, d, $J = 7.0$ Hz, H4, H5), 0.86 (6H, d, $J = 7.0$ Hz, H6, H7). ^{13}C NMR (101 MHz, CDCl_3) 108.9 (C14, C15), 65.7 (C1), 64.3 (C8), 55.2 (C13), 33.2 (C9, C10), 31.2 (C11, C12), 30.9 (C2, C3), 21.0 (C4, C5), 18.3 (C6, C7) HRMS (FTMS +p NSI) m/z : $[\text{M} + \text{H}]^+$ calculated for $\text{C}_{15}\text{H}_{30}\text{NO}_2$ 256.2271, found = 256.2271, exact match.

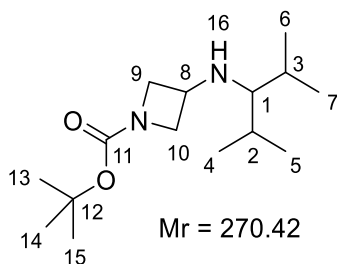
***N*-(2,4-dimethylpentan-3-yl)-2,2-dimethyl-1,3-dioxan-5-amine (29h)**



Mr = 229.36

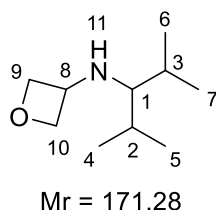
General procedure B was applied to 2,4-dimethylpentylamine (550 mg, 5 mmol), 2,4-2,2-dimethyl-1,3-dioxan-5-one (650 mg, 5 mmol) and $\text{Ti}(i\text{-PrO})_4$ (2.4 g, 10 mmol) neat. After stirring for 8 hours, the mixture was cooled to 0 °C. Absolute ethanol (20 mL) was added, followed by sodium borohydride (550 mg, 15 mmol) portion wise and the resultant mixture was stirred for another 8 hours. Purification by silica column (10% to 30% ethyl acetate / petroleum ether) gave **29h** as a colourless liquid (430 mg, 37%). IR ($\lambda_{\text{max}}/\text{cm}^{-1}$) 2957, 2870, 1471, 1379, 1369, 1245, 1197, 1155, 1039. ^1H NMR (400 MHz, CDCl_3) 3.93 (2H, dd, $J_1 = 11.3$ Hz, $J_2 = 4.1$ Hz, H9a, H10a), 3.58 (2H, dd, $J_1 = 11.8$ Hz, $J_2 = 7.0$ Hz, H9b, H10b), 2.67 (1H, sep, $J = 3.7$ Hz, H8) 1.95 (1H, t, $J = 6.0$ Hz, H1), 1.71 (2H, oct, $J = 6.2$ Hz, H2, H3), 1.42 (3H, s, H12), 1.41 (3H, s, H13), 0.90 (6H, d, $J = 6.7$ Hz, H4, H5), 0.88 (6H, d, $J = 6.7$ Hz, H6, H7) ^{13}C NMR (101 MHz, CDCl_3) 97.8 (C11), 66.6 (C1) 64.9 (C9, C10), 51.7 (C8), 30.9 (C2, C3), 25.3 (C13), 22.4 (C12), 21.0 (C4, C5), 18.1 (C6, C7) HRMS (FTMS +p NSI) m/z : $[\text{M} + \text{H}]^+$ calculated for $\text{C}_{13}\text{H}_{27}\text{NO}_2$ 230.2115, found = 230.2116, $\Delta = 0.4$ ppm.

***tert*-butyl 3-((2,4-dimethylpentan-3-yl)amino)azetidine-1-carboxylate (29i)**



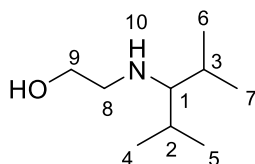
General procedure B was applied to a suspension of 2,4-dimethylpentan-3-amine hydrochloride (1.0 g, 6.6 mmol), tert-butyl 3-oxoazetidine-1-carboxylate (1.7 g, 9.9 mmol), $\text{Ti}(\text{O}i\text{Pr})_4$ (50 mL, 165 mmol), and NaHCO_3 (550 mg, 6.6 mmol) in THF (20 mL). Absolute ethanol (40 mL) was added, followed by sodium borohydride (0.5 g, 13.2 mmol) portion wise and the resultant mixture was stirred for another 8 hours. Purification by silica column (0% to 40% ethyl acetate / petroleum ether) gave **29i** as a light yellow oil (1.1 g, 62%). IR ($\lambda_{\text{max}}/\text{cm}^{-1}$): 2955, 2875, 1691, 1476. ^1H NMR (400 MHz, CDCl_3) 4.08 – 4.02 (2H, m, H9a, H10a), 3.67 – 3.54 (3H, m, H8, H9b, H10b), 1.89 (1H, t, J = 5.7 Hz, H1), 1.71 (2H, oct, J = 6.7 Hz, H2, H3), 1.43 (9H, s, H13 – H15), 0.90 (6H, d, J = 6.8 Hz, H4, H5), 0.87 (6H, d, J = 6.8 Hz, H6, H7). ^{13}C NMR (101 MHz, CDCl_3) 156.6 (C11), 79.2 (C12), 68.1 (C1), 58.0 (C9, C10), 48.9 (C8), 30.3 (C2, C3), 28.4 (C13 – C15), 20.9 (C4, C5), 18.3 (C6, C7). HRMS (ESI) m/z : calculated for $\text{C}_{15}\text{H}_{30}\text{O}_2\text{N}_2$ $[\text{M}+\text{H}]^+$ 271.2380, found 271.2378, Δ = - 0.7 ppm.

***N*-(2,4-Dimethylpentan-3-yl)oxetan-3-amine (29j)**



General procedure B was applied to a suspension of 2,4-dimethylpentan-3-amine hydrochloride (1.0 g, 6.6 mmol), oxetan-3-one (710 mg, 9.9 mmol), $\text{Ti}(\text{O}i\text{Pr})_4$ (50 mL, 165 mmol), and NaHCO_3 (550 mg, 6.6 mmol) in THF (20 mL). Absolute ethanol (40 mL) was added, followed by sodium borohydride (0.5 g, 13.2 mmol) portion wise and the resultant mixture was stirred for another 8 hours. Purification by silica column (0% to 30% ethyl acetate / petroleum ether) gave the **29j** as a light yellow oil (1.22 g, 72%). IR ($\lambda_{\text{max}}/\text{cm}^{-1}$): 2956, 2869, 1469, 969, 736. ^1H NMR (400 MHz, CDCl_3) 4.76 (2H, t, J = 6.8 Hz, H9a, H10a), 4.41 (2H, t, J = 6.7 Hz, H9b, H10b), 4.00 (1H, p, J = 7.0 Hz, H8), 1.88 (1H, t, J = 5.4 Hz, H1), 1.76 – 1.58 (2H, m, H2, H3), 1.08 (1H, br s, H11), 0.88 (6H, d, J = 6.8 Hz, H4, H5), 0.85 (6H, d, J = 6.8 Hz, H6, H7). ^{13}C NMR (101 MHz, CDCl_3) 81.4 (C9, C10), 68.7 (C1), 55.1 (C8), 30.5 (C2, C3), 21.0 (C4, C5), 18.4 (C6, C7). HRMS (ESI) m/z : calculated for $\text{C}_{10}\text{H}_{22}\text{O}_1\text{N}_1$ $[\text{M}+\text{H}]^+$ 172.1696, found 172.1692, Δ = - 2.3 ppm.

***2*-((2,4-Dimethylpentan-3-yl)amino)ethan-1-ol (29k-i)**

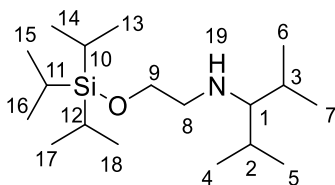


Mr = 159.27

General procedure B was applied to a 2,4-dimethylpentanone (3.9 g, 35 mmol), ethanolamine (2.0 mL, 33 mmol), and $\text{Ti}(\text{O}i\text{Pr})_4$ (50 mL, 165 mmol). Absolute ethanol (150 mL) was added, followed by sodium borohydride (5.5 g, 55 mmol) portion wise and the resultant mixture was stirred for another 8 hours. Purification by silica column (10% MeOH in DCM) gave **29k-i** as a colourless oil (0.85 g, 16%). IR ($\lambda_{\text{max}}/\text{cm}^{-1}$) 3326, 2956, 2871, 1469, 1384, 1058, 1025. ^1H NMR (400 MHz, CDCl_3) 3.54 (2H, t, $J = 5.2$ Hz, H9), 2.81 (2H, t, $J = 5.2$ Hz, H8), 1.88 (1H, t, $J = 5.5$ Hz, H1), 1.83 – 1.63 (2H, m, H2, H3), 0.90 (6H, d, $J = 6.8$ Hz, H4, H5), 0.88 (6H, d, $J = 6.8$ Hz, H6, H7). ^{13}C NMR (101 MHz, CDCl_3) 69.2 (C1), 61.7 (C9), 52.8 (C8), 30.9 (C2, C3), 21.0 (C4, C5), 18.3 (C6, C7). HRMS (ESI) m/z : calculated for $\text{C}_9\text{H}_{22}\text{N}_1\text{O}_1$ $[\text{M}+\text{H}]^+$ 160.1696, found 160.1692, $\Delta = -2.5$ ppm.

The hydrochloride salt was obtained as an off white solid by treatment of the amine with 4M HCl in dioxane, followed by removal of the solvent *in vacuo*. m.p. 82–86 °C. IR ($\lambda_{\text{max}}/\text{cm}^{-1}$): 3663, 3274, 2974, 1584, 1407, 1394, 1378, 1074. ^1H NMR (400 MHz, D_2O) 3.95 – 3.85 (2H, m, H9), 3.36 – 3.31 (2H, m, H8), 2.94 (1H, t, $J = 5.8$ Hz, H1), 2.39 – 2.12 (2H, m, H2, H3), 1.07 (6H, d, $J = 6.9$ Hz, H4, H5), 1.06 (3H, d, $J = 6.9$ Hz, H6, H7). ^{13}C NMR (101 MHz, D_2O) 70.8 (C1), 56.6 (C9), 50.7 (C8), 27.7 (C2, C3), 18.9 (C4, C5), 17.1 (C6, C7). HRMS (ESI) m/z : calculated for $\text{C}_9\text{H}_{22}\text{O}_1\text{N}_1$ $[\text{M}+\text{H}]^+$ 160.1696, found 160.1692, $\Delta = -2.5$ ppm.

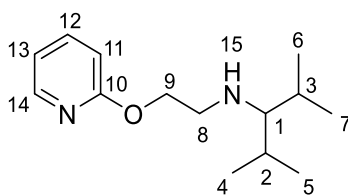
2,4-dimethyl-N-(2-((triisopropylsilyl)oxy)ethyl)pentan-3-amine (29k)



Mr = 315.62

To an ice-cold solution of **3i-i** (0.25 g, 4.8 mmol) and Et_3N (1.0 mL, 14.5 mmol) in dry CH_2Cl_2 (10 mL) was added dropwise TIPSOTf (2.0 mL, 7.3 mmol) and the resulting mixture was stirred for 16 h under an N_2 atmosphere at 21 °C. The reaction was quenched with sat. aq. NaHCO_3 (20 mL) and the aqueous phase extracted with Et_2O (3 x 25 mL). The combined organic layers were washed with brine (75 mL), dried over MgSO_4 , filtered and concentrated *in vacuo*. Purification by silica column (0% - 3% ethyl acetate / petroleum ether) gave **29k** as a colourless oil (490 mg, 95%). IR ($\lambda_{\text{max}}/\text{cm}^{-1}$) 3675, 2943, 2866, 1463, 1088, 1065, 881. ^1H NMR (400 MHz, CDCl_3) 3.77 (2H, t, $J = 5.4$ Hz, H9), 2.76 (2H, t, $J = 5.4$ Hz, H8), 1.84 (1H, t, $J = 5.7$ Hz, H1), 1.80 – 1.69 (2H, m, H2, H3), 1.29 (1H, br s, H19), 1.15 – 1.01 (21H, m, H10 – H18), 0.90 (12H, t, $J = 6.9$ Hz, H4 – H7). ^{13}C NMR (101 MHz, CDCl_3) 69.5 (C1), 63.5 (C9), 54.3 (C8), 31.0 (C2, C3), 21.0 (C4, C5), 18.3 (C6, C7), 18.2 (C13 – C18), 12.1 (C10 – C12). HRMS (ESI) m/z : calculated for $\text{C}_{18}\text{H}_{42}\text{N}_1\text{O}_1\text{Si}_1$ $[\text{M}+\text{H}]^+$ 316.3030, found 316.3029, $\Delta = 0.3$ ppm.

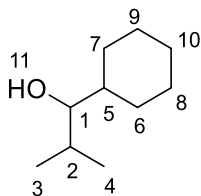
2,4-Dimethyl-N-(2-(pyridin-2-yloxy)ethyl)pentan-3-amine (29l)



Mr = 236.36

To a suspension of **3i-i**-HCl (460 mg, 3.1 mmol) in dioxane (10 mL) was added NaH (200 mg, 6.4 mmol, 60% in mineral oil) portion-wise. The mixture was refluxed for 30 min, then cooled to 21 °C. A solution of 2-chloropyridine (270 mg, 3.1 mmol) in dioxane (10 mL) was added dropwise, then refluxed for an additional 16 h. The crude was cooled, concentrated *in vacuo*, re-dissolved in EtOAc (100 mL), washed with water (100 mL) and brine (100 mL), dried over MgSO₄, filtered and concentrated *in vacuo*. Purification by silica column (0% - 5% MeOH in DCM) gave **29l** as a light yellow oil (495 mg, 89%). IR ($\lambda_{\text{max}}/\text{cm}^{-1}$) 2955, 1596, 1474, 1431, 1285, 1270, 777. ¹H NMR (400 MHz, CDCl₃) 8.16 (1H, dd, *J* = 5.0, 1.4 Hz, H14), 7.67 – 7.48 (1H, m, H12), 6.96 – 6.82 (1H, m, H13), 6.76 (1H, d, *J* = 8.4 Hz, H11), 4.42 – 3.96 (2H, m, H9), 3.12 – 3.01 (2H, t, *J* = 5.4 Hz, H8), 1.94 (1H, m, H1), 1.86 – 1.67 (2H, m, H2, H3), 1.31 (1H, br s, H15), 0.9 – 0.6 (12H, m, H4 – H7). ¹³C NMR (101 MHz, CDCl₃) 163.9 (C10), 146.9 (C14), 138.4 (C12), 116.6 (C13), 111.1 (C11), 69.4 (C9), 66.1 (C8), 50.7 (C1), 30.9 (C2, C3), 20.8 (C4, C5), 18.1 (C6, C7). HRMS (ESI) *m/z*: calculated for C₁₄H₂₅O₁N₂ [M+H]⁺ 237.1961, found 237.1963, Δ = 0.8 ppm.

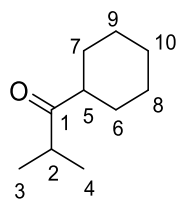
1-cyclohexyl-2-methylpropan-1-ol (29n-i)



Mr = 156.27

A solution of isobutyraldehyde (3.8 mL, 42 mmol) in THF (50 mL) was cooled to 0 °C. Cyclohexylmagnesium bromide (30 mL, 60 mmol, 2M in THF) was added portionwise. The mixture was stirred for an additional 2 hours, warming up to room temperature. The reaction mixture was quenched with sat. aq. NH₄Cl (100 mL) and extracted with EtOAc (3 x 50 mL). The combined organic layers were washed with brine (100 mL), dried over MgSO₄, filtered, and concentrated *in vacuo*. Purification by silica column (0% to 20% ethyl acetate / petroleum ether) gave the **29n-i** as a colourless liquid (2.1 g, 32%). IR ($\lambda_{\text{max}}/\text{cm}^{-1}$) 3376, 2922, 2851, 1448, 989, 976. ¹H NMR (400 MHz, CDCl₃) 3.03 (1H, t, *J* = 5.7 Hz, H4), 1.91 – 1.82 (1H, m, H5), 1.80 – 1.70 (3H, m, H6a, H7a, H10a), 1.69 – 1.61 (1H, m, H8a), 1.61 – 1.54 (1H, m, H9a), 1.46 – 1.33 (1H, m, H2), 1.30 – 0.97 6H, (m, H6b – H10b, H11), 0.91 (3H, d, *J* = 6.8 Hz, H3), 0.89 (3H, d, *J* = 6.7 Hz, H4). ¹³C NMR (101 MHz, CDCl₃) 81.3 (C1), 40.8 (C2), 30.1 (C6), 30.0 (C7), 27.9 (C5), 26.8 (C8), 26.7 (C9), 26.4 (C10), 20.1 (C3), 16.8 (C4). HRMS (ESI) *m/z*: calculated for C₁₀H₂₄O₁N₁ [M+NH₄]⁺ 174.1852, found 174.1853, Δ = 0.6 ppm.

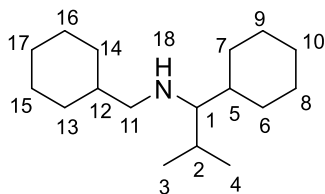
1-cyclohexyl-2-methylpropan-1-one (29n-ii)



Mr = 154.25

To an ice-cold solution of **29n-i** (1.8 g, 11.5 mmol) in dry DCM (75 mL) was added celite (5g), followed by PCC (3.1g, 14.3 mmol). The reaction mixture was warmed to room temperature and stirred for 24 hours under N₂. The crude reaction was then filtered through a pad of celite / silica, and the filtrate concentrated *in vacuo* to afford the crude **29n-ii** as a colourless oil (1.9 g, >95%). IR ($\lambda_{\text{max}}/\text{cm}^{-1}$) 2929, 2855, 1706, 1449, 996. ¹H NMR (400 MHz, CDCl₃) 2.74 (1H, hept, *J* = 6.9 Hz, H2), 2.55 – 2.42 (1H, m, H5), 1.84 – 1.61 (5H, m, H6a – H10a), 1.42 – 1.13 (5H, m, H6b – H10b), 1.06 (6H, d, *J* = 6.9 Hz, H3, H4). ¹³C NMR (101 MHz, CDCl₃) 217.9 (C1), 49.2 (C5), 39.1 (C2), 28.8 (C6, C7), 26.0 (C10), 25.9 (C8, C9), 18.6 (C3, C4).

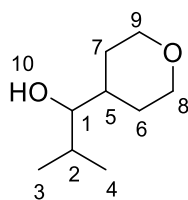
1-cyclohexyl-*N*-(cyclohexylmethyl)-2-methylpropan-1-amine (**29n**)



Mr = 251.46

General procedure B was applied to cyclohexanemethylamine (210 μL , 1.6 mmol), **29n-ii** (249 mg, 1.6 mmol), and Ti(O*i*Pr)₄ (5.0 mL, 16.6 mmol). After stirring for 8 hours, the mixture was cooled to 0 °C. Absolute ethanol (7 mL) was added, followed by sodium borohydride (0.136 g, 3.6 mmol) portion wise and the resultant mixture was stirred for another 8 hours. Purification by silica column (00% to 100% ethyl acetate / petroleum ether) gave **29n** as a colourless liquid (265 mg, 65%). IR ($\lambda_{\text{max}}/\text{cm}^{-1}$) 2919, 2850, 1448, 1129, 1112, 892. ¹H NMR (400 MHz, CDCl₃) 2.50 – 2.35 (2H, m, H11), 1.85 – 1.55 (12H, m, H1, H2, H6a – H10a, H13a – H17a), 1.44 – 1.30 (2H, m, H5, H12), 1.30 – 0.87 (10H, m, H6b – H10b, H13b – H17b), 0.89 (3H, d, *J* = 6.5 Hz, H3), 0.85 (3H, d, *J* = 6.5 Hz, H4), 0.62 (1H, br s, H18). ¹³C NMR (101 MHz, CDCl₃) 68.9 (C1), 59.5 (C11), 41.7 (C5), 39.2 (C12), 30.3 (C2), 31.9, 31.8, 31.4, 29.1, 27.0, 26.9, 26.8, 26.3, 26.3 (C6 – C10, C13 – C17), 21.0 (C3), 18.0 (C4). HRMS (ESI) *m/z*: calculated for C₁₇H₃₄N₁ [M+H]⁺ 252.2686, found 252.2684, Δ = - 0.8 ppm.

2-methyl-1-(tetrahydro-2H-pyran-4-yl)propan-1-ol (**29p-i**)

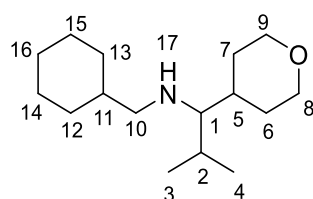


Mr = 156.27

A solution of tetrahydro-2H-pyran-4-carbaldehyde (1.7 g, 15 mmol) in THF (50 mL) was cooled to 0 °C. Isopropylmagnesium bromide (20 mL, 20 mmol, 1M in THF) was

added portionwise. The mixture was stirred for an additional 2 hours, warming up to room temperature. The reaction mixture was quenched with saturated aqueous NH_4Cl (100 mL) and extracted with EtOAc (3 x 50 mL). The combined organic layers were washed with brine (100 mL), dried over MgSO_4 , filtered, and concentrated *in vacuo*. Purification by silica column (0% to 50% ethyl acetate / petroleum ether) gave the **29p-i** as a colourless liquid (0.4 g, 17%). IR ($\lambda_{\text{max}}/\text{cm}^{-1}$): 3422, 2957, 2912, 2847.0, 1092, 1004, 987. ^1H NMR (400 MHz, CDCl_3) δ 4.12 – 3.89 (2H, m, H8a, H9a), 3.45 – 3.31 (2H, m, H8b, H9b), 3.16 – 3.02 (1H, m, H1), 1.84 – 1.73 (2H, m, H6a, H7a), 1.71 – 1.59 (1H, m, H2), 1.49 – 1.35 (3H, m, H5, H6b, H7b), 1.33 (1H, d, $J = 5.6$ Hz, H10), 0.96 (3H, d, $J = 6.8$ Hz, H3), 0.89 (3H, d, $J = 6.7$ Hz, H4). ^{13}C NMR (101 MHz, CDCl_3) δ 80.3 (C1), 68.2 (C8), 68.0 (C9), 38.3 (C5), 29.6 (C2), 29.4 (C7, C8), 28.7 (C6, C7), 20.1 (C3), 15.9 (C4). HRMS (ESI) m/z : calculated for $\text{C}_9\text{H}_{19}\text{O}_2$ $[\text{M}+\text{H}]^+$ 159.1380, found 159.1383, $\Delta = 1.9$ ppm.

***N*-(Cyclohexylmethyl)-2-methyl-1-(tetrahydro-2H-pyran-4-yl)propan-1-amine (29p)**

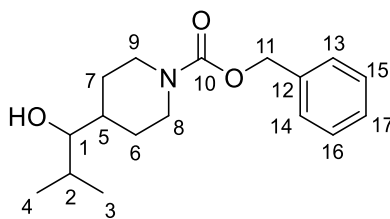


Mr = 253.43

To an ice-cold solution of **29p-i** (300 mg, 1.9 mmol), in dry CH_2Cl_2 (15 mL) was added celite (1.0 g) followed by PCC (610 mg, 2.85 mmol). The reaction mixture was allowed to warm to 21 °C and stirred for 24 h under an N_2 atmosphere. Then, the crude reaction was filtered through a pad of celite/silica and the filtrate concentrated *in vacuo* to afford the crude 2-methyl-1-(tetrahydro-2H-pyran-4-yl)propan-1-one as a brown oil (250 mg, 84%), which was used for next step without further purification.

General procedure A was applied to cyclohexanemethylamine (170 μL , 1.6 mmol), 2-methyl-1-(tetrahydro-2H-pyran-4-yl)propan-1-one (200 mg, 1.3 mmol), and sodium triacetoxyborohydride (325 mg, 1.6 mmol). Purification by silica column (0% to 15% MeOH / DCM) gave the **29p** as a colourless liquid (255 mg, 78%). IR ($\lambda_{\text{max}}/\text{cm}^{-1}$) 2920, 2848, 1448, 1123, 1095. ^1H NMR (400 MHz, CDCl_3) 4.21 – 3.74 (2H, m, H8a, H9a), 3.47 – 3.14 (2H, m, H8b, H9b), 2.53 – 2.35 (2H, m, H10), 1.87 (1H, dd, $J = 6.4, 5.0$ Hz, H1), 1.84 – 1.61 (7H, m, H2, H10, H13a – H16a), 1.60 – 1.50 (1H, m, H5), 1.49 – 1.31 (4H, m, H6, H7), 1.30 – 1.09 (3H, m, H12b, H13b, H16b), 0.93 (3H, d, $J = 6.7$ Hz, H3), 0.98 – 0.88 (2H, m, H14b, H15b), 0.86 (3H, d, $J = 6.7$ Hz, H4). ^{13}C NMR (101 MHz, CDCl_3) 68.6 (C8), 68.4 (C1), 68.3 (C9), 59.4 (C10), 39.4 (C5), 39.3 (C11), 31.8 (C12), 31.7 (C13), 31.1 (C6), 29.8 (C2), 29.7 (C7), 26.9 (C14, C15), 26.3 (C16), 21.0 (C3), 17.3 (C4). HRMS (ESI) m/z : calculated for $\text{C}_{16}\text{H}_{32}\text{O}_1\text{N}_1$ $[\text{M}+\text{H}]^+$ 254.2478, found 254.2477, $\Delta = -0.4$ ppm.

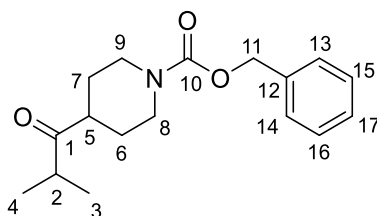
Benzyl 4-(1-hydroxy-2-methylpropyl)piperidine-1-carboxylate (29q-i)



Mr = 291.39

A solution of benzyl 4-formylpiperidine-1-carboxylate (2.47 g, 10 mmol) in DCM (100 mL) was cooled to 0 °C. Isopropylmagnesium chloride (10 mL, 20 mmol, 2M in THF) was added portionwise. The mixture was stirred for an additional 2 hours, warming up to room temperature. The reaction mixture was quenched with sat. aq. NH_4Cl (100 mL) and extracted with EtOAc (3 x 50 mL). The combined organic layers were washed with brine (100 mL), dried over MgSO_4 , filtered, and concentrated *in vacuo*. Purification by silica column (0% to 30% ethyl acetate / petroleum ether) gave the **29q-i** as a colourless liquid (2.5 g, 85%). IR ($\lambda_{\text{max}}/\text{cm}^{-1}$) 3464 (br), 2959, 2869, 1679, 1431, 1364, 1278, 1213, 1124, 1070, 976. ^1H NMR (400 MHz, CDCl_3) 7.39 – 7.27 (5H, m, H13 – H17), 5.12 (2H, s, H11), 4.23 (2H, br s, H8a, H9a), 3.08 (1H, br s, H1), 2.74 (2H, br s, H8b, H9b), 1.90 – 1.82 (1H, m, H7a), 1.77 (1H, oct, $J = 6.3$ Hz, H2), 1.63 – 1.48 (2H, m, H5, H6a), 1.47 – 1.38 (1H, br, OH), 1.36 – 1.19 (2H, m, H6b, H7b), 0.94 (3H, d, $J = 6.9$ Hz, H3), 0.90 (3H, d, $J = 6.9$ Hz, H4). ^{13}C NMR (101 MHz, CDCl_3) 155.3 (C10), 137.0 (C12), 128.5, 127.9, 127.8 (C13 – C17), 79.9 (C1), 67.0 (C11), 44.1 (C8), 44.0 (C9), 39.0 (C5), 29.7 (C2), 28.7 (C6), 27.5 (C7), 19.9 (C4), 16.1 (C3). HRMS (FTMS +p NSI) m/z : $[\text{M} + \text{H}]^+$ calculated for $\text{C}_{17}\text{H}_{26}\text{NO}_3$ 292.1907 found = 292.1908, $\Delta = 0.3$ ppm.

Benzyl 4-isobutyrylpiperidine-1-carboxylate (29q-ii)

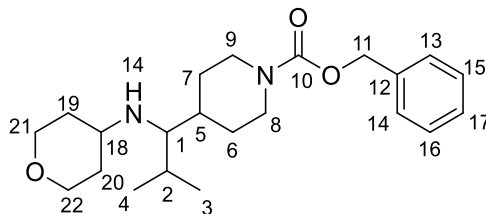


Mr = 289.37

A solution of **29q-i** (1.7 g, 6 mmol) in DCM (60 mL) was cooled to 0 °C. Dess-Martin Periodinane (2.8 g, 6.6 mmol) was added portionwise. The mixture was stirred for an additional 2 hours, warming up to room temperature. 10% aq NaOH (30 mL) was added and the mixture stirred for 30 minutes. The reaction mixture was extracted with DCM (3 X 50 mL), dried over MgSO_4 , filtered, and concentrated *in vacuo*. Purification by silica column (0% to 20% ethyl acetate / petroleum ether) gave the **29q-ii** as a colourless liquid (1.4 g, 82%). IR ($\lambda_{\text{max}}/\text{cm}^{-1}$) 2967, 1693, 1427, 1277, 1221, 1127, 1090, 1013, 994. ^1H NMR (400 MHz, CDCl_3) 7.37 – 7.28 (5H, m, H13 – H17), 5.12 (2H, s, H11), 4.19 (2H, br s, H8a, H9a), 2.93 – 2.81 (2H, m, H8b, H9b), 2.77 (1H, sep, $J = 7.2$ Hz, H2), 2.67 (1H, tt, $J_1 = 11.2$ Hz, $J_2 = 3.6$ Hz, H5), 1.75 (2H, br, H6a, H7a), 1.57 (2H, qd, $J_1 = 12.9$ Hz, $J_2 = 4.8$ Hz, H6b, H7b), 1.08 (6H, d, $J = 7.0$ Hz, H3, H4). ^{13}C NMR (101 MHz, CDCl_3) 215.8 (C1), 155.2 (C10), 136.8 (C12), 128.5, 128.0, 127.9 (C13 – C17), 67.1 (C11), 46.5 (C5), 43.5 (C8, C9), 38.9 (C2), 27.7 (C6, C7), 18.4 (C3,

C4). HRMS (FTMS +p NSI) m/z: [M + H]⁺ calculated for C₁₇H₂₃NO₃ 290.1756 found = 290.1754, Δ = - 0.6 ppm.

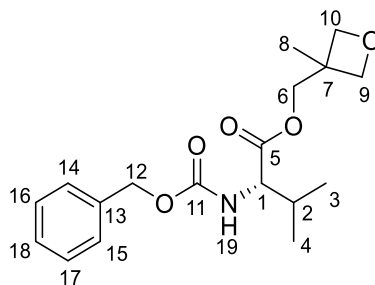
Benzyl 4-(2-methyl-1-((tetrahydro-2H-pyran-4-yl)amino)propyl)piperidine-1-carboxylate (29q)



Mr = 374.52

General procedure B was applied to 4-aminotetrahydropyran (300 mg, 3 mmol), benzyl 4-isobutyrylpiperidine-1-carboxylate (800 mg, 2.7 mmol) and Ti(*i*-PrO)₄ (1.7 g, 6 mmol) neat. After stirring for 8 hours, the mixture was cooled to 0 °C. Absolute ethanol (15 mL) was added, followed by sodium borohydride (330 mg, 10 mmol) portion wise and the resultant mixture was stirred for another 8 hours. Purification by silica column (50% to 70% ethyl acetate / petroleum ether) gave the **29q** as a colourless liquid (700 mg, 62%). IR (λ_{max}/cm⁻¹) 2953, 2850, 1690, 1469, 1431, 1363, 1278, 1250, 1215, 1121, 1088, 1010. ¹H NMR (400 MHz, CDCl₃) 7.37 – 7.26 (5H, m, H13, H14, H15, H16, H17), 5.11 (2H, s, H11) 4.21 (2H, br, H8, H9), 3.98 – 3.88 (2H, m, H21a, H22a), 3.33 (2H, td, J = 12.0 Hz, J2 = 1.8 Hz, H21b, H22b) 2.80 – 2.63 (2H, br, H8b, H9b), 2.58 (1H, tt, J1 = 10.0 Hz, J2 = 3.6 Hz, H18), 2.07 (1H, t, J = 5.9 Hz, H1), 1.83 – 1.70 (4H, m, H2, H19b, H20b), 1.61 – 1.41 (2H, m, H6a, H7a), 1.39 – 1.13 (5H, m, H5, H6b, H7b, H19b, H20b), 0.92 (3H, d, J = 6.7 Hz, H3), 0.86 (3H, d, J = 6.7 Hz, H4) ¹³C NMR (101 MHz, CDCl₃) 155.2 (C10), 137.0 (C12), 128.5, 127.9, 127.8 (C13, C14, C15, C16, C17), 67.0 (C11), 66.9 (C21, C22), 63.7 (C1), 54.4 (C18), 44.5, 44.4 (C8, C9), 40.1 (C5), 34.8, 34.6 (C19, C20), 29.9 (C2), 28.6 (C6, C7), 21.1, 17.6 (C3, C4) HRMS (FTMS +p NSI) m/z: [M + H]⁺ calculated for C₂₂H₃₄N₂O₃ 375.2642, found = 375.2642, exact match.

((Benzzyloxy)carbonyl)-L-valine (29s-i)



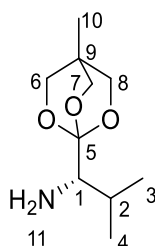
Mr = 335.40

To an ice-cold solution of L-valine (4.1 g, 16.3 mmol) in 1 M aq. NaOH (100 mL) was added dropwise a solution of benzyl chloroformate (6.4 mL, 44.8 mmol) in dioxane (40 mL). The mixture was allowed to warm to room temperature and stirred for 16 h. The crude aqueous mixture was washed with Et₂O (2 x 100 mL), neutralized with 3 M aq. HCl until pH ~ 2 and extracted with Et₂O (3 x 50 mL). The combined organic layers

were dried over MgSO_4 , filtered and concentrated *in vacuo* to afford crude ((benzyloxy)carbonyl)-L-valine as a thick colourless oil (8.1 g, 95%).

To an ice cold stirred solution of DCC (6.0 g, 29.3 mmol), 3-methyl- 3-oxetanemethanol (3.3 mL, 33.4 mmol), and DMAP (34 mg, 0.3 mmol) in dry CH_2Cl_2 (150 mL) was added dropwise a solution of ((benzyloxy)carbonyl)-L-valine (8.0 g, 27.9 mmol) in CH_2Cl_2 (50 mL). The reaction mixture was stirred for 5 h and the formed precipitate was filtered off. The filtrate was washed with water (100 mL), 0.01 M aq. HCl (2 x 100 mL), and brine (100 mL), dried over MgSO_4 , and concentrated *in vacuo*. Purification by silica column (0% – 50% ethyl acetate / petroleum ether) gave the **29s-i** as a colourless oil (7.6 g, 71%). $[\alpha]_D^{20} = +4.38^\circ$ (c. 0.89, CHCl_3). IR ($\lambda_{\text{max}}/\text{cm}^{-1}$) 3390, 2964, 2876, 1717, 1525, 979. ^1H NMR (400 MHz, CDCl_3) 7.55 – 7.14 (5H, m, H14 – H18), 5.48 (1H, d, $J = 8.9$ Hz, H12a), 5.09 (2H, s, H6), 4.5 – 4.42 (2H, m, H9a, H10a), 4.35 (2H, d, $J = 6.0$ Hz, H9b, H10b), 4.31 (1H, dd, $J = 9.0$ Hz, 4.3 Hz, H1), 4.20 (2H, q, $J = 11.1$ Hz), 2.23 – 2.11 (1H, m, H2), 1.30 (3H, s, H8), 0.97 (3H, d, $J = 6.8$ Hz, H3), 0.89 (3H, d, $J = 6.8$ Hz, H4). ^{13}C NMR (101 MHz, CDCl_3) 172.1, 156.3, 136.3, 128.5, 128.1, 128.1, 79.3, 69.4, 67.0, 59.1, 39.0, 31.1, 21.1, 19.0, 17.5.

(S)-2-Methyl-1-(4-methyl-2,6,7-trioxabicyclo[2.2.2]octan-1-yl)propan-1-amine (29s-ii)

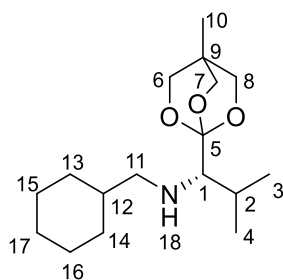


Mr = 201.27

A solution of **29s-i** (7.0 g, 20.9 mmol) in CH_2Cl_2 (100 mL) was treated with $\text{BF}_3 \cdot \text{Et}_2\text{O}$ (5 mL, 40.5 mmol) and the mixture was stirred under an N_2 atmosphere for 16 h at room temperature. Et_3N (8.0 mL, 60.7 mmol) was added to the reaction and the crude mixture concentrated *in vacuo* until dryness. The residue was dissolved in EtOAc, washed with diluted aq. K_2CO_3 (2 x 100 mL), brine (200 mL), dried over MgSO_4 , filtered, and concentrated *in vacuo* to afford crude benzyl (S)-(2-methyl-1-(4-methyl-2,6,7-trioxabicyclo[2.2.2]octan-1-yl)propyl)carbamate as a colourless oil (6.8 g, 95%).

To a solution of benzyl (S)-(2-methyl-1-(4-methyl-2,6,7-trioxabicyclo[2.2.2]octan-1-yl)propyl)carbamate (6.0 g, 17.9 mmol) in dry MeOH was added Pd/C (5.0 g, 10 wt. %) and the mixture was stirred under a H_2 atmosphere for 24 h. Then the crude was filtered through celite and concentrated *in vacuo*. Purification by silica column (0% – 20% ethyl acetate / petroleum ether) gave the **29s-ii** as a colourless oil (1.97g, 55%). $[\alpha]_D^{20} = -12.2^\circ$ (c. 1.0, CHCl_3). IR ($\lambda_{\text{max}}/\text{cm}^{-1}$) 2960, 2876, 1031, 1597, 976; ^1H NMR (400 MHz, CDCl_3) 3.87 (6H, s, H6 – H8), 2.60 (1H, d, $J = 3.2$ Hz, H1), 2.05 (1H, sept d, $J = 6.9, 3.2$ Hz, H2), 1.38 (2H, br s, H11), 0.96 (3H, d, $J = 6.9$ Hz, H3), 0.88 (3H, d, $J = 6.9$ Hz, H4), 0.78 (3H, s, H10). ^{13}C NMR (101 MHz, CDCl_3) 109.8 (C5), 72.6 (C6 – C8), 60.2 (C1), 30.6 (C9), 27.7 (C2), 21.9 (C3), 16.4 (C4), 14.6 (C10).

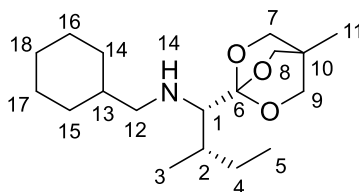
(S)-N-(Cyclohexylmethyl)-2-methyl-1-(4-methyl-2,6,7-trioxabicyclo[2.2.2]octan-1-yl)propan-1-amine (29s)



Mr = 297.44

General procedure A was applied to **29s-ii** (510 mg, 2.5 mmol), cyclohexanecarboxaldehyde (270 mg, 2.5 mmol) and sodium triacetoxyborohydride (625 mg, 3.0 mmol). Purification by silica column (0% – 10% ethyl acetate / petroleum ether) gave the **29s** as a colourless oil (595 mg, 79%). $[\alpha]_D^{20} = -8.6^\circ$ (c. 0.9, CHCl_3). IR ($\lambda_{\text{max}}/\text{cm}^{-1}$) 3370; 2923, 1043, 969, 749, 688. ^1H NMR (400 MHz, CDCl_3) 3.86 (s, 6H, H6 – H8), 2.68 (1H, dd, $J_1 = 11.3$ Hz, $J_2 = 6.4$ Hz, H11a), 2.40 (1H, d, $J = 3.0$ Hz, H1), 2.33 (1H, dd, $J = 11.3$, 6.9 Hz, H11b), 2.13 – 1.96 (1H, m, H2), 1.87 – 1.56 (5H, m, H13a – H17a), 1.45 – 1.31 (1H, m, H12), 1.30 – 1.06 (3H, m, H13b, H14b, H17b), 0.94 (3H, d, $J = 6.9$ Hz, H3), 0.98 – 0.81 (2H, m, H15b, H16b), 0.87 (3H, d, $J = 6.9$ Hz, H4), 0.78 (3H, s, H10). ^{13}C NMR (101 MHz, CDCl_3) 110.2 (C5), 72.3 (C6 – C8), 66.6 (C1), 57.3 (C11), 38.6 (C12), 31.6 (C13), 31.5 (C14), 30.4 (C9), 28.1 (C2), 26.9 (C15, C16), 26.2 (C17), 21.7 (C3), 17.0 (C4), 14.6 (C10). HRMS (ESI) m/z : calculated for $\text{C}_{17}\text{H}_{32}\text{O}_3\text{N}_1$ $[\text{M}+\text{H}]^+$ 298.2377, found 298.2379, $\Delta = 0.7$ ppm.

***N*-(cyclohexylmethyl)-2-methyl-1-(4-methyl-2,6,7-trioxabicyclo[2.2.2]octan-1-yl)butan-1-amine (29t)**



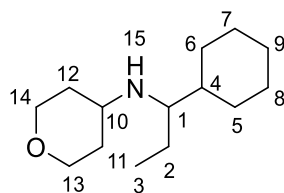
Mr = 311.47

2-methyl-1-(4-methyl-2,6,7-trioxabicyclo[2.2.2]octan-1-yl)butan-1-amine was prepared as per literature procedure²¹⁰. Spectra matches reported ^1H NMR (400 MHz, CDCl_3) 3.90 (6H, s, H7 – H9), 2.66 (1H, d, $J = 3.4$ Hz, H1), 1.79 – 1.69 (2H, m, H2, H4a), 1.39 (2H, br, NH), 1.09 – 1.00 (1H, m, H4b), 0.97 (3H, d, $J = 6.9$ Hz, H3), 0.87 (3H, t, $J = 7.0$ Hz, H5), 0.80 (3H, s, H11). ^{13}C NMR (101 MHz, CDCl_3) 109.8 (C6), 72.5 (C7 – C9), 60.2 (C1), 34.9 (C2), 30.4 (C10), 23.1 (C4), 17.5 (C3), 14.5 (C11), 12.0 (C5).

General procedure A was applied to 2-methyl-1-(4-methyl-2,6,7-trioxabicyclo[2.2.2]octan-1-yl)butan-1-amine (400 mg, 2 mmol), cyclohexanecarbaldehyde (220 mg, 2 mmol) and sodium triacetoxyborohydride (500 mg, 2.4 mmol) in DCM (40 mL). Purification by silica column (10% to 30% ethyl acetate / petroleum ether) gave the **29t** as a colourless liquid (320 mg, 52%). IR ($\lambda_{\text{max}}/\text{cm}^{-1}$) 2958, 2922, 2873, 2851, 1459, 1394, 1351, 1269, 1193, 1054. ^1H NMR (400 MHz, CDCl_3) 3.86 (6H, s, H7, H8, H9), 2.64 (1H, dd, $J_1 = 11.0$ Hz, $J_2 = 6.2$ Hz, H12a), 2.45

(1H, d, J = 3.0 Hz, H1), 2.34 (1H, dd, J1 = 11.0 Hz, J2 = 6.2 Hz, H12b), 1.83 – 1.59 (7H, m, H2, H4a, H14a, H15a, H16a, H17a, H18a), 1.45 – 1.31 (1H, m, H13), 1.29 – 0.99 (4H, m, H4b, H16b, H17b), 0.94 (3H, d, J = 6.7 Hz, H3), 0.90 – 0.81 (5H, m, H5, H14b, H15b), 0.78 (3H, s, H11). ¹³C NMR (101 MHz, CDCl₃) 72.3 (C7, C8, C9), 66.7 (C1), 57.0 (C12), 38.6 (C13), 35.4 (C2), 31.6 (C14), 31.5 (C15), 30.4 (C10), 26.9 (C18), 26.2 (C16, C17), 23.8 (C4), 17.3 (C3), 14.6 (C11), 12.4 (C5). HRMS (FTMS +p NSI) m/z: [M + H]⁺ calculated for C₁₈H₃₃NO₃ 312.2533, found = 312.2532, Δ = -0.3 ppm.

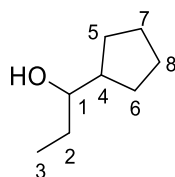
***N*-(1-cyclohexylpropyl)tetrahydro-2H-pyran-4-amine (29v)**



Mr = 225.38

General procedure B was applied to 4-aminotetrahydropyran (1.0 g, 10 mmol), 1-cyclohexylpropan-1-one (1.4 g, 10 mmol) and Ti(*i*-PrO)₄ (5.7 g, 20 mmol) neat. After stirring for 8 hours, the mixture was cooled to 0 °C. Absolute ethanol (40 mL) was added, followed by sodium borohydride (1.1 g, 30 mmol) portion wise and the resultant mixture was stirred for another 8 hours. Purification by silica column (30 % to 50% ethyl acetate / petroleum ether) gave the **29v** as a colourless liquid (1.8 g, 79%). IR (λ_{max}/cm⁻¹) 2921, 2848, 1448, 1367, 1140, 1087. ¹H NMR (400 MHz, CDCl₃) 3.95 (2H, dt, J1 = 11.6 Hz, J2 = 3.3 Hz, H13b, H14b), 3.38 (2H, tt, J1 = 11.5 Hz, J2 = 1.8 Hz, H13b, H14b), 2.65 (1H, tt, J1 = 10.2 Hz, J2 = 4.2 Hz, H10), 2.27 (1H, m, H1), 1.83 – 1.58 (7H, m, H5a, H6a, H7a, H8a, H9a, H11a, H12a) 1.51 – 1.38 (1H, m, H2), 1.39 – 0.92 (8H, m, H4, H11b, H12b, H(5-9)b), 0.87 (3H, t, J = 7.6 Hz, H3). ¹³C NMR (101 MHz, CDCl₃) 67.0 (C13, C14), 60.3 (C1), 51.9 (C10), 41.0 (C2), 34.6 (C11), 34.5 (C12), 29.2 (C5), 29.1 (C6), 26.8 (C7), 26.7 (C8), 24.3 (C4, C9), 10.7 (C3). HRMS (FTMS +p NSI) m/z: [M + H]⁺ calculated for C₁₄H₂₇NO 226.2165, found = 226.2164, Δ = - 0.4 ppm.

***1*-cyclopentylpropan-1-ol (29w-i)**

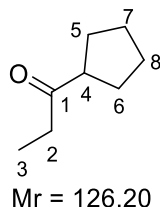


Mr = 128.22

A solution of cyclopentanecarbaldehyde (1.9 g, 20 mmol) in DCM (200 mL) was cooled to 0 °C. Ethylmagnesium bromide (5 mL, 15 mmol, 3M in ether) was added portionwise. The mixture was stirred for an additional 2 hours, warming up to room temperature. The reaction mixture was quenched with sat. aq. NH₄Cl (100 mL) and extracted with DCM (3 x 100 mL). The combined organic layers were washed with brine (100 mL), dried over MgSO₄, filtered, and concentrated *in vacuo* to give the crude **29w-i** as a colourless liquid (2.1 g, 81%). IR (λ_{max}/cm⁻¹) 3335 (br), 1708, 1452, 1313, 1115, 967. ¹H NMR (400 MHz, CDCl₃) 3.32 (1H, td, J1 = 7.8 Hz, J = 3.0 Hz, H1), 1.86

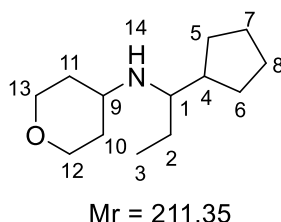
(1H, sep, , J = 8.2 Hz, H4), 1.81 – 1.13 (10H, m, H2, H5 – H8), 0.95 (3H, t, J = 7.8 Hz, H3). ¹³C NMR (101 MHz, CDCl₃) 76.7 (C1), 45.9 (C4), 29.1 (C5), 28.9 (C6), 28.5 (C2), 25.7 (C7), 25.6 (C8), 10.0 (C3). HRMS (FTMS +p NSI) m/z: [M + NH₄]⁺ calculated for C₈H₂₀NO 146.1539, found = 146.1537, Δ = -1.4 ppm.

1-cyclopentylpropan-1-one (29w-ii)



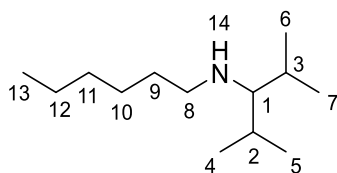
A solution of **29w-i** (1.9 g, 15 mmol) in DCM (200 mL) was cooled to 0 °C. Dess-Martin Periodinane (7.0 g, 16.5 mmol) was then added portionwise. The mixture was stirred for an additional 2 hours, warming up to room temperature. 10% aq NaOH (100 mL) was added and the mixture stirred for 30 minutes. The reaction mixture was extracted with DCM (3 X 100 mL), dried over MgSO₄, filtered, and concentrated *in vacuo* (caution, volatile) to give the crude **29w-ii** as a colourless liquid (1.5 g, 81%). IR (λ_{max}/cm⁻¹) 2953, 2869, 1708, 1451, 1413, 1362, 1128, 1023. ¹H NMR (400 MHz, CDCl₃) 2.86 (1H, p, J = 8.0 Hz, H4), 2.45 (2H, q, J = 7.6 Hz, H2), 1.86 – 1.50 (8H, m, H5 – H8), 1.04 (3H, t, J = 8.8 Hz, H3). ¹³C NMR (101 MHz, CDCl₃) 214.0 (C1), 51.1 (C4), 34.9 (C2), 28.7, 26.0 (C5, C8), 7.9 (C3). HRMS (FTMS +p NSI) m/z: [M + NH₄]⁺ calculated for C₈H₁₈NO 144.1383, found = 144.1384, Δ = 0.7 ppm.

N-(1-cyclopentylpropyl)tetrahydro-2H-pyran-4-amine (29w)



General procedure B was applied to 4-aminotetrahydropyran (1.0 g, 10 mmol), **1-29w-ii** (1.3 g, 10 mmol) and Ti(*i*-PrO)₄ (5.7 g, 20 mmol) neat. After stirring for 8 hours, the mixture was cooled to 0 °C. Absolute ethanol (40 mL) was added, followed by sodium borohydride (1.1 g, 30 mmol) portion wise and the resultant mixture was stirred for another 8 hours. Purification by silica column (60% to 80% ethyl acetate / petroleum ether) gave the **29w** as a colourless liquid (600 mg, 28%). IR (λ_{max}/cm⁻¹) 2936, 2866, 1463, 1366, 1235, 1141, 1111, 1087. ¹H NMR (400 MHz, CDCl₃) 3.95 (2H, dt, J₁ = 11.6 Hz, J₂ = 3.4 Hz, H12a, H13a), 3.38 (2H, qd, J₁ = 10.8 Hz, J₂ = 2.2 Hz, H12b, H13b), 2.67 (1H, tt, J₁ = 10.4 Hz, J₂ = 4.2 Hz, H9), 2.41 (1H, dt, J₁ = 7.4 Hz, J₂ = 5.2 Hz, H1), 1.90 – 1.11 (15H, m, H2, H4 – H8, H10, H11), 0.88 (3H, t, J = 8.2 Hz, H3). ¹³C NMR (101 MHz, CDCl₃) 67.2 (C12), 67.0 (C13), 59.3 (C1), 51.5 (C9), 44.1 (C4), 35.1 (C10), 34.2 (C11), 29.7 (C7), 29.6 (C8), 25.4 (C2), 25.4 (C5), 25.4 (C6), 9.3 (C3). HRMS (FTMS +p NSI) m/z: [M + H]⁺ calculated for C₁₃H₂₅NO 212.2009, found = 212.2011, Δ = 0.9 ppm.

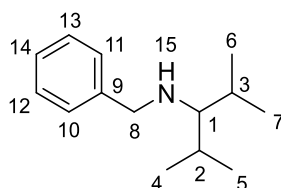
N-(2,4-dimethylpentan-3-yl)hexan-1-amine (29y)



Mr = 199.38

General procedure B was applied to 1-hexylamine (1.0 g, 10 mmol), 2,4-dimethylpentanone (1.1 g, 10 mmol) and $\text{Ti}(i\text{-PrO})_4$ (5.7 g, 20 mmol) neat. After stirring for 8 hours, the mixture was cooled to 0 °C. Absolute ethanol (40 mL) was added, followed by sodium borohydride (1.1 g, 30 mmol) portion wise and the resultant mixture was stirred for another 8 hours. Purification by kugelrohr (120 °C, 5 mbar) gave the **29y** as a colourless liquid (1.2g, 60%). IR ($\lambda_{\text{max}}/\text{cm}^{-1}$) 2956, 2924, 2871, 1466, 1381, 1115. ^1H NMR (400 MHz, CDCl_3) 2.60 (2H, t, $J = 7.2$ Hz, H8), 1.82 (1H, t, $J = 5.9$ Hz, H1), 1.74 (2H, oct, $J = 6.7$ Hz, H2, H3) 1.49 – 1.39 (2H, m, H9), 1.37 – 1.23 (6H, m, H10, H11, H12), 0.92 – 0.86 (15H, m (overlap), H4, H5, H6, H7, H13) ^{13}C NMR (101 MHz, CDCl_3) 69.5 (C1), 52.3 (C8), 31.9 (C9), 31.0 (C10), 30.8 (C2, C3), 27.1 (C11), 22.7 (C12), 20.9 (C4, C5), 18.2 (C6, C7), 14.1 (C13). HRMS (FTMS +p NSI) m/z : $[\text{M} + \text{H}]^+$ calculated for $\text{C}_{13}\text{H}_{29}\text{N}$ 200.2373, found = 200.2372, $\Delta = -0.5$ ppm.

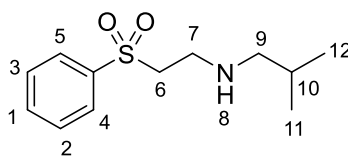
***N*-benzyl-2,4-dimethylpentan-3-amine (29z)**



Mr = 205.35

General procedure B was applied to benzylamine (1.1 g, 10 mmol), 2,4-dimethylpentanone (1.1 g, 10 mmol) and $\text{Ti}(i\text{-PrO})_4$ (5.7 g, 20 mmol) neat. After stirring for 8 hours, the mixture was cooled to 0 °C. Absolute ethanol (40 mL) was added, followed by sodium borohydride (1.1 g, 30 mmol) portion wise and the resultant mixture was stirred for another 8 hours. Purification by silica column (5% to 20% ethyl acetate / petroleum ether) gave the **29z** as a colourless liquid (1.3 g, 63%). IR ($\lambda_{\text{max}}/\text{cm}^{-1}$) 2957, 2870, 1452, 1382, 1107, 1066, 1028. ^1H NMR (400 MHz, CDCl_3) 7.37 (2H, m, H10, H11), 7.32 (2H, m, H12, H13), 7.24 (1H, m, H14), 3.82 (2H, s, H8), 2.03 (1H, t, $J = 5.5$ Hz, H1), 1.77 (2H, oct, $J = 6.6$ Hz, H2, H3) 0.95 (6H, d, $J = 5.8$ Hz, H4, H5), 0.93 (6H, d, $J = 5.5$ Hz, H6, H7). ^{13}C NMR (101 MHz, CDCl_3) 141.6 (C9), 128.3 (C10, C11), 128.2 (C12, C13), 126.8 (C14), 68.9 (C1), 56.1 (C8), 30.9 (C2, C3), 20.9 (C4, C5), 18.2 (C6, C7). HRMS (FTMS +p NSI) m/z : $[\text{M} + \text{H}]^+$ calculated for $\text{C}_{14}\text{H}_{23}\text{N}$ 206.1903, found = 206.1901, $\Delta = -1.0$ ppm.

***2*-methyl-*N*-(2-(phenylsulfonyl)ethyl)propan-1-amine (29ab)**

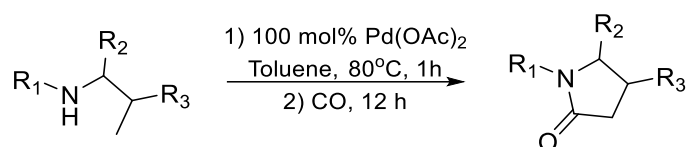


Mr = 241.35

A solution of phenylvinylsulfone (168 mg, 1 mmol) and isobutylamine (100 mg, 1.4 mmol) in ethanol (5 mL) was stirred at room temperature for 12 hours. Removal of the solvent *in vacuo* gave **29ab** as a colourless liquid (239 mg, 99 %) which was used without further purification. IR ($\lambda_{\text{max}}/\text{cm}^{-1}$) 2954.8, 2871.1, 1447.1, 1304.4, 1142.8, 1085.3. ^1H NMR (400 MHz, CDCl_3) 7.92 (2H, d, $J = 8.2$ Hz, H4, H5), 7.66 (1H, t, $J = 7.57$ Hz, H1), 7.58 (2H, t, $J = 7.06$ Hz, H2, H3), 3.29 (2H, t, $J = 6.3$ Hz, H6 or H7), 3.00 (2H, t, $J = 6.3$ Hz, H6 or H7), 2.39 (2H, d, $J = 7.1$ Hz, H10), 1.67 (1H, spt, $J = 6.7$ Hz, H11), 1.42 (1H, br, H9), 0.87 (6H, d, $J = 6.6$ Hz, H12, H13) ^{13}C NMR (101 MHz, CDCl_3) 139.43 (C6 or C7), 133.78 (C1), 129.34 (C2, C3), 127.97 (C4, C5), 57.62 (C6 or C7), 56.15 (C8), 43.33 (C10), 28.30 (C11), 20.54 (C12, C13). HRMS (FTMS +p NSI) m/z : $[\text{M} + \text{H}]^+$ calculated for $\text{C}_{12}\text{H}_{19}\text{NO}_2\text{S}$ 242.1210, found 242.1209, $\Delta = -0.4$ ppm.

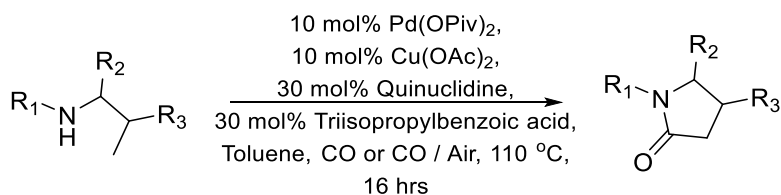
4.4 Carbonylation of Amines

General Procedure C for Stoichiometric Palladium Catalysed Carbonylation of Amines



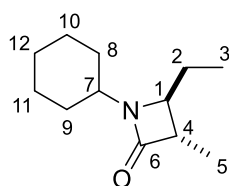
To a 10 mL round-bottomed flask with large oval stirrer bar was added palladium (II) acetate (66 mg, 0.3 mmol, 1 eq), the amine (0.3 mmol, 1 eq) and anhydrous toluene (3 mL). The flask was sealed with a new septum and Teflon tape. The flask was placed into an oil bath at 80 °C and stirred at 400 rpm for 1 hour. A balloon of carbon monoxide was placed on top, and the flask was stirred for a further 12 hours. The reaction mixture was cooled, and the contents were filtered through celite and washed with ethyl acetate. The solvent was removed *in vacuo* and the crude mixture was purified by column chromatography to obtain the corresponding γ lactam.

General Procedure D for Catalytic Palladium Catalysed Carbonylation of Amines



To a 100 mL round-bottomed flask with large oval stirrer bar was added palladium (II) pivalate (9.0 mg, 0.03 mmol, 0.1 eq), copper acetate (5.4 mg, 0.03 mmol, 0.1 eq), quinuclidine (9.9 mg, 0.09 mmol, 0.3 eq), triisopropylbenzoic acid (22.5 mg, 0.09 mmol, 0.3 eq), the amine (0.3 mmol, 1 eq) and anhydrous toluene (6 mL). The flask was sealed with a new septum and parafilm. A balloon of CO was placed on top. The flask was placed into an oil bath at 110 °C, and stirred at 400 rpm for 16 hour. The reaction mixture was cooled, and the contents were filtered through celite and washed with ethyl acetate. The solvent was removed *in vacuo* and the crude mixture was purified by column chromatography to obtain the corresponding γ lactam.

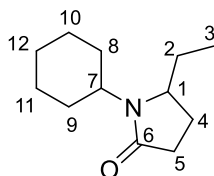
Trans-1-Cyclohexyl-4-ethyl-3-methylazetidin-2-one (**27ai**)



Mr = 195.30

To a 10 mL round-bottomed flask with large oval stirrer bar was added palladium (II) acetate (66 mg, 0.3 mmol, 1 eq), di(pentan-3-yl)amine (47.1 mg, 0.3 mmol, 1 eq) silver (I) acetate (150 mg, 0.9 mmol, 3 eq), Xantphos (17.4 mg, 0.03 mmol, 0.1 eq) 1,4-benzoquinone (66 mg, 0.6 mmol, 0.2 eq) and anhydrous toluene (3 mL). The flask was sealed with a new septum and Teflon tape. A balloon of carbon monoxide was placed on top, and the system was evacuated and backfilled with CO three times. The flask was placed into an oil bath at 80 °C and stirred at 400 rpm for 18 hours. The reaction mixture was cooled, then filtered through celite and washed with ethyl acetate. The organic solvents were removed in vacuo and the crude mixture was purified by column chromatography to obtain **27ai** as a yellow oil (29.9 mg, 51 %, d.r. > 20:1). IR ($\lambda_{\text{max}}/\text{cm}^{-1}$) 2928, 2855, 1736, 1451, 1394, 1371. ^1H NMR (400 MHz, CDCl_3) 3.42 (1H, tt, $J_1 = 11.4$ Hz, $J_2 = 3.5$ Hz, H7), 3.11 (1H, dq, $J_1 = 9.6$ Hz, $J_2 = 0.9$ Hz, H1), 2.65 (1H, qd, $J_1 = 7.4$ Hz, $J_2 = 1.9$ Hz, H4), 1.94 – 1.58 (6H, m, H2b, H8b, H9b, H10b, H11b, H12b), 1.57 – 1.28 (4H, m, H2a, H8a, H9a, H12a), 1.25 (3H, d, $J = 8.2$ Hz, H5), 1.23 – 1.05 (2H, m, H10a, H11a), 0.93 (3H, t, $J = 7.7$ Hz, H3). ^{13}C NMR (101 MHz, CDCl_3) 170.2 (C6), 60.5 (C1), 51.4 (C7), 48.6 (C4), 32.3 (C8, C9), 30.7 (C12), 27.0 (C2), 25.4 (C10), 25.3 (C11), 13.4 (C5, 9.5 (C3). HRMS (FTMS +p NSI) m/z : $[\text{M} + \text{H}]^+$ calculated for $\text{C}_{12}\text{H}_{21}\text{NO}$ 196.1696, found = 196.1696, $\Delta = 1.0$ ppm.

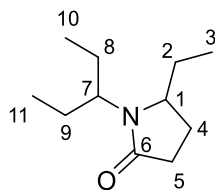
1-Cyclohexyl-5-ethylpyrrolidin-2-one (**27aii**)



Mr = 195.30

General procedure D was applied to N-(pentan-3-yl)cyclohexylamine (50.8 mg, 0.3 mmol) with 2-methyl-6-nitrobenzoic acid (16.3 mg, 0.09 mmol) in place of triisopropylbenzoic acid, and 6.25% CO / Air in place of CO. The crude reaction product was purified by column chromatography (0 to 25% ethyl acetate / petroleum ether) to give **27aii** as a yellow oil (23.4 mg, 42 %). IR ($\lambda_{\text{max}}/\text{cm}^{-1}$) 2929, 2854, 1673, 1418, 1266. ^1H NMR (400 MHz, CDCl_3) 3.66 (1H, tt, $J_1 = 11.9$ Hz, $J_2 = 3.9$ Hz, H7), 3.60 (1H, tt, $J_1 = 8.7$ Hz, $J_2 = 3.0$ Hz, H1), 2.42 (1H, m, H5b), 2.25 (1H, m, H5a), 2.05 (1H, m, H4a), 1.88 – 1.61 (8H, m, H2b, H4b, H8a, H8b, H9a, H9b, H10b, H11b), 1.56 – 1.40 (2H, m, H2a, H12b), 1.37 – 1.27 (2H, m, H10a, H11a), 1.14 (1H, m, 12a), 0.89 (3H, t, $J = 8.0$, H3). ^{13}C NMR (101 MHz, CDCl_3) 174.8 (C6), 58.5 (C1, 52.9 (C7), 31.6 (C9), 30.7 (C5), 29.9 (C8), 28.0 (C2), 26.0 (C10, C11), 25.5 (C12), 23.7 (C4), 9.0 (C3). HRMS (FTMS +p NSI) m/z : $[\text{M} + \text{H}]^+$ calculated for $\text{C}_{12}\text{H}_{21}\text{NO}$ 196.1696, found = 196.1694, $\Delta = -1.0$ ppm.

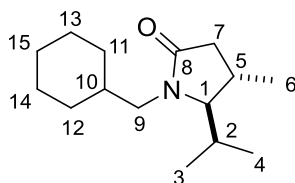
5-Ethyl-1-(pentan-3-yl)pyrrolidin-2-one (**27bii**)



Mr = 183.30

General procedure C was applied to di(pentan-3-yl)amine (47.1 mg, 0.3 mmol). The crude reaction product was purified by column chromatography (100% petroleum ether to 25 % ethyl acetate / petroleum ether) to give **27bii** as a yellow oil (30.2 mg, 55 %). IR ($\lambda_{\text{max}}/\text{cm}^{-1}$) 2965, 1933, 2876, 1678, 1417, 1263. ^1H NMR (400 MHz, CDCl_3) 3.56 (1H, p, $J = 7.6$ Hz, H7) 3.46 (1H, tt, $J_1 = 8.5$ Hz, $J_2 = 3.5$ Hz, H1) 2.45 (1H, m, H5b), 2.29 (1H, m, H5a), 2.09 (1H, m, H4a), 1.78 (1H, m, H2b), 1.67 (2H, m, H8, H9), 1.54 (1H, spt, $J = 7.0$ Hz, H4b), 1.39 (1H, m, H2a), 0.95 (6H, t, $J = 7.5$ Hz, H10, H11) 0.85 (3H, t, $J = 7.6$ Hz, H3) ^{13}C NMR (101 MHz, CDCl_3) 175.6 (C6), 59.4 (C7), 57.0 (C1), 30.6 (C5), 27.7 (C2), 27.0 (C9), 24.5 (C9), 24.0 (C4), 11.5 (C10), 11.4 (C11), 9.7 (C3) HRMS (FTMS +p NSI) m/z : $[\text{M} + \text{H}]^+$ calculated for $\text{C}_{11}\text{H}_{21}\text{NO}$ 184.1696, found = 184.1695, $\Delta = -0.5$ ppm.

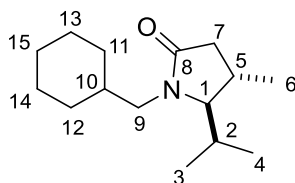
Trans-1-(cyclohexylmethyl)-5-isopropyl-4-methylpyrrolidin-2-one (30a)



Mr = 237.39

General procedure C was applied to N-(cyclohexylmethyl)-2,4-dimethylpentan-3-amine (63.4 mg, 0.3 mmol). The crude reaction product was purified by alumina column chromatography (0% - 20% ethyl acetate / petroleum ether) to give **30a** as a yellow oil (38.5 mg, 54 %, *d.r.* = 8:1). IR ($\lambda_{\text{max}}/\text{cm}^{-1}$) 2959, 2923, 2852, 1682, 1423, 1260. ^1H NMR (400 MHz, CDCl_3) 3.58 (1H, dd, $J_1 = 15.0$ Hz, $J_2 = 10.3$ Hz, H9a), 3.07 (1H, t, $J = 2.7$ Hz, H1), 2.62 – 2.52 (2H, m, H7a, H9b), 2.19 – 2.10 (1H, m, H5), 2.10 – 2.02 (1H, m, H2), 1.96 (1H, dd, $J_1 = 17.5$ Hz, $J_2 = 3.5$ Hz, H7b) 1.77 – 1.54 (8H, m, H10, H11b, H12b, H13, H14, H15b), 1.30 – 1.13 (3H, m, H11a, H12a, H15a), 1.10 (3H, d, $J = 7.0$ Hz, H6), 0.96 (3H, d, $J = 7.1$ Hz, H3), 0.74 (3H, d, $J = 7.0$ Hz, H4). ^{13}C NMR (100 MHz, CDCl_3) 174.4 (C8), 70.4 (C1), 45.8 (C9), 39.4 (C7), 35.2 (C10), 31.2 (C13), 30.5 (C11), 28.2 (C2), 26.4 (C14), 25.9 (C12), 15.6 (C15), 25.1 (C5), 23.2 (C6), 18.5 (C3), 14.9 (C4). HRMS (FTMS +p NSI) m/z : $[\text{M} + \text{H}]^+$ calculated for $\text{C}_{15}\text{H}_{27}\text{NO}$ 238.2165, found = 238.2165, exact match.

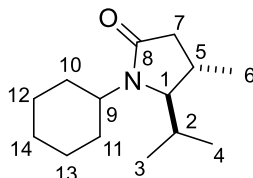
Trans-1-(cyclohexylmethyl)-5-isopropyl-4-methylpyrrolidin-2-one (30a)



Mr = 237.39

General procedure D was applied to N-(cyclohexylmethyl)-2,4-dimethylpentan-3-amine (63.4 mg, 0.3 mmol). The crude reaction product was purified by alumina column chromatography (0% - 20% ethyl acetate / petroleum ether) to give **30a** as a yellow oil (50.1 mg, 70 %, *d.r.* = 10:1).

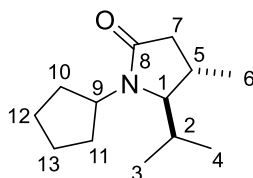
Trans-1-cyclohexyl-5-isopropyl-4-methylpyrrolidin-2-one (30b)



Mr = 223.36

General procedure D was applied to N-(2,4-dimethylpentan-3-yl)cyclohexanamine 238 (59.1 mg, 0.3 mmol). The crude reaction product was purified by silica column chromatography (0% - 30% ethyl acetate / petroleum ether) to give **30b** as a yellow oil (44.0 mg, 66 %, *d.r.* = 8:1). IR ($\lambda_{\text{max}}/\text{cm}^{-1}$) 2958, 2930, 1675, 1420, 1253, 894, 751, 663. ^1H NMR (400 MHz, CDCl_3) 3.63 (1H, tt, $J = 12.0, 3.9$ Hz, H9), 3.09 (1H, d, $J = 2.2$ Hz, H1), 2.58 (1H, dd, $J_1 = 17.1$ Hz, $J_2 = 8.9$ Hz, H7a), 2.13 – 1.94 (2H, m, H2, H5), 1.93 – 1.59 (6H, m, H7b, H10a – H14a), 1.51 (1H, dq, $J_1 = 12.3$ Hz, $J_2 = 3.5$ Hz, H14b), 1.39 – 1.10 (4H, m, H10b – H13b), 1.03 (3H, d, $J = 7.1$ Hz, H6), 0.94 (3H, d, $J = 6.9$ Hz, H3), 0.80 (3H, d, $J = 6.8$ Hz, H4). ^{13}C NMR (1001 MHz, CDCl_3) 174.3 (C8), 71.1 (C1), 53.3 (C9), 40.2 (C7), 31.6 (C10), 31.4 (C11), 29.9 (C2), 26.2 (C12), 25.7 (C13), 25.6 (C14), 23.3 (C6), 19.0 (C3), 15.1 (C4). HRMS (ESI) m/z : calculated for $\text{C}_{14}\text{H}_{26}\text{O}_1\text{N}_1$ $[\text{M}+\text{H}]^+$ 224.2009, found 224.2008, $\Delta = -0.4$ ppm.

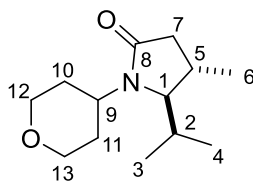
Trans-1-cyclopentyl-5-isopropyl-4-methylpyrrolidin-2-one (30c)



Mr = 209.33

General procedure D was applied to N-(2,4-dimethylpentan-3-yl)cyclopentanamine (55.0 mg, 0.3 mmol). The crude reaction product was purified by alumina column chromatography (5% - 25% ethyl acetate / petroleum ether) to give **30c** as a yellow oil (40.8 mg, 65%, *d.r.* = 11:1). IR ($\lambda_{\text{max}}/\text{cm}^{-1}$) 2957, 2869, 1674, 1449, 1422, 1373, 1322, 1263, 1234. ^1H NMR (400 MHz, CDCl_3) 3.96 – 3.81 (1H, m, H9), 3.06 (1H, d, $J = 2.1$ Hz, H1), 2.58 (1H, dd, $J_1 = 17.5$ Hz, $J_2 = 8.6$ Hz, H7a), 2.14 – 2.09 (1H, m, H5), 2.04 – 1.97 (1H, m, H2), 1.96 – 1.48 (9H, m, H7b, H10 – H13), 1.05 (3H, d, $J = 7.5$ Hz, H6), 0.94 (3H, d, $J = 6.8$ Hz, H3), 0.80 (3H, d, $J = 7.0$ Hz, H4). ^{13}C NMR (101 MHz, CDCl_3) 174.3 (C8), 72.2 (C1), 55.1 (C9), 40.2 (C7), 30.9 (C2), 29.7 (C10), 28.3 (C11), 25.5 (C5), 23.9 (C12), 23.8 (C13), 23.2 (C6), 18.8 (C3), 15.0 (C4). HRMS (FTMS +p NSI) m/z : $[\text{M} + \text{H}]^+$ calculated for $\text{C}_{15}\text{H}_{27}\text{NO}$ 210.1852, found = 210.1852, exact match.

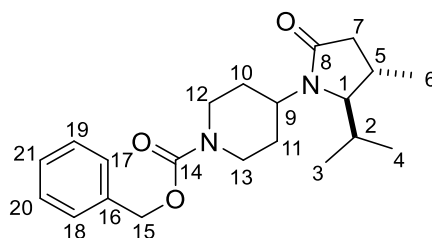
Trans 5-isopropyl-4-methyl-1-(tetrahydro-2H-pyran-4-yl)pyrrolidin-2-one (30d)



Mr = 225.33

General procedure D was applied to N-(2,4-dimethylpentan-3-yl)tetrahydro-2H-pyran-4-amine (59.8 mg, 0.3 mmol). The crude reaction product was purified by alumina column chromatography (50% - 90% ethyl acetate / petroleum ether) to give **30d** as a yellow oil (55.0 mg, 74%, *d.r.* = 8:1). IR ($\lambda_{\text{max}}/\text{cm}^{-1}$) 2957, 2870, 1673, 1421, 1375, 1145. ^1H NMR (400 MHz, CDCl_3) 4.08 – 3.92 (3H, m, H9, H12a, H13a), 3.50 – 3.40 (2H, m, H12b, H13b), 3.11 (1H, dd, J_1 = 3.2 Hz, J_2 = 1.0 Hz, H1), 2.60 (1H, dd, J_1 = 17.6 Hz, J_2 = 9.0 Hz, H7a), 2.19 – 1.99 (3H, m, H5, H10a, H11a), 1.88 (1H, dd, J_1 = 16.8 Hz, J_2 = 2.4 Hz, H7b), 1.87 – 1.77 (2H, m, H2, H10b), 1.59 – 1.52 (1H, m, H11), 1.04 (3H, d, J = 7.3 Hz, H6), 0.95 (3H, d, J = 7.0 Hz, H3), 0.80 (3H, d, J = 7.0 Hz, H4). ^{13}C NMR (101 MHz, CDCl_3) 174.5 (C8), 70.7 (C1), 67.9 (C12), 67.7 (C13), 50.1 (C9), 39.8 (C7), 31.6 (C2), 31.2 (C10), 29.7 (C11), 25.5 (C5), 23.1 (C6), 18.9 (C3), 14.8 (C4). HRMS (FTMS +p NSI) m/z : $[\text{M} + \text{H}]^+$ calculated for $\text{C}_{13}\text{H}_{23}\text{NO}_2$ 226.1802, found = 226.1801, Δ = -0.4 ppm.

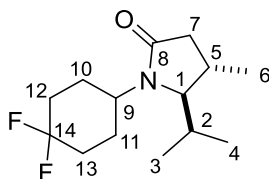
Benzyl-4-(trans-2-isopropyl-3-methyl-5-oxopyrrolidin-1-yl)piperidine-1-carboxylate (30e)



Mr = 358.48

General procedure D was applied to benzyl 4-((2,4-dimethylpentan-3-yl)amino)piperidine-1-carboxylate (99.7 mg, 0.3 mmol). The crude reaction product was purified by alumina column chromatography (70% - 100% ethyl acetate / petroleum ether) to give **30e** as a yellow oil (71.7 mg, 70%, *d.r.* = 8:1). IR ($\lambda_{\text{max}}/\text{cm}^{-1}$) 2959, 2871, 1671, 1422, 1233, 1127. ^1H NMR (400 MHz, CDCl_3) 7.37 – 7.27 (5H, m, H17 – H21), 5.11 (2H, s, H15), 4.27 (2H, br, H12, H13), 3.86 (2H, tt, J_1 = 12.5 Hz, J_2 = 4.0 Hz, H9), 3.05 (1H, d, J = 2.5 Hz, H1), 2.81 (2H, br, H12, H13), 2.58 (1H, dd, J_1 = 17.0 Hz, J_2 = 9.2 Hz, H7a), 2.17 – 2.07 (1H, m, H5), 2.00 – 1.81 (3H, m, H10a, H11a, H7b), 1.73 – 1.57 (2H, m, H10b, H11b), 1.02 (3H, d, J = 7.5 Hz, H6), 0.92 (3H, d, J = 7.1 Hz, H3), 0.77 (3H, d, J = 7.1 Hz, H4). ^{13}C NMR (101 MHz, CDCl_3) 174.4 (C8), 155.1 (C1), 136.7 (C16), 128.49, 128.03, 127.99, 127.94 (C17 – C21), 70.7 (C1), 67.2 (C15), 51.2 (C9), 13.8 (C12), 43.7 (C13), 39.8 (C7), 31.2 (C2), 28.7 (C10, C11), 25.5 (C5), 23.1 (C6), 18.2 (C3), 14.8 (C4). HRMS (FTMS +p NSI) m/z : $[\text{M} + \text{H}]^+$ calculated for $\text{C}_{21}\text{H}_{30}\text{N}_2\text{O}_3$ 359.2329, found = 359.2332, Δ = 0.8 ppm.

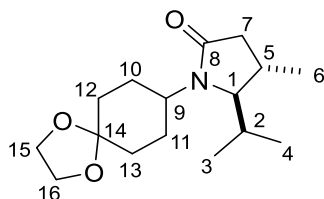
Trans-1-(4,4-difluorocyclohexyl)-5-isopropyl-4-methylpyrrolidin-2-one (30f)



Mr = 259.34

General procedure D was applied to N-(2,4-dimethylpentan-3-yl)-4,4-difluorocyclohexan-1-amine (70.0 mg, 0.3 mmol). The crude reaction product was purified by alumina column chromatography (50% - 20% ethyl acetate / petroleum ether) to give **30f** as a yellow oil (52.0 mg, 67%, *d.r.* = 11 : 1). IR ($\lambda_{\text{max}}/\text{cm}^{-1}$) 2962, 2877, 1670, 1443, 1423, 1378, 1269, 1105, 956. ^1H NMR (400 MHz, CDCl_3) 3.93 - 3.81 (1H, m, H9), 3.10 (1H, d, J = 2.9 Hz, H1), 2.59 (1H, dd, J_1 = 17.1 Hz, J_2 = 9.6 Hz, H7a), 2.27 - 1.61 (11H, m, H2, H5, H7b, H10 - H13), 1.04 (3H, d, J = 6.7 Hz, H6), 0.96 (3H, d, J = 6.6 Hz, H3), 0.80 (3H, d, J = 6.7 Hz, H4). ^{13}C NMR (101 MHz, CDCl_3) 174.5 (C8), 70.6 (C1), 50.5 (C9), 39.6 (C7), 33.1 (C14, t), 31.4 (C10), 27.1 (C12), 25.5 (C11), 25.4 (C13), 23.2 (C6), 18.9 (C3), 14.8 (C4). ^{19}F NMR (377 MHz, CDCl_3) -94.0 (d), -103.5 (d) HRMS (FTMS +p NSI) m/z : $[\text{M} + \text{H}]^+$ calculated for $\text{C}_{14}\text{H}_{23}\text{F}_2\text{NO}$ 260.1820, found = 260.1822, Δ = 0.8 ppm.

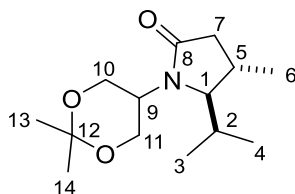
Trans-5-isopropyl-4-methyl-1-(1,4-dioxaspiro[4.5]decan-8-yl)pyrrolidin-2-one (30g)



Mr = 281.40

General procedure D was applied to N-(2,4-dimethylpentan-3-yl)-1,4-dioxaspiro[4.5]decan-8-amine (76.6 mg, 0.3 mmol). The crude reaction product was purified by alumina column chromatography (50% - 70% ethyl acetate / petroleum ether) to give **30g** as a yellow oil (59.1 mg, 70%, *d.r.* = 13 : 1). IR ($\lambda_{\text{max}}/\text{cm}^{-1}$) 2957, 2874, 1671, 1420, 1265, 1102. ^1H NMR (400 MHz, CDCl_3) 3.98 - 3.84 (5H, m H9, H15, H16), 3.12 (1H, s, H1), 2.58 (1H, dd, J_1 = 17.4 Hz, J_2 = 9.1 Hz, H7a), 2.17 - 1.60 (11H, m, H2, H5, H7b, H10 - H13), 1.02 (3H, d, J = 7.1 Hz, H6), 0.94 (3H, d, J = 7.1 Hz, H3), 0.79 (3H, d, J = 6.9 Hz, H4). ^{13}C NMR (101 MHz, CDCl_3) 174.3 (C8), 107.9 (C14), 70.2 (C1), 64.4 (C15, C16), 51.2 (C9), 39.8 (C7), 34.1 (C12), 34.1 (C13), 31.4 (C2), 28.6 (C10), 26.6 (C11), 25.4 (C5), 23.2 (C6), 18.9 (C3), 14.8 (C4). HRMS (FTMS +p NSI) m/z : $[\text{M} + \text{H}]^+$ calculated for $\text{C}_{16}\text{H}_{27}\text{NO}_3$ 282.2064, found = 282.2065, Δ = 0.4 ppm.

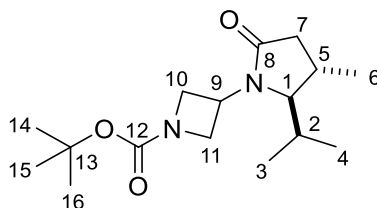
Trans-1-(2,2-dimethyl-1,3-dioxan-5-yl)-5-isopropyl-4-methylpyrrolidin-2-one (30h)



Mr = 255.36

General procedure D was applied to N-(2,4-dimethylpentan-3-yl)-2,2-dimethyl-1,3-dioxan-5-amine (68.8 mg, 0.3 mmol). The crude reaction product was purified by alumina column chromatography (10% - 40% ethyl acetate / petroleum ether) to give **30h** as a yellow oil (54.2 mg, 71%, *d.r.* = 14 : 1). IR ($\lambda_{\text{max}}/\text{cm}^{-1}$) 2961, 2875, 1675, 1423, 1372, 1257, 1199, 1123, 1092. ^1H NMR (400 MHz, CDCl_3) 4.51 (1H, dd, $J_1 = 10.6$ Hz, $J_2 = 8.5$ Hz, H10a) 4.37 (1H, dd, $J_1 = 11.6$ Hz, $J_2 = 8.1$ Hz, H11a), 3.87 – 3.80 (2H, m, H10b, H11b), 3.70 – 3.62 (1H, m, H9) 3.17 (1H, d, $J = 2.4$ Hz, H1), 2.59 (1H, dd, $J_1 = 17.5$ Hz, $J_2 = 9.5$ Hz, H7a) 2.26 – 2.14 (2H, m, H2, H5), 1.87 (1H, $J_1 = 17.5$ Hz, $J_2 = 1.8$ Hz, H7b), 1.55 (3H, s, H13), 1.43 (3H, s, H14), 1.09 (3H, d, $J = 7.0$ Hz, H6), 0.98 (3H, d, $J = 6.7$ Hz, H3), 0.83 (3H, d, $J = 7.0$ Hz, H4). ^{13}C NMR (101 MHz, CDCl_3) 175.2 (C8), 98.1 (C12), 73.0 (C1), 60.7 (C10), 59.9 (C11), 48.0 (C9), 39.7 (C7), 30.3 (C2), 26.0 (C5), 25.9 (C14), 23.1 (C6), 21.8 (C13), 18.8 (C3), 15.1 (C4). HRMS (FTMS +p NSI) m/z : $[\text{M} + \text{H}]^+$ calculated for $\text{C}_{14}\text{H}_{25}\text{NO}_3$ 256.1907, found = 256.1910, $\Delta = 1.2$ ppm.

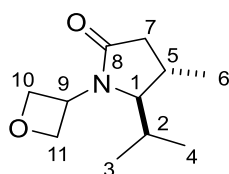
Tert-butyl 3-((trans-2-isopropyl-3-methyl-5-oxopyrrolidin-1-yl)azetidine-1-carboxylate (30i)



Mr = 296.41

General procedure D was applied to tert-butyl 3-((2,4-dimethylpentan-3-yl)amino)azetidine-1-carboxylate (81.1 mg, 0.3 mmol). The crude reaction product was purified by alumina column chromatography (40% - 60% ethyl acetate / petroleum ether) to give **30i** as a yellow oil (44.3 mg, 50%, *d.r.* = 11:1). IR ($\lambda_{\text{max}}/\text{cm}^{-1}$) 2963, 1685, 1390, 1364, 1255, 1132. ^1H NMR (400 MHz, CDCl_3) 4.37 – 4.02 (5H, m, H9 – H11), 3.16 (1H, dd, 3.7 Hz, 1.4 Hz, H1), 2.57 (1H, dd, $J_1 = 17.3$ Hz, $J_2 = 9.3$ Hz, H7a), 2.21 – 2.12 (1H, m, H5), 1.93 (1H, dd, $J_1 = 17.1$ Hz, $J_2 = 2.7$ Hz, H7b), 1.89 – 1.82 (1H, m, H2), 1.10 (3H, d, $J = 6.9$ Hz, H6), 0.94 (3H, d, $J = 7.1$ Hz, H3), 0.78 (3H, d, $J = 6.9$ Hz, H4). ^{13}C NMR (101 MHz, CDCl_3) 175.0 (C8), 156.4 (C12), 79.8 (C13), 71.4 (C1), 53.8 (C10 – C11), 42.9 (C9), 39.6 (C7), 30.9 (C2), 28.4 (C14 – C16), 25.9 (C5), 23.1 (C6), 18.5 (C3), 15.5 (C4). HRMS (FTMS +p NSI) m/z : $[\text{M} + \text{H}]^+$ calculated for $\text{C}_{16}\text{H}_{28}\text{N}_2\text{O}_3$ 297.2173, found = 297.2174, $\Delta = 0.3$ ppm.

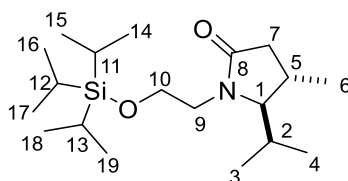
Trans-5-isopropyl-4-methyl-1-(oxetan-3-yl)pyrrolidin-2-one (30j)



Mr = 197.28

General procedure D was applied to N-(2,4-dimethylpentan-3-yl)oxetan-3-amine (51.3 mg, 0.3 mmol). The crude reaction product was purified by alumina column chromatography (50% - 70% ethyl acetate / petroleum ether) to give **30j** as a yellow oil (16.8 mg, 28%, *d.r.* = 7:1). IR ($\lambda_{\text{max}}/\text{cm}^{-1}$) 2960, 2876, 1678, 1421, 1389, 1377, 1265, 972. ^1H NMR (400 MHz, CDCl_3) 4.96 – 4.71 (5H, m, H9 – H11), 3.21 (1H, dd, $J_1 = 3.7$ Hz, $J_2 = 1.7$ Hz), 2.58 (1H, dd, $J_1 = 17.6$ Hz, $J_2 = 9.6$ Hz, H7a), 2.24 – 2.14 (1H, m, H5), 1.95 (1H, dd, $J_1 = 17.5$ Hz, $J_2 = 2.3$ Hz, H7b), 1.90 – 1.81 (1H, m, H2), 1.13 (3H, d, $J = 7.3$ Hz, H6), 0.94 (3H, d, $J = 7.1$ Hz, H3), 0.78 (3H, d, $J = 7.1$ Hz, H4). ^{13}C NMR (101 MHz, CDCl_3) 174.8 (C8), 76.1 (C10), 74.7 (C11), 70.8 (C1), 47.8 (C9), 39.4 (C7), 30.9 (C2), 26.0 (C5), 23.1 (C6), 18.5 (C3), 15.5 (C4). HRMS (FTMS +p NSI) m/z : $[\text{M} + \text{H}]^+$ calculated for $\text{C}_{11}\text{H}_{29}\text{NO}_2$ 198.1489, found = 198.1488, $\Delta = -0.5$ ppm.

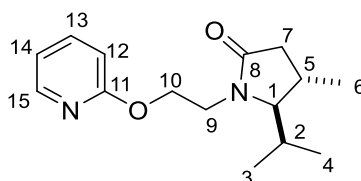
Trans-5-isopropyl-4-methyl-1-(2-((triisopropylsilyl)oxy)ethyl)pyrrolidin-2-one (30k)



Mr = 341.61

General procedure D was applied to 2,4-dimethyl-N-(2-((triisopropylsilyl)oxy)ethyl)pentan-3-amine (94.7 mg, 0.3 mmol) with 2-methyl-6-nitrobenzoic acid (16.3 mg, 0.09 mmol) in place of triisopropylbenzoic acid. The crude reaction product was purified by alumina column chromatography (10% - 30% ethyl acetate / petroleum ether) to give **30k** as a yellow oil (48.1 mg, 47%, *d.r.* = 5:1). IR ($\lambda_{\text{max}}/\text{cm}^{-1}$) 2959, 2942, 2866, 1682, 1462, 1258, 1104. ^1H NMR (400 MHz, CDCl_3) 3.90 – 3.77 (3H, m, H9a, H10), 3.39 (1H, t, $J = 3.0$ Hz, H1), 3.02 – 2.93 (1H, m, H9b), 2.56 (1H, dd, $J_1 = 17.8$ Hz, $J_2 = 9.2$ Hz, H7a), 2.21 – 2.08 (2H, m, H2, H5), 1.93 (1H, dd, $J_1 = 17.4$ Hz, $J_2 = 3.4$ Hz, H7b), 1.09 (3H, d, $J = 7.0$ Hz, H6), 1.07 – 1.03 (21H, m, H11-H19), 0.94 (3H, d, $J = 7.0$ Hz, H3), 0.74 (3H, d, $J = 7.0$ Hz, H4). ^{13}C NMR (101 MHz, CDCl_3) 174.4 (C8), 71.5 (C1), 62.1 (C10), 42.8 (C9), 39.2 (C7), 28.4 (C5), 25.4 (C2), 23.0 (C6), 18.5 (C3), 18.0 (C14 – C19), 15.0 (C4), 11.9 (C11 – C13). HRMS (FTMS +p NSI) m/z : $[\text{M} + \text{H}]^+$ calculated for $\text{C}_{19}\text{H}_{39}\text{NO}_2\text{Si}$ 342.2823, found = 342.2824, $\Delta = 0.3$ ppm.

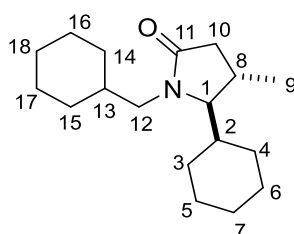
Trans-5-isopropyl-4-methyl-1-(2-(pyridin-2-yloxy)ethyl)pyrrolidin-2-one (30l)



Mr = 262.35

General procedure D was applied to 2,4-dimethyl-N-(2-(pyridin-2-yloxy)ethyl)pentan-3-amine (70.9 mg, 0.3 mmol) with 2-methyl-6-nitrobenzoic acid (16.3 mg, 0.09 mmol) in place of triisopropylbenzoic acid. The crude reaction product was purified by alumina column chromatography (30% - 50% ethyl acetate / petroleum ether) to give **30l** as a yellow oil (60.0 mg, 76%, *d.r.* = 5:1). IR ($\lambda_{\text{max}}/\text{cm}^{-1}$) 2960, 1680, 1595, 1570, 1466, 1431, 1273, 1142. ^1H NMR (400 MHz, CDCl_3) 8.14 – 8.10 (1H, m, H15), 7.58 – 7.52 (1H, m, H13), 6.87 – 6.83 (1H, m, H14), 4.53 – 4.45 (1H, m, H10a), 4.46 – 4.38 (1H, m, H10b), 4.07 (1H, ddd, $J_1 = 14.5$ Hz, $J_2 = 6.3$ Hz, $J_3 = 5.7$ Hz, H9a), 3.29 – 3.25 (1H, m, H9b), 3.23 (1H, t, $J = 3.1$ Hz, H1), 2.57 (1H, dd, $J_1 = 17.7$ Hz, $J_2 = 9.3$ Hz, H7a), 2.19 – 2.04 (2H, m, H2, H5), 1.92 (1H, dd, $J_1 = 17.4$ Hz, $J_2 = 2.9$ Hz, H7b), 1.04 (3H, d, $J = 6.5$ Hz, H6), 0.94 (3H, d, $J = 7.4$ Hz, H3), 0.76 (3H, d, $J = 7.5$ Hz, H4). ^{13}C NMR (101 MHz, CDCl_3) 174.7 (C8), 163.3 (C11), 146.9 (C15), 138.7 (C13), 117.0 (C14), 111.0 (C12), 71.2 (C1), 63.0 (C10), 39.7 (C9), 39.2 (C7), 28.7 (C2), 25.7 (C5), 22.9 (C6), 18.5 (C3), 15.2 (C4). HRMS (FTMS +p NSI) m/z : $[\text{M} + \text{H}]^+$ calculated for $\text{C}_{15}\text{H}_{22}\text{N}_2\text{O}_2$ 263.1754, found = 263.1756, $\Delta = 0.8$ ppm.

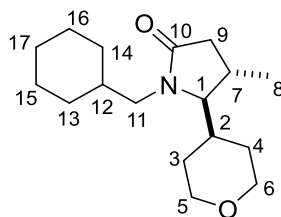
Trans-5-cyclohexyl-1-(cyclohexylmethyl)-4-methylpyrrolidin-2-one (30n)



Mr = 277.45

General procedure D was applied to 1-cyclohexyl-N-(cyclohexylmethyl)-2-methylpropan-1-amine (75.4 mg, 0.3 mmol). The crude reaction product was purified by silica column chromatography (0% - 30% ethyl acetate / petroleum ether) to give **30n** as a yellow oil (53 mg, 62%, *d.r.* = 8 : 1). IR ($\lambda_{\text{max}}/\text{cm}^{-1}$) 2923, 2847, 1672, 1448, 1424, 1271, 1250, 894; ^1H NMR (400 MHz, CDCl_3) 3.56 (1H, dd, $J_1 = 13.8$ Hz, $J_2 = 9.1$ Hz, H12a), 3.07 – 2.93 (1H, m, H4), 2.63 – 2.51 (2H, m, H9b, H10a), 2.23 – 2.11 (1H, m, H8), 1.94 (1H, dd, $J_1 = 17.2$ Hz, $J_2 = 2.8$ Hz, H10b), 1.86 – 1.40 (12H, m, H2a – H7a, H13a – H18a), 1.37 – 1.10 (6H, m, H3b, H4b, H7b, H14b, H15b, H18b), 1.08 (3H, d, $J = 7.0$ Hz, H9), 1.05 – 0.77 (4H, m, H5b, H6b, H16b, H17b). ^{13}C NMR (101 MHz, CDCl_3) 174.5, 70.4, 46.1, 39.5, 39.2, 35.5, 31.4, 30.7, 29.4, 26.7, 26.7, 26.6, 26.2, 26.0, 25.9, 25.8, 23.3. HRMS (ESI) m/z : calculated for $\text{C}_{18}\text{H}_{32}\text{O}_1\text{N}_1$ $[\text{M} + \text{H}]^+$ 278.2478, found 278.2478, exact match.

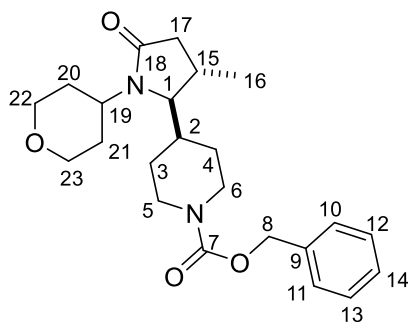
Trans-1-(cyclohexylmethyl)-4-methyl-5-(tetrahydro-2H-pyran-4-yl)pyrrolidin-2-one (30p)



Mr = 279.42

General procedure D was applied to N-(cyclohexylmethyl)-2-methyl-1-(tetrahydro-2H-pyran-4-yl)propan-1-amine (76.0 mg, 0.3 mmol). The crude reaction product was purified by silica column chromatography (100% ethyl acetate) to give **30p** as a yellow oil (49.1 mg, 55%). IR ($\lambda_{\text{max}}/\text{cm}^{-1}$) 2914, 2847, 1674, 1435, 1423, 1091. ^1H NMR (400 MHz, CDCl_3) 4.12 – 3.93 (2H, m, H5a, H6a), 3.60 (1H, dd, $J_1 = 13.8$ Hz, $J_2 = 9.2$ Hz, H11a), 3.40 (1H, td, $J_1 = 11.7$ Hz, $J_2 = 2.3$ Hz, H5b), 3.36 – 3.25 (1H, m, H6b), 3.13 – 3.02 (1H, m, H1), 2.65 – 2.48 (2H, m, H9a, H11b), 2.27 – 2.17 (1H, m, H7), 1.97 (1H, dd, $J_1 = 17.3$ Hz, $J_2 = 2.7$ Hz, H9b), 1.98 – 1.86 (1H, m, H2), 1.78 – 1.48 (7H, m, H3a, H4a, H13a - H17a), 1.45 – 1.37 (1H, m, H12a), 1.35 – 1.13 (5H, m, H3b, H4b, H13b, H14b, H17b), 1.11 (3H, d, $J = 7.0$ Hz, H8), 1.06 – 0.86 (2H, m, H15b, H16b). ^{13}C NMR (101 MHz, CDCl_3) 174.5 (C10), 69.6 (C1), 68.1 (C5), 68.1 (C6), 46.2 (C11), 39.2 (C9), 36.7 (C2), 35.5 (C12), 31.4 (C13), 30.6 (C4), 29.0 (C3), 26.6 (C7), 26.5 (C17), 26.3 (C10), 26.0 (C15), 25.8 (C16), 23.2 (C8). HRMS (ESI) m/z : calculated for $\text{C}_{17}\text{H}_{30}\text{O}_2\text{N}_1$ $[\text{M}+\text{H}]^+$ 280.2271, found 280.2274, $\Delta = 1.0$ ppm.

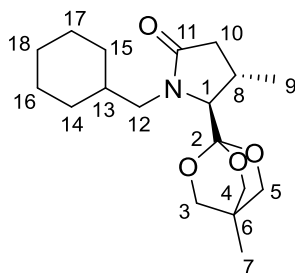
Benzyl 4-(trans-3-methyl-5-oxo-1-(tetrahydro-2H-pyran-4-yl)piperolidin-2-yl)piperidine-1-carboxylate (30q)



Mr = 400.52

General procedure D was applied to benzyl 4-(2-methyl-1-((tetrahydro-2H-pyran-4-yl)amino)propyl)piperidine-1-carboxylate (112.3 mg, 0.3 mmol). The crude reaction product was purified by alumina column chromatography (70% - 100% ethyl acetate / petroleum ether) to give **30q** as a yellow oil (66.1 mg, 55%, $d.r. = 8:1$). IR ($\lambda_{\text{max}}/\text{cm}^{-1}$) 2958, 1680, 1423, 1274, 1224, 1144, 1085. ^1H NMR (400 MHz, CDCl_3) 7.39 – 7.27 (5H, m, H10 – H14), 5.12 (2H, s, H8), 4.30 (2H, br, H5a, H6a), 4.10 – 3.95 (3H, m, H19, H22a, H23a), 3.51 – 3.41 (2H, m, H22b, H23b), 3.14 (1H, d, $J = 2.7$ Hz, H1), 2.76 (1H, br, H5b), 2.63 (1H, br, H6b), 2.55 (1H, dd, $J_1 = 16.9$ Hz, $J_2 = 6.7$ Hz, H17a), 2.17 – 1.96 (3H, m, H15, H17b, H21), 1.93 – 1.70 (5H, m, H2, H3a, H4a, H20), 1.61 – 1.47 (3H, m, H3b, H4b, H21), 1.03 (3H, d, $J = 6.9$ Hz, H16). ^{13}C NMR (101 MHz, CDCl_3) 174.3 (C18), 155.2 (C7), 136.7 (C9), 128.5, 128.1, 128.0 (C10 – C14), 69.3 (C1), 67.6 (C22), 67.5 (C23), 67.2 (C8), 50.1 (C19), 44.2 (C5), 44.2 (C6), 40.7 (C15), 39.5 (C17), 31.9 (C20), 29.8 (C21), 28.5 (C3), 26.8 (C15), 25.1 (C4), 22.9 (C16). HRMS (FTMS +p NSI) m/z : $[\text{M} + \text{H}]^+$ calculated for $\text{C}_{15}\text{H}_{27}\text{NO}$ 401.2135, found = 401.2432, $\Delta = -0.7$ ppm.

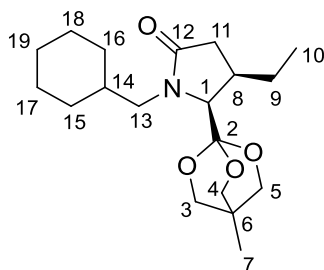
(4S,5S)-1-(cyclohexylmethyl)-4-methyl-5-(4-methyl-2,6,7-trioxabicyclo[2.2.2]octan-1-yl)pyrrolidin-2-one (30s)



Mr = 323.43

General procedure D was applied to N-(cyclohexylmethyl)-2-methyl-1-(4-methyl-2,6,7-trioxabicyclo[2.2.2]octan-1-yl)propan-1-amine (89.1 mg, 0.3 mmol). The crude reaction product was purified by silica column chromatography (0% - 40% ethyl acetate / petroleum ether) to give **30s** as a yellow oil (52.8 mg, 54%, d.r. = 5 : 1). $[\alpha]_D^{20} = -8.6^\circ$ (c. 0.9, CHCl₃). IR ($\lambda_{\max}/\text{cm}^{-1}$) 2925, 1683, 1046, 987, 736; ¹H NMR (400 MHz, CDCl₃) 3.89 (6H, s, H3 - H6), 3.56 (1H, dd, $J_1 = 13.6$ Hz, $J_2 = 9.2$ Hz, H12a), 3.22 (1H, d, $J = 1.1$ Hz, H1), 3.05 (1H, dd, $J_1 = 13.6$ Hz, $J_2 = 5.0$ Hz, H12b), 2.73 (1H, dd, $J_1 = 16.5$ Hz, $J_2 = 8.7$ Hz, H10a), 2.59 – 2.48 (1H, m, H8), 1.83 (1H, dd, $J_1 = 16.6$ Hz, $J_2 = 1.7$ Hz, H10b), 1.80 – 1.50 (6H, m, H13a – H18a), 1.38 – 1.12 (3H, m, H13b, H14b, H18b), 1.10 (3H, d, $J = 7.2$ Hz, H9), 1.06 – 0.85 (2H, m, H16b, H17b), 0.82 (3H, s, H7). ¹³C NMR (101 MHz, CDCl₃) 176.0 (C11), 109.3 (C2), 72.5 (C3 - C6), 68.1 (C1), 47.7 (C12), 38.5 (C10), 35.0 (C13), 31.1 (C6), 30.7 (C14), 30.5 (C15), 27.5 (C8), 26.5 (C18), 26.0 (C16), 25.7 (C17), 22.0 (C9), 14.4 (C7). HRMS (ESI) m/z : calculated for C₁₈H₃₀O₄N₁ [M+H]⁺ 324.2169, found 324.2161, $\Delta = -2.5$ ppm.

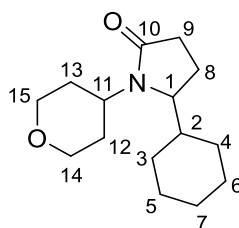
(4R,5S)-1-(cyclohexylmethyl)-4-ethyl-5-(4-methyl-2,6,7-trioxabicyclo[2.2.2]octan-1-yl)pyrrolidin-2-one (30t)



Mr = 337.46

General procedure D was applied to (1S,2S)-N-(cyclohexylmethyl)-2-methyl-1-(4-methyl-2,6,7-trioxabicyclo[2.2.2]octan-1-yl)butan-1-amine (93.4 mg, 0.3 mmol) with 2-methyl-6-nitrobenzoic acid (16.3 mg, 0.09 mmol) in place of triisopropylbenzoic acid. The crude reaction product was purified by alumina column chromatography (10% - 40% ethyl acetate / petroleum ether) to give **30t** as a yellow oil (57.5 mg, 57%). IR ($\lambda_{\max}/\text{cm}^{-1}$) 2959, 2923, 2874, 1683, 1452, 1419, 1266, 1065, 1042. ¹H NMR (400 MHz, CDCl₃) 3.81 (6H, s, H3 – H5), 3.59 (1H, dd, $J_1 = 14.2$ Hz, $J_2 = 9.2$ Hz, H13a), 3.49 (1H, d, $J = 6.3$ Hz, H1), 3.05 (1H, dd, $J_1 = 14.6$ Hz, $J_2 = 6.3$ Hz, H13b), 2.30 – 2.18 (2H, m, H8, H11a), 1.83 – 1.48 (9H, m, H9 H11b, H14a, H15a, H16a, H17a, H18a, H19a), 1.28 – 1.09 (3H, m, H15b, H16b, H19b), 0.99 – 0.81 (5H, m, H17b, H18b, H10), 0.78 (3H, s, H7). ¹³C NMR (101 MHz, CDCl₃) 176.4 (C12), 110.1 (C2), 72.5 (C3 – C5), 62.9 (C1), 48.6 (C13), 40.3 (C8), 36.5 (C11), 36.4 (C14), 31.0 (C6), 30.6, 30.5, 26.6, 26.0, 25.8 (C15 – C19), 22.8 (C9), 14.5 (C7), 13.2 (C10). HRMS (FTMS +p NSI) m/z : [M + H]⁺ calculated for C₁₅H₂₇NO 280.2271, found = 280.2272, $\Delta = 0.4$ ppm.

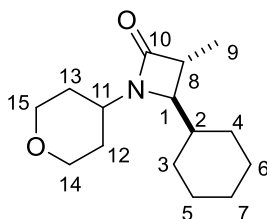
5-Cyclohexyl-1-(tetrahydro-2H-pyran-4-yl)pyrrolidin-2-one (30v)



Mr = 251.37

General procedure D was applied to N-(1-cyclohexylpropyl)tetrahydro-2H-pyran-4-amine (67.6 mg, 0.3 mmol) with 2-methyl-6-nitrobenzoic acid (16.3 mg, 0.09 mmol) in place of triisopropylbenzoic acid, and 6.25% CO / Air in place of CO. The crude reaction product was purified by alumina column chromatography (50% - 75% ethyl acetate / petroleum ether) to give **30v** as a yellow oil (30.1 mg, 40%,). IR ($\lambda_{\text{max}}/\text{cm}^{-1}$) 2925, 2852, 1666, 1451, 1421, 1382, 1281, 1145, 1087, 1009. ^1H NMR (400 MHz, CDCl_3) 4.10 – 3.88 (3H, m, H11, H14a, H15a), 3.59 (1H, dt, $J_1 = 9.1$ Hz, $J_2 = 2.8$ Hz, H1), 3.49 – 3.41 (2H, m, H14, H15), 2.42 – 2.20 (2H, m, H9), 2.10 (1H, qd, $J_1 = 12.1$ Hz, $J_2 = 4.9$ Hz, H8a), 1.97 – 1.47 (11H, m, H2, H(3 – 7)a, H8b, H12, H13), 1.35 – 0.86 (5H, m, H(3 – 7)b). ^{13}C NMR (101 MHz, CDCl_3) 175.2 (C10), 67.7 (C14), 67.6 (C15), 62.1 (C1), 50.2 (C11), 41.9 (C2), 31.6 (C12), 31.4 (C9), 29.8 (C8), 29.6 (C13), 26.6 (C3), 26.5 (C4), 25.9 (C5), 25.0 (C6), 19.7 (C7). HRMS (FTMS +p NSI) m/z : $[\text{M} + \text{H}]^+$ calculated for $\text{C}_{15}\text{H}_{25}\text{NO}_2$ 252.1958, found = 252.1961, $\Delta = 1.2$ ppm.

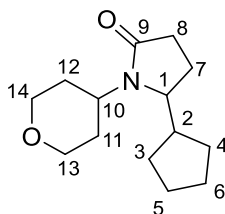
Trans-4-cyclohexyl-3-methyl-1-(tetrahydro-2H-pyran-4-yl)azetidin-2-one (31v)



Mr = 251.37

General procedure D was applied to N-(1-cyclohexylpropyl)tetrahydro-2H-pyran-4-amine (67.6 mg, 0.3 mmol). The crude reaction product was purified by alumina column chromatography (50% - 75% ethyl acetate / petroleum ether) to give **31v** as a yellow oil (19.6 mg, 26%,). IR ($\lambda_{\text{max}}/\text{cm}^{-1}$) 2923, 2851, 1734, 1449, 1376, 1358, 1142, 1088, 1008. ^1H NMR (400 MHz, CDCl_3) 4.01 – 3.93 (2H, m, H14, H15), 3.63 (1H, tt, $J_1 = 10.8$ Hz, $J_2 = 4.1$ Hz, H1), 3.45 – 3.34 (2H, m, H14, H15), 3.12 (1H, dd, $J_1 = 4.7$ Hz, $J_2 = 2.1$ Hz, H1), 2.83 (1H, qd, $J_1 = 7.4$ Hz, $J_2 = 2.3$ Hz, H8), 1.99 (1H, qd, $J_1 = 12.1$ Hz, $J_2 = 4.5$ Hz, H2), 1.84 – 1.58 (9H, m, H3a – H7a, H12, H13), 1.22 (3H, d, $J = 7.7$ Hz, H9), 1.33 – 1.09 (3H, m, H3b, H4b, H7b), 1.06 – 0.92 (2H, m, H5b, H6b). ^{13}C NMR (101 MHz, CDCl_3) 171.1 (C10), 67.0 (C14), 66.9 (C15), 64.3 (C1), 49.4 (C11), 44.9 (C8), 39.9 (C2), 31.8 (C12), 30.6 (C13), 30.0 (C7), 26.6 (C3), 26.4 (C4), 26.2 (C5), 25.8 (C6), 13.8 (C9). HRMS (FTMS +p NSI) m/z : $[\text{M} + \text{H}]^+$ calculated for $\text{C}_{15}\text{H}_{25}\text{NO}_2$ 252.1958, found = 252.1959, $\Delta = 0.4$ ppm.

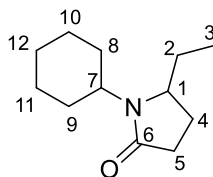
5-Cyclopentyl-1-(tetrahydro-2H-pyran-4-yl)pyrrolidin-2-one (30w)



Mr = 237.34

General procedure D was applied to N-(1-cyclopentylpropyl)tetrahydro-2H-pyran-4-amine (63.4 mg, 0.3 mmol) with 2-methyl-6-nitrobenzoic acid (16.3 mg, 0.09 mmol) in place of triisopropylbenzoic acid, and 6.25% CO / Air in place of CO. The crude reaction product was purified by alumina column chromatography (60% - 80% ethyl acetate / petroleum ether) to give **30w** as a yellow oil (44.0 mg, 62%). IR ($\lambda_{\text{max}}/\text{cm}^{-1}$) 2953, 2868, 1666, 1448, 1421, 1144, 1087, 1008. ^1H NMR (400 MHz, CDCl_3) 4.78 – 3.80 (4H, m, H1, H10, H13, H14), 3.43 (2H, td, $J_1 = 11.9$ Hz, $J_2 = 1.8$ Hz, H13, H14), 2.50 – 2.24 (3H, m, H7a, H11a, H12a), 2.18 (1H, tq, $J_1 = 12.5$ Hz, $J_2 = 4.8$ Hz, H8a), 2.06 – 1.86 (2H, H2, H8b), 1.87 – 1.52 (9H, m, H3, H4, H5a, H6a, H7b, H11b, H12b), 1.27 – 1.13 (2H, m, H5b, H6b). ^{13}C NMR (101 MHz, CDCl_3) 175.1 (C9), 67.8 (C13), 67.7 (C14), 59.7 (C1), 50.4 (C10), 43.5 (C2), 31.4 (C11), 31.3 (C8), 31.0 (C12), 30.2 (C7), 25.9 (C3, C4), 25.8 (C5), 19.7 (C6). HRMS (FTMS +p NSI) m/z : $[\text{M} + \text{H}]^+$ calculated for $\text{C}_{15}\text{H}_{25}\text{NO}_2$ 238.1802, found = 238.1804, $\Delta = 0.8$ ppm.

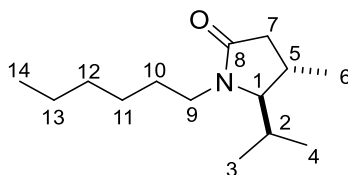
1-Cyclohexyl-5-ethylpyrrolidin-2-one (30x)



Mr = 195.30

General procedure D was applied to N-(pentan-3-yl)cyclohexylamine (50.8 mg, 0.3 mmol) with 2-methyl-6-nitrobenzoic acid (16.3 mg, 0.09 mmol) in place of triisopropylbenzoic acid, and 6.25% CO / Air in place of CO. The crude reaction product was purified by column chromatography (0 to 25% ethyl acetate / petroleum ether) to give **30x** as a yellow oil (23.4 mg, 42 %). IR ($\lambda_{\text{max}}/\text{cm}^{-1}$) 2929, 2854, 1673, 1418, 1266. ^1H NMR (400 MHz, CDCl_3) 3.66 (1H, tt, $J_1 = 11.9$ Hz, $J_2 = 3.9$ Hz, H7), 3.60 (1H, tt, $J_1 = 8.7$ Hz, $J_2 = 3.0$ Hz, H1), 2.42 (1H, m, H5b), 2.25 (1H, m, H5a), 2.05 (1H, m, H4a), 1.88 – 1.61 (8H, m, H2b, H4b, H8a, H8b, H9a, H9b, H10b, H11b), 1.56 – 1.40 (2H, m, H2a, H12b), 1.37 – 1.27 (2H, m, H10a, H11a), 1.14 (1H, m, 12a), 0.89 (3H, t, $J = 8.0$, H3) ^{13}C NMR (101 MHz, CDCl_3) 174.8 (C6), 58.58 (C1), 52.91 (C7), 31.64 (C9), 30.74 (C5), 29.98 (C8), 28.01 (C2), 26.01 (C10, C11), 25.58 (C12), 23.72 (C4), 9.07 (C3). HRMS (FTMS +p NSI) m/z : $[\text{M} + \text{H}]^+$ calculated for $\text{C}_{12}\text{H}_{21}\text{NO}$ 196.1696, found = 196.1694, $\Delta = -1.0$ ppm.

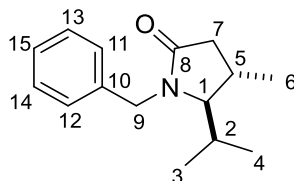
Trans-1-hexyl-5-isopropyl-4-methylpyrrolidin-2-one (30y)



Mr = 225.38

General procedure D was applied to N-(2,4-dimethylpentan-3-yl)hexan-1-amine (59.8 mg, 0.3 mmol) with a 6.25% CO / air balloon in place of the CO balloon. The crude reaction product was purified by alumina column chromatography (0% - 20% ethyl acetate / petroleum ether) to give **30y** as a yellow oil (37.2 mg, 55%, *d.r.* = 9:1). IR ($\lambda_{\text{max}}/\text{cm}^{-1}$) 2958, 2927, 2871, 1683, 1441, 1423, 1259, 1066. ^1H NMR (400 MHz, CDCl_3) 3.68 (1H, ddd, $J_1 = 15.0$ Hz, $J_2 = 9.1$ Hz, $J_3 = 7.2$ Hz, H9a), 3.07 (1H, t, $J = 3.0$ Hz, H1), 2.78 (1H, ddd, $J_1 = 13.9$ Hz, $J_2 = 8.7$ Hz, $J_3 = 5.0$ Hz, H9b), 2.57 (1H, dd, $J_1 = 17.2$ Hz, $J_2 = 9.2$ Hz, H7a), 2.19 – 2.09 (1H, m, H5), 2.09 – 1.99 (1H, m, H2), 1.93 (1H, dd, $J_1 = 17.2$ Hz, $J_2 = 3.0$ Hz, H7b), 1.60 – 1.38 (2H, m, H10), 1.34 – 1.22 (6H, m, H11 – H12), 1.08 (3H, d, $J = 7.5$ Hz, H6), 0.96 (3H, d, $J = 7.5$ Hz, H3), 0.88 (3H, t, $J = 6.5$ Hz, H14), 0.76 (3H, d, $J = 6.5$ Hz, H4). ^{13}C NMR (101 MHz, CDCl_3) 174.2 (C8), 70.4 (C1), 40.2 (C9), 39.4 (C7), 31.5 (C10), 28.7 (C2), 26.9 (C11), 26.6 (C12), 25.3 (C5), 23.0 (C13), 22.6 (C14), 18.5 (C6), 15.1 (C3), 14.0 (C4). HRMS (FTMS +p NSI) m/z : $[\text{M} + \text{H}]^+$ calculated for $\text{C}_{14}\text{H}_{27}\text{NO}$ 226.2165, found = 226.2165, exact match.

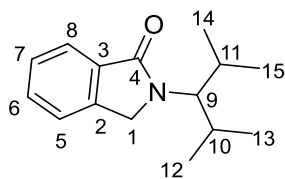
Trans-1-benzyl-5-isopropyl-4-methylpyrrolidin-2-one (30z)



Mr = 231.34

General procedure D was applied to N-benzyl-2,4-dimethylpentan-3-amine (61.5 mg, 0.3 mmol). The crude reaction product was purified by alumina column chromatography (5% - 25% ethyl acetate / petroleum ether) to give **30z** as a yellow oil (15.3 mg, 22%, *d.r.* = 7:1). IR ($\lambda_{\text{max}}/\text{cm}^{-1}$) 2961, 1679, 1422, 1253, 1078. ^1H NMR (400 MHz, CDCl_3) 7.35 – 7.18 (5H, m, H11 – H15), 5.09 (1H, d, $J = 15.2$ Hz, H9a), 3.82 (1H, d, $J = 15.2$ Hz, H9b), 2.87 (1H, t, $J = 3.0$ Hz, H1), 2.66 (1H, dd, $J_1 = 17.8$ Hz, $J_2 = 9.6$ Hz, H7a), 2.18 – 2.09 (1H, m, H5), 2.09 – 2.00 (1H, m, H2), 2.00 (1H, dd, $J_1 = 17.8$ Hz, $J_2 = 3.0$ Hz, H7b), 0.98 (3H, d, $J = 7.1$ Hz, H6), 0.87 (3H, d, $J = 7.3$ Hz, H3), 0.76 (3H, d, $J = 7.1$ Hz, H4). ^{13}C NMR (101 MHz, CDCl_3) 174.4 (C8), 136.6 (C10), 128.6 (C11, C12), 128.1 (C13, C14), 127.4 (C15), 69.4 (C1), 44.0 (C9), 39.3 (C7), 28.3 (C2), 25.2 (C5), 22.8 (C6), 18.4 (C3), 15.0 (C4). HRMS (FTMS +p NSI) m/z : $[\text{M} + \text{H}]^+$ calculated for $\text{C}_{15}\text{H}_{21}\text{NO}$ 232.1696, found = 232.1696, exact match.

2-(2,4-Dimethylpentan-3-yl)isoindolin-1-one (30z-i)

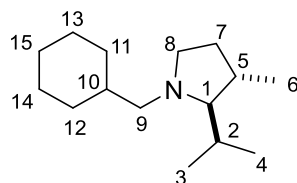


Mr = 231.34

In the same reaction, **30z-i** was also isolated as a yellow oil (38.2 mg, 55%). IR ($\lambda_{\text{max}}/\text{cm}^{-1}$) 2961, 2873, 1678, 1468, 1405, 1214, 1148. ^1H NMR (400 MHz, CDCl_3) 7.86 (1H, d, $J = 7.4$ Hz, H8), 7.54 – 7.49 (1H, m, H6), 7.47 – 7.41 (2H, m, H5, H7), 4.38 (2H, s, H1), 4.01 (1H, t, $J = 8.0$ Hz, H1), 2.13 (2H, oct, $J = 7.0$ Hz, H10, H11), 0.99 (6H, d $J = 7.2$ Hz, H12, H13), 0.88 (6H, d, $J = 7.1$ Hz, H14, H15). ^{13}C NMR (101 MHz, CDCl_3) 169.8 (C4), 141.3 (C2), 132.5 (C3), 131.1 (C6), 127.9 (C5), 123.9 (C7), 122.5 (C8), 61.5 (C9), 48.5 (C1), 28.7 (C10, C11), 20.2 (C12, C13), 18.8 (C14, C15). HRMS (FTMS +p NSI) m/z : $[\text{M} + \text{H}]^+$ calculated for $\text{C}_{15}\text{H}_{21}\text{NO}$ 232.1696, found = 232.1696, exact match.

4.5 Functionalisation of Lactams

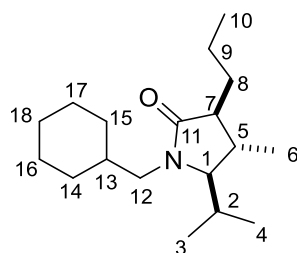
Trans-1-(cyclohexylmethyl)-2-isopropyl-3-methylpyrrolidine (32a-i)



Mr = 223.40

To an ice-cold solution of *trans*-1-(cyclohexylmethyl)-5-isopropyl-4-methylpyrrolidin-2-one (0.2 g, 0.8 mmol) in dry Et₂O (15 mL) was added LiAlH₄ (128 mg, 3.4 mmol) and the reaction mixture was stirred for 48 h under an N₂ atmosphere at room temperature. The reaction was diluted with Et₂O (50 mL) and quenched with dropwise addition sat. aq. NaHCO₃ at 0 °C. The aqueous phase was extracted with Et₂O (2 x 50 mL), and the combined organic layers washed with brine (50 mL), dried over MgSO₄, filtered, and concentrated *in vacuo*. The crude reaction product was purified by alumina column chromatography (0% - 10% ethyl acetate / petroleum ether) to give **32a-i** as a yellow oil (155 mg, 82%). IR ($\lambda_{\text{max}}/\text{cm}^{-1}$) 2956, 2916, 2785, 1448. ¹H NMR (400 MHz, CDCl₃) 3.05 – 2.95 (1H, m, H_{9a}), 2.42 – 2.30 (1H, m, H_{8a}), 2.13 (1H, ddd, *J*₁ = 11.0 Hz, *J*₂ = 8.7 Hz, *J*₃ = 6.1 Hz, H_{9b}), 2.03 (1H, dd, *J*₁ = 11.9 Hz, *J*₂ = 4.1 Hz, H_{8b}), 2.02 – 1.58 (8H, m, H₅, H_{7a}, H_{10a} – H_{15a}), 1.48 – 1.33 (1H, m, H₁₀), 1.30 – 1.07 (4H, m, H_{7b}, H_{11b}, H_{12b}, H_{15b}), 0.93 (3H, d, *J* = 6.8 Hz, H₆), 0.88 (3H, d, *J* = 6.8 Hz, H₃), 0.84 (3H, d, *J* = 6.5 Hz, H₄), 1.00 – 0.70 (2H, m, H_{13b}, H_{14b}). ¹³C NMR (101 MHz, CDCl₃) 78.5 (C₁), 63.3 (C₈), 52.9 (C₉), 37.5 (C₁₀), 32.9 (C₇), 32.4 (C₅), 32.4 (C₁₁), 31.8 (C₁₂), 29.9 (C₂), 27.2 (C₁₅), 26.5 (C₁₃), 26.3 (C₁₄), 22.9 (C₆), 20.0 (C₃), 16.7 (C₄). HRMS (ESI) *m/z*: calculated for C₁₅H₃₀N₁ [*M*+*H*]⁺ 224.2373, found 224.2374, Δ = 0.4 ppm.

1-(Cyclohexylmethyl)-5-isopropyl-4-methyl-3-propylpyrrolidin-2-one (32a-ii)

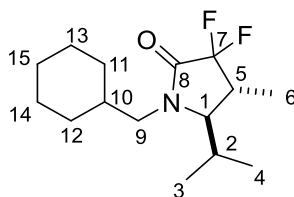


Mr = 279.47

Trans-1-(cyclohexylmethyl)-5-isopropyl-4-methylpyrrolidin-2-one (71.1 mg, 0.3 mmol) was dissolved in THF (6 mL) and cooled to -78 °C. LDA (2.0 M in THF / heptane/ ethylbenzene, 0.16 mL, 1.1 eq) was added dropwise and stirred for 10 mins. 1-Iodopropane (56.1 mg 1.1 eq) was then added to the solution and stirred for another 1 hour, warming up to room temperature. The mixture was then quenched with saturated ammonium chloride (20 mL), extracted with DCM (3 x 20 mL), washed with brine and dried with MgSO₄. The solvent was then removed *in vacuo*. The crude reaction product was purified by alumina column chromatography (5% ethyl acetate / petroleum ether) to give **32a-ii** as a yellow oil (68.7 mg, 82%, *d.r.* = 5 : 1). IR ($\lambda_{\text{max}}/\text{cm}^{-1}$) 2957, 2923, 2852, 1677, 1443, 1257, 1188. ¹H NMR (400 MHz, CDCl₃) 3.59 (1H, dd, *J*₁ = 14.2 Hz, *J*₂ = 9.4 Hz, H_{12a}), 3.05 (1H, dd, *J*₁ = 5.8 Hz, *J*₂ = 3.9 Hz, H₁), 2.54

(1H, dd, $J_1 = 14.1$ Hz, $J_2 = 9.4$ Hz), 2.13 – 2.03 (1H, m, H2), 2.01 – 1.94 (1H, m, H7), 1.84 – 1.27 (9H, m, H5, H8, H(13-18)a), 1.21 – 1.09 (6H, m, H10, H14b, H15b, H18b) 0.99 – 0.87 (10H, m, H3, H6, H9, H16b, H17b), 0.71 (3H, d, $J = 5.4$ Hz, H4). ^{13}C NMR (101 MHz, CDCl_3) 176.7 (C11), 68.0 (C1), 49.6 (C7), 45.7 (C12), 35.0 (C13), 33.7 (C18), 31.8 (C5), 31.2 (C14), 30.4 (C15), 27.4 (C2), 26.4 (C8), 25.9 (C16), 25.7 (C17), 22.9 (C10), 20.4 (C9), 18.4 (C6), 15.1 (C4), 14.2 (C3). HRMS (FTMS +p NSI) m/z : $[\text{M} + \text{H}]^+$ calculated for $\text{C}_{18}\text{H}_{33}\text{NO}$ 280.2635, found = 280.2633, $\Delta = -0.7$ ppm.

Trans-1-(cyclohexylmethyl)-3,3-difluoro-5-isopropyl-4-methylpyrrolidin-2-one (32a-iii)

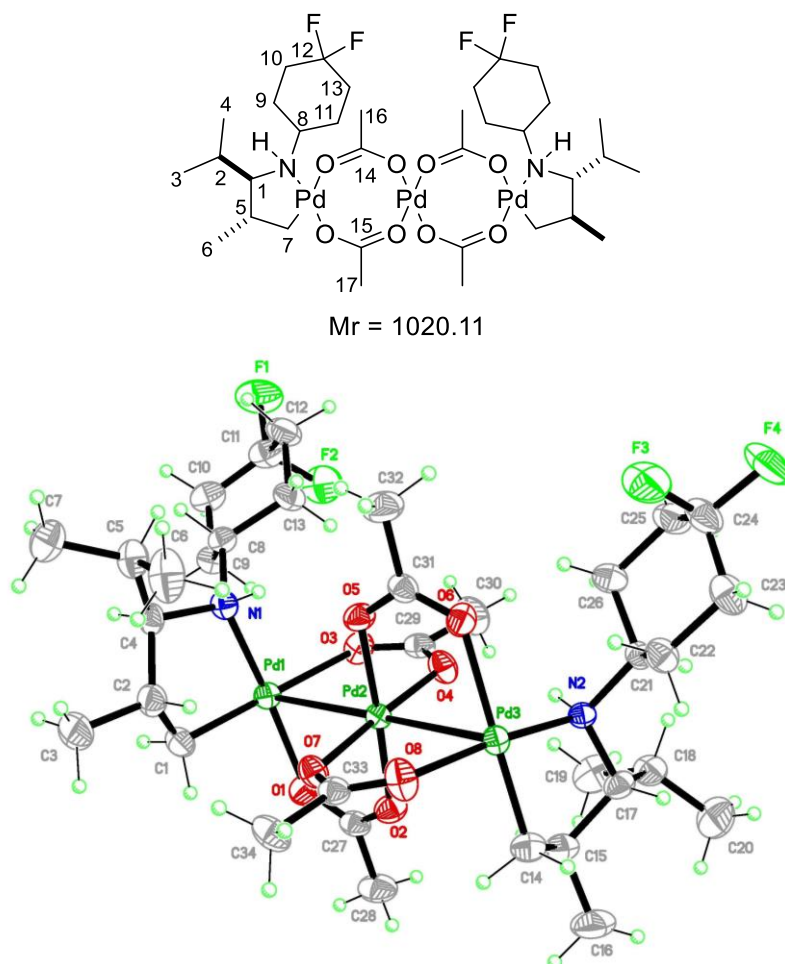


$\text{Mr} = 273.37$

Trans-1-(cyclohexylmethyl)-5-isopropyl-4-methylpyrrolidin-2-one (71.1 mg, 0.3 mmol) was dissolved in THF (6 mL) and cooled to -78°C . LDA (2.0 M in THF / heptane/ ethylbenzene, 0.32 mL, 2.2 eq) was added dropwise and stirred for 10 mins. NFSI (208 mg 2.2 eq) was then added to the solution and stirred for another 1 hour, warming up to room temperature. The mixture was then quenched with saturated ammonium chloride (20 mL), extracted with DCM (3 x 20 mL), washed with brine and dried with MgSO_4 . The solvent was then removed *in vacuo*. The crude reaction product was purified by alumina column chromatography (5% ethyl acetate / petroleum ether) to give **32a-iii** as a yellow oil (67.3 mg, 82%). IR ($\lambda_{\text{max}}/\text{cm}^{-1}$) 2925, 2851, 1719, 1450, 1394, 1331, 1249, 1180, 1107, 1045. ^1H NMR (400 MHz, CDCl_3) 3.66 (1H, dd, $J_1 = 13.5$ Hz, $J_2 = 9.5$ Hz, H9a), 3.16 (1H, q, $J = 4.0$ Hz, H1), 2.69 (1H, ddd, $J_1 = 14.0$ Hz, $J_2 = 5.2$ Hz, $J_3 = 2.2$ Hz, H9b), 2.40 – 2.25 (1H, m, H5), 2.23 – 2.12 (1H, m, H2), 1.78 – 1.51 (6H, m, H(10-15)a), 1.21 (3H, dd, $J_1 = 7.4$ Hz, $J_2 = 2.8$ Hz, H6), 1.28 – 1.13 (3H, m, H11b, H12b, H15b), 1.02 (3H, d, $J = 7.0$ Hz, H3), 1.10 – 0.88 (2H, m, H13, H14), 0.78 (3H, d, $J = 7.0$ Hz, H4). ^{13}C NMR (101 MHz, CDCl_3) 164.1 (C8), 118.3 (C7), 65.2 (C1), 46.3 (C9), 34.9 (C10), 34.5 (C5), 31.0 (C11), 30.1 (C13), 27.3 (C2), 26.2 (C14), 25.7 (C12), 25.5 (C15), 18.8 (C3), 14.5 (C4), 13.5 (C6). ^{19}F NMR (376.5 MHz, CDCl_3) -103.5 (d), -115.4 (d). HRMS (FTMS +p NSI) m/z : $[\text{M} + \text{H}]^+$ calculated for $\text{C}_{15}\text{H}_{25}\text{F}_2\text{NO}$ 274.1977, found = 274.1977, exact match.

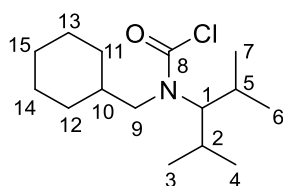
4.6 Palladacycle Studies

N-(2,4-dimethylpentan-3-yl)-4,4-difluorocyclohexan-1-amine-palladacycle-trimer (**33f**)



N-(2,4-dimethylpentan-3-yl)-4,4-difluorocyclohexan-1-amine (70.0 mg, 1 mmol) and palladium acetate (331 mg, 1.5 mmol, 1.5 eq) were dissolved in toluene (6 mL) and heated to 60 °C for 16 hours. The mixture was cooled, filtered through celite (eluting with ethyl acetate, 20 mL), concentrated *in vacuo*. The crude product was purified by recrystallisation in DCM / Hexane mixture to give a **33f** as a green solid (72%, 240 mg). Crystals were grown by diffusion of hexane in a DCM solution of the palladacycle. IR ($\lambda_{\text{max}}/\text{cm}^{-1}$) 2967, 1586, 1537, 1396, 1336, 1104, 975. ^1H NMR (400 MHz, CDCl_3) 4.46 (1H, d, $J = 10.0$ Hz, H7a), 3.22 – 3.04 (1H, m, H7b), 2.63 – 2.23 (6H, m, H5, H8, H9a – H12a), 2.12 – 1.90 (5H, m, H2, H9b – H12b), 1.86 (3H, s, H16), 1.72 (3H, s, H17), 1.03 (3H, d, $J = 7.5$ Hz, H3), 0.92 (3H, d, $J = 7.5$ Hz, H4), 0.88 (3H, t, $J = 7.0$ Hz, H6). ^{13}C NMR (101 MHz, CDCl_3) 184.11 (C14), 180.3 (C15), 76.7 (C1), 59.5 (C8), 39.3 (C5), 32.7 (C13), 31.6 (C2), 30.5 (C7), 23.3 (C9), 23.0 (C10), 22.7 (C11, C12), 20.7 (C6), 18.2 (C3), 16.6 (C4). ^{19}F NMR (376 MHz, CDCl_3) -94.5 (d, $J = 236.9$ Hz), -102.7 (d, $J = 236.4$ Hz). HRMS (FTMS +p NSI) m/z : $[\text{M} + \text{H}]^+$ calculated for $\text{C}_{34}\text{H}_{60}\text{F}_4\text{N}_2\text{O}_8\text{Pd}_3$ 1020.1420, found = 1020.1406, $\Delta = -1.3$ ppm.

(Cyclohexylmethyl)(2,4-dimethylpentan-3-yl)carbamic chloride (**34a**)

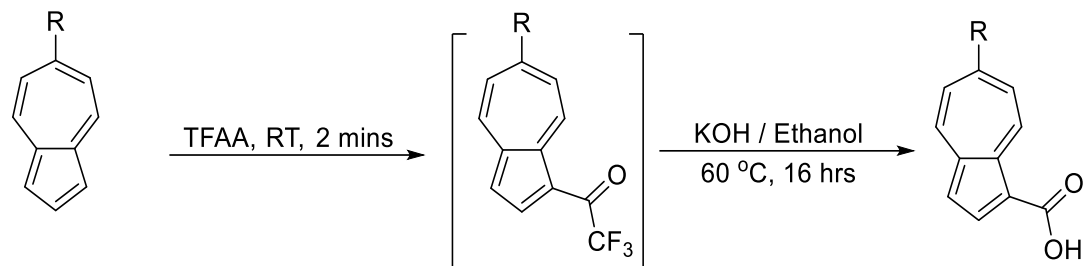


Mr = 273.85

To a slurry of sodium bicarbonate (250 mg, 3 mmol) and triphosgene (300 mg, 1 mmol) in anhydrous DCM at - 10 °C was added a solution of N-(cyclohexylmethyl)-2,4-dimethylpentan-3-amine (211 mg, 1 mmol) in DCM dropwise under N₂. The mixture was allowed to warm up to room temperature overnight, then filtered and the solvent removed *in vacuo*. The product **34a** was obtained without further purification as a white liquid (220 mg, 80 %). IR ($\lambda_{\text{max}}/\text{cm}^{-1}$) 2965, 2852, 2924, 1729, 1448, 1387, 1298, 1250, 1220, 1127, 1103. ¹H NMR (400 MHz, CDCl₃) 3.91 (1H, t, J = 6.3 Hz, H1), 3.26 (1H, d, J = 7.0 Hz, H8a), 3.07 (1H, d J = 7.0 Hz, H8b), 2.37 – 2.20 (1H, m, H2), 2.00 (1H, oct, J = 7.0 Hz, H3), 1.81 – 1.53 (6H, m, H(9-14)a), 1.31 – 1.03 (5H, m, H10 - 14)b), 1.00 (d, 6H, J = 6.9 Hz, H4, H5), 0.97 (d, 6H, J = 6.9 Hz, H6, H7). ¹³C NMR (101 MHz, CDCl₃) 151.6 (C15), 71.8 (C1), 53.7 (C8), 37.9 (C9), 31.7 (C2), 31.4 (C3), 29.2, 26.2, 26.1, 26.0 (C10 – C14), 20.1 (C4, C5), 19.5 (C6, C7). HRMS (FTMS +p NSI) m/z: [M + H]⁺ calculated for C₁₅H₂₉NCIO 274.1938, found = 274.1937, Δ = - 0.4 ppm.

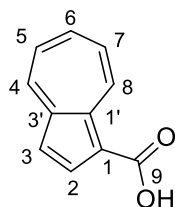
4.7 Synthesis of Azulene-1-Carboxylic Acids

General Procedure E for 1-Carboxylation of Azulenes



Azulene-1-carboxylic acids were synthesised by method of Mathias and Overberger.¹⁸³ To a solution of azulene derivatives (1 eq) in hexane (minimum volume) was added trifluoroacetic acid (8 eq) dropwise. The solution was stirred at room temperature for 2 mins. The red solution formed was then quenched by adding it into a solution of 1 M potassium hydroxide. The mixture was extracted with dichloromethane and the combined organic extracts was dried *in vacuo* to yield a red solid. The red solid was dissolved in ethanol and equal volume of 2.5 M potassium hydroxide was added to it. The mixture was then heated at 60 °C for 16 hours, turning from dark red to dark purple. The reaction was cooled to RT, then concentrated *in vacuo* to remove excess ethanol. Dilute HCl was added to it, yielding a purple precipitate. The mixture was then extracted with ethyl acetate until the aqueous layer turns pale purple. The combined organic extracts was dried with magnesium sulphate, then concentrated *in vacuo* to give the crude carboxylic acid. Further purification by column chromatography (20% ethyl acetate / hexane) gave the pure azulene-1-carboxylic acid as a purple solid.

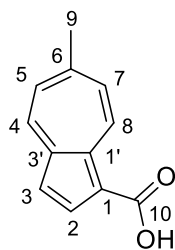
Azulene-1-carboxylic acid (**47**)¹⁸³



Mr = 172.18

General procedure E was applied to azulene (1.28 mg, 10 mmol). The crude reaction product was purified by silica column chromatography (5% - 10% ethyl acetate / hexane) to give **47** as a blue solid (1.30 g, 76 %). Spectrums correspond to previous reports IR ($\lambda_{\text{max}}/\text{cm}^{-1}$) 3368, 1638 (C=O), 1498, 1467, 1396, 1242, 1036. ¹H NMR (500 MHz, CDCl₃) 9.71 (1H, d, J = 8.0 Hz, H8), 8.51 (1H, d, J = 7.6 Hz, H4), 8.49 (1H, d, J = 3.2 Hz, H2), 7.85 (1H, t, J = 7.6 Hz, H6), 7.62 (1H, t, J = 8.0 Hz, H7), 7.52 (1H, t, J = 8.0 Hz, H5), 7.34 (1H, d, J = 3.2 Hz, H3) ¹³C NMR (100.6 MHz, CDCl₃) 170.8 (C9), 145.7 (C1'), 141.6 (C3'), 141.3 (C2), 139.3 (C6), 138.5 (C4), 138.2 (C8), 128.3 (C7), 127.5 (C5), 118.1 (C3), 116.1 (C1).

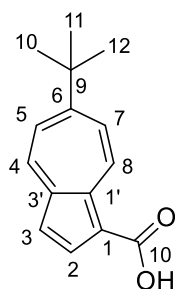
6-Methylazulene-1-carboxylic acid (**50**)



Mr = 186.21

General procedure E was applied to 6-methylazulene (711 mg, 5 mmol). The crude reaction product was purified by silica column chromatography (5% - 10% ethyl acetate / hexane) to give **50** as a blue solid (750 mg, 81 %). IR ($\lambda_{\text{max}}/\text{cm}^{-1}$) 3567, 1634 (C=O), 1552, 1498, 1455, 1400, 1291, 1232, 1041. ^1H NMR (500 MHz, CDCl_3) 9.51 (1H, d, J = 8.4 Hz, H8), 8.36 (1H, d, J = 5.2 Hz, H4), 8.34 (1H, d, J = 3.2 Hz, H2), 7.51 (1H, d, J = 8.4 Hz, H7), 7.41 (1H, d, J = 8.0 Hz, H5), 7.25 (1H, d, J = 3.6 Hz, H3) 2.75 (3H, s, H9). ^{13}C NMR (101 MHz, CDCl_3) 170.2 (C10), 151.5 (C1'), 144.1 (C3'), 140.2 (C6), 139.7 (C2), 137.5 (C4), 137.2 (C8), 129.7 (C7), 128.9 (C5), 117.9 (C3), 115.8 (C1), 28.1 (C9). Melting point 211 - 212 °C (melts). HRMS (FTMS +p NSI) m/z : $[\text{M} + \text{H}]^+$ calculated for $\text{C}_{12}\text{H}_{11}\text{O}_2$ 187.0754, found = 187.0754, exact match.

6-*Tert*-butylazulene-1-carboxylic acid (**51**)

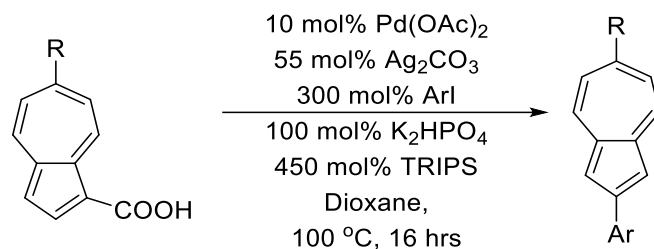


Mr = 228.29

General procedure E was applied to 6-*tert*-butylazulene (921 mg, 5 mmol). The crude reaction product was purified by silica column chromatography (5% - 10% ethyl acetate / hexane) to give **51** as a blue solid (915 mg, 80 %). IR ($\lambda_{\text{max}}/\text{cm}^{-1}$) 2963, 1648, 1581, 1558, 1542, 1451, 1407, 1563, 1557, 1537, 1455, 1415, 1356, 1286, 1236, 1020. ^1H NMR (500 MHz, CDCl_3) 9.63 (1H, d, J = 8.0 Hz, H8), 8.43 (1H, d, J = 8.4 Hz, H4), 8.40 (dH, d, J = 3.2 Hz, H2), 7.80 (1H, d, J = 8.4 Hz, H7), 7.68 (1H, d, J = 8.4 Hz, H5), 7.25 (1H, d, J = 3.2 Hz, H3) 1.50 (9H, s, H10 – H12). ^{13}C NMR (101 MHz, CDCl_3) 171.0 (C13), 163.7 (C1), 144.4 (C3'), 140.5 (C6), 140.3 (C2), 137.5 (C4), 137.2 (C8), 126.5 (C7), 125.7 (C5), 117.5 (C3), 115.6 (C1), 39.0 (C9), 32.0 (C10 – C12). Melting point 223 – 225 °C (melts). HRMS (FTMS +p NSI) m/z : $[\text{M} + \text{H}]^+$ calculated for $\text{C}_{15}\text{H}_{17}\text{O}_2$ 229.1223, found = 229.1222, Δ = - 0.3 ppm.

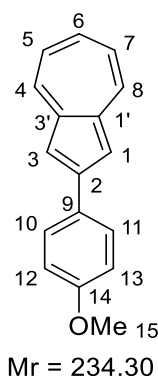
4.8 C-H Arylation of Azulene-1-Carboxylic Acid

General Procedure F for Arylation of Azulene-1-Carboxylic Acids



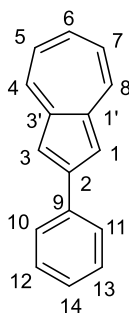
To a 100 mL round-bottomed flask with large oval stirrer bar was added palladium (II) acetate (11.2 mg, 0.05 mmol, 0.1 eq), azulene-1-carboxylic acid (86.1 mg, 0.5 mmol, 1 eq), silver carbonate (75.8 mg, 0.255 mmol, 0.55 eq), aryl-iodide (1.5 mmol, 3 eq), K₂HPO₄ (87.1 mg, 0.5 mmol, 1eq), triisopropylbenzoic acid (558.0 mg, 2.25 mmol, 4.5 eq) and dioxane (5 mL). The flask was sealed with a new septum, then heated at 100 °C for 16 hours. The reaction mixture was cooled, hydrochloric acid (20 mL, 1M) was added to it, then extracted with chloroform, and dried with magnesium sulphate. The solvent was then removed *in vacuo* and the crude mixture was purified by column chromatography to obtain the corresponding 2-arylazulene.

2-(4-Methoxyphenyl)azulene (**49a**)²¹¹



General procedure F was applied to 4-iodoanisole (351 mg, 1.5 mmol). The crude reaction product was purified by silica column chromatography (0% - 20% dichloromethane / hexane) to give **49a** as a blue solid (82.0 mg, 70 %). Spectrums correspond to previous reports IR ($\lambda_{\text{max}}/\text{cm}^{-1}$) 3031, 1604, 1557, 1542, 1457, 1404, 1296, 1256, 1182. ¹H NMR (500 MHz, CDCl₃) 8.25 (2H, d, J = 7.6 Hz, H4, H8), 7.98 (2H, d, J = 6.4 Hz, H10, H11), 7.62 (2H, br s, H1, H3), 7.48 (1H, t, J = 8.0 Hz, H6), 7.15 (2H, t, J = 8.0 Hz, H5, H7), 7.01 (2H, d, J = 6.8 Hz, H12, H13), 3.88 (3H, s, H15). ¹³C NMR (101 MHz, CDCl₃) 160.0 (C14), 149.8 (C2), 141.4 (C1', C3'), 135.7 (C6), 135.2 (C4, C8), 129.2 (C9), 128.9 (C10, C11), 123.8 (C5, C7), 114.4 (C12, C13), 113.8 (C1, C3). Melting point 225 – 227 °C, decomposes (lit. 229 – 234). HRMS (FTMS +p NSI) m/z: [M + H]⁺ calculated for C₁₇H₁₅O 235.1117, found = 235.1118, Δ = 0.2 ppm.

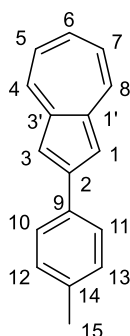
2-Phenylazulene (**49b**)



Mr = 204.27

General procedure F was applied to iodobenzene (306 mg, 1.5 mmol). The crude reaction product was purified by silica column chromatography (0% - 30% dichloromethane / hexane) to give **49b** as a blue solid (68.4 mg, 67 %). IR ($\lambda_{\text{max}}/\text{cm}^{-1}$) 3046, 1600, 1532, 1455, 1407, 1328, 1296, 1216. ^1H NMR (500 MHz, CDCl_3) 8.30 (2H, d, $J = 7.2$ Hz, H4, H8), 7.97 (2H, d, $J = 5.6$ Hz, H10, H11), 7.69 (2H, br s, H1, H3), 7.52 (1H, t, $J = 7.2$ Hz, H6) 7.48 (2H, t, $J = 5.2$ Hz, H12, H13), 7.36 (1H, t, $J = 6.0$ Hz, H14), 7.17 (2H, $J = 8.0$ Hz, H5, H7). ^{13}C NMR (101 MHz, CDCl_3) 150.0 (C2), 141.4 (C1', C3'), 136.6 (C6), 136.1 (C4, C8), 129.0 (C12, C13), 128.3 (C14), 127.7 (C10, C11), 123.8 (C5, C7), 114.6 (C1, C3). Melting point 198 - 199 °C, sublimes. HRMS (FTMS +p NSI) m/z : $[\text{M} + \text{H}]^+$ calculated for $\text{C}_{16}\text{H}_{13}$ 205.1015, found = 205.1012, $\Delta = -1.5$ ppm.

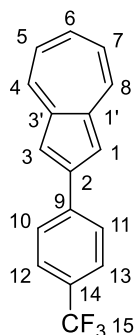
2-(*p*-Tolyl)azulene (**49c**)²¹



Mr = 218.30

General procedure F was applied to 4-iodotoluene (327 mg, 1.5 mmol). The crude reaction product was purified by silica column chromatography (0% - 5% dichloromethane / hexane) to give **49c** as a blue solid (82.0 mg, 75 %). IR ($\lambda_{\text{max}}/\text{cm}^{-1}$) 3024, 2911, 1609, 1572, 1524, 1474, 1406, 1316, 1210, 1106, 1116. ^1H NMR (500 MHz, CDCl_3) 8.27 (2H, d, $J = 8.0$ Hz, H4, H8), 7.89 (2H, d, $J = 4.8$ Hz, H10, H11), 7.68 (2H, br s, H1, H3), 7.50 (1H, t, $J = 8.0$ Hz, H6), 7.29 (2H, d, $J = 6.4$ Hz, H12, H13), 7.16 (2H, t, $J = 8.0$ Hz, H5, H7), 2.43 (3H, s, H15). ^{13}C NMR (101 MHz, CDCl_3) 150.1 (C2), 141.4 (C1', C3'), 138.4 (C14), 136.2 (C6), 135.7 (C4, C8), 133.7 (C9), 129.8 (C12, C13), 127.6 (C10, C11), 123.8 (C5, C7), 114.4 (C1, C3), 21.5 (C15). Melting point 195 - 198 °C, sublimes (lit 214). HRMS (FTMS +p NSI) m/z : $[\text{M} + \text{H}]^+$ calculated for $\text{C}_{17}\text{H}_{14}$ 219.1168, found = 219.1166, $\Delta = -1.2$ ppm.

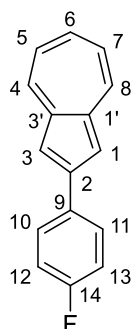
2-(4-(Trifluoromethyl)phenyl)azulene (**49d**)



Mr = 272.27

General procedure F was applied to 1-iodo-4-(trifluoromethyl)benzene (408 mg, 1.5 mmol). The crude reaction product was purified by silica column chromatography (0% - 10% dichloromethane / hexane) to give **49d** as a blue solid (42.1 mg, 31 %). IR ($\lambda_{\text{max}}/\text{cm}^{-1}$) 1615, 1575, 1542, 1408, 1328, 1164, 1114, 1069, 1014. ^1H NMR (500 MHz, CDCl_3) 8.34 (2H, d, $J = 7.2$ Hz, H4, H8), 8.05 (2H, d, $J = 6.8$ Hz, H12, H13), 7.71 (2H, d, $J = 6.4$ Hz, H10, H11), 7.69 (2H, br s, H1, H3), 7.57 (1H, t, $J = 8.0$ Hz, H6), 7.20 (2H, t, $J = 8.0$ Hz, H5, H7). ^{13}C NMR (101 MHz, CDCl_3) 148.0 (C2), 141.4 (C1', C3'), 140.1 (C9), 137.5 (C6), 137.0 (C4, C8), 127.8 (C10, C11), 125.9 (C12, C13), 124.2 (C5, C7), 114.8 (C1, C3). ^{19}F NMR (376 MHz, CDCl_3) -62.4 (CF_3). Melting point 190 – 191 °C, sublimes. HRMS (FTMS +p NSI) m/z : $[\text{M} + \text{H}]^+$ calculated for $\text{C}_{17}\text{H}_{12}\text{F}_3$ 273.0886, found = 273.0884, $\Delta = -0.7$ ppm.

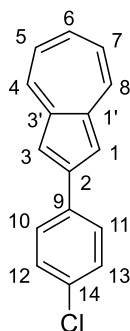
2-(4-Fluorophenyl)azulene (49e)



Mr = 222.26

General procedure F was applied to 1-iodo-4-fluorobenzene (333 mg, 1.5 mmol). The crude reaction product was purified by silica column chromatography (0% - 10% dichloromethane / hexane) to give **49e** as a blue solid (71.0 mg, 64 %). IR ($\lambda_{\text{max}}/\text{cm}^{-1}$) 3049, 1602, 1592, 1522, 1470, 1406, 1296, 1238, 1217, 1156, 1086, 1010. ^1H NMR (500 MHz, CDCl_3) 8.29 (2H, d, $J = 8.0$ Hz, H4, H8), 7.95 – 7.91 (2H, m, H10, H11), 7.62 (2H, br s, H1, H3), 7.52 (1H, t, $J = 8.0$ Hz, H6), 7.20 – 7.14 (4H, m, H5, H7, C12, C13). ^{13}C NMR (101 MHz, CDCl_3) 163.0 (d, $J = 197.4$ Hz, C14), 148.6 (C2), 141.4 (C1', C3'), 136.6 (C6), 136.0 (C4, C8), 132.8 (C9), 129.3 (C10, C11), 124.0 (C5, C7), 116.0 (d, $J = 17.1$ Hz, C12, C13), 114.3 (C1, C3). ^{19}F NMR (376 MHz, CDCl_3) -113.6. Melting point 201 – 205 °C, sublimes. HRMS (FTMS +p NSI) m/z : $[\text{M} + \text{H}]^+$ calculated for $\text{C}_{16}\text{H}_{12}\text{F}$ 223.0918, found = 223.0913, $\Delta = -2.2$ ppm.

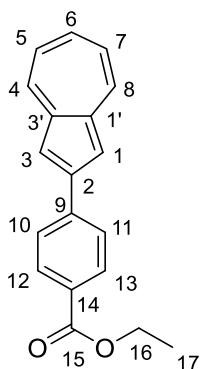
2-(4-Chlorophenyl)azulene (49f)



Mr = 238.71

General procedure F was applied to 1-chloro-4-iodobenzene (357 mg, 1.5 mmol). The crude reaction product was purified by silica column chromatography (0% - 20% dichloromethane / hexane) to give **49f** as a blue solid (57.0 mg, 48 %). IR ($\lambda_{\text{max}}/\text{cm}^{-1}$) 3046, 1592, 1536, 1467, 1449, 1409, 1400, 1296, 1207, 1031, 1010. ^1H NMR (500 MHz, CDCl_3) 8.29 (2H, d, $J = 7.6$ Hz, H4, H8), 7.89 (2H, d, $J = 6.8$ Hz, H10, H11), 7.63 (2H, br s, H1, H3), 7.53 (1H, t, $J = 8.0$ Hz, H6), 7.44 (2H, d, $J = 6.8$ Hz, H12, H13), 7.18 (2H, t, $J = 8.0$ Hz, H5, H7). ^{13}C NMR (101 MHz, CDCl_3) 148.5 (C2), 141.4 (C1', C3'), 136.9 (C6), 136.3 (C4, C8), 135.1 (C14), 134.2 (C9), 129.2 (C12, C13), 128.9 (C10, C11), 124.1 (C5, C7), 114.4 (C1, C3). Melting point 201 – 202 °C, melts. HRMS (FTMS +p NSI) m/z : $[\text{M} + \text{H}]^+$ calculated for $\text{C}_{16}\text{H}_{12}\text{Cl}$ 239.0622, found = 239.0625, $\Delta = 1.1$ ppm.

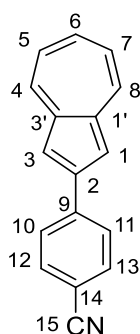
Ethyl 4-(azulen-2-yl)benzoate (49g)



Mr = 276.34

General procedure F was applied to ethyl 4-iodobenzoate (414mg, 1.5 mmol). The crude reaction product was purified by silica column chromatography (0% - 5% dichloromethane / hexane) to give **49g** as a blue solid (100.5 mg, 73 %). IR ($\lambda_{\text{max}}/\text{cm}^{-1}$) 2976, 1712 (C=O), 1600, 1574, 1464, 1406, 1364, 1297, 1272, 1108, 1016. ^1H NMR (500 MHz, CDCl_3) 8.32 (2H, d, $J = 8.4$ Hz, H4, H8), 8.14 (2H, d, $J = 6.0$ Hz, H12, H13), 8.01 (2H, d, $J = 6.8$ Hz, H10, H11), 7.71 (2H, br s, H1, H3), 7.55 (1H, t, $J = 7.6$ Hz, H6), 7.18 (2H, J = 8.0 Hz, H5, H7). ^{13}C NMR (101 MHz, CDCl_3) 166.6 (C15), 148.4 (C2), 141.4 (C1', C3'), 140.8 (C14), 137.4 (C6), 136.9 (C4, C8), 130.3 (C10, C11), 129.8 (C9), 127.5 (C12, C13), 124.1 (C5, C7), 115.0 (C1, C3). Melting point 211 -214 °C, melts. HRMS (FTMS +p NSI) m/z : $[\text{M} + \text{H}]^+$ calculated for $\text{C}_{19}\text{H}_{17}\text{O}_2$ 277.1229, found = 277.1223, $\Delta = - 2.2$ ppm.

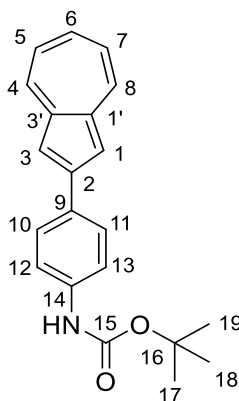
4-(Azulen-2-yl)benzonitrile (49h)



Mr = 229.28

General procedure F was applied to 4-iodobenzonitrile (344 mg, 1.5 mmol). The crude reaction product was purified by silica column chromatography (0% - 30% dichloromethane / hexane) to give **49h** as a blue solid (45.6 mg, 40 %). IR ($\lambda_{\text{max}}/\text{cm}^{-1}$) 2963, 2225, 1575, 1470, 1407, 1259, 1020. ^1H NMR (500 MHz, CDCl_3) 8.34 (2H, d, J = 8.0 Hz, H5, H7), 8.02 (2H, d, J = 6.4 Hz, H12, H13), 7.73 (2H, d, J = 6.4 Hz, H10, H11), 7.67 (2H, s, H1, H3), 7.57 (1H, t, J = 8.0 Hz, H6), 7.21 (2H, t, J = 7.6 Hz, H5, H7). ^{13}C NMR (101 MHz, CDCl_3) 147.1 (C2) < 141.4 (C1', C3'), 141.0 (C9), 138.0 (C6), 137.5 (C4, C8), 132.8 (C12, C13), 128.1 (C10, C11), 124.4 (C5, C7), 119.2 (C15), 114.8 (C1, C3), 111.3 (C14). Melting point 211 - 213 °C, melts. HRMS (FTMS +p NSI) m/z : $[\text{M} + \text{H}]^+$ 230.0967 calculated for $\text{C}_{17}\text{H}_{12}\text{N}$ 230.0964, Δ = 1.4 ppm.

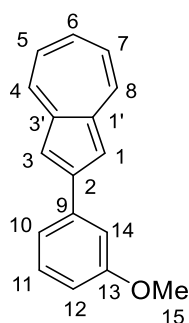
Tert-butyl (4-(azulen-2-yl)phenyl)carbamate (49i)



Mr = 319.40

General procedure F was applied to tert-butyl (4-iodophenyl)carbamate (478 mg, 1.5 mmol). The crude reaction product was purified by silica column chromatography (0% - 10% dichloromethane / hexane) to give **49i** as a blue solid (121.7 mg, 76 %). IR ($\lambda_{\text{max}}/\text{cm}^{-1}$) 2970, 1739 (C=O), 1558, 1365, 1217. ^1H NMR (500 MHz, CDCl_3) 8.25 (2H, d, J = 7.6 Hz, H5, H7), 7.90 (2H, d, J = 8.0 Hz, H10, H11), 7.63 (2H, br, H1, H3), 7.50 - 7.45 (3H, m, H6, H12, H13), 7.15 (2H, t, J = 7.6 Hz, H5, H7), 6.56 (1H, br s, NH), 1.55 (9H, s, H17 - H19). ^{13}C NMR (101 MHz, CDCl_3) 149.6 (C2), 141.5 (C1', C3'), 138.6 (C9), 136.0 (C6), 135.5 (C4, C8), 131.3 (C14), 128.4 (C10, C11), 123.9 (C5, C7), 118.8 (C12, C13), 114.0 (C1, C3), 81.0 (C16), 28.4 (C17 - C19). Melting point 252 - 255 °C, sublimes. HRMS (FTMS +p NSI) m/z : $[\text{M} + \text{H}]^+$ 320.1644 calculated for $\text{C}_{21}\text{H}_{22}\text{NO}_2$ 320.1845, Δ = - 0.4 ppm.

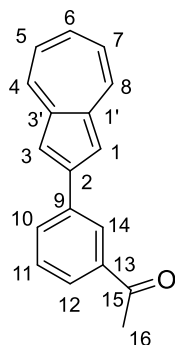
2-(3-Methoxyphenyl)azulene (49j)



Mr = 234.30

General procedure F was applied to 3-iodoanisole (351 mg, 1.5 mmol). The crude reaction product was purified by silica column chromatography (0% - 10% dichloromethane / hexane) to give **49j** as a blue solid (79.1 mg, 69 %). IR ($\lambda_{\text{max}}/\text{cm}^{-1}$) 3045, 2433, 1514, 1535, 1459, 1405, 1292, 1245, 1210, 1176. ^1H NMR (500 MHz, CDCl_3) 8.31 (2H, d, $J = 8.0$ Hz, H4, H8), 7.70 (2H, br s, H1, H3), 7.60, (1H, d, $J = 6.0$ Hz, H10), 7.55 – 7.51 (2H, m, H6, H14), 7.42 (1H, t, $J = 6.4$ Hz, H11), 7.18 (2H, t, $J = 8.0$ Hz, H5, H7), 6.96 (1H, d, $J = 2.0$ Hz), H12), 3.95 (3H, s, H15). ^{13}C NMR (101 MHz, CDCl_3) 160.2 (C13), 149.9 (C2), 141.4 (C1', C3'), 138.0 (C9), 136.7 (C6), 136.2 (C4, C8), 130.0 (C11), 123.9 (C5, C7), 120.4 (C10), 114.8 (C1, C3), 113.9 (C14), 113.2 (C12). Melting point 123 - 124 °C, melts. HRMS (FTMS +p NSI) m/z : $[\text{M} + \text{H}]^+$ calculated for $\text{C}_{17}\text{H}_{15}\text{O}$ 235.1122, found = 235.1117, $\Delta = 2.1$ ppm.

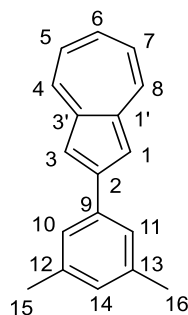
1-(3-(Azulen-2-yl)phenyl)ethan-1-one (49k)



Mr = 246.31

General procedure F was applied to 1-(3-iodophenyl)ethan-1-one (369 mg, 1.5 mmol). The crude reaction product was purified by silica column chromatography (0% - 5% dichloromethane / hexane) to give **49k** as a blue solid (44.1 mg, 36 %). IR ($\lambda_{\text{max}}/\text{cm}^{-1}$) 2963, 1679 (C=O), 1590, 1560, 1465, 1398, 1354, 1262, 1022. ^1H NMR (500 MHz, CDCl_3) 8.54 (1H, s, H14), 8.32 (2H, d, $J = 8.0$ Hz, H4, H8), 8.15 (1H, d, $J = 6.0$ Hz, H12), 7.93 (1H, d, $J = 6.0$ Hz, H10), 7.72 (2H, s, H1, H3), 7.58 – 7.53 (2H, m, H6, H11), 7.20 (2H, $J = 7.6$ Hz, H5, H7) 2.70 (3H, s, H16). ^{13}C NMR (101 MHz, CDCl_3) 198.3 (C15), 148.6 (C2), 141.4 (C1', C3'), 137.8 (C9), 137.1 (C13), 137.1 (C6), 136.6 (C4, C8), 132.1 (C12), 129.3 (C11), 128.1 (C10), 127.4 (C14), 124.1 (C5, C7), 114.6 (C1, C3), 26.9 (C16). Melting point 150 – 152 °C, melts. HRMS (FTMS +p NSI) m/z : $[\text{M} + \text{H}]^+$ 247.1117 calculated for $\text{C}_{18}\text{H}_{15}\text{O}$ 247.1118, $\Delta = 0.1$ ppm.

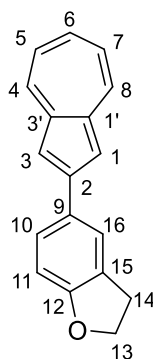
2-(3,5-Dimethylphenyl)azulene (49l)



Mr = 232.33

General procedure F was applied to 1-iodo-3,5-dimethylbenzene (348 mg, 1.5 mmol). The crude reaction product was purified by silica column chromatography (0% - 5% dichloromethane / hexane) to give **49l** as a blue solid (95.1 mg, 82 %). IR ($\lambda_{\text{max}}/\text{cm}^{-1}$) 3036, 2914, 1599, 1534, 1455, 1401, 1294, 1203, 1105, 1019. ^1H NMR (500 MHz, CDCl_3) 8.31 (2H, d, $J = 8.0$ Hz, H4, H8), 7.73 (2H, br s, H1, H3), 7.66 (2H, br, H10, H11), 7.53 (1H, t, $J = 7.8$ Hz, H6), 7.18 (2H, t, $J = 8.0$ Hz, H5, H7), 7.05 (1H, br, H14), 2.47 (6H, s, H15, H16). ^{13}C NMR (101 MHz, CDCl_3) 150.4 (C2), 141.4 (C1', C3'), 138.5 (C12, C13), 136.5 (C9), 136.5 (C6), 135.9 (C4, C8), 130.2 (C14), 125.7 (C5, C7), 123.8 (C10, C11), 114.8 (C1, C3). Melting point 122 - 123 °C, melts. HRMS (FTMS +p NSI) m/z : $[\text{M} + \text{H}]^+$ calculated for $\text{C}_{18}\text{H}_{17}$ 233.1322, found = 233.1325, $\Delta = 1.0$ ppm.

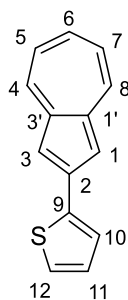
5-(Azulen-2-yl)-2,3-dihydrobenzofuran (49m)



Mr = 246.31

General procedure F was applied to 5-iodo-2,3-dihydrobenzofuran (369 mg, 1.5 mmol). The crude reaction product was purified by silica column chromatography (0% - 20% dichloromethane / hexane) to give **49m** as a blue solid (50.0 mg, 40 %). IR ($\lambda_{\text{max}}/\text{cm}^{-1}$) 2961, 1608, 1558, 1542, 1465, 1407, 1293, 1239, 1030. ^1H NMR (500 MHz, CDCl_3) 8.23 (2H, d, $J = 7.6$ Hz, H4, H8), 7.83 (1H, s, H16), 7.76 (1H, d, $J = 6.8$ Hz, H10), 7.60 (2H, br, H1, H3), 7.46 (1H, t, $J = 7.6$ Hz, H6), 7.143 (2H, t, $J = 8.0$ Hz, H5, H7), 6.88 (2H, d, $J = 6.4$ Hz, H11), 4.65 (2H, t, $J = 8.0$ Hz, H13), 3.31 (2H, t, $J = 6.8$ Hz, H11). ^{13}C NMR (101 MHz, CDCl_3) 160.8 (C12), 150.4 (C2), 141.5 (C1', C3'), 135.6 (C6), 135.0 (C4, C8), 129.4 (C9), 128.0 (C10), 124.4 (C16), 123.8 (C5, C7), 113.9 (C1, C3), 109.9 (C11), 71.7 (C13), 29.7 (C14). Melting point 207 - 210 °C, melts. HRMS (FTMS +p NSI) m/z : $[\text{M} + \text{H}]^+$ calculated for $\text{C}_{18}\text{H}_{15}\text{O}$ 247.1117, found = 247.1116, $\Delta = -0.6$ ppm.

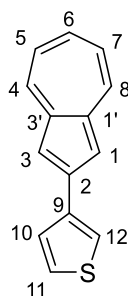
2-(Azulen-2-yl)thiophene (49n)



Mr = 210.29

General procedure F was applied to 2-iodothiophene (315 mg, 1.5 mmol). The crude reaction product was purified by silica column chromatography (0% - 15% dichloromethane / hexane) to give **49n** as a blue solid (27.3 mg, 26 %). IR ($\lambda_{\text{max}}/\text{cm}^{-1}$) 2960, 1575, 1537, 1470, 1399, 1362, 1031. ^1H NMR (500 MHz, CDCl_3) 8.21 (2H, d, J = 8.0 Hz, H4, H8), 7.59 (1H, d, J = 2.8 Hz, H12) 7.54 (2H, s, H1, H3), 7.48 (1H, J = 7.6 Hz, H6), 7.37 (1H, d, J = 4.0 Hz, H10), 7.17 – 7.13 (3H, m, H5, H7, H11). ^{13}C NMR (101 MHz, CDCl_3) 143.3 (C9), 141.3 (C1', C3'), 141.0 (C2), 136.1 (C6), 135.4 (C4, C8), 128.4 (C12), 126.5 (C11), 125.6 (C10), 124.1 (C5, C7), 114.0 (C1, C3). Melting point 164 - 165 °C, melts. HRMS (FTMS +p NSI) m/z : $[\text{M} + \text{H}]^+$ calculated for $\text{C}_{14}\text{H}_{11}\text{S}$ 211.0576, found = 211.0576, exact match.

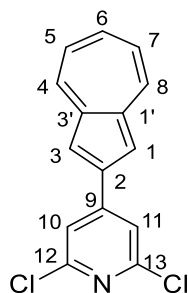
3-(Azulen-2-yl)thiophene (49o)



Mr = 210.29

General procedure F was applied to 3-iodothiophene (315 mg, 1.5 mmol). The crude reaction product was purified by silica column chromatography (0% - 15% dichloromethane / hexane) to give **49o** as a blue solid (21.0 mg, 20 %). IR ($\lambda_{\text{max}}/\text{cm}^{-1}$) 2961, 1646, 1542, 1455, 1408, 1261, 1132, 1030. ^1H NMR (500 MHz, CDCl_3) 8.25 (2H, d, J = 7.6 Hz, H4, H8), 7.78 (1H, d, J = 2.4 Hz, H12), 7.64 (1H, d, J = 4.0 Hz, H11), 7.56 (2H, br s, H1, H3), 7.49 (1H, t, J = 7.6 Hz, H6), 7.42 (1H, dd, J_1 = 4.0 Hz, J_2 = 2.0 Hz, H10), 7.16 (2H, t, J = 8.0 Hz, H5, H7). ^{13}C NMR (101 MHz, CDCl_3) 144.9 (C2), 141.4 (C1', C3'), 138.9 (C9), 136.1 (C6), 135.6 (C4, C8), 127.1 (C10), 126.3 (C11), 123.9 (C5, C7), 122.8 (C12), 114.6 (C1, C3). Melting point 207 – 209 °C, melts. HRMS (FTMS +p NSI) m/z : $[\text{M} + \text{H}]^+$ calculated for $\text{C}_{14}\text{H}_{11}\text{S}$ 211.0576, found = 211.0578, Δ = 0.9 ppm.

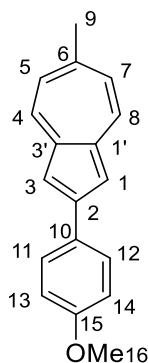
4-(Azulen-2-yl)-2,6-dichloropyridine (49p)



Mr = 274.14

General procedure F was applied to 2,6-dichloro-4-iodopyridine (410 mg, 1.5 mmol). The crude reaction product was purified by silica column chromatography (0% - 20% dichloromethane / hexane) to give **49p** as a green solid (99.6 mg, 73 %). IR ($\lambda_{\text{max}}/\text{cm}^{-1}$) 2963, 1575, 1531, 1400, 1261, 1094, 1030. ^1H NMR (500 MHz, CDCl_3) 8.35 (2H, d, $J = 8.0$ Hz, H5, H7), 7.71 (2H, s, H1, H3), 7.64 (1H, t, $J = 7.6$ Hz, H6), 7.62 (2H, s, H10, H11), 7.24 (2H, t, $J = 8.0$ Hz, H5, H7). ^{13}C NMR (101 MHz, CDCl_3) 151.2 (C12, C13), 149.4 (C2), 143.1 (C9), 141.2 (C1', C3'), 139.3 (C6), 138.8 (C4, C8), 124.7 (C5, C7), 120.8 (C10, C11), 115.1 (C1, C3). Melting point 206 – 207 °C, melts. HRMS (FTMS +p NSI) m/z : $[\text{M} + \text{H}]^+$ 274.0178 calculated for $\text{C}_{15}\text{H}_{10}\text{Cl}_2\text{N}$ 274.0185, $\Delta = -2.6$ ppm.

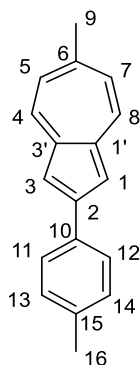
2-(4-Methoxyphenyl)-6-methylazulene (50a)



Mr = 248.33

General procedure F was applied to 4-iodoanisole (351 mg, 1.5 mmol) and 6-methylazulene-1-carboxylic acid (93.1 mg, 0.5 mmol) in place of azulene-1-carboxylic acid. The crude reaction product was purified by silica column chromatography (0% - 20% dichloromethane / hexane) to give **50a** as a blue solid (61.9 mg, 50 %). IR ($\lambda_{\text{max}}/\text{cm}^{-1}$) 2962, 1558, 1261, 1029. ^1H NMR (500 MHz, CDCl_3) 8.11 (2H, d, $J = 8.0$ Hz, H4, H8), 7.88 (2H, d, $J = 6.8$ Hz, H10, H11), 7.54 (2H, s, H1, H3), 7.05 (2H, d, $J = 8.0$ Hz, H5, H7), 6.99 (2H, d, $J = 6.8$ Hz, H12, H13), 3.87 (3H, s, H16), 2.62 (3H, s, H9). ^{13}C NMR (101 MHz, CDCl_3) 159.7 (C14), 148.4 (C2), 147.2 (C6), 140.0 (C1', C3'), 134.5 (C4, C8), 129.4 (C9), 128.6 (C10, C11), 125.2 (C5, C7), 114.3 (C12, C13), 113.8 (C1, C3), 55.3 (C16), 28.0 (C9). Melting point 239 - 243 °C, sublimes. HRMS (FTMS +p NSI) m/z : $[\text{M} + \text{H}]^+$ calculated for $\text{C}_{18}\text{H}_{17}\text{O}$ 249.1270, found = 249.1274, $\Delta = 1.5$ ppm.

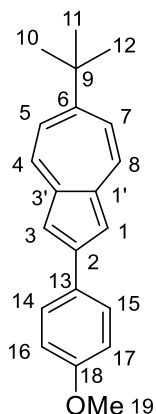
6-Methyl-2-(p-tolyl)azulene (50b)



Mr = 232.33

General procedure F was applied to 4-iodotoluene (327 mg, 1.5 mmol) and 6-methylazulene-1-carboxylic acid (93.1 mg, 0.5 mmol) in place of azulene-1-carboxylic acid. The crude reaction product was purified by silica column chromatography (0% - 5% dichloromethane / hexane) to give **50b** as a blue solid (61.9 mg, 57 %). IR ($\lambda_{\text{max}}/\text{cm}^{-1}$) 2962, 1558, 1533, 1468, 1411, 1259, 1030. ^1H NMR (500 MHz, CDCl_3) 8.13 (2H, d, $J = 7.6$ Hz, H4, H8), 7.86 (2H, d, $J = 5.2$ Hz, H11, H12), 7.59 (2H, s, H1, H3), 7.26 (2H, d, $J = 7.6$ Hz, H13, H14), 7.06 (2H, d, $J = 7.6$ Hz, H5, H7), 2.63 (3H, s, H9), 2.41 (3H, s, H16). ^{13}C NMR (101 MHz, CDCl_3) 148.7 (C2), 147.7 (C6), 140.0 (C1', C3'), 138.0 (C15), 134.9 (C4, C8), 133.9 (C10), 129.7 (C13, C14), 127.4 (C11, C12), 125.3 (C5, C7), 114.3 (C1, C3), 28.1 (C9), 21.4 (C16). Melting point 214 – 217 °C, sublimes. HRMS (FTMS +p NSI) m/z : $[\text{M} + \text{H}]^+$ calculated for $\text{C}_{18}\text{H}_{17}$ 233.1325, found = 233.1325, exact match.

6-(*Tert*-butyl)-2-(4-methoxyphenyl)azulene (**51a**)

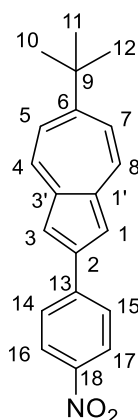


Mr = 290.41

General procedure F was applied to 4-iodoanisole (351 mg, 1.5 mmol) and 6-*tert*-butylazulene-1-carboxylic acid (114.1 mg, 0.5 mmol) in place of azulene-1-carboxylic acid. The crude reaction product was purified by silica column chromatography (0% - 10% dichloromethane / hexane) to give **51a** as a blue solid (54.9 mg, 45 %). IR ($\lambda_{\text{max}}/\text{cm}^{-1}$) 2961, 1605, 1549, 1488, 1418, 1259, 1094, 1028. ^1H NMR (500 MHz, CDCl_3) 8.19 (2H, d, $J = 8.8$ Hz, H4, H8), 7.89 (2H, d, $J = 7.2$ Hz, H14, H15), 7.32 (2H, d, $J = 8.8$ Hz, H5, H7), 6.99 (2H, d, $J = 7.2$ Hz, H16, H17), 3.87 (3H, s, H19), 1.45 (9 H, s, H10 – H12). ^{13}C NMR (101 MHz, CDCl_3) 159.7 (C18), 149.0 (C2), 140.3 (C1', C3'), 134.4 (C4, C8), 129.6 (C9), 128.8 (C14, C15), 122.0 (C5, C7), 114.4 (C16, C17), 113.2 (C1, C3), 55.4 (C19), 38.5 (C9), 32.0 (C10 – C12). Melting point 272 - 274 °C,

melts. HRMS (FTMS +p NSI) m/z: [M + H]⁺ calculated for C₂₁H₂₃O 291.1743, found = 291.1746, Δ = 1.0 ppm.

6-(*Tert*-butyl)-2-(4-nitrophenyl)azulene (51b)



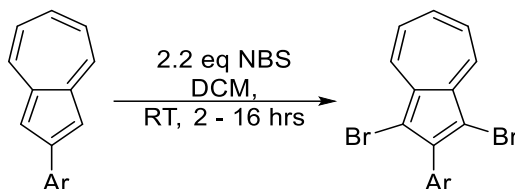
Mr = 305.38

General procedure F was applied to 1-iodo-4-nitrobenzene (374 mg, 1.5 mmol) and 6-*tert*-butylazulene-1-carboxylic acid (114.1 mg, 0.5 mmol) in place of azulene-1-carboxylic acid. The crude reaction product was purified by silica column chromatography (0% - 20% dichloromethane / hexane) to give **51b** as a blue solid (54.9 mg, 45 %). IR (λ_{max} /cm⁻¹) 2932, 1558, 1515, 1333, 1198. ¹H NMR (500 MHz, CDCl₃) 8.28 – 8.31 (4H, m, H4, H8, H16, H17), 8.05 (2H, d, J = 7.2 Hz, H14, H15), 7.61 (2H, br s, H1, H3), 7.39 (2H, d, J = 7.6 Hz, H5, H7), 1.47 (9H, s, H10 – H12). ¹³C NMR (101 MHz, CDCl₃) 162.5 (C6), 147.1 (C2), 145.7 (C13), 143.4 (C18), 140.2 (C1', C3'), 136.9 (C4, C8), 127.9 (C14, C15), 124.3 (C16, C17), 122.7 (C5, C7), 114.5 (C1, C3), 38.8 (C9), 31.9 (C10 – C12). Melting point 289 – 291 °C, melts. HRMS (FTMS +p NSI) m/z: [M + H]⁺ calculated for C₂₀H₂₀NO₂ 306.1489, found = 306.1491, Δ = 0.8 ppm.

4.9 Bromination of 2-Functionalised Azulene

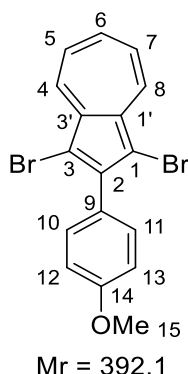
2-arylazulenes were prepared as previously described on a 5 mmol scale. The yields were found to be similar that obtained when carried out on the 0.5 mmol scale (~ 50 – 75%).

General Procedure G for Bromination of Azulenes



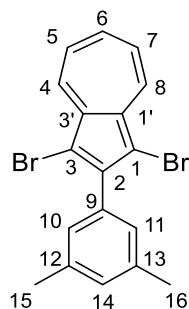
To a 500 mL round-bottomed flask with a large oval stirrer bar was added 2-arylazulene (2 mmol) and DCM (100 mL). NBS (783 mg, 2.2 mmol, 2.2 eq) was dissolved in 50 mL DCM and added portionwise to the azulene solution. The reaction was stirred at room temperature for 2 hours. The reaction was quenched with NaHCO₃ (100mL, 1M), then extracted with DCM, and dried with magnesium sulphate. The solvent was then removed *in vacuo*, and the crude mixture was purified by column chromatography to obtain the corresponding 1,3-dibromo-2-arylazulene.

1,3-Dibromo-2-(4-methoxyphenyl)azulene (57b)



General procedure G was applied to 2-(4-methoxyphenyl)azulene (469 mg, 2 mmol). The crude reaction product was purified by silica column chromatography (0% - 15% dichloromethane / hexane) to give **57b** as a green solid (569 mg, 73%). IR (λ_{max} /cm⁻¹) 2961, 1607, 1572, 1455, 1388, 1250, 1173, 1031. ¹H NMR (500 MHz, CO(CD₃)₂) 8.41 (2H, dd, J₁ = 9.8 Hz, J₂ = 1.2 Hz, H4, H8), 7.83 (1H, tt, J₁ = 9.9 Hz, J₂ = 1.0 Hz, H6), 7.58 – 7.45 (2H, m, H10, H11), 7.49 (2H, td, J₁ = 9.6 Hz, J₂ = 0.8 Hz, H5, H7), 7.12 – 7.09 (2H, m, H12, H13), 3.88 (3H, s, H15). ¹³C NMR (101 MHz, CO(CD₃)₂) 160.2 (C14), 146.6 (C2), 139.7 (C6), 136.4 (C4, C8), 132.0 (C10, C11), 131.0 (C1', C3'), 126.6 (C9), 125.4 (C5, C7), 113.6 (C12, C13), 102.6 (C1, C3), 54.9 (C15). Melting point 211 – 213 °C, melts. HRMS (FTMS +p NSI) m/z: [M + H]⁺ calculated for C₁₇H₁₃Br₂O₃ 390.9328, found = 390.9325, Δ = 0.6 ppm.

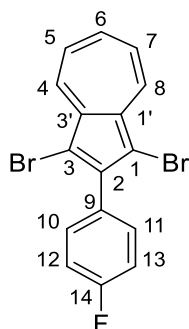
1,3-Dibromo-2-(3,5-dimethylphenyl)azulene (57c)



Mr = 390.1

General procedure G was applied to 2-(3,5-dimethylphenyl)azulene (465 mg, 2 mmol). The crude reaction product was purified by silica column chromatography (0% - 15% dichloromethane / hexane) to give **57c** as a green solid (468 mg, 60%). IR (λ_{max} /cm⁻¹) 2911, 1573, 1450, 1386, 1256, 1024 ¹H NMR (500 MHz, CO(CD₃)₂) 8.42 (2H, dd, J_1 = 10.0 Hz, J_2 = 1.0 Hz, H4, H8), 7.85 (1H, tt, J_1 = 9.9 Hz, J_2 = 1.0 Hz, H6), 7.50 (2H, t, J = 9.7 Hz, H5, H7), 7.17 (2H, s, H10, H11), 7.11 (1H, s, H14), 2.37 (6H, s, H15, H16). ¹³C NMR (101 MHz, CO(CD₃)₂) 147.3 (C2), 140.0 (C6), 137.5 (C12, C13), 136.7 (C4, C8), 136.3 (C1', C3'), 130.1 (C14), 128.2 (C10, C11), 127.4 (C9), 125.4 (C5, C7), 102.6 (C1, C3), 20.5 (C15, C16). Melting point 109 – 111 °C, melts. HRMS (FTMS +p NSI) m/z: [M + H]⁺ calculated for C₁₈H₁₅Br₂ 388.9535, found = 388.9535, Δ = - 0.1 ppm.

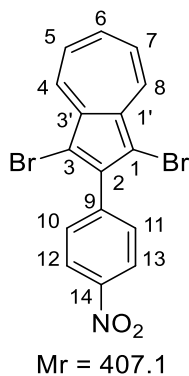
1,3-Dibromo-2-(4-fluorophenyl)azulene (**57d**)



Mr = 380.1

General procedure G was applied to 2-(4-fluorophenyl)azulene (444 mg, 2 mmol). The crude reaction product was purified by silica column chromatography (0% - 25% dichloromethane / hexane) to give **57d** as a green solid (483 mg, 64%). IR (λ_{max} /cm⁻¹) 1604, 1574, 1519, 1451, 1386, 1228, 1218, 1156, 1096, 1012. ¹H NMR (500 MHz, CO(CD₃)₂) 8.44 (2H, dd, J_1 = 10.0 Hz, J_2 = 1.0 Hz, H4, H8), 7.87 (1H, tt, J_1 = 10.0 Hz, J_2 = 1.0 Hz, H6), 7.67 – 7.62 (2H, m, H12, H13), 7.52 (2H, t, J = 10.0 Hz, H5, H7), 7.36 – 7.30 (2H, m, H10, H11). ¹³C NMR (101 MHz, CO(CD₃)₂) 162.9 (d, J = 246 Hz, C14), 145.8 (C2), 140.3 (C6), 137.0 (C4, C8), 136.3 (C1', C3'), 132.7 (d J = 8 Hz, H10, H11), 130.9 (d, J = 3 Hz, C9), 125.6 (C5, C7), 115.1 (d, 22 Hz, H12, H13), 102.4 (C1, C3). ¹⁹F NMR (376 MHz, CDCl₃) -114.2. Melting point 190 – 191 °C, melts. HRMS (FTMS +p NSI) m/z: [M + H]⁺ calculated for C₁₆H₁₀Br₂F 378.9128, found = 378.9126, Δ = 0.4.

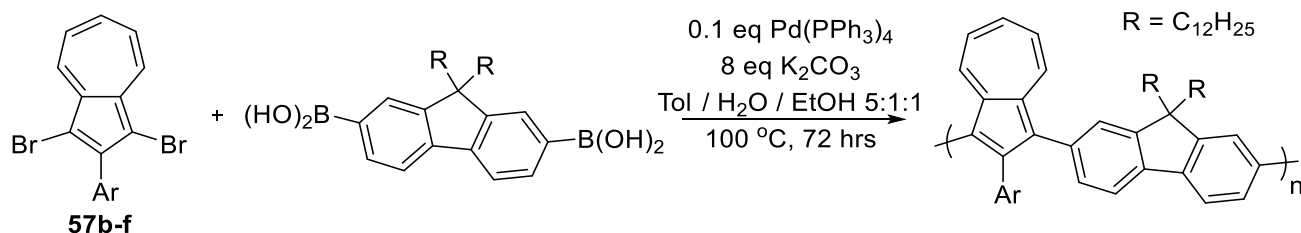
1,3-Dibromo-2-(4-nitrophenyl)azulene (**57e**)



General procedure G was applied to 2-(4-nitrophenyl)azulene (498 mg, 2 mmol) for 16 hours. The crude reaction product was purified by silica column chromatography (30% - 70% dichloromethane / hexane) to give **57e** as a green solid (472 mg, 58%). IR ($\lambda_{\text{max}}/\text{cm}^{-1}$) 2919, 1573, 1450, 1386, 1256, 1024. ^1H NMR (500 MHz, $\text{CO}(\text{CD}_3)_2$) 8.51 (2H, dd, $J_1 = 10.1$ Hz, $J_2 = 1.0$ Hz, H4, H8), 8.45 – 8.42 (2H, m, H12, H13), 7.94 (1H, tt, $J_1 = 9.9$ Hz, $J_2 = 0.9$ Hz, H6), 7.91 – 7.88 (2H, m, H10, H11), 7.57 (2H, t, $J = 10.0$ Hz, H5, H7). ^{13}C NMR (101 MHz, $\text{CO}(\text{CD}_3)_2$) 147.9 (C14), 144.3 (C9), 141.3 (C2), 141.2 (C6), 137.9 (C4, C8), 136.3 (C1', C3'), 131.9 (C10, C11), 126.0 (C5, C7), 123.3 (C12, C13), 102.1 (C1, C3). Melting point 200 – 202 °C, melts. HRMS (FTMS +p NSI) m/z : $[\text{M} + \text{H}]^+$ calculated for $\text{C}_{16}\text{H}_{10}\text{Br}_2\text{NO}_2$ 405.9073, found = 405.9066, $\Delta = 1.6$ ppm.

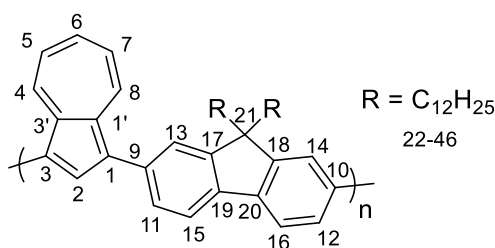
4.10 Suzuki Polymerisation

General Procedure H for Suzuki Polymerisation



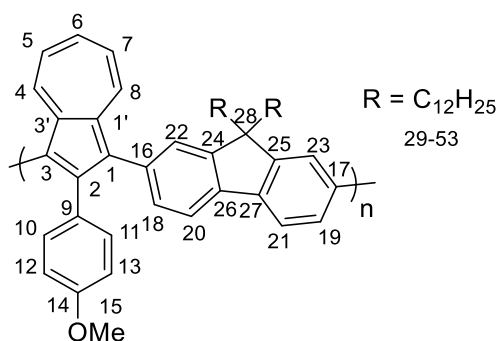
To a 100 mL round-bottomed flask with a large oval stirrer bar was added 1,3-dibromo-2-arylazulene (0.5 mmol), (9,9-didodecyl-9H-fluorene-2,7-diyl)diboronic acid (295 mg, 0.5 mmol), potassium carbonate (552 mg, 4 mmol), and tetrakis(triphenylphosphine)palladium(0) (23.1 mg, 0.02 mmol). The flask was sealed with a septum and evacuated / backfilled with nitrogen three times. Degassed toluene (10 mL), water (2 mL), and ethanol (2 mL) were then added via syringe. The mixture was heated at 100 °C for 72 hours. The solution was allowed to cool, then precipitated in methanol (100 mL). Filtration gave the crude polymer as a solid powder. The polymer was purified by Soxhlet extraction by acetone (3 hours), hexane (3 hours), and finally chloroform (3 hours). Chloroform was then removed in *vacuo* and the polymer was redissolved in minimum amount of chloroform. The polymer was then reprecipitated in methanol, filtered, and dried under vacuum.

Poly[2,7-(9,9-didodecylfluorenyl)-alt-(1',3'-azuleneyl)] (P16a)¹²⁵



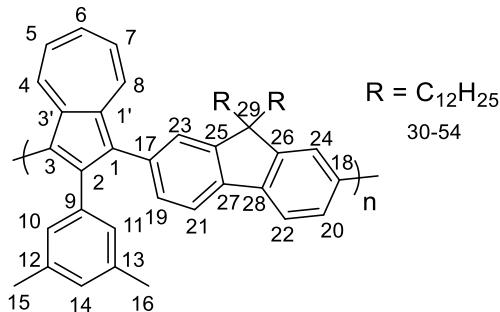
General procedure H was applied to 1,3-dibromoazulene (143 mg, 0.5 mmol). The purified polymer was obtained as a greenish yellow solid (94 mg, 30%). Spectrums match those previously reported. IR ($\lambda_{\text{max}}/\text{cm}^{-1}$) 2923, 2852, 1744, 1570, 1466, 1376, 1260, 1100. ¹H NMR (500 MHz, CDCl₃) 8.62 – 8.65 (2H, m, H4, H8), 8.32 – 8.35 (1H, m, H2), 7.90 – 7.93 (2H, m, H15, H16), 7.58 – 7.78 (5H, m, H6, H11 – H14), 7.10 – 7.20 (2H, m, H5, H7) 2.20 – 2.00 (4H, m, H22, H23), 0.80 – 1.30 (46H, m, H24 – H46). ¹³C NMR (101 MHz, CDCl₃) 151.6 (C17, C18), 139.6 (C19, C20), 139.2 (C1', C3'), 137.0 (C9, C10), 137.0 (C4, C8), 135.8 (C2), 131.4 (C5, C7), 128.8 (C13, C14), 124.5 (C11, C12), 123.6 (C6), 120.0 (C15, C16), 55.4 (C21), 40.6 (C22, C23), 32.0 (C24, C25), 32.0, 30.3, 29.4 – 29.9, 22.8, (C24 – C44), 14.2 (C45, C46). Mn ~ 15.1 kDa, Mw ~ 30.6 kDa, PDI = 2.0, T_d = 405 °C.

Poly[2,7-(9,9-didodecylfluorenyl)-alt-(1',3'-(2-(4-methoxyphenyl)azuleneyl))] (P16b)



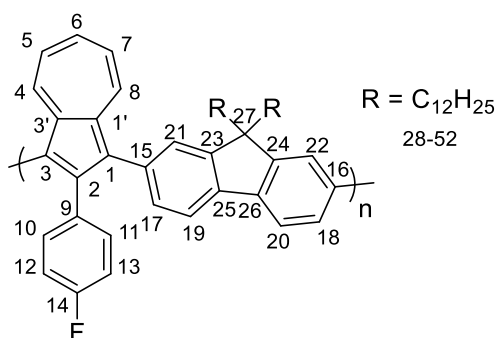
General procedure H was applied to 1,3-dibromo-2-(4-methoxyphenyl)azulene (196 mg, 0.5 mmol). The purified polymer was obtained as a greenish yellow solid (238 mg, 65%). IR ($\lambda_{\text{max}}/\text{cm}^{-1}$) 3004, 2923, 2852, 1609, 1573, 1519, 1463, 1411, 1294, 1248, 1176, 1037. ^1H NMR (500 MHz, CDCl_3) 8.41 – 8.38 (2H, m, H4, H8), 7.45 – 7.83 (5H, m, H6, H18, H19, H22, H23), 7.27 – 7.41 (2H, m, H10, H11), 7.05 – 7.21 (4H, m, H5, H7, H20, H21), 6.61 – 6.65 (2H, m, H12, H13), 3.71 (3H, m, H15), 1.80 – 2.00 (4H, H29, H30), 0.70 – 1.22 (46H, m, H31 – H53). ^{13}C NMR (101 MHz, CDCl_3) 158.5 (C14), 150.9 (C24, C25), 139.4 (C26, C27), 137.7 (C4, C8), 135.5 (C2), 132.7 (C10, C11), 131.2 (C5, C7), 130.2 (C1', C3'), 129.5 (C9), 128.8 (C22, C23), 126.4 (C6), 123.8 (C18, C19), 119.4 (C20, C21), 113.2 (C12, C13), 55.2 (C28), 55.0 (C15), 40.4 (C29, C30), 32.0, 30.3, 29.4 – 29.9, 22.8, (C31 – C51), 14.2 (C52, C53). $M_n \sim 10.3$ kDa, $M_w \sim 23.4$ kDa, PDI = 2.3, $T_d = 437$ °C.

Poly[2,7-(9,9-didodecylfluorene)-alt-(1',3'-(2-(3,5-dimethylphenyl)azuleneyl))]
(P16c)



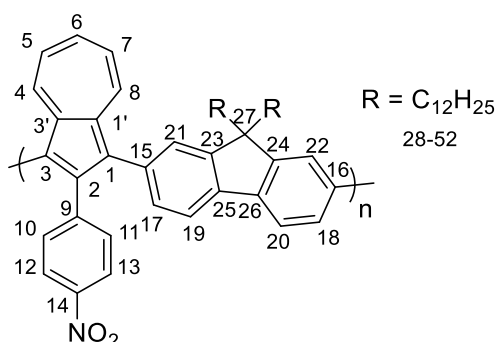
General procedure H was applied to 1,3-dibromo-2-(3,5-dimethylphenyl)azulene (195 mg, 0.5 mmol). The purified polymer was obtained as a greenish yellow solid (190 mg, 52%). IR ($\lambda_{\text{max}}/\text{cm}^{-1}$) 3006, 2852, 1569, 1463, 1377, 1294, 1215. ^1H NMR (500 MHz, CDCl_3) 8.45 – 8.38 (2H, m, H4, H8), 7.85 – 7.50 (5H, m, H6, H21 – H24), 7.27 – 7.35 (2H, m, H19, H20), 7.07 – 7.15 (2H, m, H5, H7), 6.70 – 6.78 (3H, m, H10, H11, H14), 2.01 – 2.20 (4H, H30, H31), 0.70 – 1.22 (46H, m, H32 – H54), 0.86 (6H, m, H15, H16). ^{13}C NMR (101 MHz, CDCl_3) 150.8 (C25, C26), 148.7 (C2), 139.4 (C27, C28), 137.6 (C4, C8), 136.6 (C12, C13), 135.8 (C2), 130.2 (C5, C7), 130.0 (C14), 129.4 (C9), 128.4 (C6), 128.0 (C10, C11), 126.3 (C19, C20), 123.6 (C9), 119.2 (C21, C22), 54.8 (C29), 40.4 (C30, C31), 32.0, 30.5 – 29.3, 22.8 (C32–C52), 21.4 (C15, C16), 14.2 (C53, C54). $M_n \sim 11.2$ kDa, $M_w \sim 15.6$ kDa, PDI = 1.4, $T_d = 423$ °C.

Poly[2,7-(9,9-didodecylfluorene)-alt-(1',3'-(2-(4-fluorophenyl)azuleneyl))]
(P16d)



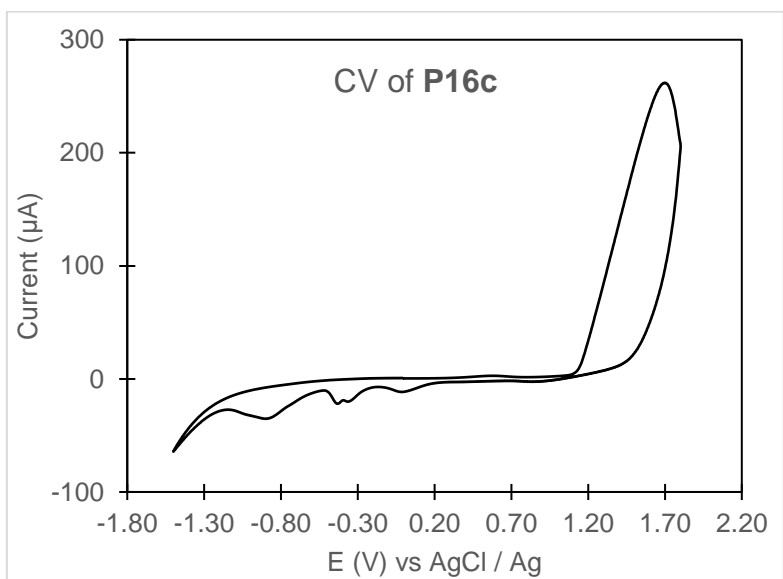
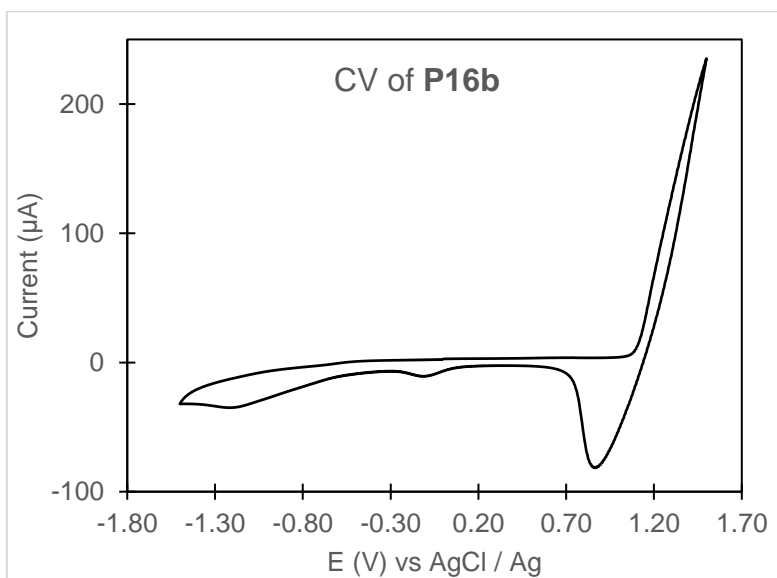
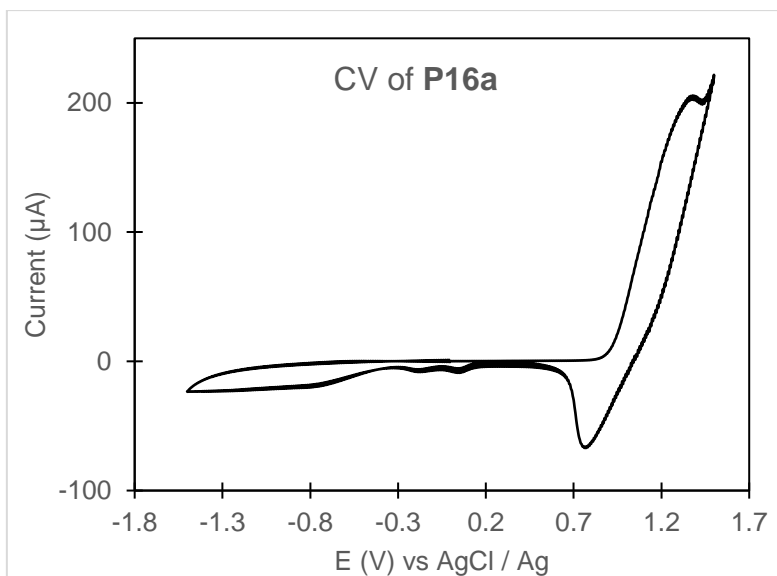
General procedure H was applied to 1,3-dibromo-2-(4-fluorophenyl)azulene (190 mg, 0.5 mmol). The purified polymer was obtained as a green solid (241 mg, 67%). IR ($\lambda_{\text{max}}/\text{cm}^{-1}$) 2925, 2853, 1890, 1605, 1571, 1516, 1460, 1410, 1232, 1156, 1014. ^1H NMR (500 MHz, CDCl_3) 8.48 – 8.40 (2H, m, H4, H8), 7.84 – 7.52 (5H, m, H6, H17, H18, H21, H22), 7.38 – 7.44 (2H, m, H10, H11), 7.07 – 7.16 (4H, m, H5, H7, H19, H20), 6.75 – 6.82 (2H, H12, H13), 1.80 – 2.00 (4H, H28, H29), 0.70 – 1.22 (46H, m, H30 – H52). ^{13}C NMR (101 MHz, CDCl_3) 160.8 (C14), 151.0 (C23, C24), 146.8 (C2), 139.4 (C26, C27), 137.6 (C4, C8), 136.1 (C1', C3'), 134.8 (C5, C7), 133.0 (C12, C13), 130.2 (C9), 129.6 (C21, C22), 126.3 (C6), 123.9 (C17, C18), 119.4 (C19, C20), 114.9 (C10, C11), 55.0 (C27), 40.6 (C28, C29), 32.0, 30.5 – 29.3, 22.8 (C30–C50), 14.2 (C51, C52). ^{19}F NMR (376 MHz, CDCl_3) -114.5. $M_n \sim 8.2$ kDa, $M_w \sim 12.1$ kDa, PDI = 1.5, $T_d = 437$ °C.

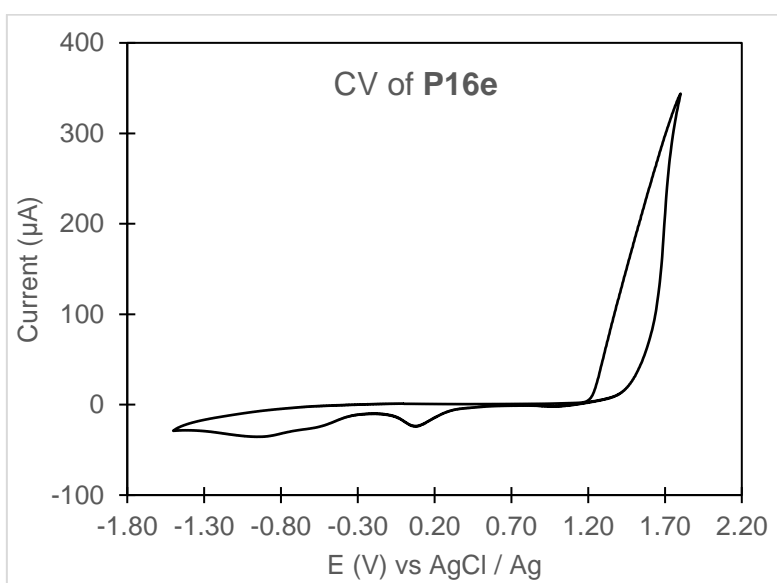
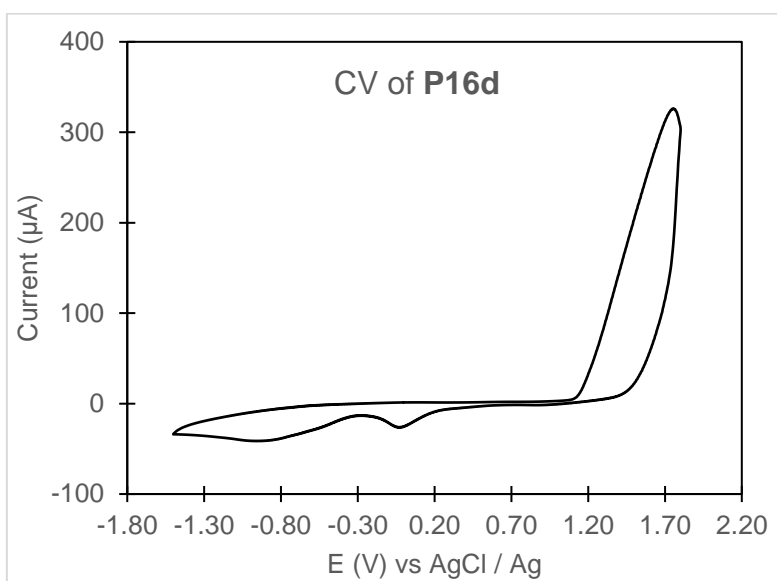
Poly[2,7-(9,9-didodecylfluorenyl)-alt-(1',3'-(2-(4-nitrophenyl)azuleneyl)]] (P16e)

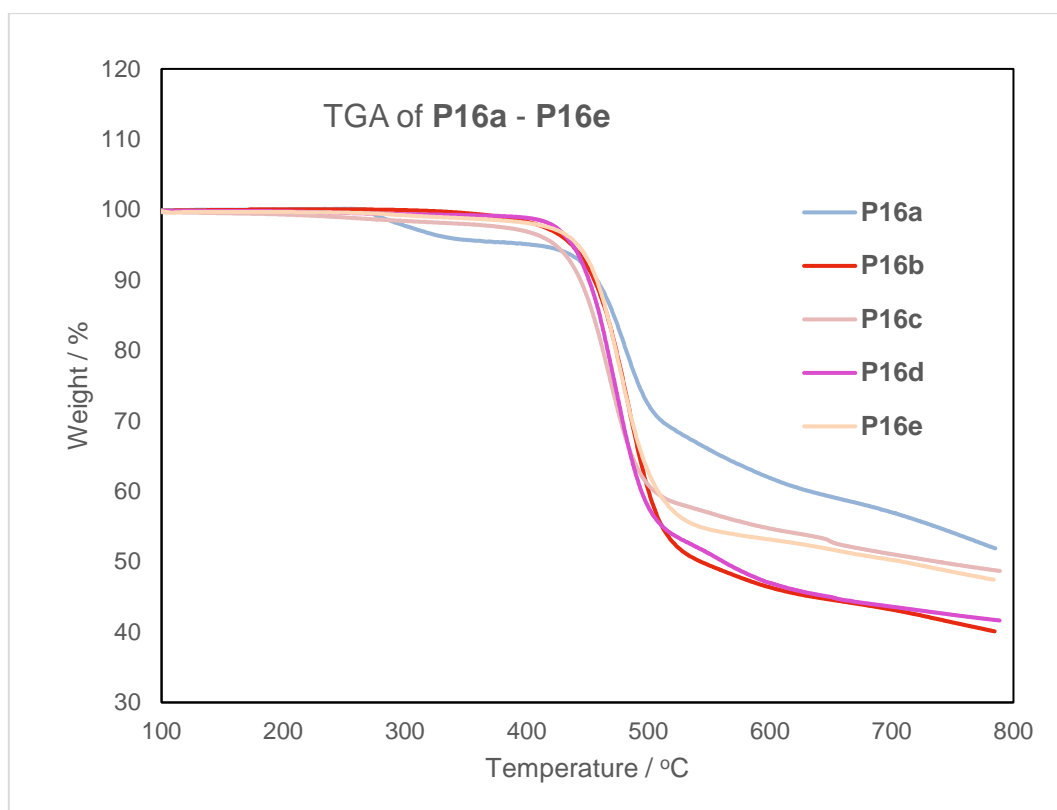


General procedure H was applied to 1,3-dibromo-2-(4-nitrophenyl)azulene (203 mg, 0.5 mmol). The purified polymer was obtained as a green solid (191 mg, 51%). IR ($\lambda_{\text{max}}/\text{cm}^{-1}$) 2925, 2853, 1744, 1597, 1571, 1520, 1463, 1341, 1246, 1109. ^1H NMR (500 MHz, CDCl_3) 8.40 – 8.46 (2H, m, H4, H8), 7.93 – 7.98 (2H, m, H12, H13), 7.60 – 7.81 (5H, m, H6, H17, H18, H21, H22), 7.28 – 7.33 (4H, m, H5, H7, H10, H11), 7.13 – 7.20 (2H, m, H19, H20), 1.80 – 2.00 (4H, H28, H29), 0.70 – 1.22 (46H, m, H30 – H52). ^{13}C NMR (101 MHz, CDCl_3) 151.2 (C23, C24), 146.2 (C14), 144.7 (C25, C26), 144.00 (C9), 139.6 (C1', C3'), 137.7 (C4, C8), 137.3 (C2), 134.3 (C19, C20), 132.3 (C6), 130.0 (C5, C7), 126.3 (C21, C22), 124.4 (C17, C18), 123.0 (C12, C13), 119.9 (C1, C3), 55.1 (C27), 40.6 (C28, C29), 32.0, 30.5 – 29.3, 22.8 (C30–C50), 14.2 (C51, C52). $M_n \sim 12.9$ kDa, $M_w \sim 21.0$ kDa, PDI = 1.6, $T_d = 442$ °C.

4.11 Miscellaneous Spectra







5. REFERENCES

- (1) Miyaura, N.; Yamada, K.; Suzuki, A. *Tetrahedron Lett.* **1979**, 20 (36), 3437–3440.
- (2) King, A. O.; Okukado, N.; Negishi, E. *J. Chem. Soc. Chem. Commun.* **1977**, No. 19, 683–684.
- (3) Heck, R. F. *J. Am. Chem. Soc.* **1968**, 90 (20), 5518–5526.
- (4) Blanksby, S. J.; Ellison, G. B. *Acc. Chem. Res.* **2003**, 36 (4), 255–263.
- (5) Bordwell, F. G. *Acc. Chem. Res.* **1988**, 21 (12), 456–463.
- (6) Olah, G. A.; Halpern, Y.; Shen, J.; Mo, Y. K. *J. Am. Chem. Soc.* **1973**, 95 (15), 4960–4970.
- (7) Tabushi, I.; Hamuro, J.; Oda, R. *J. Am. Chem. Soc.* **1967**, 89 (26), 7127–7129.
- (8) Davies, H. M. L.; Beckwith, R. E. *J. Chem. Rev.* **2003**, 103 (8), 2861–2904.
- (9) Lebel, H.; Huard, K.; Lectard, S. *J. Am. Chem. Soc.* **2005**, 127 (41), 14198–14199.
- (10) Groves, J. T. *Nat Chem* **2014**, 6 (2), 89–91.
- (11) Kleiman, J. P.; Dubeck, M. *J. Am. Chem. Soc.* **1963**, 85 (10), 1544–1545.
- (12) Murahashi, S. *J. Am. Chem. Soc.* **1955**, 77 (23), 6403–6404.
- (13) Murai, S.; Kakiuchi, F.; Sekine, S.; Tanaka, Y.; Kamatani, A.; Sonoda, M.; Chatani, N. *Nature* **1993**, 366 (6455), 529–531.
- (14) Wasa, M.; Chan, K. S. L.; Zhang, X.-G.; He, J.; Miura, M.; Yu, J.-Q. *J. Am. Chem. Soc.* **2012**, 134 (45), 18570–18572.
- (15) Zhang, F.-L.; Hong, K.; Li, T.-J.; Park, H.; Yu, J.-Q. *Science* **2016**, 351 (6270), 252–256.
- (16) Lu, L.; Shi, R.; Liu, L.; Yan, J.; Lu, F.; Lei, A. *Chem. – A Eur. J.* **2016**, 22 (41), 14484–14488.
- (17) Xin, Z.; Gøsgsig, T. M.; Lindhardt, A. T.; Skrydstrup, T. *Org. Lett.* **2012**, 14 (1), 284–287.
- (18) Kalogirou, A. S.; Koutentis, P. A. *Tetrahedron* **2014**, 70 (38), 6796–6802.
- (19) Sloan, N. L.; Sutherland, A. *Synthesis* **2016**, 48 (18), 2969–2980.
- (20) Moghimi, S.; Mahdavi, M.; Shafiee, A.; Foroumadi, A. *Eur. J. Org. Chem.* **2016**, 2016 (20), 3282–3299.
- (21) Wang, Q.; Takita, R.; Kikuzaki, Y.; Ozawa, F. *J. Am. Chem. Soc.* **2010**, 132 (33), 11420–11421.
- (22) Zhu, R.-Y.; Farmer, M. E.; Chen, Y.-Q.; Yu, J.-Q. *Angew. Chem Int. Ed.* **2016**, 55 (36), 10578–10599.
- (23) Pulis, A. P.; Procter, D. J. *Angew. Chemie Int. Ed.* **2016**, 55 (34), 9842–9860.
- (24) Zaitsev, V. G.; Shabashov, D.; Daugulis, O. *J. Am. Chem. Soc.* **2005**, 127 (38), 13154–13155.
- (25) Thalji, R. K.; Ellman, J. A.; Bergman, R. G. *J. Am. Chem. Soc.* **2004**, 126 (23), 7192–7193.
- (26) Brasche, G.; García-Fortanet, J.; Buchwald, S. L. *Org. Lett.* **2008**, 10 (11), 2207–2210.
- (27) Chotana, G. A.; Rak, M. A.; Smith, M. R. *J. Am. Chem. Soc.* **2005**, 127 (30), 10539–10544.
- (28) Zhao, X.; Yeung, C. S.; Dong, V. M. *J. Am. Chem. Soc.* **2010**, 132 (16), 5837–5844.
- (29) Wan, L.; Dastbaravardeh, N.; Li, G.; Yu, J.-Q. *J. Am. Chem. Soc.* **2013**, 135 (48), 18056–18059.
- (30) Yang, G.; Lindovska, P.; Zhu, D.; Kim, J.; Wang, P.; Tang, R.-Y.; Movassaghi, M.; Yu, J.-Q. *J. Am. Chem. Soc.* **2014**, 136 (30), 10807–10813.
- (31) Wang, X.-C.; Gong, W.; Fang, L.-Z.; Zhu, R.-Y.; Li, S.; Engle, K. M.; Yu, J.-Q. *Nature* **2015**, 519 (7543), 334–338.
- (32) Wencel-Delord, J.; Droge, T.; Liu, F.; Glorius, F. *Chem. Soc. Rev.* **2011**, 40 (9), 4740–4761.
- (33) Smalley, A. P.; Gaunt, M. J. *J. Am. Chem. Soc.* **2015**, 137 (33), 10632–10641.
- (34) Ryabov, A. D. *Chem. Rev.* **1990**, 90 (2), 403–424.
- (35) Niu, S.; Hall, M. B. *Chem. Rev.* **2000**, 100 (2), 353–406.
- (36) Balcells, D.; Clot, E.; Eisenstein, O. *Chem. Rev.* **2010**, 110 (2), 749–823.
- (37) Gorelsky, S. I.; Lapointe, D.; Fagnou, K. *J. Am. Chem. Soc.* **2008**, 130 (33), 10848–10849.
- (38) Labinger, J. A.; Bercaw, J. E. *Nature* **2002**, 417 (6888), 507–514.
- (39) Davies, D. L.; Donald, S. M. A.; Macgregor, S. A. *J. Am. Chem. Soc.* **2005**, 127 (40), 13754–13755.
- (40) Vicente, J.; Saura-Llomas, I. *Inorg. Chem.* **2007**, 28 (1–2), 39–72.
- (41) Ryabov, A. D.; Sakodinskaya, I. K.; Yatsimirsky, A. K. *J. Chem. Soc. Dalt. Trans.* **1985**, No. 12, 2629–2638.
- (42) Brookhart, M.; Green, M. L. H.; Parkin, G. *Proc. Natl. Acad. Sci.* **2007**, 104 (17), 6908–6914.
- (43) Oxgaard, J.; Tenn, W. J.; Nielsen, R. J.; Periana, R. A.; Goddard, W. A. *Organometallics* **2007**, 26 (7), 1565–1567.
- (44) Boutadla, Y.; Davies, D. L.; Macgregor, S. A.; Poblador-Bahamonde, A. I. *Dalt. Trans.* **2009**, No. 30, 5887–5893.
- (45) Bruce, M. I. *Angew. Chemie Int. Ed. English* **1977**, 16 (2), 73–86.
- (46) Pasunooti, K. K.; Banerjee, B.; Yap, T.; Jiang, Y.; Liu, C.-F. *Org. Lett.* **2015**, 17 (24), 6094–6097.
- (47) Thacker, N. C.; Shoba, V. M.; Geis, A. E.; Takacs, J. M. *Tetrahedron Lett.* **2015**, 56 (23), 3306–3310.
- (48) Neufeldt, S. R.; Sanford, M. S. *Org. Lett.* **2010**, 12 (3), 532–535.
- (49) Cho, S. H.; Hwang, S. J.; Chang, S. *J. Am. Chem. Soc.* **2008**, 130 (29), 9254–9256.
- (50) Simmons, E. M.; Hartwig, J. F. *Nature* **2012**, 483 (7387), 70–73.
- (51) Dastbaravardeh, N.; Toba, T.; Farmer, M. E.; Yu, J.-Q. *J. Am. Chem. Soc.* **2015**, 137 (31), 9877–9884.
- (52) Huang, L.; Weix, D. J. *Org. Lett.* **2016**, 18 (20), 5432–5435.
- (53) Samanta, R.; Antonchick, A. P. *Angew. Chemie Int. Ed.* **2011**, 50 (22), 5217–5220.
- (54) Zhang, Y.; Li, Z.; Liu, Z.-Q. *Org. Lett.* **2012**, 14 (1), 226–229.
- (55) Xiao, B.; Fu, Y.; Xu, J.; Gong, T.-J.; Dai, J.-J.; Yi, J.; Liu, L. *J. Am. Chem. Soc.* **2010**, 132 (2), 468–469.
- (56) Feng, R.; Yu, W.; Wang, K.; Liu, Z.; Zhang, Y. *Adv. Synth. Catal.* **2014**, 356 (7), 1501–1508.
- (57) Keshri, P.; Bettadapur, K. R.; Lanke, V.; Prabhu, K. R. *J. Org. Chem.* **2016**, 81 (14), 6056–6065.

- (58) Salvatore, R. N.; Yoon, C. H.; Jung, K. W. *Tetrahedron* **2001**, 57 (37), 7785–7811.
- (59) Baxter, E. W.; Reitz, A. B. In *Organic Reactions*; John Wiley & Sons, Inc., 2004.
- (60) Bariwal, J.; der Eycken, E. *Chem. Soc. Rev.* **2013**, 42 (24), 9283–9303.
- (61) Müller, T. E.; Hultzs, K. C.; Yus, M.; Foubelo, F.; Tada, M. *Chem. Rev.* **2008**, 108 (9), 3795–3892.
- (62) Beatty, J. W.; Stephenson, C. R. J. *Acc. Chem. Res.* **2015**, 48 (5), 1474–1484.
- (63) Orito, K.; Horibata, A.; Nakamura, T.; Ushito, H.; Nagasaki, H.; Yuguchi, M.; Yamashita, S.; Tokuda, M. *J. Am. Chem. Soc.* **2004**, 126 (44), 14342–14343.
- (64) Lazareva, A.; Daugulis, O. *Org. Lett.* **2006**, 8 (23), 5211–5213.
- (65) Feng, R.; Yao, J.; Liang, Z.; Liu, Z.; Zhang, Y. *J. Org. Chem.* **2013**, 78 (8), 3688–3696.
- (66) Tan, P. W.; Haughey, M.; Dixon, D. J. *Chem. Commun.* **2015**, 51 (21), 4406–4409.
- (67) Cai, G.; Fu, Y.; Li, Y.; Wan, X.; Shi, Z. *J. Am. Chem. Soc.* **2007**, 129 (24), 7666–7673.
- (68) Vicente, J.; Saura-Llomas, I.; Palin, M. G.; Jones, P. G.; Ramírez de Arellano, M. C. *Organometallics* **1997**, 16 (5), 826–833.
- (69) Wang, J.-R.; Fu, Y.; Zhang, B.-B.; Cui, X.; Liu, L.; Guo, Q.-X. *Tetrahedron Lett.* **2006**, 47 (47), 8293–8297.
- (70) Shabashov, D.; Daugulis, O. *Org. Lett.* **2005**, 7 (17), 3657–3659.
- (71) He, G.; Chen, G. *Angew. Chemie Int. Ed.* **2011**, 50 (22), 5192–5196.
- (72) He, G.; Zhao, Y.; Zhang, S.; Lu, C.; Chen, G. *J. Am. Chem. Soc.* **2012**, 134 (1), 3–6.
- (73) Zhang, S.-Y.; He, G.; Nack, W. A.; Zhao, Y.; Li, Q.; Chen, G. *J. Am. Chem. Soc.* **2013**, 135 (6), 2124–2127.
- (74) Zhao, Y.; Chen, G. *Org. Lett.* **2011**, 13 (18), 4850–4853.
- (75) Hamilton, G. L.; Kanai, T.; Toste, F. D. *J. Am. Chem. Soc.* **2008**, 130 (45), 14984–14986.
- (76) Rodríguez, N.; Romero-Revilla, J. A.; Fernández-Ibáñez, M. Á.; Carretero, J. C. *Chem. Sci.* **2013**, 4 (1), 175–179.
- (77) García-Rubia, A.; Urones, B.; Gómez Arrayás, R.; Carretero, J. C. *Chem. – A Eur. J.* **2010**, 16 (31), 9676–9685.
- (78) García-Rubia, A.; Arrayás, R. G.; Carretero, J. C. *Angew. Chemie Int. Ed.* **2009**, 48 (35), 6511–6515.
- (79) García-Rubia, A.; Urones, B.; Gómez Arrayás, R.; Carretero, J. C. *Angew. Chemie Int. Ed.* **2011**, 50 (46), 10927–10931.
- (80) Reddy, B. V. S.; Reddy, L. R.; Corey, E. J. *Org. Lett.* **2006**, 8 (15), 3391–3394.
- (81) Fan, M.; Ma, D. *Angew. Chemie Int. Ed.* **2013**, 52 (46), 12152–12155.
- (82) Ye, X.; He, Z.; Ahmed, T.; Weise, K.; Akhmedov, N. G.; Petersen, J. L.; Shi, X. *Chem. Sci.* **2013**, 4 (9), 3712–3716.
- (83) Wang, C.; Chen, C.; Zhang, J.; Han, J.; Wang, Q.; Guo, K.; Liu, P.; Guan, M.; Yao, Y.; Zhao, Y. *Angew. Chemie Int. Ed.* **2014**, 53 (37), 9884–9888.
- (84) L., C. S.; Wasa, M.; Chu, L.; Laforteza, B. N.; Miura, M.; Yu, J.-Q. *Nat. Chem.* **2014**, 6 (2), 146–150.
- (85) Jiang, H.; He, J.; Liu, T.; Yu, J.-Q. *J. Am. Chem. Soc.* **2016**, 138 (6), 2055–2059.
- (86) Wang, P.-L.; Li, Y.; Wu, Y.; Li, C.; Lan, Q.; Wang, X.-S. *Org. Lett.* **2015**, 17 (15), 3698–3701.
- (87) Nakata, K.; Yamaoka, Y.; Miyata, T.; Taniguchi, Y.; Takaki, K.; Fujiwara, Y. *J. Organomet. Chem.* **1994**, 473 (1), 329–334.
- (88) Bennett, M. I.; Laird, B.; van Litsenburg, C.; Nimour, M. *Pain Med.* **2013**, 14 (11), 1681–1688.
- (89) Wang, C.; Zhang, L.; Chen, C.; Han, J.; Yao, Y.; Zhao, Y. *Chem. Sci.* **2015**, 6 (8), 4610–4614.
- (90) Lafrance, M.; Gorelsky, S. I.; Fagnou, K. *J. Am. Chem. Soc.* **2007**, 129 (47), 14570–14571.
- (91) Hernando, E.; Villalva, J.; Manu, A.; Rodr, N. *ACS Catal.* **2016**, 6 (10), 6868–6882.
- (92) McNally, A.; Haffemayer, B.; Collins, B. S. L.; Gaunt, M. J. *Nature* **2014**, 510 (7503), 129–133.
- (93) Zakrzewski, J.; Smalley, A. P.; Kabeshov, M. A.; Gaunt, M. J.; Lapkin, A. A. *Angew. Chemie Int. Ed.* **2016**, 55 (31), 8878–8883.
- (94) Smalley, A. P.; Cuthbertson, J. D.; Gaunt, M. J. *J. Am. Chem. Soc.* **2017**, 139 (4), 1412–1415.
- (95) Manuel, N.; Chuan, H.; Whitehurst, W.G.; Chappell, B.C.; Gaunt, M.J. *Angew. Chemie Int. Ed.* **2018**, 57 (12), 3178–3182.
- (96) Koser, G. F.; Wettach, R. H. *J. Org. Chem.* **1980**, 45 (24), 4988–4989.
- (97) Buettner, C. S.; Willcox, D.; Chappell, B. G. N.; Gaunt, M. J. *Chem. Sci.* **2019**, 10 (1), 83–89.
- (98) He, C.; Gaunt, M. J. *Chem. Sci.* **2017**, 8 (5), 3586–3592.
- (99) He, C.; Gaunt, M. J. *Angew. Chemie - Int. Ed.* **2015**, 54 (52), 15840–15844.
- (100) Engle, K. M.; Wang, D.-H.; Yu, J.-Q. *J. Am. Chem. Soc.* **2010**, 132 (40), 14137–14151.
- (101) Calleja, J.; Pla, D.; Gorman, T. W.; Domingo, V.; Haffemayer, B.; Gaunt, M. J. *Nat. Chem.* **2015**, 7 (12), 1009–1016.
- (102) Ho, D. K. H.; Calleja, J.; Gaunt, M. J. *Synlett* **2019**, 30 (04), 454–458.
- (103) Topczewski, J. J.; Cabrera, P. J.; Saper, N. I.; Sanford, M. S. *Nature* **2016**, 531 (7593), 220–224.
- (104) Coe, J. W.; Brooks, P. R.; Vetelino, M. G.; Wirtz, M. C.; Arnold, E. P.; Huang, J.; Sands, S. B.; Davis, T. I.; Lebel, L. A.; Fox, C. B.; Shrikhande, A.; Heym, J. H.; Schaeffer, E.; Rollemma, H.; Lu, Y.; Mansbach, R. S.; Chambers, L. K.; Rovetti, C. C.; Schulz, D. W.; Tingley, F. D.; O'Neill, B. T. *J. Med. Chem.* **2005**, 48 (10), 3474–3477.
- (105) Cabrera, P. J.; Lee, M.; Sanford, M. S. *J. Am. Chem. Soc.* **2018**, 140 (16), 5599–5606.
- (106) Willcox, D.; Chappell, B. G. N.; Hogg, K. F.; Calleja, J.; Smalley, A. P.; Gaunt, M. J. *Science* **2016**, 354 (6314), 851–857.

- (107) Cabrera-Pardo, J. R.; Trowbridge, A.; Nappi, M.; Ozaki, K.; Gaunt, M. J. *Angew. Chemie Int. Ed.* **2017**, 56 (39), 11958–11962.
- (108) Hogg, K. F.; Trowbridge, A.; Alvarez-Perez, A.; Gaunt, M. J. *Chem. Sci.* **2017**, 8 (12), 8198–8203.
- (109) Xu, Y.; Young, M. C.; Wang, C.; Magness, D. M.; Dong, G. *Angew. Chemie Int. Ed.* **2016**, 55 (31), 9084–9087.
- (110) Wu, Y.; Chen, Y.-Q.; Liu, T.; Eastgate, M. D.; Yu, J.-Q. *J. Am. Chem. Soc.* **2016**, 138 (44), 14554–14557.
- (111) Liu, Y.; Ge, H. *Nat. Chem.* **2016**, 9, 26.
- (112) Yada, A.; Liao, W.; Sato, Y.; Murakami, M. *Angew. Chemie Int. Ed.* **2017**, 56 (4), 1073–1076.
- (113) Kapoor, M.; Liu, D.; Young, M. C. *J. Am. Chem. Soc.* **2018**, 140 (22), 6818–6822.
- (114) Chen, K.; Wang, D.; Li, Z.-W.; Liu, Z.; Pan, F.; Zhang, Y.-F.; Shi, Z.-J. *Org. Chem. Front.* **2017**, 4 (11), 2097–2101.
- (115) Cabrera-Pardo, J. R.; Trowbridge, A.; Nappi, M.; Ozaki, K.; Gaunt, M. J. *Angew. Chemie Int. Ed.* **2017**, 56 (39), 11958–11962.
- (116) McDermott, J. X.; White, J. F.; Whitesides, G. M. *J. Am. Chem. Soc.* **1976**, 98 (21), 6521–6528.
- (117) Kamimura, A.; Omata, Y.; Tanaka, K.; Shirai, M. *Tetrahedron* **2003**, 59 (33), 6291–6299.
- (118) Lee, K. L.; Ambler, C. M.; Anderson, D. R.; Boscoe, B. P.; Bree, A. G.; Brodfuehrer, J. I.; Chang, J. S.; Choi, C.; Chung, S.; Curran, K. J.; Day, J. E.; Dehnhardt, C. M.; Dower, K.; Drozda, S. E.; Frisbie, R. K.; Gavrin, L. K.; Goldberg, J. A.; Han, S.; Hegen, M.; Hepworth, D.; Hope, H. R.; Kamtekar, S.; Kilty, I. C.; Lee, A.; Lin, L.-L.; Lovering, F. E.; Lowe, M. D.; Mathias, J. P.; Morgan, H. M.; Murphy, E. A.; Papaioannou, N.; Patny, A.; Pierce, B. S.; Rao, V. R.; Saiah, E.; Samardjiev, I. J.; Samas, B. M.; Shen, M. W. H.; Shin, J. H.; Soutter, H. H.; Strohbach, J. W.; Symanowicz, P. T.; Thomason, J. R.; Trzuppek, J. D.; Vargas, R.; Vincent, F.; Yan, J.; Zapf, C. W.; Wright, S. W. *J. Med. Chem.* **2017**, 60 (13), 5521–5542.
- (119) Anderson, A. G.; Steckler, B. M. *J. Am. Chem. Soc.* **1959**, 81 (18), 4941–4946.
- (120) Morgante, C. G.; Struve, W. S. *Chem. Phys. Lett.* **1979**, 68 (2), 267–271.
- (121) Liu, R. S. H. *J. Chem. Educ.* **2002**, 79 (2), 183.
- (122) Tsurui, K.; Murai, M.; Ku, S.; Hawker, C. J.; Robb, M. J. *Adv. Funct. Mater.* **2014**, 24 (46), 7338–7347.
- (123) He, N.; Höfler, L.; Latonen, R.-M.; Lindfors, T. *Sensors Actuators B Chem.* **2015**, 207, 918–925.
- (124) Wang, F.; Lin, T. T.; He, C.; Chi, H.; Tang, T.; Lai, Y.-H. *J. Mater. Chem.* **2012**, 22 (21), 10448–10451.
- (125) Tang, T.; Ding, G.; Lin, T.; Chi, H.; Liu, C.; Lu, X.; Wang, F.; He, C. *Macromol. Rapid Commun.* **2013**, 34 (5), 431–436.
- (126) Wang, X.; Ng, J. K.-P.; Jia, P.; Lin, T.; Cho, C. M.; Xu, J.; Lu, X.; He, C. *Macromolecules* **2009**, 42 (15), 5534–5544.
- (127) Ding, G.; Cho, C. M.; Chen, C.; Zhou, D.; Wang, X.; Tan, A. Y. X.; Xu, J.; Lu, X. *Org. Electron.* **2013**, 14 (11), 2748–2755.
- (128) Yao, J.; Cai, Z.; Liu, Z.; Yu, C.; Luo, H.; Yang, Y.; Yang, S.; Zhang, G.; Zhang, D. *Macromolecules* **2015**, 48 (7), 2039–2047.
- (129) Umeyama, T.; Watanabe, Y.; Miyata, T.; Imahori, H. *Chem. Lett.* **2015**, 44 (1), 47–49.
- (130) Ghasimi, S.; Landfester, K.; Zhang, K. A. I. *ChemCatChem* **2016**, 8 (4), 694–698.
- (131) Wang, F.; Lai, Y.-H.; Kocherginsky, N. M.; Kostecki, Y. Y. *Org. Lett.* **2003**, 5 (7), 995–998.
- (132) Estdale, S. E.; Brett, R.; A. Dunmur, D.; Marson, C. M. *J. Mater. Chem.* **1997**, 7 (3), 391–401.
- (133) Grodzka, E.; Winkler, K.; Esteban, B. M.; Kvarnstrom, C. *Electrochim. Acta* **2010**, 55 (3), 970–978.
- (134) Peet, J.; Selyutina, A.; Bredihhin, A. *Bioorg. Med. Chem.* **2016**, 24 (8), 1653–1657.
- (135) Ohshima, N.; Akatsu, Y.; Nishishiro, M. *Anticancer Res.* **2006**, 2928, 2921–2927.
- (136) Akatsu, Y.; Ohshima, N.; Yamagishi, Y.; Nishishiro, M. *Anticancer Res.* **2006**, 1924, 1917–1923.
- (137) Takekuma, S.; Matsubara, Y.; Yamamoto, H.; Nozoe, T. *Bull. Chem. Soc. Jpn.* **1987**, 60 (10), 3721–3730.
- (138) Matsubara, Y.; Yamamoto, H.; Nozoe, T. *Stereoselective Synthesis (Part I)*; Elsevier, **1994**; Vol. 14, pp 313–354.
- (139) Tang, T.; Lin, T.; Erden, F.; Wang, F.; He, C. *J. Mater. Chem. C* **2018**, 6 (19), 5153–5160.
- (140) Brown, R. D. *Trans. Faraday Soc.* **1948**, 44 (0), 984–987.
- (141) Anderson, A. G.; Nelson, J. A. *J. Am. Chem. Soc.* **1950**, 72 (8), 3824–3825.
- (142) Anderson, A. G.; Nelson, J. A.; Tazuma, J. J. *J. Am. Chem. Soc.* **1953**, 75 (20), 4980–4989.
- (143) Muthyala, R. S.; Liu, R. S. H. *J. Fluor. Chem.* **1998**, 89 (2), 173–175.
- (144) Porsch, M.; Sigl-Seifert, G.; Daub, J. *Adv. Mater.* **2004**, 9 (8), 635–639.
- (145) Kurotobi, K.; Tabata, H.; Miyauchi, M.; Murafuji, T.; Sugihara, Y. *Synthesis* **2002**, 2002 (08), 1013–1016.
- (146) Cowper, P.; Jin, Y.; Turton, M. D.; Kociok-Köhn, G.; Lewis, S. E. *Angew. Chemie Int. Ed.* **2016**, 55 (7), 2564–2568.
- (147) Dyker, G.; Borowski, S.; Heiermann, J.; Körning, J.; Opwis, K.; Henkel, G.; Köckerling, M. *J. Organomet. Chem.* **2000**, 606 (2), 108–111.
- (148) Murai, M.; Yanagawa, M.; Nakamura, M.; Takai, K. *Asian J. Org. Chem.* **2016**, 5 (5), 629–635.
- (149) Zhao, L.; Bruneau, C.; Doucet, H. *Chem. Commun.* **2013**, 49 (49), 5598–5600.
- (150) Ho, T.-I.; Ku, C.-K.; Liu, R. S. H. *Tetrahedron Lett.* **2001**, 42 (4), 715–717.
- (151) Nozoe, T.; Seto, S.; Matsumura, S.; Asano, T. *Proc. Jpn. Acad.* **1956**, 32 (5), 339–343.
- (152) Nozoe, T.; Takase, K.; Shimazaki, N. *Bull. Chem. Soc. Jpn.* **1964**, 37 (11), 1644–1648.
- (153) Yang, P.-W.; Yasunami, M.; Takase, K. *Tetrahedron Lett.* **1971**, 12 (45), 4275–4278.
- (154) Hafner, K. *Angew. Chemie* **1955**, 67 (11), 301–302.

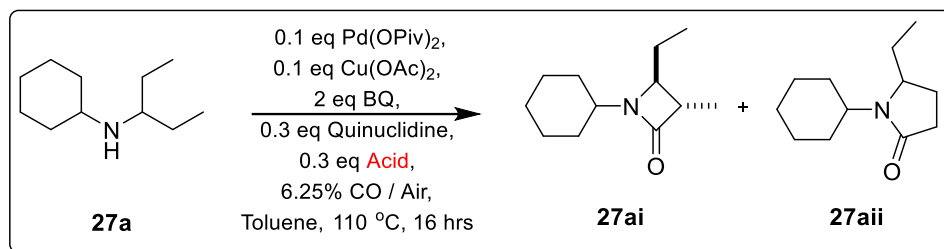
- (155) Reiter, S. E.; Dunn, L. C.; Houk, K. N. *J. Am. Chem. Soc.* **1977**, 99 (12), 4199–4201.
- (156) Xin, H.; Ge, C.; Yang, X.; Gao, H.; Yang, X.; Gao, X. *Chem. Sci.* **2016**, 7 (11), 6701–6705.
- (157) Rudolf, K.; Robinette, D.; Koenig, T. *J. Org. Chem.* **1987**, 52 (4), 641–647.
- (158) Leino, T. O.; Baumann, M.; Yli-Kauhaluoma, J.; Baxendale, I. R.; Wallén, E. A. A. *J. Org. Chem.* **2015**, 80 (22), 11513–11520.
- (159) Gromov, S. P. *Heterocycles* **2000**, 53 (7), 1607–1630.
- (160) Székely, A.; Péter, Á.; Aradi, K.; Tolnai, G. L.; Novák, Z. *Org. Lett.* **2017**, 19 (4), 954–957.
- (161) Muth, C. W.; DeMatte, M. L.; Urbanik, A. R.; Isner, W. G. *J. Org. Chem.* **1966**, 31 (9), 3013–3015.
- (162) Kurokawa, S.; Anderson Arthur G., J. *Bull. Chem. Soc. Jpn.* **1979**, 52 (1), 257–258.
- (163) Copland, D.; Leaver, D.; Menzies, W. B. *Tetrahedron Lett.* **1977**, 18 (7), 639–640.
- (164) Amir, E.; Amir, R. J.; Campos, L. M.; Hawker, C. J. *J. Am. Chem. Soc.* **2011**, 133 (26), 10046–10049.
- (165) Murai, M.; Amir, E.; Amir, R. J.; Hawker, C. J. *Chem. Sci.* **2012**, 3 (9), 2721–2725.
- (166) Amir, E.; Murai, M.; Amir, R. J.; Cowart, J. S.; Chabiny, M. L.; Hawker, C. J. *Chem. Sci.* **2014**, 5 (11), 4483–4489.
- (167) Kurotobi, K.; Takakura, K.; Murafuji, T.; Sugihara, Y. *Synthesis (Stuttg.)* **2001**, 2001 (09), 1346–1350.
- (168) Nozoe, T.; Seto, S.; Matsumura, S. *Bull. Chem. Soc. Jpn.* **1962**, 35 (12), 1990–1998.
- (169) Kurotobi, K.; Tabata, H.; Miyauchi, M.; Mustafizur, R. A. F. M.; Migita, K.; Murafuji, T.; Sugihara, Y.; Shimoyama, H.; Fujimori, K. *Synthesis* **2003**, 1 (01), 30–34.
- (170) Kurotobi, K.; Miyauchi, M.; Takakura, K.; Murafuji, T.; Sugihara, Y. *European J. Org. Chem.* **2003** (18), 3663–3665.
- (171) Ishiyama, T.; Takagi, J.; Hartwig, J. F.; Miyauchi, N. *Angew. Chemie Int. Ed.* **2002**, 41 (16), 3056–3058.
- (172) Ishiyama, T.; Takagi, J.; Ishida, K.; Miyauchi, N.; Anastasi, N. R.; Hartwig, J. F. *J. Am. Chem. Soc.* **2002**, 124 (3), 390–391.
- (173) Cho, J.-Y.; Tse, M. K.; Holmes, D.; Maleczka, R. E.; Smith, M. R. *Science* **2002**, 295 (5553), 305–308.
- (174) Cho, J.-Y.; Iverson, C. N.; Smith, M. R. *J. Am. Chem. Soc.* **2000**, 122 (51), 12868–12869.
- (175) Xia, J.; Capozzi, B.; Wei, S.; Strange, M.; Batra, A.; Moreno, J. R.; Amir, R. J.; Amir, E.; Solomon, G. C.; Venkataraman, L.; Campos, L. M. *Nano Lett.* **2014**, 14 (5), 2941–2945.
- (176) Koide, T.; Takesue, M.; Murafuji, T.; Satomi, K.; Suzuki, Y.; Kawamata, J.; Terai, K.; Suzuki, M.; Yamada, H.; Shiota, Y.; Yoshizawa, K.; Tani, F. *Chempluschem* **2016**, 82 (7), 1010–1014.
- (177) Murai, M.; Iba, S.; Ota, H.; Takai, K. *Org. Lett.* **2017**, 19 (20), 5585–5588.
- (178) Ninomiya, K.; Harada, Y.; Kanetou, T.; Suenaga, Y.; Murafuji, T.; Tsunashima, R. *New J. Chem.* **2015**, 39 (12), 9079–9085.
- (179) Narita, M.; Murafuji, T.; Yamashita, S.; Fujinaga, M.; Hiyama, K.; Oka, Y.; Tani, F.; Kamijo, S.; Ishiguro, K. *J. Org. Chem.* **2018**, 83 (3), 1298–1303.
- (180) Murai, M.; Takami, K.; Takeshima, H.; Takai, K. *Org. Lett.* **2015**, 17 (7), 1798–1801.
- (181) Drapeau, M. P.; Gooßen, L. J. *Chem. A Eur. J.* **2016**, 22 (52), 18654–18677.
- (182) Shen, P.-X.; Hu, L.; Shao, Q.; Hong, K.; Yu, J.-Q. *J. Am. Chem. Soc.* **2018**, 140 (21), 6545–6549.
- (183) Font, M.; Quibell, J. M.; Perry, G. J. P.; Larrosa, I. *Chem. Commun.* **2017**, 53 (41), 5584–5597.
- (184) Pichette Drapeau, M.; Gooßen, L. J. *Chem. – A Eur. J.* **2016**, 22 (52), 18654–18677.
- (185) Mathias, L. J.; Overberger, C. G. *J. Org. Chem.* **1980**, 45 (9), 1701–1703.
- (186) Zhu, C.; Zhang, Y.; Kan, J.; Zhao, H.; Su, W. *Org. Lett.* **2015**, 17 (14), 3418–3421.
- (187) Giri, R.; Maugel, N.; Li, J.-J.; Wang, D.-H.; Breazzano, S. P.; Saunders, L. B.; Yu, J.-Q. *J. Am. Chem. Soc.* **2007**, 129 (12), 3510–3511.
- (188) Wang, D.-H.; Mei, T.-S.; Yu, J.-Q. *J. Am. Chem. Soc.* **2008**, 130 (52), 17676–17677.
- (189) Arroniz, C.; Ironmonger, A.; Rassias, G.; Larrosa, I. *Org. Lett.* **2013**, 15 (4), 910–913.
- (190) Arroniz, C.; Denis, J. G.; Ironmonger, A.; Rassias, G.; Larrosa, I. *Chem. Sci.* **2014**, 5 (9), 3509–3514.
- (191) Whitaker, D.; Burés, J.; Larrosa, I. *J. Am. Chem. Soc.* **2016**, 138 (27), 8384–8387.
- (192) He, N.; Gyurcsanyi, R. E.; Lindfors, T. *Analyst* **2016**, 141 (10), 2990–2997.
- (193) Florina Teodorescu, Cecilia Lete, Mariana Marin, Cornel Munteanu, N. T. *Rev. Chim.* **2013**, 64 (1), 15–21.
- (194) Lete, C.; Gadgil, B.; Kvarnström, C. *J. Electroanal. Chem.* **2015**, 742, 30–36.
- (195) Lupu, S.; Lete, C.; Marin, M.; Totir, N.; Balaure, P. C. *Electrochim. Acta* **2009**, 54 (7), 1932–1938.
- (196) Suominen, M.; Lehtimäki, S.; Yewale, R.; Damlin, P.; Tuukkanen, S.; Kvarnström, C. *J. Power Sources* **2017**, 356, 181–190.
- (197) Yang, C.; Schellhammer, K. S.; Ortmann, F.; Sun, S.; Dong, R.; Karakus, M.; Mics, Z.; Löffler, M.; Zhang, F.; Zhuang, X.; Cánovas, E.; Cuniberti, G.; Bonn, M.; Feng, X. *Angew. Chemie Int. Ed.* **2017**, 56 (14), 3920–3924.
- (198) Yamamoto, T. *Bull. Chem. Soc. Jpn.* **1999**, 72 (4), 621–638.
- (199) Wang, F.; Lai, Y.-H. *Macromolecules* **2003**, 36 (3), 536–538.
- (200) Wang, F.; Lai, Y.-H.; Han, M.-Y. *Macromolecules* **2004**, 37 (9), 3222–3230.
- (201) Tang, T.; Lin, T.; Wang, F.; He, C. *Polym. Chem.* **2014**, 5 (8), 2980–2989.
- (202) Xin, H.; Ge, C.; Jiao, X.; Yang, X.; Rundel, K.; McNeill, C. R.; Gao, X. *Angew. Chemie Int. Ed.* **2018**, 57 (5), 1322–1326.
- (203) Gao, H.; Ge, C.; Hou, B.; Xin, H.; Gao, X. *ACS Macro Lett.* **2019**, 8 (10), 1360–1364.
- (204) Wada, E.; Nakai, T.; Okawara, M. *J. Polym. Sci. Polym. Chem. Ed.* **1978**, 16 (8), 2085–2087.
- (205) Puodziukynaite, E.; Wang, H.-W.; Lawrence, J.; Wise, A. J.; Russell, T. P.; Barnes, M. D.; Emrick, T. J.

- Am. Chem. Soc.* **2014**, 136 (31), 11043–11049.
- (206) Koch, M.; Blacque, O.; Venkatesan, K. *Org. Lett.* **2012**, 14 (6), 1580–1583.
- (207) Cooksey, C. J.; Courtneidge, J. L.; Davies, A. G.; Gregory, P. S.; Evans, J. C.; Rowlands, C. C. *J. Chem. Soc. Perkin Trans. 2* **1988**, No. 5, 807–813.
- (208) Gerson, F.; Scholz, M.; Hansen, H.-J.; Uebelhart, P. *J. Chem. Soc. Perkin Trans. 2* **1995**, No. 2, 215–220.
- (209) Kashima, C.; Harada, K.; Fujioka, Y.; Maruyama, T.; Omote, Y. *J. Chem. Soc. Perkin Trans. 1* **1988**, No. 3, 535–539.
- (210) Zhdanko, A. G.; Nenajdenko, V. G. *J. Org. Chem.* **2009**, 74 (2), 884–887.
- (211) Ito, S.; Terazono, T.; Kubo, T.; Okujima, T.; Morita, N.; Murafuji, T.; Sugihara, Y.; Fujimori, K.; Kawakami, J.; Tajiri, A. *Tetrahedron* **2004**, 60 (25), 5357–5366.

APPENDIX A

The following section contains other results obtained while optimising for improved reactivity (section 1.2.3). The original conditions were found to be optimal at the end of the optimisation process.

Acid screen (figure 43) comprising different steric, and electronic environment around the acid.



| Entry | Acid | 27ai / % | 27aii / % | 27aii : 27ai | Entry | Acid | 27ai / % | 27aii / % | 27aii : 27ai |
|-------|------|----------|-----------|--------------|-------|------|----------|-----------|--------------|
| 1 | A1 | 42 | 29 | 0.7 : 1 | 11 | A30 | 44 | Traces | - |
| 2 | A23 | 32 | Traces | - | 12 | A5 | 69 | Traces | - |
| 3 | A24 | 29 | 24 | 0.8 : 1 | 13 | A31 | 48 | Traces | - |
| 4 | A25 | 62 | 13 | 0.2 : 1 | 14 | A2 | 45 | Traces | - |
| 5 | A26 | 57 | Traces | - | 15 | A32 | 60 | Traces | - |
| 6 | A27 | 15 | 8 | 0.5 : 1 | 16 | A33 | 68 | Traces | - |
| 7 | A28 | - | - | - | 17 | A9 | 39 | 8 | 0.2 : 1 |
| 8 | A29 | 44 | 9 | 0.2 : 1 | 18 | A34 | 28 | 8 | 0.3 : 1 |
| 9 | AcOH | 45 | 8 | 0.2 : 1 | 19 | A20 | 28 | 10 | 0.4 : 1 |
| 10 | A6 | 54 | Traces | - | | | | | |

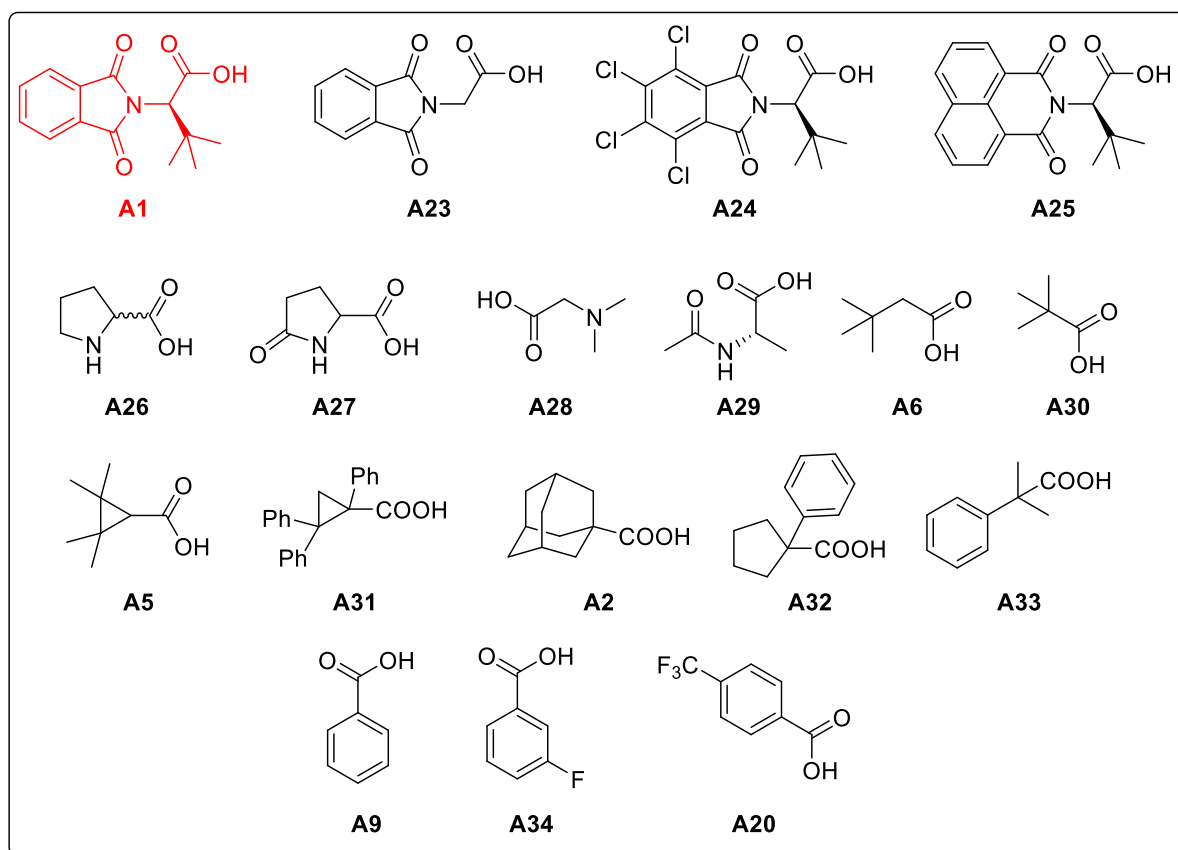
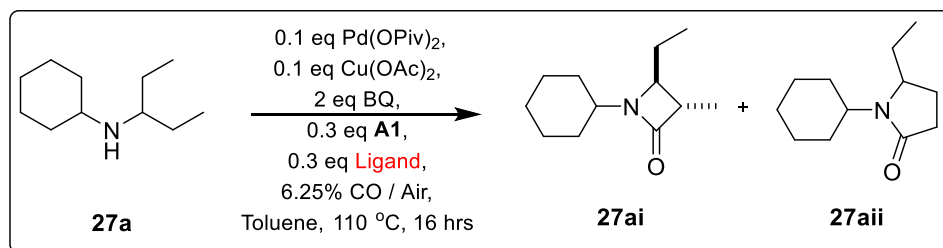


Figure 43: Screen of a various carboxylic acids for reaction optimisation. Yields determined by ^1H NMR of the crude reaction sample against TCE as an internal standard.

Ligand screen using various analogues of quinuclidine and pyridine (figure 44).



| Entry | Ligand | 27ai / % | 27aii / % | 27aii : 27ai |
|-------|------------|----------|-----------|--------------|
| 1 | L8 | 3 | Traces | - |
| 2 | L39 | - | - | - |
| 3 | L40 | 7 | 6 | 0.9 : 1 |
| 4 | L21 | 39 | 21 | 0.5 : 1 |
| 5 | L41 | 28 | 19 | 0.7 : 1 |
| 6 | L42 | 23 | 18 | 0.8 : 1 |

| | | | | |
|---|------------|----|--------|---------|
| 7 | L43 | 25 | Traces | - |
| 8 | L44 | 39 | 26 | 0.7 : 1 |

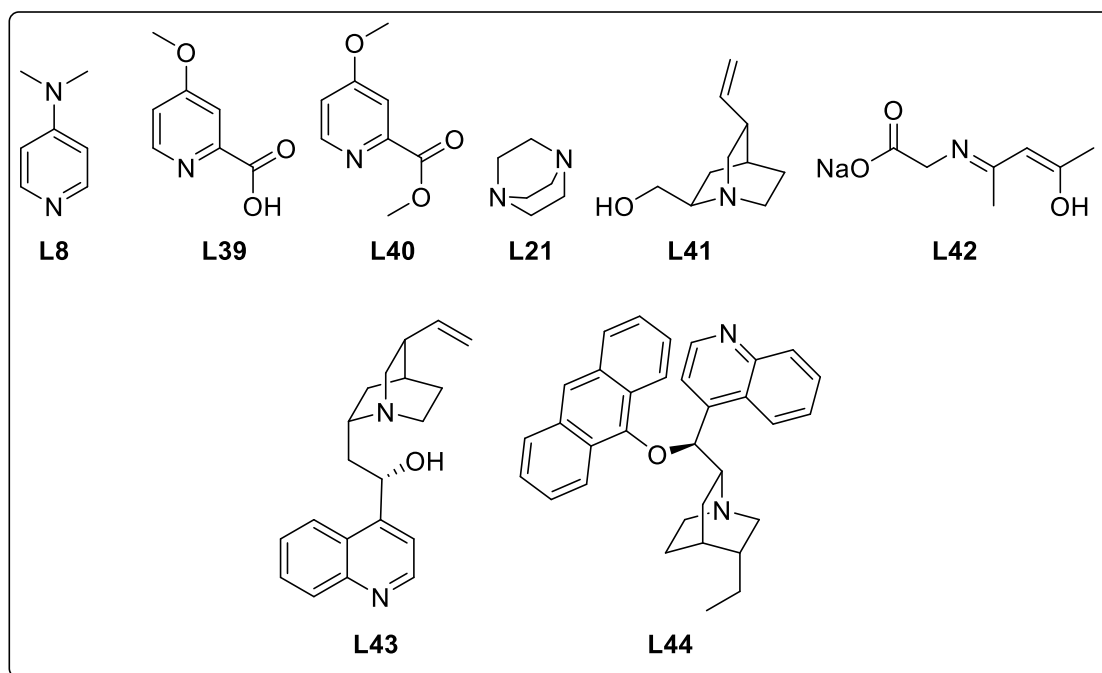
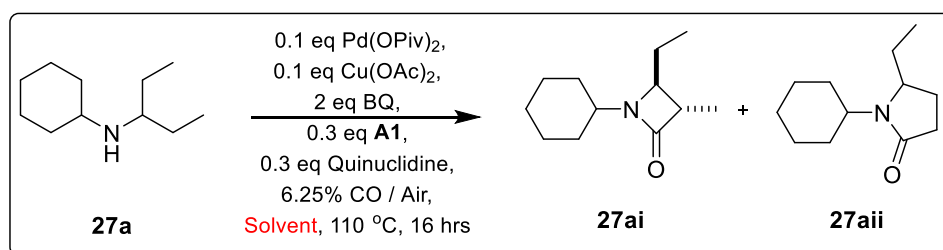


Figure 44: Screen of a various ligands for reaction optimisation. Yields determined by ^1H NMR of the crude reaction sample against TCE as an internal standard.

Screen of solvent and temperature (figure 45)



| Entry | Solvent | T / °C | 27ai / % | 27aai / % | 27aai : 27ai |
|-------|-------------------|--------|----------|-----------|--------------|
| 1 | Dioxane | 110 | 31 | Traces | - |
| 2 | Dibutylether | 110 | 11 | Traces | - |
| 3 | DMF | 110 | - | - | - |
| 4 | Isopropyl acetate | 110 | Traces | - | - |
| 6 | Toluene | 120 | 31 | 26 | 0.8 : 1 |
| 7 | Xylene | 120 | 30 | 20 | 0.7 : 1 |
| 8 | Toluene | 130 | 21 | 13 | 0.6 : 1 |

| | | | | | |
|---|---------------|-----|----|----|---------|
| 9 | Xylene | 130 | 18 | 15 | 0.8 : 1 |
|---|---------------|-----|----|----|---------|

Figure 45: Solvent and temperature screen for reaction optimisation. Yields determined by ^1H NMR of the crude reaction sample against TCE as an internal standard.

Screen of different quinones (figure 46).

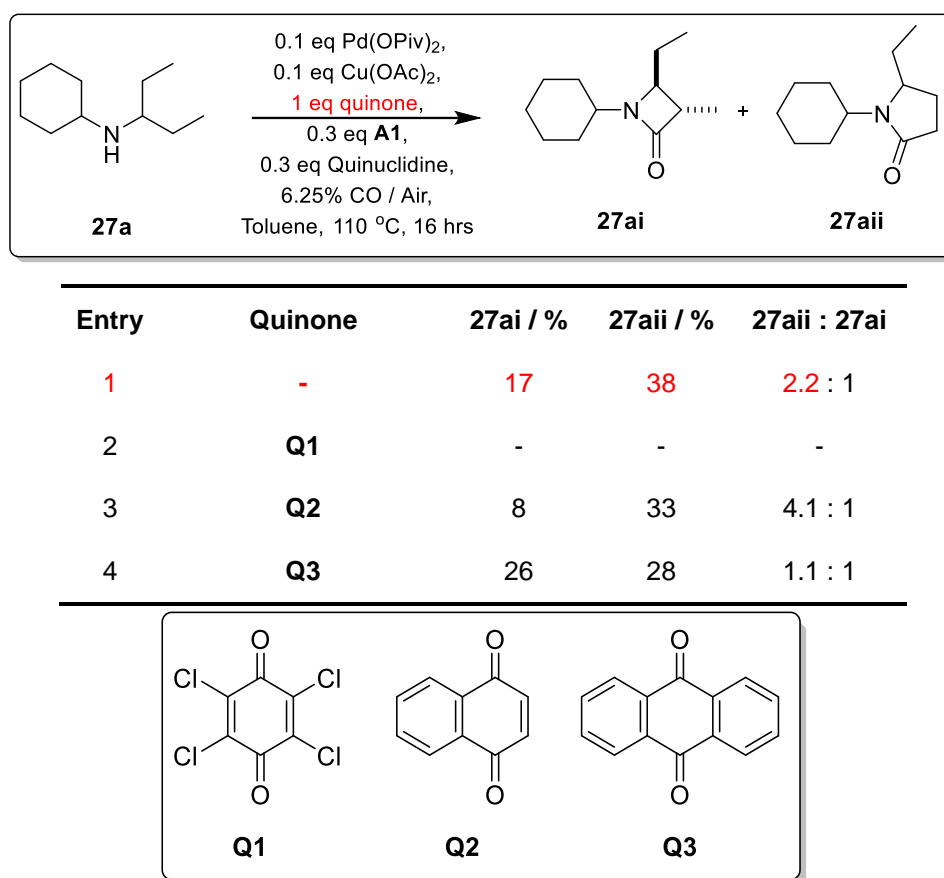
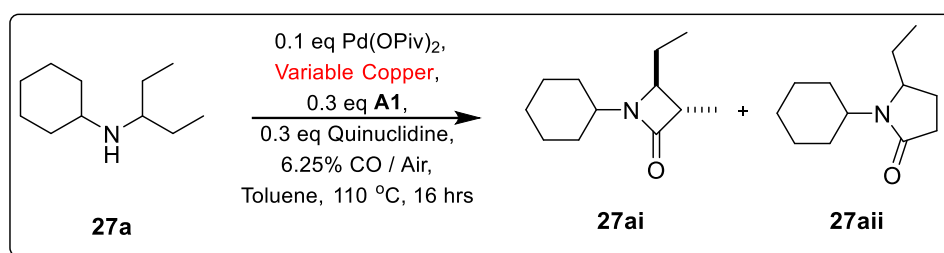


Figure 46: Quinone screen for reaction optimisation. Yields determined by ¹H NMR of the crude reaction sample against TCE as an internal standard.

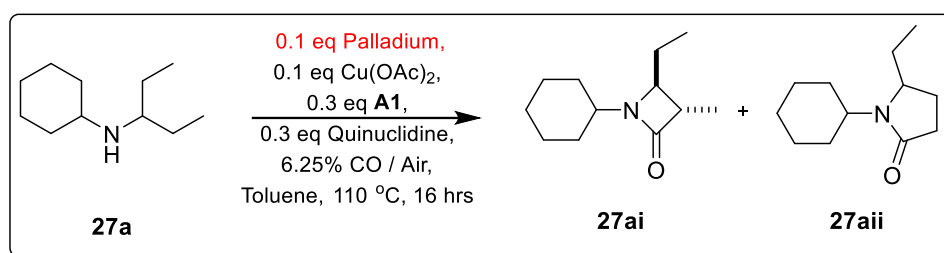
Changing the loading and counterion of the copper salt (figure 47)



| Entry | Copper salt | Loading / mol% | 27ai / % | 27aai / % | 27aai : 27ai |
|-------|-----------------------------------|----------------|----------|-----------|--------------|
| 1 | Cu(OAc) ₂ | 5 | Traces | 28 | - |
| 2 | Cu(OAc) ₂ | 10 | 17 | 38 | 2.2 : 1 |
| 3 | Cu(OAc) ₂ | 20 | 14 | 31 | 2.2 : 1 |
| 4 | Cu(OAc) ₂ | 50 | 8 | 27 | 3.4 : 1 |
| 5 | Cu(OAc) ₂ | 100 | 4 | 17 | 4.3 : 1 |
| 6 | CuCl ₂ | 10 | - | - | - |
| 7 | CuBr ₂ | 10 | - | - | - |
| 8 | Cu(OTFA) ₂ | 10 | 21 | 23 | 1.1 : 1 |
| 9 | Cu(NO ₃) ₂ | 10 | 6 | 33 | 5.5 : 1 |

Figure 47: Copper salt type and loading screening. Yields determined by ¹H NMR of the crude reaction sample against TCE as an internal standard.

Optimisation of palladium source (figure 48)



| Entry | Palladium source | 27ai / % | 27aii / % | 27aii : 27ai |
|-------|---------------------------------|----------|-----------|--------------|
| 1 | Pd(OPiv) ₂ | 17 | 38 | 2.2 |
| 2 | Pd(OAc) ₂ | Traces | 28 | - |
| 3 | Pd(OAc) ₂ L45 | 14 | 22 | 1.6 |
| 4 | Pd(Acac) ₂ | 16 | 19 | 1.2 |
| 5 | PdCl ₂ | - | - | - |

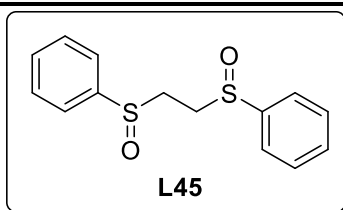
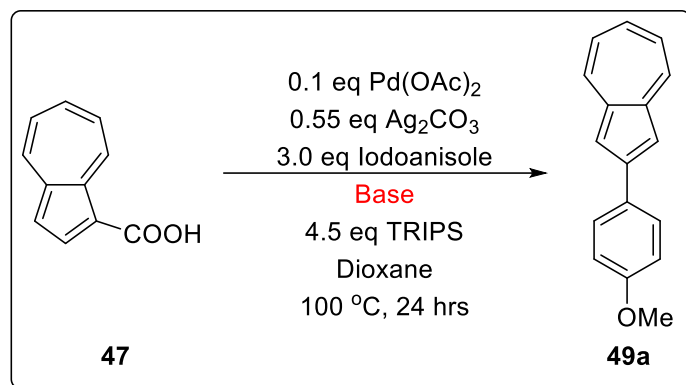


Figure 48: Palladium source screening for optimisation. Yields determined by ¹H NMR of the crude reaction sample against TCE as an internal standard.

APPENDIX B

The following section contains control experiments done to ensure that the reaction conditions obtained were indeed optimal.

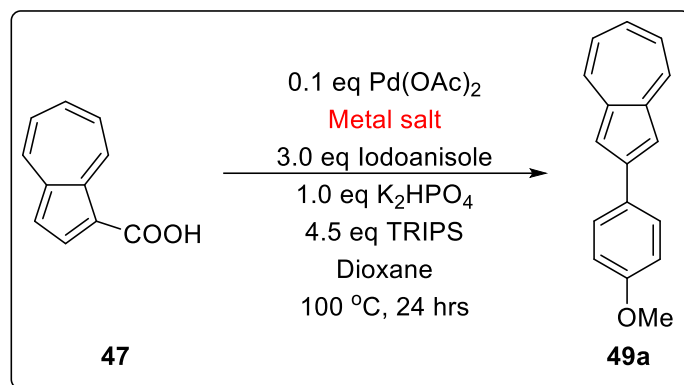
The base used and the equivalence was checked. Removal of the base led to almost complete inhibition of the reaction (entry 8). Reasonable yields were obtained between 0.5 eq and 3 eq of K_2HPO_4 used, with 1 eq being slightly better than the other results.



| Entry | Base | Eq | 49a / % |
|-------|--------------------------|-----|---------|
| 1 | KOH | 1 | 34 |
| 2 | KOAc | 1 | 17 |
| 3 | K_2CO_3 | 1 | 3 |
| 4 | Na_2CO_3 | 1 | 28 |
| 5 | Li_2CO_3 | 1 | 33 |
| 6 | Cs_2CO_3 | 1 | 15 |
| 7 | Quinuclidine | 1 | - |
| 8 | No Base | - | 6 |
| 9 | K_2HPO_4 | 0.5 | 68 |
| 10 | K_2HPO_4 | 1 | 72 |
| 11 | K_2HPO_4 | 1.5 | 63 |
| 12 | K_2HPO_4 | 2 | 70 |
| 13 | K_2HPO_4 | 3 | 71 |

Figure 71: Control reaction to check base used for reaction. Yields determined by ^1H NMR of the crude reaction sample against TCE as an internal standard.

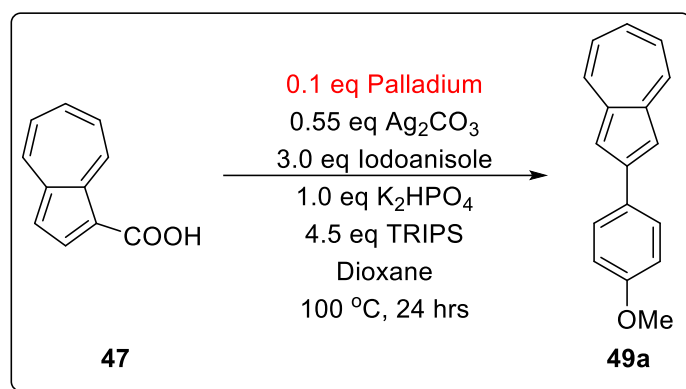
Apart from silver carbonate, silver acetate also performed quite well with a yield of 60% (entry 4). The loading of silver was found to be important, with too much silver leading to significant drops in yield. Removal of the silver salt also led to almost complete inhibition of the reaction (entry 8). Copper salts also did not perform well in the reaction (entry 6, 7).



| Entry | Silver or copper salt | Eq | 49a / % |
|----------|-------------------------------------|-------------|-----------|
| 1 | Ag₂CO₃ | 0.55 | 72 |
| 2 | Ag ₂ CO ₃ | 1.1 | 16 |
| 3 | Ag ₂ CO ₃ | 2.2 | 5 |
| 4 | AgOAc | 1.1 | 60 |
| 5 | AgOAc | 2.2 | 15 |
| 6 | Cu(OAc) ₂ | 1.1 | 12 |
| 7 | CuCl ₂ | 1.1 | - |
| 8 | None | | 5 |

Figure 72: Control reaction to check metal salt used for reaction. Yields determined by ¹H NMR of the crude reaction sample against TCE as an internal standard.

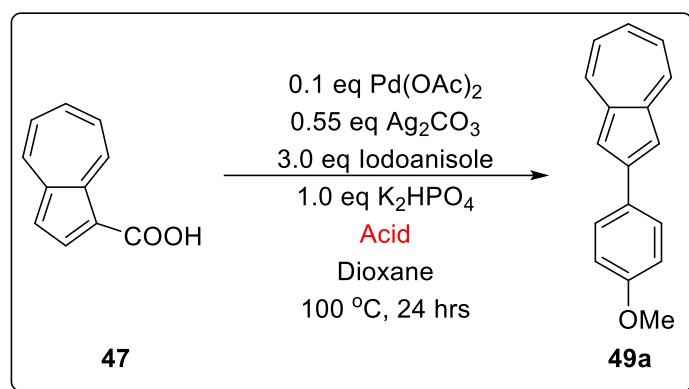
Various palladium (II) sources give moderate yields (entry 2, 3), though pairing them up with ligands inhibited the reaction (entry 5, 6). As before, palladium (0) sources performed significantly worse in the reaction (entry 4). As expected, removal of palladium saw that no reaction takes place.



| Entry | Palladium source | 49a / % |
|----------|---|-----------|
| 1 | $\text{Pd}(\text{OAc})_2$ | 72 |
| 2 | $\text{Pd}(\text{OPiv})_2$ | 65 |
| 3 | PdCl_2 | 56 |
| 4 | $\text{Pd}(\text{PPh}_3)_4$ | 16 |
| 5 | $\text{PdCl}_2(2,2'\text{-Bipyridine})$ | - |
| 6 | $\text{PdCl}_2(\text{Bisbenzonitrile})$ | - |
| 8 | No palladium | - |

Figure 73: Control reaction to check catalyst used for reaction. Yields determined by ^1H NMR of the crude reaction sample against TCE as an internal standard.

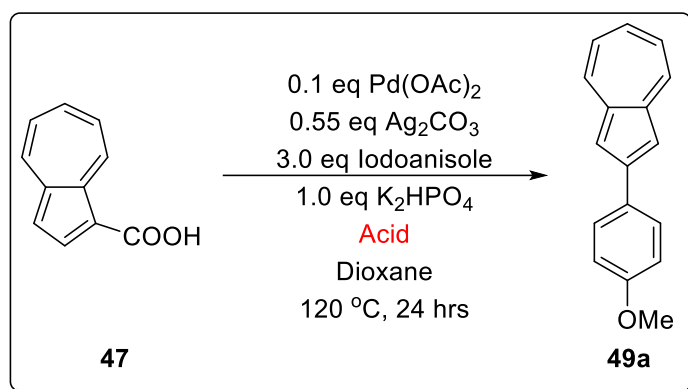
Employing other acids, including acetic acid gave significantly lower yields (entry 1-4, 10). Removal of the acid also inhibited the reaction (entry 11). Loading of TRIPS was studied (entry 5-9), and the 4.5 eq was found to be optimal, with both lower and higher loadings giving lower yields.



| Entry | Acid | Eq | 49a / % |
|----------|------------------------------|------------|-----------|
| 1 | AcOAc | 4.5 | 4 |
| 2 | TFA | 4.5 | 14 |
| 3 | p-toluenesulfonic acid | 4.5 | 5 |
| 4 | N-Acetyl isoleucine | 4.5 | 6 |
| 5 | TRIPS | 1 | 4 |
| 6 | TRIPS | 2 | 5 |
| 8 | TRIPS | 4.5 | 72 |
| 9 | TRIPS | 6 | 52 |
| 10 | 2-methyl-6-nitrobenzoic acid | 4.5 | 20 |
| 11 | No acid | - | 5 |

Figure 74: Control reaction to check acid used for reaction. Yields determined by ¹H NMR of the crude reaction sample against TCE as an internal standard.

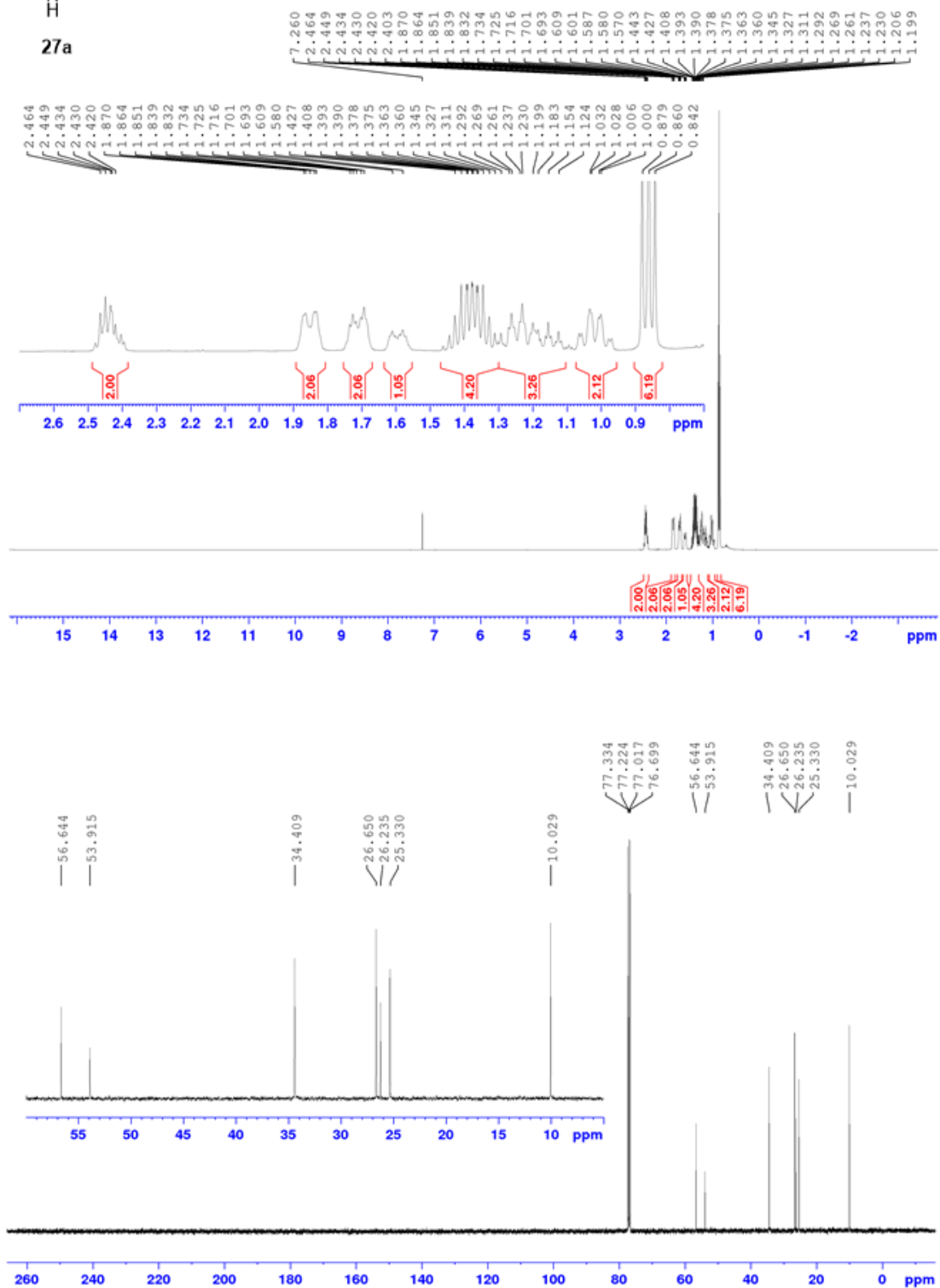
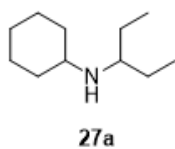
Use of dichloroethane (entry 2), and toluene (entry 3) still gave similar yields, though dioxane was slightly higher. These can be alternate solvents for the reaction. Using acetic acid completely inhibited the reaction (entry 1). *t*-Butanol only gave moderate yields (entry 4), while hexanol gave drastically lower yields (entry 5).

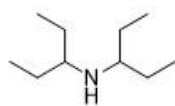


| Entry | Solvent | 49a / % |
|----------|-------------------|-----------|
| 1 | Acetic Acid | - |
| 2 | Dichloroethane | 71 |
| 3 | Toluene | 68 |
| 4 | <i>t</i> -Butanol | 54 |
| 5 | Hexanol | 5 |
| 6 | Dioxane | 72 |

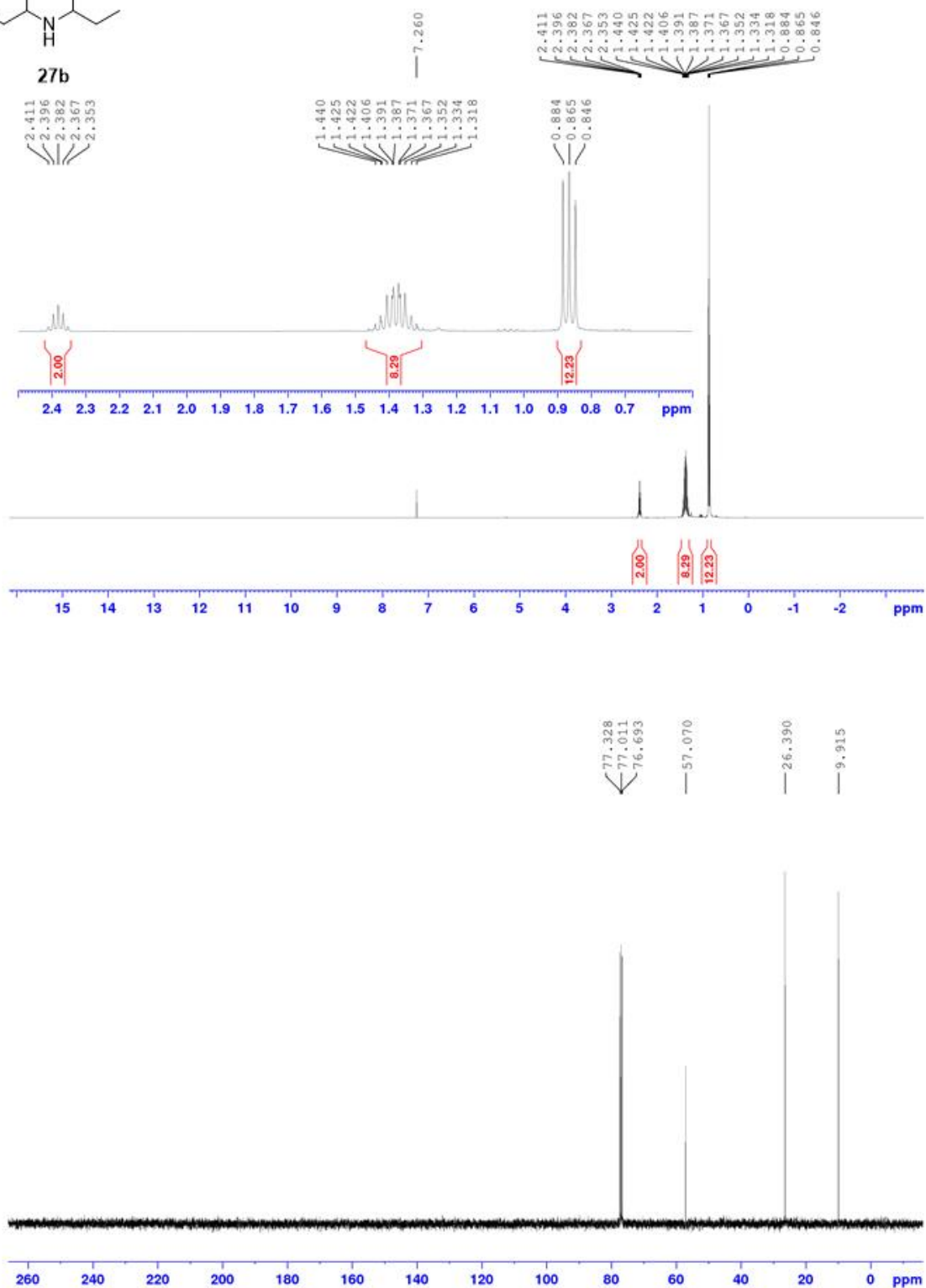
Figure 75: Control reaction to check solvent used for reaction. Yields determined by ¹H NMR of the crude reaction sample against TCE as an internal standard.

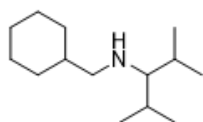
APPENDIX C: PROTON AND CARBON NMRS



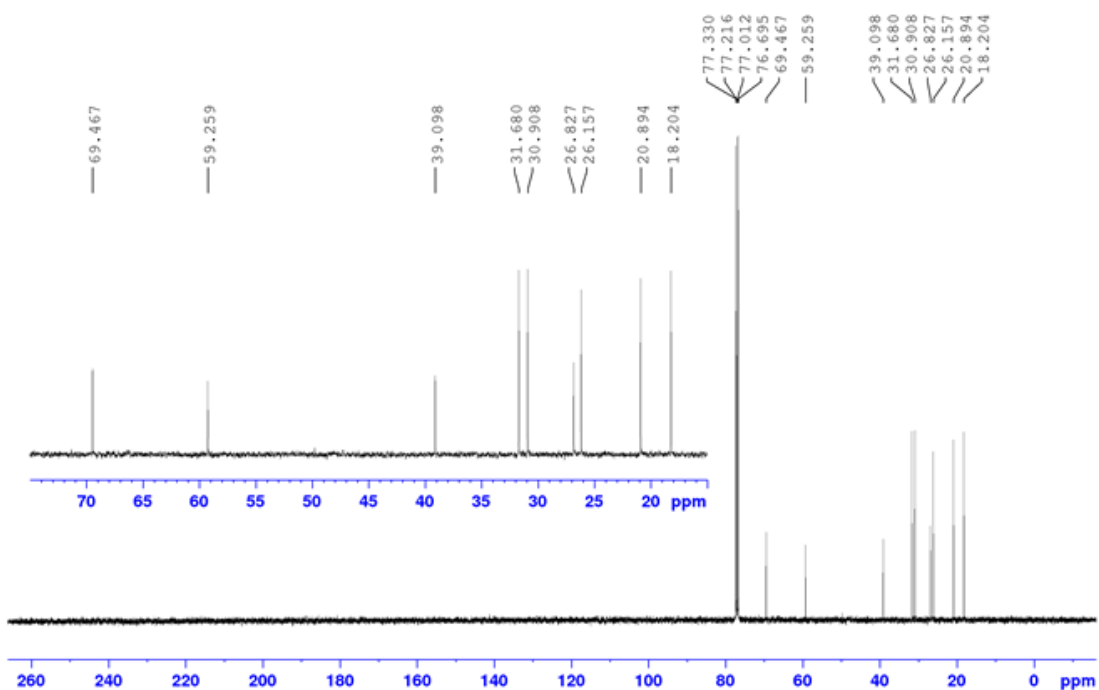
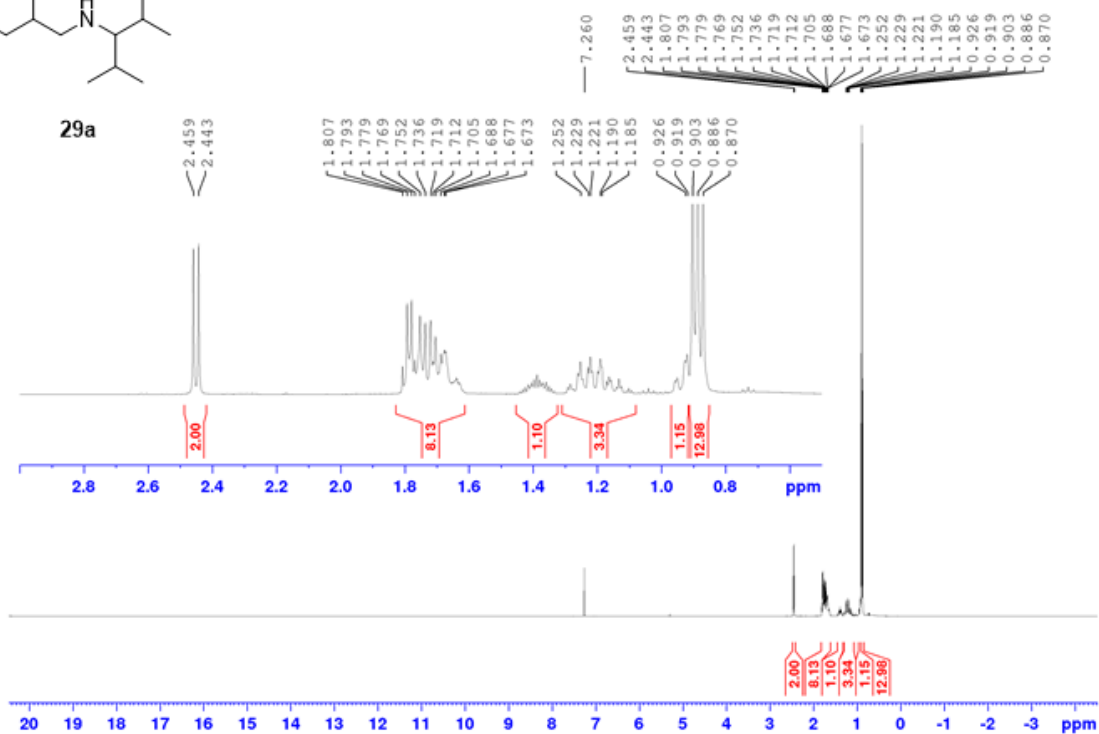


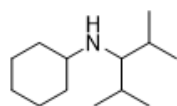
27b



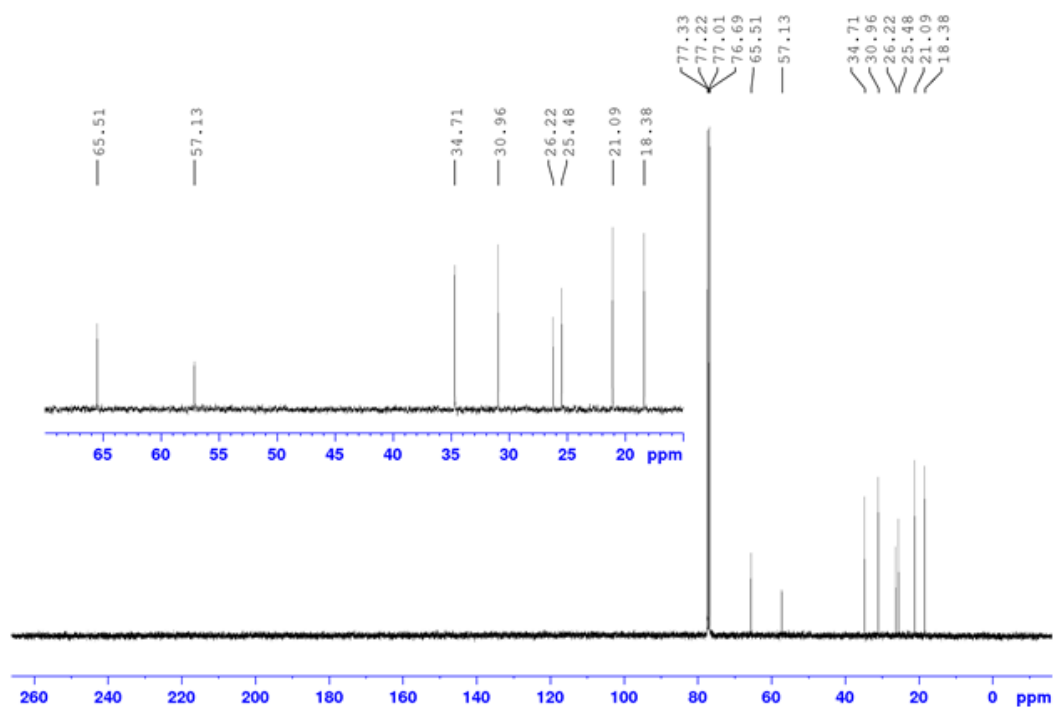
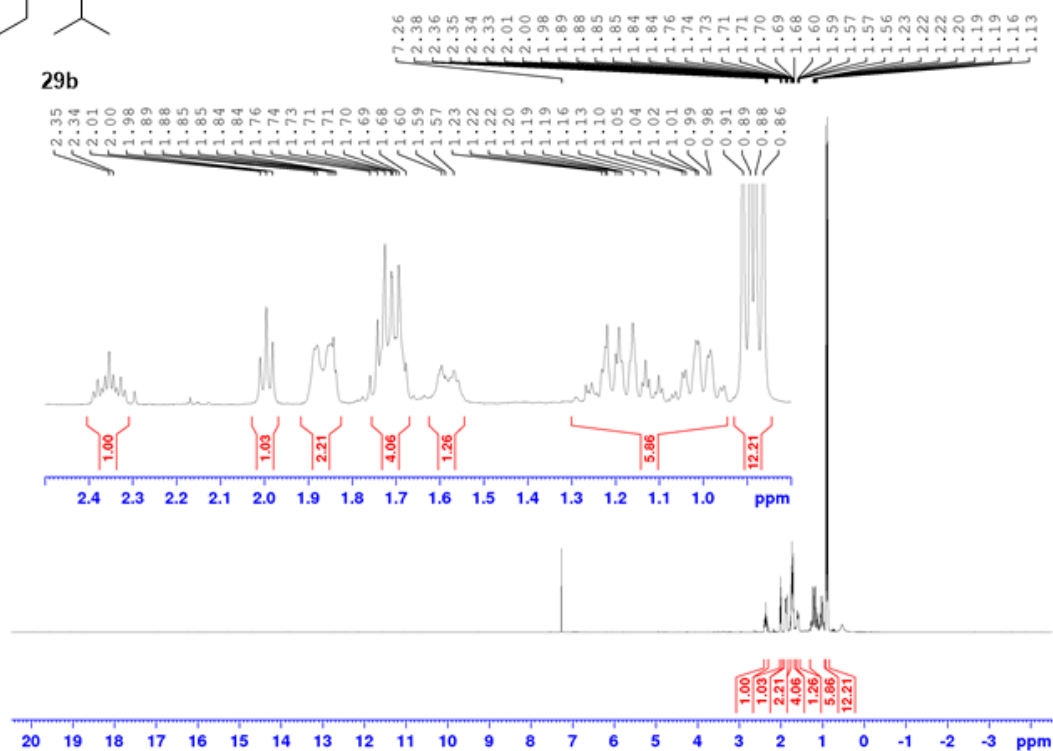


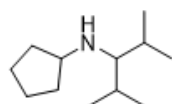
29a



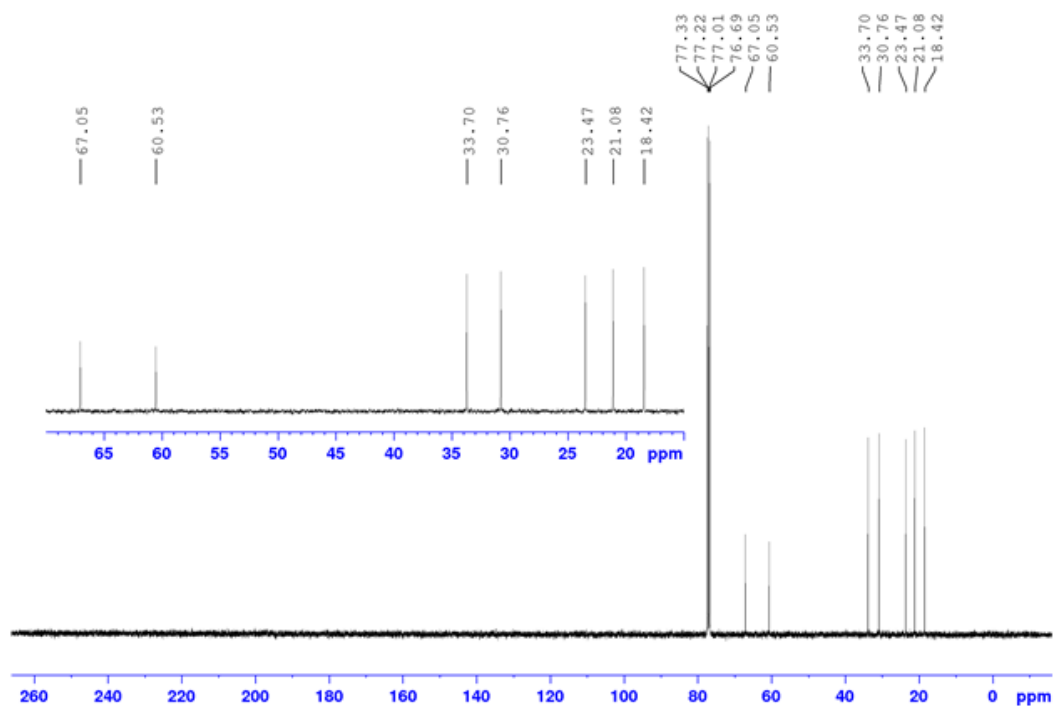
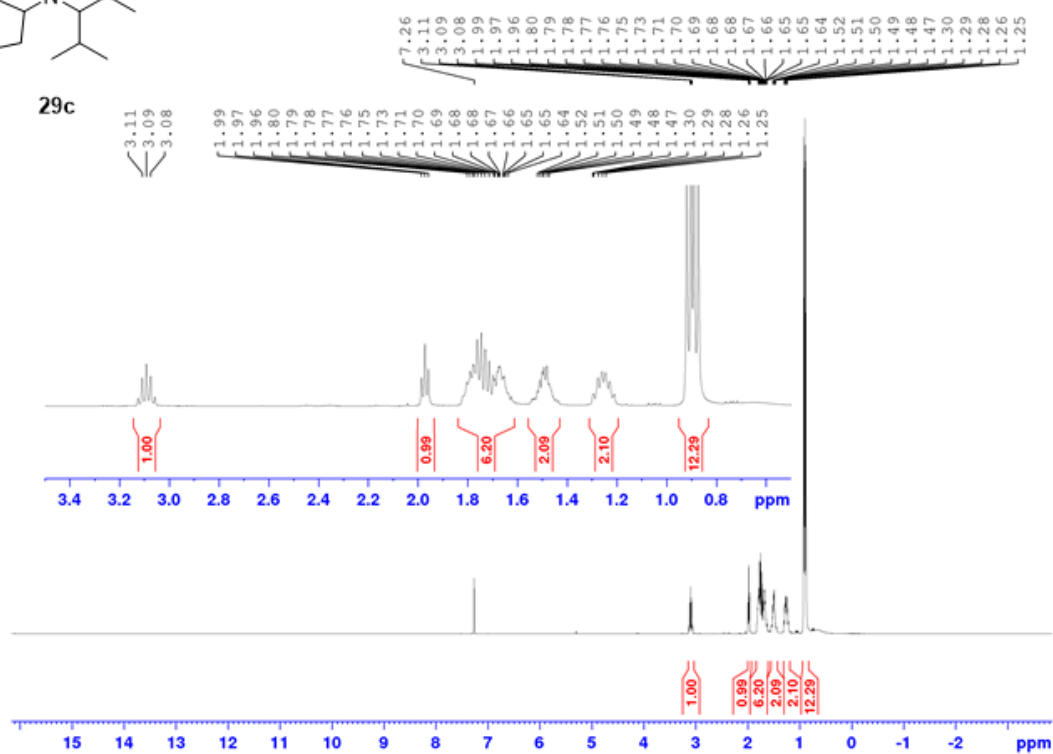


29b

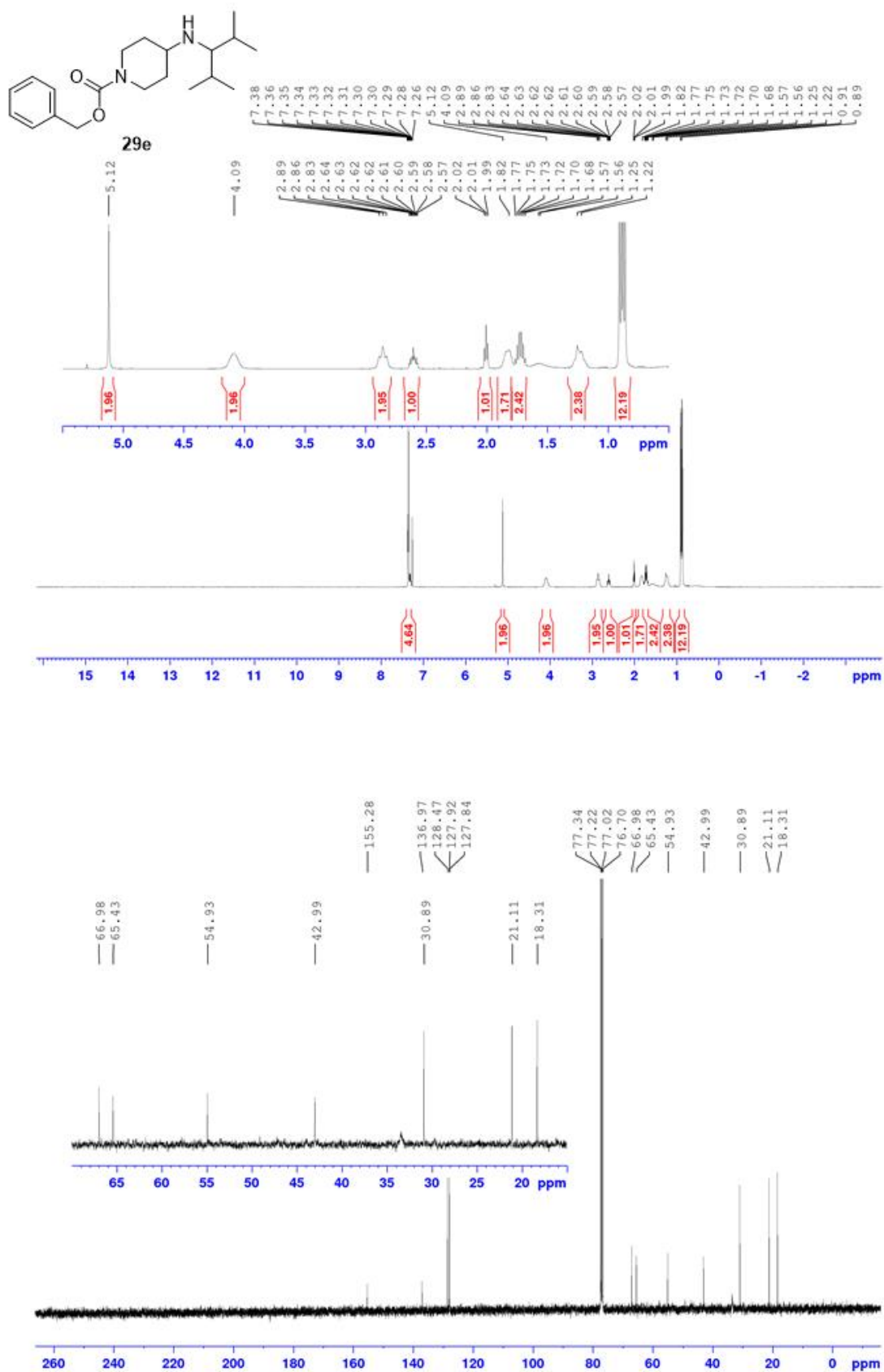


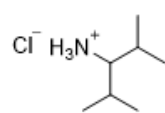


29c

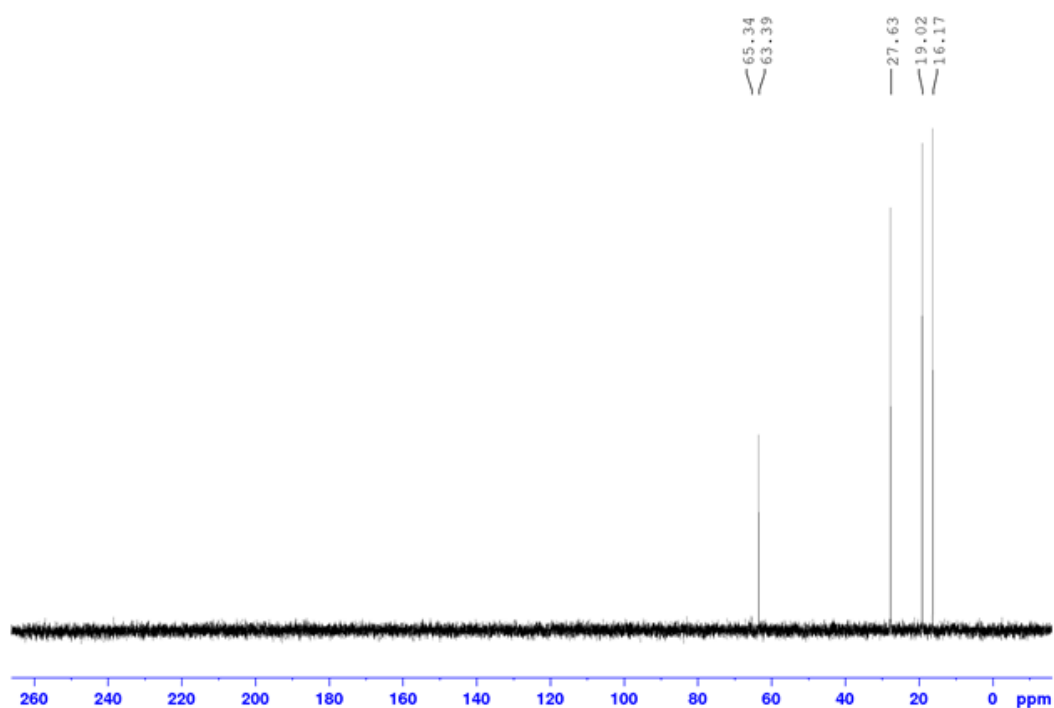
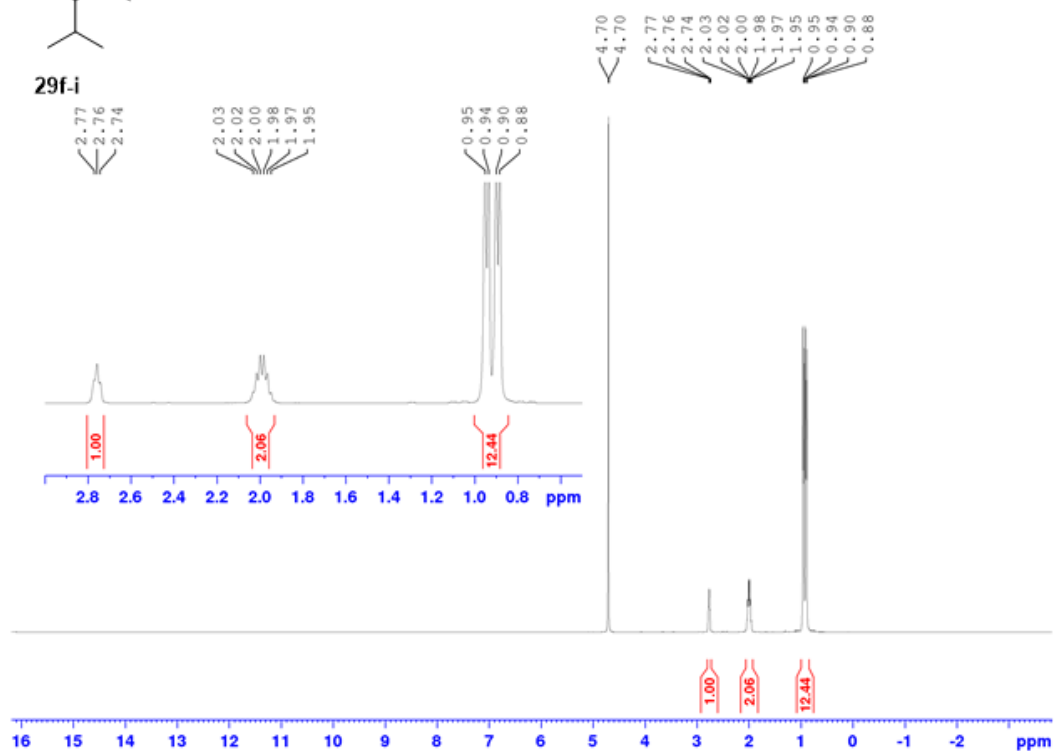


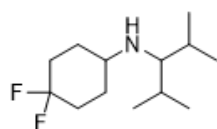




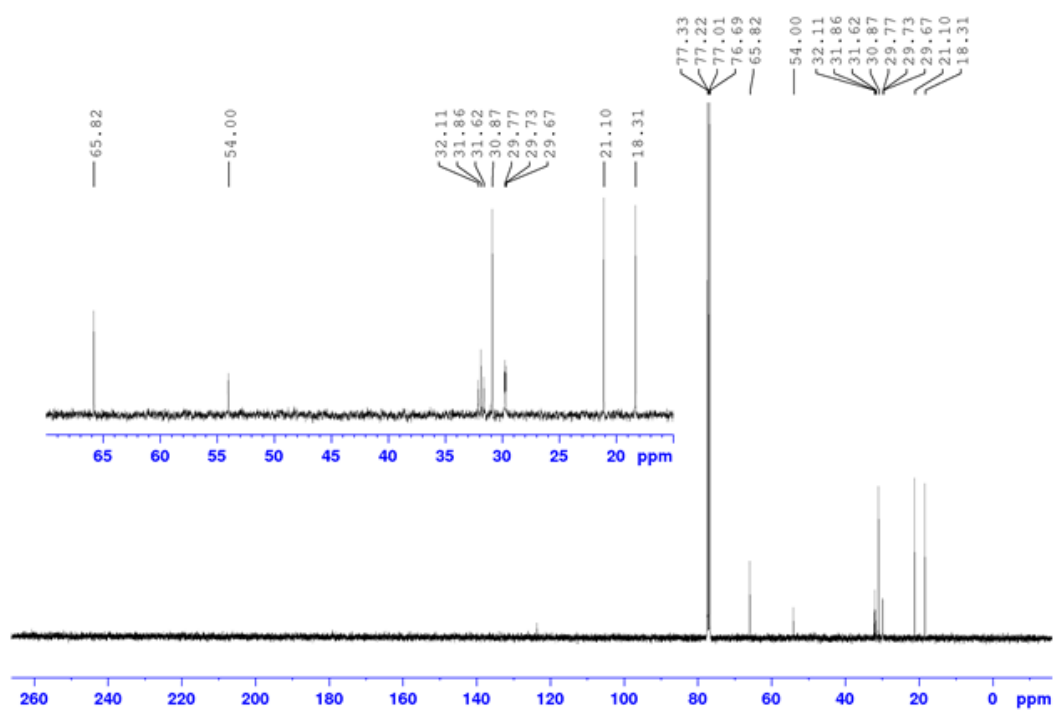
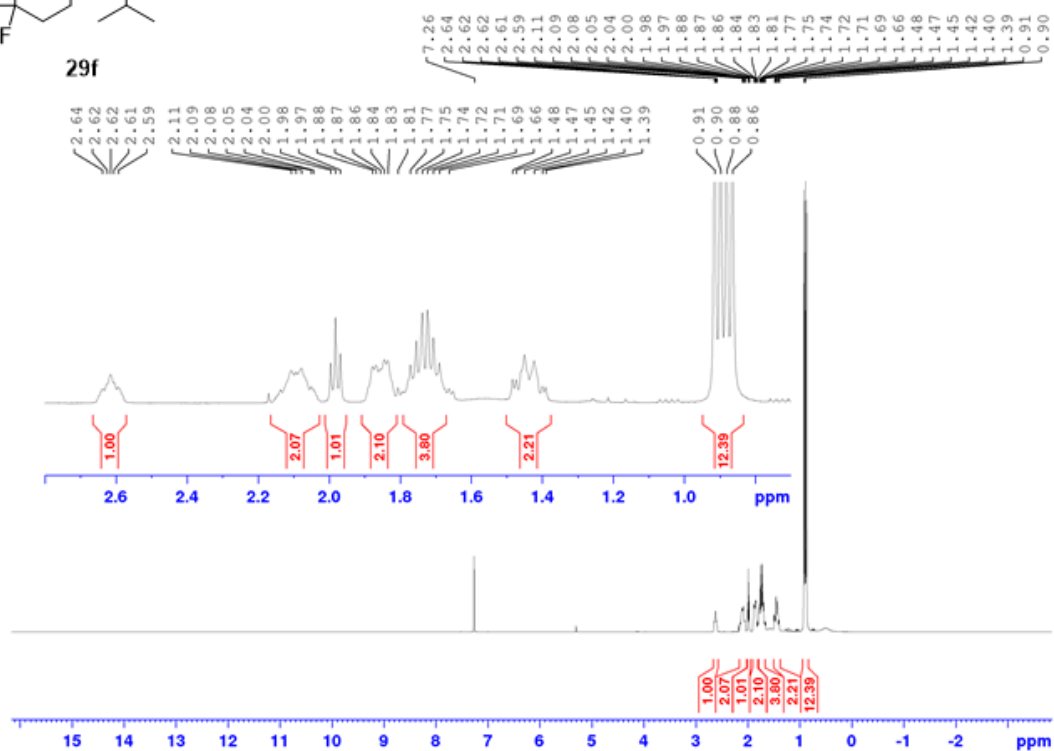


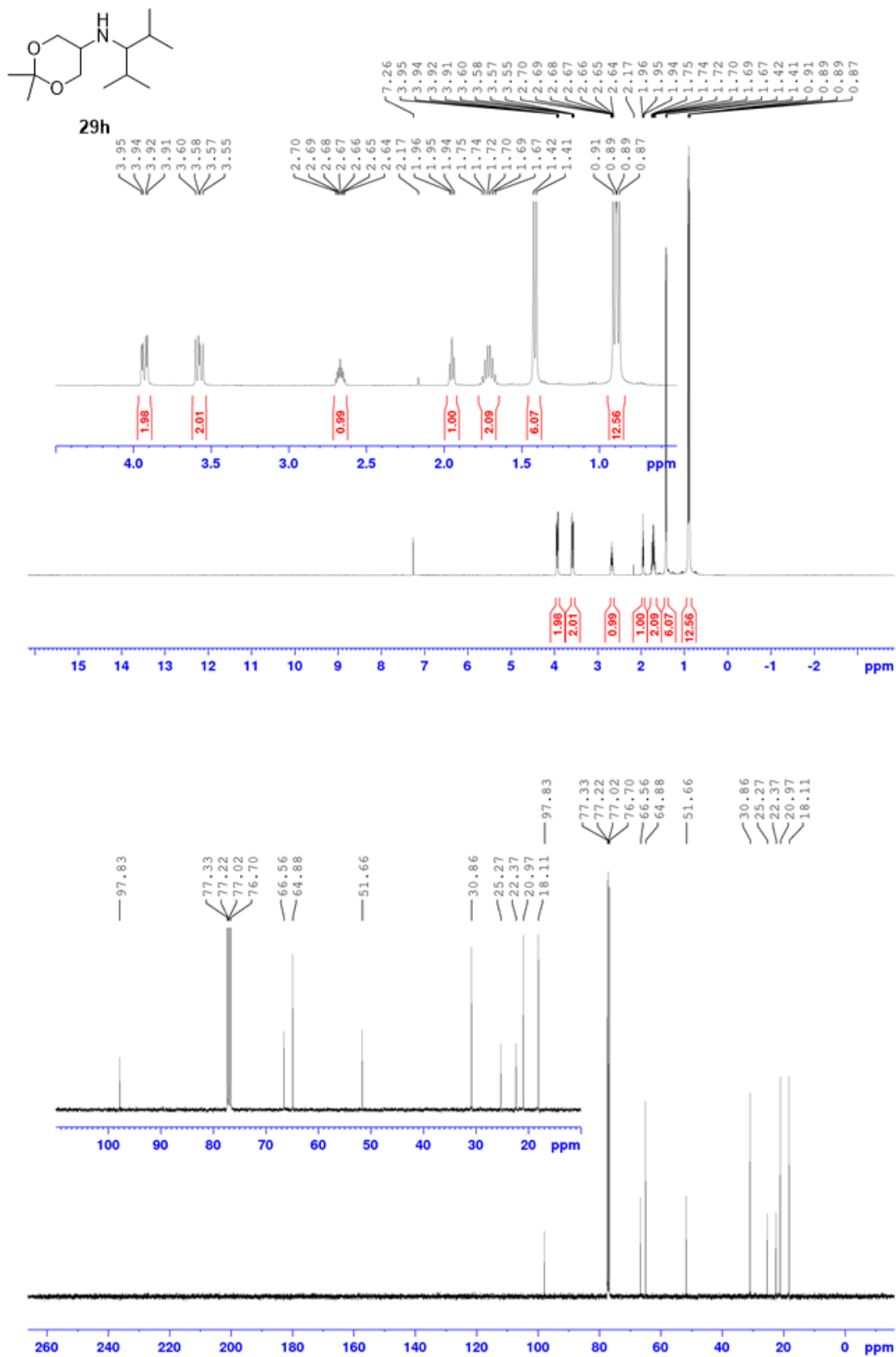
29f-i

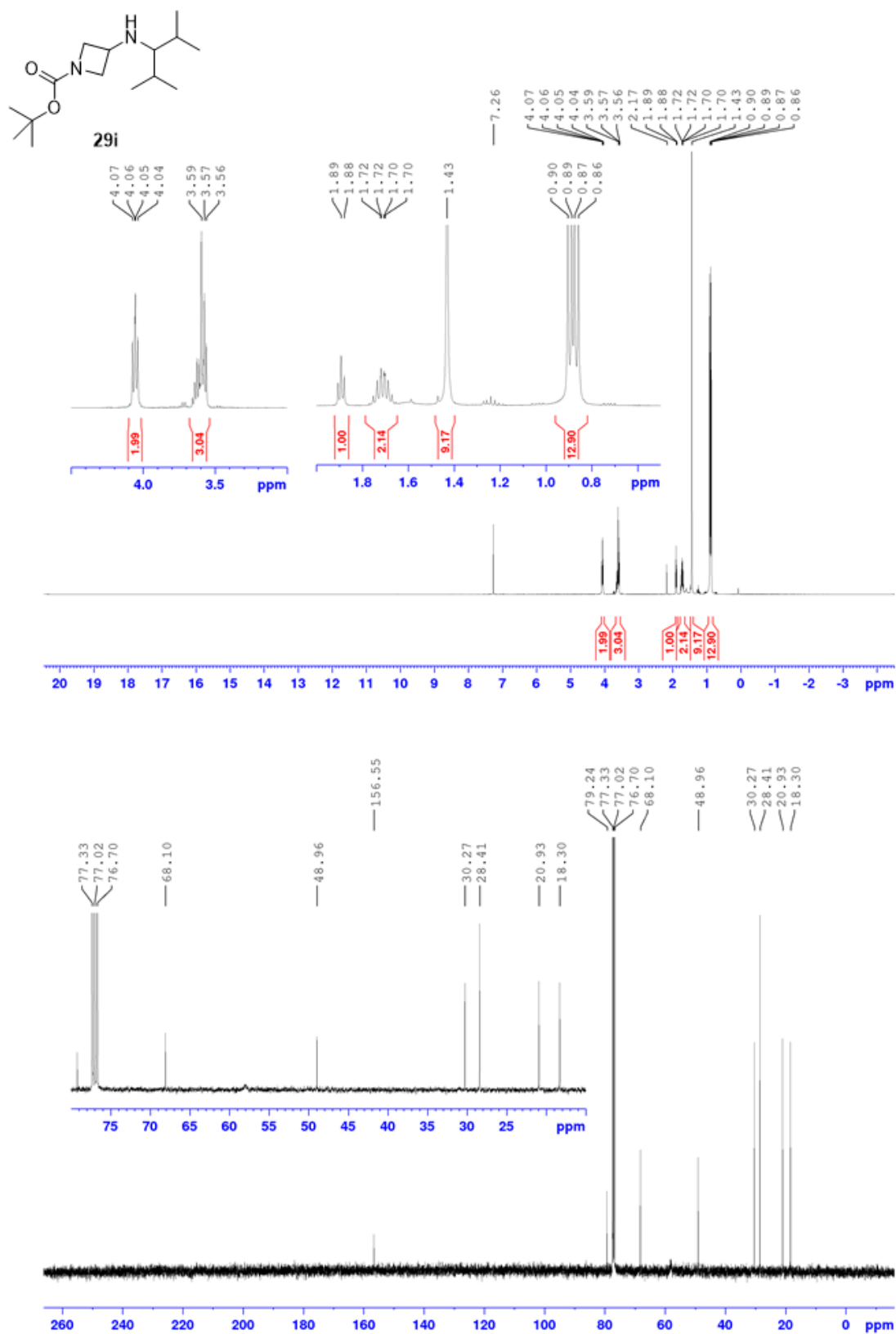




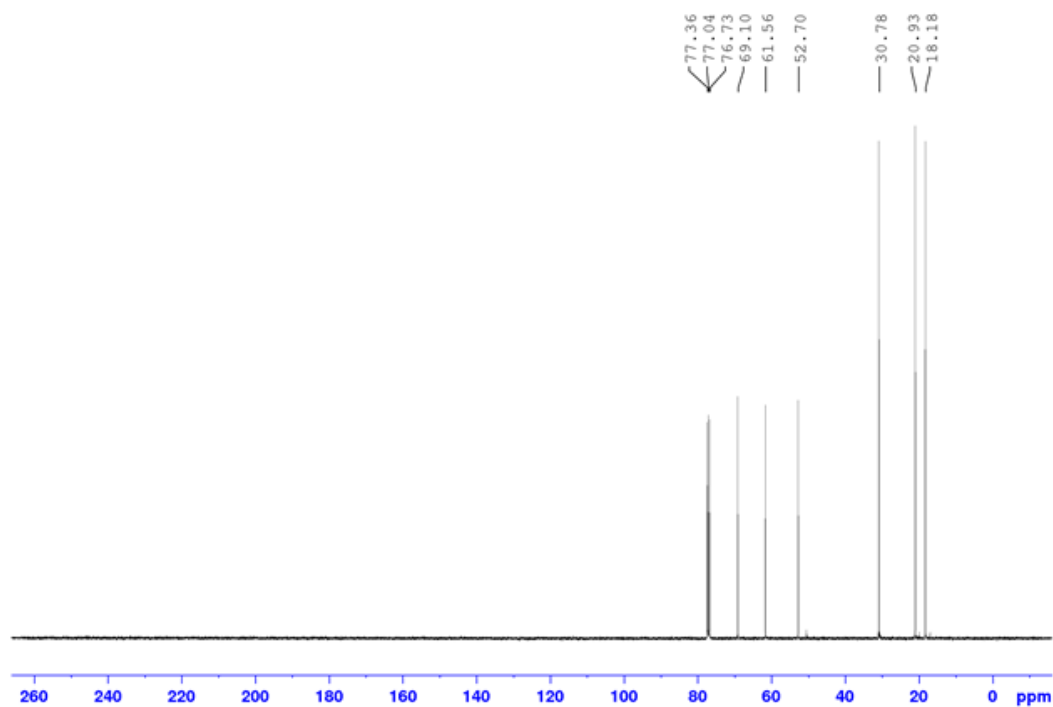
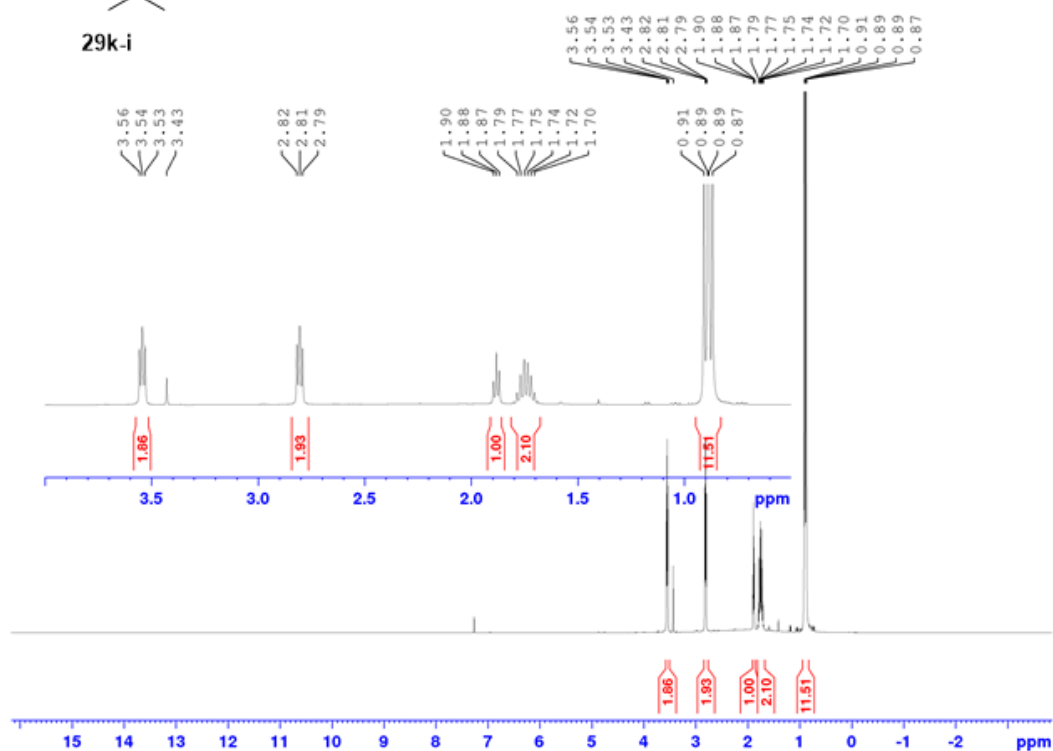
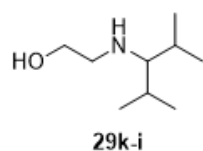
29f

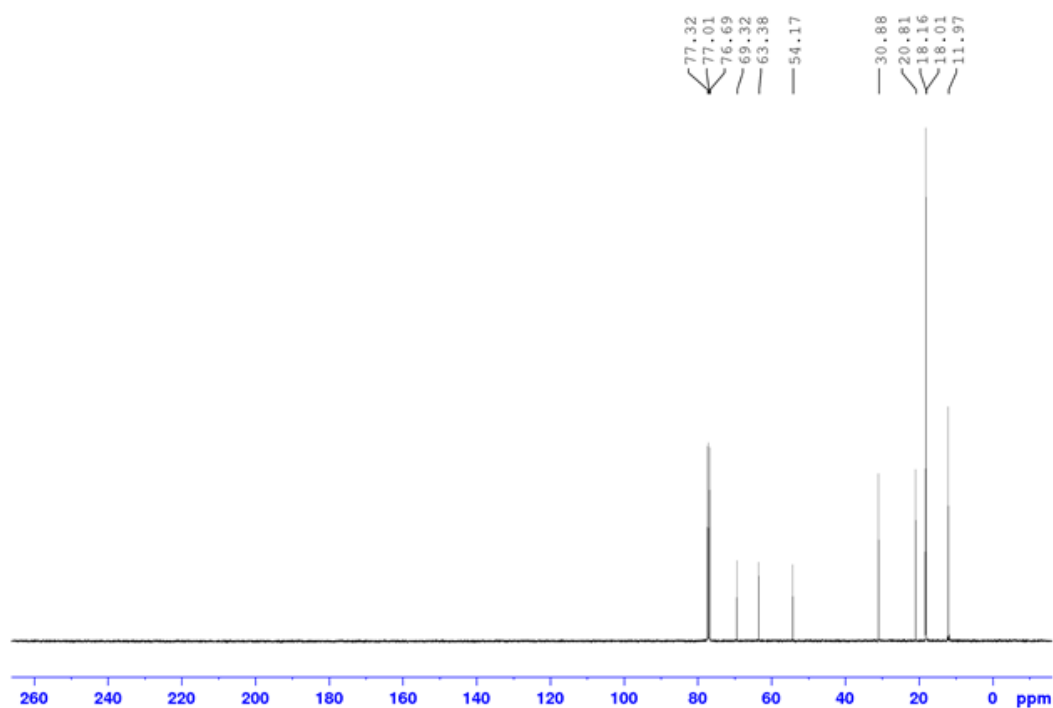
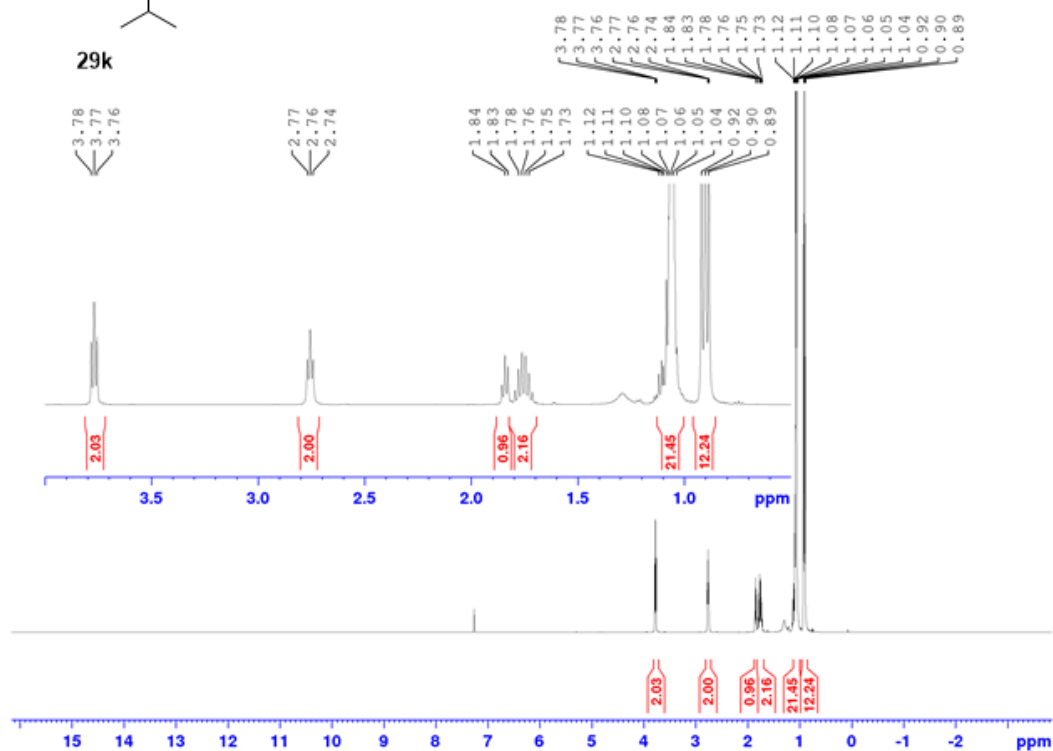
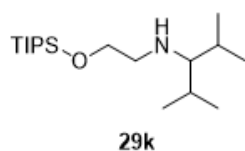


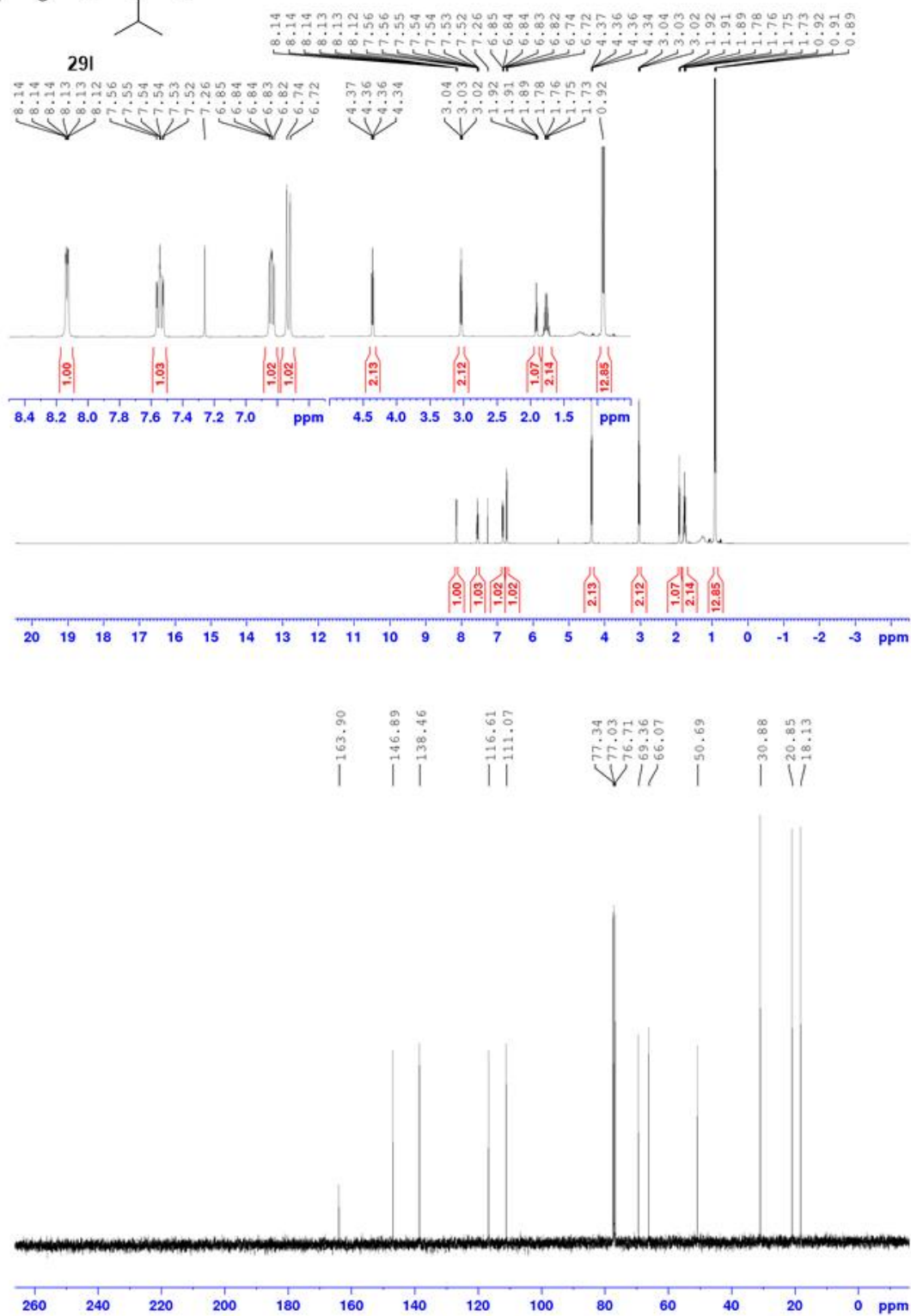


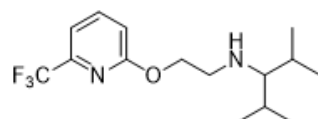




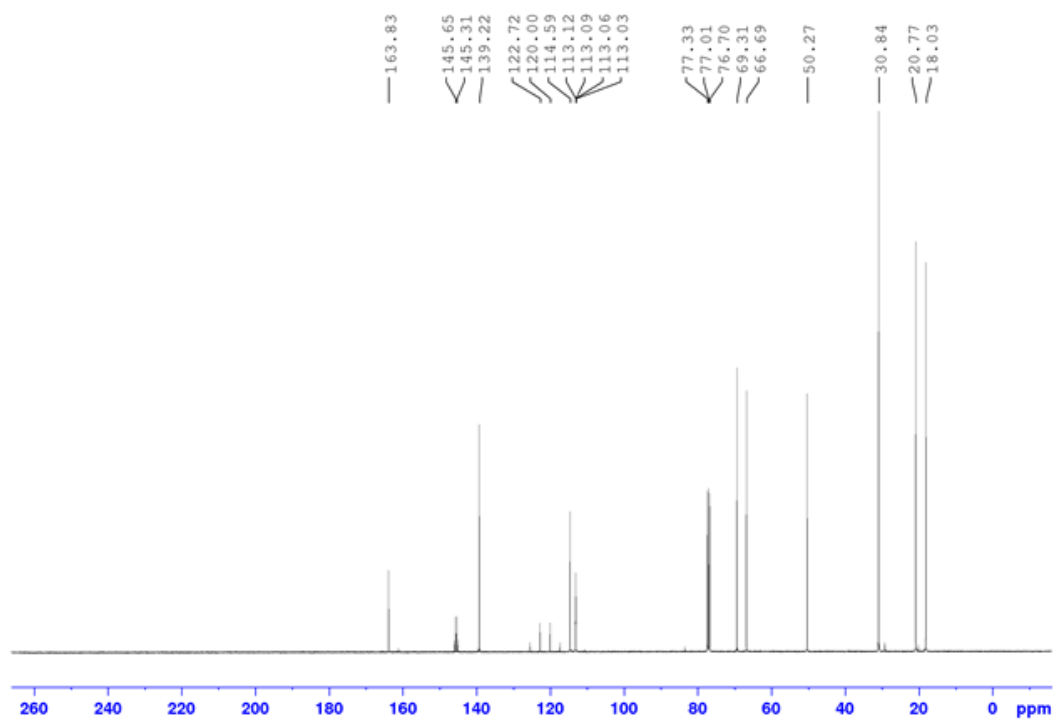
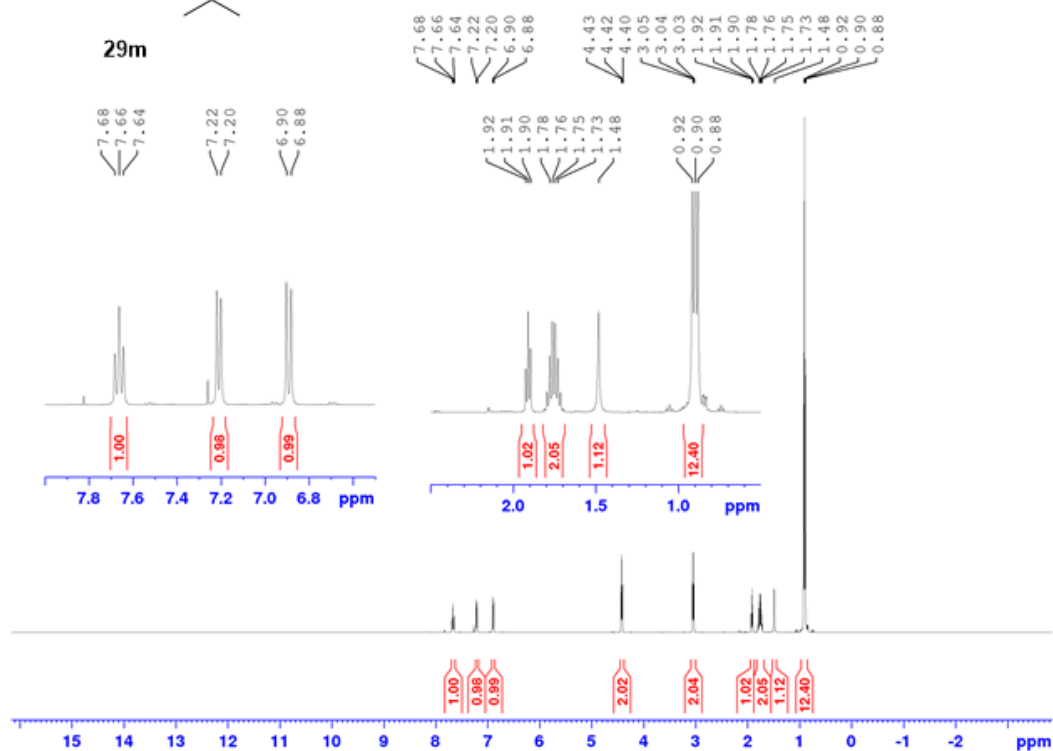


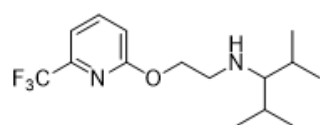




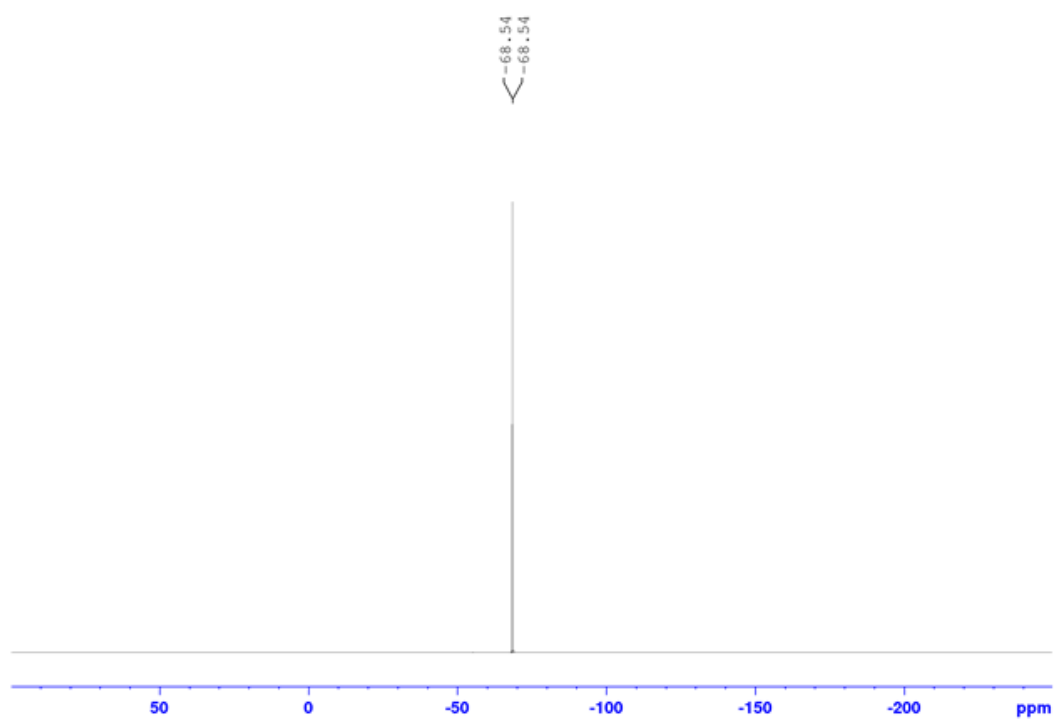


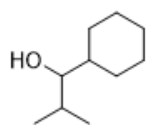
29m



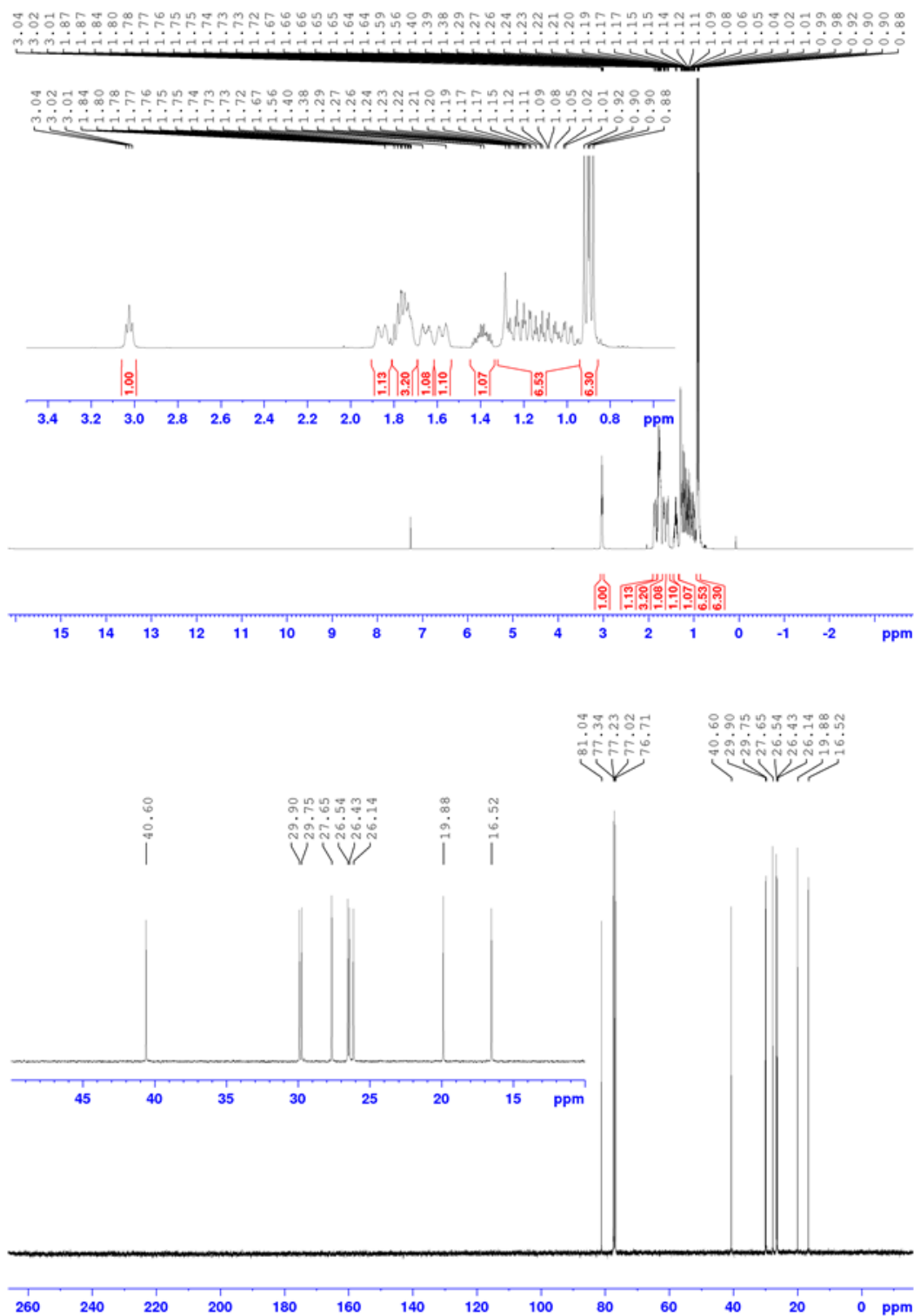


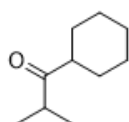
29m



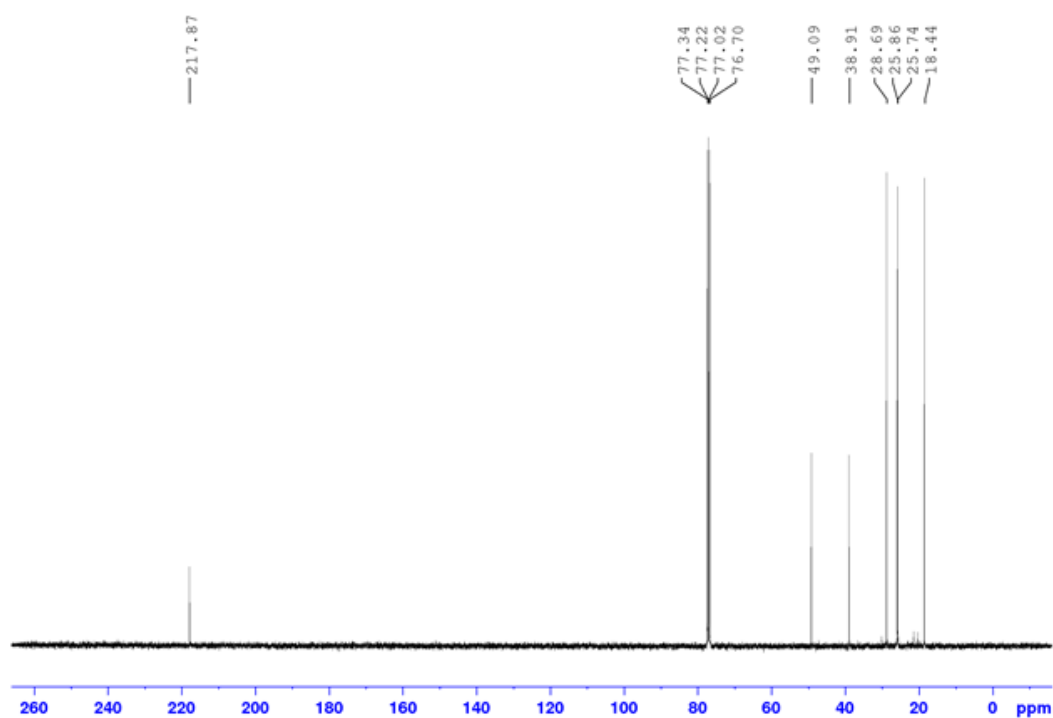
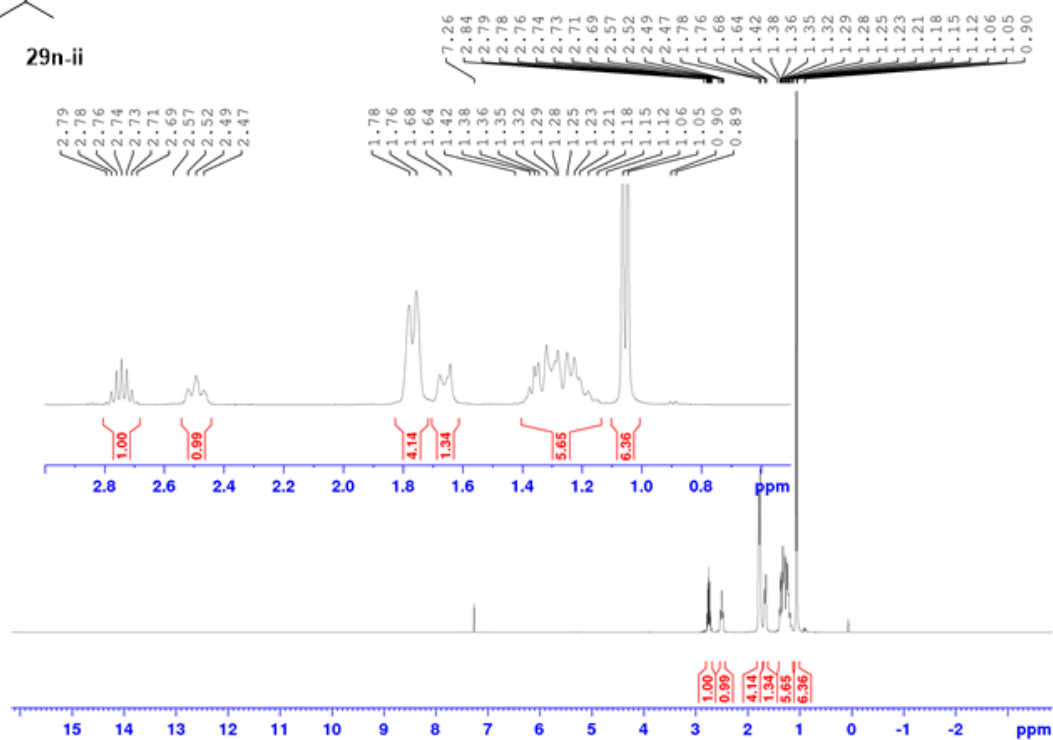


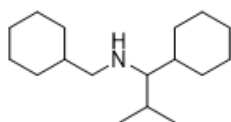
29n-i



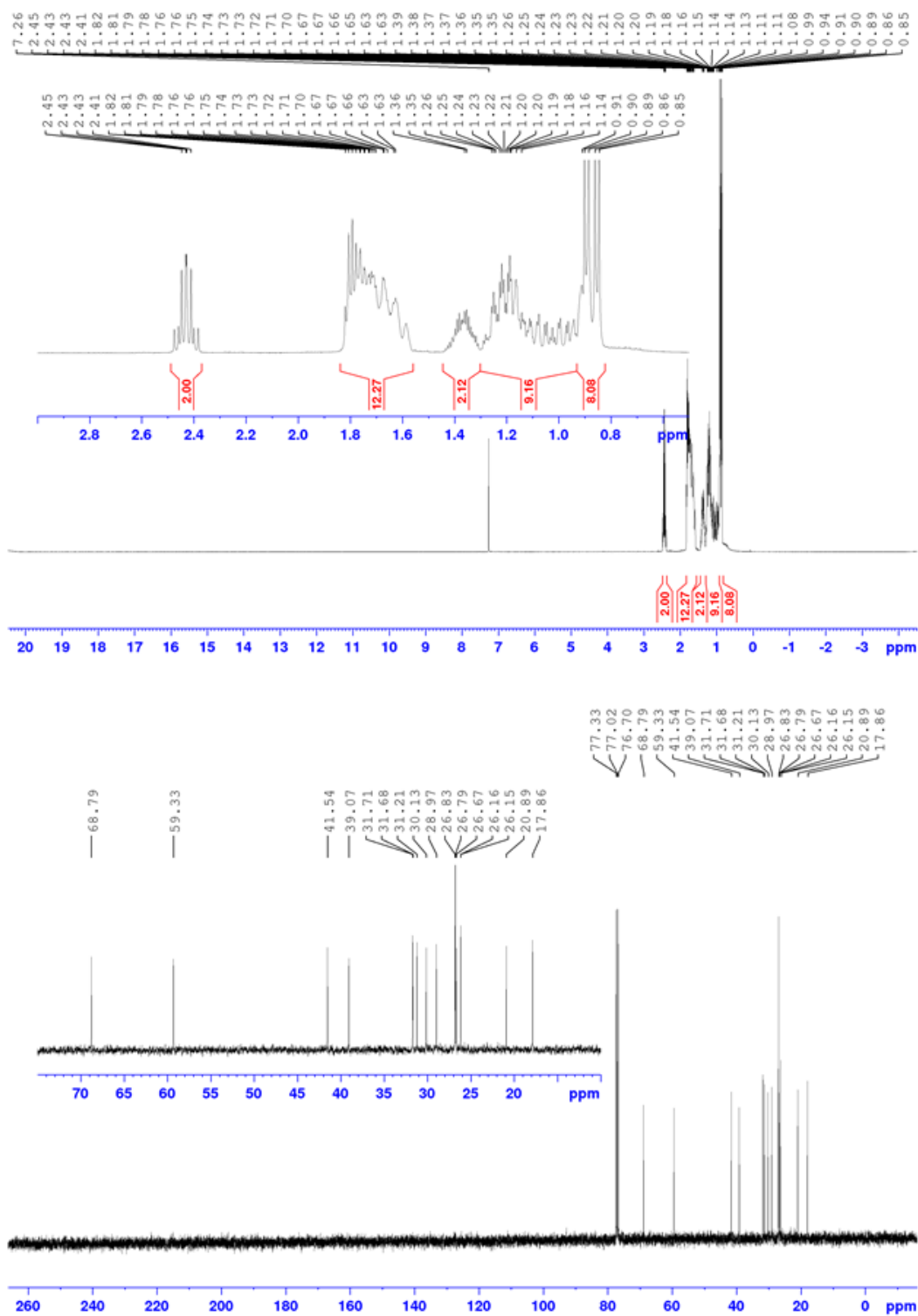


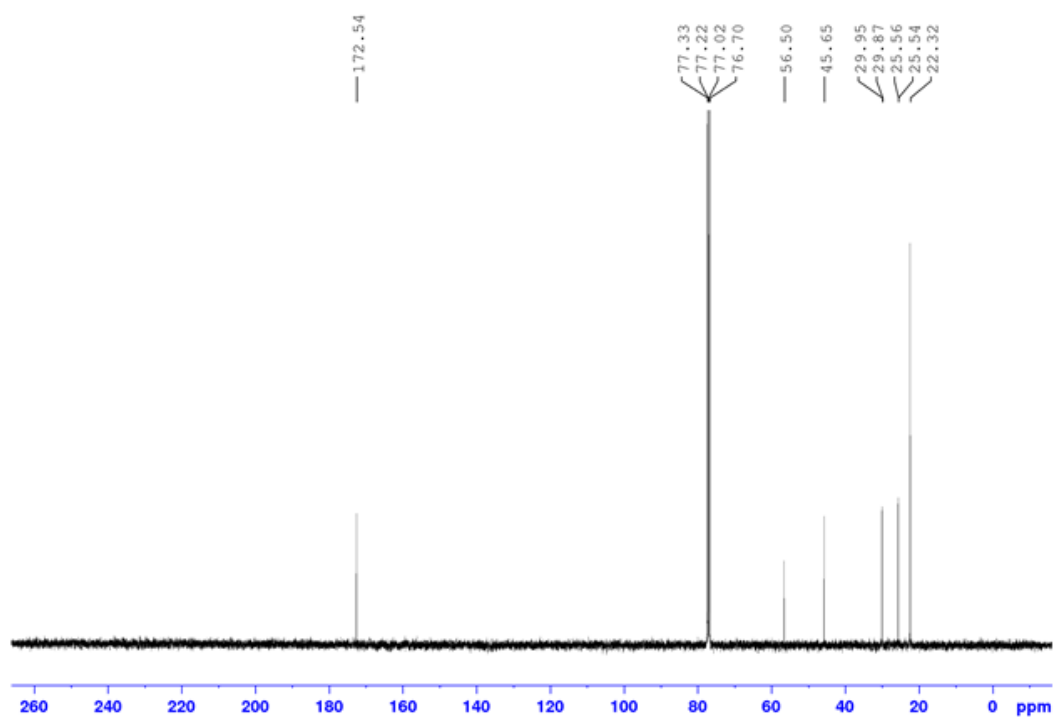
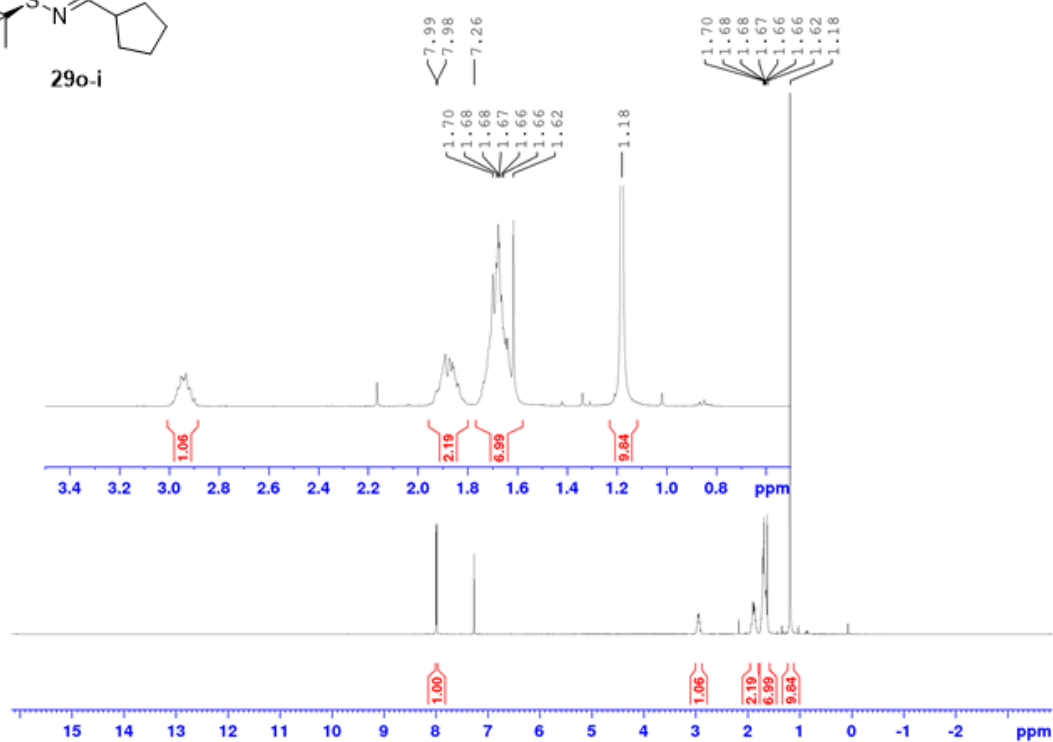
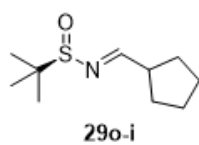
29n-ii

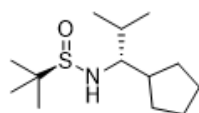




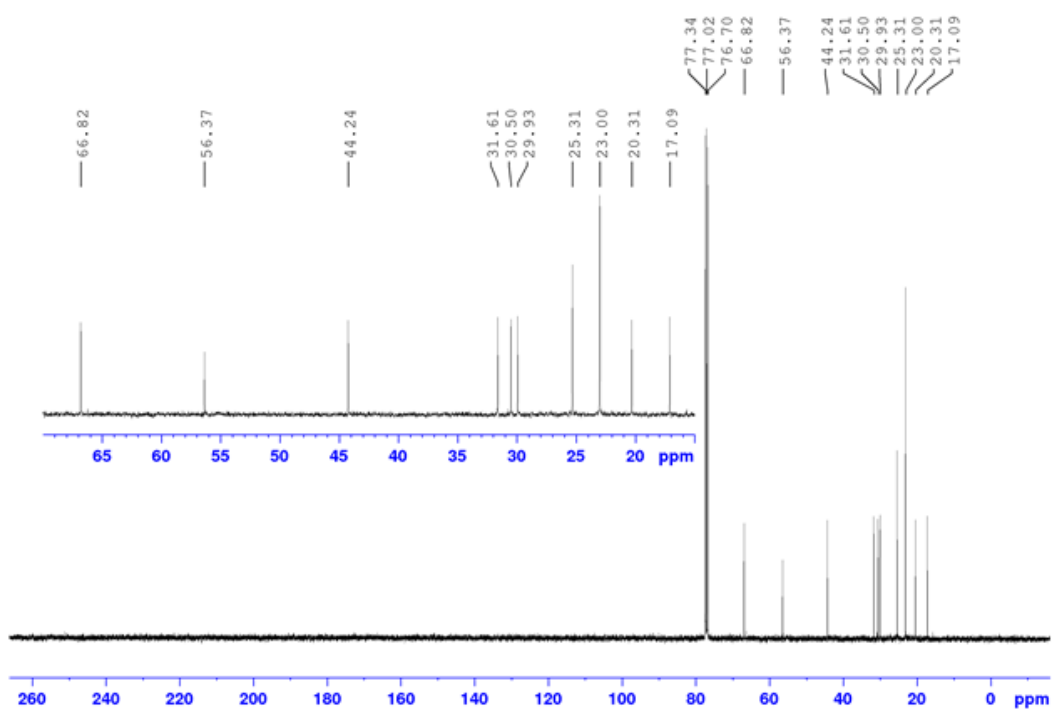
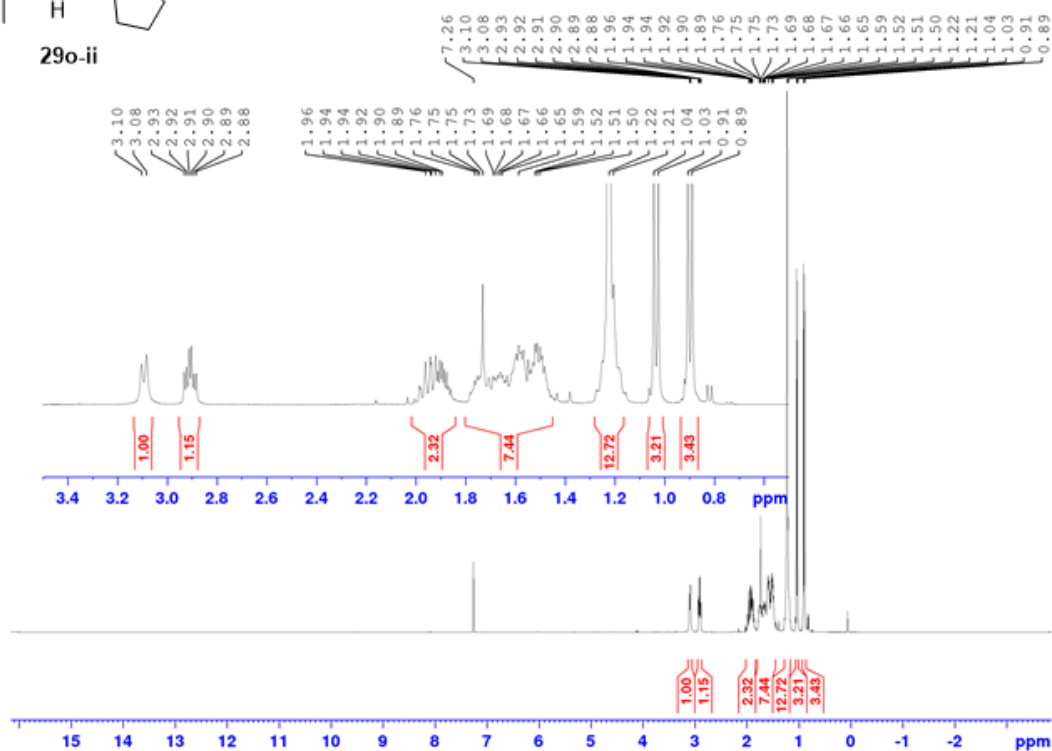
29n

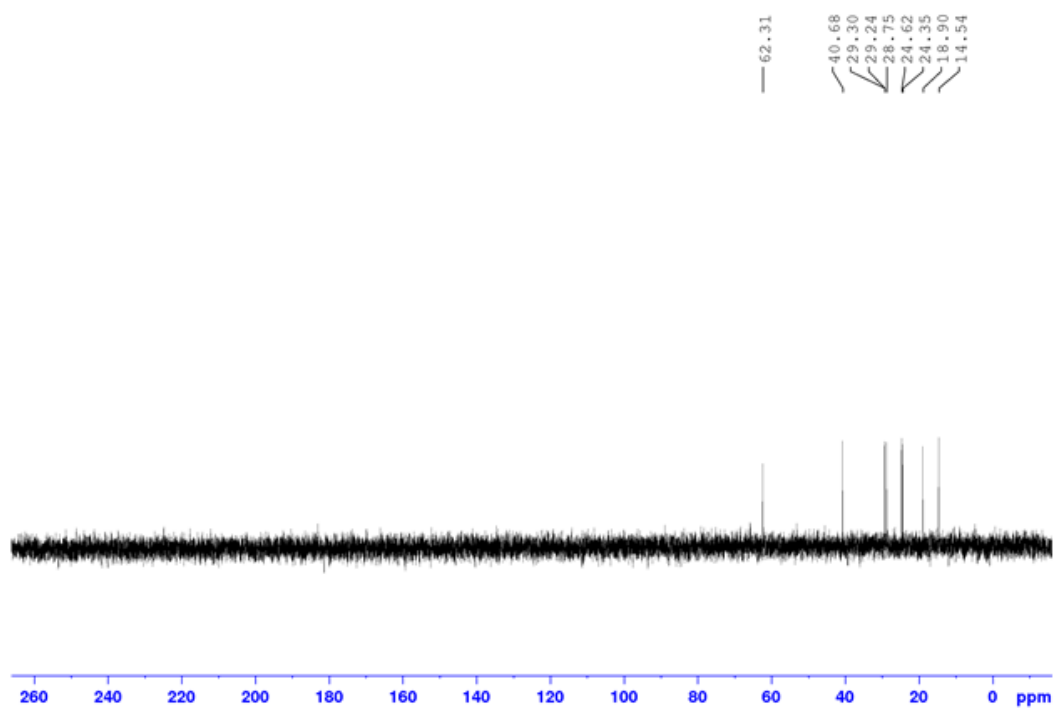
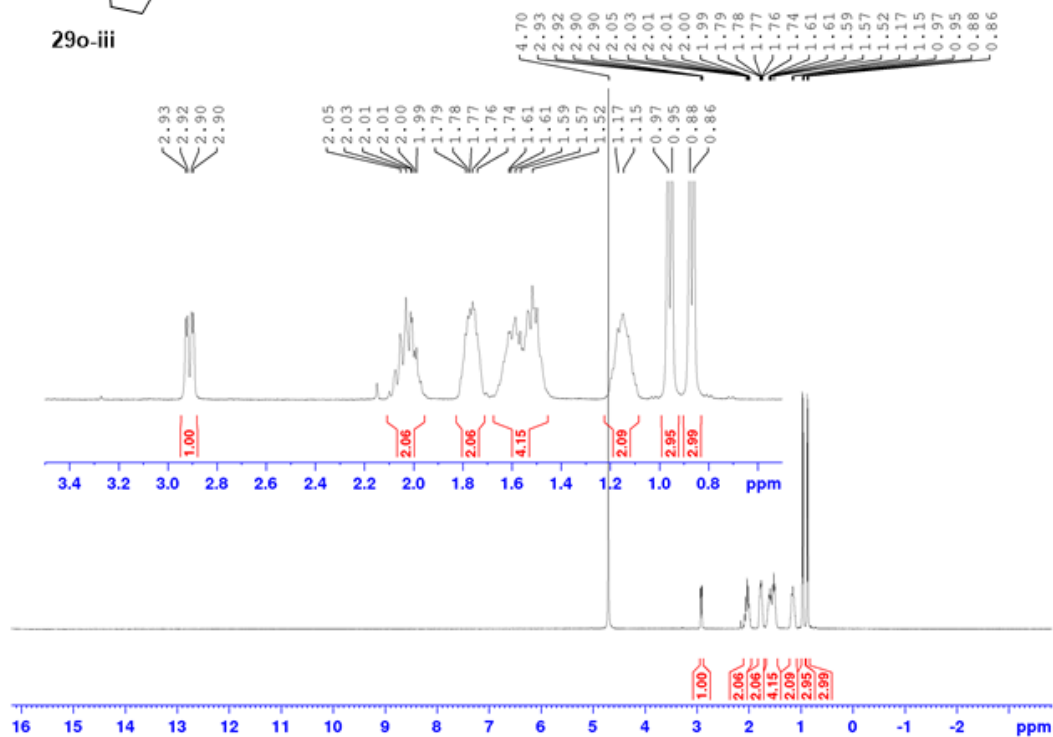
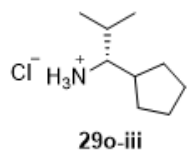


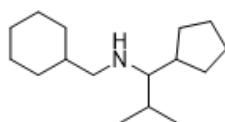




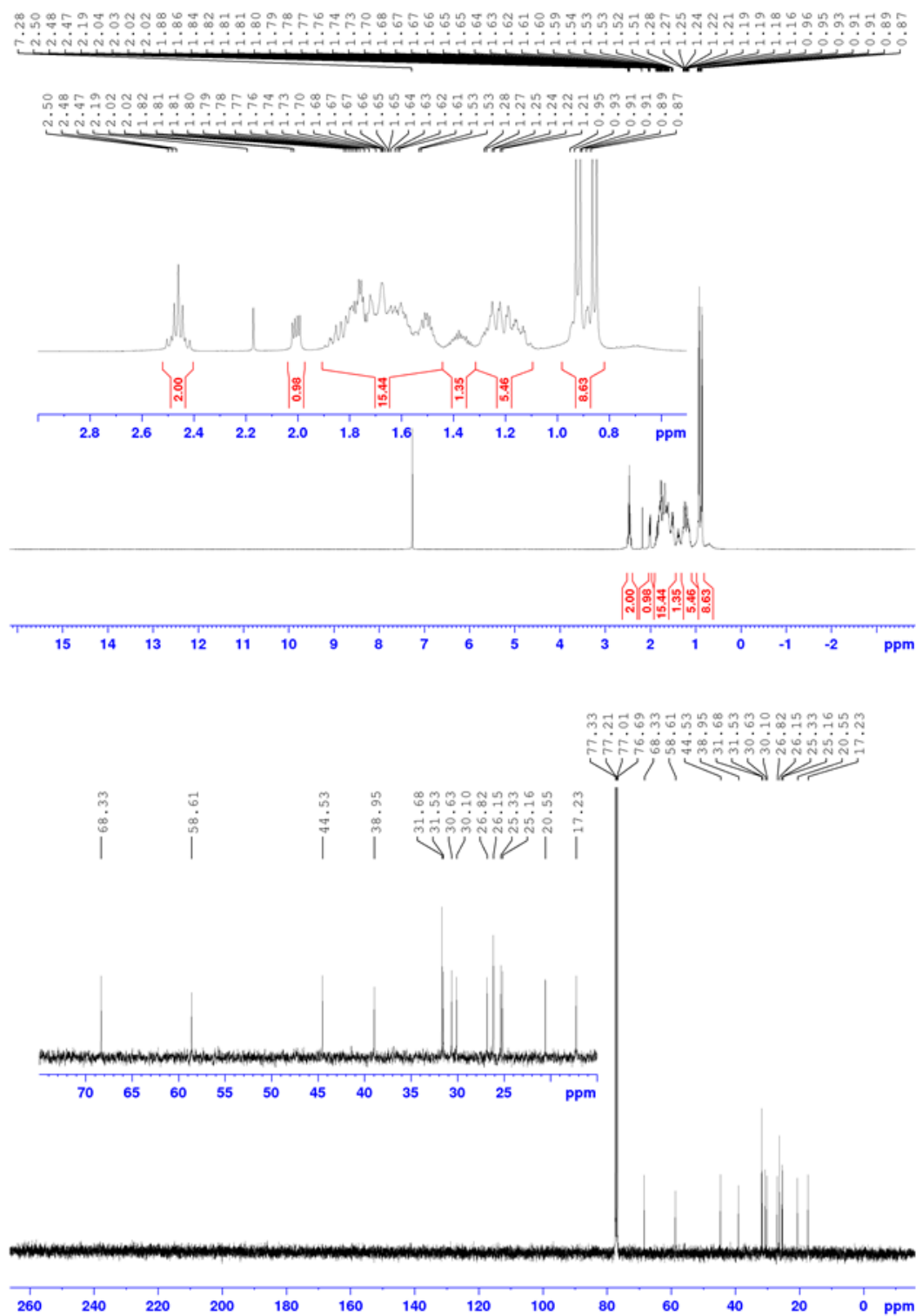
29o-ii

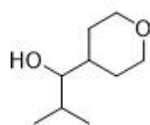




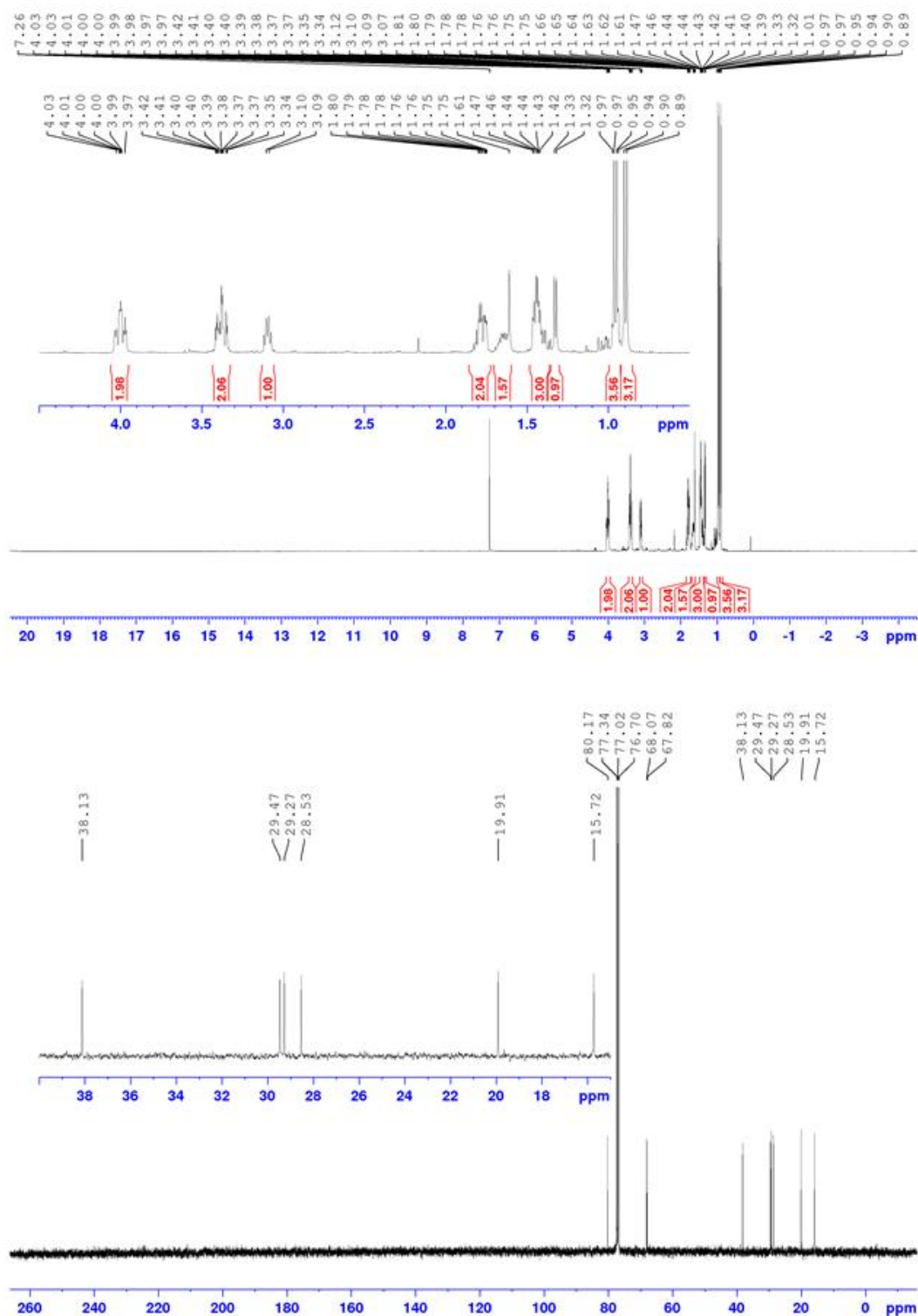


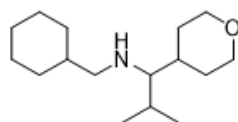
29o



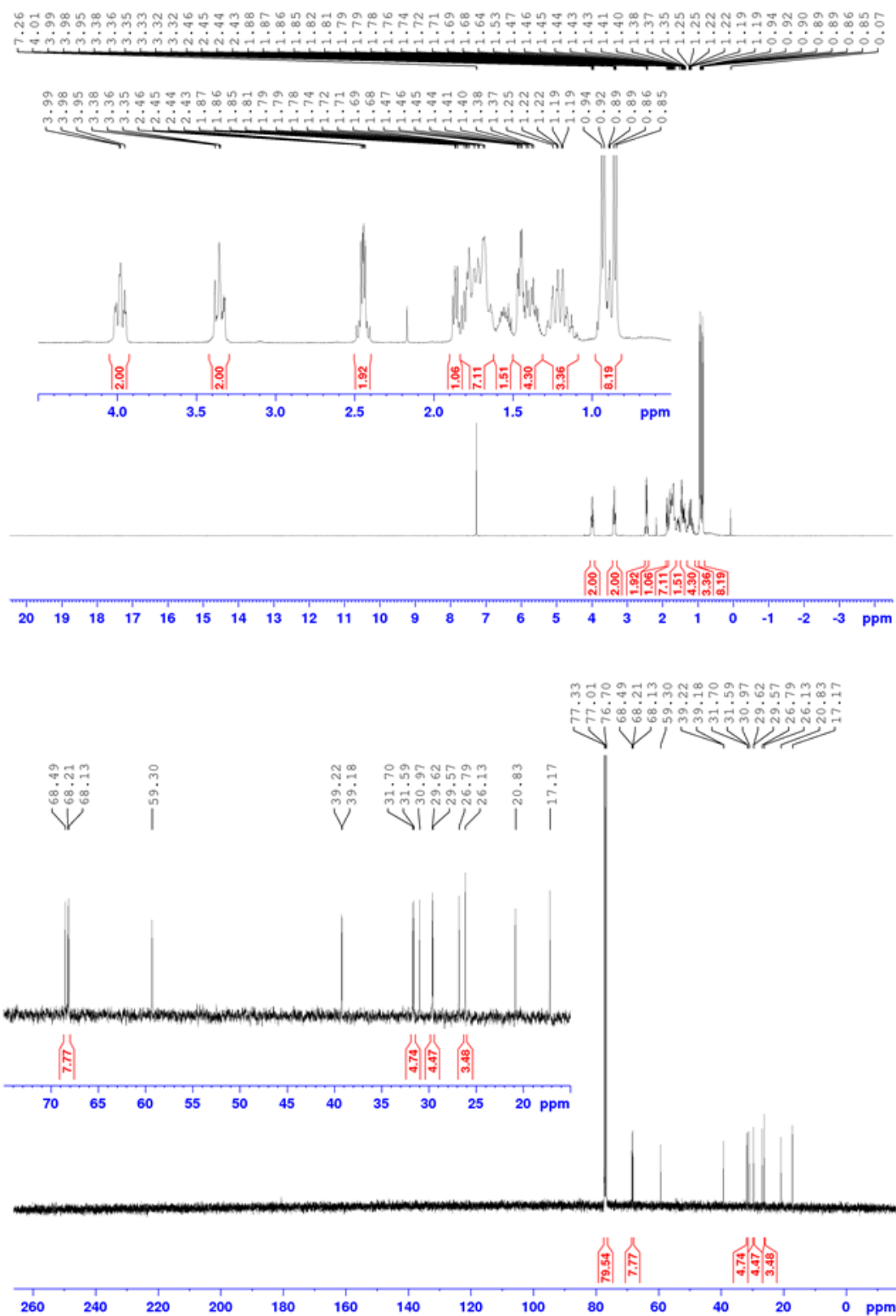


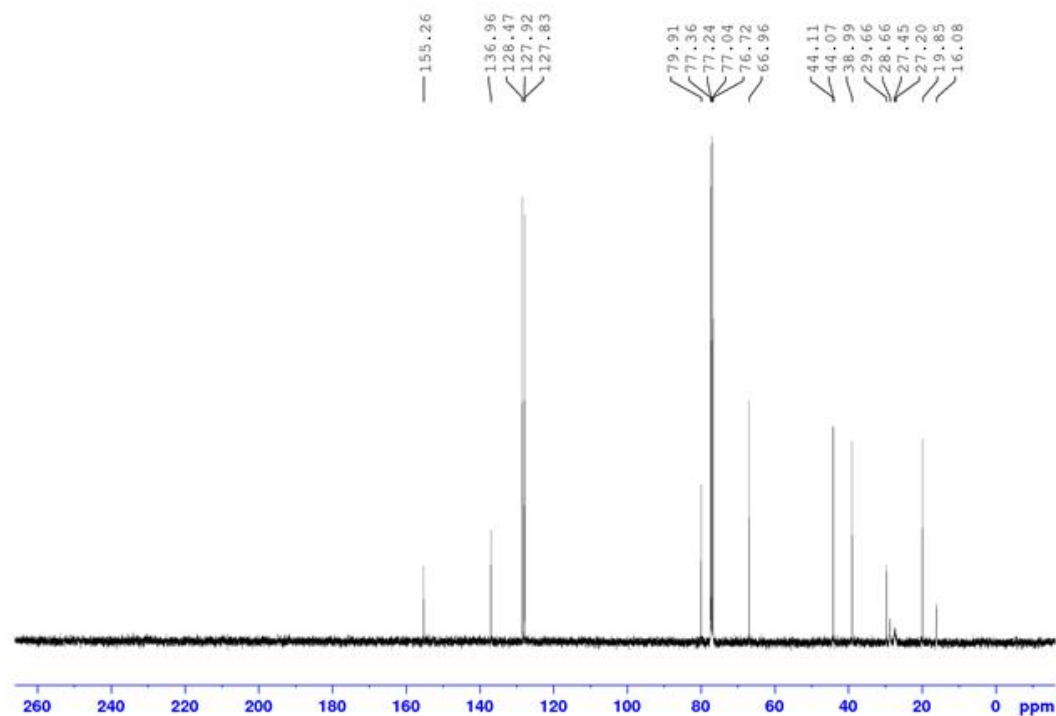
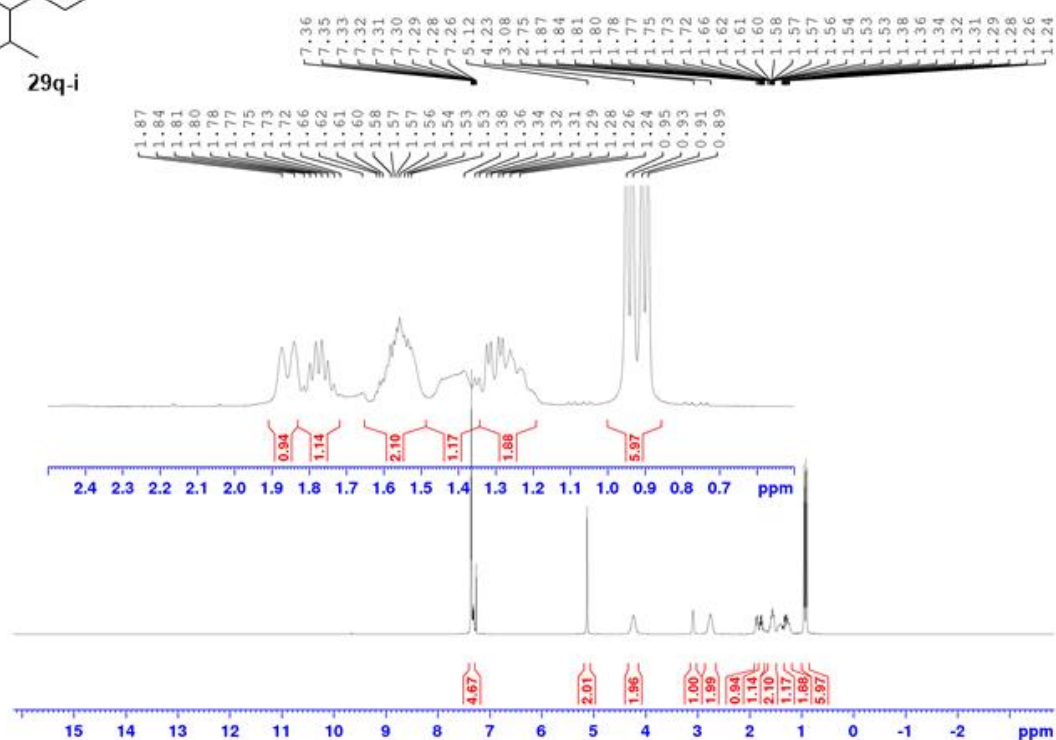
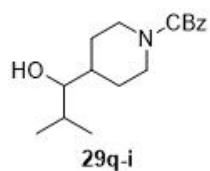
29p-i

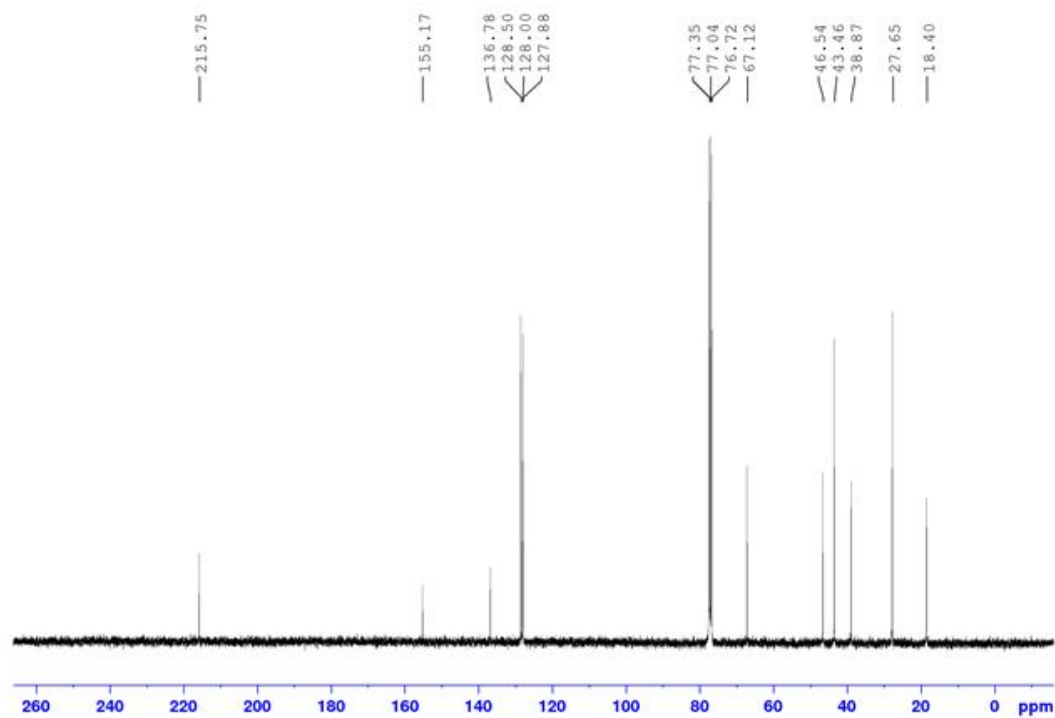
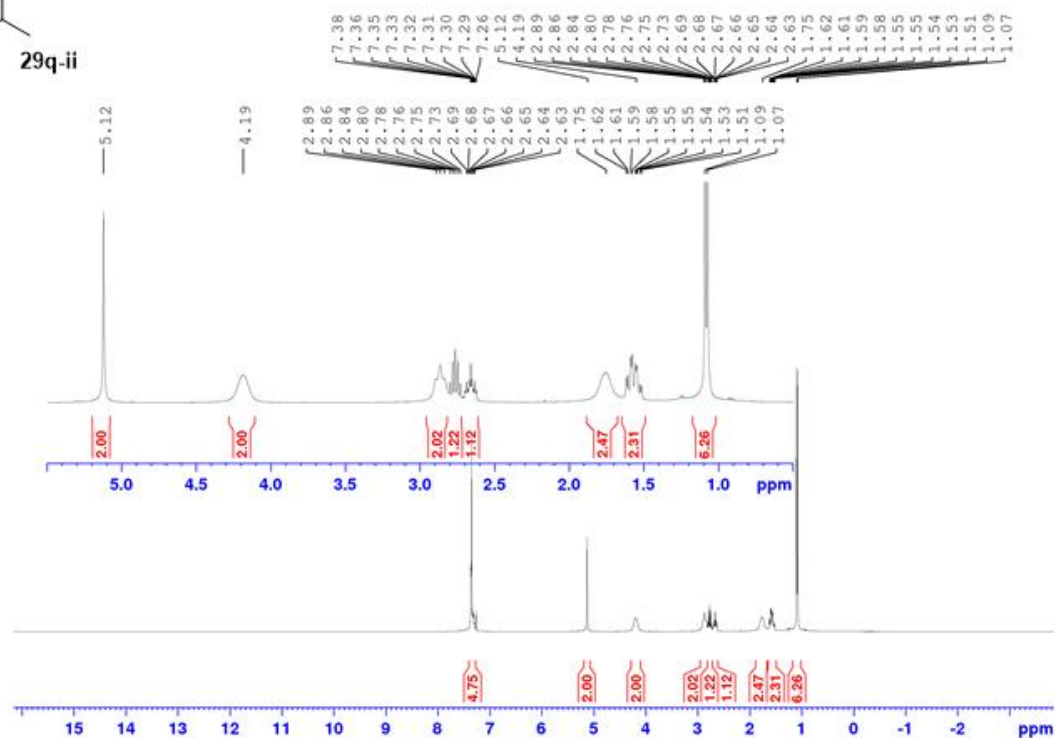
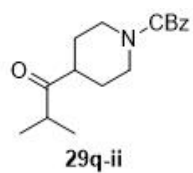


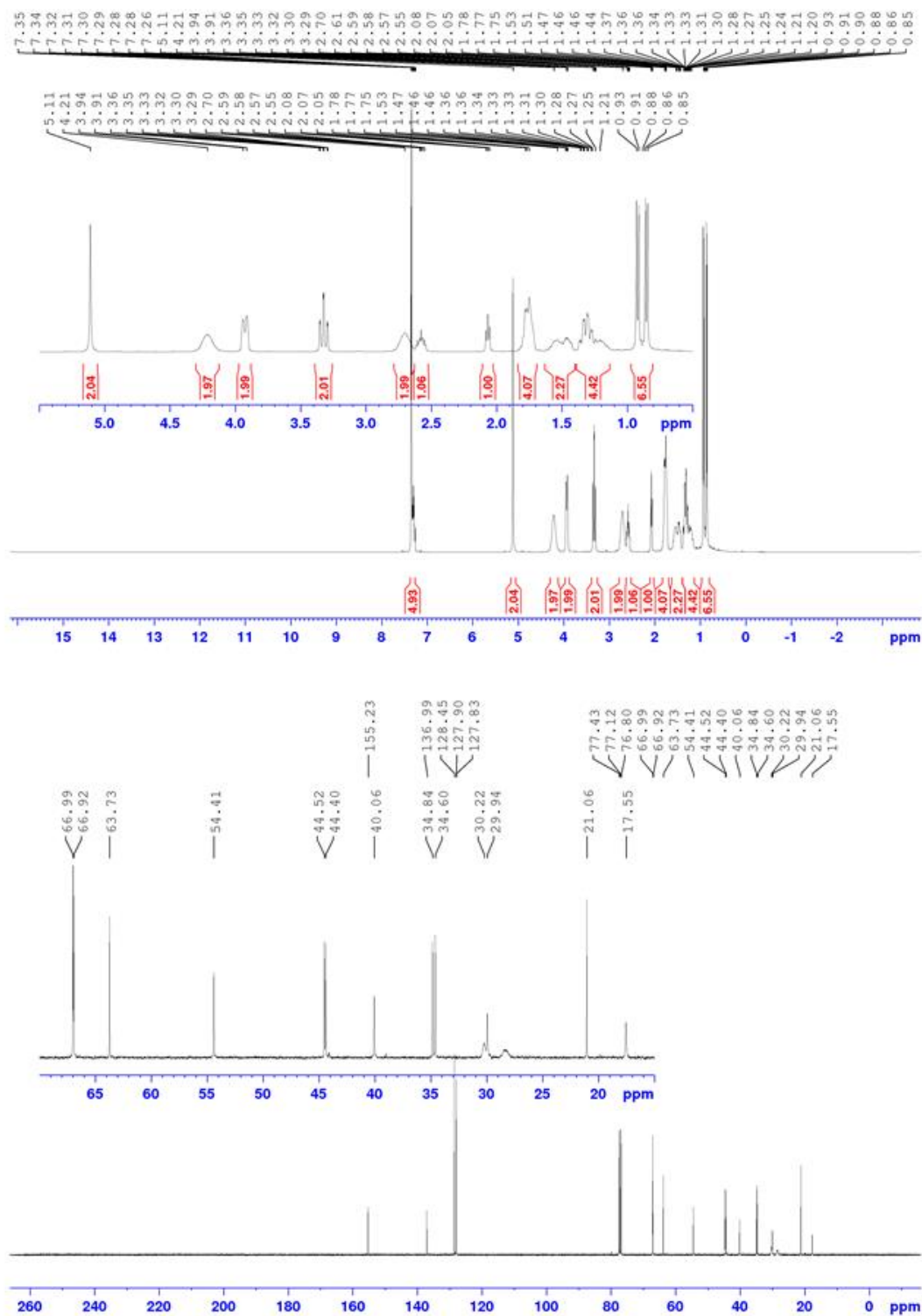
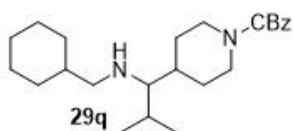


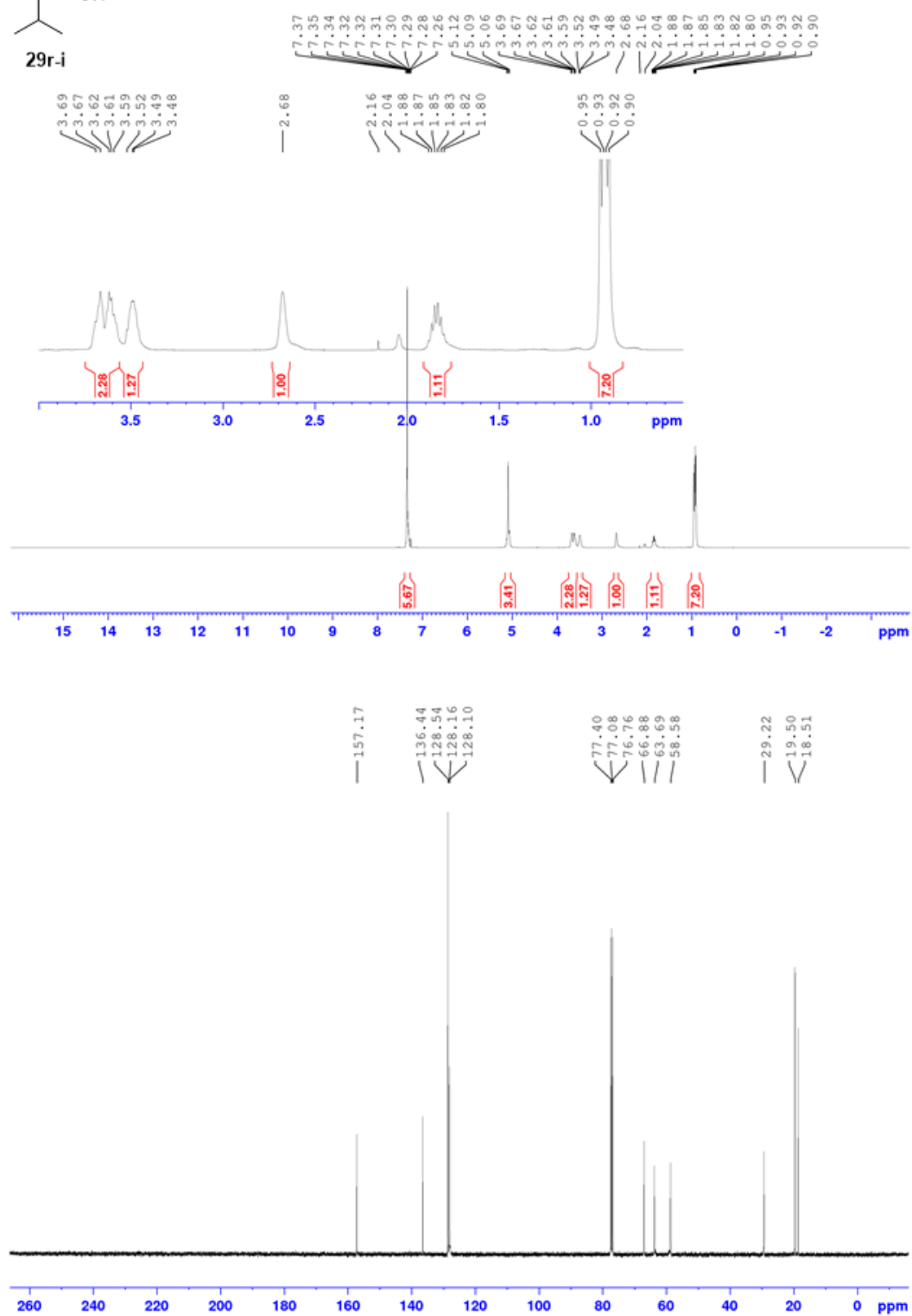
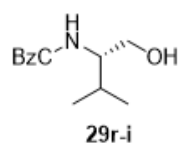
29p

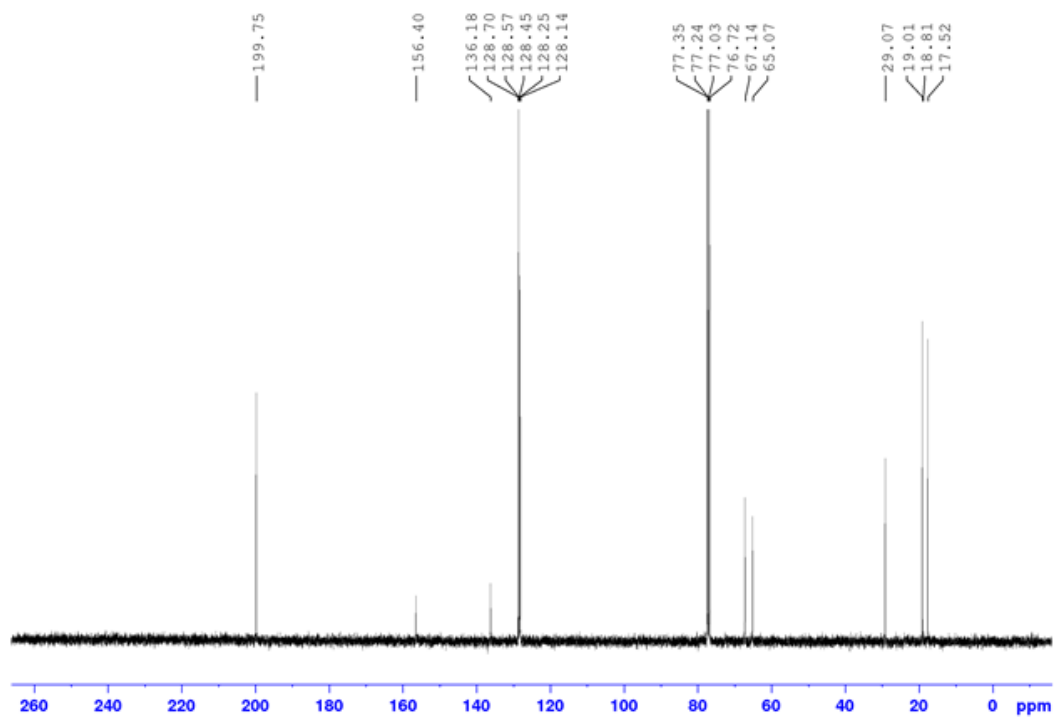
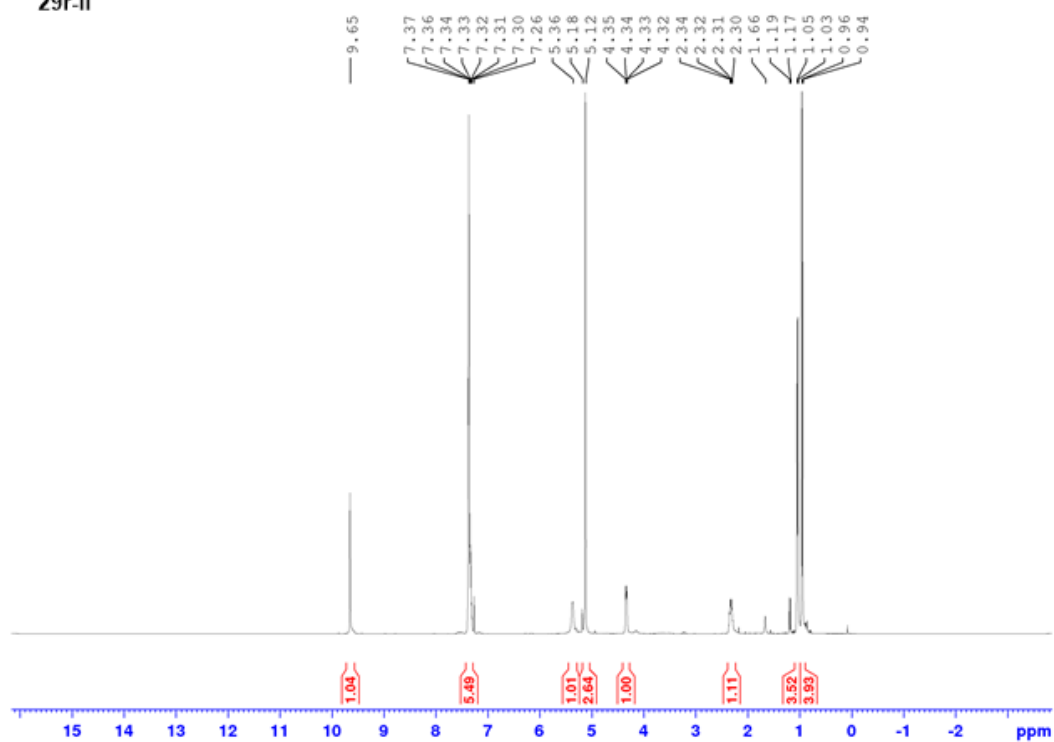
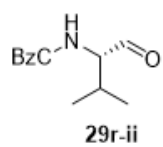


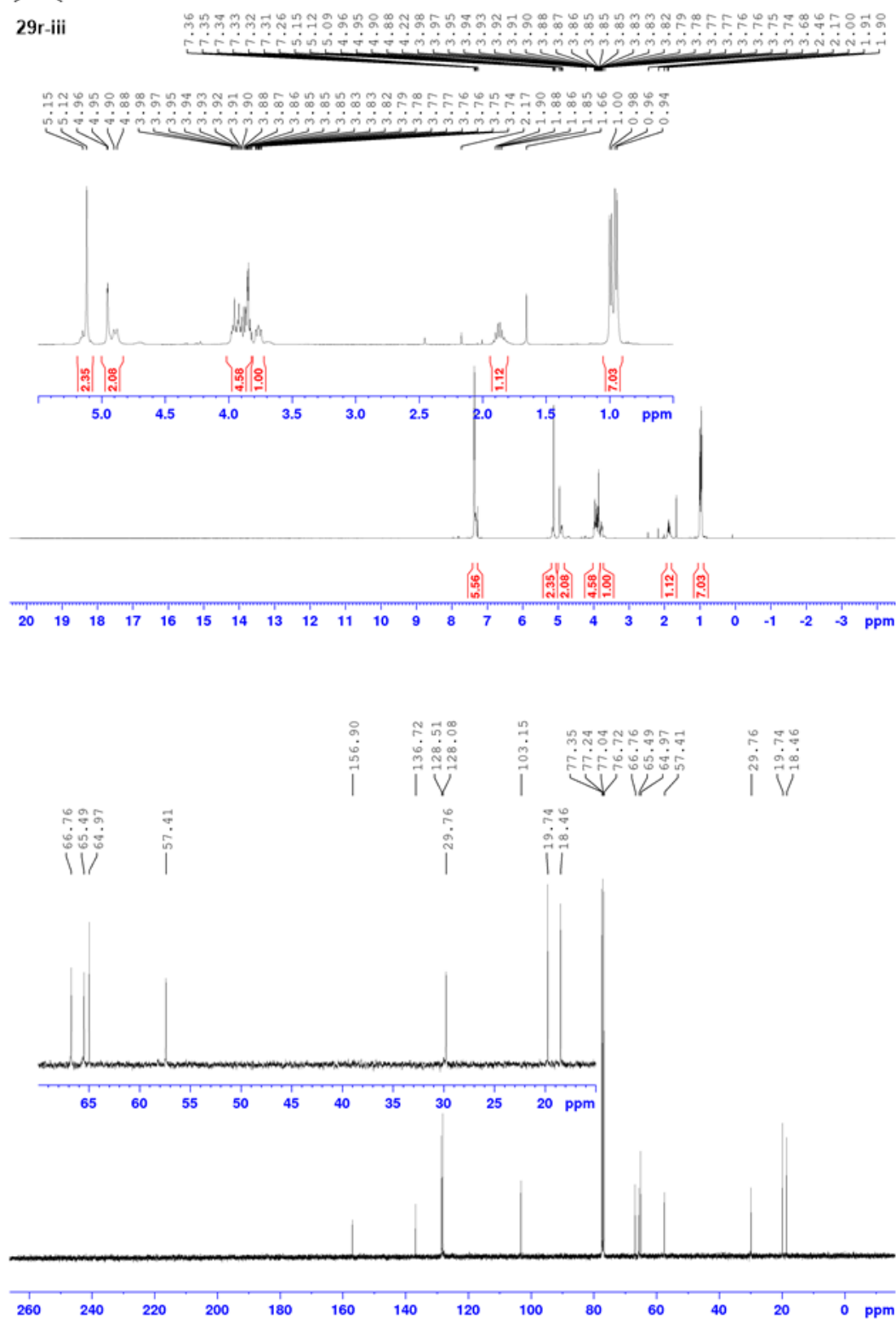
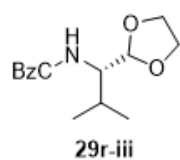


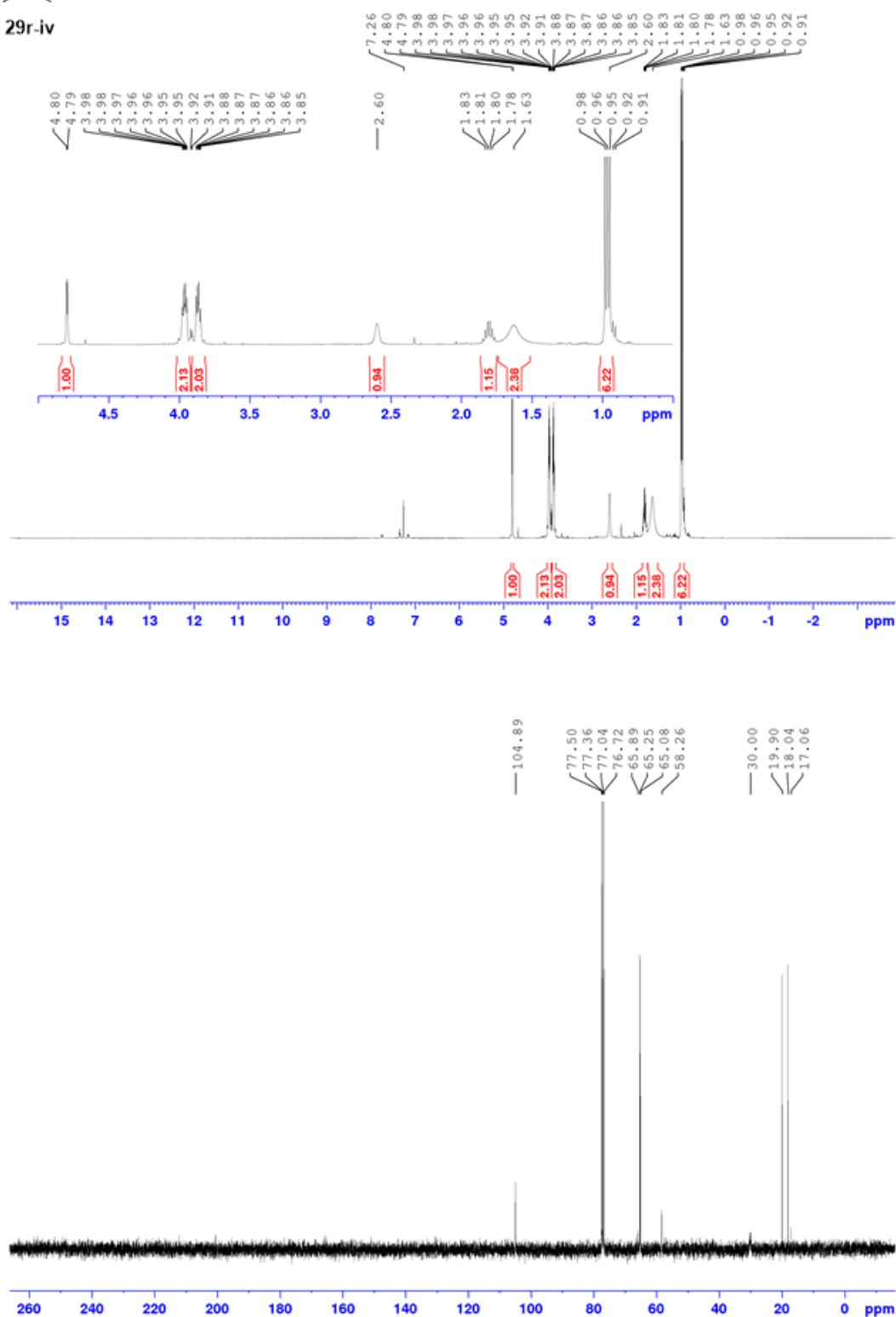
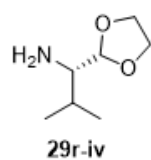


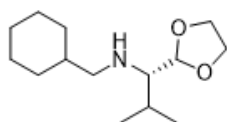




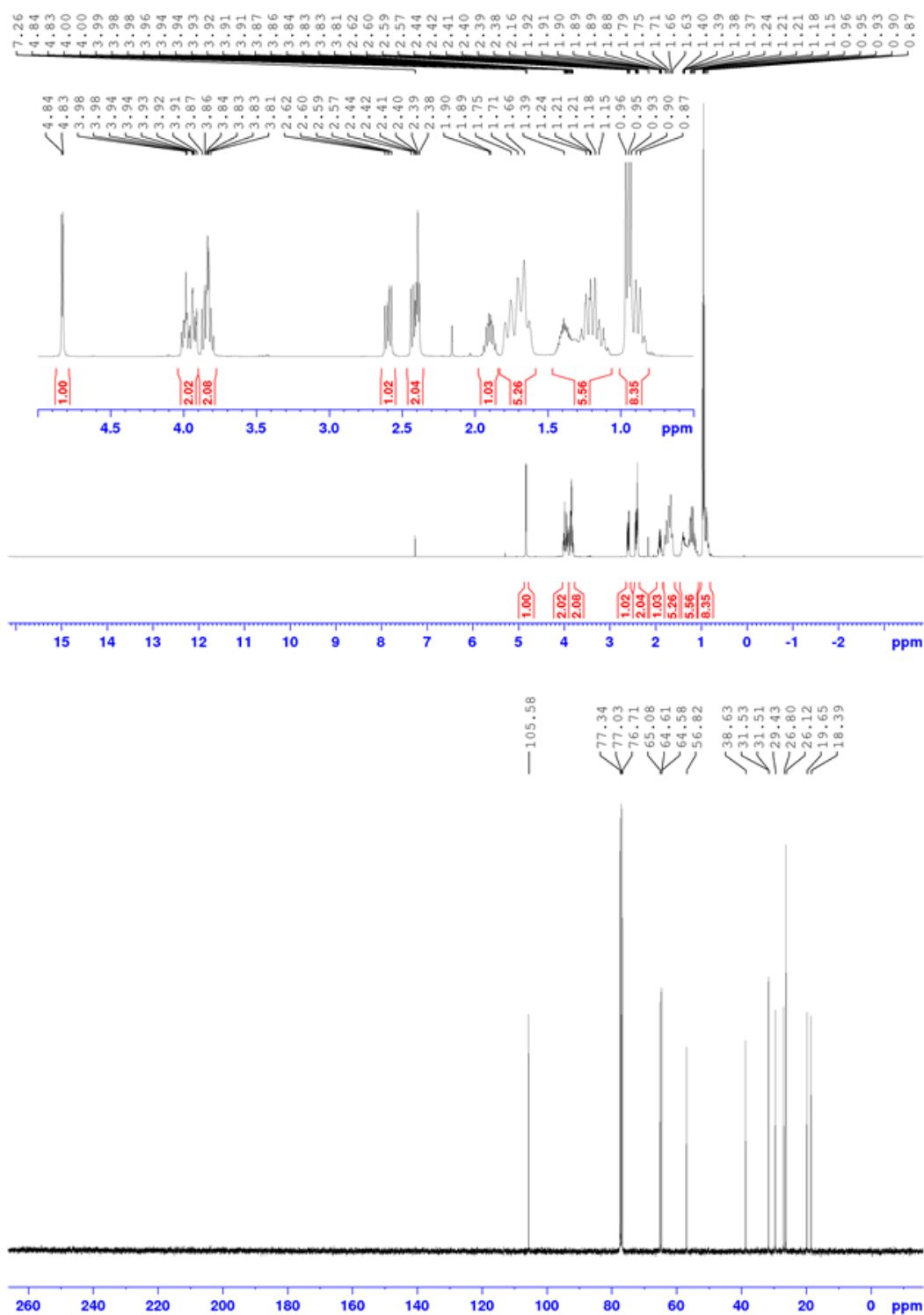


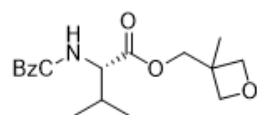




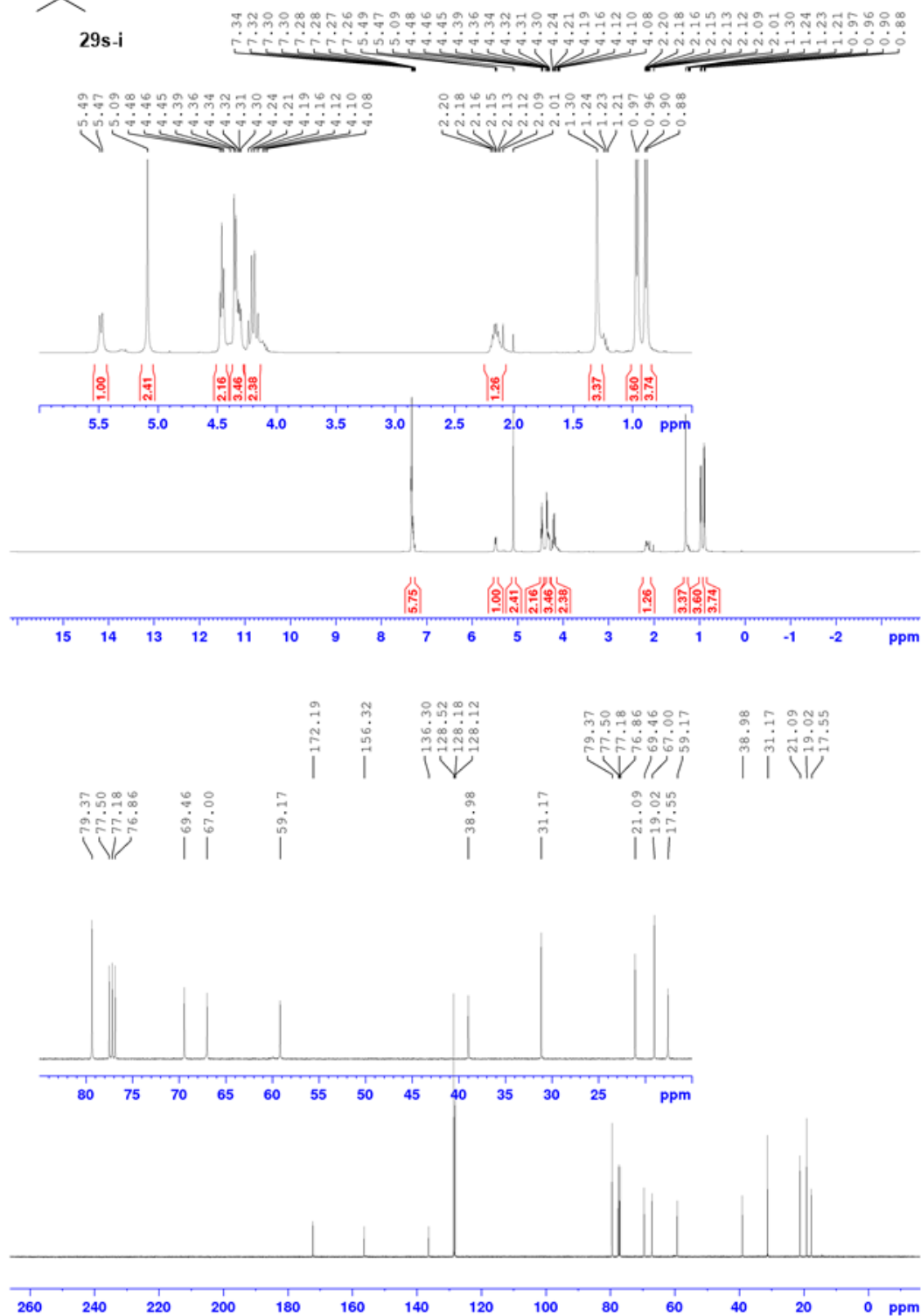


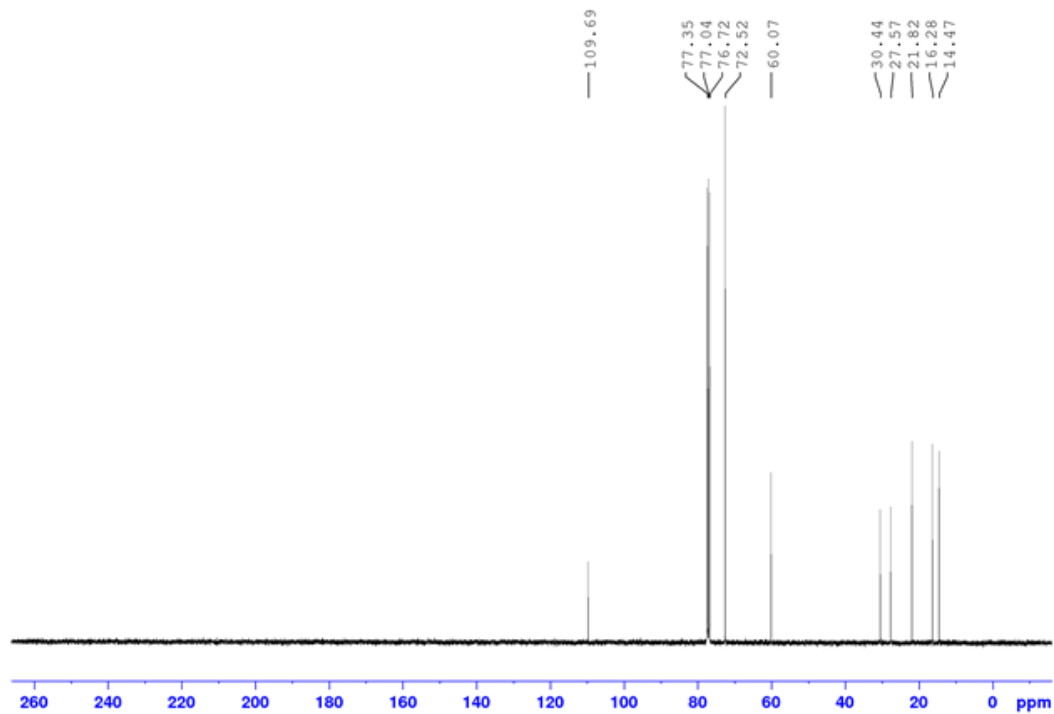
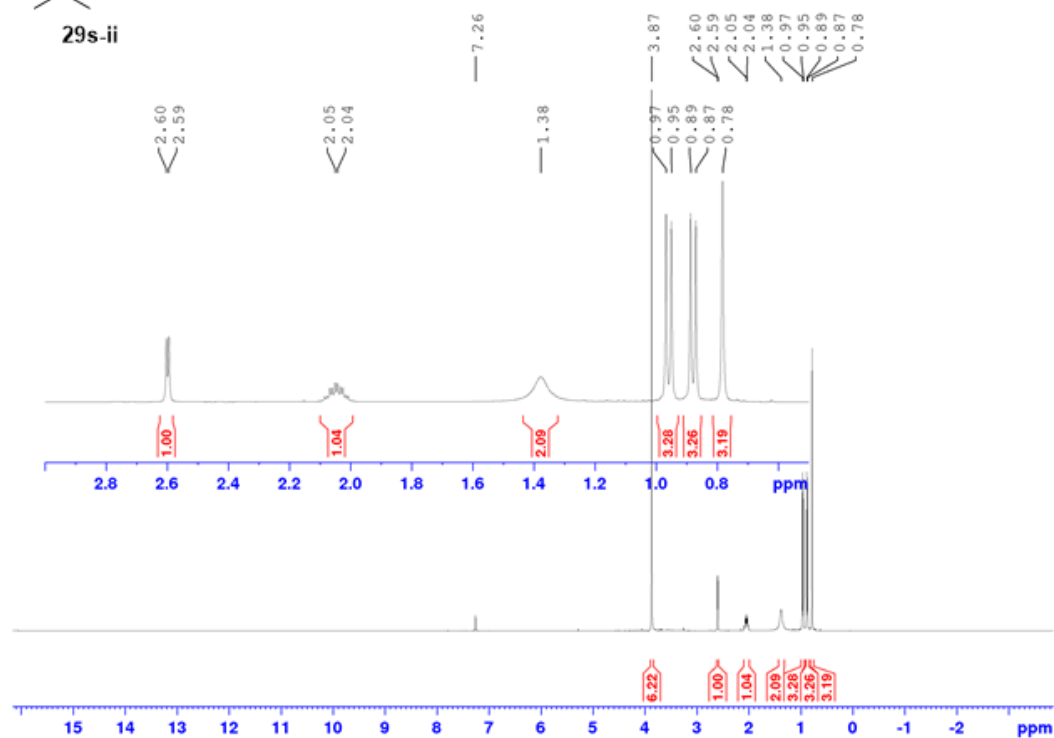
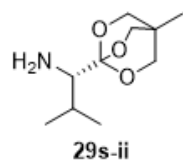
29r

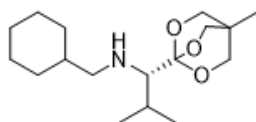




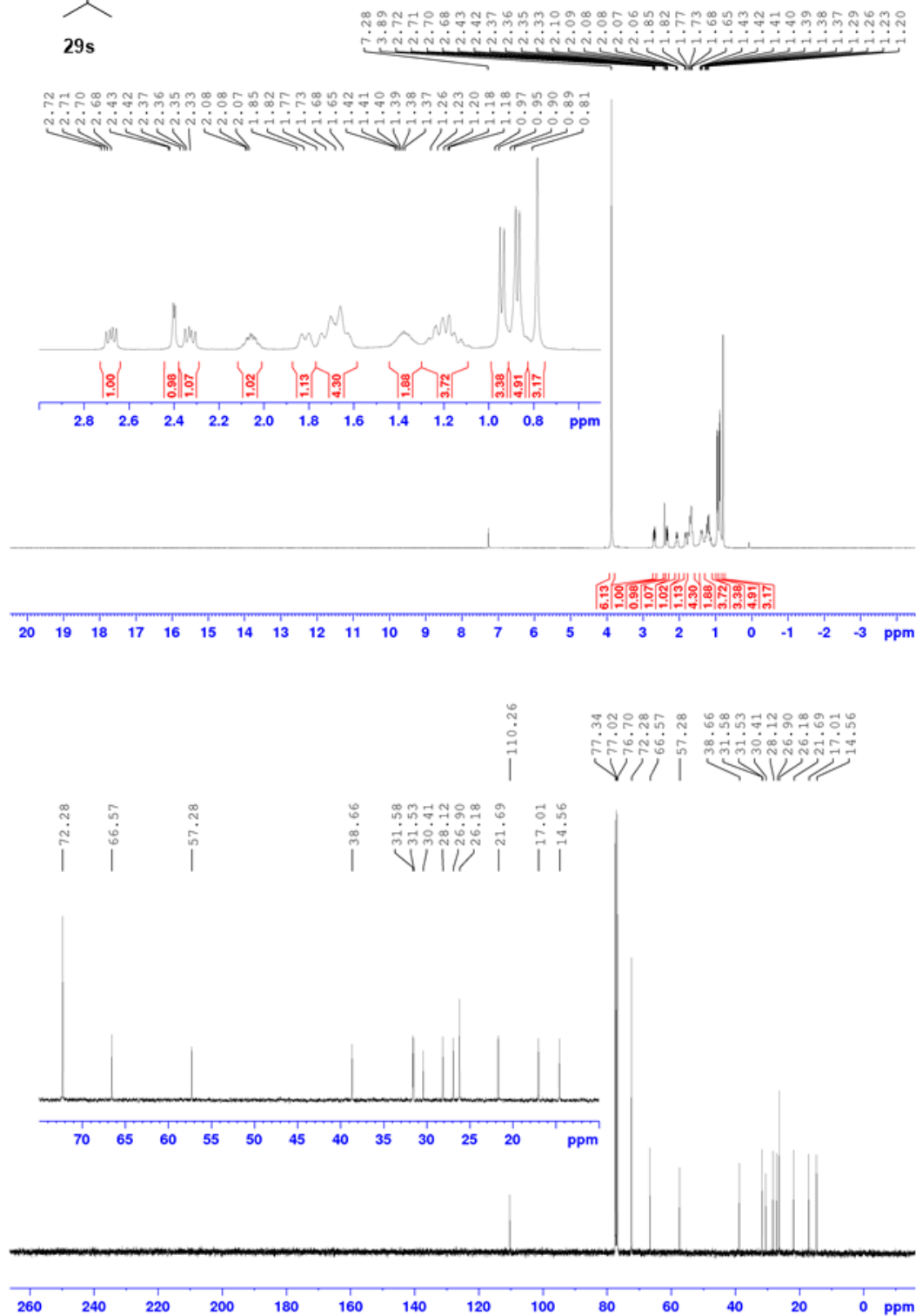
29s-i



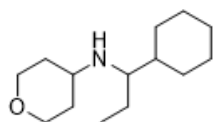




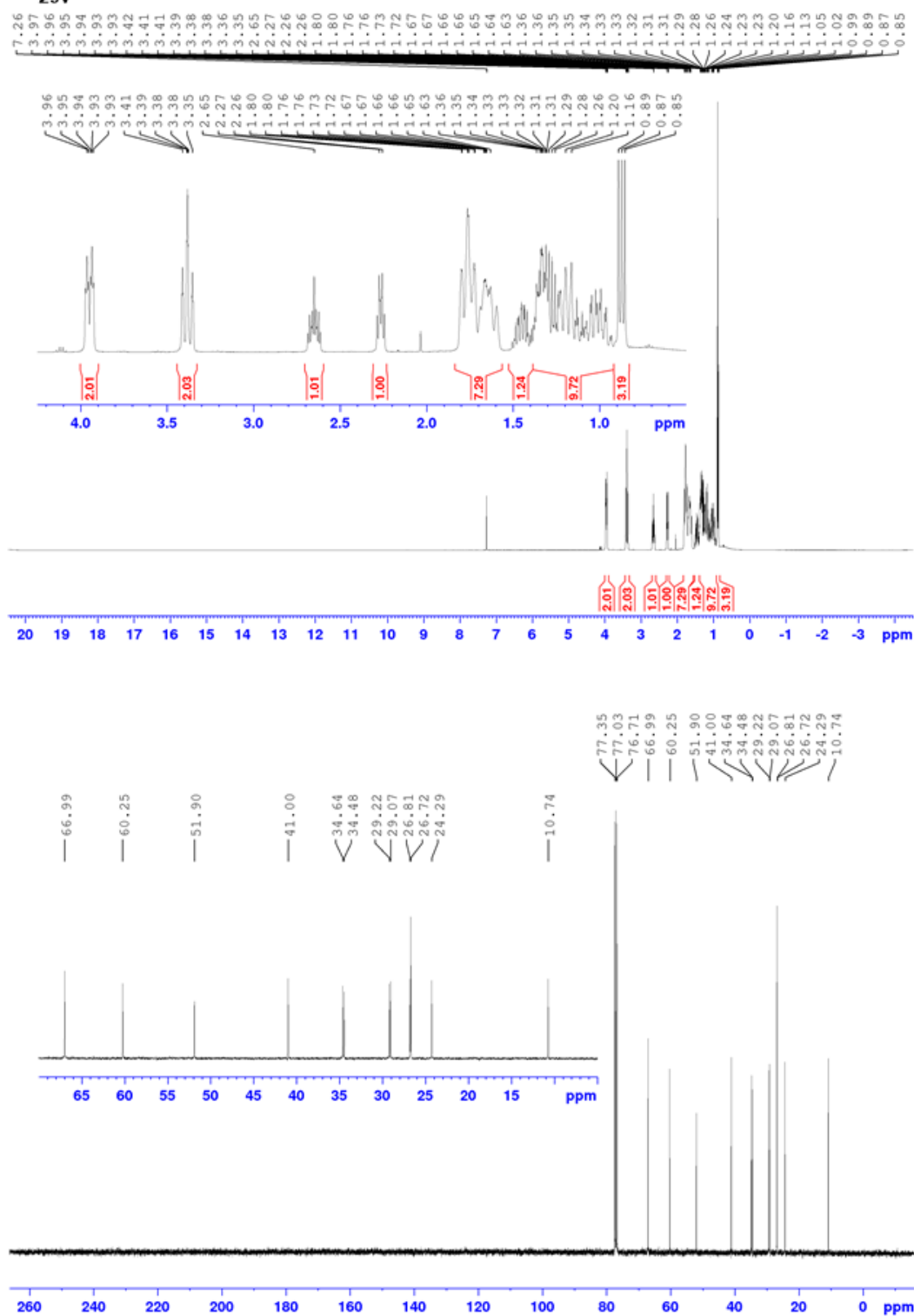
29s

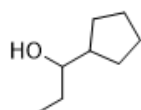




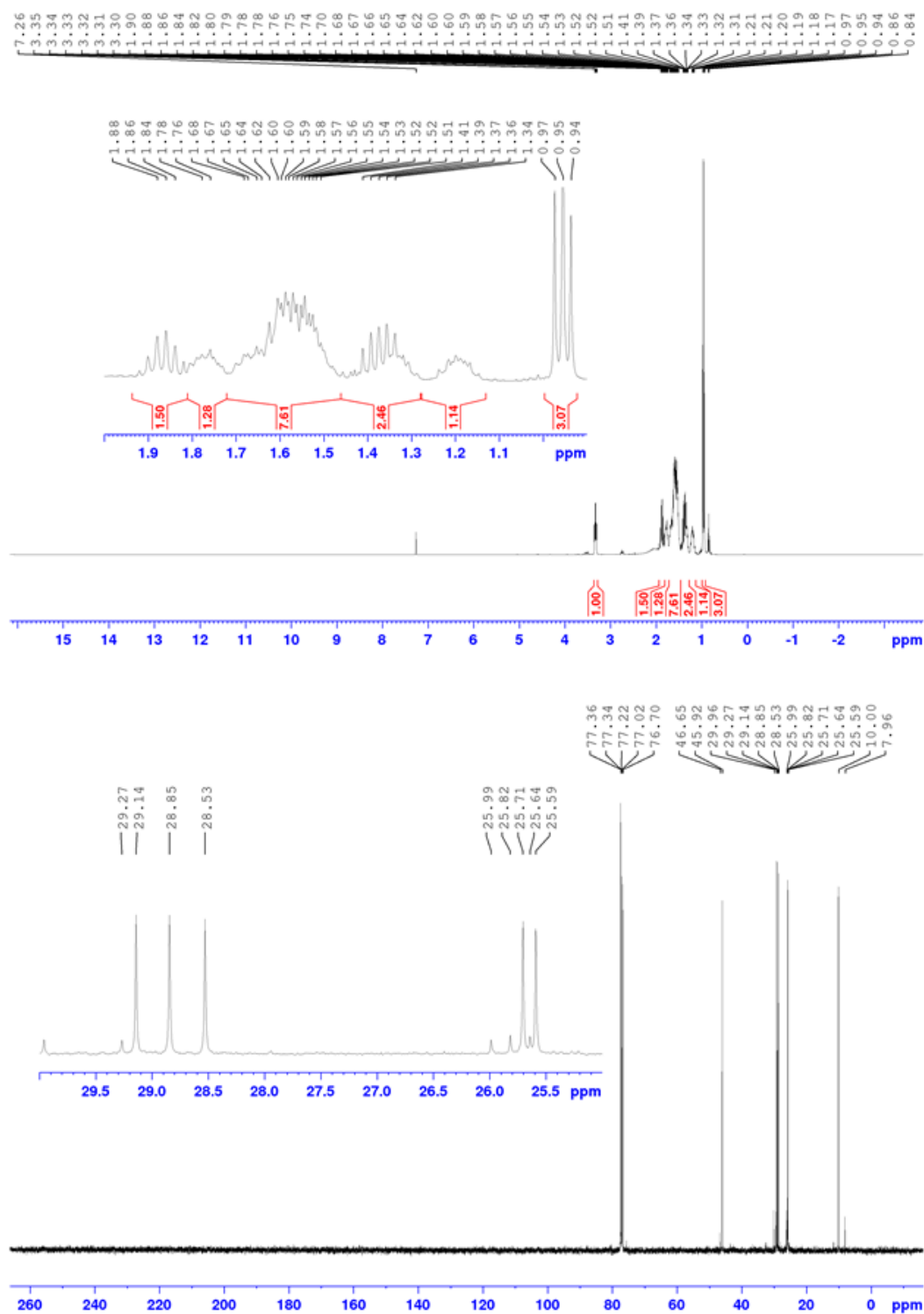


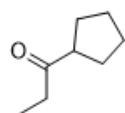
29v



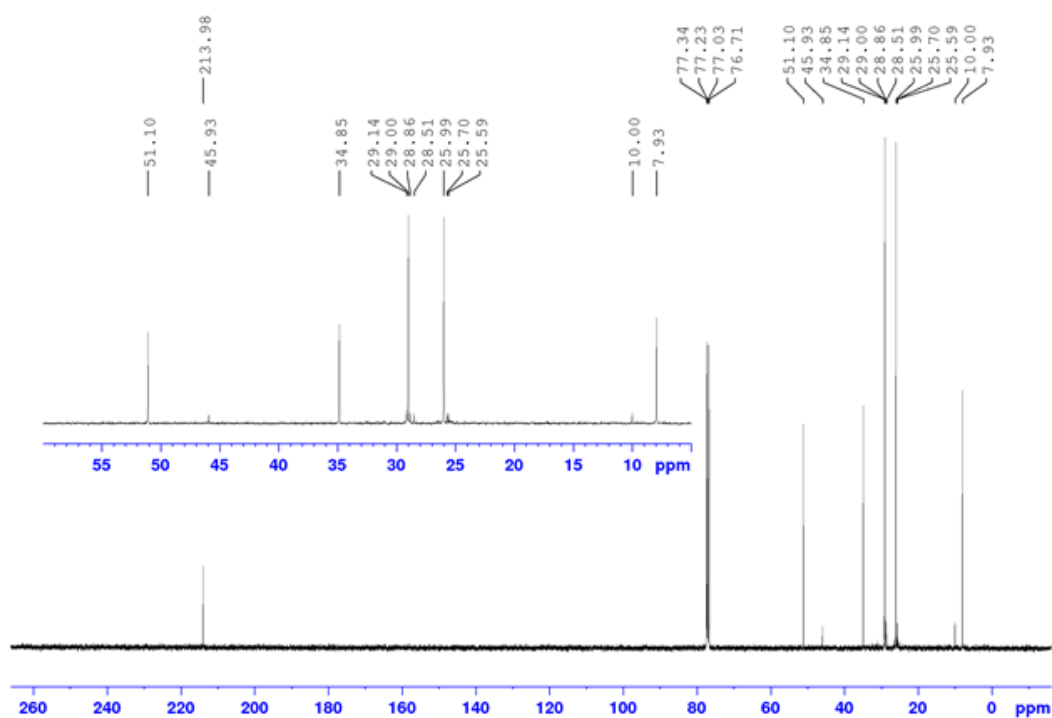
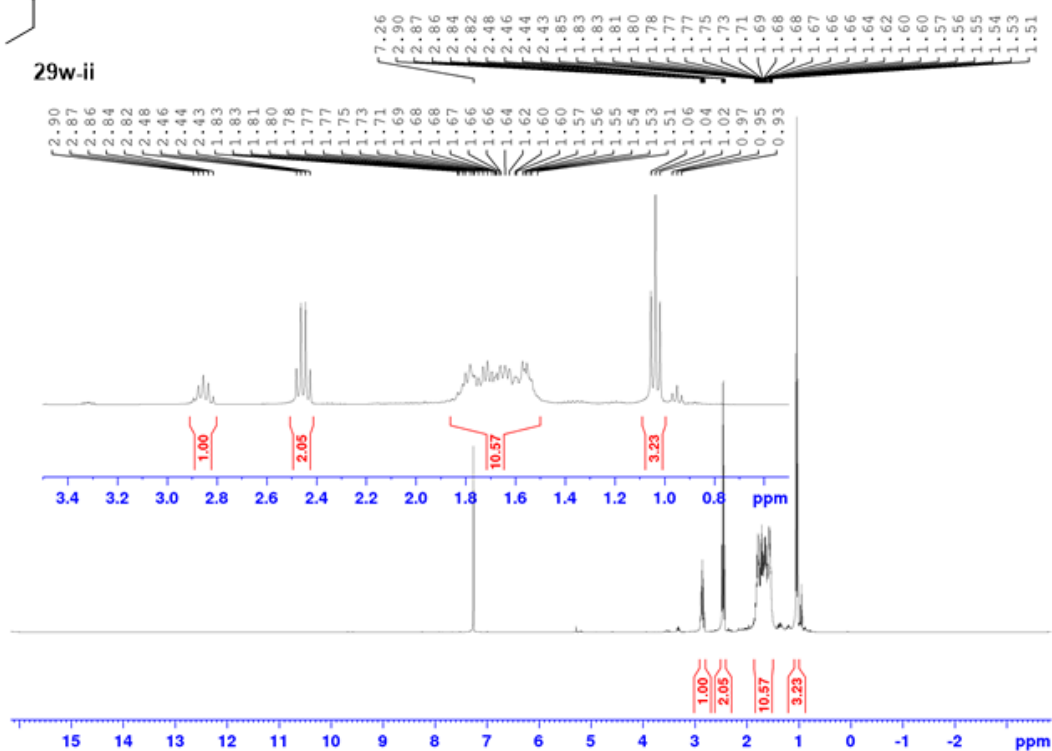


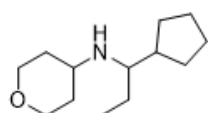
29w-i



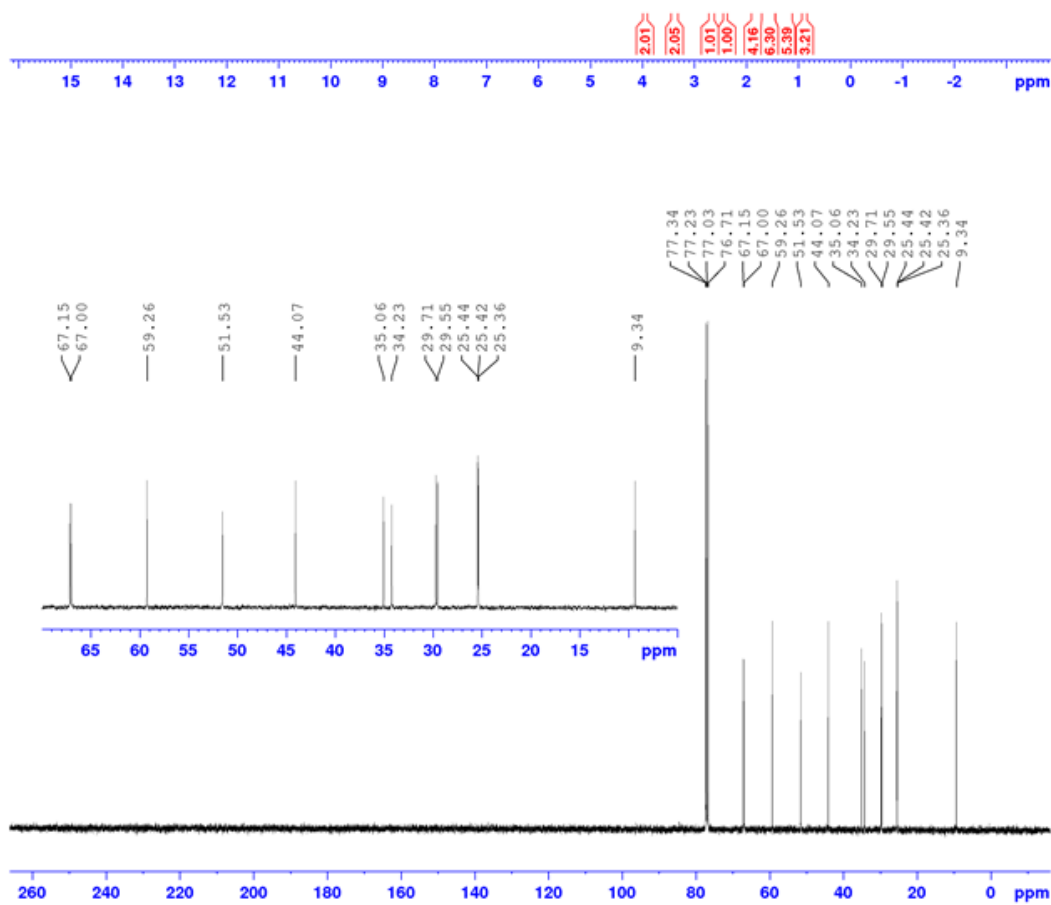
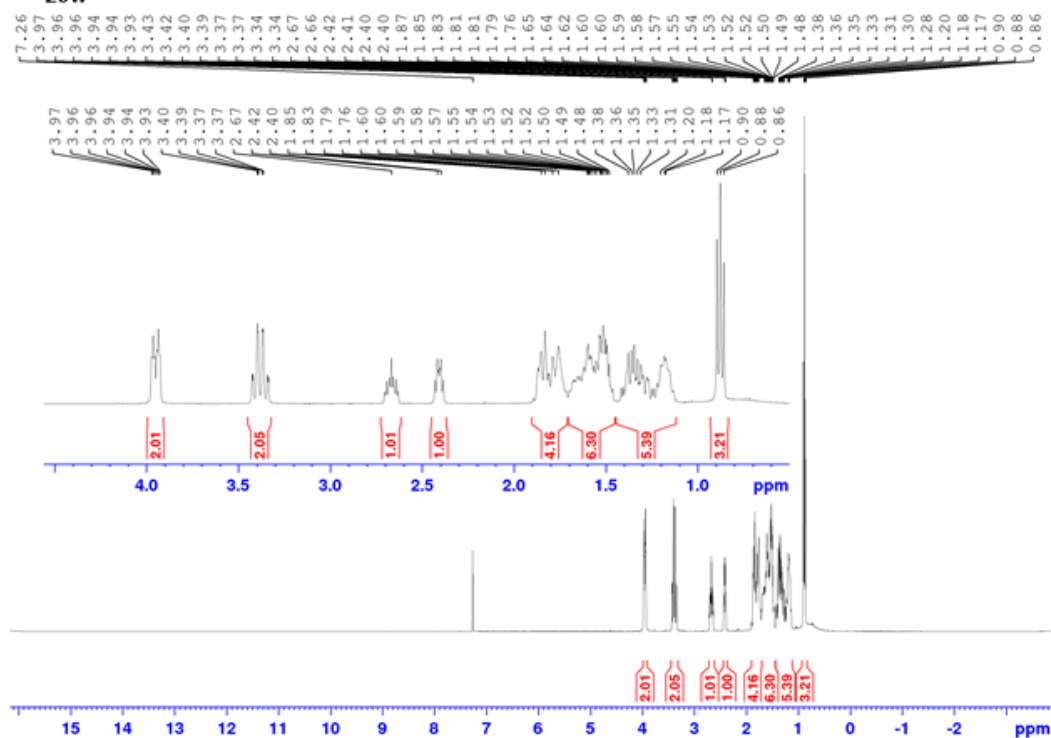


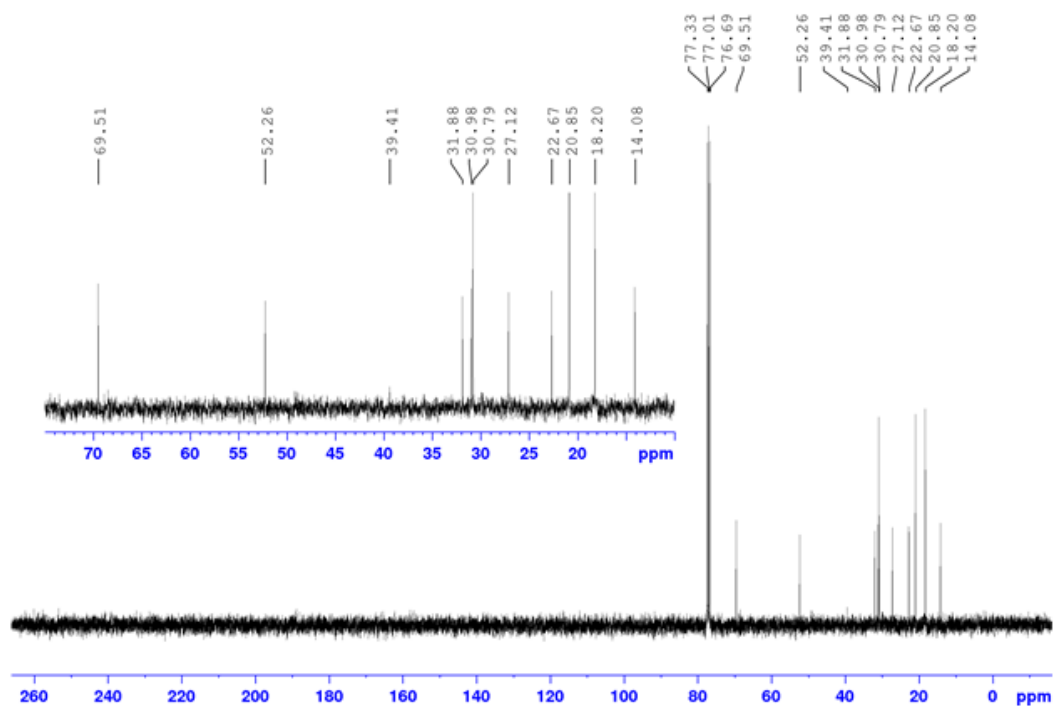
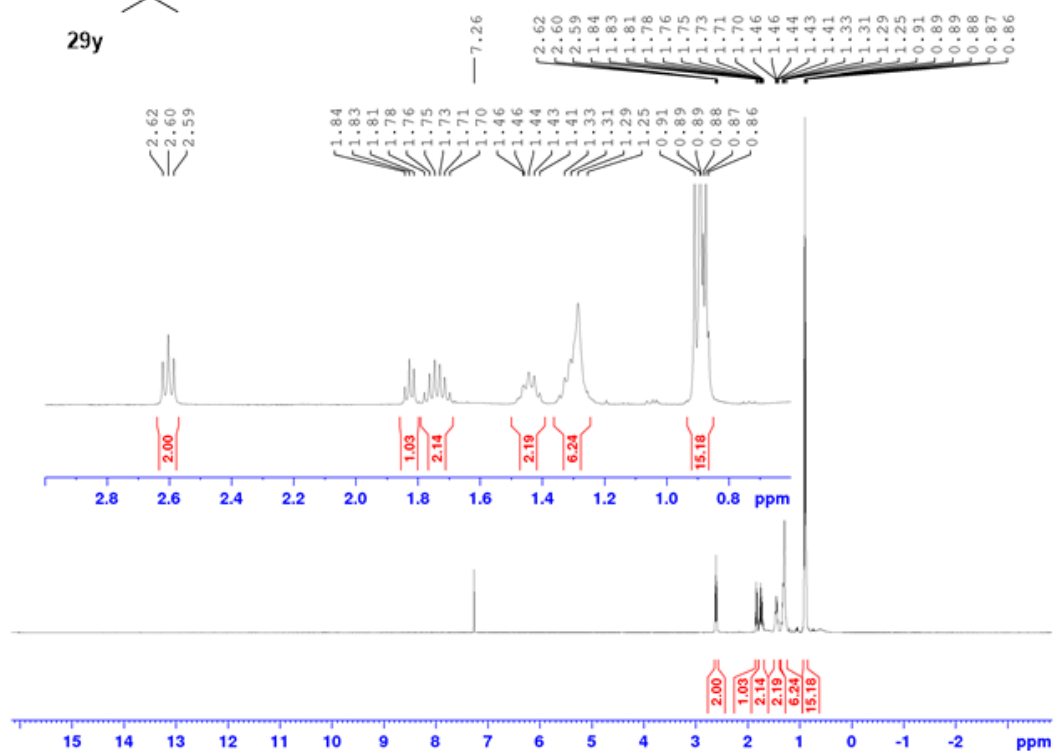
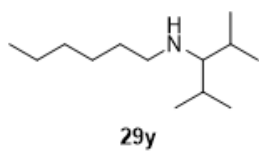
29w-ii

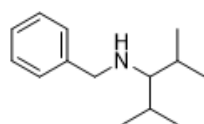




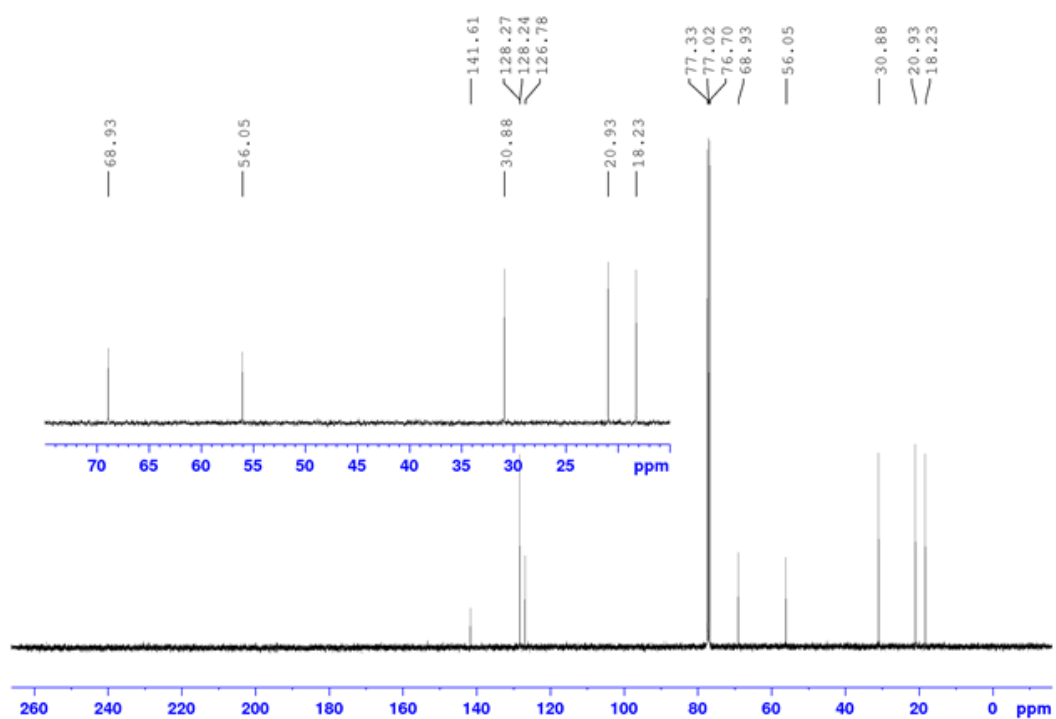
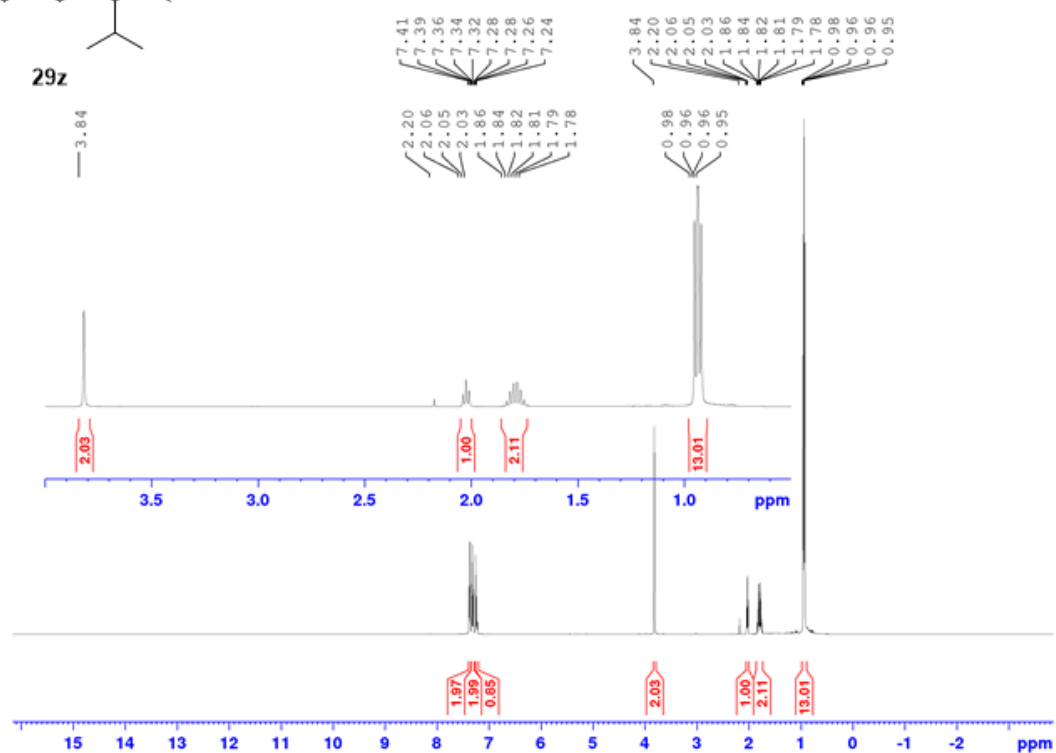
29w

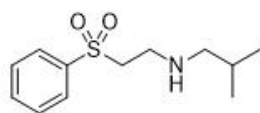




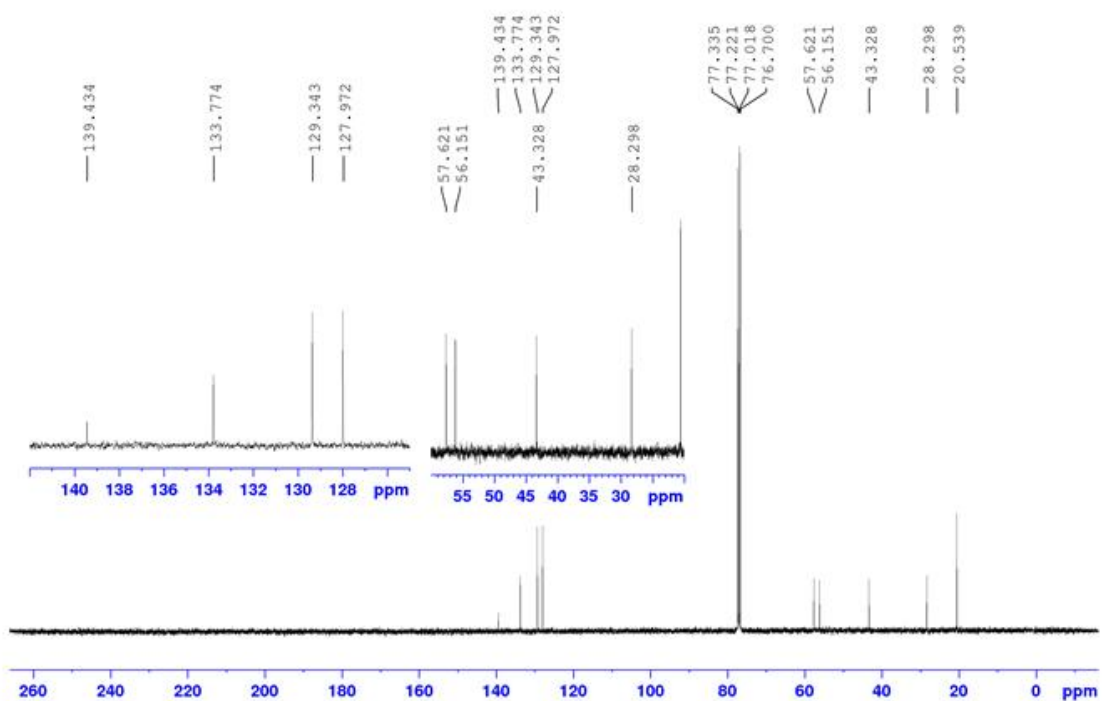
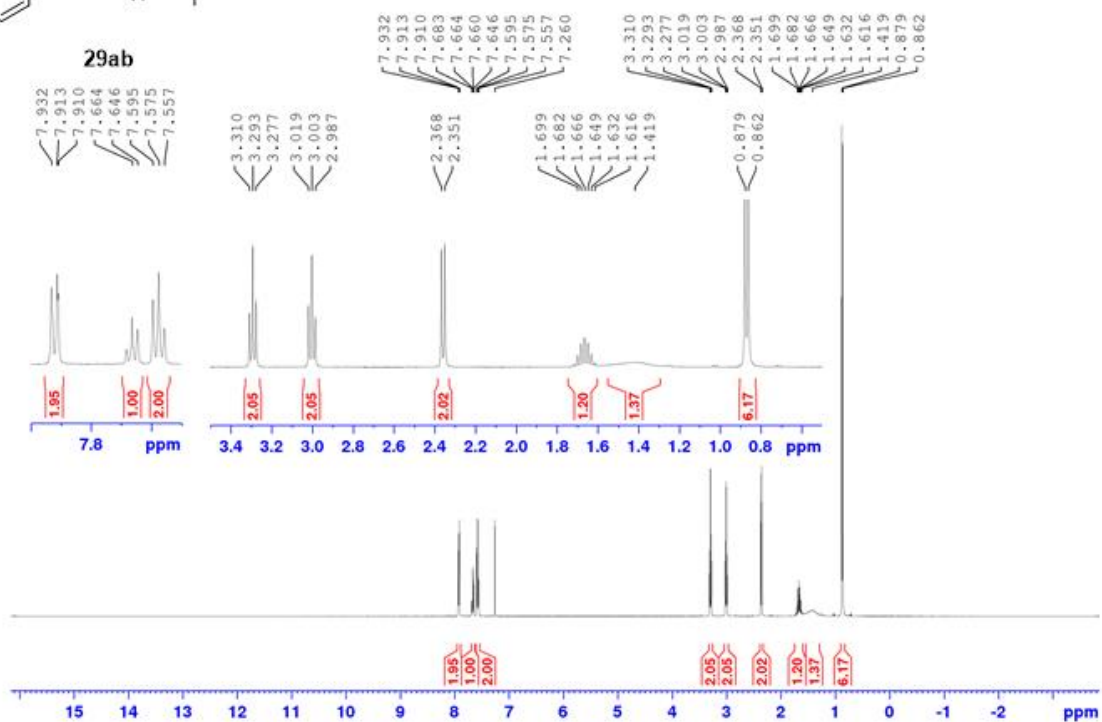


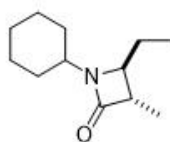
29z



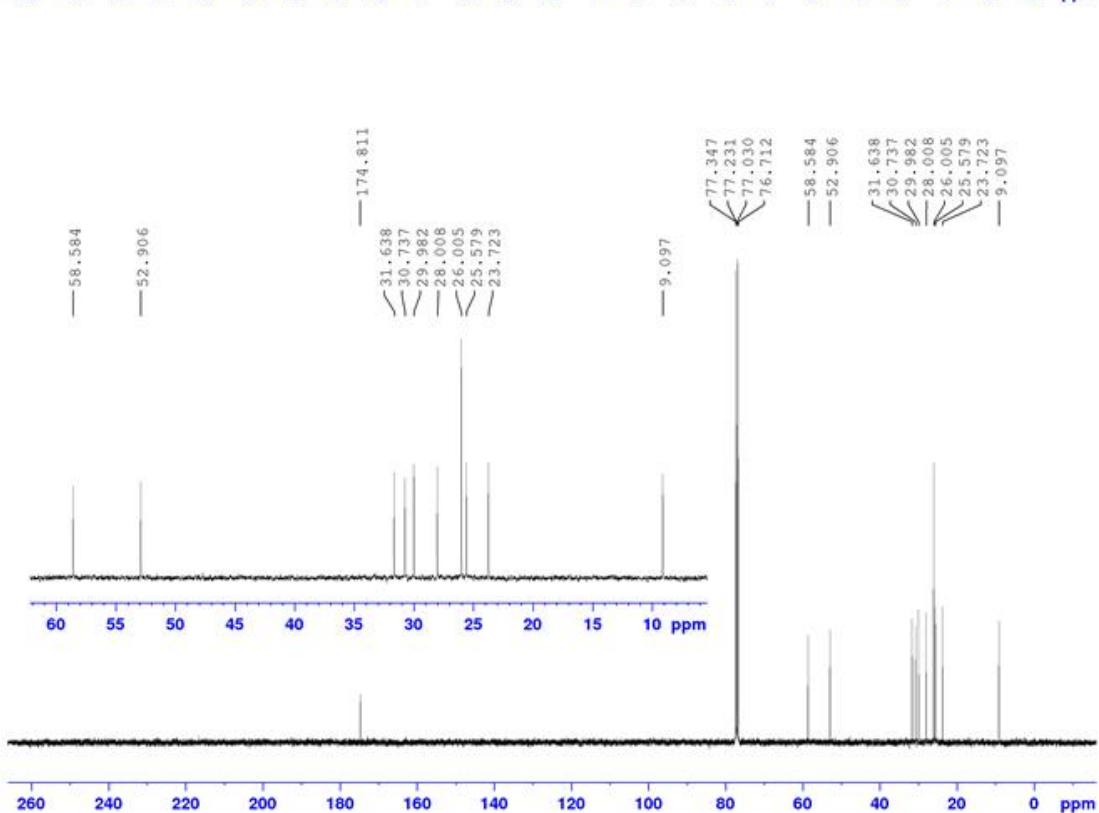
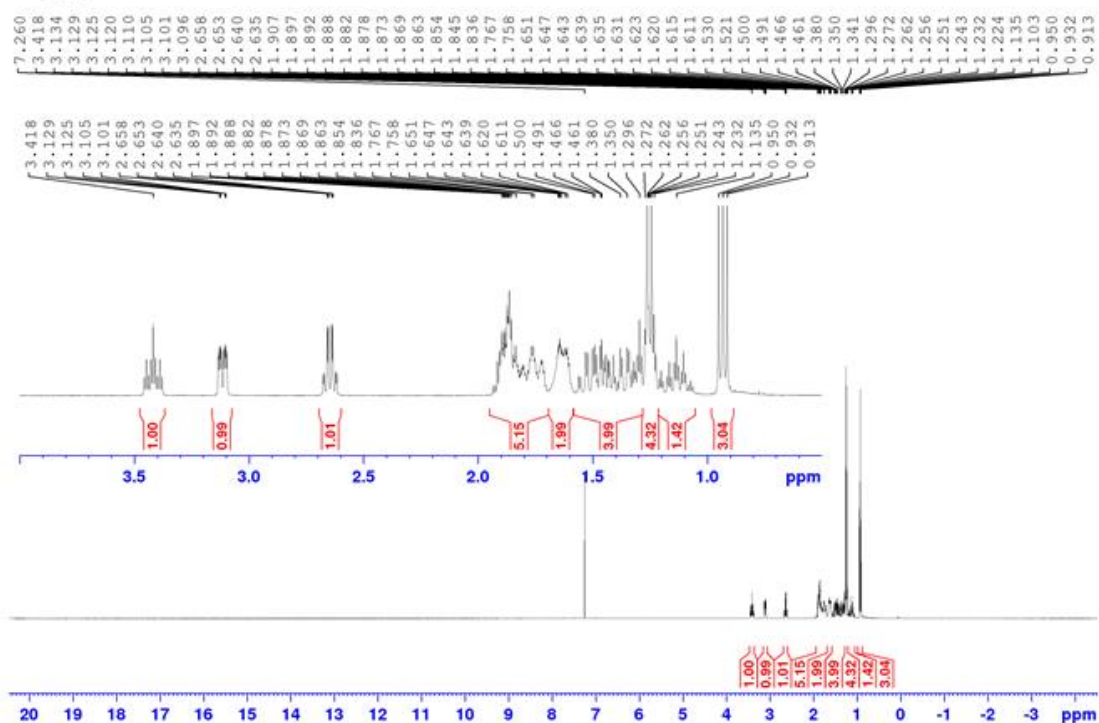


29ab



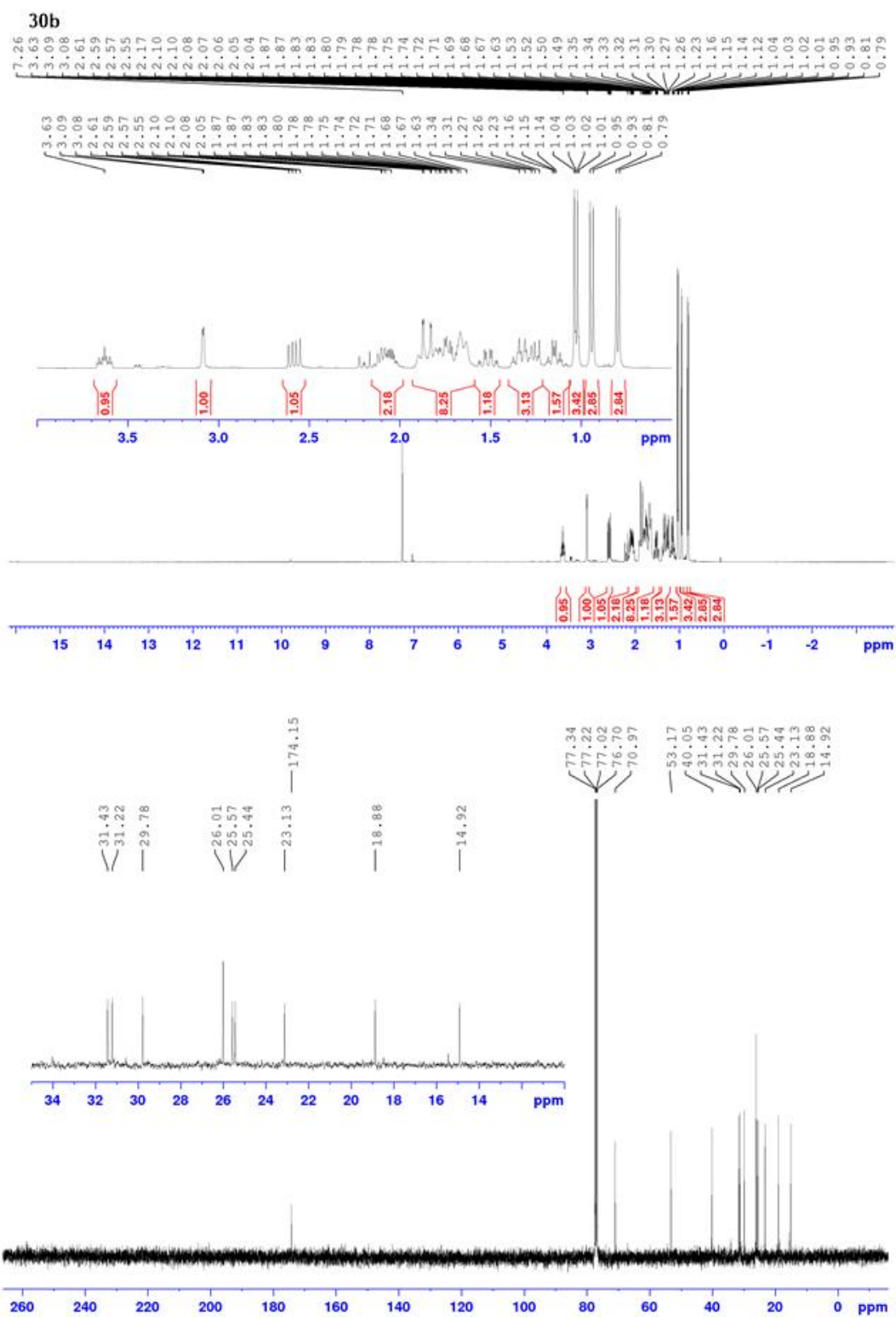
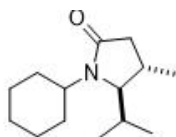


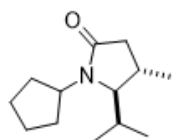
27ai



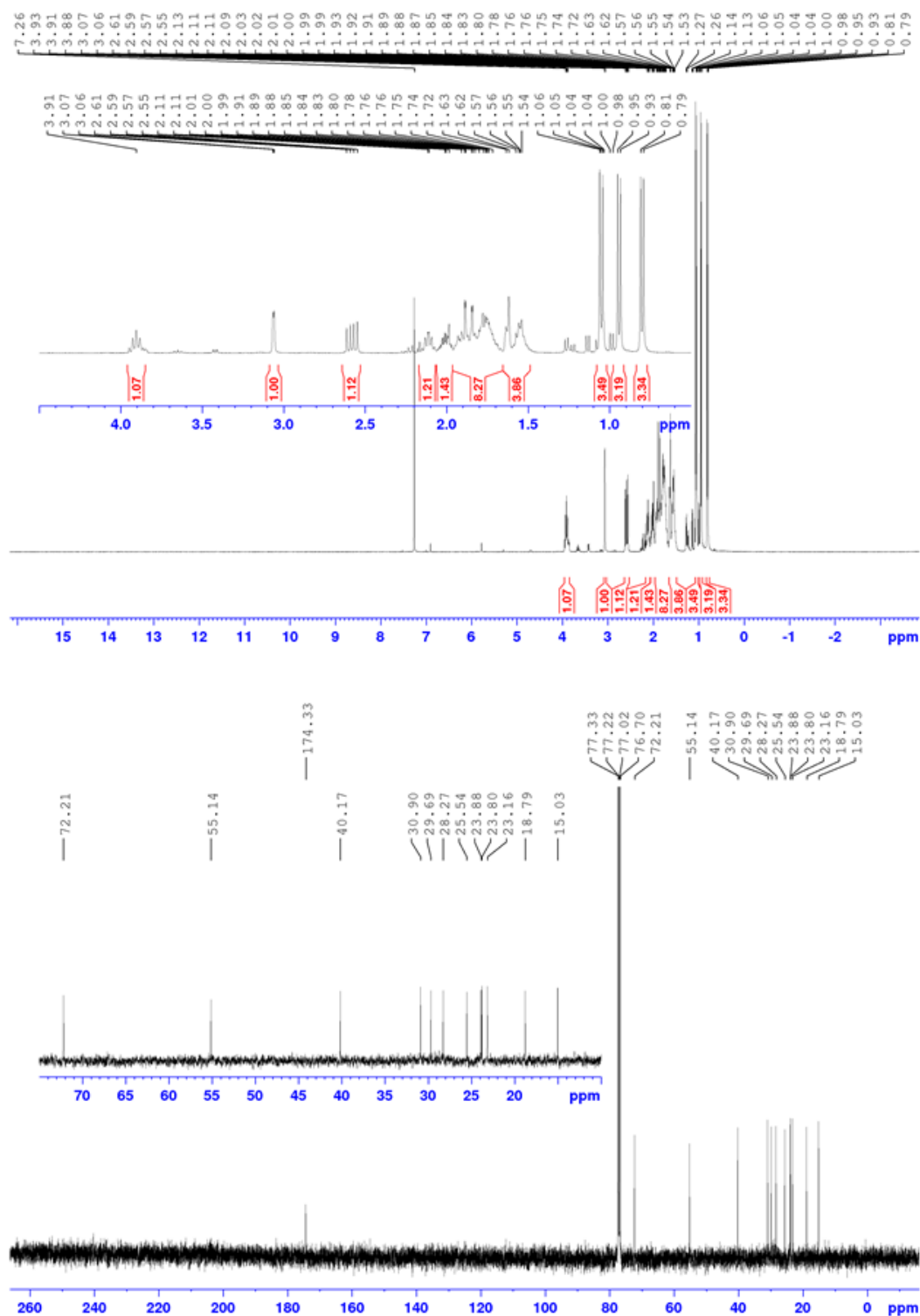


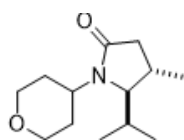




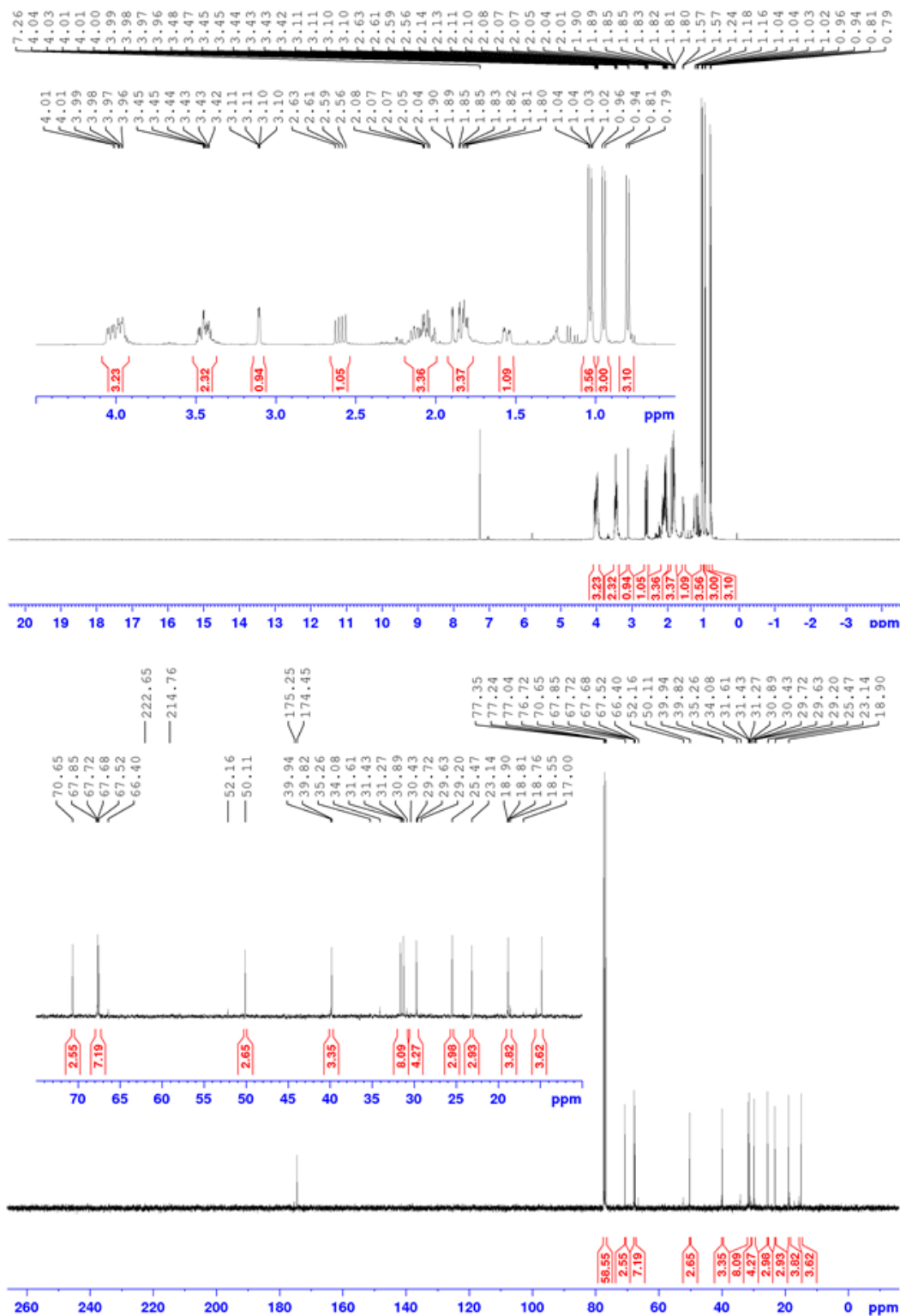


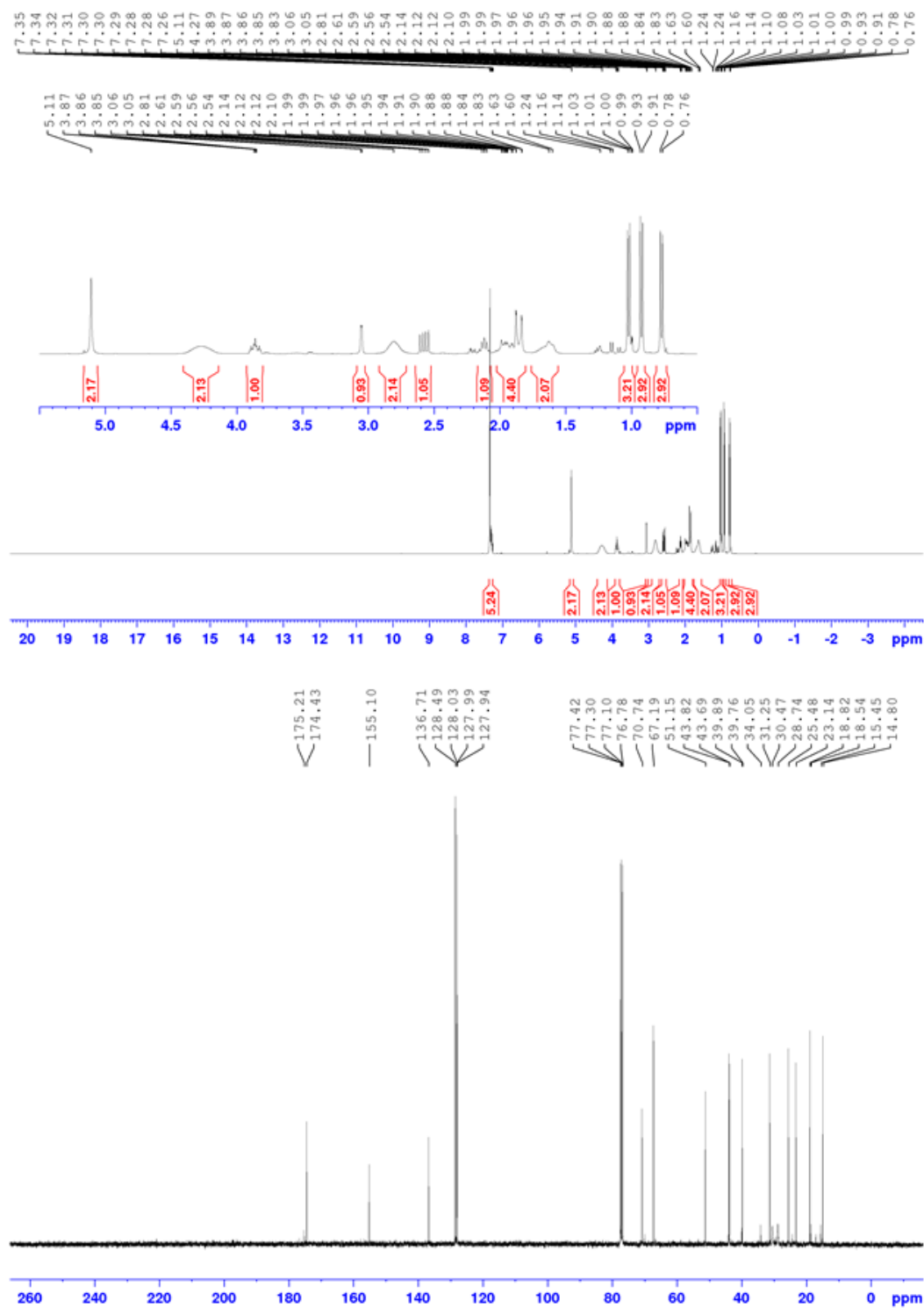
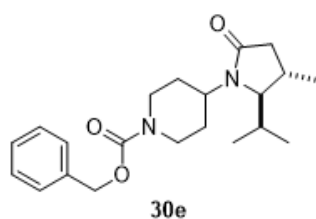
30c

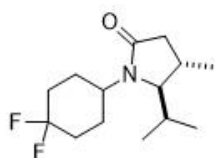




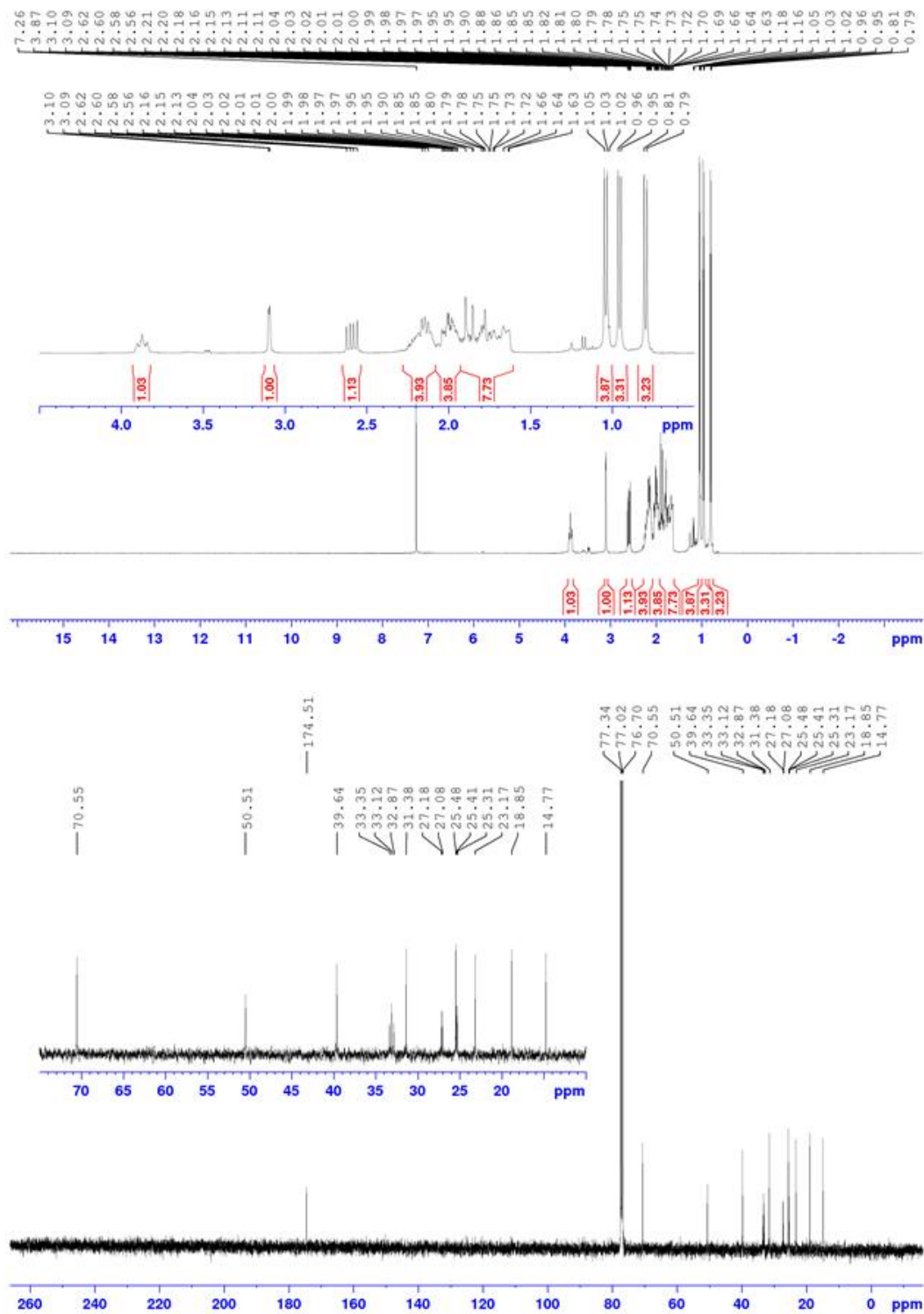
30d

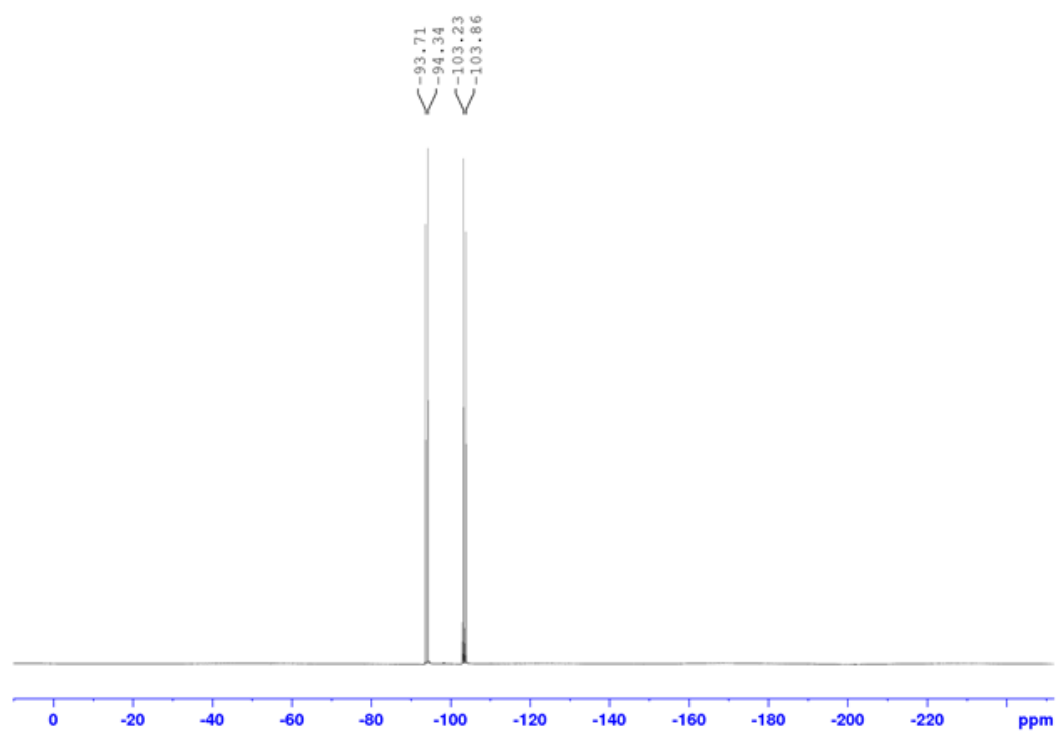
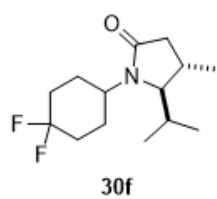


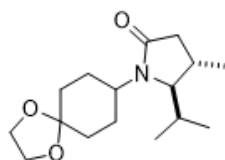




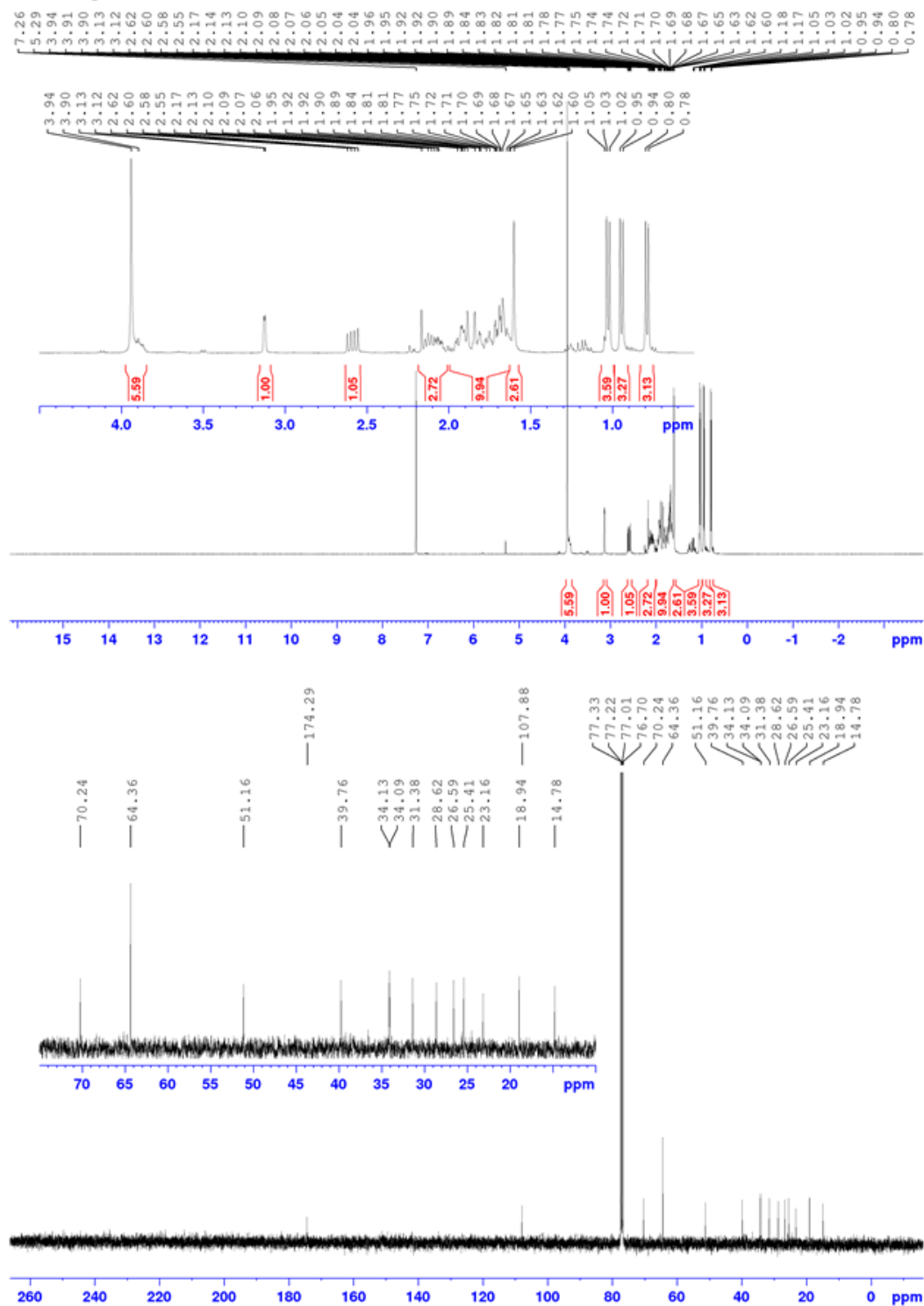
30f

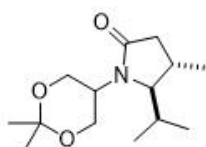




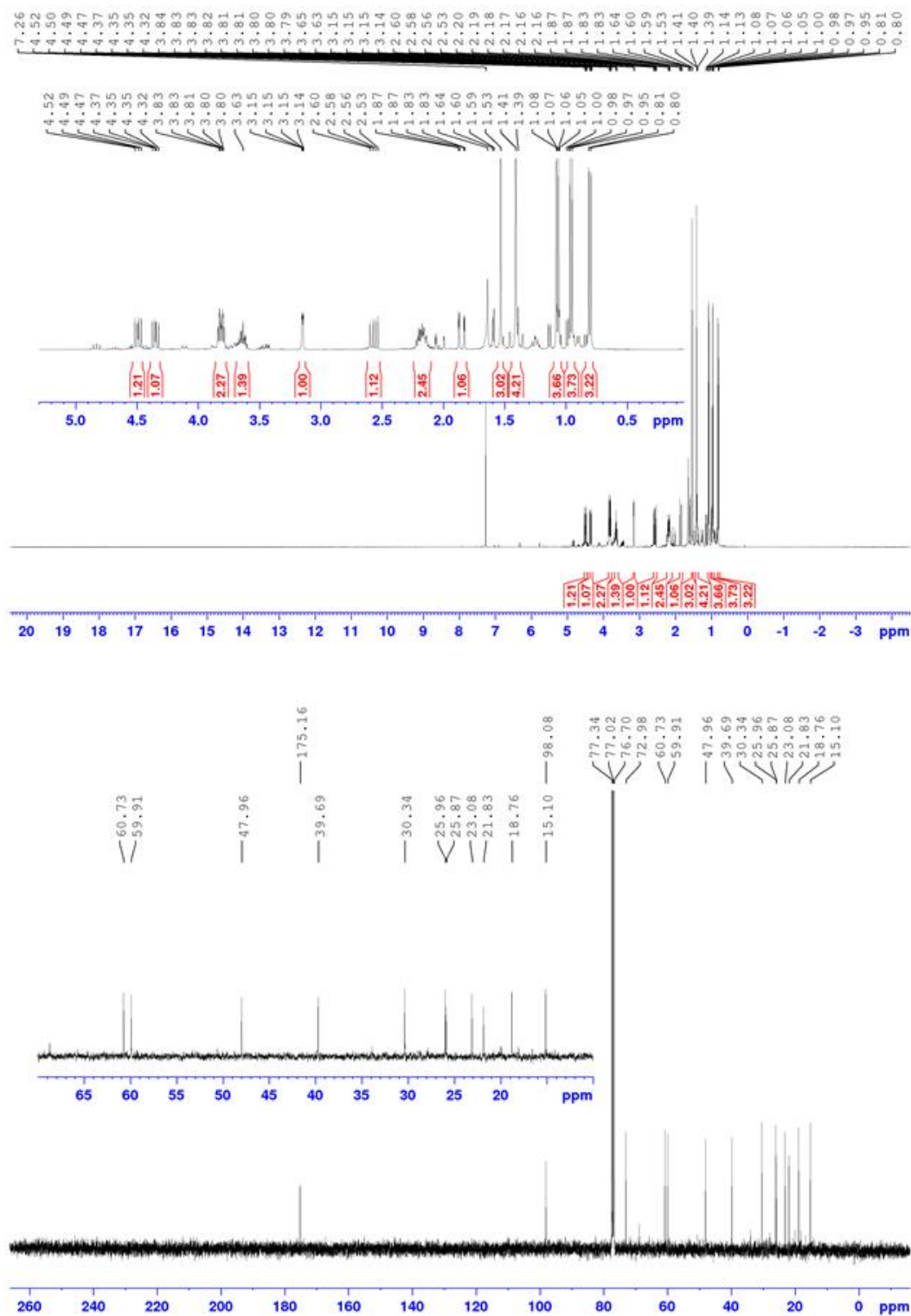


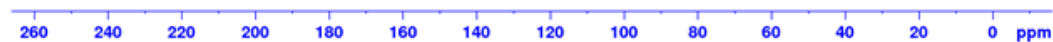
30g

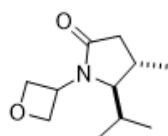




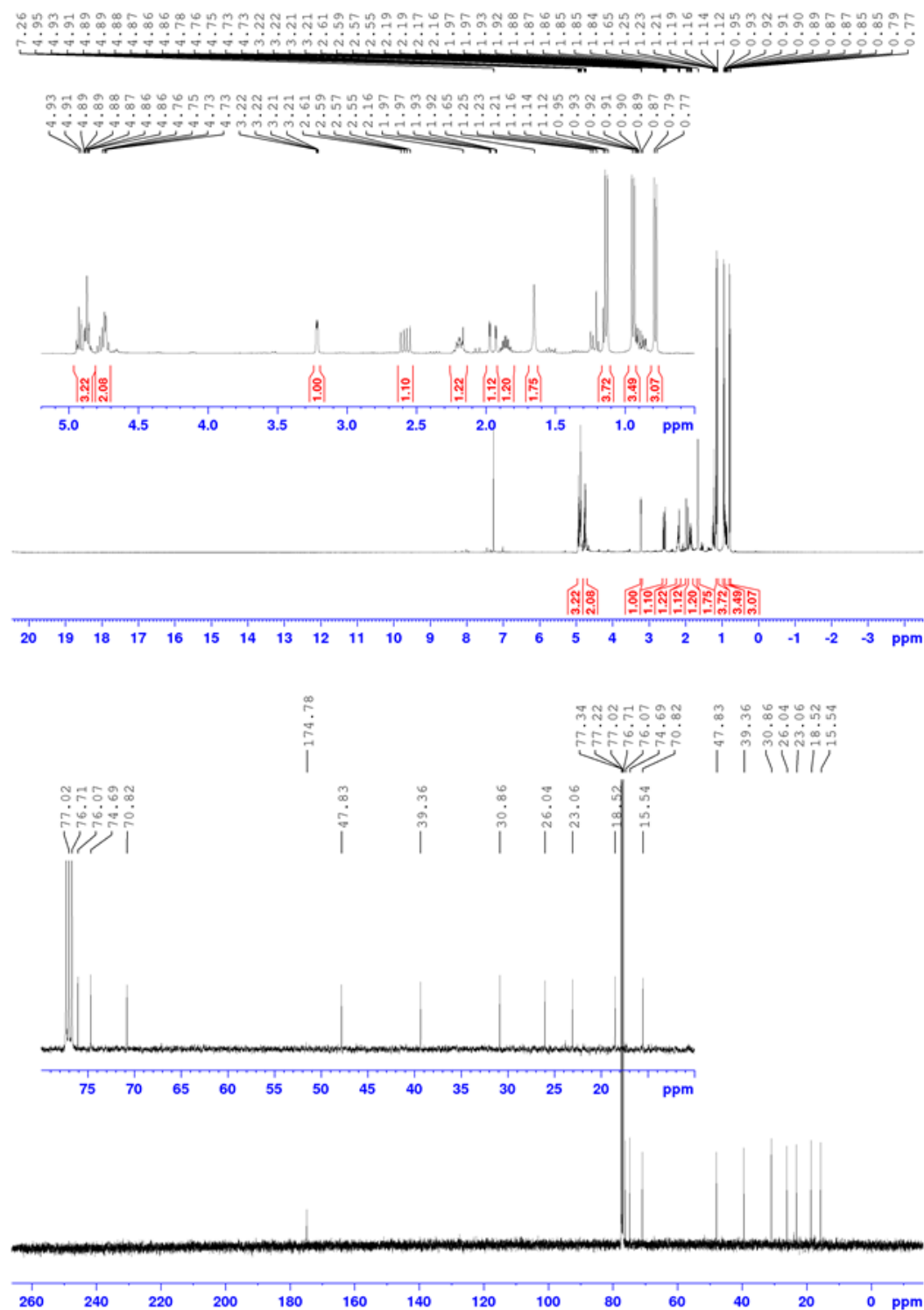
30h



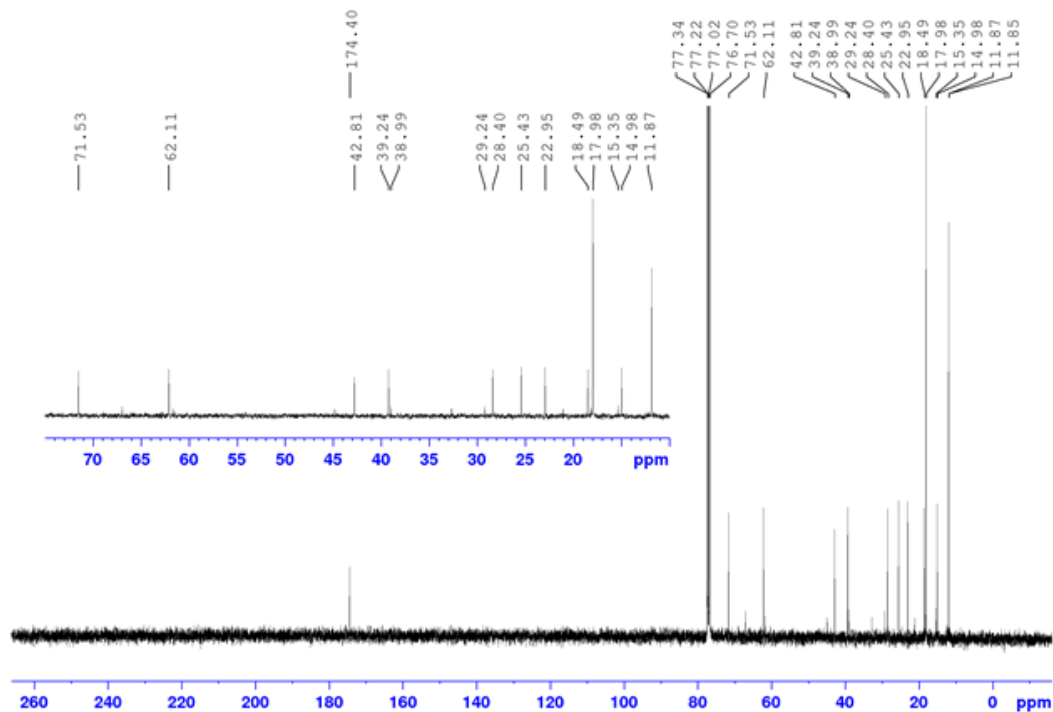
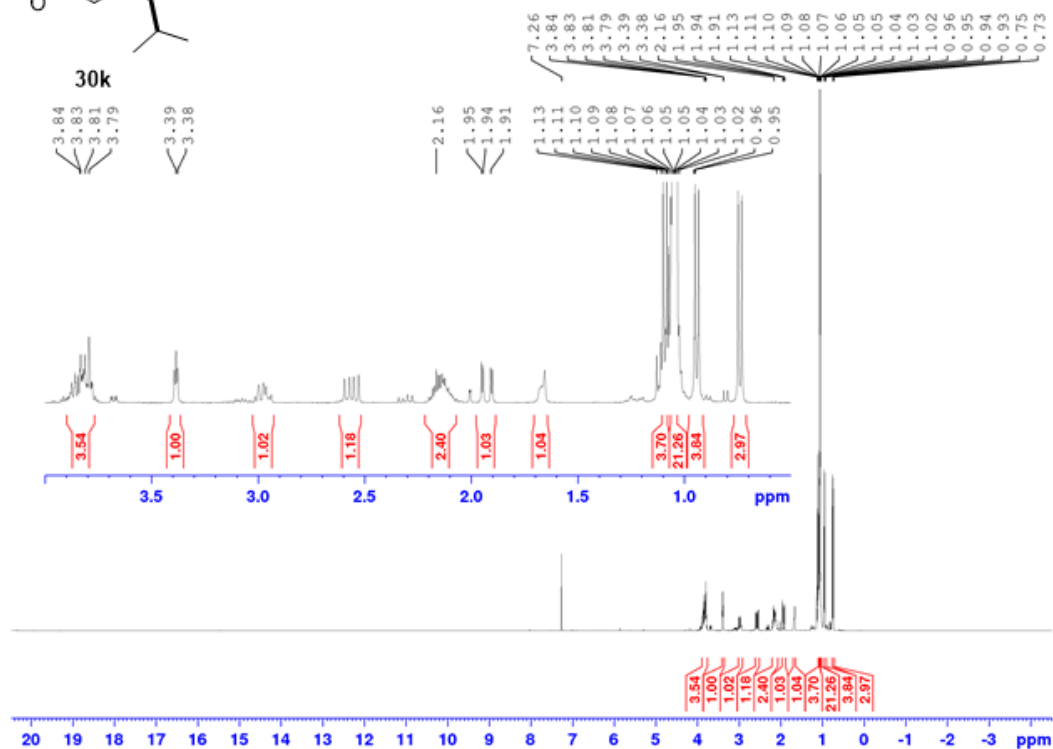




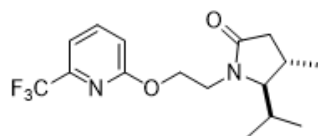
30j



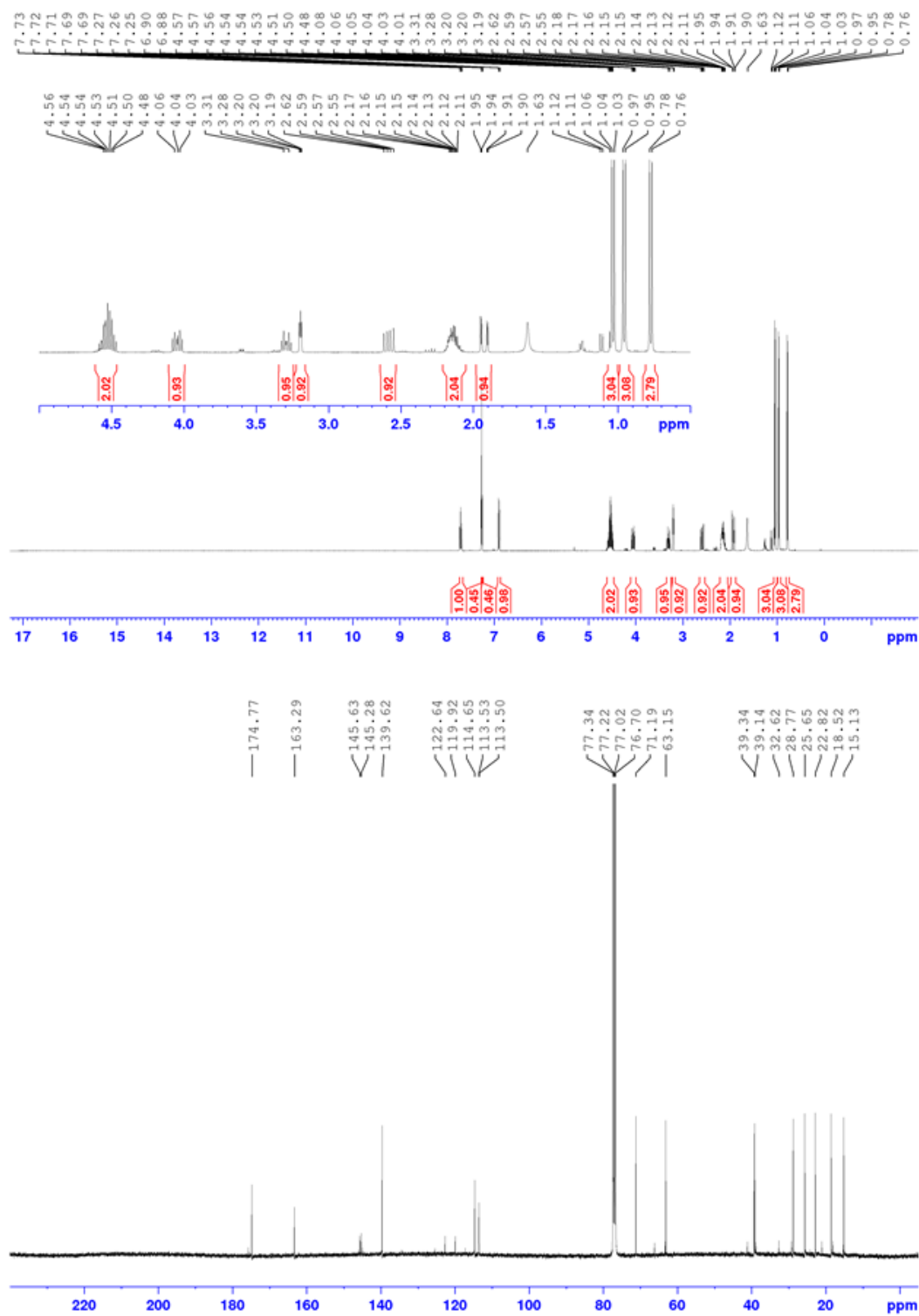
30k

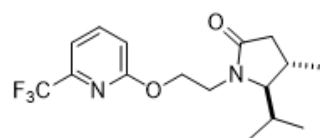




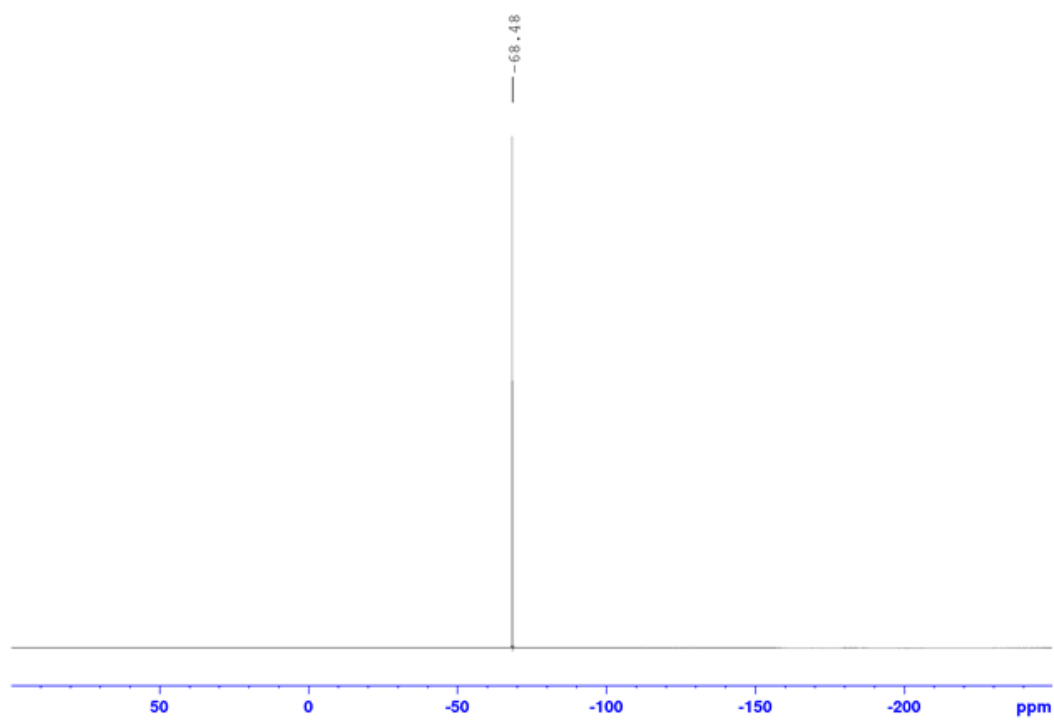


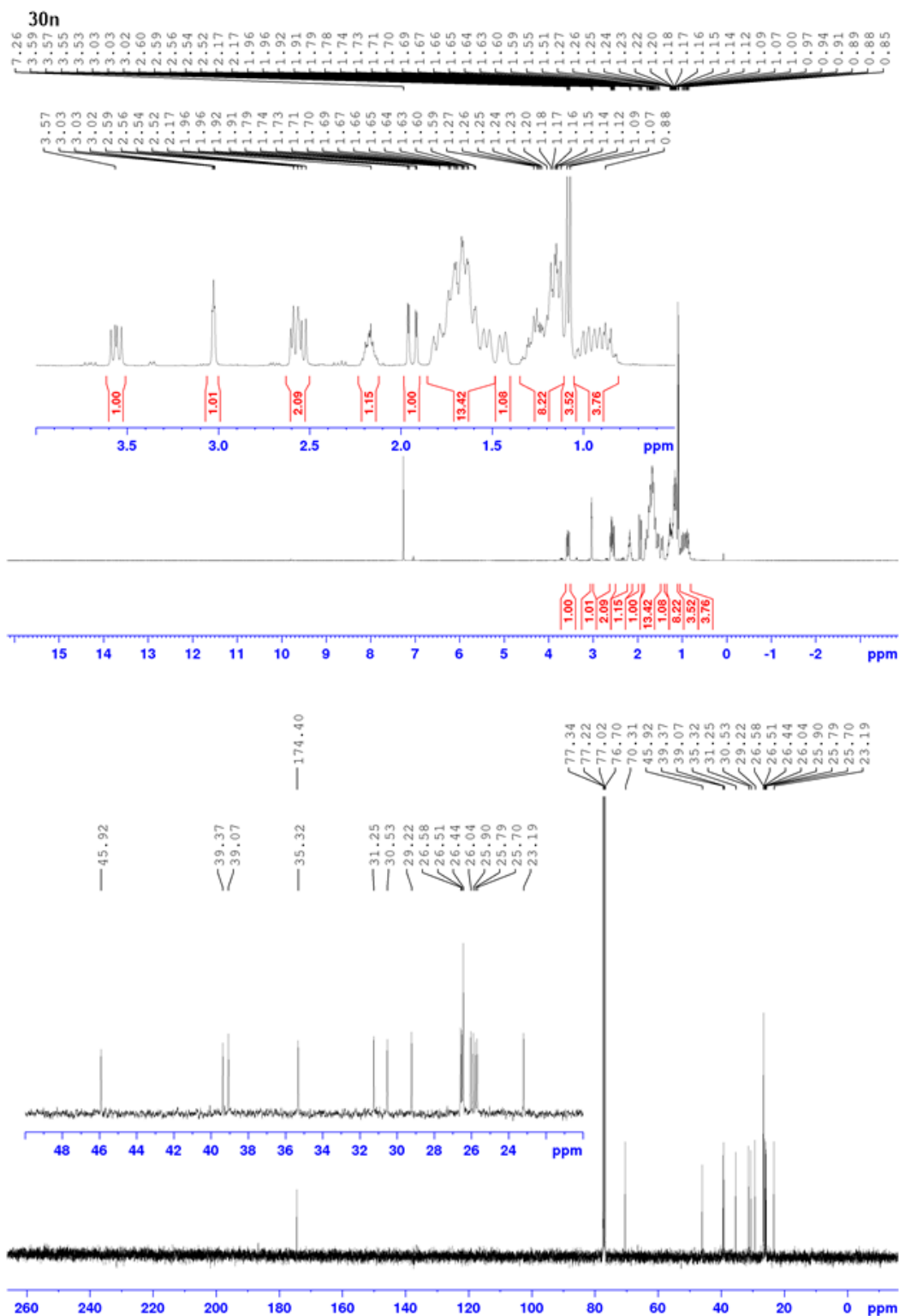
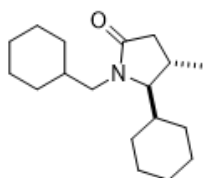
30m

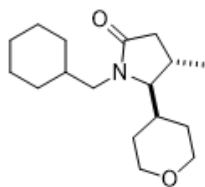




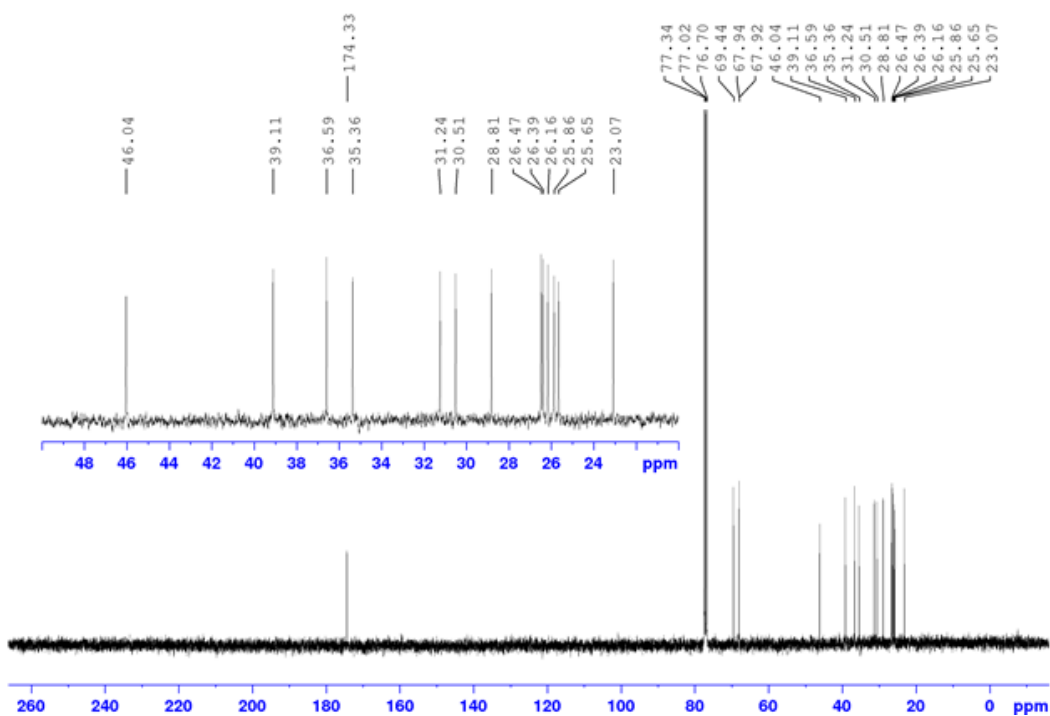
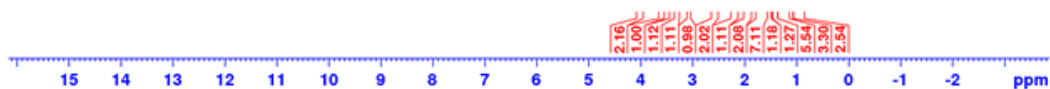
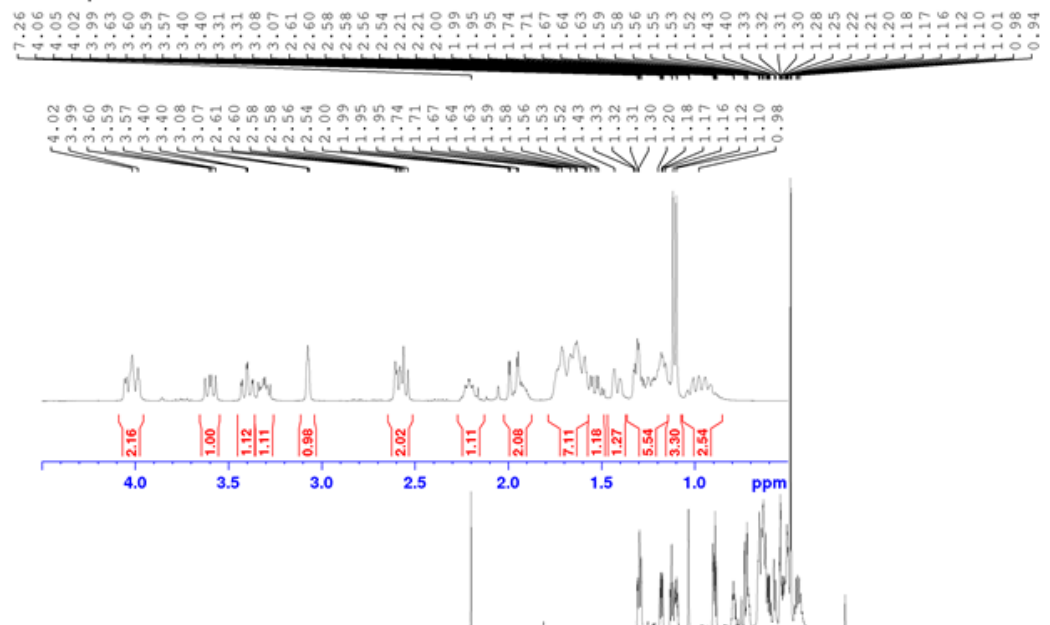
30m

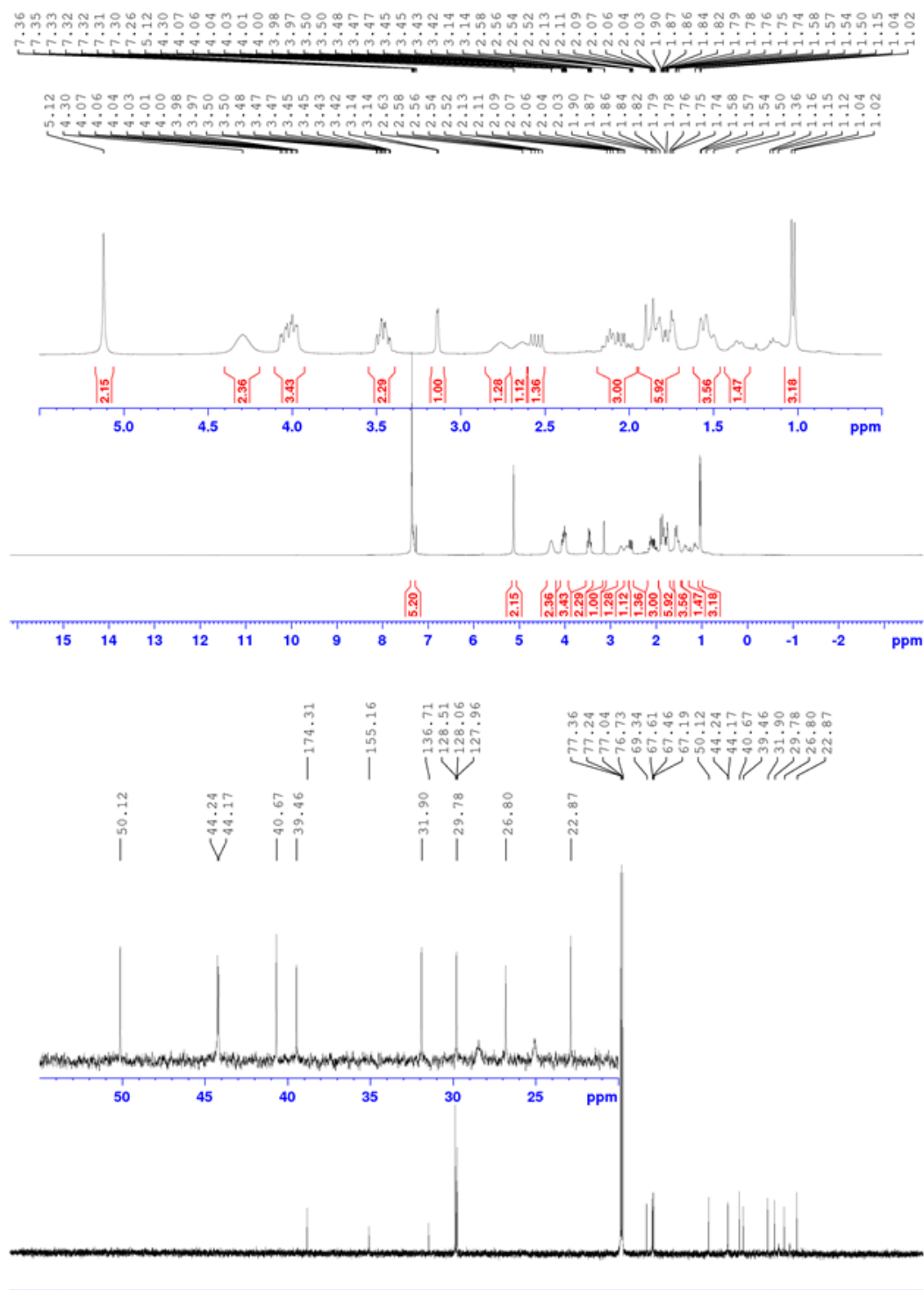
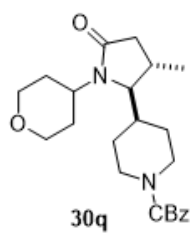




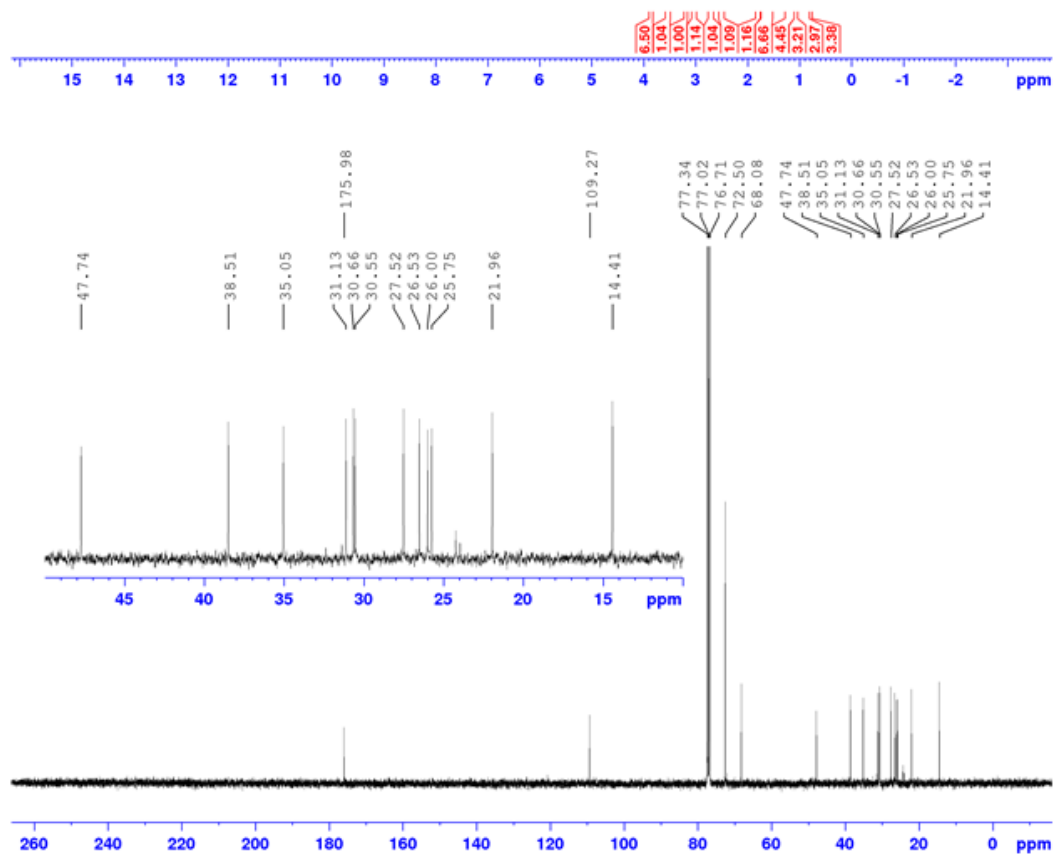
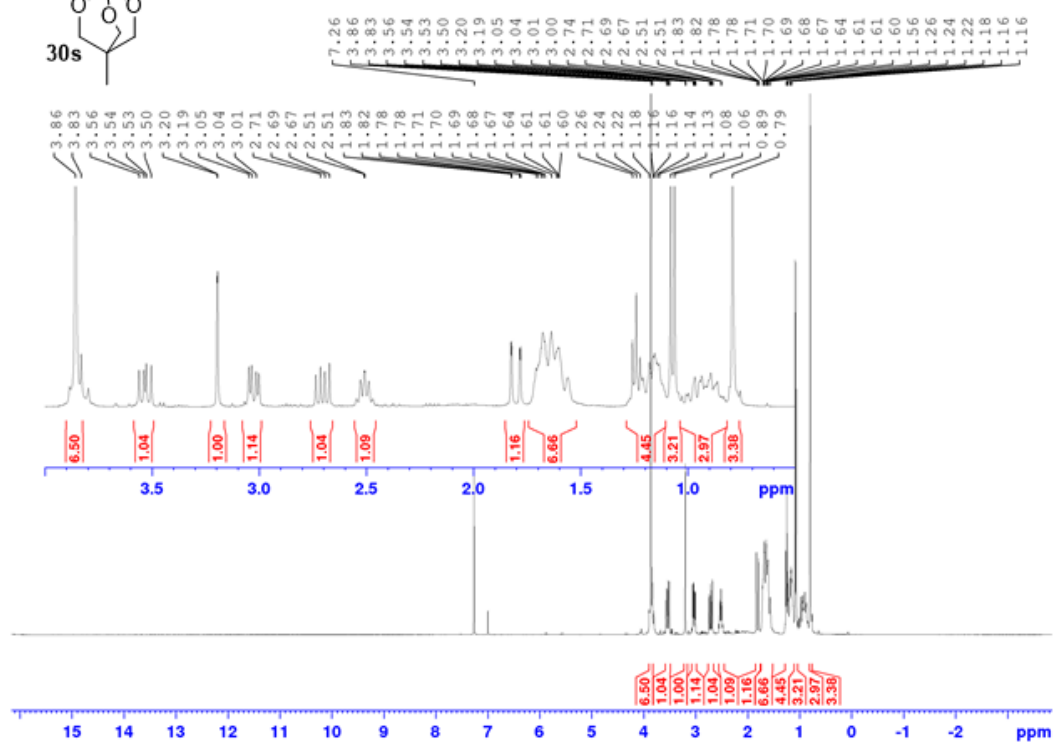
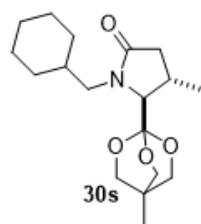


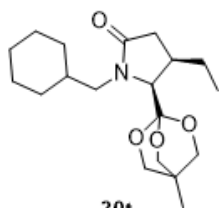
30p



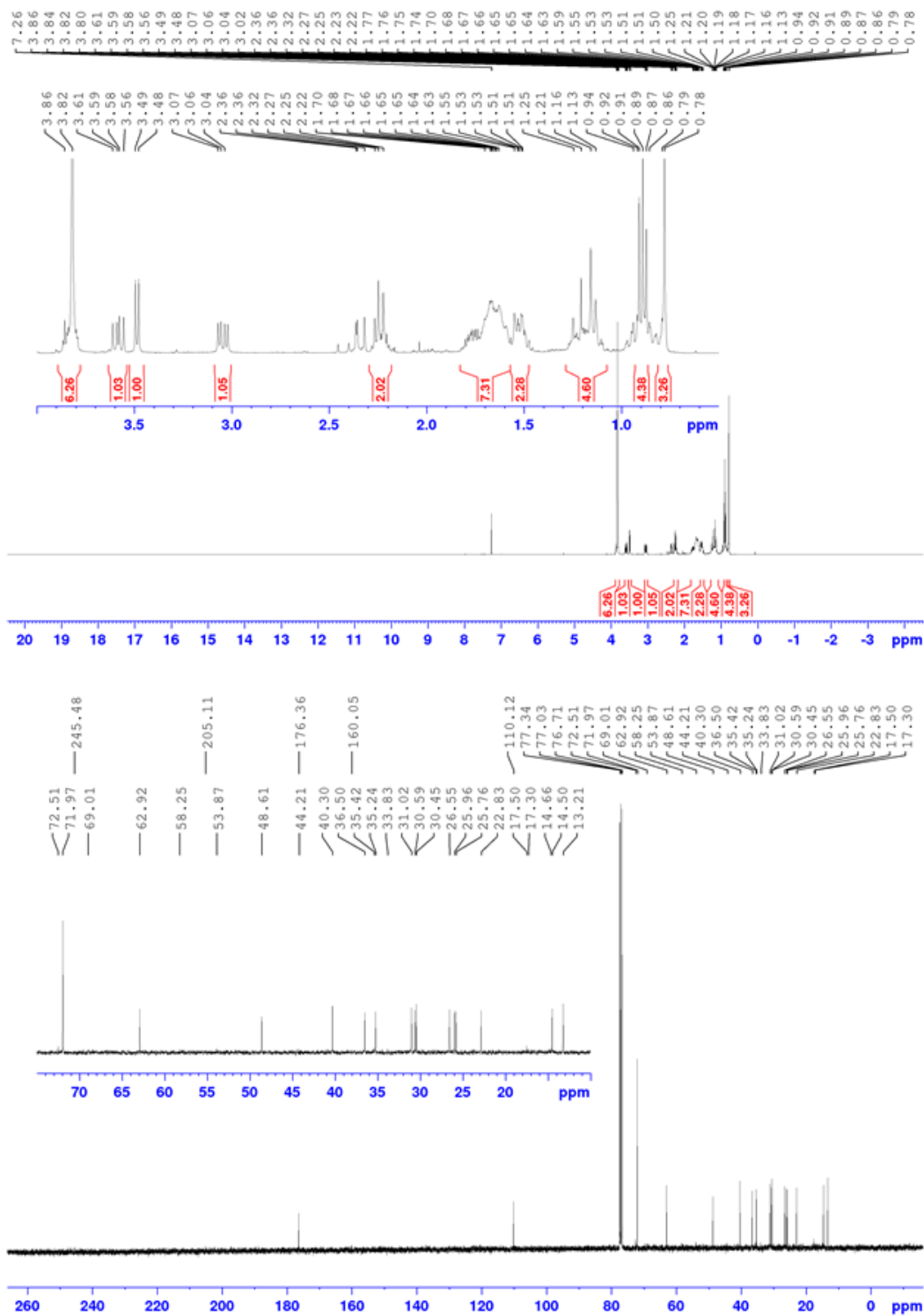


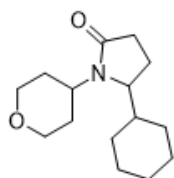




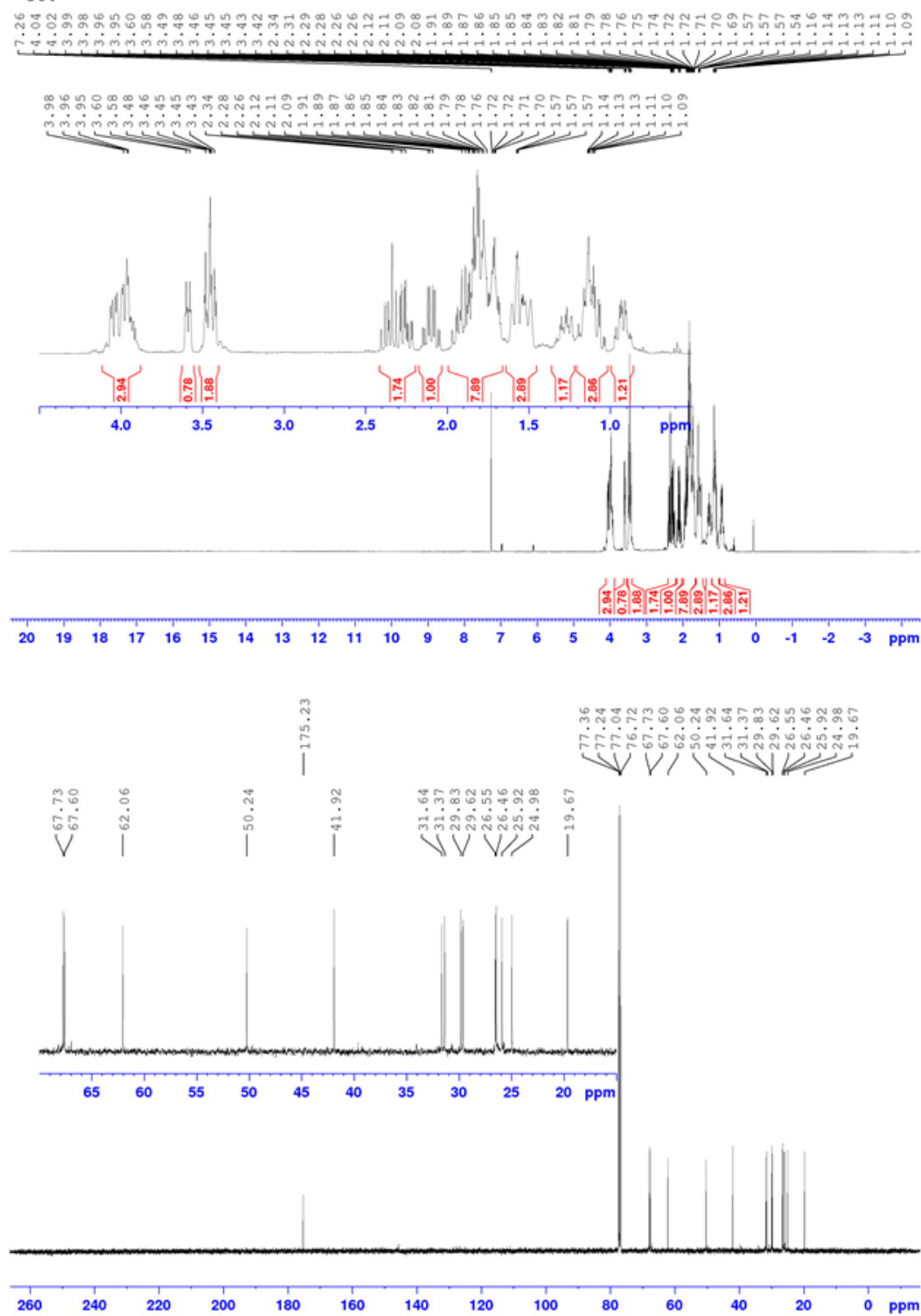


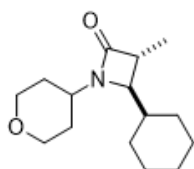
30t



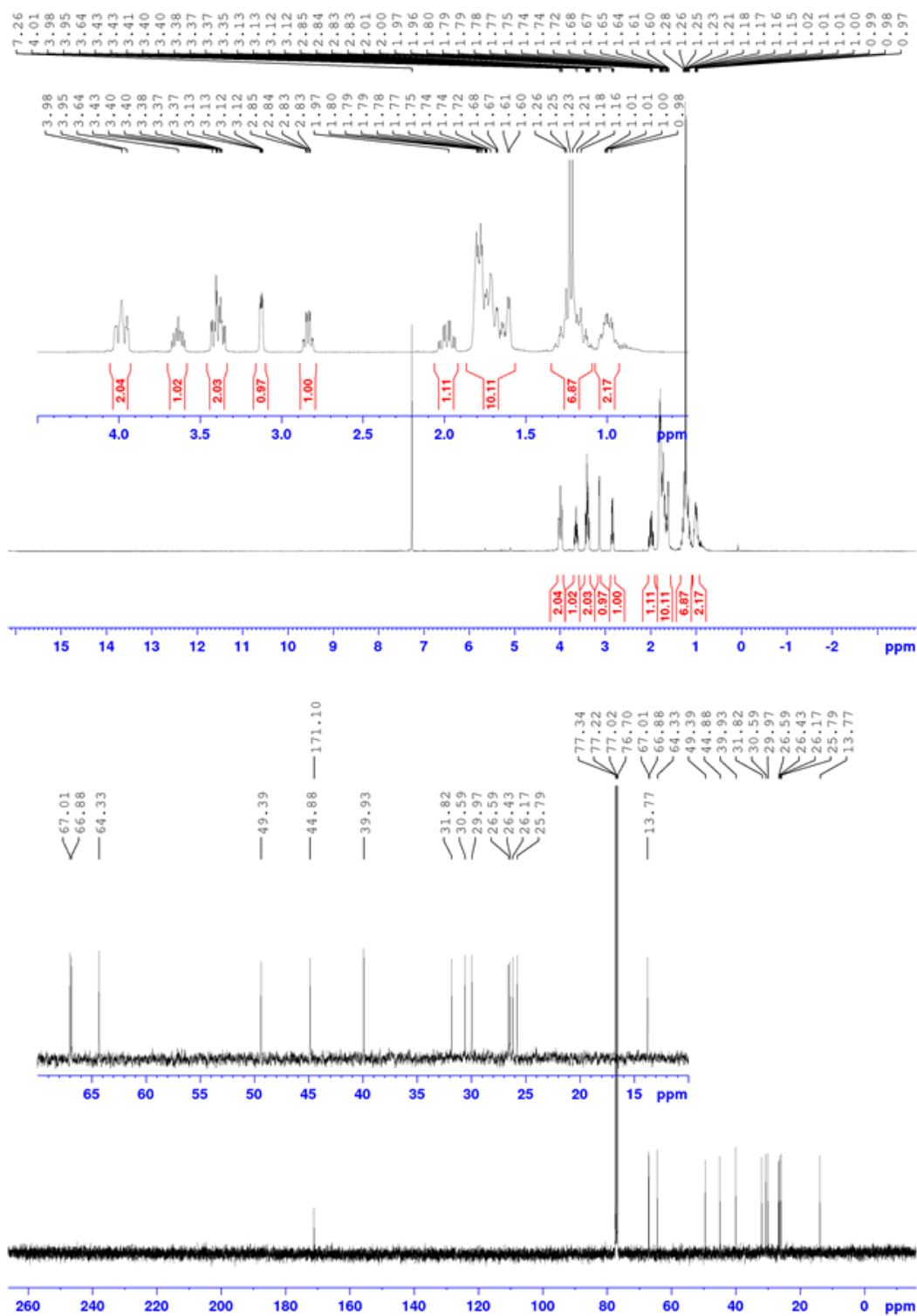


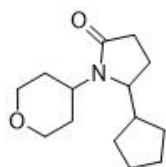
30v



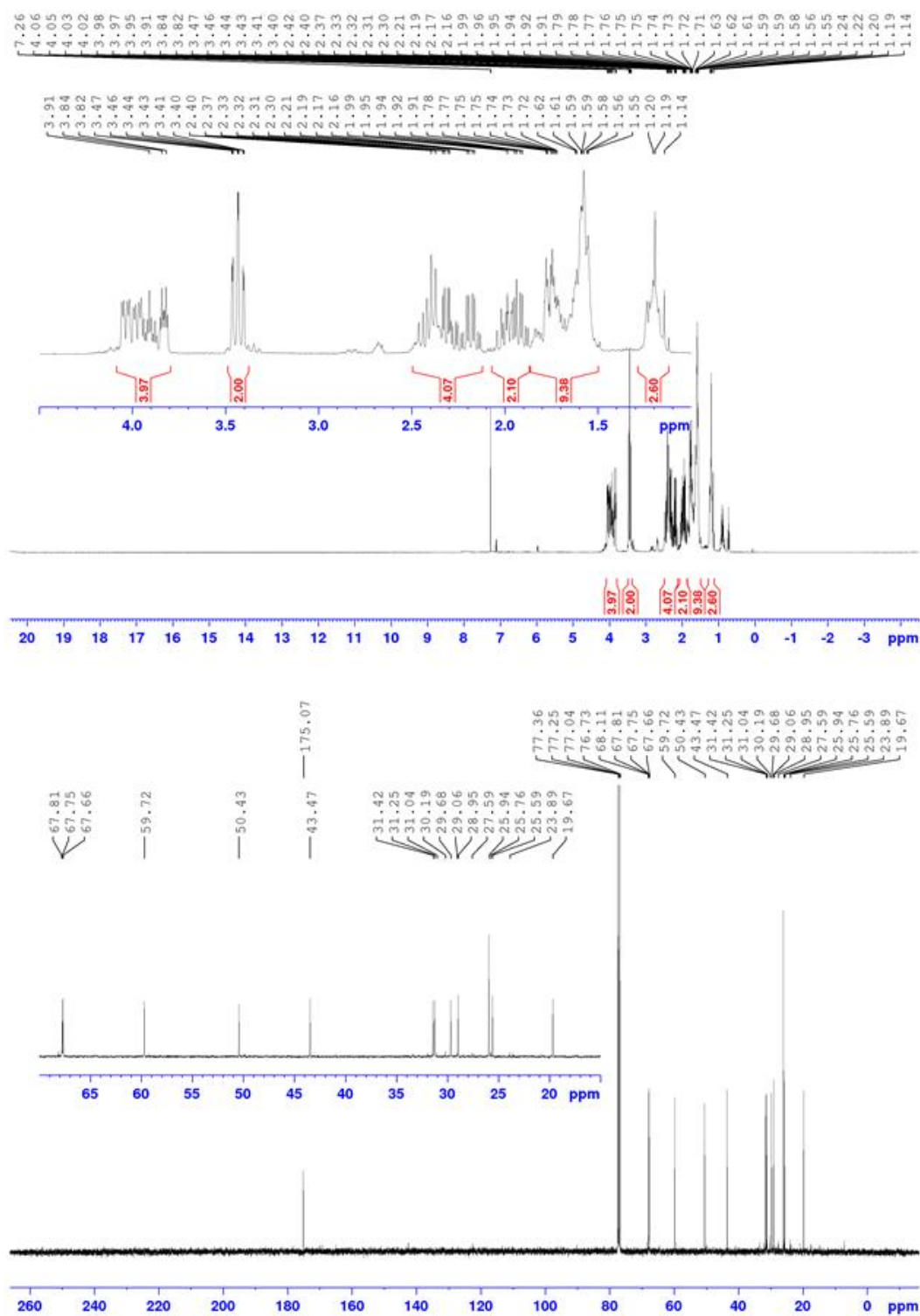


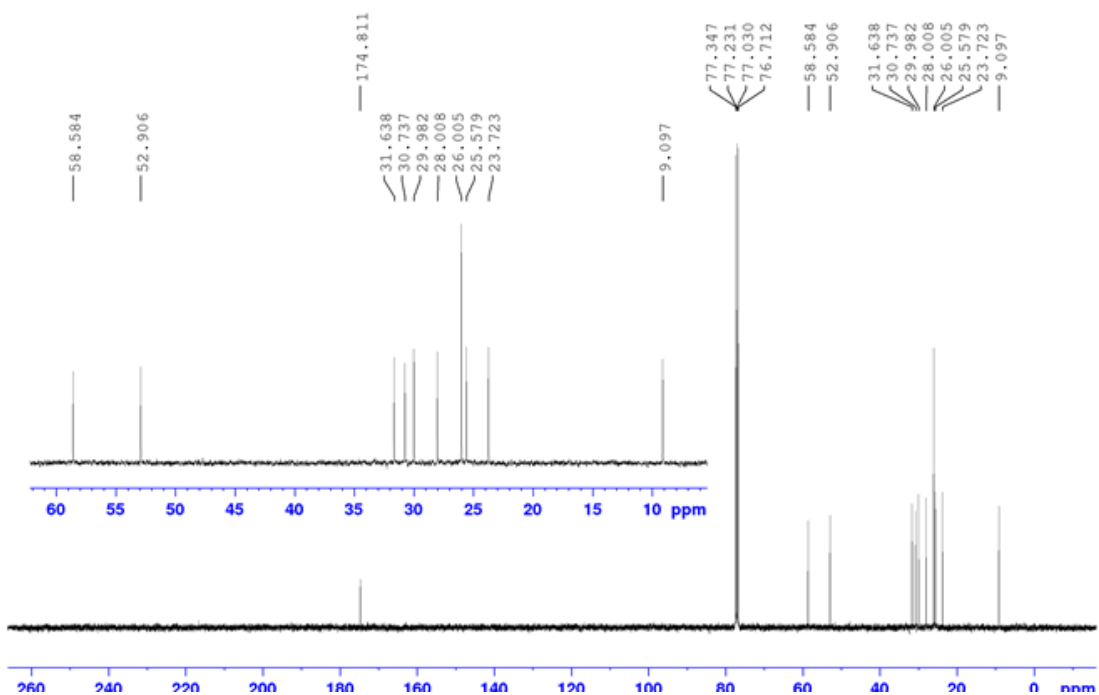
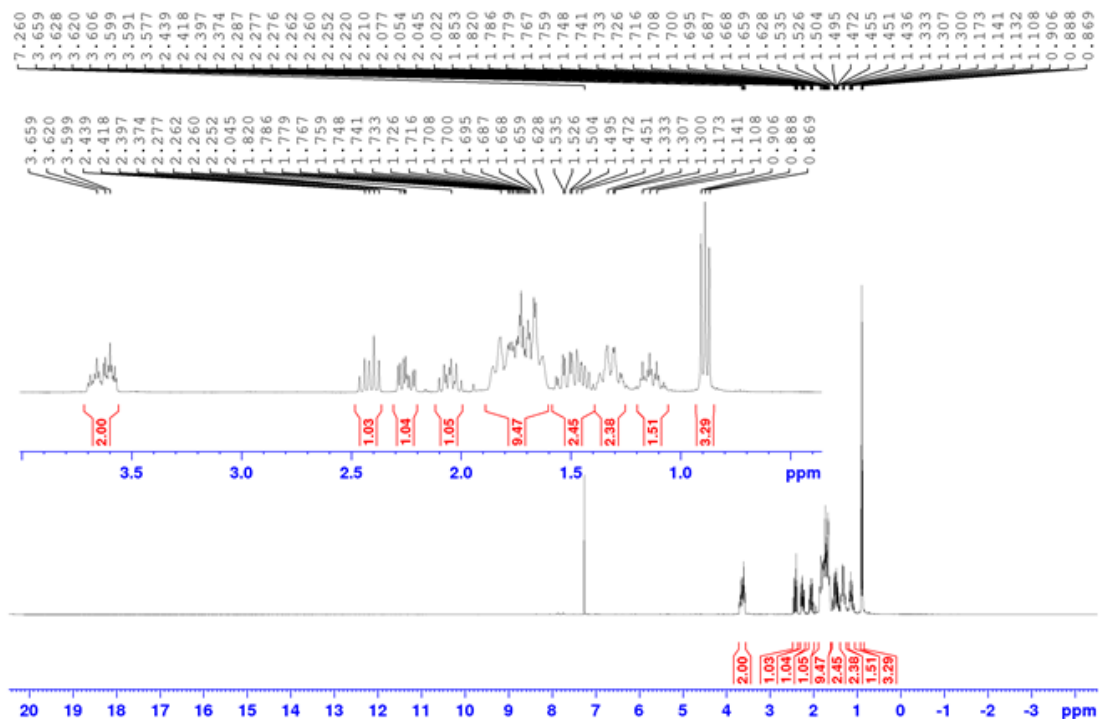
31v

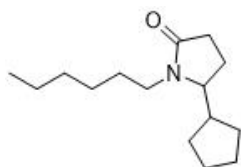




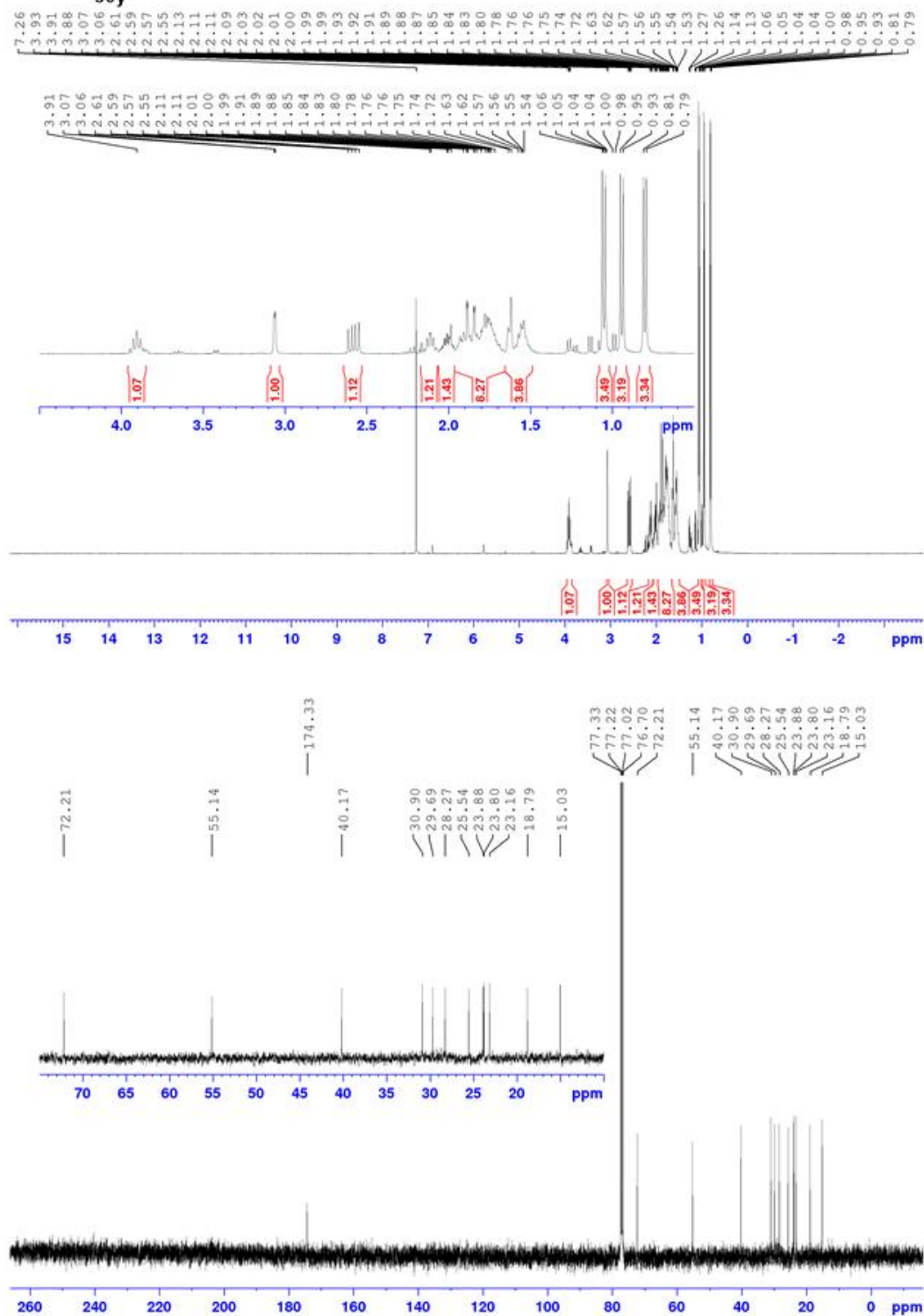
30w

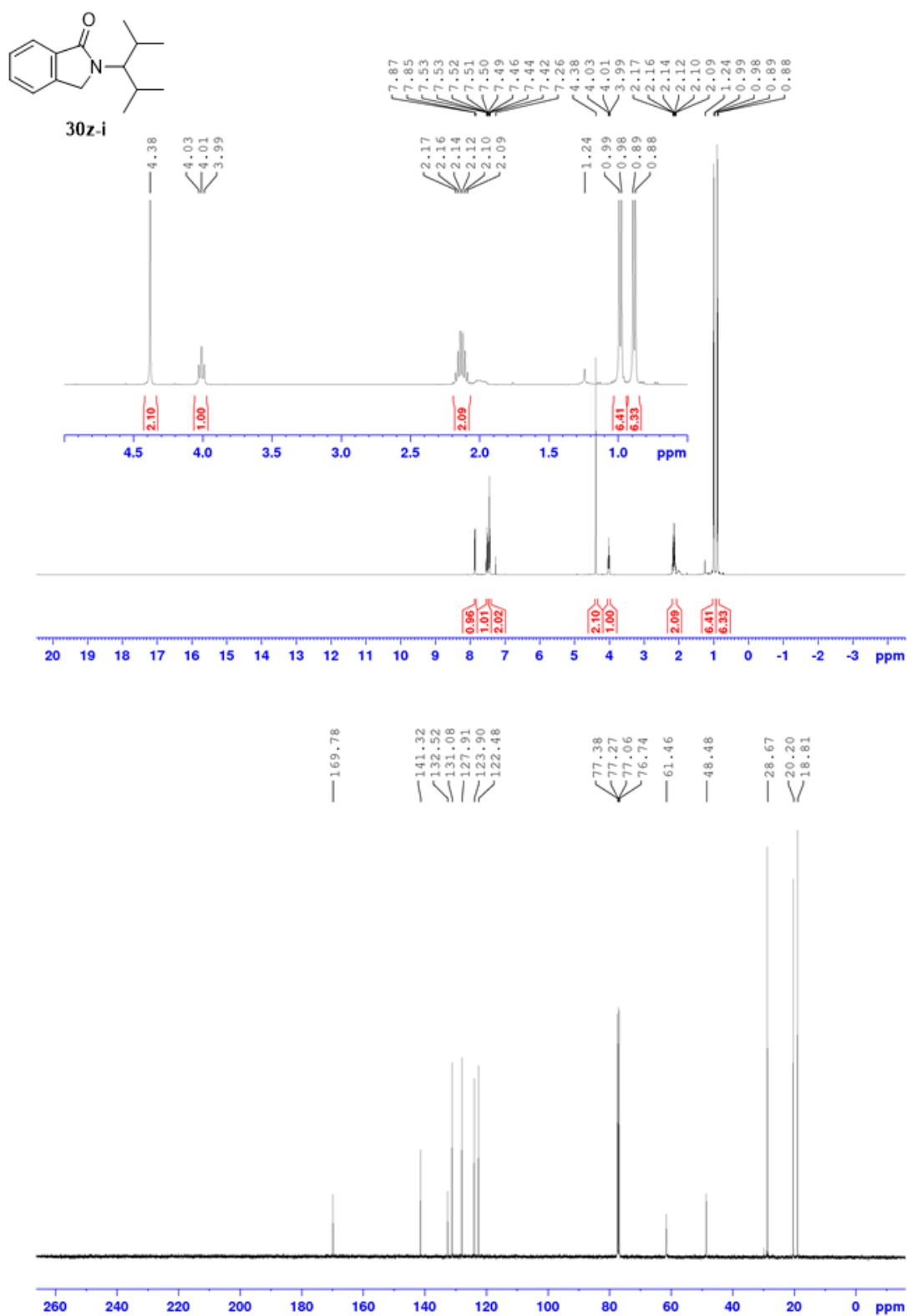


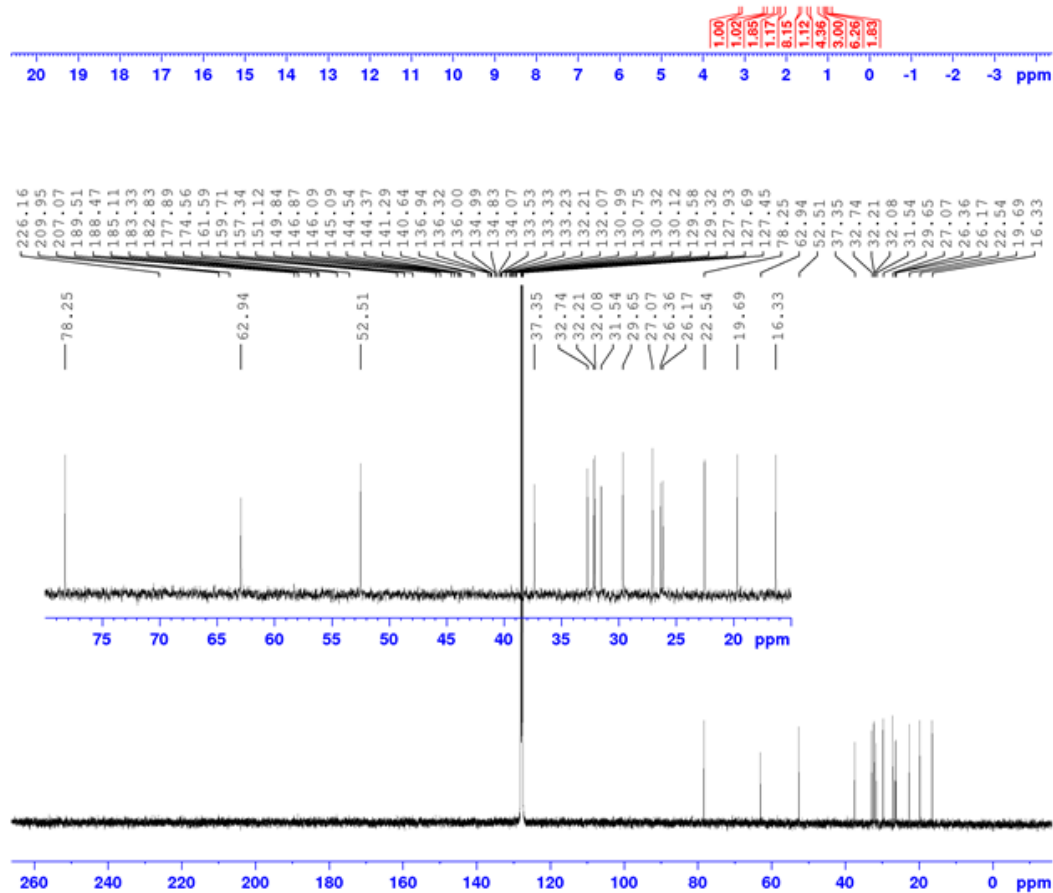
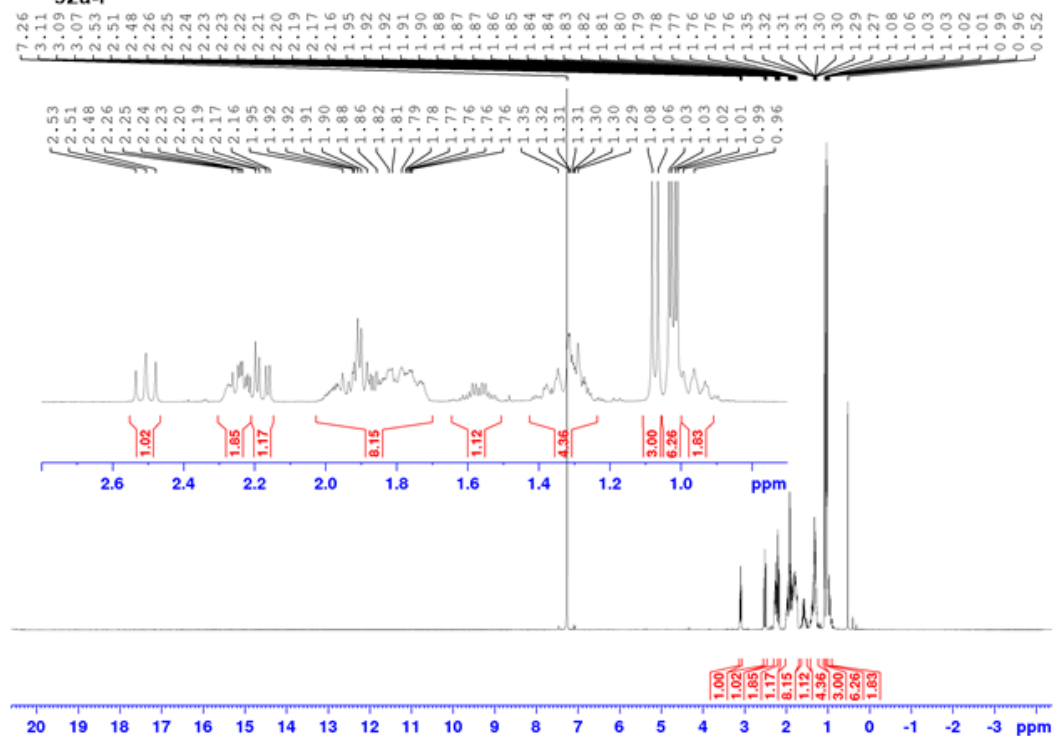
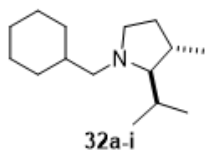


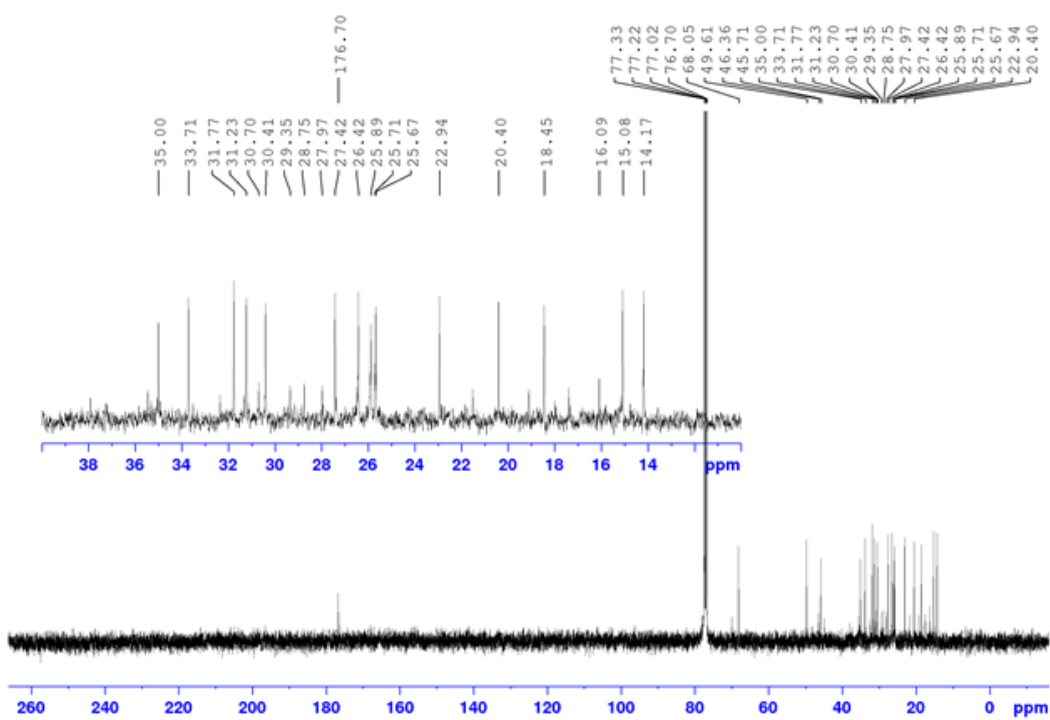
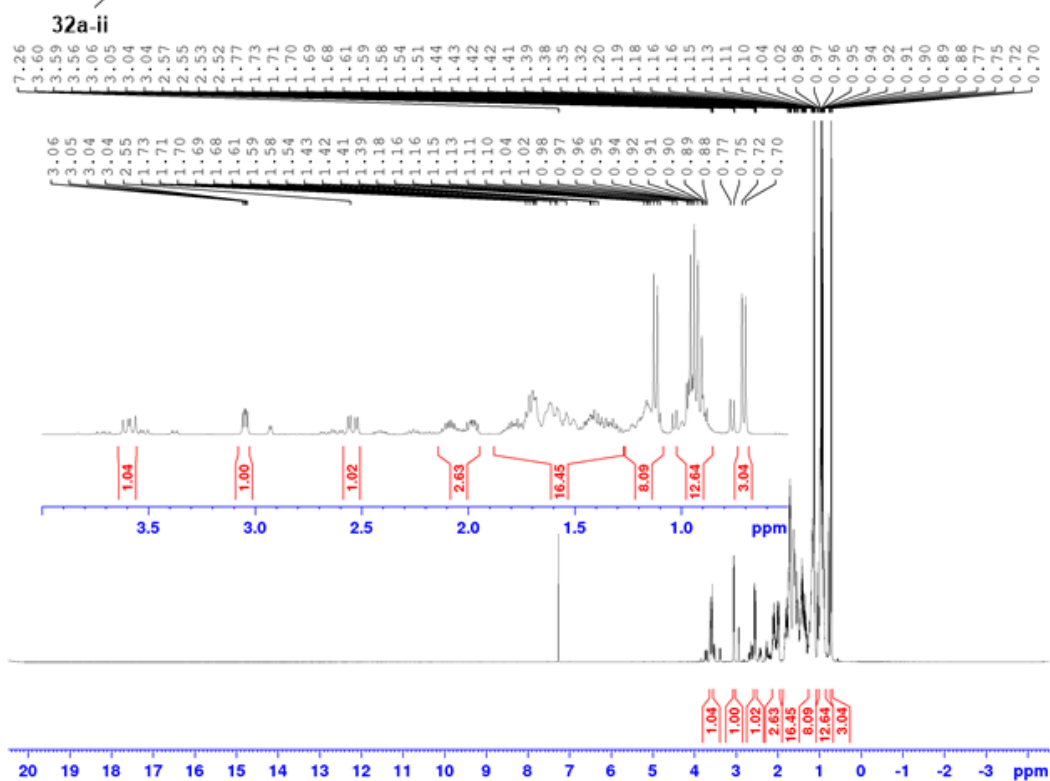
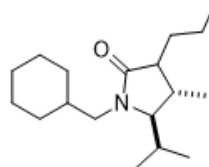


30y

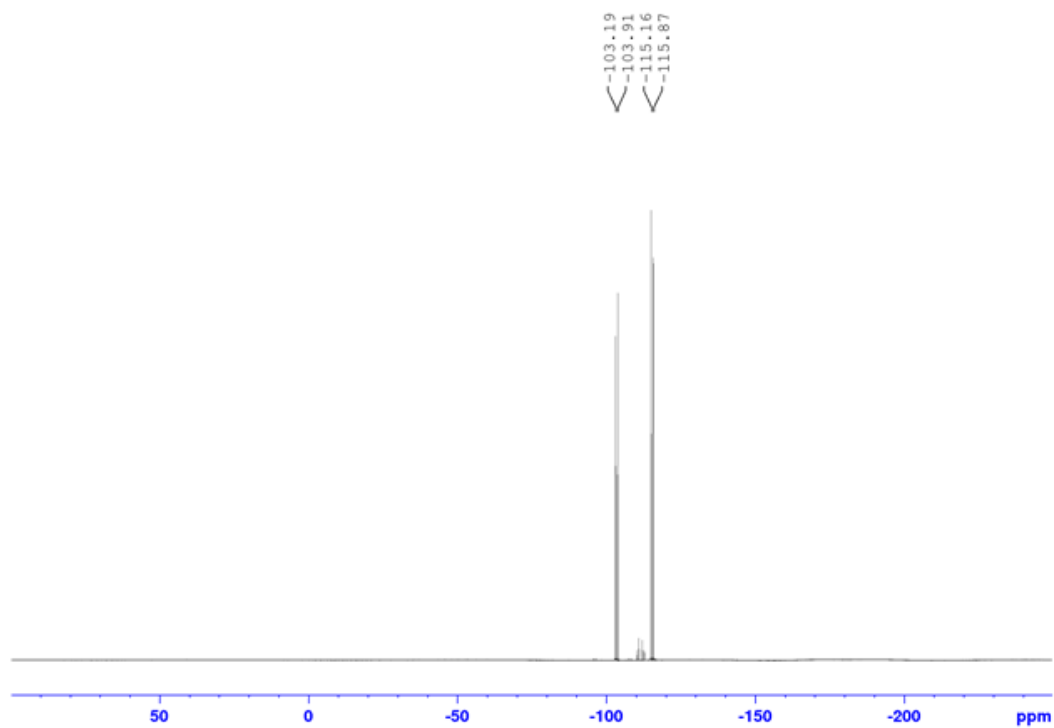
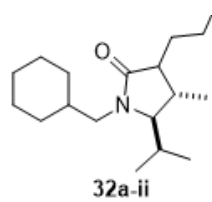


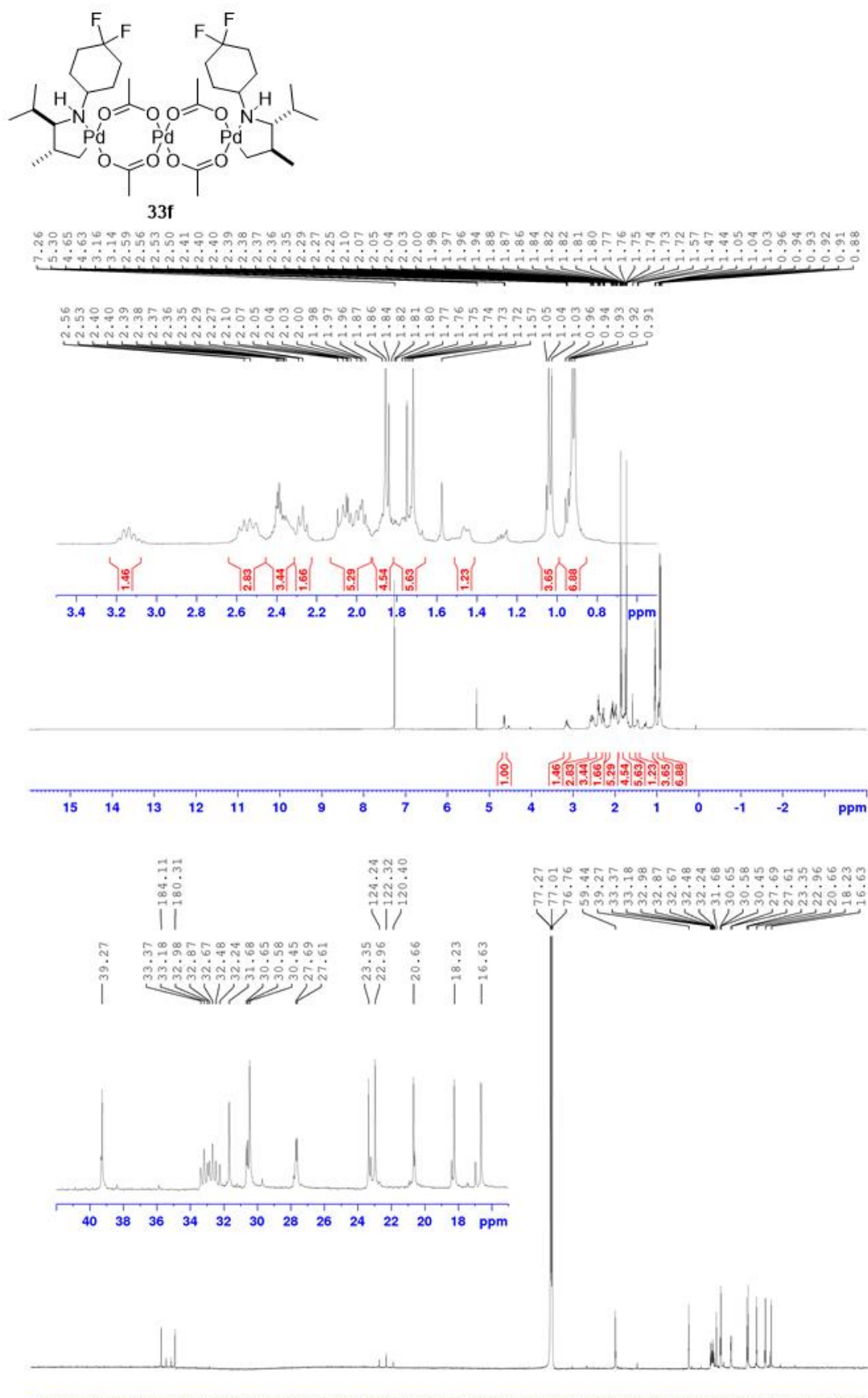


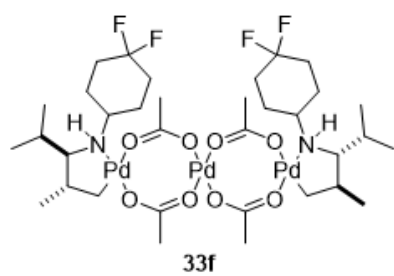












Chemical shift data (ppm):

- 94.15
- 94.18
- 94.78
- 94.81
- 102.26
- 102.41
- 102.88
- 103.03

